THE PATHOGENETIC MECHANISMS AT THE BASIS OF AORTOPATHY ASSOCIATED WITH BICUSPID AORTIC VALVE: INSIGHTS FROM "OMICS", MODELS OF DISEASE AND EMERGENT TECHNOLOGIES

EDITED BY: Amalia Forte and Alessandro Della Corte
PUBLISHED IN: Frontiers in Physiology

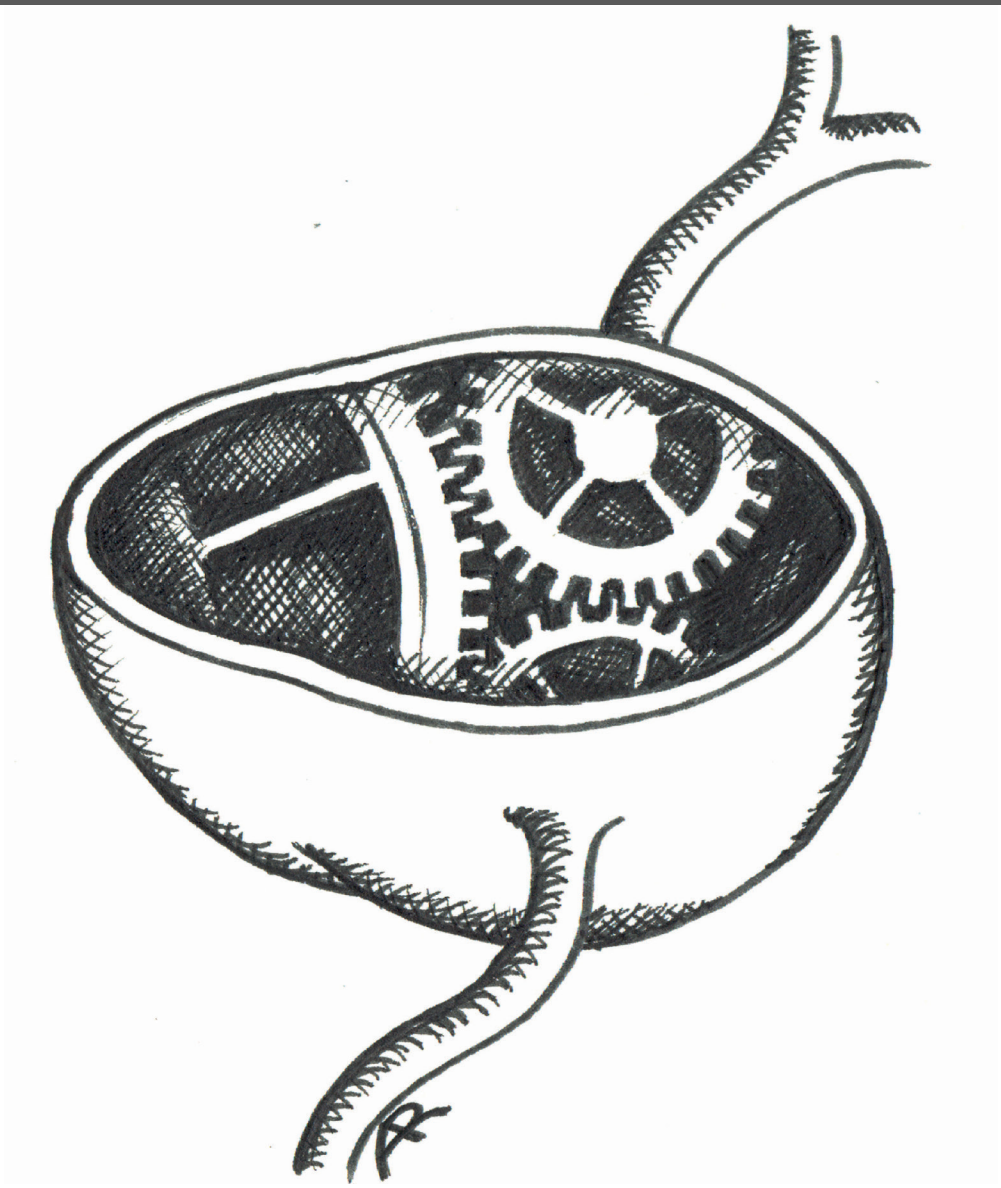

frontiers Research Topics

ISSN 1664-8714
ISBN 978-2-88945-395-5
DOI 10.3389/978-2-88945-395-5

About Frontiers

Frontiers is more than just an open-access publisher of scholarly articles: it is a pioneering approach to the world of academia, radically improving the way scholarly research is managed. The grand vision of Frontiers is a world where all people have an equal opportunity to seek, share and generate knowledge. Frontiers provides immediate and permanent online open access to all its publications, but this alone is not enough to realize our grand goals.

Frontiers Journal Series

The Frontiers Journal Series is a multi-tier and interdisciplinary set of open-access, online journals, promising a paradigm shift from the current review, selection and dissemination processes in academic publishing. All Frontiers journals are driven by researchers for researchers; therefore, they constitute a service to the scholarly community. At the same time, the Frontiers Journal Series operates on a revolutionary invention, the tiered publishing system, initially addressing specific communities of scholars, and gradually climbing up to broader public understanding, thus serving the interests of the lay society, too.

Dedication to Quality

Each Frontiers article is a landmark of the highest quality, thanks to genuinely collaborative interactions between authors and review editors, who include some of the world's best academicians. Research must be certified by peers before entering a stream of knowledge that may eventually reach the public - and shape society; therefore, Frontiers only applies the most rigorous and unbiased reviews.
Frontiers revolutionizes research publishing by freely delivering the most outstanding research, evaluated with no bias from both the academic and social point of view.
By applying the most advanced information technologies, Frontiers is catapulting scholarly publishing into a new generation.

What are Frontiers Research Topics?

Frontiers Research Topics are very popular trademarks of the Frontiers Journals Series: they are collections of at least ten articles, all centered on a particular subject. With their unique mix of varied contributions from Original Research to Review Articles, Frontiers Research Topics unify the most influential researchers, the latest key findings and historical advances in a hot research area! Find out more on how to host your own Frontiers Research Topic or contribute to one as an author by contacting the Frontiers Editorial Office: **researchtopics@frontiersin.org**

THE PATHOGENETIC MECHANISMS AT THE BASIS OF AORTOPATHY ASSOCIATED WITH BICUSPID AORTIC VALVE: INSIGHTS FROM "OMICS", MODELS OF DISEASE AND EMERGENT TECHNOLOGIES

Topic Editors:
Amalia Forte, University of Campania "L. Vanvitelli" Naples, Italy
Alessandro Della Corte, University of Campania "L. Vanvitelli" Naples, Italy

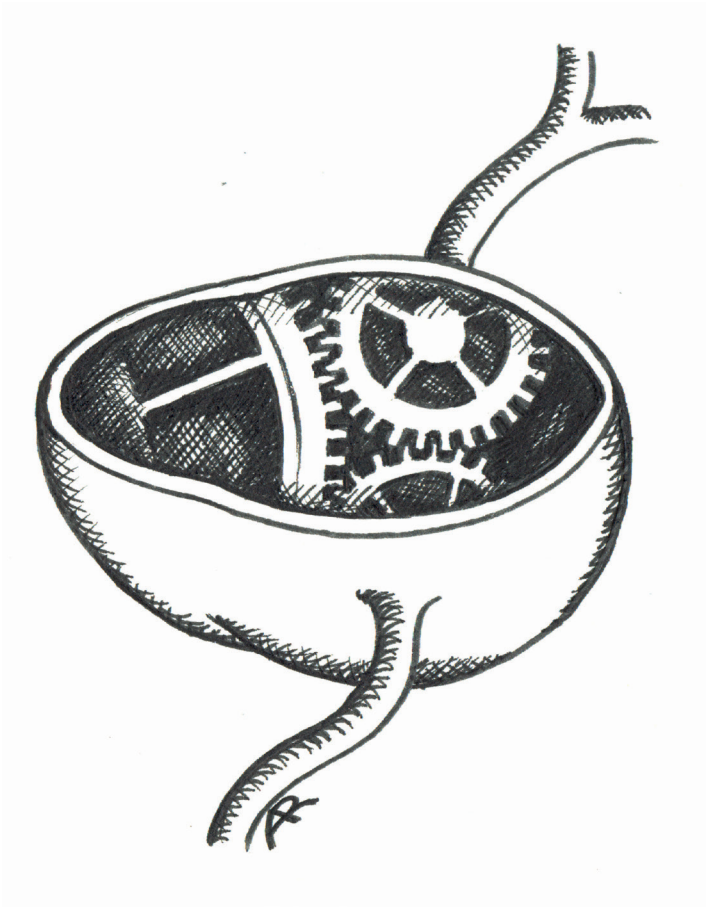

Which pathogenetic mechanisms underlie bicuspid aortopathy?

Image: Dr Rasul Ashurov, from the Cardiac Surgery School of the Department of Cardiothoracic and Respiratory Sciences, University of Campania "L. Vanvitelli", Naples, Italy.

This forum of comprehensive reviews and research studies on distinct aspects of the pathophysiology of BAV aortopathy provides both the state of the art in the knowledge on this complex disease and novel insights into its causes and consequences. The present collection of focused papers also envisions and proposes new therapeutic strategies, novel biomarkers and original risk stratification criteria, for the improvement of patient management.

Citation: Forte, A., Della Corte, A., eds. (2018). The Pathogenetic Mechanisms at the Basis of Aortopathy Associated with Bicuspid Aortic Valve: Insights from "Omics", Models of Disease and Emergent Technologies. Lausanne: Frontiers Media. doi: 10.3389/978-2-88945-395-5

Table of Contents

Section 2: Biomechanics and Clinical Applications

frontiers in Physiology

EDITORIAL
published: 04 December 2017
doi: 10.3389/fphys.2017.01002

Editorial: The Pathogenetic Mechanisms at the Basis of Aortopathy Associated with Bicuspid Aortic Valve: Insights from "Omics", Models of Disease and Emergent Technologies

Amalia Forte[1]* *and Alessandro Della Corte*[2]*

[1] Department of Experimental Medicine, University of Campania "L. Vanvitelli," Naples, Italy, [2] Department of Cardiothoracic and Respiratory Sciences, University of Campania "L. Vanvitelli," Naples, Italy

Keywords: bicuspid aortic valve, aortopathy, pathogenesis, hemodynamics, genetics, epigenetics, smooth muscle cells, endothelial cells

Editorial on the Research Topic

The Pathogenetic Mechanisms at the Basis of Aortopathy Associated with Bicuspid Aortic Valve: Insights from "Omics", Models of Disease and Emergent Technologies

OPEN ACCESS

Edited and reviewed by:
John D. Imig,
Medical College of Wisconsin,
United States

***Correspondence:**
Amalia Forte
amalia.forte@unicampania.it
Alessandro Della Corte
aledellacorte@libero.it

Specialty section:
This article was submitted to Vascular Physiology, a section of the journal Frontiers in Physiology

Received: *07 November 2017*
Accepted: *20 November 2017*
Published: *04 December 2017*

Citation:
Forte A and Della Corte A (2017) Editorial: The Pathogenetic Mechanisms at the Basis of Aortopathy Associated with Bicuspid Aortic Valve: Insights from "Omics", Models of Disease and Emergent Technologies. Front. Physiol. 8:1002. doi: 10.3389/fphys.2017.01002

The bicuspid aortic valve (BAV) represents the most frequent congenital cardiovascular malformation among live births, with a prevalence of 1–2% in the general population (Ward, 2000).

BAV aortopathy is characterized by a complex, multifactorial pathophysiology, involving alterations in genetics, epigenetics, hemodynamics, as well as in cellular and molecular pathways (Forte et al., 2013, 2016). All these factors contribute to BAV aortopathy with different levels of interaction and impacts in patients. BAV aortopathy is associated with a 6-9-fold increased risk of aortic complications (e.g. dissection) with respect to the general population, leading to higher morbidity and mortality (Michelena et al., 2011). Currently, the only available treatment of aortic aneurysm is surgical intervention (Calero and Illig, 2016).

In this Research Topic of *Frontiers in Vascular Physiology*, Authors with different background and expertise in the field of BAV aortopathy, examined different aspects of this disease, including the clinical, hemodynamic and biomechanic aspects, the identification of key molecular pathways involved in alterations of the phenotype of endothelial (ECs) and smooth muscle cells (SMCs) and in mechanosensing, and the identification of potential early biomarkers of aortopathy, with the aim of collecting and summarizing the most updated research findings.

It is believed that different combinations of BAV phenotypes and valvular dysfunctions lead to different alterations in wall shear stress in distinct regions (Della Corte et al., 2014; Sievers et al., 2016), which in turn can cause consequent specific molecular and histological changes. An in-depth characterization of BAV aortopathy is still missing, at least in part because of the heterogeneity described above, thus leading to limitations in the clinical approach, i.e., risk stratification criteria and standardization of surgical treatment. Fatehi Hassanabad et al. addressed in an interesting review the risk stratification of BAV patients through non-invasive hemodynamic biomarkers derived from novel imaging techniques. Among them, the *in vivo* assessment of time-resolved 3D blood velocity, using a volumetric imaging method referred to as 4D flow magnetic resonance imaging (MRI), can be utilized to accurately identify altered flow patterns secondary to BAV, even

if aortic stenosis is present. As a result, 4D flow MRI revealed that aortic wall shear stress (WSS) is increased in BAV subjects independently from the degree of stenosis, and is dependent on aortic valve fusion phenotype. The study summarized by the Authors in their review demonstrates the potential utility of 4D flow MRI to identify areas with more advanced aortopathy in patients. Advanced models of risk prediction, i.e., based not only on aortic size and growth criteria, could lead to the development of individualized surgical approaches for patients with BAV and associated aortic disease.

The importance of hemodynamics in BAV aortopathy and the role of 4D flow MRI in the identification of alterations of WSS distribution in patients in relation with BAV morphotype and before the onset of aortopathy has been underlined also by a research study conducted by Piatti et al. In addition, the relevance of BAV morphotype in pulsatile flow characteristics has been investigated and confirmed *in vitro* in a study conducted on porcine tissue models of tricuspid aortic valve (TAV) and BAV using particle image velocimetry (PIV) (McNally et al.).

Of interest, Kim et al. focused their investigations not on the aorta but on the structure and mechanical function of the common carotids of BAV and TAV patients using ultrasound and velocity vector imaging (VVI), revealing differences for carotids in BAV patients and thus suggesting intrinsic vascular alterations in these subjects.

While abnormal flow patterns in the aortas of patients with BAV are increasingly recognized as important in the pathogenesis of aortic dilatation, pulmonary flow patterns in bicuspid pulmonary valves have not been investigated so far. Bicuspid pulmonary valve disease is rare and a small numbers of case reports describe concomitant pulmonary artery dilation similar to the dilation of the ascending aorta. Bissell et al. focused their research study on the 4D flow MRI assessment of the flow pattern in bicuspid *vs.* tricuspid pulmonary valves, revealing haemodynamic alterations similar to recent studies in BAV aortopathy, thus suggesting the importance of flow patterns in the pathophysiology of vessel dilation in both aortic and pulmonary bicuspid valve disease.

Along with hemodynamics, surely genetics contributes to BAV aortopathy pathogenesis, as intuitively suggested by BAV malformation being characterized by an autosomal dominant pattern of inheritance with reduced penetrance and variable expressivity. Few genes have been robustly linked to the BAV phenotype to date. In the present Research Topic, Giusti et al. reviewed the genes and *loci* proven or candidate to be associated with BAV (e.g., NOTCH1, GATA5, ACTA2 and a locus containing AXIN1 and PDIA2). Interestingly, the Authors reported also data for the gene FBN1, whose alteration is already known to be causative of Marfan syndrome (MFS), but some variants have now been associated with aortic dilation also in some BAV patients not fulfilling the clinical criteria for MFS. In addition, the impact of novel high-throughput sequencing technologies and of methods for data analysis on research and diagnosis of BAV genetic alterations has been addressed by Giusti et al. Among them, the haloplex target enrichment system has been used by Gillis et al. for targeted resequencing of 22 BAV-associated genes and for evaluation of their contribution to the etiology of BAV-associated thoracic aortic aneurysm (TAA), starting from the hypothesis that rare genetic variants in these genes may be enriched in patients presenting both BAV and TAA. The Authors identified SMAD6 as the strongest candidate susceptibility gene, showing different types of mutations in 2.5% of the large BAV/TAA cohort they analyzed. Additional considerations about the different influence of genetics and hemodynamics in the different phenotypes (root *vs.* tubular ascending) of BAV aortopathy have been proposed by Yassine et al.

Mutations in the NOTCH1 gene mentioned above are proven to be associated with non-syndromic forms of BAV. Ignatieva et al. tested in a research study the hypothesis that Notch-dependent pathways and TGF-β and BMP differentiation pathways exhibit different alterations in SMCs isolated from aortic tissue of BAV and TAV patients, with SMCs from BAV aortas more prone to osteogenic differentiation in response to Notch signal.

Currently, there are no effective strategies to prevent or limit the progression of BAV-related diseases, including aortic dilation. The development of novel therapeutic strategies requires a more detailed comprehension of the underlying molecular mechanisms. In this context, this Research Topic counts in some interesting studies focusing on molecular players whose knowledge about their role in cardiovascular pathogenesis is increasing: the non-coding RNAs (ncRNAs), a class of molecules that includes the micro-ribonucleic acids (miRNAs) and the long non-coding RNAs (lncRNAs). miRNAs are endogenously expressed, 19–23-nt-long RNAs that regulate gene expression at post-transcriptional level, mostly via base-pairing interactions that occur preferentially within the 3′ untranslated regions (UTRs) of target mRNAs. Martínez-Micaelo et al. identified a specific pattern of miRNAs associated with plasmatic endothelial microparticles (EMPs) that is specific for BAV disease, and in particular a cluster of 19 highly co-expressed miRNAs located in the 14q32 locus that could play a role as effectors of the intercellular communication carried out by EMPs in endothelial damage in BAV aortopathy. A relevant role for endothelium in the development of TAA associated with stenotic BAV has been highlighted also in a review by van de Pol et al. with particular reference to the role of communication between ECs and SMCs. miRNAs have been also the focus of the review by Alajbegovic et al., and specifically the small RNA molecules expressed by SMCs and influencing actin polymerization during the progression of aneurysm in BAV. Actin polymerization is important to maintain the contractile phenotype of SMCs through the promotion of specific gene expression *via* the transcriptional co-activator MRTF, which is translocated to the nucleus when released from monomeric actin.

lncRNAs are longer than 200 nt and, differently from miRNAs, their distinct functions are still largely unexplored. Li and Maegdefessel summarized in their review the current knowledge about the regulatory roles of lncRNAs in the fate of SMCs and in development and progression of TAA, with particular reference to HIF1α-antisense RNA 1.

Finally, Norton and Yang provided an overview of the phenotypical heterogeneity of BAV, and the associated complications and also propose a classification of BAV patients on the basis of their clinical phenotype, suggesting a conservative approach or a surgical resection depending on the involvement of aortic root in TAA.

This forum of comprehensive reviews and research studies on distinct aspects of the pathophysiology of BAV aortopathy provides both the state of the art in the knowledge on this complex disease and novel insights into its causes and consequences. The present collection of focused papers also envisions and proposes new therapeutic strategies, novel biomarkers and original risk stratification criteria, for the improvement of patient management.

AUTHOR CONTRIBUTIONS

AF and AD reviewed all the papers accepted for publication in the Research Topic of Frontiers in Vascular Physiology and summarized them in the Editorial, together with a general commentary on the status of current knowledge in BAV aortopathy.

ACKNOWLEDGMENTS

We would like to thank all the contributing Authors, the Reviewers, the *Frontiers in Vascular Physiology* Editor in-chief and the members of the editorial team for their competence and support.

REFERENCES

Calero, A., and Illig, K. A. (2016). Overview of aortic aneurysm management in the endovascular era. *Semin. Vasc. Surg.* 29:3. doi: 10.1053/j.semvascsurg.2016.07.003

Della Corte, A., Body, S. C., Booher, A. M., Schaefers, H. J., Milewski, R. K., Michelena, H. I., et al. (2014). International Bicuspid Aortic Valve Consortium (BAVCon) Investigators. Surgical treatment of bicuspid aortic valve disease: knowledge gaps and research perspectives. *J. Thorac. Cardiovasc. Surg.* 147:1749. doi: 10.1016/j.jtcvs.2014.01.021

Forte, A., Della Corte, A., Grossi, M., Bancone, C., Provenzano, R., Finicelli, M., et al. (2013). Early cell changes and TGFβ pathway alterations in the aortopathy associated with bicuspid aortic valve stenosis. *Clin. Sci.* 124:97. doi: 10.1042/CS20120324

Forte, A., Galderisi, U., Cipollaro, M., De Feo, M., and Della Corte, A. (2016). Epigenetic regulation of TGF-β1 signalling in dilative aortopathy of the thoracic ascending aorta. *Clin. Sci.* 130:1389. doi: 10.1042/CS20160222

Michelena, H. I., Khanna, A. D., Mahoney, D., Margaryan, E., Topilsky, Y., Suri, R. M., et al. (2011). Incidence of aortic complications in patients with bicuspid aortic valves. *JAMA* 306:1104. doi: 10.1001/jama.2011.1286

Sievers, H. H., Stierle, U., Hachmann, R. M., and Charitos, E. I. (2016). New insights in the association between bicuspid aortic valve phenotype, aortic configuration and valve haemodynamics. *Eur. J. Cardiothorac. Surg.* 49:439. doi: 10.1093/ejcts/ezv087

Ward, C. (2000). Clinical significance of the bicuspid aortic valve. *Heart* 83:81. doi: 10.1136/heart.83.1.81

Conflict of Interest Statement: The authors declare that the research was conducted in the absence of any commercial or financial relationships that could be construed as a potential conflict of interest.

frontiers in Physiology

ORIGINAL RESEARCH
published: 13 June 2017
doi: 10.3389/fphys.2017.00400

Candidate Gene Resequencing in a Large Bicuspid Aortic Valve-Associated Thoracic Aortic Aneurysm Cohort: *SMAD6* as an Important Contributor

Elisabeth Gillis[1†], Ajay A. Kumar[1†], Ilse Luyckx[1], Christoph Preuss[2], Elyssa Cannaerts[1], Gerarda van de Beek[1], Björn Wieschendorf[1,3], Maaike Alaerts[1], Nikhita Bolar[1], Geert Vandeweyer[1], Josephina Meester[1], Florian Wünnemann[2], Russell A. Gould[4], Rustam Zhurayev[5], Dmytro Zerbino[5], Salah A. Mohamed[3], Seema Mital[6], Luc Mertens[6], Hanna M. Björck[7], Anders Franco-Cereceda[8], Andrew S. McCallion[4], Lut Van Laer[1], Judith M. A. Verhagen[9], Ingrid M. B. H. van de Laar[9], Marja W. Wessels[9], Emmanuel Messas[10], Guillaume Goudot[10], Michaela Nemcikova[11], Alice Krebsova[12], Marlies Kempers[13], Simone Salemink[13], Toon Duijnhouwer[13], Xavier Jeunemaitre[10], Juliette Albuisson[10], Per Eriksson[7], Gregor Andelfinger[2], Harry C. Dietz[4,14], Aline Verstraeten[1], Bart L. Loeys[1,13] and Mibava Leducq Consortium*

[1] Faculty of Medicine and Health Sciences, Center of Medical Genetics, University of Antwerp and Antwerp University Hospital, Antwerp, Belgium, [2] Cardiovascular Genetics, Department of Pediatrics, CHU Sainte-Justine, Université de Montreal, Montreal, QC, Canada, [3] Department of Cardiac and Thoracic Vascular Surgery, University Hospital Schleswig-Holstein, Lübeck, Germany, [4] McKusick-Nathans Institute of Genetic Medicine, Johns Hopkins University School of Medicine, Baltimore, MD, United States, [5] Department of Clinical pathology, Lviv National Medical University after Danylo Halytsky, Lviv, Ukraine, [6] Cardiovascular Research, SickKids University Hospital, Toronto, ON, Canada, [7] Cardiovascular Medicine Unit, Department of Medicine, Karolinska Institute, Stockholm, Sweden, [8] Cardiothoracic Surgery Unit, Department of Molecular Medicine and Surgery, Karolinska Institute, Stockholm, Sweden, [9] Department of Clinical Genetics, Erasmus University Medical Center, Rotterdam, Netherlands, [10] Assistance Publique–Hôpitaux de Paris, Hôpital Européen Georges Pompidou; Université Paris Descartes, Paris Sorbonne Cité; Institut National de la Santé et de la Recherche Médicale, UMRS, Paris, France, [11] Department of Biology and Medical Genetics, 2nd Faculty of Medicine-Charles University and Motol University Hospital, Prague, Czechia, [12] Institute of Clinical and Experimental Medicine, Prague, Czechia, [13] Department of Human Genetics, Radboud University Medical Centre, Nijmegen, Netherlands, [14] Howard Hughes Medical Institute, Baltimore, MD, United States

Bicuspid aortic valve (BAV) is the most common congenital heart defect. Although many BAV patients remain asymptomatic, at least 20% develop thoracic aortic aneurysm (TAA). Historically, BAV-related TAA was considered as a hemodynamic consequence of the valve defect. Multiple lines of evidence currently suggest that genetic determinants contribute to the pathogenesis of both BAV and TAA in affected individuals. Despite high heritability, only very few genes have been linked to BAV or BAV/TAA, such as *NOTCH1*, *SMAD6,* and *MAT2A*. Moreover, they only explain a minority of patients. Other candidate genes have been suggested based on the presence of BAV in knockout mouse models (e.g., *GATA5, NOS3*) or in syndromic (e.g., *TGFBR1/2, TGFB2/3*) or non-syndromic (e.g., *ACTA2*) TAA forms. We hypothesized that rare genetic variants in these genes may be enriched in patients presenting with both BAV and TAA. We performed targeted resequencing of 22 candidate genes using Haloplex target enrichment in a strictly defined BAV/TAA cohort (n = 441; BAV in addition to an aortic root or ascendens

OPEN ACCESS

Edited by:
Alessandro Della Corte, Second University of Naples, Monaldi Hospital, Italy

Reviewed by:
Simon Body, Brigham and Women's Hospital, United States
Bengt-Olof Nilsson, Lund University, Sweden

***Correspondence:**
Bart L. Loeys
bart.loeys@uantwerpen.be

[†] *These authors have contributed equally to this work.*

Specialty section:
This article was submitted to Vascular Physiology, a section of the journal Frontiers in Physiology

Received: *14 April 2017*
Accepted: *26 May 2017*
Published: *13 June 2017*

Citation:
Gillis E, Kumar AA, Luyckx I, Preuss C, Cannaerts E, van de Beek G, Wieschendorf B, Alaerts M, Bolar N, Vandeweyer G, Meester J, Wünnemann F, Gould RA, Zhurayev R, Zerbino D, Mohamed SA, Mital S, Mertens L, Björck HM, Franco-Cereceda A, McCallion AS, Van Laer L, Verhagen JMA, van de Laar IMBH, Wessels MW, Messas E, Goudot G, Nemcikova M, Krebsova A, Kempers M, Salemink S, Duijnhouwer T, Jeunemaitre X, Albuisson J, Eriksson P, Andelfinger G, Dietz HC, Verstraeten A, Loeys BL and Mibava Leducq Consortium (2017) Candidate Gene Resequencing in a Large Bicuspid Aortic Valve-Associated Thoracic Aortic Aneurysm Cohort: SMAD6 as an Important Contributor. Front. Physiol. 8:400. doi: 10.3389/fphys.2017.00400

diameter ≥ 4.0 cm in adults, or a Z-score ≥ 3 in children) and in a collection of healthy controls with normal echocardiographic evaluation ($n = 183$). After additional burden analysis against the Exome Aggregation Consortium database, the strongest candidate susceptibility gene was *SMAD6* ($p = 0.002$), with 2.5% ($n = 11$) of BAV/TAA patients harboring causal variants, including two nonsense, one in-frame deletion and two frameshift mutations. All six missense mutations were located in the functionally important MH1 and MH2 domains. In conclusion, we report a significant contribution of *SMAD6* mutations to the etiology of the BAV/TAA phenotype.

Keywords: bicuspid aortic valve, thoracic aortic aneurysm, SMAD6, targeted gene panel, variant burden test

INTRODUCTION

With a prevalence of 1–2% in the general population, bicuspid aortic valve (BAV) is the most common congenital heart defect. It has a 3:1 male preponderance and is characterized by an aortic valve with two cusps instead of the normal three. BAV often coincides with aortic manifestations such as coarctation of the aorta and thoracic aortic aneurysm (TAA) (Verstraeten et al., 2016). The latter can lead to lethal dissections if left untreated. Although first described over 400 years ago and high heritability (89%) (Cripe et al., 2004), the genetic etiology of BAV, with or without TAA, remains largely elusive. It was initially suggested that TAA results from altered blood flow dynamics imposed by the abnormal bicuspid valve. Changes in shear stress were presumed to weaken the aortic wall, resulting in dilatation and rupture. At present, common genetic risk factors for BAV and TAA are proposed (Hinton, 2012), based on the following observations: (i) the aortic valve and the aorta share common embryologic origins [i.e., the cardiac neural crest (CNC) and the second heart field] (Martin et al., 2015), (ii) family members of BAV/TAA probands show TAA without valve abnormalities and/or BAV without aneurysmal disease (Loscalzo et al., 2007), and (iii) TAA formation in BAV probands that previously underwent valve replacement has been reported (Braverman et al., 2005).

Transmission of BAV/TAA mostly complies with an autosomal dominant inheritance pattern, displaying reduced penetrance and variable expressivity (Clementi et al., 1996; Huntington et al., 1997). Few genes have been robustly linked to the BAV phenotype to date. *NOTCH1* is often considered the sole established BAV gene, either as an isolated finding or in association with early onset valve calcification, TAA, or other left-sided heart defects (Mohamed et al., 1797; Garg et al., 2005; McKellar et al., 2007; Foffa et al., 2013; Kent et al., 2013; Bonachea et al., 2014; Freylikhman et al., 2014; Kerstjens-Frederikse et al., 2016). *SMAD6* (Tan et al., 2012) and *MAT2A* (Guo et al., 2015) have also been implicated in BAV, but only in a very limited number of patients. A dozen candidate genes emanated from knockout mouse models with increased BAV occurrence (Biben et al., 2000; Lee et al., 2000; Laforest and Nemer, 2011; Laforest et al., 2011; Thomas et al., 2012; Mommersteeg et al., 2015; Quintero-Rivera et al., 2015). The prevalence of BAV in these knockout models is often low (range: 2–42% in single knockouts) (**Table 1**), probably due to reduced penetrance and/or activation of compensatory mechanisms. Mutations in some syndromic (Attias et al., 2009; Callewaert et al., 2011; Lindsay et al., 2012; Nistri et al., 2012; van de Laar et al., 2012; Pepe et al., 2014) or non-syndromic (Guo et al., 2007) TAA genes also associate with increased BAV occurrence (**Table 1**).

To date, no major BAV/TAA gene has emerged. The described genes have been associated with BAV, but their contribution to the etiology of BAV/TAA has never been examined systematically. Here, we evaluate this contribution in 22 BAV-associated genes (**Table 1**) using a targeted gene panel and variant burden approach.

MATERIALS AND METHODS

Study Cohort

Genomic DNA (gDNA) of 441 BAV/TAA patients was collected through a collaborative effort involving 8 different centers (Supplementary Table 1). Patients were selected based on the presence of BAV and either an aortic diameter at the sinus of Valsalva or the ascending aorta of at least 4.0 cm in adults, or a Z-score exceeding 3 in children. Aortic diameter dimensions were determined using echocardiography, computed tomography or magnetic resonance imaging. A positive family history was defined as having at least one first- or second-degree relative with BAV and/or TAA. Control gDNA was obtained from 183 cancer patients who presented at the SickKids Hospital, Toronto, Canada. None of the controls showed structural heart disease upon examination with echocardiography. All study participants or their legal guardians gave informed consent at the respective sample-contributing centers.

Targeted Enrichment

Genes ($n = 22$) were selected for targeted resequencing based on the following criteria: (i) mutations occur in human BAV cases ($n = 3$), (ii) knockout mouse models present with incomplete penetrance of BAV ($n = 9$), and (iii) occasional or increased BAV manifestation occurs in patients with mutations in known TAA genes ($n = 10$) (**Table 1**). Enrichment of all exons of these candidate genes, including ±10 nucleotides of adjacent intronic sequence, was performed with a custom Haloplex target enrichment kit per instructions of the manufacturer (Agilent Technologies, USA). Probe design covered a theoretical 99.7% of the complete target region (560 kb). Pooled samples were sequenced either on a HiSeq 2500 (Illumina, USA) with 2 × 150

TABLE 1 | Genes included in the targeted gene panel and the criteria on which their selection was based.

Context	Gene	Incidence	References
BAV in humans	*NOTCH1*	Mutations found in 27 BAV patients	Mohamed et al., 1797; Garg et al., 2005; McKellar et al., 2007; Foffa et al., 2013; Kent et al., 2013; Bonachea et al., 2014; Freylikhman et al., 2014; Kerstjens-Frederikse et al., 2016
	SMAD6	Mutations found in 2 BAV patients	Tan et al., 2012
	MAT2A	Mutations found in 1 BAV patient	Guo et al., 2015
BAV in mice	*ACVR1*	BAV in 78–83% of $Alk2^{FXKO}/Gata5^{-Cre+}$ mice	Thomas et al., 2012
	GATA4	BAV in 43% of $Gata4^{+/-}$;$Gata5^{+/-}$ mice	Laforest and Nemer, 2011
	GATA5	BAV in 25% of $Gata5^{-/-}$ mice	Laforest et al., 2011
	GATA6	BAV in 25% $Gata5^{+/-}$;$Gata6^{+/-}$ mice	Laforest and Nemer, 2011
	MATR3	BAV in 12% in $Matr3^{+/-}$ mice	Quintero-Rivera et al., 2015
	NKX2-5	BAV in 2–20% of $Nkx2\text{-}5^{+/-}$ mice	Biben et al., 2000
	NOS3	BAV in 42% of $Nos3^{-/-}$ mice	Lee et al., 2000
	ROBO1	BAV in 100% of $Robo1^{-/-}$;$Robo2^{-/-}$ mice	Mommersteeg et al., 2015
	ROBO2	BAV in 100% of $Robo1^{-/-}$;$Robo2^{-/-}$ mice	Mommersteeg et al., 2015
BAV in (non)syndromic TAA cases	*FBN1*	Occasional BAV in Marfan syndrome	Attias et al., 2009; Nistri et al., 2012; Pepe et al., 2014
	ACTA2	7% BAV in non-syndromic TAA	Guo et al., 2007
	ELN	Occasional BAV in cutis laxa	Callewaert et al., 2011
	FLNA	Occasional BAV in X-linked valve disease	Jefferies et al., 2010
	MYH11	Occasional BAV in non-syndromic TAA	Personal observation
	SMAD3	3–11% BAV in Loeys-Dietz syndrome	van de Laar et al., 2012
	TGFB2	8–13% BAV in Loeys-Dietz syndrome	Lindsay et al., 2012
	TGFB3	4% BAV in Loeys-Dietz syndrome	Personal observation
	TGFBR1	8–12% BAV in Loeys-Dietz syndrome	Personal observation
	TGFBR2	8–12% BAV in Loeys-Dietz syndrome	Personal observation

BAV, Bicuspid aortic valve; TAA, Thoracic aortic aneurysm.

bp reads or on a HiSeq 1500 (Illumina, USA) with 2 × 100 bp reads.

Data Analysis and Filtering

The raw data were processed using an in-house-developed Galaxy-based pipeline, followed by variant calling with the Genome Analysis Toolkit Unified Genotyper (DePristo et al., 2011). Variants were subsequently annotated and filtered with the in-house developed database VariantDB (Vandeweyer et al., 2014), which uses ANNOVAR. Heterozygous coding or splice site (±2 bp from exon-intron boundaries for nucleotide substitution, and ±5 bp for multi-bp deletions or insertions) variants with an allelic balance between 0.25 and 0.85 (*FLNA* in males: 0.75–1) and a minimum coverage of 10 reads were selected. Finally, we included variants that fitted within at least one of the following three categories; unique variants [absent in the Exome Aggregation Consortium (ExAC) database (Lek et al., 2016)], variants with an ExAC Minor Allele Frequency (MAF) lower than 0.01% or variants with an ExAC MAF between 0.01% and 0.1% that had a Combined Annotation Dependent Depletion (CADD) (Kircher et al., 2014) score above 20. All splice region variants underwent splice site effect prediction using ALAMUT (Interactive Biosoftware, France). Synonymous variants outside of splicing regions were not taken into account.

The ExAC database was used as an independent control dataset. The raw data of variants (∼all ExAC datasets) fulfilling ExAC's quality control parameters ("PASS") were extracted from the offline version of ExAC v0.3.1. Since the ExAC variants were annotated using VEP, whereas our patient variant annotation was ANNOVAR-based, we re-annotated the ExAC variants with ANNOVAR. The same variant filtering strategy as described for the patient cohort was subsequently applied. For each selected ExAC variant, the allele frequency was determined by computing the ratio of the Mutant Allele Count (mAC) and Total Allele Count (tAC). Next, we re-scaled each variant's mAC by multiplying its computed allele frequency by its respective tAC_Adj, i.e., the tAC average of all variants in that specific gene. Finally, the variant counts for each panel gene were obtained by summing up the re-scaled mACs.

Validation by Sanger Sequencing

Variants discussed in the results section were confirmed with Sanger sequencing. Primers were designed using Primer3 software (Untergasser et al., 2012) v4.0.0 and polymerase chain reaction (PCR) products were purified with Calf Intestinal Alkaline Phosphatase (Sigma-Aldrich, USA). Sequencing reactions were performed using the BigDye Terminator Cycle Sequencing kit (Applied Biosystems, Life Technologies, USA), followed by capillary electrophoresis on an ABI3130XL (Applied

Biosystems, Life Technologies, USA). The obtained sequences were analyzed with CLC DNA Workbench v5.0.2 (CLC bio, Denmark).

Segregation Analysis

When family members were available, Sanger sequencing of the *SMAD6* variants identified in the proband was performed in additional relatives to check if the phenotype segregated with the variant.

Statistical Analysis

We performed burden analyses comparing frequencies of the variants fulfilling the three criteria that were mentioned in "Section Data Analysis and Filtering" between patients and controls. Whereas the Fisher's Exact Test was used to statistically compare variant frequencies in the patient cohort to those in the study control cohort, the Chi-Square Test with Yates' correction was used for the patient-ExAC comparison. No *p*-values were calculated if the number of variants in patients and/or controls was zero. Fisher's Exact statistics were also used to determine if significant variant type enrichment and/or domain clustering of variants occurs in patients. Statistical significance was considered when $p < 0.05$.

RESULTS

The patient cohort consisted of 441 BAV/TAA patients (75% males and 25% females) with an average age at inclusion of 63.5 ± 14.4 years. For these patients, the most common associated feature was coarctation of the aorta (2.9%, $n = 13$). About 3% ($n = 14$) had other additional findings such as mitral valve prolaps, aortic stenosis, dilated cardiomyopathy, aortic insufficiency, patent ductus arteriosus or intracranial aneurysm. 46.7% ($n = 206$) had a left-right leaflet BAV orientation, 15.9% ($n = 70$) had a right-non-coronary leaflet BAV orientation and for 37.4% ($n = 165$) of the patients the subtype of valve leaflet morphology was not specified. A positive family history was known for 9.3% of the patients, whereas for the remainder the family history was negative or unknown. The study control cohort ($n = 183$) consisted of 58% males and 42% females. The average age at inclusion of this control cohort was 13.1 ± 5.1 years.

Targeted gene panel sequencing reached an overall coverage at 10x of 99.13% of the targeted regions. In total, 169 variants passed our selection criteria in our patient and control group (Supplementary Table 2). Of these, 112 variants were identified in 441 patients. They included 101 missense, 2 nonsense, 2 splice-site, 5 in-frame indel, and 2 frameshift variants. The 183 study controls contained 57 variants including 53 missense, 1 nonsense, 2 splice-site, and 1 frameshift variant. After applying the identical filtering criteria to the ExAC control cohort, 15,660 variants were retained in on average 54,940 individuals: i.e., 14,931 missense, 190 splice-site, 72 nonsense, 10 no-stop, 204 frameshift, and 253 in-frame indel variants.

To validate our control cohort, we compared its variant frequencies for the 22 selected candidate genes to those of the ExAC cohort. No significant differences were observed (**Figure 1**). We then performed a variant burden analysis equating the numbers of patient variants per gene to the numbers found in the control cohort (**Table 2**). Results are graphically presented in **Figure 1**, showing the proportion of variants per gene in the three different cohorts. Although a few genes (e.g., *FLNA*) showed trends toward significance when comparing our study patient and control cohort, we decided to focus on the patient-ExAC comparison because of the larger number of controls in the ExAC cohort and hence, higher power. Only *SMAD6* reached significance ($p = 0.002$) in the patient-ExAC comparison. Remarkably, a protective effect for *NOS3* and *NOTCH1* variants was suggested ($p = 0.06$ and $p = 0.05$, respectively).

We identified 11 *SMAD6* variants in 441 patients (2.5%). These included two frameshift deletions, two nonsense mutations, one in-frame deletion, and six missense variants (**Figure 2**). Only a single individual (0.55%) in the study control cohort harbored a *SMAD6* missense variant. The ExAC database harbored 450 *SMAD6* variants in 47,389 individuals (0.9%). Whereas 36.4% ($n = 4/11$) of the *SMAD6* mutations in the patient cohort were loss of function (LOF; frameshift, nonsense or splice site) mutations, truncating *SMAD6* mutations were found in only 4.0% ($n = 18/450$) of the ExAC individuals, demonstrating a clear enrichment in BAV/TAA patients compared to controls ($p = 0.001$).

The *SMAD6* c.726del variant leads to a frameshift (p.Lys242Asnfs*300) and a predicted protein with a C-terminal extension due to loss of the intended stop codon. The c.454_461del frameshift variant (p.Gly166Valfs*23) causes the introduction of a premature stop codon, most likely resulting in haploinsufficiency due to nonsense-mediated mRNA decay (NMD). Also the two nonsense variants (p.Tyr279* and p.Tyr288*) are predicted to lead to NMD. All of the missense variants cluster in the functionally important MH1 and MH2 domains (Makkar et al., 2009) (amino acids 148–275 and 331–496, respectively), which is not the case for the sole missense variant (p.Ser130Leu) found in a control individual (**Figure 2**). All but one (p.Arg443His) of the identified variants were absent in the ExAC control cohort (v0.3.1; Supplementary Table 2). Moreover, the missense variants in the patient cohort (7/7) are enriched in the MH1 and MH2 domains when compared to ExAC controls ($n = 228/430$; $p = 0.02$).

For two *SMAD6* mutation carriers (P89, p.Gly271Glu; P99, p.Gly166Valfs*23), gDNA of family members was available for segregation analysis (Supplementary Figure 1). Although neither of these probands had a documented family history of BAV/TAA, a brother of P89 has been diagnosed with a sinus of Valsalva aneurysm (45 mm) and carried the *SMAD6* mutation. The mutation was also observed in an unaffected daughter (age 28) of the proband (Supplementary Figure 1). Three unaffected siblings at ages 54, 58, and 64 did not carry the mutation. No gDNA was available from a sister of P99 with unspecified aortic valve problems. The p.Gly166Valfs*23 mutation was found in an unaffected daughter (age 39) of P99 but was absent in his 39 year-old unaffected son (Supplementary Figure 1).

Intriguingly, two genes (*NOTCH1* and *NOS3*) that previously had been associated with increased BAV risk in humans

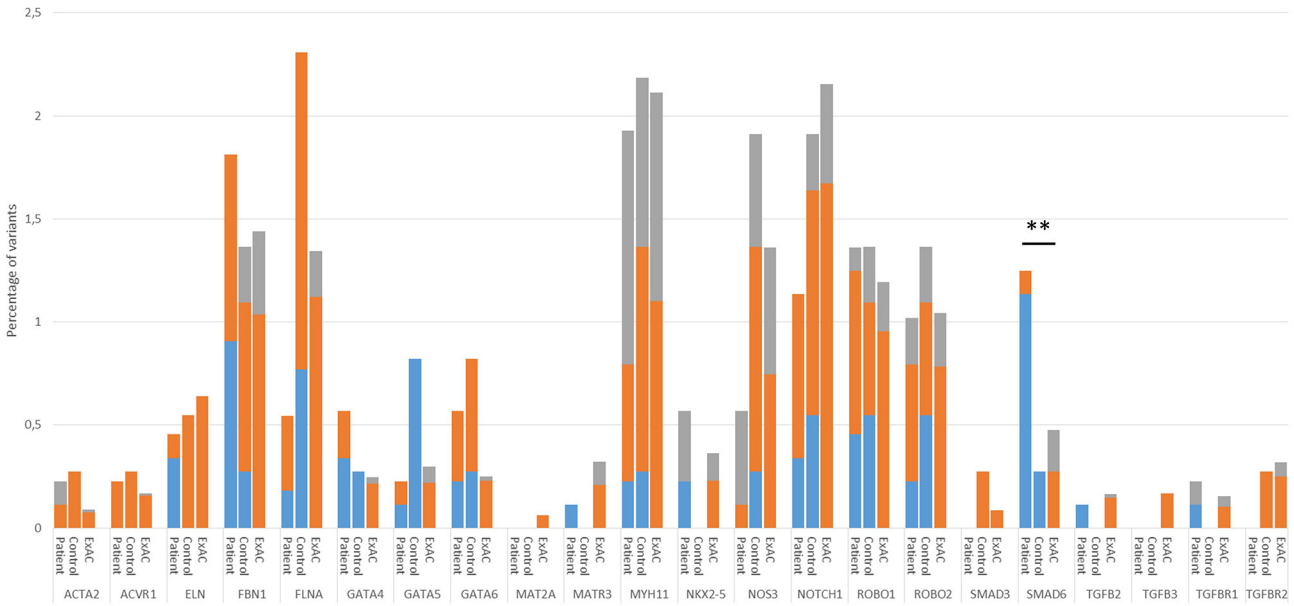

FIGURE 1 | Proportion of variant alleles per gene in the patient group, control group and ExAC cohort. Variants were selected as follows: First, we selected heterozygous coding or splice site variants with an allelic balance between 0.25 and 0.85 (*FLNA* in males: 0.75–1) and a minimum coverage of 10x. Next, we made three variant groups based on their frequency in the ExAC database; that is, variants that are absent from the ExAC control dataset (blue), variants with an ExAC MAF lower than 0.01% (orange) and variants with an ExAC MAF between 0.01% and 0.1% that had a CADD score above 20 (gray). Only statistics of the patient-ExAC comparison are shown (**$p \leq 0.01$). No statistically significant differences in allele frequencies were observed between our control cohort and the ExAC controls. Abbreviations: ExAC, Exome Aggregation Consortium; MAF, Minor Allele frequency; CADD, Combined Annotation Dependent Depletion.

(Mohamed et al., 1797; Garg et al., 2005; McKellar et al., 2007; Foffa et al., 2013) and/or mice (Lee et al., 2000; Bosse et al., 2013) revealed borderline significance for protection from BAV/TAA ($p = 0.05$ and $p = 0.06$, respectively). Analysis of *NOTCH1* identified 10 variants in patients (2.3%), including two splice-site variants, vs. seven variants (all missense) in controls (3.8%) and 2,181 (4.3%) variants in ExAC. One variant in the patient cohort (c.5167+3_5167+6del) leads to complete loss of the 5' donor splice site of intron 27, predicted to result in skipping of exon 27 (149 bp) and hence a frameshift. For the second variant (p.S784S), the predicted effect on splicing is more ambiguous. If loss of the 5' donor splice site of intron 14 would occur, skipping of exon 14 (146 bp) would again lead to a frameshift event. Unfortunately, cDNA to reliably determine the precise effect of these mutations on splicing is not available. None of the *NOTCH1* variants that we identified in BAV/TAA patients has previously been reported in the literature. We did not observe any variant-domain clustering or significant differences in CADD scores when comparing the patient and control *NOTCH1* variants. Similarly, for *NOS3* a total of five missense variants (1.1%) was found in patients, whereas the control cohort harbored seven variants (3.8%), including one out-of-frame mutation (p.Leu927Hisfs*32). In the ExAC control cohort, 1,390 *NOS3* variants (2.7%) were found in 51,035 individuals.

Based on statistical analyses of BAV/TAA heritability and the fact that BAV/TAA shows prominent gender bias, oligogenic inheritance of BAV/TAA is an emerging concept (Andelfinger et al., 2016; Verstraeten et al., 2016). To test for such oligogenic patterns, we determined the number of patients and controls in our study cohort with variants in at least two out of the 22 analyzed genes. In the patient cohort, 10 patients presented with two variants (2.3%), while the control group harbored 7 individuals that carried two variants (3.8%). Based on these data, there is no evidence for a digenic or multigenic model in the analyzed genes ($p = 0.29$).

DISCUSSION

So far, no gene with a contribution of more than 1% to BAV or BAV/TAA has been identified in humans. Gene identification has been hampered by low penetrance, variable clinical expressivity, the likelihood of BAV-phenocopies within individual families and, most likely, substantial locus heterogeneity (Verstraeten et al., 2016). *NOTCH1* has been suggested as a BAV(/TAA) gene, but does not contribute greatly to disease etiology. About 20 other genes have been associated with BAV in humans and mice (**Table 1**), but few of them also showed association with TAA. This suggests that whereas some disease genes might be linked to both BAV and TAA, others increase risk for only one of the component phenotypes. In this study, we used a targeted gene panel approach to study the prevalence of mutations in genes that previously have been associated with BAV and/or TAA in people or mice in a cohort of BAV/TAA patients. In total, 22 genes were sequenced in 441 BAV/TAA patients and 183 controls. *SMAD6* was identified as the most important known gene in the etiology of BAV with associated TAA. With 11 mutation-carrying

TABLE 2 | Variant burden comparisons per gene between patients and either study controls or ExAC controls.

Gene	Number of variants in 882 patient alleles	Number of variants in 366 control alleles	Number of variants in ExAC alleles	*p*-value patients-controls	*p*-value patients-ExAC
ACTA2	2	1	109 in 120,631	1.00	0.44
ACVR1	2	1	202 in 120,994	1.00	0.98
ELN	4	2	728 in 113,954	1.00	0.63
FBN1	16	5	1,740 in 120,988	0.81	0.43
FLNA	3*	6*	1,133 in 84,359*	**0.03**	0.15
GATA4	5	1	260 in 105,980	0.68	0.11
GATA5	2	3	259 in 86,819	0.15	0.94
GATA6	5	3	240 in 95,775	0.70	0.13
MAT2A	0	0	74 in 116,667	/	/
MATR3	1	0	382 in 119,089	/	0.43
MYH11	17	8	2,513 in 119,001	0.82	0.79
NKX2-5	5	0	360 in 98,978	/	0.47
NOS3	5	7	1,390 in 102,070	0.05	0.06
NOTCH1	10	7	2,181 in 101,245	0.29	0.05
ROBO1	12	5	1,354 in 113,390	1.00	0.77
ROBO2	9	5	1,245 in 119,282	0.57	0.95
SMAD3	0	1	95 in 111,500	/	/
SMAD6	11	1	450 in 94,779	0.20	**0.002**
TGFB2	1	0	192 in 117,070	/	0.71
TGFB3	0	0	205 in 121,315	/	/
TGFBR1	2	0	181 in 118,320	/	0.90
TGFBR2	0	1	366 in 115,147	/	/

Variant burden analyses were performed comparing frequencies of the variants fulfilling the three criteria that were mentioned in "Section Data Analysis and Filtering" between patients and controls. Whereas, the Fisher's Exact Test was used to statistically compare variant frequencies in the patient cohort to those in the study control cohort, the Chi-Square Test with Yates' correction was used for the patient-ExAC comparison. No p-values were calculated if the number of variants in patients and/or controls was zero. Statistical significance was considered when $p < 0.05$. The asterisks denote that in these cases the number of alleles is consistent with the number of X-chromosomes, i.e., 553 patient alleles and 260 control alleles were checked for variants. Statistically significant p-values are represented in bold.

probands, *SMAD6* offers a molecular explanation for 2.5% of our study population. For two of the variants segregation analysis in relatives could be performed, revealing the presence of one of the respective *SMAD6* mutations in a TAA patient and two rather young individuals (age 28 & 39) that might still develop TAA later in life. Four unaffected individuals (age 37, 54, 58, 64) did not carry a *SMAD6* mutation. As two nonsense and two frameshift *SMAD6* variants in our cohort are predicted to lead to haploinsufficiency, LOF is the most likely mechanism. All the patient-specific missense variants ($n = 7$) are in the functionally important MH1 and MH2 domains of SMAD6 (Makkar et al., 2009). LOF missense mutations in *SMAD2* and *SMAD3* causing Loeys-Dietz syndrome, another syndromic TAA form, are also located in the MH1 and MH2 domains (van de Laar et al., 2011; Micha et al., 2015). The MH1 domain of SMAD6 binds DNA (Bai and Cao, 2002), while the MH2 domain interacts with key components of the transforming growth factor (TGF)-β and bone morphogenetic protein (BMP) signaling cascades (Hanyu et al., 2001; Lin et al., 2003; Jung et al., 2013). In 2012, two missense variants in the MH2 domain of SMAD6 were identified in two patients with BAV in association with mild to moderate aortic stenosis (Tan et al., 2012). Interestingly, in our cohort, one *SMAD6* patient (p.Tyr288*) presented with coarctation in addition to BAV and TAA. Moreover, mice lacking expression of the murine orthologue of *SMAD6*, i.e., *Madh6*$^{-/-}$ mice, also present with cardiovascular pathologies, including abnormal vascular smooth muscle cell relaxation, thickening of the cardiac valves and misplaced septation and ossification of the outflow tract (OFT) (Galvin et al., 2000). As such, our findings confirm a role for *SMAD6* mutations in the etiology of BAV and expand the spectrum of *SMAD6*-related cardiovascular manifestations with BAV-related TAA.

SMAD6 is highly expressed in the cardiac valves and OFT of the embryonic heart, in the late-embryonic, and adult vascular endothelium as well as in the vascular smooth muscle cells of the adult aortic root (Galvin et al., 2000; Dickel et al., 2016). Upregulation in response to laminar shear stress has been reported (Topper et al., 1997). *SMAD6* encodes an inhibitory SMAD protein which negatively regulates BMP signaling by binding to BMP type I receptors or by establishing competitive interactions for SMAD4 (Imamura et al., 1997; Hata et al., 1998). In doing so, SMAD1/5/8 phosphorylation and/or nuclear translocation are prevented. Additionally, SMAD6 cooperates with SMURF E3 ubiquitin ligases to prime ubiquitin-mediated proteasomal degradation of BMP receptors and SMAD effector proteins (Murakami et al., 2003), including SMAD1 and 5. BMP signaling has previously been independently implicated in BAV- and TAA-related processes (Cai et al., 2012; Garside

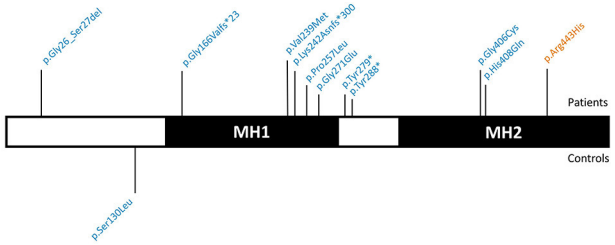

FIGURE 2 | Graphical representation of the identified *SMAD6* variants. SMAD6 has two major protein domains, a DNA-binding MH1 domain and a MH2 domain that interacts with components of the TGF-β and BMP signaling pathways. Variants above the protein have been found in patients, while those below the protein occurred in control individuals. Variants in blue are absent from the ExAC database, variants in orange have an ExAC MAF below 0.01%. Abbreviations: TGF-β, Transforming growth factor-β; BMP, Bone morphogenetic protein; ExAC, Exome Aggregation Consortium; MAF, Minor Allele frequency.

et al., 2013). In addition to mediating CNC cell migration into the cardiac cushions and differentiation to smooth muscle cells, BMP signaling promotes endothelial-to-mesenchymal transition and instigates mesenchymal cell invasion (Kaartinen et al., 2004; Garside et al., 2013). While SMAD6 and SMAD7 are thought to have a predominant negative regulatory effect on BMP and TGF-β signaling, respectively, there is strong evidence that this specificity is not absolute and that SMAD6 can directly suppress the TGF-β signaling cascade. Important crosstalk between BMP, TGF-β and NOTCH signaling has been reported (Garside et al., 2013). Many syndromic forms of TAA are caused by mutations in genes encoding effectors or regulators of the TGF-β signaling pathway (including *TGFB2/3*, *TGFBR1/2*, *SMAD2/3*, *SKI*) (Loeys et al., 2005; van de Laar et al., 2011; Boileau et al., 2012; Carmignac et al., 2012; Doyle et al., 2012; Lindsay et al., 2012; Bertoli-Avella et al., 2015; Micha et al., 2015), with increased activity observed in aortic specimens from people and mice with these conditions. An increased prevalence of BAV has been observed in patients carrying mutations in these genes (**Table 1**). Overall, these results imply that mutations in *SMAD6* likely cause BAV/TAA through impaired negative regulation of BMP and/or TGF-β signaling.

Multiple studies have previously reported a link between *NOTCH1* mutations and BAV (Mohamed et al., 1797; Garg et al., 2005; McKellar et al., 2007; Foffa et al., 2013). In 2005, a nonsense and a frameshift *NOTCH1* mutation were found to segregate with BAV associated with early onset valve calcification in the respective families (Garg et al., 2005). Since the initial report, multiple *NOTCH1*, mostly missense, variants have been associated with BAV, BAV/TAA, aortic valve stenosis, coarctation, and hypoplastic left heart (Mohamed et al., 1797; McKellar et al., 2007; Iascone et al., 2012; Foffa et al., 2013; Freylikhman et al., 2014; Preuss et al., 2016; Irtyuga et al., 2017). In addition to these mutations in association with left-sided heart defects, frameshift and nonsense mutations were also identified in patients with right-sided heart defects affecting the pulmonary valve and conotruncal disease including pulmonary atresia with intact ventricular septum, tetralogy of Fallot, and truncus arteriosus, and other congenital heart diseases, such as anomalous pulmonary venous return, atrial septal defect, and ventricular septal defect (Kerstjens-Frederikse et al., 2016). Mouse models have confirmed a role for Notch1 in the development of the aortic valve and the cardiac OFT (Koenig et al., 2016). Unexpectedly, in our dataset *NOTCH1* did not stand out as a prominent BAV/TAA gene, with the suggestion that *NOTCH1* variants might even be protective. Sample selection bias might contribute to this observation as *NOTCH1* variants appear to associate with early and severe valve calcification and seem to be enriched in families with highly penetrant BAV but far lower penetrance of TAA (Kent et al., 2013). Given that our study did not select for valve calcification and prioritized the BAV/TAA phenotype, it is understandable that *NOTCH1* variants would be underrepresented. It also seems notable that only missense variants were seen in controls, while multiple variants in the patient cohort are predicted to have a more overt impact on protein expression and function.

Similarly, our variant burden test suggested that *NOS3* variants might be protective for BAV/TAA development. NOS3, the endothelial specific nitric oxide (NO) synthase, is important in balancing NO production and in the reduction of oxidative stress (Forstermann and Munzel, 2006). Its role in cardiac development is demonstrated by the formation of BAV in *Nos3*-targeted mice (**Table 1**). Furthermore, it has already been shown that specific *NOS3* polymorphisms can affect NO production (Oliveira-Paula et al., 2016), and increased NO levels have been found in a MFS mouse model and in *Adamts1*-deficient mice that develop TAA (Oller et al., 2017). Pharmacological inhibition of NOS2 in mice led to a protective effect in aortic aneurysm development (Oller et al., 2017). This supports the importance of NO levels and nitric oxide synthases in aneurysm pathology. The variants in *NOS3* identified in the current study may lead to less active NOS3 and as such may protect against development of aortic aneurysm.

Our study has several methodological limitations: (i) The small number of genes included in our study, as well as the patient cohort size, precludes the ability to detect oligogenic inheritance or gene-gene interactions involved in BAV/TAA. An extended experiment in a larger BAV/TAA cohort, including BAV-related pathways instead of selected genes, could give us more insight regarding how genes work together in BAV and/or TAA development; (ii) The size of the patient and study/ExAC control cohort only allows us to detect BAV/TAA genes with a fairly large contribution (variant burden in patients: $\geq$3% & $\geq$2%, respectively); (iii) The control cohort consists of younger, adolescent patients that did not show cardiac complications at the time of investigation but may still develop complications such as TAA later-on in life. Therefore, the ExAC database was used as an additional dataset for allele frequencies in a cohort without gross developmental defects.

Our study specifically assesses the presence of pathogenic variants in BAV-associated genes in a large BAV/TAA cohort. We conclude that *SMAD6* is currently the most important contributor to the genetic architecture of BAV/TAA. More research and larger cohorts will be needed to fully elucidate the

genetic architecture of this common but complex cardiovascular pathology.

ETHICS STATEMENT

This study was carried out in accordance with written informed consent from all subjects. All subjects gave written informed consent in accordance with the Declaration of Helsinki. The protocol was approved by the Ethics Committee of the Antwerp University Hospital and all participating centers.

AUTHOR CONTRIBUTIONS

All authors revised the work critically. All authors provided final approval of the version for publication. All authors agreed to be accountable for all aspects of the work and ensure that questions related to the accuracy or integrity of any part of the work are appropriately investigated and resolved. More specific contributions to the work are: EG, AAK, IL, CP, EC, NB, FW, RG, LV, SAM, SM, LM, HB, AF, AM, PE, GA, HD, AV, and BL contributed to conception and design of the work. EG, AAK, IL, EC, MA, NB, GvdB, BW, GV, JM, RZ, DZ, SAM, SM, LM, JV, IV, MW, EM, GG, MN, AK, MK, SS, TD, XJ, JA, PE, AV, and BL contributed to acquisition of the data. EG, AAK, CP, FW, GA, LV, HD, AV, and BL contributed to analysis of the data. EG, IL, CP, EC, MA, FW, RG, RZ, DZ, SAM, SM, LM, HB, AF, AM, LV, JV, IV, MW, EM, GG, MN, AK, MK, SS, TD, XJ, JA, PE, HD, AV, and BL contributed to interpretation of the data.

FUNDING

This research was supported by funding from the University of Antwerp (Lanceringsproject), the Fund for Scientific Research, Flanders (FWO, Belgium, G.0221.12), The Dutch Heart Foundation (2013T093), the Foundation Leducq (MIBAVA—Leducq 12CVD03). BL is senior clinical investigator of the Fund for Scientific Research, Flanders (FWO). AV and GV are FWO postdoctoral researchers and JM (FWO) and IL (FWO-SB) hold a PhD mandate. BL holds a starting grant from the European Research Council (ERC- StG-2012-30972-BRAVE).

SUPPLEMENTARY MATERIAL

The Supplementary Material for this article can be found online at: http://journal.frontiersin.org/article/10.3389/fphys.2017.00400/full#supplementary-material

REFERENCES

Andelfinger, G., Loeys, B., and Dietz, H. (2016). A decade of discovery in the genetic understanding of thoracic aortic disease. *Can. J. Cardiol.* 32, 13–25. doi: 10.1016/j.cjca.2015.10.017

Attias, D., Stheneur, C., Roy, C., Collod-Beroud, G., Detaint, D., Faivre, L., et al. (2009). Comparison of clinical presentations and outcomes between patients with TGFBR2 and FBN1 mutations in Marfan syndrome and related disorders. *Circulation* 120, 2541–2549. doi: 10.1161/CIRCULATIONAHA.109.887042

Bai, S., and Cao, X. (2002). A nuclear antagonistic mechanism of inhibitory Smads in transforming growth factor-beta signaling. *J. Biol. Chem.* 277, 4176–4182. doi: 10.1074/jbc.M105105200

Bertoli-Avella, A. M., Gillis, E., Morisaki, H., Verhagen, J. M., de Graaf, B. M., van de Beek, G., et al. (2015). Mutations in a TGF-β ligand, TGFB3, cause syndromic aortic aneurysms and dissections. *J. Am. Coll. Cardiol.* 65, 1324–1336. doi: 10.1016/j.jacc.2015.01.040

Biben, C., Weber, R., Kesteven, S., Stanley, E., McDonald, L., Elliott, D. A., et al. (2000). Cardiac septal and valvular dysmorphogenesis in mice heterozygous for mutations in the homeobox gene Nkx2-5. *Circ. Res.* 87, 888–895. doi: 10.1161/01.RES.87.10.888

Boileau, C., Guo, D. C., Hanna, N., Regalado, E. S., Detaint, D., Gong, L., et al. (2012). TGFB2 mutations cause familial thoracic aortic aneurysms and dissections associated with mild systemic features of Marfan syndrome. *Nat. Genet.* 44, 916–921. doi: 10.1038/ng.2348

Bonachea, E. M., Zender, G., White, P., Corsmeier, D., Newsom, D., Fitzgerald-Butt, S., et al. (2014). Use of a targeted, combinatorial next-generation sequencing approach for the study of bicuspid aortic valve. *BMC Med. Genomics* 7:56. doi: 10.1186/1755-8794-7-56

Bosse, K., Hans, C. P., Zhao, N., Koenig, S. N., Huang, N., Guggilam, A., et al. (2013). Endothelial nitric oxide signaling regulates Notch1 in aortic valve disease. *J. Mol. Cell. Cardiol.* 60, 27–35. doi: 10.1016/j.yjmcc.2013.04.001

Braverman, A. C., Guven, H., Beardslee, M. A., Makan, M., Kates, A. M., and Moon, M. R. (2005). The bicuspid aortic valve. *Curr. Probl. Cardiol.* 30, 470–522. doi: 10.1016/j.cpcardiol.2005.06.002

Cai, J., Pardali, E., Sanchez-Duffhues, G., and ten Dijke, P. (2012). BMP signaling in vascular diseases. *FEBS Lett.* 586, 1993–2002. doi: 10.1016/j.febslet.2012.04.030

Callewaert, B., Renard, M., Hucthagowder, V., Albrecht, B., Hausser, I., Blair, E., et al. (2011). New insights into the pathogenesis of autosomal-dominant cutis laxa with report of five ELN mutations. *Hum. Mutat.* 32, 445–455. doi: 10.1002/humu.21462

Carmignac, V., Thevenon, J., Ades, L., Callewaert, B., Julia, S., Thauvin-Robinet, C., et al. (2012). In-frame mutations in exon 1 of SKI cause dominant Shprintzen-Goldberg syndrome. *Am. J. Hum. Genet.* 91, 950–957. doi: 10.1016/j.ajhg.2012.10.002

Clementi, M., Notari, L., Borghi, A., and Tenconi, R. (1996). Familial congenital bicuspid aortic valve: a disorder of uncertain inheritance. *Am. J. Med. Genet.* 62, 336–338. doi: 10.1002/(SICI)1096-8628(19960424)62:4<336::AID-AJMG2>3.0.CO;2-P

Cripe, L., Andelfinger, G., Martin, L. J., Shooner, K., and Benson, D. W. (2004). Bicuspid aortic valve is heritable. *J. Am. Coll. Cardiol.* 44, 138–143. doi: 10.1016/j.jacc.2004.03.050

DePristo, M. A., Banks, E., Poplin, R., Garimella, K. V., Maguire, J. R., Hartl, C., et al. (2011). A framework for variation discovery and genotyping using next-generation DNA sequencing data. *Nat. Genet.* 43, 491–498. doi: 10.1038/ng.806

Dickel, D. E., Barozzi, I., Zhu, Y., Fukuda-Yuzawa, Y., Osterwalder, M., Mannion, B. J., et al. (2016). Genome-wide compendium and functional assessment of *in vivo* heart enhancers. *Nat. Commun.* 7:12923. doi: 10.1038/ncomms12923

Doyle, A. J., Doyle, J. J., Bessling, S. L., Maragh, S., Lindsay, M. E., Schepers, D., et al. (2012). Mutations in the TGF-beta repressor SKI cause Shprintzen-Goldberg syndrome with aortic aneurysm. *Nat. Genet.* 44, 1249–1254. doi: 10.1038/ng.2421

Foffa, I., Ait Ali, L., Panesi, P., Mariani, M., Festa, P., Botto, N., et al. (2013). Sequencing of NOTCH1, GATA5, TGFBR1 and TGFBR2 genes in familial cases of bicuspid aortic valve. *BMC Med. Genet.* 14:44. doi: 10.1186/1471-2350-14-44

Forstermann, U., and Munzel, T. (2006). Endothelial nitric oxide synthase in vascular disease: from marvel to menace. *Circulation* 113, 1708–1714. doi: 10.1161/CIRCULATIONAHA.105.602532

Freylikhman, O., Tatarinova, T., Smolina, N., Zhuk, S., Klyushina, A., Kiselev, A., et al. (2014). Variants in the NOTCH1 gene in patients with aortic coarctation. *Congenit. Heart Dis.* 9, 391–396. doi: 10.1111/chd.12157

Galvin, K. M., Donovan, M. J., Lynch, C. A., Meyer, R. I., Paul, R. J., Lorenz, J. N., et al. (2000). A role for smad6 in development and homeostasis of the cardiovascular system. *Nat. Genet.* 24, 171–174. doi: 10.1038/72835

Garg, V., Muth, A. N., Ransom, J. F., Schluterman, M. K., Barnes, R., King, I. N., et al. (2005). Mutations in NOTCH1 cause aortic valve disease. *Nature*. 437, 270–274. doi: 10.1038/nature03940

Garside, V. C., Chang, A. C., Karsan, A., and Hoodless, P. A. (2013). Co-ordinating Notch BMP and TGF-β signaling during heart valve development. *Cell. Mol. Life Sci.* 70, 2899–2917. doi: 10.1007/s00018-012-1197-9

Guo, D. C., Gong, L., Regalado, E. S., Santos-Cortez, R. L., Zhao, R., Cai, B., et al. (2015). MAT2A mutations predispose individuals to thoracic aortic aneurysms. *Am. J. Hum. Genet.* 96, 170–177. doi: 10.1016/j.ajhg.2014.11.015

Guo, D. C., Pannu, H., Tran-Fadulu, V., Papke, C. L., Yu, R. K., Avidan, N., et al. (2007). Mutations in smooth muscle α-actin (ACTA2) lead to thoracic aortic aneurysms and dissections. *Nat. Genet.* 39, 1488–1493. doi: 10.1038/ng.2007.6

Hanyu, A., Ishidou, Y., Ebisawa, T., Shimanuki, T., Imamura, T., and Miyazono, K. (2001). The N domain of Smad7 is essential for specific inhibition of transforming growth factor-beta signaling. *J. Cell Biol.* 155, 1017–1027. doi: 10.1083/jcb.200106023

Hata, A., Lagna, G., Massague, J., and Hemmati-Brivanlou, A. (1998). Smad6 inhibits BMP/Smad1 signaling by specifically competing with the Smad4 tumor suppressor. *Genes Dev.* 12, 186–197. doi: 10.1101/gad.12.2.186

Hinton, R. B. (2012). Bicuspid aortic valve and thoracic aortic aneurysm: three patient populations, two disease phenotypes, and one shared genotype. *Cardiol. Res. Pract.* 2012:926975. doi: 10.1155/2012/926975

Huntington, K., Hunter, A. G., and Chan, K. L. (1997). A prospective study to assess the frequency of familial clustering of congenital bicuspid aortic valve. *J. Am. Coll. Cardiol.* 30, 1809–1812. doi: 10.1016/S0735-1097(97)00372-0

Iascone, M., Ciccone, R., Galletti, L., Marchetti, D., Seddio, F., Lincesso, A. R., et al. (2012). Identification of *de novo* mutations and rare variants in hypoplastic left heart syndrome. *Clin. Genet.* 81, 542–554. doi: 10.1111/j.1399-0004.2011.01674.x

Imamura, T., Takase, M., Nishihara, A., Oeda, E., Hanai, J., Kawabata, M., et al. (1997). Smad6 inhibits signalling by the TGF-beta superfamily. *Nature* 389, 622–626.

Irtyuga, O., Malashicheva, A., Zhiduleva, E., Freylikhman, O., Rotar, O., Back, M., et al. (2017). NOTCH1 mutations in aortic stenosis: association with osteoprotegerin/RANK/RANKL. *Biomed. Res. Int.* 2017:6917907. doi: 10.1155/2017/6917907

Jefferies, J. L., Taylor, M. D., Rossano, J., Belmont, J. W., and Craigen, W. J. (2010). Novel cardiac findings in periventricular nodular heterotopia. *Am. J. Med. Genet. A.* 152A, 165–168. doi: 10.1002/ajmg.a.33110

Jung, S. M., Lee, J. H., Park, J., Oh, Y. S., Lee, S. K., Park, J. S., et al. (2013). Smad6 inhibits non-canonical TGF-β1 signalling by recruiting the deubiquitinase A20 to TRAF6. *Nat. Commun.* 4:2562. doi: 10.1038/ncomms3562

Kaartinen, V., Dudas, M., Nagy, A., Sridurongrit, S., Lu, M. M., and Epstein, J. A. (2004). Cardiac outflow tract defects in mice lacking ALK2 in neural crest cells. *Development* 131, 3481–3490. doi: 10.1242/dev.01214

Kent, K. C., Crenshaw, M. L., Goh, D. L., and Dietz, H. C. (2013). Genotype-phenotype correlation in patients with bicuspid aortic valve and aneurysm. *J. Thorac. Cardiovasc. Surg.* 146, 158–1565. doi: 10.1016/j.jtcvs.2012.09.060

Kerstjens-Frederikse, W. S., van de Laar, I. M., Vos, Y. J., Verhagen, J. M., Berger, R. M., Lichtenbelt, K. D., et al. (2016). Cardiovascular malformations caused by NOTCH1 mutations do not keep left: data on 428 probands with left-sided CHD and their families. *Genet. Med.* 18, 914–923. doi: 10.1038/gim.2015.193

Kircher, M., Witten, D. M., Jain, P., O'Roak, B. J., Cooper, G. M., and Shendure, J. (2014). A general framework for estimating the relative pathogenicity of human genetic variants. *Nat. Genet.* 46, 310–315. doi: 10.1038/ng.2892

Koenig, S. N., Bosse, K., Majumdar, U., Bonachea, E. M., Radtke, F., and Garg, V. (2016). Endothelial notch1 is required for proper development of the semilunar valves and cardiac outflow tract. *J. Am. Heart Assoc.* 5:e003075. doi: 10.1161/JAHA.115.003075

Laforest, B., Andelfinger, G., and Nemer, M. (2011). Loss of Gata5 in mice leads to bicuspid aortic valve. *J. Clin. Invest.* 121, 2876–2887. doi: 10.1172/JCI44555

Laforest, B., and Nemer, M. (2011). GATA5 interacts with GATA4 and GATA6 in outflow tract development. *Dev. Biol.* 358, 368–378. doi: 10.1016/j.ydbio.2011.07.037

Lee, T. C., Zhao, Y. D., Courtman, D. W., and Stewart, D. J. (2000). Abnormal aortic valve development in mice lacking endothelial nitric oxide synthase. *Circulation* 101, 2345–2348. doi: 10.1161/01.CIR.101.20.2345

Lek, M., Karczewski, K. J., Minikel, E. V., Samocha, K. E., Banks, E., Fennell, T., et al. (2016). Analysis of protein-coding genetic variation in 60,706 humans. *Nature* 536, 285–291. doi: 10.1038/nature19057

Lin, X., Liang, Y. Y., Sun, B., Liang, M., Shi, Y., Brunicardi, F. C., et al. (2003). Smad6 recruits transcription corepressor CtBP to repress bone morphogenetic protein-induced transcription. *Mol. Cell. Biol.* 23, 9081–9093. doi: 10.1128/MCB.23.24.9081-9093.2003

Lindsay, M. E., Schepers, D., Bolar, N. A., Doyle, J. J., Gallo, E., Fert-Bober, J., et al. (2012). Loss-of-function mutations in TGFB2 cause a syndromic presentation of thoracic aortic aneurysm. *Nat. Genet.* 44, 922–927. doi: 10.1038/ng.2349

Loeys, B. L., Chen, J., Neptune, E. R., Judge, D. P., Podowski, M., Holm, T., et al. (2005). A syndrome of altered cardiovascular, craniofacial, neurocognitive and skeletal development caused by mutations in TGFBR1 or TGFBR2. *Nat. Genet.* 37, 275–281. doi: 10.1038/ng1511

Loscalzo, M. L., Goh, D. L., Loeys, B., Kent, K. C., Spevak, P. J., and Dietz, H. C. (2007). Familial thoracic aortic dilation and bicommissural aortic valve: a prospective analysis of natural history and inheritance. *Am. J. Med. Genet. A* 143A, 1960–1967. doi: 10.1002/ajmg.a.31872

Makkar, P., Metpally, R. P., Sangadala, S., and Reddy, B. V. (2009). Modeling and analysis of MH1 domain of Smads and their interaction with promoter DNA sequence motif. *J. Mol. Graph. Model.* 27, 803–812. doi: 10.1016/j.jmgm.2008.12.003

Martin, P., Kloesel, B., Norris, R., Lindsay, M., Milan, D., and Body, S. (2015). Embryonic development of the bicuspid aortic valve. *J. Cardiovasc. Dev. Dis.* 2:248. doi: 10.3390/jcdd2040248

McKellar, S. H., Tester, D. J., Yagubyan, M., Majumdar, R., Ackerman, M. J., Sundt, T. M., et al. (2007). Novel NOTCH1 mutations in patients with bicuspid aortic valve disease and thoracic aortic aneurysms. *J. Thorac. Cardiovasc. Surg.* 134, 290–296. doi: 10.1016/j.jtcvs.2007.02.041

Micha, D., Guo, D. C., Hilhorst-Hofstee, Y., van Kooten, F., Atmaja, D., Overwater, E., et al. (2015). SMAD2 mutations are associated with arterial aneurysms and dissections. *Hum. Mutat.* 36, 1145–1149. doi: 10.1002/humu.22854

Mohamed, S. A., Aherrahrou, Z., Liptau, H., Erasmi, A. W., Hagemann, C., Wrobel, S., et al. (1797). Novel missense mutations (p.T596M and p.PH) in NOTCH1 in patients with bicuspid aortic valve. *Biochem. Biophys. Res. Commun.* 345, 1460–1465.

Mommersteeg, M. T., Yeh, M. L., Parnavelas, J. G., and Andrews, W. D. (2015). Disrupted Slit-Robo signalling results in membranous ventricular septum defects and bicuspid aortic valves. *Cardiovasc. Res.* 106, 55–66. doi: 10.1093/cvr/cvv040

Murakami, G., Watabe, T., Takaoka, K., Miyazono, K., and Imamura, T. (2003). Cooperative inhibition of bone morphogenetic protein signaling by Smurf1 and inhibitory Smads. *Mol. Biol. Cell.* 14, 2809–2817. doi: 10.1091/mbc.E02-07-0441

Nistri, S., Porciani, M. C., Attanasio, M., Abbate, R., Gensini, G. F., and Pepe, G. (2012). Association of Marfan syndrome and bicuspid aortic valve: frequency and outcome. *Int. J. Cardiol.* 155, 324–325. doi: 10.1016/j.ijcard.2011.12.009

Oliveira-Paula, G. H., Lacchini, R., and Tanus-Santos, J. E. (2016). Endothelial nitric oxide synthase: from biochemistry and gene structure to clinical implications of NOS3 polymorphisms. *Gene* 575(2 Pt 3), 584–99. doi: 10.1016/j.gene.2015.09.061

Oller, J., Mendez-Barbero, N., Ruiz, E. J., Villahoz, S., Renard, M., Canelas, L. I., et al. (2017). Nitric oxide mediates aortic disease in mice deficient in the metalloprotease Adamts1 and in a mouse model of Marfan syndrome. *Nat. Med.* 23, 200–212. doi: 10.1038/nm.4266

Pepe, G., Nistri, S., Giusti, B., Sticchi, E., Attanasio, M., Porciani, C., et al. (2014). Identification of fibrillin 1 gene mutations in patients with bicuspid aortic valve (BAV) without Marfan syndrome. *BMC Med. Genet.* 15:23. doi: 10.1186/1471-2350-15-23

Preuss, C., Capredon, M., Wunnemann, F., Chetaille, P., Prince, A., Godard, B., et al. (2016). Family based whole exome sequencing reveals the multifaceted role of notch signaling in congenital heart disease. *PLoS Genet.* 12:e1006335. doi: 10.1371/journal.pgen.1006335

Quintero-Rivera, F., Xi, Q. J., Keppler-Noreuil, K. M., Lee, J. H., Higgins, A. W., Anchan, R. M., et al. (2015). MATR3 disruption in human and mouse associated with bicuspid aortic valve, aortic coarctation and patent ductus arteriosus. *Hum. Mol. Genet.* 24, 2375–2389. doi: 10.1093/hmg/ddv004

Tan, H. L., Glen, E., Topf, A., Hall, D., O'Sullivan, J. J., Sneddon, L., et al. (2012). Nonsynonymous variants in the SMAD6 gene predispose to congenital cardiovascular malformation. *Hum. Mutat.* 33, 720–727. doi: 10.1002/humu.22030

Thomas, P. S., Sridurongrit, S., Ruiz-Lozano, P., and Kaartinen, V. (2012). Deficient signaling via Alk2 (Acvr1) leads to bicuspid aortic valve development. *PLoS ONE* 7:e35539. doi: 10.1371/journal.pone.0035539

Topper, J. N., Cai, J., Qiu, Y., Anderson, K. R., Xu, Y. Y., Deeds, J. D., et al. (1997). Vascular MADs: two novel MAD-related genes selectively inducible by flow in human vascular endothelium. *Proc. Natl. Acad. Sci. U.S.A.* 94, 9314–9319. doi: 10.1073/pnas.94.17.9314

Untergasser, A., Cutcutache, I., Koressaar, T., Ye, J., Faircloth, B. C., Remm, M., et al. (2012). Primer3–new capabilities and interfaces. *Nucleic Acids Res.* 40:e115. doi: 10.1093/nar/gks596

van de Laar, I. M., Oldenburg, R. A., Pals, G., Roos-Hesselink, J. W., de Graaf, B. M., Verhagen, J. M., et al. (2011). Mutations in SMAD3 cause a syndromic form of aortic aneurysms and dissections with early-onset osteoarthritis. *Nat. Genet.* 43, 121–126. doi: 10.1038/ng.744

van de Laar, I. M., van der Linde, D., Oei, E. H., Bos, P. K., Bessems, J. H., Bierma-Zeinstra, S. M., et al. (2012). Phenotypic spectrum of the SMAD3-related aneurysms-osteoarthritis syndrome. *J. Med. Genet.* 49, 47–57. doi: 10.1136/jmedgenet-2011-100382

Vandeweyer, G., Van Laer, L., Loeys, B., Van den Bulcke, T., and Kooy, R. F. (2014). VariantDB: a flexible annotation and filtering portal for next generation sequencing data. *Genome Med.* 6:746. doi: 10.1186/s13073-014-0074-6

Verstraeten, A., Roos-Hesselink, J., and Loeys, B. (2016). "Bicuspid aortic valve," in *Clinical Cardiogenetics,* eds H. F. Baars, P. A. F. M. Doevendans, A. C. Houweling, and J. P. van Tintelen (Cham: Springer International Publishing), 295–308.

Conflict of Interest Statement: The authors declare that the research was conducted in the absence of any commercial or financial relationships that could be construed as a potential conflict of interest.

frontiers in Physiology

REVIEW
published: 24 August 2017
doi: 10.3389/fphys.2017.00612

Genetic Bases of Bicuspid Aortic Valve: The Contribution of Traditional and High-Throughput Sequencing Approaches on Research and Diagnosis

Betti Giusti[1, 2, 3, 4]*, *Elena Sticchi*[1, 2, 3, 4], *Rosina De Cario*[1, 2], *Alberto Magi*[1, 3], *Stefano Nistri*[4, 5] *and Guglielmina Pepe*[1, 2, 4]

[1] Department of Experimental and Clinical Medicine, Section of Critical Medical Care and Medical Specialities, University of Florence, Florence, Italy, [2] Marfan Syndrome and Related Disorders Regional (Tuscany) Referral Center, Careggi Hospital, Florence, Italy, [3] Advanced Molecular Genetics Laboratory, Atherothrombotic Diseases Center, Careggi Hospital, Florence, Italy, [4] Center of Excellence for the Study at Molecular and Clinical Level of Chronic, Degenerative and Neoplastic Diseases to Develop Novel Therapies (DENOTHE), University of Florence, Florence, Italy, [5] Cardiology Service, Centro Medico Strumentale Riabilitativo (CMSR) Veneto Medica, Altavilla Vicentina, Italy

OPEN ACCESS

Edited by:
Amalia Forte,
Università degli Studi della Campania "Luigi Vanvitelli" Caserta, Italy

Reviewed by:
Martin Ingi Sigurdsson,
Duke University Health System, United States
Simon Body,
Brigham and Women's Hospital, United States

***Correspondence:**
Betti Giusti
betti.giusti@unifi.it

Specialty section:
This article was submitted to Vascular Physiology, a section of the journal Frontiers in Physiology

Received: *15 May 2017*
Accepted: *09 August 2017*
Published: *24 August 2017*

Citation:
Giusti B, Sticchi E, De Cario R, Magi A, Nistri S and Pepe G (2017) Genetic Bases of Bicuspid Aortic Valve: The Contribution of Traditional and High-Throughput Sequencing Approaches on Research and Diagnosis. Front. Physiol. 8:612. doi: 10.3389/fphys.2017.00612

Bicuspid aortic valve (BAV) is a common (0.5–2.0% of general population) congenital heart defect with increased prevalence of aortic dilatation and dissection. BAV has an autosomal dominant inheritance with reduced penetrance and variable expressivity. BAV has been described as an isolated trait or associated with syndromic conditions [e.g., Marfan Marfan syndrome or Loeys-Dietz syndrome (MFS, LDS)]. Identification of a syndromic condition in a BAV patient is clinically relevant to personalize aortic surgery indication. A 4-fold increase in BAV prevalence in a large cohort of unrelated MFS patients with respect to general population was reported, as well as in LDS patients (8-fold). It is also known that BAV is more frequent in patients with thoracic aortic aneurysm (TAA) related to mutations in *ACTA2*, *FBN1*, and *TGFBR2* genes. Moreover, in 8 patients with BAV and thoracic aortic dilation, not fulfilling the clinical criteria for MFS, *FBN1* mutations in 2/8 patients were identified suggesting that *FBN1* or other genes involved in syndromic conditions correlated to aortopathy could be involved in BAV. Beyond loci associated to syndromic disorders, studies in humans and animal models evidenced/suggested the role of further genes in non-syndromic BAV. The transcriptional regulator *NOTCH1* has been associated with the development and acceleration of calcium deposition. Genome wide marker-based linkage analysis demonstrated a linkage of BAV to loci on chromosomes 18, 5, and 13q. Recently, a role for *GATA4/5* in aortic valve morphogenesis and endocardial cell differentiation has been reported. BAV has also been associated with a reduced *UFD1L* gene expression or involvement of a locus containing *AXIN1*/*PDIA2*. Much remains to be understood about the genetics of BAV. In the last years, high-throughput sequencing technologies, allowing the analysis of large number of genes or entire exomes or genomes, progressively became available. The latter issue together with the development of "BigData" analysis methods improving their interpretation and integration with clinical data represents a promising opportunity to increase the disease

knowledge and diagnosis in monogenic and multifactorial complex traits. This review summarized the main knowledge on the BAV genetic bases, the role of genetic diagnosis in BAV patient managements and the crucial challenges for the comprehension of genetics of BAV in research and diagnosis.

Keywords: bicuspid aortic valve, genetics, high-throughput sequencing, next generation sequencing, gene, modifier gene, mendelian inheritance, multifactorial inheritance

INTRODUCTION

Bicuspid aortic valve (BAV) represents a common congenital heart defect (0.5–2.0% of the adult general population) (Prakash et al., 2014). Complications of BAV are: aortic regurgitation (13–30%), aortic stenosis (12–37%), infective endocarditis (2–5%), and dilatation of the thoracic ascending aorta (20–50%) (Cecconi et al., 2006; Della Corte et al., 2013; Masri et al., 2017); an increased risk of aortic dissection has been also documented in BAV population (De Cario et al., 2014; Verma and Siu, 2014; Masri et al., 2017). This is especially relevant as a large part of BAV patients encounter a valve damage requiring aortic surgery (the cumulative 25-years risk including 25% of aortic surgery and 53% of receiving valve replacement) and the high incidence of associated thoracic aortic aneurysm (TAA) formation (Michelena et al., 2011). Such BAV complications, if not early identified and appropriately managed, may indeed represent long-term health risks. The surveillance approach to the disease and the prophylactic surgical management of patients resulted in a survival rate similar to that of the comparable general population (Masri et al., 2017). A male preponderance (M:F = 3:1) has been noted among BAVs. The latter issue is of interest in relation also to the fact that BAV is frequent in the XO Turner syndrome where it may be the most common cardiac defect: >30% of patients with Turner syndrome had BAV (Miller et al., 1983; De Cario et al., 2014; Masri et al., 2017). Beyond the well-known hemodynamic bases of BAV, whereby an altered blood flow through the valve during its formation determines an abnormal cups formation, a role for genetics in contributing to the development of the disease has also been recognized (Longobardo et al., 2016). Although BAV usually represents an isolated feature, its association with other clinical manifestations suggestive of a syndromic disorder, has also been described (Prakash et al., 2014). Moreover, both mathematical algorithms and familial studies support the hypothesis that BAV could be heritable (Cripe et al., 2004; Loscalzo et al., 2007; Laforest and Nemer, 2012; Longobardo et al., 2016), even though the genetic bases of BAV largely remain to be elucidated. Actually, different molecular signaling pathways—involved in the formation of the outflow tract (OFT) and in the endocardial-mesenchymal transition (Laforest et al., 2011; Laforest and Nemer, 2012), migration of neural crest cells (Jain et al., 2011), or extracellular matrix (ECM) remodeling (Fedak et al., 2003)—have been demonstrated to be involved in aortic valve embryogenesis. Therefore, this issue supports the possible contribution of different loci in influencing the development of an abnormal valve formation and of other non-valvular complications associated with the disease. The present review will focus on up to date information concerning the genetic loci found to be associated with BAV (both syndromic and non-syndromic cases), and on the progressive advancements in massive parallel sequencing approaches able to generate a large volume of genetic data, thus representing a substantial challenge in contributing to faster elucidate the molecular bases of the disease, and to allow differential diagnosis for a better BAV patients management.

GENETICS OF BAV

What We Know So Far

The initial insight of a strong genetic component participating in the pathogenesis of this cardiac malformation has been provided by several studies revealing a high incidence of familial clustering. Early studies showed the aortic valve disease, probably resulting from BAV, to have a prevalence of 24% in families with more than one family member carrying the valve malformation (Glick and Roberts, 1994; Clementi et al., 1996). Shortly thereafter, a 9.1% prevalence of BAV was observed among 190 first-degree relatives in families screened by echocardiography (Huntington et al., 1997). More recent studies, that made use of a variance component methodology and a mathematical model, established the heritability of BAV up to 89% indicating the disease as almost entirely genetically determined (Cripe et al., 2004; Lewin et al., 2004; Freeze et al., 2016). Family data were consistent with an autosomal dominant pattern of inheritance with reduced penetrance and variable expressivity (Laforest and Nemer, 2012; De Cario et al., 2014).

Despite the well-established notion of a heritability associated with BAV, no single gene model exists that could explain the inheritance of this cardiac malformation. In fact, a role of many discrete genes with divergent inheritance pattern which might also act in combination as polygenic trait may be derived by the analysis of literature data (Laforest and Nemer, 2012; De Cario et al., 2014). Hence, during the last decades, a number of studies on animal models, together with various genetic and biochemical approaches, have been performed allowing the identification of a large number of genes suggested to be implied in BAV pathogenesis in its sporadic or syndromic presentation (**Table 1**). The products of these genes are represented by transcription factors, components of the ECM, and proteins involved in several signaling pathways regulating various cellular processes, such as proliferation or apoptosis, in cardiac tissues (Laforest and Nemer, 2012; De Cario et al., 2014; Freeze et al., 2016). Furthermore, over recent years, the wide heterogeneity in BAV has been suggested to be the result of a combination between genetic, functional and hemodynamic factors acting as modulators of the phenotype

TABLE 1 | Genetic loci associated with BAV in humans and animal models.

HUMANS	
NON-SYNDROMIC BAV	**SYNDROMIC BAV**
NOTCH1	*FBN1* (Marfan syndrome)
GATA5	*TGFBR1/2* (Loeys-Dietz syndrome)
GATA4	*ACTA2* (Thoracic aortic aneurysm and dissection syndrome)
ACTA2	
Linkage loci on:	*KCNJ2* (Andersen syndrome)
Chr 15q	45 × 0 karyotype (Turner syndrome)
Chr18q	Deletion of 1.5-1.8Mb region (7q11.3) including
Chr 5q	*CLIP2*, *ELN*, *GTF2I*, *GTF2IRD1*, and *LIMK1* (William
UFD1L	Beuren syndrome)
AXIN1/PDIA2	*HOXA1* (Bosley-Salih-Alorainy syndrome,
ENG	Athabaskan brainstem dysgenesis syndrome)
EGFR	*COL3A1* (Vascular Ehlers Danlos syndrome)
SMAD6	
ANIMAL MODELS	
Notch1	
Gata5	
Nos3	
Nkx2.5	

expression (Nistri et al., 2008, 2016; Conti et al., 2010; Della Corte et al., 2012; De Cario et al., 2014; Michelena et al., 2015; Fedak and Barker, 2016; Fedak et al., 2016; Longobardo et al., 2016; Masri et al., 2017). In most cases, BAV presents itself as an isolated trait but its association with other genetic syndromes, such as Andersen syndrome, Turner syndrome, William Beuren, Bosley-Salih-Alorainy, Athabascan Brainstem Dysgenesis syndromes is well established. In particular, it may occur as component of connective tissue disorders, such as familial TAA and dissection (FTAA/D), Marfan syndrome (MFS), Loeys-Dietz syndrome (LDS) and vascular Ehlers-Danlos syndrome (vEDS) (Duran et al., 1995). In fact, the identification of a syndromic condition in a BAV patient is relevant as it can affect the rate of progression to clinically evident disease and has led, for example, to the definition of distinct guidelines, with respect to aortic diameter thresholds, for elective surgery in MFS and BAV patients (Erbel et al., 2014; Nishimura et al., 2014). A recent study, carried out on a cohort of 257 MFS patients, allowed the unequivocal diagnosis of BAV in 12 patients (4.7%) revealing a prevalence of the cardiac valve malformation exceeding four times that observed in the general population screened by echocardiography (0.5%) (Basso et al., 2004; Nistri et al., 2005, 2012). In patients with LDS, BAV has been also noted as a clinical finding more prevalent (8%) than in the general population (Patel et al., 2017). These results suggest how aortic valve morphology in MFS patients should be better pursued during clinical examination. On the other hand, due to the wide range variability and severity of clinical manifestations in inherited connective tissue disorders patients often leading to a late definite diagnosis of syndromic phenotypes, such as MFS or LDS, the evaluation of the coexistence of a syndromic condition in BAV patients by an expert clinician/geneticist should be encouraged in order to better decide the follow-up and surgical timing. Genetic testing could therefore provide a valuable tool in order to detect not only genetic variants causative of BAV, furthering knowledge of the mechanisms underlying its pathogenesis, but also to predict and prevent the aforementioned BAV-associated complications and to identify at-risk asymptomatic family members.

In 2012, in 2 out of 3 BAV/MFS patients undergoing mutation-screening analysis, genetic variants in *FBN1* gene were found (Nistri et al., 2012). Moreover, our group next identified for the first time pathogenetic *FBN1* gene (fibrillin 1, 15q21.1, OMIM*134797) mutations in patients with BAV and aortic dilation/aneurysm in whom MFS and other more severe type 1 fibrillinopathies were clinically excluded (Pepe et al., 2014). *FBN1* encodes a glycoprotein component of the ECM involved in the maintenance of elastic fibers and in the anchorage of epithelial cells to the interstitial matrix and a decreased *FBN1* mRNA or protein content has been demonstrated in a subgroup of BAV patients, suggesting this gene to be one of those possibly associated with BAV. In addition, it has been demonstrated that targeted deletion of *Fbn1* in mice recapitulates the vascular defects observed in MFS suggesting valve malformation to be the result of *FBN1* mutations (Pereira et al., 1997; Ng et al., 2004). An up-regulated transforming growth factor beta (TGF-ß) signaling was observed in these mice who showed mitral valve prolapse and died shortly after birth for aortic dissection as a consequence of aortic wall weakening (Ng et al., 2004). TGF-ß represents the key regulator of vascular matrix remodeling and vascular smooth muscle cells (VSMCs) activity, and a wide number of studies provided evidences of the association between the dysregulation of its signaling and aneurysm formation, including-BAV associated TAA (Kurtovic et al., 2011). Mutations in the TGF-β receptors, *TGFBR1* (transforming growth factor beta receptor, type 1, 9q22.33, OMIM*190181) and *TGFBR2* (transforming growth factor beta receptor, type 2, 3p24.1, OMIM*190182) have been described in MFS-like conditions and have been consistently associated with LDS (Loeys et al., 2005; Mátyás et al., 2006; Attias et al., 2009; Wei et al., 2016). A missense mutation in *TGFBR2* has been shown to segregate in a family with non-syndromic associated BAV and proximal aortic aneurysm which was identical to the one found in MFS patients who tested negative for mutation in *FBN1* (Girdauskas et al., 2011). More recent sequencing experiments on familial and isolated BAV cases failed to identify mutations in the two receptors suggesting their contribution to be probably very low in the overall BAV population (Arrington et al., 2008; Foffa et al., 2013; Bonachea et al., 2014b).

Mutations in *ACTA2* gene, encoding smooth muscle α-actin and known to be associated with familial TAA, have been also detected in patients with BAV (Jondeau and Boileau, 2012; Martín et al., 2017).

Moreover, further data from genetics studies (candidate gene as well as genome wide analyses) allowed to deepen the knowledge concerning the genetic bases of the disease, thus evidencing a role for other candidate loci not previously associated with syndromic BAV. *NOTCH1* (Notch, Drosophila, homolog of, 1, chr 9q34.3, OMIM*190198) mutations have been firstly associated with aortic valve abnormalities, such as aortic valve calcium deposition, suggesting their potential role in cardiac disease in humans. These studies suggested

that mutations in this gene, identified in a small number of families, may represent the genetic basis for hypoplastic left heart syndrome in some patients (Garg et al., 2005). Further evidences of a *NOTCH1* haploinsufficiency as possible cause of aortic valve disease were provided by shortly subsequent studies in which targeted mutational analyses were performed, allowing the identification of not previously described missense mutations in patients with BAV and/or aortic aneurysms (Mohamed et al., 2006; McKellar et al., 2007; Foffa et al., 2013). These studies also unraveled the role of *NOTCH1* mutations in familial BAV as well as in approximately 4% of sporadic cases. Recently, genetic screening of 428 probands with left-sided congenital heart disease (LS-CHD) allowed the identification of 14 *NOTCH1* mutations (11 in familial and 3 in isolated cases), 10 out of 11 families and 1 out of 3 isolated cases showed BAV (Kerstjens-Frederikse et al., 2016). Interestingly, this datum suggests a higher prevalence of *NOTCH1* mutations among familial cases [11/148 (7%)] than among sporadic forms [3/280 (1%)] of LS-CHD. The Notch signaling pathway is highly conserved across species. *NOTCH1* encodes a large protein containing an extracellular domain with 36 tandem epidermal growth factor (EGF)-like repeats and three cysteine-rich Notch/LIN-12 repeats, an intracellular domain with six ankyrin repeats, and a transactivation domain (Artavanis-Tsakonas et al., 1999). Since the discovery of *NOTCH1* as a potential candidate gene underlying BAV formation, a number of studies carried out analysis of aortic valves in genetically engineered mice in an attempt to unravel the molecular mechanisms associated with valve development. Murine model studies indicate that targeted inactivation of Notch impairs endocardial epithelial-to mesenchyme transition *in vivo* and in explant assays. Notably, Notch1 null mice developed serious cardiac alterations which led them to an early death; one of these defects results in imperfect epithelial-to-mesenchymal transition (EMT). EMT, occurring in the developing cardiac valves, represents an important process determining the transition from primordial to mature valves (von Gise and Pu, 2012). In addition, mutations involving components of the Notch pathway affect the expression of some TGF-ß signaling members, indicating that Notch activity is needed for the normal functioning of several elements acting in these key intracellular processes (Timmerman et al., 2004). This is of particular importance since a large number of evidences support the key role of a dysregulated TGF-ß signaling in vascular matrix remodeling. BAV patients with dilated ascending aorta showed indeed a distinctive TGF-β pathway gene expression pattern with respect to dilated subjects with normal three leaflet valve, resulting, in turn, to modulate phenotypic heterogeneity of thoracic aneurysm in BAV. This is likely to represent one of the most frequent events implicated in aneurysm formation, which can occur in association with BAV in a more severe clinical phenotype. These findings provided initial insights on developmentally regulated EMT processes, including the occurrence of congenital cardiac valve abnormalities. Subsequently, Notch1 signaling has also been described as affecting molecular processes involved in aortic valve calcification. Engineered Notch1$^{+/-}$ mice have in fact been shown to endure a >5-fold aortic valve calcification level with respect to their wild-type counterparts comparable for age and sex. These studies provided evidence of the repression mechanism, generally played by Notch1 in murine aortic valves *in vivo* and in aortic valve cells *in vitro*, on *BMP2* gene (bone morphogenic protein, 220p12.3, OMIM*112261), which partly stall the progression of aortic valve calcification (Nigam and Srivastava, 2009). In a more recent aortic valve calcification *in vitro* model, addition of Sox9 was found to prevent Notch signaling, implying Notch1 to act as a regulator of aortic valve calcification through a Sox-9-dependent pathway (Acharya et al., 2011). All together, these results strengthen the hypothesis according to which *NOTCH1* haploinsufficiency plays a fundamental part during the embryonic development of cardiac valves and also in maintaining their regular function in the mature heart. Its dysregulation may therefore predispose to BAV as well as other congenital cardiac malformations affecting both the left and right-sided cardiac OFTs in humans (Koenig et al., 2017).

Besides Notch, which appears to be critical for normal tricuspid formation, *Nos3* pathway has been implicated as a regulator of BAV formation in animal models. *Nos3* is expressed in endocardial cells of the heart and is shear-stress-dependent. *Nos3*$^{-/-}$mice were reported to carry CHD in early studies (Lee et al., 2000). The relevance of *NOS3* (Nitric oxide synthase 3, 7q36.1, OMIM*163729) as possible regulator in BAV formation was also supported by other studies showing a significant reduction of its expression in patients with BAV (Aicher et al., 2007). *NOS3* activation is mediated by members of the GATA family of transcription factors (German et al., 2000), such as GATA5, encoded by *GATA5* gene (Gata-binding protein 5, 20q13.33, OMIM*611496).

Alongside *NOTCH1*, *GATA5* has been linked to BAV in humans as a number of studies reported several rare sequence variants of this gene in BAV and its associated aortopathy (Padang et al., 2012; Bonachea et al., 2014a; Shi et al., 2014), accounting for up to 4% of sporadic cases. *GATA5* has an essential role in cardiogenesis and aortic valve development as a mediator of cellular mechanisms participating in endocardial cell differentiation, some of these processes being regulated by *Bmp4*, *Tbx20* as well as *NOS3* and *NOTCH1* (Padang et al., 2012). A recent *Gata5* null mouse model showed partial penetrance of BAV with a prevalence of 26%; a decrease in *Nos3* expression was also observed in the endocardial cushions of the OFT together with a significant downregulation of Notch1 pathway (Laforest et al., 2011). In addition to that, a deleterious mutation in *NKX2.5* gene (Nk2 Homeobox 5; 5q35.1, OMIM*600584) that completely abolished its interaction with GATA5 was found to segregate with disease in a family with BAV and a small proportion (11%) of mice carrying cardiac homeobox *Nkx2-5* haploinsufficiency (Groenendijk et al., 2004) have been associated with a higher incidence of the disease. Homeobox protein Nkx-2.5 activity is critically required during cardiac morphogenesis and it's also involved in modulation of the ECM of the aorta due to its role as a regulator of the collagen type I availability (Ponticos et al., 2004). All together, these findings seem to support the notion of Notch1 and Nos3 pathways, mediated by GATA5, as possible relevant elements in BAV pathogenesis. Other genes encoding GATA family cardiac factors, such as *GATA4* (GATA-binding protein,

4; 8p23.1; OMIM*6005769) and *GATA6* (GATA-binding protein, 6; 18q11.2; OMIM*601656) were observed in human congenital heart defects (Garg et al., 2003; Lepore et al., 2006; Rajagopal et al., 2007; Hamanoue et al., 2009; Maitra et al., 2010). Recently, a low frequency noncoding variant 151 kb from *GATA4*, together with a missense mutation involving the same gene, showed an association with the BAV phenotype that reached genome wide significance. The case-control genome wide association study was carried out on 466 BAV patients and 4,660 controls, replicated in up to 1,326 cases and 8,103 controls. These identified variants are thought to affect cardiac valves development and increase the risk of cardiac malformations as they seem to disrupt some regulatory elements involved in *GATA4* expression during cardiac embryogenesis (Yang et al., 2017). Several other genes have been implicated in isolated BAV or in BAV-TAA (Laforest and Nemer, 2012; De Cario et al., 2014; Freeze et al., 2016). One of these is *UFD1L* (ubiquitin fusion degradation 1-like, 22q11.21, OMIM*601754), whose expression has been demonstrated to be down-regulated in BAV patients. Its product is a component of a multi-enzyme complex involved in the degradation of ubiquitin fusion proteins during embryogenesis, with an important role in the development of ectoderm-derived structures; it has been observed to be diminished in BAV patients (Mohamed et al., 2005).

Its important function in aortic leaflets formation indicates a possible role of *UFD1L* in BAV pathogenesis even if no causal relationship, but only an association, between mutations involving this gene and the cardiac malformation has been established so far. A missense mutation in the MH2 domain of the SMAD6 protein (p.Cys484Phe) in a man with BAV, aortic valve stenosis, and coarctation and calcification of the aorta was identified (Tan et al., 2012). Resequencing of the MH2 domain of SMAD6 gene (homolog of mothers against decapentaplegic, drosophila, 6 chr 15q22.31, OMIM *602931) in a replication cohort consisting of 346 additional probands with a broad range of cardiovascular malformation phenotypes revealed another missense mutation (p.Pro415Leu) in an infant with BAV and moderate aortic stenosis. Gene network analysis identified haplotypes for *ENG* (endoglin, 9q34.11, OMIM*13195), a gene known to be important in heart valve formation, and for *AXIN1* (axis inhibitor 1; 16p13.3, OMIM*603816) and *PDIA2* (Protein Disulfide Isomerase Family A Member 2; 16p13.3, OMIM*608012) to be associated with BAV in a cohort of 68 probands (Wooten et al., 2010). AXIN1 is member of the Wnt pathway, which mediates TGF-β signaling and acts as a crucial regulator of both heart valve formation and cardiac neural crest development (Armstrong and Bischoff, 2004). The role of PDIA2 in heart valve formation is not yet unveiled.

Recently, next generation sequencing (NGS) approaches on nine genes previously associated with BAV (*NOTCH1*, *AXIN1*, *EGFR*, *ENG*, *GATA5*, *NKX2-5*, *NOS3*, *PDIA2*, and *TGFBR2*) has been performed on 48 BAV patients (Dargis et al., 2016), allowing the identification of previously known potentially pathogenic variants in *AXIN1*, *EGFR*, *ENG*, *GATA5*, *NOTCH1*, and *PDIA2*. The most promising variants were subsequently evaluated in a case-control study showing men and women to carry some distinct genetic variants associated with BAV. These findings led to the hypothesis of the involvement of some gender-specific variants in BAV onset and advancement. Mutations in *ACTA2* (Actin, alpha 2, smooth muscle, aorta;10q23.3, OMIM*102620) were identified in 7 family members with aortic aneurysms and dissection, of whom 3 had BAVs, their aortic tissue displaying increased proteoglycans accumulation, fragmentation, loss of elastic fibers, and decreased numbers of smooth muscle cells, consistent with aortic wall degeneration. These findings could lead to the hypothesis of a unique pathogenetic basis for BAV-TAA patients (as BAV has been observed to occur more frequently in patients with TAA who have mutations in his gene) (Guo et al., 2007; Jondeau and Boileau, 2012) even if, at present, whether *ACTA2* mutations may cause BAV remains uncertain. Targeted NGS approach identified 31 rare non-synonymous, exonic variants classified as putative disease-causing changes by *in-silico* analysis in the 97 candidate genes. These study evidenced variants in 25 genes (*APC, AXIN2, FLT1, GATA4, GLI1, JAG1, MCTP2, MSX1, NFATC1, NOS1, NOTCH2, NOTCH3, PAX6, PIGF, PPP3CA, PTCH1, PTCH2, SLC35B2, SNAI3, SOX9, TBX5, VEGFB, VEGFC, WNT4, and ZNF236*) not previously associated with human BAV (Bonachea et al., 2014b). Finding these genetic variants in index cases did not imply a definitive association of these genes with the BAV phenotype, thus requiring further functional analyses and segregation data in families. Ultimately, BAV seems to display a substantial genetic heterogeneity, suggesting the role of many discrete genes in its pathogenesis, which is challenging for researchers whose aim is to discover genetic variants causative of BAV as well as patients at risk to develop the most feared BAV-associated complications (**Figure 1**). The aforementioned animal studies provided evidences of a combination between multiple genetic variants acting as a burden and epigenetic plus environmental factors. This complex array of genetic and non-genetic factors may be responsible for the extremely variable phenotypic expression of BAV. This is especially relevant considering those conditions that often accompany BAV as TAA/D.

Due to the evidence that BAV and TAAD frequently occur together, we might hypothesize that BAV genetic profile may be determined by an additive contribution of many different genetic variants increasing both the risk for BAV occurrence and for its complications (Prakash et al., 2014). Therefore, successful gene discovery may help in situations in which the identification of the leading factor, hemodynamic or genetic, playing a relevant role in the disease development, determines different surgical decisions (Padang et al., 2012). In fact, wherever a genetic alteration is identified as the dominant factor, this may lead to a more aggressive disease phenotype and earlier aortic intervention (Erbel et al., 2014; Nishimura et al., 2014). To that purpose, large families with inherited predisposition to BAV currently represent the most promising opportunities for the consolidation of suspected and novel discovery of gene association even considering (1) the known difficulties in recruiting well clinically evaluated relatives, together with (2) the reduced penetrance and variable expressivity associated with the BAV phenotype. Even and above all, in the era of high-throughput technologies, segregation analyses represent the gold standard approach to identify causative mutations in genes of distantly related

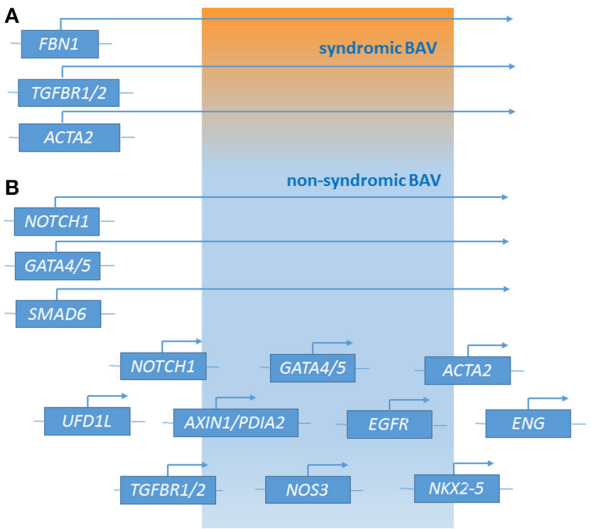

FIGURE 1 | Genetic loci associated with syndromic BAV **(A)** and non-syndromic BAV **(B)** [effect of major genes or contribution of multiple minor loci (polygenic form of the disease)].

subjects, also providing and optimizing the statistical power in genotype-phenotype correlations (Michelena et al., 2014). As thousands of cases are needed to identify substantial genetic contributors, constant advances in NGS technologies provide an unprecedented opportunity to unravel the genetic complexity of BAV and its associated aortopathies (Andreassi and Della Corte, 2016). Targeted NGS of a carefully selected part of the genome (a specific set of genes relevant to a disease phenotype) produces a more manageable data set compared with broader approaches, making analysis easier and faster (Wooderchak-Donahue et al., 2015). This kind of approach may lead to the identification of novel genetic variants whose biological role in BAV is yet to be determined; these variants could be tested for a possible association with the disease also when assessed together in intracellular signaling pathways (Michelena et al., 2014). Nevertheless, it should be considered that the comprehension of the pathogenesis of BAV could be further supported by different mechanisms not addressed in this review. In fact, beyond the presence of mutations in exons or splice site consensus regions of protein-coding genes, mutations in introns and regulatory 5′ promoter and UTR regions, intergenic variants, as well as epigenetic mechanisms involving miRNAs expression profiles alterations or DNA methylation and histone modifications may also have a role in BAV development.

High-Throughput Sequencing (HTS) Technologies:

The achievement of information on the genetic bases of BAV has been allowed by the progressive acquisition of novel technologies able to produce a large volume of data. Actually, first studies were based on the evaluation of the heritability of BAV, thus providing information on the contribution of genetics to this phenotypic trait. To that end, family-based approach has revealed useful in identifying loci segregating with the disease. Afterwards, genome wide association studies (GWAS) investigating a wide number of genetic variants in genes supposed to be associated with the disease added a further support in identifying novel candidate loci (Wang et al., 2009; De Cario et al., 2014; Freeze et al., 2016). Although a number of information on genetic contribution to BAV disease have been obtained through these approaches, most remains to be discovered and understood concerning genetics of BAV. At this purpose a relevant contribution in deepening the molecular bases of BAV may derive from high-throughput sequencing (HTS) technologies also identified as next generation sequencing (NGS), allowing the parallel analysis of large number of genes or entire exomes or genomes. Advancements in DNA sequencing technologies led to the progressive availability of several platforms, each one exhibiting differences in detection methods and throughput, in order to cover needs ranging from target genes panel sequencing approach to exomes/genomes analyses. The resulting availability of large volume of data determined also the development of novel "BigData" analysis methods, able to integrate genetic and clinical data, thus representing a promising opportunity, at present and in the next few years, to significantly increase the knowledge on the genetic bases of BAV. Actually, since 2008, the diffusion of HTS allowed reduction in costs per run and time of analysis, thus raising interest in the use of HTS approach both as a research and clinical tool (https://www.genome.gov/27541954/dna-sequencing-costs-data/; Goodwin et al., 2016; Magi et al., 2017).

Each platform exhibits specific chemistry and detection methods, thus differently contributing to the overall performance of the sequencing approach and then differently adapting to the needs and peculiarities of research and diagnostics.

The first HTS technology to be widespread is represented by the Roche 454 (GS FLX) platform (Roche Diagnostics; **Table 2**), released in 2005 (Margulies et al., 2005) and just discontinued (Levy and Myers, 2016), a sequencing-by-synthesis (SBS) approach based on *single nucleotide addition* (SNA) sequencing principle. In this approach clonal template populations are generated after sample DNA fragmentation followed by ligation with an oligonucleotide adaptor, complementary to an oligonucleotide fragment immobilized on the surface of a capture bead, and emulsion PCR (emPCR), carried out in aqueous droplets (Shendure et al., 2005). Consequently, multiple copies of the same DNA sequence will cover each capture bead. The beads are next arrayed in the wells of a fiber optic slide (PicoTiterPlate) for the pyrosequencing reaction (Leamon et al., 2004).

Among SBS approaches, Ion Torrent and Illumina platforms are currently used (**Table 2**). Ion torrent technology also shares with the Roche 454 system the SNA principle and the emulsion PCR step to achieve the clonal amplification of the DNA template, whereas Illumina technology foresees a solid-phase bridge amplification and a *cyclic reversible termination* (CRT) approach (Goodwin et al., 2016).

Ion Torrent platform, although representing a very similar technology with respect to Roche 454, it does not rely on the optical detection of incorporating nucleotide through imaging technology, but it is based on a semiconductor sequencing approach, as proton release detection during

TABLE 2 | High-Throughput sequencing (HTS) platforms characteristics.

Platform	Chemistry	Read length (bp)	Throughput	Error rate (%)	Primary error type
ROCHE 454*					
GS FLX Titanium XLR70	*Sequencing-by-synthesis*	Up to 600	450 Mb	1	indel
GS FLX Titanium XL+	*Sequencing-by-synthesis*	Up to 1000	700 Mb	1	indel
ION TORRENT^					
Ion PGM 314	*Sequencing-by-synthesis*	200	30–50 Mb	1	indel
		400	60–100 Mb		
Ion PGM 316	*Sequencing-by-synthesis*	200	300–500 Mb	1	indel
		400	600 Mb-1 Gb		
Ion PGM 318	*Sequencing-by-synthesis*	200	600 Mb–1 Gb	1	indel
		400	1–2 Gb		
Ion Proton	*Sequencing-by-synthesis*	Up to 200	Up to 10 Gb	1	indel
Ion S5 520	*Sequencing-by-synthesis*	200	600 Mb–1 Gb	1	indel
		400	1.2–2 Gb		
Ion S5 530	*Sequencing-by-synthesis*	200	3–4 Gb	1	indel
		400	6–8 Gb		
Ion S5 540	*sequencing-by-synthesis*	200	10–15 Gb	1	indel
ILLUMINA^					
MiniSeq	*Sequencing-by-synthesis*	Up to 150	1.65–7.5 Gb	<1	substitutions
MiSeq	*sequencing-by-synthesis*	Up to 300	540 Mb–15 Gb	0.1	substitution
NextSeq 500/550	*Sequencing-by-synthesis*	Up to 150	16.25–120 Gb	<1	substitution
HiSeq 2500	*Sequencing-by-synthesis*	Up to 250	9–1000 Gb	0.1	substitution
HiSeq 3000/4000	*Sequencing-by-synthesis*	Up to 150	105–1500 Gb	0.1	substitution
HiSeqX	*Sequencing-by-synthesis*	Up to 150	1600–1800 Gb	0.1	substitution
PACIFIC BIOSCIENCES*					
RSII	*Single-molecule real-time long-reads*	∼20,000	500 Mb–1 Gb	13 (single-pass); ≤1% circular consensus read*	indel
Sequel	*Single-molecule real-time long-reads*	8,000–12,000	3.5–7 Gb	–	–
OXFORD NANOPORE‡					
Mk1 MinION	*Single-molecule real-time long-reads*	Up to 1 Mb*	Up to 20 Gb^ (1-D yield)	–	–

Goodwin et al., 2016; ^Goodwin et al., 2016 and manifacturers's data (http://www.thermosisher.com/it/en/Home/brands/ion-torrent.html);
†*Goodwin et al. (2016) and manifacturers's data manifacturers's data (http://www.illumina.com);*
‡*Manifacturers's data (http://www.nanoporetech.com).*

nucleotide incorporation may be permitted by the use of ion sensors. Therefore, this approach requires smaller instrument size and may result in higher speed of sequencing analysis and lower costs with respect to Roche 454 (Metzker, 2010; Liu et al., 2012; van Dijk et al., 2014). Ion Torrent platform appears particularly useful for targeted sequencing approached in which a panel of specific genes is analyzed for diagnosis and research purpose.

Differently from previously described sequencing approaches, Illumina technology is based on the "bridge amplification" principle, in which DNA fragments, ligated to oligonucleotide adapters complementary to Illumina flow-cell anchors, are amplified *in-situ* on the flow-cell surface. This amplification step relies on arching of the captured DNA strand and its subsequent hybridization to an adjacent anchor oligonucleotide, thus contributing to generate clonally amplified clusters, each one including thousands of clonal molecules (Voelkerding et al., 2009). Afterwards, sequencing is performed through CRT approach, based on the use of fluorescent reversible dye terminators, in which the presence of a chemical modification of the ribose at the 3′-hydroxyl position of the nucleotide, allows a single-base extension during each sequencing cycle. After image acquisition, the reversible dye terminators are unblocked and the next cycle may be performed (Voelkerding et al., 2009). At present, Illumina platform, with its wide range of instruments with different through-put and lower costs, is the widespread HTS technology in research as well as diagnosis laboratories.

Although advancements in generating longer reads are currently being developed, the abovementioned platforms achieved significant results in providing sequencing data, with different strengths and weaknesses depending of each platform characteristics.

The Illumina technology (read length 35–300 bp) is shared by a large number of instruments, ranging from lower throughput benchtop units, such as MiniSeq (<7.5 Gb) or MiSeq v3 (<15 Gb), to ultra-high-throughput instruments, such as HiSeq × (800–900 Gb per flow cell) (Goodwin et al., 2016), useful for providing whole genome sequencing data at a population level. The different chemistry (CRT approach) of Illumina technology contributes to make it less susceptible to homopolymers errors, as observed in other platforms (Roche 454 and Ion Torrent). Nevertheless, although an overall accuracy of >99.5% could be recognized for this approach, under-representation in both AT- and GC-rich regions and substitution error have been observed (Bentley et al., 2008; Dohm et al., 2008; Harismendy et al., 2009; Minoche et al., 2011; Nakamura et al., 2011). The availability of different Illumina platforms contributes to render this technology suitable for a large number of applications, ranging from target gene panel/whole exome/whole genome sequencing to epigenomics (Park, 2009) as well as transcriptomics (Wang et al., 2009) applications.

If compared with Illumina technology, both Roche 454 and Ion Torrent HTS sequencing platforms generate higher length reads (up to 1,000 and 400 bp, respectively), thus offering a better efficiency in providing information concerning complex /repetitive DNA regions. Nevertheless, although their overall error higher rate in non-homopolymeric DNA regions could be considered comparable with that of other platforms, a higher prevalence of false positives in insertion/deletion (indel) variants detections is more commonly observed (Loman et al., 2012; Forgetta et al., 2013).

Over the last years, further advancements in HTS technologies have allowed to improve read length, thus possibly overcoming limitations of short read sequencing, such as *de-novo sequencing* and detection of structural features of the genome, by spanning these regions with a single continuous read. Actually, a wider resolution of genomic variations might be achieved in the presence of a complete, reference-free, genome assembly. The generation of longer reads could also be useful in the transcriptomics field, in order to correctly discern gene isoforms by spanning an entire mRNA transcript (Goodwin et al., 2016). Moreover, the short reads (100–50 bp) generated by previously mentioned platforms are not enough adequate to resolve complex genomic structures, such as long repetitive elements, copy number alterations and structural variations that could play a crucial role in the pathogenesis of BAV as well as other diseases in all the fields of medicine (Magi et al., 2017).

To date, long-read sequencing is primarily based on a *single-molecule real-time* (SMRT) sequencing approach, in which the generation of a clonally amplified DNA fragments population is no longer required in the sequencing protocol. The most widely adopted SMRT approach is that developed by Pacific Biosciences (**Table 2**) (read length average >14 kb) (Eid et al., 2009; Reuter et al., 2015; Levy and Myers, 2016), which foresees the use of specialized flow cells including thousands of picolitre wells (*zero-mode waveguide*, ZMW), at whose transparent bottom a polymerase is fixed, thus allowing labeled dNTP incorporation on each single molecule template. After the fluorescence signal is recorded by the instrument imaging system, the enzyme removes the fluorophore from the nucleotide and permits the next labeled dNTP to be added. Of interest, the present approach uses a unique circular DNA template, thus allowing to consecutively sequence the same DNA molecule several times (Eid et al., 2009; Loomis et al., 2013).

The use of nanopores in sequencing technologies was widely discussed from 1996 (Kasianowicz et al., 1996; Branton et al., 2008), thus providing new challenges in the sequencing technology field.

In 2014 the Oxford Nanopore Technology (ONT) developed a handheld sequencer based on nanopore sequencing technology, the MinION system (**Table 2**), able to directly detect the DNA base composition of a native single strand DNA molecule. It is a disposable device containing a sensor chip, application specific integrated circuits (ASIC) and nanopores that are needed to perform single molecule DNA sequencing experiments. The DNA sequencing with Nanopore instrument relies on the conversion of electrical signal of nucleotides passing through a nanopore in a membrane between two electrolytes. The experimental protocol foresees the use of a leader-hairpin library structure, with the reverse strand linked by a hairpin adaptor to the forward strand, thus allowing, when DNA passes throughout the pore, the consecutive sequencing of both strands (2D-reads) (Goodwin et al., 2016). Data from literature showed that the current MinION platform is able to generate approximately 100 Mb of data per 16-h run, with an average read length of about 6 kb (Ashton et al., 2015). Moreover, the ONT PromethION platform, more recently released (Levy and Myers, 2016; Gigante, 2017), represent an ultra-high-throughput platform including 48 individual flow cells, each one including 3000 nanopores, thus providing a large volume of data (about 2–4 Tb) in a 2-day run.

A recent study showed a significant improvement in *de novo* genomes' assembly and in exploration of structural variants by nanopore technology application (Magi et al., 2017). This approach might represent a further challenge to improve the comprehension of genetics of BAV.

CONCLUSIONS AND FUTURE PERSPECTIVES

During the last decades, the hypothesis of an underlying genetic contribution in the pathogenesis of BAV has been supported by a growing number of evidences resulting from both human and animal models, even though no precise association between specific genes and the disease has been established in the majority of cases.

As other vascular and cardiovascular diseases, beside the mendelian inheritance observed in some families due to mutations in some genes (e.g., *NOTCH1*) with a strong pathogenetic effect, in the large part of BAV patients the disease is likely to have a multifactorial nature. The latter condition is the result of complex interactions among genetic alterations (from common to rare genetic variants and chromosomal abnormalities), hemodynamic shear stress (produced by the abnormal leaflets), and other environmental

and stochastic factors. To further complicate the pathogenic complexity, BAV often accompanies syndromic disorders, such as MFS or LDS thus being difficult to distinguish whether the pathogenetic variants determining the syndromic picture are also responsible for BAV or they represent two different pathogenetic conditions due to genetic variants in different genes (**Figure 1**). The availability of high-throughput sequencing (HTS) technologies, enabling rapid and relatively cheap analyses of panel of genes or whole exome/genome, plays a fundamental role in achieving a better comprehension of the genetic bases of isolated and syndromic BAV. In this context, alongside the study of large cohorts of probands, the definite contribution deriving from functional analyses and segregation data in families should be encouraged.

At present, from a diagnostic point of view, performing differential genetic diagnosis through HTS techniques in order to exclude syndromic traits in BAV patients with suggestive manifestations should be considered.

Indeed, the greatest interest in obtaining more insights on the genetic contributors of aortic valve malformations lies in the opportunity to translate this knowledge in the clinical practice, aimed to predict BAV most feared complications (mainly aortic aneurysm and dissection), and make decisions on the best options and timing for aortic surgery (based on individualized genetic risk profiles) as well as on global patients management.

AUTHOR CONTRIBUTIONS

All the Authors substantially contributed to (1) the conception or design of the work, acquisition a revision of literature data; (2) drafting the work or revising it critically for important intellectual content; (3) final approval of the version to be published; AND All Authors agree to be accountable for all aspects of the work in ensuring that questions related to the accuracy or integrity of any part of the work are appropriately investigated and resolved.

REFERENCES

Acharya, A., Hans, C. P., Koenig, S. N., Nichols, H. A., Galindo, C. L., Garner, H. R., et al. (2011). Inhibitory role of Notch1 in calcific aortic valve disease. *PLoS ONE* 6:e27743. doi: 10.1371/journal.pone.0027743

Aicher, D., Urbich, C., Zeiher, A., Dimmeler, S., and Schäfers, H. J. (2007). Endothelial nitric oxide synthase in bicuspid aortic valve disease. *Ann. Thorac. Surg.* 83, 1290–1294. doi: 10.1016/j.athoracsur.2006.11.086

Andreassi, M. G., and Della Corte, A. (2016). Genetics of bicuspid aortic valve aortopathy. *Curr. Opin. Cardiol.* 31, 585–592. doi: 10.1097/HCO.0000000000000328

Armstrong, E. J., and Bischoff, J. (2004). Heart valve development: endothelial cell signaling and differentiation. *Circ. Res.* 95, 459–470. doi: 10.1161/01.RES.0000141146.95728.da

Arrington, C. B., Sower, C. T., Chuckwuk, N., Stevens, J., Leppert, M. F., Yetman, A. T., et al. (2008). Absence of TGFBR1 and TGFBR2 mutations in patients with bicuspid aortic valve and aortic dilation. *Am. J. Cardiol.* 102, 629–631. doi: 10.1016/j.amjcard.2008.04.044

Artavanis-Tsakonas, S., Rand, M. D., and Lake, R. J. (1999). Notch signaling: cell fate control and signal integration in development. *Science* 284, 770–776.

Ashton, P. M., Nair, S., Dallman, T., Rubino, S., Rabsch, W., Mwaigwisya, S., et al. (2015). MinIONnanopore sequencing identifies the position and structure of a bacterial antibiotic resistance island. *Nat. Biotechnol.* 33, 296–300. doi: 10.1038/nbt.3103

Attias, D., Stheneur, C., Roy, C., Collod-Béroud, G., Detaint, D., Faivre, L., et al. (2009). Comparison of clinical presentations and outcomes between patients with TGFBR2 and FBN1 mutations in Marfan syndrome and related disorders. *Circulation* 120, 2541–2549. doi: 10.1161/CIRCULATIONAHA.109.887042

Basso, C., Boschello, M., Perrone, C., Mecenero, A., Cera, A., Bicego, D., et al. (2004). An echocardiographic survey of primary schoolchildren for bicuspid aortic valve. *Am. J. Cardiol.* 93, 661–663. doi: 10.1016/j.amjcard.2003.11.031

Bentley, D. R., Balasubramanian, S., Swerdlow, H. P., Smith, G. P., Milton, J., Brown, C. G., et al. (2008). Accurate whole human genome sequencing using reversible terminator chemistry. *Nature* 456, 53–59. doi: 10.1038/nature07517

Bonachea, E. M., Chang, S. W., Zender, G., LaHaye, S., Fitzgerald-Butt, S., McBride, K. L., et al. (2014a). Rare GATA5 sequence variants identified in individuals with bicuspid aortic valve. *Pediatr. Res.* 76, 211–216. doi: 10.1038/pr.2014.67

Bonachea, E. M., Zender, G., White, P., Corsmeier, D., Newsom, D., Fitzgerald-Butt, S., et al. (2014b). Use of a targeted, combinatorial next-generation sequencing approach for the study of bicuspid aortic valve. *BMC Med. Genomics* 7:56. doi: 10.1186/1755-8794-7-56

Branton, D., Deamer, D. W., Marziali, A., Bayley, H., Benner, S. A., Butler, T., et al. (2008). The potential and challenges of nanopore sequencing. *Nat. Biotechnol.* 26, 1146–1153. doi: 10.1038/nbt.1495

Cecconi, M., Nistri, S., Quarti, A., Manfrin, M., Colonna, P. L., Molini, E., et al. (2006). Aortic dilatation in patients with bicuspid aortic valve. *J. Cardiovasc. Med.* 7, 11–20. doi: 10.2459/01.JCM.0000199777.85343.ec

Clementi, M., Notari, L., Borghi, A., and Tenconi, R. (1996). Familial congenital bicuspid aortic valve: a disorder of uncertain inheritance. *Am. J. Med. Genet.* 62, 336–338. doi: 10.1002/(SICI)1096-8628(19960424)62:4<336::AID-AJMG2>3.0.CO;2-P

Conti, C. A., Della Corte, A., Votta, E., Del Viscovo, L., Bancone, C., De Santo, L. S., et al. (2010). Biomechanical implications of the congenital bicuspid aortic valve: a finite element study of aortic root function from *in vivo* data. *J. Thorac. Cardiovasc. Surg.* 140, 890–896. doi: 10.1016/j.jtcvs.2010.01.016

Cripe, L., Andelfinger, G., Martin, L. J., Shooner, K., and Benson, D. W. (2004). Bicuspid aortic valve is heritable. *J. Am. Coll. Cardiol.* 44, 138–143. doi: 10.1016/j.jacc.2004.03.050

Dargis, N., Lamontagne, M., Gaudreault, N., Sbarra, L., Henry, C., Pibarot, P., et al. (2016). Identification of gender-specific genetic variants in patients with bicuspid aortic valve. *Am. J. Cardiol.* 117, 420–426. doi: 10.1016/j.amjcard.2015.10.058

De Cario, R., Sticchi, E., Giusti, B., Abbate, R., Gensini, G. F., Nistri, S., et al. (2014). Bicuspid aortic valve syndrome and fibrillinopathies: potential impact on clinical approach. *Int. Cardiovasc. Forum J.* 4, 167–174. doi: 10.17987/icfj.v1i4.45

Della Corte, A., Bancone, C., Buonocore, M., Dialetto, G., Covino, F. E., Manduca, S., et al. (2013). Pattern of ascending aortic dimensions predicts the growth rate of the aorta in patients with bicuspid aortic valve. *JACC Cardiovasc. Imaging* 6, 1301–1310. doi: 10.1016/j.jcmg.2013.07.009

Della Corte, A., Bancone, C., Conti, C. A., Votta, E., Redaelli, A., Del Viscovo, L., et al. (2012). Restricted cusp motion in right-left type of bicuspid aortic valves: anew risk marker for aortopathy. *J. Thorac. Cardiovasc. Surg.* 144, 360–369. doi: 10.1016/j.jtcvs.2011.10.014

Dohm, J. C., Lottaz, C., Borodina, T., and Himmelbauer, H. (2008). Substantial biases in ultra-short read data sets from high-throughput DNA sequencing. *Nucleic Acids Res.* 36:e105. doi: 10.1093/nar/gkn425

Duran, A. C., Frescura, C., Sans-Coma, V., Angelini, A., Basso, C., and Thiene, G. (1995). Bicuspid aortic valves in hearts with other congenital heart disease. *J. Heart Valve Dis.* 4, 581–590.

Eid, J., Fehr, A., Gray, J., Luong, K., Lyle, J., Otto, G., et al. (2009). Real-time DNA sequencing from single polymerase molecules. *Science* 323, 133–138. doi: 10.1126/science.1162986

Erbel, R., Aboyans, V., Boileau, C., Bossone, E., Bartolomeo, R. D., Eggebrecht, H., et al. (2014). 2014 ESC Guidelines on the diagnosis and treatment of aortic diseases: document covering acute and chronic aortic diseases of the thoracic and abdominal aorta of the adult. The task force for the diagnosis and treatment of aortic diseases of the European Society of Cardiology (ESC). *Eur. Heart J.* 35, 2873–2926. doi: 10.1093/eurheartj/ehu281

Fedak, P. W., and Barker, A. J. (2016). Is concomitantaortopathy unique with bicuspid aortic valve stenosis? *J. Am. Coll. Cardiol.* 67, 1797–1799. doi: 10.1016/j.jacc.2016.02.038

Fedak, P. W., Barker, A. J., and Verma, S. (2016). Year in review: bicuspid aortopathy. *Curr. Opin. Cardiol.* 31, 132–138. doi: 10.1097/HCO.0000000000000258

Fedak, P. W., de Sa, M. P., Verma, S., Nili, N., Kazemian, P., Butany, J., et al. (2003). Vascular matrix remodeling in patients with bicuspid aortic valve malformations: implications for aortic dilatation. *J. Thorac. Cardiovasc. Surg.* 126, 797–806. doi: 10.1016/S0022-5223(03)00398-2

Foffa, I., Ait Alì, L., Panesi, P., Mariani, M., Festa, P., Botto, N., et al. (2013). Sequencing of NOTCH1, GATA5, TGFBR1 and TGFBR2 genes in familial cases of bicuspid aortic valve. *BMC Med. Genet.* 14:44. doi: 10.1186/1471-2350-14-44

Forgetta, V., Leveque, G., Dias, J., Grove, D., Lyons, R. Jr., Genik, S., et al. (2013). Sequencing of the Dutch elm disease fungus genome using the Roche/454 GS-FLX Titanium System in a comparison of multiple genomics core facilities. *J. Biomol. Tech.* 24, 39–49. doi: 10.7171/jbt.12-2401-005

Freeze, S. L., Landis, B. J., Ware, S. M., and Helm, B. M. (2016). Bicuspid aortic valve: a review with recommendations for genetic counseling. *J. Genet. Couns.* 25, 1171–1178. doi: 10.1007/s10897-016-0002-6

Garg, V., Kathiriya, I. S., Barnes, R., Schluterman, M. K., King, I. N., Butler, C. A., et al. (2003). GATA4 mutations cause human congenital heart defects and reveal an interaction with TBX5. *Nature* 424, 443–447. doi: 10.1038/nature01827

Garg, V., Muth, A. N., Ransom, J. F., Schluterman, M. K., Barnes, R., King, I. N., et al. (2005). Mutations in NOTCH1 cause aortic valve disease. *Nature* 437, 270–274. doi: 10.1038/nature03940

German, Z., Chambliss, K. L., Pace, M. C., Arnet, U. A., Lowenstein, C. J., and Shaul, P. W. (2000). Molecular basis of cell-specific endothelial nitric-oxide synthase expression in airway epithelium. *J. Biol. Chem.* 275, 8183–8189. doi: 10.1074/jbc.275.11.8183

Gigante, S. (2017). Picopore: a tool for reducing the storage size of Oxford Nanopore Technologies datasets without loss of functionality. *F1000Res* 6:227. doi: 10.12688/f1000research.11022.2

Girdauskas, E., Schulz, S., Borger, M. A., Mierzwa, M., and Kuntze, T. (2011). Transforming growth factor-beta receptor type II mutation in a patient with bicuspid aortic valve disease and intraoperative aortic dissection. *Ann. Thorac. Surg.* 91, e70–e71. doi: 10.1016/j.athoracsur.2010.12.060

Glick, B. N., and Roberts, W. C. (1994). Congenitally bicuspid aortic valve in multiple family members. *Am. J. Cardiol.* 73, 400–404. doi: 10.1016/0002-9149(94)90018-3

Goodwin, S., McPherson, J. D., and McCombie, W. R. (2016). Coming of age: ten years of next-generation sequencing technologies. *Nat. Rev. Genet.* 17, 333–351. doi: 10.1038/nrg.2016.49

Groenendijk, B. C., Hierck, B. P., Gittenberger-De Groot, A. C., and Poelmann, R. E. (2004). Development-related changes in the expression of shear stress responsive genes KLF-2, ET-1, and NOS-3 in the developing cardiovascular system of chicken embryos. *Dev. Dyn.* 230, 57–68. doi: 10.1002/dvdy.20029

Guo, D. C., Pannu, H., Tran-Fadulu, V., Papke, C. L., Yu, R. K., Avidan, N., et al. (2007). Mutations in smooth muscle alpha-actin (ACTA2) lead to thoracic aortic aneurysms and dissections. *Nat. Genet.* 39, 1488–1493. doi: 10.1038/ng.2007.6

Hamanoue, H., Rahayuningsih, S. E., Hirahara, Y., Itoh, J., Yokoyama, U., Mizuguchi, T., et al. (2009). Genetic screening of 104 patients with congenitally malformed hearts revealed a fresh mutation of GATA4 in those with atrial septal defects. *Cardiol. Young* 19, 482–485. doi: 10.1017/S1047951109990813

Harismendy, O., Ng, P. C., Strausberg, R. L., Wang, X., Stockwell, T. B., Beeson, K. Y., et al. (2009). Evaluation of next generation sequencing platforms for population targeted sequencing studies. *Genome Biol.* 10:R32. doi: 10.1186/gb-2009-10-3-r32

Huntington, K., Hunter, M. D., Alasdair, G. W., and Chan, M. D. (1997). A prospective study to assess the frequency of familial clustering of congenital bicuspid aortic valve. *J. Am. Coll. Cardiol.* 30, 1809–1812. doi: 10.1016/S0735-1097(97)00372-0

Jain, R., Engleka, K. A., Rentschler, S. L., Manderfield, L. J., Li, L., Yuan, L., et al. (2011). Cardiac neural crest orchestrates remodeling and functional maturation of mouse semilunar valves. *J. Clin. Invest.* 121, 422–430. doi: 10.1172/JCI44244

Jondeau, G., and Boileau, C. (2012). Genetics of thoracic aortic aneurysms. *Curr. Atheroscler. Rep.* 14, 219–226. doi: 10.1007/s11883-012-0241-4

Kasianowicz, J. J., Brandin, E., Branton, D., and Deamer, D. W. (1996). Characterization of individual polynucleotide molecules using a membrane channel. *Proc. Natl. Acad. Sci. U.S.A.* 93, 13770–13773. doi: 10.1073/pnas.93.24.13770

Kerstjens-Frederikse, W. S., van de Laar, I. M., Vos, Y. J., Verhagen, J. M., Berger, R. M., Lichtenbelt, K. D., et al. (2016). Cardiovascular malformations caused by NOTCH1 mutations do not keep left: data on 428 probands with left-sided CHD and their families. *Genet. Med.* 18, 914–923. doi: 10.1038/gim.2015.193

Koenig, S. N., Lincoln, J., and Garg, V. (2017). Genetic basis of aortic valvular disease. *Curr. Opin. Cardiol.* 32, 239–245. doi: 10.1097/HCO.0000000000000384

Kurtovic, S., Paloschi, V., Folkersen, L., Gottfries, J., Franco-Cereceda, A., and Eriksson, P. (2011). Diverging alternative splicing fingerprints in the transforming growth factor-β signaling pathway identified in thoracic aortic aneurysms. *Mol. Med.* 17, 665–675. doi: 10.2119/molmed.2011.00018

Laforest, B., and Nemer, M. (2012). Genetic insights into bicuspid aortic valve formation. *Cardiol. Res. Pract.* 2012:180297. doi: 10.1155/2012/180297

Laforest, B., Andelfinger, G., and Nemer, M. (2011). Loss of Gata5 in mice leads to bicuspid aortic valve. *J. Clin. Invest.* 121, 2876–2887. doi: 10.1172/JCI44555

Leamon, J. H., Lee, W. L., Tartaro, K. R., Lanza, J. R., Sarkis, G. J., deWinter, A. D., et al. (2004). A massively parallel PicoTiterPlate based platform for discrete picoliter-scale polymerase chain reactions. *Electrophoresis* 25:1176. doi: 10.1002/elps.200490004

Lee, T. C., Zhao, Y. D., Courtman, D. W., and Stewart, D. J. (2000). Abnormal aortic valve development in mice lacking endothelial nitric oxide synthase. *Circulation* 101, 2345–2348. doi: 10.1161/01.CIR.101.20.2345

Lepore, J. J., Mericko, P. A., Cheng, L., Lu, M. M., Morrisey, E. E., and Parmacek, M. S. (2006). GATA-6 regulates semaphorin 3C and is required in cardiac neural crest for cardiovascular morphogenesis. *J. Clin. Invest.* 116, 929–939. doi: 10.1172/JCI27363

Levy, S. E., and Myers, R. M. (2016). Advancements in next-generation, sequencing. *Annu. Rev. Genomics Hum. Genet.* 17, 95–115. doi: 10.1146/annurev-genom-083115-022413

Lewin, M. B., McBride, K. L., Pignatelli, R., Fernbach, S., Combes, A., Menesses, A., et al. (2004). Echocardiographic evaluation of asymptomatic parental and sibling cardiovascular anomalies associated with congenital left ventricular outflow tract lesions. *Pediatrics* 114, 691–696. doi: 10.1542/peds.2003-0782-L

Liu, L., Li, Y., Li, S., Hu, N., He, Y., Pong, R., et al. (2012). Comparison of next-generation sequencing systems. *J. Biomed. Biotechnol.* 2012:251364. doi: 10.1155/2012/251364

Loeys, B. L., Chen, J., Neptune, E. R., Judge, D. P., Podowski, M., Holm, T., et al. (2005). A syndrome of altered cardiovascular, craniofacial, neurocognitive and skeletal development caused by mutations in TGFBR1 or TGFBR2. *Nat. Genet.* 37, 275–281. doi: 10.1038/ng1511

Loman, N. J., Misra, R. V., Dallman, T. J., Constantinidou, C., Gharbia, S. E., Wain, J., et al. (2012). Performance comparison of benchtop high-throughput sequencing platforms. *Nat. Biotechnol.* 30, 434–439. doi: 10.1038/nbt.2198

Longobardo, L., Jain, R., Carerj, S., Zito, C., and Khandheria, B. K. (2016). Bicuspid aortic valve: unlocking the morphogenetic puzzle. *Am. J. Med.* 129, 796–805. doi: 10.1016/j.amjmed.2016.03.009

Loomis, E. W., Eid, J. S., Peluso, P., Yin, J., Hickey, L., Rank, D., et al. (2013). Sequencing the unsequenceable: expanded CGG-repeat alleles of the fragile X gene. *Genome Res.* 23, 121–128. doi: 10.1101/gr.141705.112

Loscalzo, M. L., Goh, D. L., Loeys, B., Kent, K. C., Spevak, P. J., and Dietz, H. C. (2007). Familial thoracic aortic dilation and bicommissural aortic valve: a prospective analysis of natural history and inheritance. *Am. J. Med. Genet. A* 143A, 1960–1967. doi: 10.1002/ajmg.a.31872

Magi, A., Semeraro, R., Mingrino, A., Giusti, B., and D'Aurizio, R. (2017). Nanopore sequencing data analysis: state of the art, applications and challenges. *Brief. Bioinform.* doi: 10.1093/bib/bbx062. [Epub ahead of print].

Maitra, M., Koenig, S. N., Srivastava, D., and Garg, V. (2010). Identification of GATA6 sequence variants in patients with congenital heart defects. *Pediatr. Res.* 68, 281–285. doi: 10.1203/PDR.0b013e3181ed17e4

Margulies, M., Egholm, M., Altman, W. E., Attiya, S., Bader, J. S., Bemben, L. A., et al. (2005). Genome sequencing in microfabricated high-density picolitre reactors. *Nature* 437, 376–380. doi: 10.1038/nature03959

Martín, M., Lorca, R., Rozado, J., Alvarez-Cabo, R., Calvo, J., Pascual, I., et al. (2017). Bicuspid aortic valve syndrome: a multidisciplinary approach for a complex entity. *J. Thorac. Dis.* 9(Suppl. 6), S454–S464. doi: 10.21037/jtd.2017.05.11

Masri, A., Svensson, L. G., Griffin, B. P., and Desai, M. Y. (2017). Contemporary natural history of bicuspid aortic valve disease: a systematic review. *Heart*. 103, 1323–1330. doi: 10.1136/heartjnl-2016-309916

Mátyás, G., Arnold, E., Carrel, T., Baumgartner, D., Boileau, C., Berger, W., et al. (2006). Identification and *in silico* analyses of novel TGFBR1 and TGFBR2 mutations inMarfan syndrome-related disorders. *Hum. Mutat.* 27, 760–769. doi: 10.1002/humu.20353

McKellar, S. H., Tester, D. J., Yagubyan, M., Majumdar, R., Ackerman, M. J., and Sundt, T. M. III. (2007). Novel NOTCH1 mutations in patients with bicuspid aortic valve disease and thoracic aortic aneurysms. *J. Thorac. Cardiovasc. Surg.* 134, 290–296. doi: 10.1016/j.jtcvs.2007.02.041

Metzker, M. L. (2010). Sequencing technologies-the next generation. *Nat. Rev. Genet.* 11, 31–46. doi: 10.1038/nrg2626

Michelena, H. I., Della Corte, A., Prakash, S. K., Milewicz, D. M., Evangelista, A., and Enriquez-Sarano, M. (2015). Bicuspid aortic valve aortopathy in adults: Incidence, etiology, and clinical significance. *Int. J. Cardiol.* 201, 400–407. doi: 10.1016/j.ijcard.2015.08.106

Michelena, H. I., Khanna, A. D., Mahoney, D., Margaryan, E., Topilsky, Y., Suri, R. M., et al. (2011). Incidence of aortic complications in patients with bicuspid aortic valves. *JAMA* 306, 1104–1112. doi: 10.1001/jama.2011.1286

Michelena, H. I., Prakash, S. K., Della Corte, A., Bissell, M. M., Anavekar, N., Mathieu, P., et al. (2014). BAVCon Investigators. Bicuspid aortic valve: identifying knowledge gaps and rising to the challenge from the International Bicuspid Aortic Valve Consortium(BAVCon). *Circulation* 129, 2691–2704. doi: 10.1161/CIRCULATIONAHA.113.007851

Miller, M. J., Geffner, M. E., Lippe, B. M., Itami, R. M., Kaplan, S. A., DiSessa, T. G., et al. (1983). Echocardiography reveals a high incidence of bicuspid aortic valve in Turner syndrome. *J. Pediatr.* 102, 47–50.

Minoche, A. E., Dohm, J. C., and Himmelbauer, H. (2011). Evaluation of genomic high-throughput sequencing data generated on Illumina HiSeq and genome analyzer systems. *Genome Biol.* 12:R112. doi: 10.1186/gb-2011-12-11-r112

Mohamed, S. A., Aherrahrou, Z., Liptau, H., Erasmi, A. W., Hagemann, C., Wrobel, S., et al. (2006). Novel missense mutations (p.T596M andp.P1797H) in NOTCH1 in patients with bicuspid aortic valve. *Biochem. Biophys. Res. Commun.* 345, 1460–1465. doi: 10.1016/j.bbrc.2006.05.046

Mohamed, S. A., Hanke, T., Schlueter, C., Bullerdiek, J., and Sievers, H. H. (2005). Ubiquitin fusion degradation 1-like gene dysregulation in bicuspid aortic valve. *J. Thorac. Cardiovasc. Surg.* 130, 1531–1536. doi: 10.1016/j.jtcvs.2005.08.017

Nakamura, K., Oshima, T., Morimoto, T., Ikeda, S., Yoshikawa, H., Shiwa, Y., et al. (2011). Sequence-specific error profile of Illumina sequencers. *Nucleic Acids Res.* 39:e90. doi: 10.1093/nar/gkr344

Ng, C. M., Cheng, A., Myers, L. A., Martinez-Murillo, F., Jie, C., Bedja, D., et al. (2004). TGF-beta-dependent pathogenesis of mitral valve prolapse in a mouse model of Marfan syndrome. *J. Clin. Invest.* 114, 1586–1592. doi: 10.1172/JCI200422715

Nigam, V., and Srivastava, D. (2009). Notch1 represses osteogenic pathways in aortic valvecells. *J. Mol. Cell. Cardiol.* 47, 828–834. doi: 10.1016/j.yjmcc.2009.08.008

Nishimura, R. A., Otto, C. M., Bonow, R. O., Carabello, B. A., Erwin, J. P. III., Guyton, R. A., et al. (2014). 2014 AHA/ACC guideline for the management of patients with valvular heart disease: executive summary: a report of the American College of Cardiology/American Heart Association Task Force on Practice Guidelines. *J. Am. Coll. Cardiol.* 63, 2438–2488. doi: 10.1016/j.jacc.2014.02.537

Nistri, S., Basso, C., Marzari, C., Mormino, P., and Thiene, G. (2005). Frequency of bicuspid aortic valve in young male conscripts by echocardiogram. *Am. J. Cardiol.* 96, 718–721. doi: 10.1016/j.amjcard.2005.04.051

Nistri, S., Giusti, B., Pepe, G., and Cademartiri, F. (2016). Another piece in the puzzle of bicuspid aortic valve syndrome. *Eur. Heart J. Cardiovasc. Imaging* 17, 1248–1249. doi: 10.1093/ehjci/jew169

Nistri, S., Grande-Allen, J., Noale, M., Basso, C., Siviero, P., Maggi, S., et al. (2008). Aortic elasticity and size in bicuspid aortic valve syndrome. *Eur Heart J.* 29, 472–479. doi: 10.1093/eurheartj/ehm528

Nistri, S., Porciani, M. C., Attanasio, M., Abbate, R., Gensini, G. F., and Pepe, G. (2012). Association of Marfan syndrome and bicuspid aortic valve: frequency and outcome. *Int. J. Cardiol.* 155, 324–325. doi: 10.1016/j.ijcard.2011.12.009

Padang, R., Bagnall, R. D., Richmond, D. R., Bannon, P. G., and Semsarian, C. (2012). Rare non-synonymous variations in the transcriptional activation domains of GATA5 in bicuspid aortic valve disease. *J. Mol. Cell. Cardiol.* 53, 277–281. doi: 10.1016/j.yjmcc.2012.05.009

Park, P. J. (2009). ChIP-seq: advantages and challenges of a maturing technology. *Nat. Rev. Genet.* 10, 669–680. doi: 10.1038/nrg2641

Patel, N. D., Crawford, T., Magruder, J. T., Alejo, D. E., Hibino, N., Black, J., et al. (2017). Cardiovascular operations for Loeys-Dietz syndrome: intermediate-term results. *J. Thorac. Cardiovasc. Surg.* 153, 406–412. doi: 10.1016/j.jtcvs.2016.10.088

Pepe, G., Nistri, S., Giusti, B., Sticchi, E., Attanasio, M., Porciani, C., et al. (2014). Identification of fibrillin1 gene mutations in patients with bicuspid aortic valve (BAV) without Marfan syndrome. *BMC Med. Genet.* 15:23. doi: 10.1186/1471-2350-15-23

Pereira, L., Andrikopoulos, K., Tian, J., Lee, S. Y., Keene, D. R., Ono, R., et al. (1997). Targetting of the gene encoding fibrillin-1 recapitulates the vascular aspect of Marfan syndrome. *Nat. Genet.* 17, 218–222. doi: 10.1038/ng1097-218

Ponticos, M., Partridge, T., Black, C. M., Abraham, D. J., and Bou-Gharios, G. (2004). Regulation of collagen type I in vascular smooth muscle cells by competition between Nkx2.5 and deltaEF1/ZEB1. *Mol. Cell. Biol.* 24, 6151–6161. doi: 10.1128/MCB.24.14.6151-6161.2004

Prakash, S. K., Bossé, Y., Muehlschlegel, J. D., Michelena, H. I., Limongelli, G., Della Corte, A., et al. (2014). A roadmap to investigate the genetic basis of bicuspid aortic valve and its complications: insights from the International BAVCon (Bicuspid Aortic Valve Consortium). *J. Am. Coll. Cardiol.* 64, 832–839. doi: 10.1016/j.jacc.2014.04.073

Rajagopal, S. K., Ma, Q., Obler, D., Shen, J., Manichaikul, A., Tomita-Mitchell, A., et al. (2007). Spectrum of heart disease associated with murine and human GATA4 mutation. *J. Mol. Cell. Cardiol.* 43, 677–685. doi: 10.1016/j.yjmcc.2007.06.004

Reuter, J. A., Spacek, D. V., and Snyder, M. P. (2015). High-throughput sequencing technologies. *Mol. Cell* 58, 586–597. doi: 10.1016/j.molcel.2015.05.004

Shendure, J., Porreca, G. J., Reppas, N. B., Lin, X., McCutcheon, J. P., Rosenbaum, A. M., et al. (2005). Accurate multiplex polony sequencing of an evolved bacterial genome. *Science* 309, 1728–1732. doi: 10.1126/science.1117389

Shi, L. M., Tao, J. W., Qiu, X. B., Wang, J., Yuan, F., Xu, L., et al. (2014). GATA5 loss-of-function mutations associated with congenital bicuspid aortic valve. *Int. J. Mol. Med.* 33, 1219–1226. doi: 10.3892/ijmm.2014.1700

Tan, H. L., Glen, E., Töpf, A., Hall, D., O'Sullivan, J. J., Sneddon, L., et al. (2012). Non-synonymous variants in the SMAD6 gene predispose to congenital cardiovascular malformation. *Hum. Mutat.* 33, 720–727. doi: 10.1002/humu.22030

Timmerman, L. A., Grego-Bessa, J., Raya, A., Bertrán, E., Pérez-Pomares, J. M., Díez, J., et al. (2004). Notch promotes epithelial-mesenchymal transition during cardiac development and oncogenic transformation. *Genes Dev.* 18, 99–115. doi: 10.1101/gad.276304

van Dijk, E. L., Auger, H., Jaszczyszyn, Y., and Thermes, C. (2014). Ten years of next-generation sequencing technology. *Trends Genet.* 30, 418–426. doi: 10.1016/j.tig.2014.07.001

Verma, S., and Siu, S. C. (2014). Aortic dilatation in patients with bicuspid aortic valve. *N. Engl. J. Med.* 370, 1920–1929. doi: 10.1056/NEJMra1207059

Voelkerding, K. V., Dames, S. A., and Durtschi, J. D. (2009). Next-generation sequencing: from basic research to diagnostics. *Clin. Chem.* 55, 641–658. doi: 10.1373/clinchem.2008.112789

von Gise, A., and Pu, W. T. (2012). Endocardial and epicardial epithelial to mesenchymal transitions in heart development and disease. *Circ. Res.* 110, 1628–1645. doi: 10.1161/CIRCRESAHA.111.259960

Wang, Z., Gerstein, M., and Snyder, M. (2009). RNA-Seq: a revolutionary tool for transcriptomics. *Nat. Rev. Genet.* 10, 57–63. doi: 10.1038/nrg2484

Wei, S., Huang, X., Hu, S., Yang, Y., and Liu, F. (2016). Successful single-stage operation for loeys-dietz syndrome with critical coarctation of the descending aorta in a young adult. *Can. J. Cardiol.* 32, 1260. doi: 10.1016/j.cjca.2015.11.015

Wooderchak-Donahue, W., VanSant-Webb, C., Tvrdik, T., Plant, P., Lewis, T., Stocks, J., et al. (2015). Clinical utility of a next generation sequencing panel assay for Marfan and Marfan-like syndromes featuring aortopathy. *Am. J. Med. Genet. A* 167A, 1747–1757. doi: 10.1002/ajmg.a.37085

Wooten, E. C., Iyer, L. K., Montefusco, M. C., Hedgepeth, A. K., Payne, D. D., Kapur, N. K., et al. (2010). Application of gene network analysis techniques identifies AXIN1/PDIA2 and endoglin haplotypes associated with bicuspid aortic valve. *PLoS ONE* 5:e8830. doi: 10.1371/journal.pone.0008830

Yang, B., Zhou, W., Jiao, J., Nielsen, J. B., Mathis, M. R., and Heydarpour, M. (2017). Protein-altering and regulatory genetic variants near GATA4 implicated in bicuspid aortic valve. *Nat. Commun.* 8:15481. doi: 10.1038/ncomms15481

Conflict of Interest Statement: The authors declare that the research was conducted in the absence of any commercial or financial relationships that could be construed as a potential conflict of interest.

frontiers in Physiology

ORIGINAL RESEARCH
published: 05 September 2017
doi: 10.3389/fphys.2017.00648

MicroRNAs Clustered within the 14q32 Locus Are Associated with Endothelial Damage and Microparticle Secretion in Bicuspid Aortic Valve Disease

Neus Martínez-Micaelo[1], Raúl Beltrán-Debón[1], Gerard Aragonés[1], Marta Faiges[1] and Josep M. Alegret[1,2]**

[1] Grup de Recerca Cardiovascular, Institut d'Investigació Sanitària Pere Virgili, Universitat Rovira i Virgili, Reus, Spain, [2] Servei de Cardiologia, Hospital Universitari de Sant Joan, Universitat Rovira i Virgili, Reus, Spain

OPEN ACCESS

Edited by:
Amalia Forte,
Università degli Studi della Campania "Luigi Vanvitelli" Caserta, Italy

Reviewed by:
Gayathri Krishnamoorthy,
Nutriflour International Inc. LLC, United States
Lars Maegdefessel,
Karolinska Institute (KI), Sweden

***Correspondence:**
Neus Martínez-Micaelo
neus.martinez@urv.cat
Josep M. Alegret
josepmaria.alegret@urv.cat

Specialty section:
This article was submitted to Vascular Physiology, a section of the journal Frontiers in Physiology

Received: *31 March 2017*
Accepted: *16 August 2017*
Published: *05 September 2017*

Citation:
Martínez-Micaelo N, Beltrán-Debón R, Aragonés G, Faiges M and Alegret JM (2017) MicroRNAs Clustered within the 14q32 Locus Are Associated with Endothelial Damage and Microparticle Secretion in Bicuspid Aortic Valve Disease. Front. Physiol. 8:648. doi: 10.3389/fphys.2017.00648

Background: We previously described that PECAM$^+$ circulating endothelial microparticles (EMPs) are elevated in bicuspid aortic valve (BAV) disease as a manifestation of endothelial damage. In this study, we hypothesized that this endothelial damage, is functionally related to the secretion of a specific pattern of EMP-associated miRNAs.

Methods: We used a bioinformatics approach to correlate the PECAM$^+$ EMP levels with the miRNA expression profile in plasma in healthy individuals and BAV patients (n = 36). In addition, using the miRNAs that were significantly associated with PECAM$^+$ EMP levels, we inferred a miRNA co-expression network using a Gaussian graphical modeling approach to identify highly co-expressed miRNAs or miRNA clusters whose expression could functionally regulate endothelial damage.

Results: We identified a co-expression network composed of 131 miRNAs whose circulating expression was significantly associated with PECAM$^+$ EMP levels. Using a topological analysis, we found that miR-494 was the most important hub within the co-expression network. Furthermore, through positional gene enrichment analysis, we identified a cluster of 19 highly co-expressed miRNAs, including miR-494, that was located in the 14q32 locus on chromosome 14 ($p = 1.9 \times 10^{-7}$). We evaluated the putative biological role of this miRNA cluster by determining the biological significance of the genes targeted by the cluster using functional enrichment analysis. We found that this cluster was involved in the regulation of genes with various functions, specifically the "cellular nitrogen compound metabolic process" ($p = 2.34 \times 10^{-145}$), "immune system process" ($p = 2.57 \times 10^{-6}$), and "extracellular matrix organization" ($p = 8.14 \times 10^{-5}$) gene ontology terms and the "TGF-β signaling pathway" KEGG term ($p = 2.59 \times 10^{-8}$).

Conclusions: Using an integrative bioinformatics approach, we identified the circulating miRNA expression profile associated with secreted PECAM$^+$ EMPs in BAV disease. Additionally, we identified a highly co-expressed miRNA cluster that could mediate crucial

biological processes in BAV disease, including the nitrogen signaling pathway, cellular activation, and the transforming growth factor beta signaling pathway. In conclusion, EMP-associated and co-expressed miRNAs could act as molecular effectors of the intercellular communication carried out by EMPs in response to endothelial damage.

Keywords: microRNA, bicuspid aortic valve, aortic dilation, circulating endothelial microparticles, bioinformatics, endothelial damage, co-expression network

INTRODUCTION

Bicuspid aortic valve (BAV), the most common cardiac congenital malformation (occurs in 1–2% of the population), is associated with valve dysfunction and is a risk factor for aortopathy (Tzemos et al., 2008; Alegret et al., 2013). The progressive dilation of the aorta, if untreated, can lead to fatal consequences such as aortic dissection and/or rupture. The mechanisms that underlie aortic dilatation have been a matter of debate for years (Padang et al., 2013); the proposed causes include anomalous flow in the ascending aorta generated by the anomalous dynamics of BAV (Kim et al., 2012; Bissell et al., 2013) and genetic causes responsible for the anomalous structure of the aortic media (Biner et al., 2009; Pepe et al., 2014).

In a previous study, we reported that circulating endothelial microparticles (EMPs) are elevated in BAV patients and related to aortic dilation (Alegret et al., 2016). Circulating EMPs are a type of extracellular microvesicle (100–1,000 nm) that bud directly from the plasma membranes of endothelial cells upon activation, injury, or apoptosis and that are involved in intercellular communication. Specifically, we identified $PECAM^+$ EMPs, which are a kind of EMP that express CD31 and are released in endothelial damage, as those related to BAV disease.

Micro-ribonucleic acids (miRNAs) are endogenously expressed, 19- to 23-nt-long noncoding RNAs that regulate gene expression at the post-transcriptional level, mostly via imperfect base-pairing interactions that occur preferentially within the 3′ untranslated regions (UTRs) of target mRNAs. MiRNA genes are distributed across diverse genomic locations, and although some miRNAs are isolated, ∼50% are found in clusters transcribed as polycistronic miRNA transcripts (Mourelatos et al., 2002). MiRNAs are considered potent post-transcriptional regulators because each miRNA has multiple to several 100 target genes; therefore, inhibition of a single miRNA can lead to the activation of multifactorial physiological processes. In addition to functioning intracellularly, miRNAs can be exported or released by cells into the circulating blood in very stable forms. Microparticles are reportedly the major carriers of miRNAs in the blood (Diehl et al., 2012). MiRNA signatures have been proposed as potentials with the potential to improve disease diagnosis and prognosis in clinical practice and have been identified as useful biomarkers for a wide range of cardiovascular diseases. For example, in a previous study, we proposed miR-122, miR-130a, miR-486, and miR-718 as molecular features associated with BAV and aortic dilation (Martínez-Micaelo et al., 2017).

Currently, there are no effective strategies to prevent the progression of BAV disease, including the aortic dilation, and the development of new strategies requires more detailed understanding of the molecular mechanisms associated with BAV and progressive dilation of the aorta. Therefore, in this study, we hypothesized that changes in blood flow in the ascending aorta caused by the bicuspid morphology of the aortic valve would induce endothelial damage, resulting in the secretion of a specific signature of EMP-associated miRNAs. We used a bioinformatics approach to integrate the $PECAM^+$ EMP levels with the miRNA expression profile in plasma of healthy individuals and BAV patients. In addition, from the miRNAs that were significantly associated with $PECAM^+$ EMP levels, we inferred a miRNA co-expression network using a Gaussian graphical modeling approach.

METHODS

Study Population

The patients included in this study belonged to a cohort of BAV patients who were prospectively included and followed-up in our facilities. Upon enrolment, the participants were informed and prospectively entered into a specific database, underwent a blood draw and provided informed written consent. The samples were stored in our biological samples bank (Biobanc IISPV—HUSJR) until they were needed. A BAV diagnosis was made when two aortic leaflets were clearly visualized, with or without a raphe, in the parasternal short-axis view of a transthoracic echocardiogram (Alegret et al., 2005), on a transesophageal echocardiogram (Alegret et al., 2005), or on a cardiac magnetic resonance image (Gleeson et al., 2008). Explorations were performed or supervised by the same observer (JMA). Our database and biobank also included a group of healthy tricuspid aortic valve (TAV) controls. This study was approved by the Institutional Review Board (the Clinical Ethics Committee) of our institution.

This study was designed in two evaluations in which EMP levels and the miRNA expression profile were determined in two independent cohorts of TAV individuals and BAV patients with or without aortic dilation ($n = 60$). In the first evaluation, plasma from the patients diagnosed with BAV, with or without aortic dilation, and healthy TAV control subjects ($n = 24$) was used to determine the levels of EMPs and the miRNA profile using microarrays. To improve the study's power, for this stage, we selected groups composed of patients with characteristics that were extremely homogeneous (Supplementary Table 1) to exclude possible confounding factors, such as age, sex, or BMI. We included subjects in whom high levels of circulating $PECAM^+$ EMPs were expected, the BAV patients, and subjects in whom low levels of $PECAM^+$ EMPs were expected, the healthy TAV controls, to study miRNAs whose expression levels could be related to $PECAM^+$ EMPs. Patients diagnosed with cardiovascular diseases, Marfan syndrome, aortic stenosis, hypertension, or diabetes mellitus or who were receiving

pharmacologic treatment (including statins, ACE/ARII, and/or β-blockers) were excluded. In the second evaluation, the EMP-associated miRNA candidates were validated by RT-qPCR in a new cohort ($n = 36$) of TAV healthy controls and BAV patients with or without aortic dilation (Supplementary Table 2).

Blood Sampling

Blood samples were collected under overnight fasting conditions and were processed within 90 min after collection. The samples were centrifuged at 1,500 g for 15 min to obtain plasma, which was further centrifuged at 4,000 g for 10 min to obtain platelet-poor plasma. The plasmas were stored at −80°C in our biological samples bank (Biobanc IISPV—HUSJR) until they were needed.

Determination of Circulating Levels of EMPs

The circulating PECAM$^+$ EMP levels were determined in the same cohorts used for the microarray and RT-qPCR validation analyses that were previously phenotyped (Alegret et al., 2016), but for this study, individuals were selected to maximize the power of the miRNA analysis. The levels of EMPs were characterized based on the presence of endothelial-specific surface antigens, the composition of which depends on the cellular origin of the microparticles and the generating process (Jimenez et al., 2003). In our previous study (Alegret et al., 2016), we determined that the presence of CD31 (PECAM) is a marker that can discriminate between microparticles released from endothelial cells subjected to endothelial damage produced by haemodynamic causes due to the anomalous aortic flow associated with BAV and microparticles released by other triggering stimuli, including cell activation or apoptosis, in TAV and BAV patients. The concentration of circulating PECAM$^+$ EMPs was determined on an EPICS-XL (Beckman Coulter) flow cytometer at a low rate setting and a 30 s stop time. The Nano Fluorescent Particle Size Standard Kit (Spherotech) was used for instrument standardization, and Flow-Count fluorospheres (Beckman Coulter) were added as an internal calibrator to calculate microparticle amounts.

Plasma EMPs were labeled by incubating 50 μl of platelet-poor plasma with the corresponding antibody, anti-CD31-PE (Beckman Coulter), anti-CD42b-FITC (Beckman Coulter), or anti-CD45-PE (Beckman Coulter), at room temperature in the dark for 20 min as previously described (Ci et al., 2013). Then, 500 μl of PBS was subsequently added, and the EMP levels were determined as previously described (Jimenez et al., 2003; Sutherland et al., 2010; Ci et al., 2013). EMPs were defined as particles >0.1 and <1 μm in size, and their endothelial origin was identified based on their affinity to specific cell surface antigens, namely, CD31 and CD42b. To evaluate the extent of possible contamination with leukocyte-derived microparticles, the circulating levels of CD31$^+$CD45$^+$ microparticles were determined in all samples. We found that <4.5% of CD31$^+$ microparticles co-expressed CD45$^+$; this result is consistent with previous reports by other authors (Amabile et al., 2005; Pirro et al., 2006). EMP levels were measured by trained technicians who were blind to the clinical status of the patients as well as to the results.

RNA Isolation and Preparation of miRNA Microarrays

Total RNA was extracted from 250 μl of plasma using TRIzol reagent according to the manufacturer's instructions (Invitrogen) and purified using an RNeasy minikit (Qiagen). To increase RNA recovery, 1 μg of MS2 carrier RNA was added to each plasma sample. The quality of total isolated RNA was determined using the Agilent 2100 Bioanalyzer.

The plasma miRNA expression levels were assessed using Sure Print G3 human 8 × 60 k miRNA microarrays (Agilent Technologies) covering 1,205 human miRNAs (Sanger miRBase release 16). The miRNAs were dephosphorylated and labeled with cyanine 3-cytidine biphosphate including a labeling spike-in solution (Agilent Technologies) to assess labeling efficiency. The samples were hybridized on the arrays with the inclusion of a hybridization spike-in solution (Agilent Technologies) to monitor hybridization efficiency. The arrays were scanned with a G2565CA Microarray Scanner System with SureScan High-Resolution Technology (Agilent Technologies) using Scan Control software. The Feature Extraction 11.5.11 (Agilent Technologies) and GeneSpring 12.6.1. software packages were used for data processing.

Analysis of miRNA Microarray Expression Data and Integrative Analysis and Gene Co-expression Network

The data from microarrays (deposited at Gene Expression Omnibus under GEO Series accession number GSE101616) were normalized using the robust multi-array average (RMA) method (Irizarry et al., 2003) implemented in the AgiMicroRna Bioconductor package, and the fold changes in circulating miRNAs were determined using the linear model implemented in the limma Bioconductor package (Ritchie et al., 2015). The Benjamini and Hochberg methods were used to adjust p-values for multiple testing and to control the false discovery rate (Benjamini and Hochberg, 1995). The miRNA co-expression network was constructed from the expression profiles of those miRNAs whose expression was significantly associated with PECAM$^+$ EMPs (Spearman $p < 0.05$). The co-expression network was inferred using graphical Gaussian models (GGMs) implemented in the R package GeneNet (Schäfer and Strimmer, 2005). Briefly, a partial-correlation matrix was estimated by computing the partial correlation between the expression profiles of each miRNA pair. Bayesian posterior edge probability >0.95 (corresponding to a local false discovery rate of <5%) was used to determine the significance of the resulting pairwise partial correlations. In the resulting co-expression network, which was visualized using Cytoscape software (Cline et al., 2007), the nodes represent the set of miRNAs that were significantly correlated with PECAM$^+$ EMP levels, and the edges link the pairs of miRNAs whose expression was not conditionally independent, defined as the pairwise partial correlation once the common effects of the other miRNAs in the subset were removed (Opgen-Rhein and Strimmer, 2007).

MiRNA Quantification by Real-Time qRT-PCR

TaqMan microRNA assays (Applied Biosystems) were used to quantify the expression of selected miRNAs. Briefly, reverse transcription was performed using the TaqMan MicroRNA Reverse Transcription Kit (Applied Biosystems) and the miRNA-specific oligonucleotides provided with the TaqMan MicroRNA Assay (Applied Biosystems). The final concentration of total RNA used was 2.5 ng/μL. The reaction was performed at 16°C for 30 min, 42°C for 30 min, and 85°C for 5 min. We used 1.33 μL of the obtained cDNAs in a subsequent quantitative qRT-PCR amplification using the TaqMan Universal PCR master mix (Applied Biosystems, Madrid, Spain) and the associated specific probe provided in the TaqMan® MicroRNA Assay Kit (Applied Biosystems). Specific TaqMan probes were used for each gene: let-7d (hsa-let-7d-5p), let-7g (hsa-let-7g-5p), miR-122 (hsa-mir-122-5p), miR-130a (hsa-mir-130a-3p), miR-337 (hsa-mir-337-5p), miR-409 (hsa-mir-409-3p), miR-486 (hsa-mir-486-5p), miR-494 (hsa-mir-494), and miR-718 (hsa-mir-718). The results were normalized to the expression of the U6 small nuclear RNA (U6 snRNA), which was used as an endogenous control. Amplification was performed in a 7900HT thermocycler (Applied Biosystems) at 95°C for 10 min, followed by 40 cycles of 95°C for 15 s and 60°C for 1 min. The fold change in the miRNA level was calculated by the log 2 scale according to the equation $2^{-\Delta\Delta Ct}$, where ΔCt = Ct miRNA-Ct U6 and $\Delta\Delta Ct$ = ΔCt treated samples-ΔCt untreated controls. Negative control reactions, with no RNA, had undetectable quantification cycle values (C_q).

Genomic Region Overrepresentation Analysis

The genetic loci visualization of co-expressed miRNAs across chromosomes was performed using PhenoGram (Wolfe et al., 2013). To determine the significance of the overrepresentation of chromosome regions in the generated co-expressed miRNA set, we applied a hypergeometric test.

Target Prediction and Functional Pathway Analysis

Putative miRNA target sites for the miRNA candidates were identified by bioinformatics analysis using miRNA target prediction databases, including DIANA-microT-CDS (Paraskevopoulou et al., 2013), DIANA-TarBase v7.0 (Vlachos et al., 2015a), and TargetScan v6.2 (Agarwal et al., 2015). Functional enrichment analysis of miRNA target genes was conducted using miRPath v3.0 (Vlachos et al., 2015b). Visualization and topological analysis of the network was done using R and Cytoscape software.

Statistical Analysis

Because of the right-skewed distribution of the values, the $PECAM^+$ EMP plasma levels underwent a natural logarithmic transformation and were expressed as log-transformed counts per μl (log $PECAM^+$ EMPs/μl). EMP levels are presented as the mean ± SEM. Chi-squared tests, or Fisher exact tests when appropriate, were used to compare the frequencies of the categorical variables. The effects of valve morphology and aortic root dilation were assessed using ANOVA. Tukey's test was utilized for pairwise comparisons. $p < 0.05$ were considered significant. The statistical analysis was performed using SPSS software, version 21.0 (IBM, Chicago, IL, USA).

RESULTS

Identification of Circulating miRNA Sets Associated with $PECAM^+$ EMP Levels

To explore the circulating $PECAM^+$ EMP-associated miRNAs, we first corroborated our previously reported finding that BAV patients have increased levels of $PECAM^+$ EMPs in plasma compared with TAV healthy controls (Supplementary Figure 1A). Furthermore, the results of this analysis also supported the role of $PECAM^+$ EMP circulating levels as a biomarker of aortic dilation in BAV disease, as an increased diameter of the aortic root or ascending aorta was associated with higher levels of $PECAM^+$ EMPs (Supplementary Figure 1B).

We used a microarray-based screening approach to determine the miRNA expression pattern that could be related to endothelial damage. The expression of 1,205 miRNAs were evaluated in plasma samples from BAV patients and TAV healthy controls, and after the miRNA microarray expression data were processed, 277 miRNAs were identified as expressed in at least 5% of the samples. We prioritized the potential miRNA candidates based on the linear relationship between $PECAM^+$ EMP circulating levels and the miRNA expression (Supplementary Figure 1C), and based on this analysis, we found that the expression of 175 miRNAs was significantly associated with the circulating levels of $PECAM^+$ EMPs ($p < 0.05$).

Construction of a miRNA Co-expression Network Based on the EMP-Associated miRNAs

Once we identified the 175 miRNAs whose expression patterns in plasma significantly correlated with the levels of $PECAM^+$ EMPs, we took into consideration that about half of all described miRNAs are co-expressed in clusters of miRNAs. For this reason, we used a Gaussian graphical model approach to map the simultaneous expression of miRNA pairs into a co-expression network.

The resulting miRNA co-expression network is composed of a single connected component formed by 131 miRNAs (FDR<5%) linked by 391 edges (**Figure 1A**). We first evaluated the biological implications of these co-expressed miRNAs in terms of intercellular communication in BAV-induced endothelial damage (e.g., whether they are expressed in endothelial cells and whether their expression levels have been previously associated with cardiovascular diseases; **Figure 1B**). More interestingly, we also focused on miRNAs that were described in previous studies as related to BAV or whose expression might be sensitive to blood flow. We found in the literature that 98 of the 131 co-expressed miRNAs were previously reported as expressed in

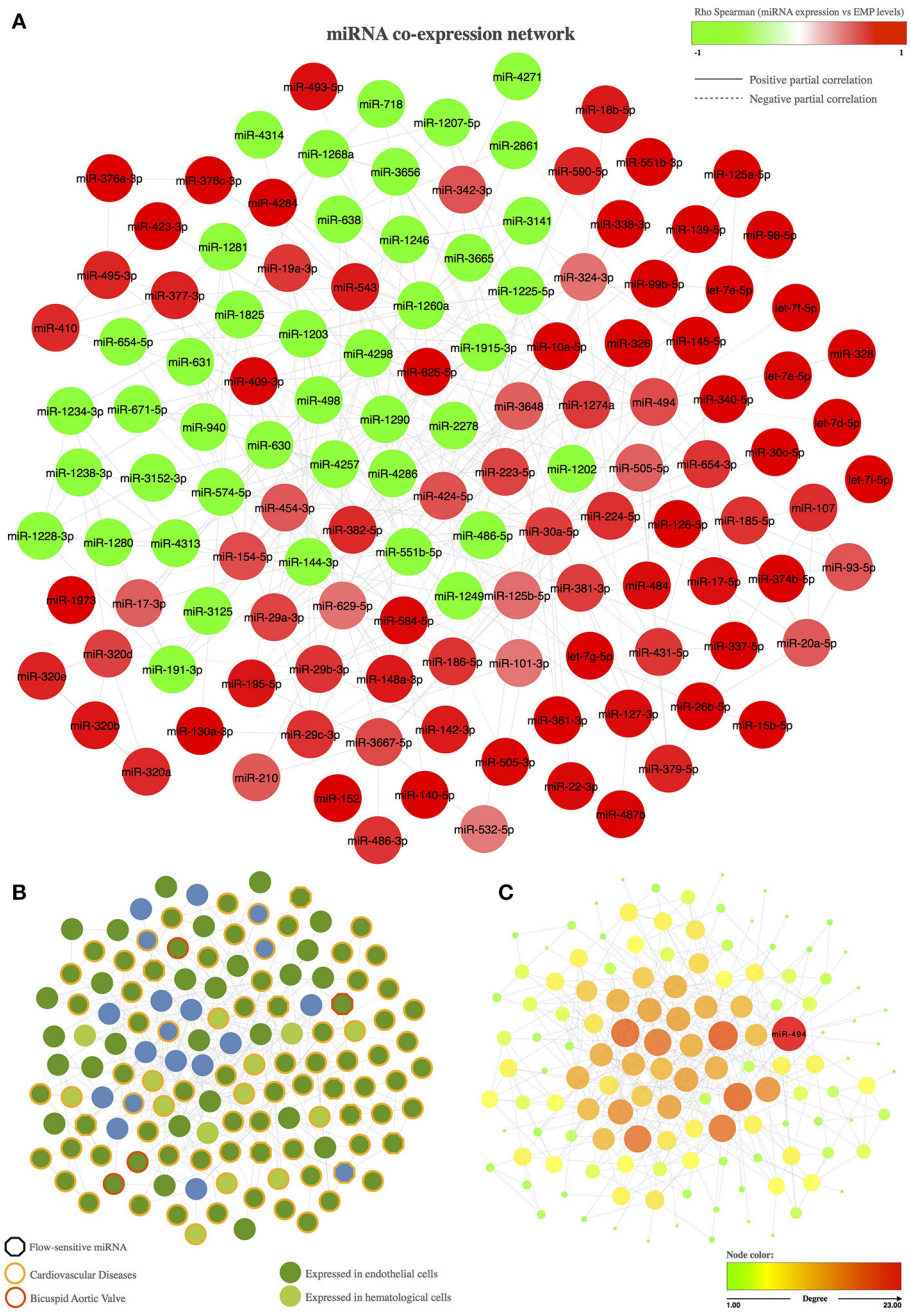

FIGURE 1 | Co-expression network of miRNAs associated with the circulating levels of EMPs. **(A)** Representation of the miRNA co-expression network. The node color represents the Spearman correlation between the expression of the corresponding miRNA and PECAM+ EMP levels; red nodes correspond to miRNAs that are positively correlated with PECAM+ EMPs, and green nodes correspond to miRNAs that are negatively correlated with PECAM+ EMPs. The edge shape is related to the direction of the partial correlation; the continuous lines represent partial positive correlations, and dotted lines refer to partial negative correlation. **(B)** Biological implications of the miRNAs included in the co-expression network based on previous knowledge. The border color of the node represent miRNAs involved in cardiovascular diseases or in bicuspid aortic valve. The hexagon node shape corresponds to flow-sensitive miRNAs. The node color represents miRNA expression in endothelial or hematological cells. **(C)** Topological analysis of the miRNA co-expression network. miR-494 was identified as the master switch based on its role as the most important hub in the co-expression network. The color and the size of the node refer the topological importance of the miRNA within the network. Node positions are conserved between networks.

endothelial cells. Moreover, 88 miRNAs included in the co-expression network had been related to cardiovascular disease. More specifically, modulation of the expression of 4 of them had been associated with BAV, and 9 miRNAs had been described as blood flow sensitive. We also carried out a topological analysis of the network and identified miR-494 as the most important

hub within the co-expression network, that is, the miRNA with the largest degree; the highest betweenness, stress, and closeness scores; and the highest radiality coefficient (**Figure 1C**).

To further validate the results obtained in the microarray analysis and the EMP-miRNA correlations, we determined the expression of 7 of miRNAs included in the miRNA co-expression network (let-7d, let-7g, miR-130a, miR-337, miR-409, miR-494, and miR-718; **Figure 2**) by RT-qPCR in a new cohort of TAV individuals and BAV patients ($n = 36$). In this way, by correlating the RT-qPCR-determined expression data for each of the selected miRNAs with the circulating levels of $PECAM^+$ EMPs, we validated and reaffirmed the sensitivity and power of our bioinformatics approach for the identification and selection of $PECAM^+$ EMP-associated miRNA candidates.

Genomic Region Enrichment Analysis for the miRNA Co-expression Network

Because co-expressed miRNA pairs tend to reside in close genomic proximity, we performed a positional gene enrichment analysis to identify chromosome regions that were overrepresented among the $PECAM^+$ EMPs-associated and co-expressed miRNAs.

We constructed chromosome ideograms to map the genomic locus of each of the miRNAs included in the co-expression network (**Figure 3A**). We found that 21 of the 131 $PECAM^+$ EMP-associated co-expressed miRNAs were located on chromosome 14 and that 19 of them were located in the same chromosome region, the 14q32 locus. We confirmed the statistical significance of this 14q32 genomic region overrepresentation using a hypergeometric test ($p = 1.90 \times 10^{-7}$). This genomic location consists of the miRNA clusters A and B and is also known as the *Dlk1-Dio3* miRNA cluster. Specifically, we identified 4 of the 8 miRNAs located within miRNA cluster A (miR-127-3p, miR-337-3p, miR-431-5p, and miR-493-5p) and 15 of the 42 miRNAs located within miRNA cluster B (miR-154-5p, miR-376a-3p, miR-376c-3p, miR-377-3p, miR-379-5p, miR-381-3p, miR-382-5p, miR-409-3p, miR-410, miR-487b, miR-494, miR-495-3p, miR-543, miR-654-3p, and miR-654-5p; **Figures 3B–C**).

Functional Analysis of the 14q32 miRNA Cluster

To gain deeper insight into the biological significance of these findings, we determined the biological significance of the regulation of the 14q32 miRNA cluster based on the functional implications of the genes targeted by the selected miRNAs. We carried out a functional enrichment analysis of the set of genes putatively targeted by the 19 EMP-related miRNAs located in the 14q32 cluster. Interestingly, this functional analysis revealed that the genes targeted by the 14q32 co-expressed miRNAs were categorized with the "cellular nitrogen compound metabolic process" ($p = 2.34 \times 10^{-145}$), "immune system process" ($p = 2.57 \times 10^{-6}$), and "extracellular matrix organization" ($p = 8.14 \times 10^{-5}$) GO terms as well as the "TGF-β signaling pathway" ($p = 2.59 \times 10^{-8}$) KEGG term, among others (**Figure 4**).

DISCUSSION

Using a bioinformatics approach, our study reported that the endothelial damage observed in BAV disease results in the differential regulation of a post-transcriptional regulatory miRNA network associated with the increased release of endothelial-derived microparticles. By determining the circulating miRNAs associated with $PECAM^+$ EMP levels, we inferred a miRNA co-expression network. Furthermore, based on the results of genomic enrichment analysis, we focused on a cluster of highly co-expressed miRNAs located at the 14q32 locus on chromosome 14 that could be acting as molecular effectors in BAV-related pathophysiological processes, including endothelial damage. We showed that the miRNAs contained within the 14q32 miRNA cluster could mediate crucial biological processes in BAV disease, such as nitric oxide biosynthesis, immune activation, reorganization of the extracellular matrix and TGF-β signaling.

Bicuspid morphology of the aortic valve is associated with haemodynamic abnormalities that result in increased wall shear stress on the endothelial layer, which contributes to dilation of the ascending aorta (Braverman et al., 2005). At the cellular level, this disturbed blood flow is associated with rearrangement of the extracellular matrix and with endothelial damage and dysfunction (Davignon and Ganz, 2004). Furthermore, in our previous studies, we demonstrated that BAV and dilation of the aorta are associated with endothelial-mediated release of microparticles (Alegret et al., 2016). Thereby, when designing this study, we hypothesized that the characteristics of blood flow through the ascending aorta in patients with BAV disease are related to aortic endothelial damage and play key a role in EMP generation.

It is important to consider that on the one hand, circulating miRNAs take very stable forms, mainly packaged in transport particles; circulating microparticles have been reported as the major carriers of miRNAs in the blood (Diehl et al., 2012). On the other hand, although most published studies have focused mainly on differences in the expression of single miRNAs instead of studying miRNA co-expression networks, miRNAs are significantly enriched in clusters in discrete genomic regions (Lau, 2001; Kim and Nam, 2006), and miRNAs in the same cluster might be transcribed in a polycistronic manner (Baskerville, 2005; Wang et al., 2016) and likely regulate functionally related genes (Kim et al., 2009; Wang et al., 2011). We considered the determination and analysis of the miRNA co-expression network resulting from the integration of $PECAM^+$ EMP levels with the expression of circulating miRNAs as an advantageous strategy to unravel the molecular mechanisms underlying the pathophysiological processes in BAV disease for the following reasons: changes in haemodynamic forces in the vascular system might alter the expression of miRNAs in endothelial cells (Marin et al., 2013); BAV promotes endothelial dysfunction, which results in the release of $PECAM^+$ EMPs in plasma; microparticles are the main carriers of miRNAs in plasma; and miRNA-coding genes are enriched in discrete genomic regions.

Using a bioinformatics approach, we identified 175 miRNAs that were significantly associated with $PECAM^+$ EMP levels.

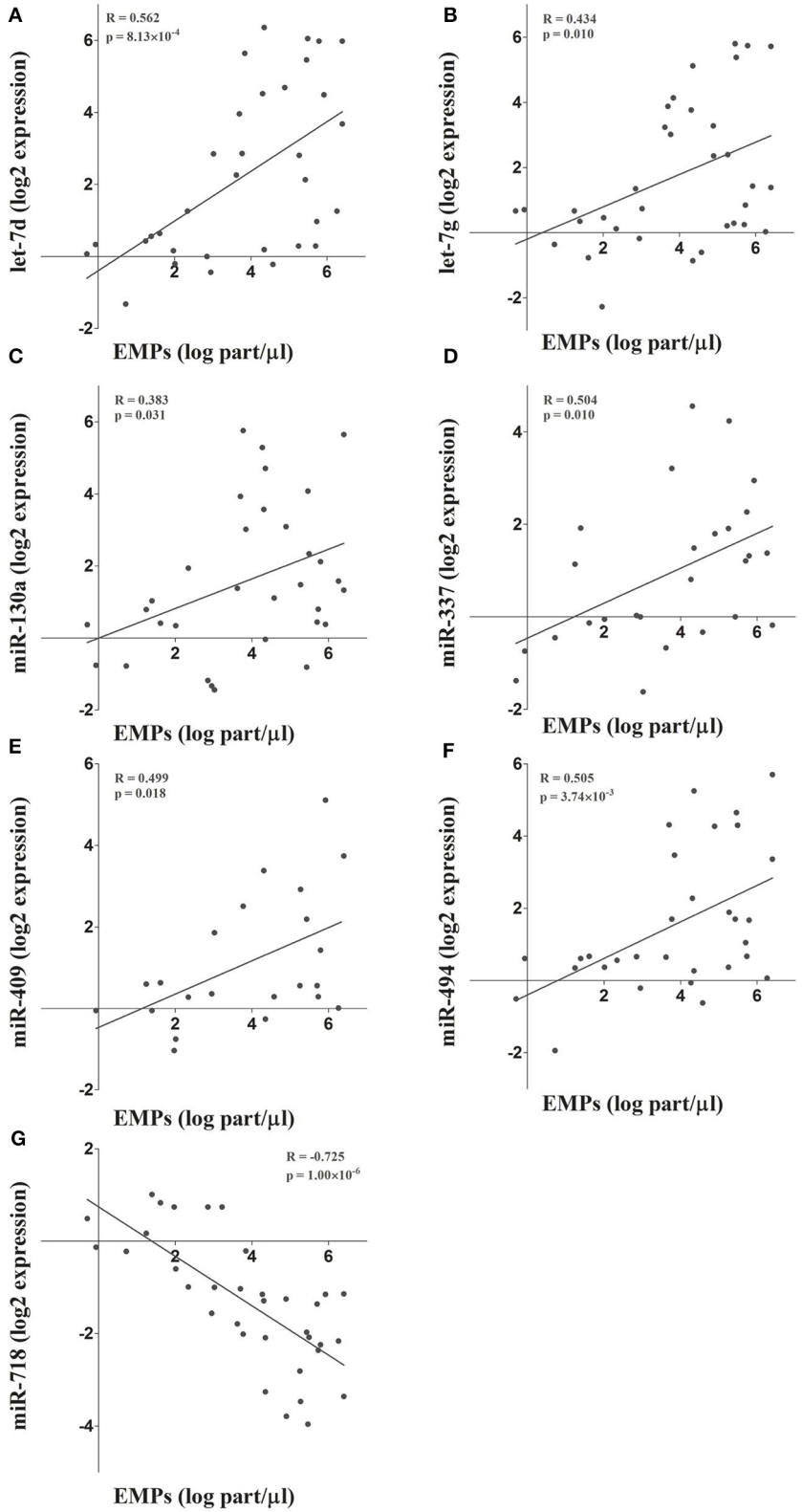

FIGURE 2 | (A-G) The microarray results and the integrative analysis were further validated by determining the expression of 7 miRNAs included in the co-expression network. The expression of these miRNAs was determined by RT-qPCR and correlated with circulating PECAM+ EMP levels.

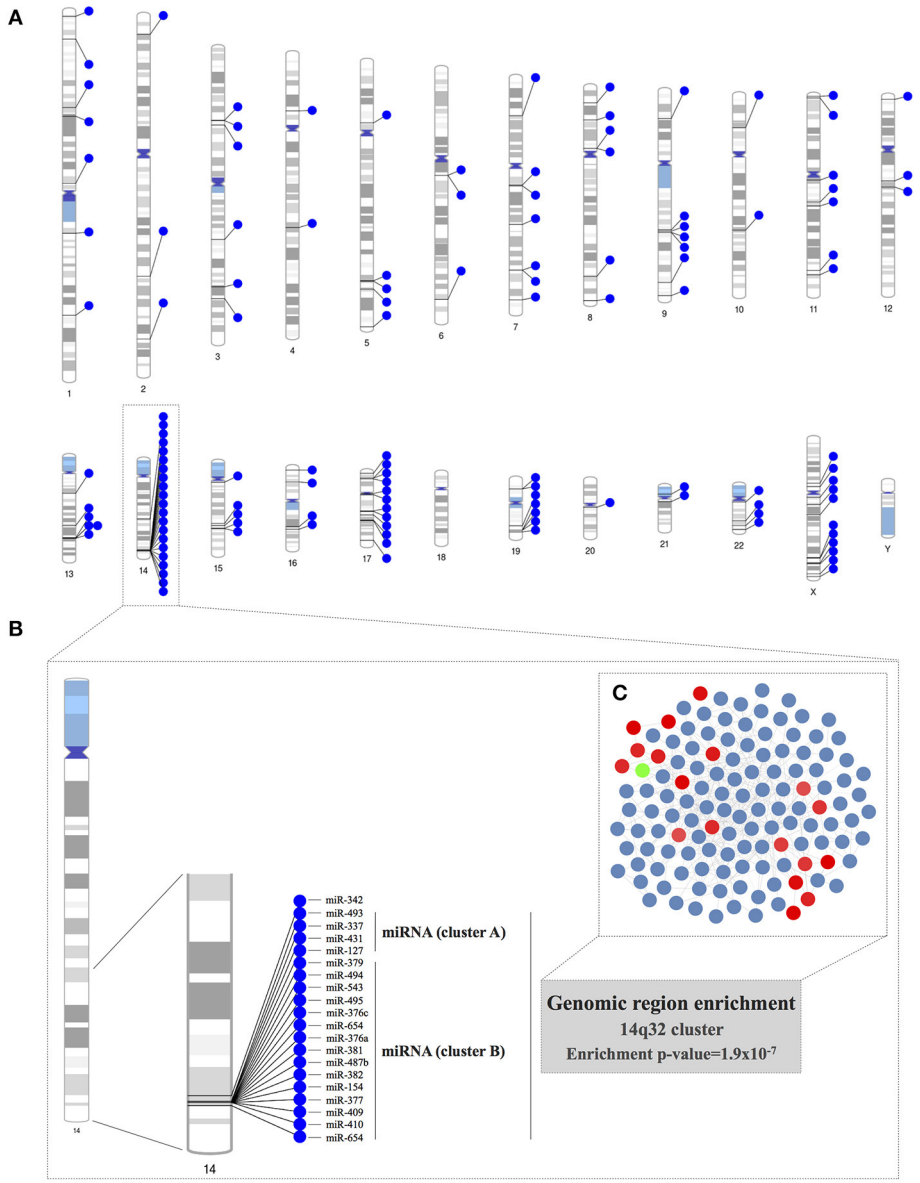

FIGURE 3 | Genomic region enrichment analysis of the miRNA co-expression network. **(A)** The locus of each of the miRNAs included in the co-expression network was mapped in the chromosome ideograms to visualize the genomic loci of co-expressed miRNAs. **(B)** Detailed genomic localization of the co-expressed miRNAs located on chromosome 14. The genomic region overrepresentation was corroborated by the results of a hypergeometric test ($p = 1.9 \times 10^{-7}$). **(C)** The miRNAs located in the 14q32 locus are highlighted within the miRNA co-expression network.

Of these miRNAs, 131 exhibited significant pairwise partial correlations and were inferred into a co-expression network to analyse miRNA co-expression patterns. Co-expression network analysis is considered a powerful method to extract strong regulatory associations that could be responsible for modulating transcriptional networks underlying biological processes. Accordingly, we first analyzed previous knowledge regarding the biological implications of the inferred network and found that 75% of the co-expressed miRNAs had been previously described as miRNAs expressed in endothelial cells and that 67% of them had been associated with cardiovascular diseases. We also analyzed the topology of the co-expression network and found that miR-494 was the most important hub of the network because it was the most highly connected miRNA. miR-494 was also the most influential miRNA within the network based on centrality parameters, which showed that miR-494 was most often found on the shortest path between two other miRNAs. These results indicate that miR-494 might have a large regulatory impact on the biological functions that could be modulated by the co-expression network.

We further analyzed the miRNA co-expression network in terms of enrichment for specific genomic locations, and we

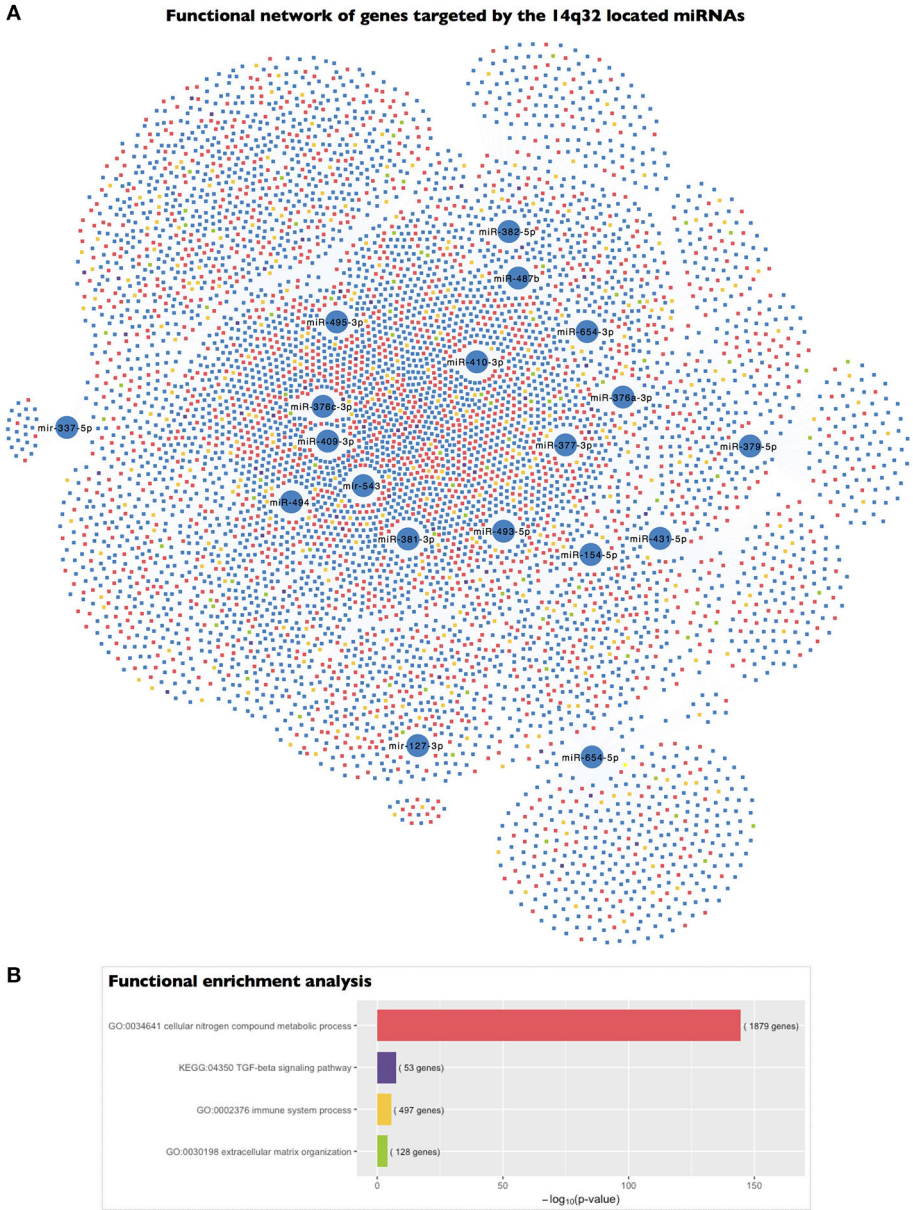

FIGURE 4 | Functional enrichment analysis of the genes targeted by the 14q32 miRNAs represented in the miRNA co-expression analysis. **(A)** A network representing the genes targeted by each of the miRNAs included in the miRNA co-expression network and located within the 14q32 locus and their association with the highlighted biological process gene ontologies. **(B)** The significance of the functional enrichment analysis of the genes targeted by the 14q32-located miRNAs.

found that the 14q32 locus on chromosome 14 was significantly overrepresented as a highly co-expressed miRNA cluster for the PECAM^{+} EMP-associated and co-expressed miRNAs in BAV. This genomic region contains the largest miRNA cluster found in the human genome (Benetatos et al., 2013). Specifically, we found that 19 of the 131 miRNAs inferred in the co-expression network, including miR-494, are located within this chromosome region. This 14q32 miRNA cluster is also known as the imprinted *DLK1-MEG3* genomic region. This region contains the protein-coding genes *DLK1*, *RTL1*, and *DIO3*, which are expressed from the paternally inherited chromosome. The region also contains multiple long and short non-protein coding RNAs, including *MEG3*, *MEG8*, the miRNA cluster and small nucleolar RNA (snoRNA) genes, which are expressed from the maternally inherited chromosome. The imprinting of a genomic region refers to biased expression of the genes contained in either the paternally or maternally inherited chromosome instead of the more common biallelic expression. Although, miRNAs located within the 14q32 region have been proposed as candidates for various diseases, including cancer, psychiatric illness, alcoholism, and non-alcoholic fatty liver disease, to date, there is no published data relating the 14q32 miRNA cluster with

cardiovascular diseases (Benetatos et al., 2013; Okamoto et al., 2016).

Based on the functional enrichment of the genes targeted by the PECAM$^+$ EMP-associated and co-expressed miRNAs located within the 14q32 locus, we could determine the biological significance of the regulation of this miRNA cluster. We found that the genes targeted by the 14q32 co-expressed miRNAs are strongly involved in the regulation of genes in categories such as "cellular nitrogen compound metabolic process," "immune system process," "extracellular matrix organization," and "TGF-β signaling pathway." The "cellular nitrogen compound metabolic process" gene ontology term includes the "nitric oxide biosynthetic pathway" subcategory. Nitric oxide (NO) is a pivotal endothelium-derived substance that plays a crucial role in the homeostasis of the cardiovascular system by modulating endothelium-dependent vasodilation; in fact, impairment of NO production or activity has been proposed as a major mechanism of endothelial dysfunction (Davignon and Ganz, 2004). Moreover, modulation of the expression and activity of endothelial nitric oxide synthase (eNOS), the specific enzyme that produces NO in endothelial cells, by fluid shear stress and the implication of this modulation in the development of BAV are well established (Ranjan et al., 1995; Aicher et al., 2007; Vion et al., 2013). Thus, in the context of BAV, the valvulopathy and the associated abnormal haemodynamics are related to the altered distribution of aortic wall shear stress, which promotes regional disruption of the eNOS pathway in a manner that is primarily mediated by the differential expression and activity of eNOS. Endothelial cells release EMPs in response to cellular stress and cell activation (Dignat-George and Boulanger, 2011). Consistent with this fact and the role of PECAM$^+$ EMP-related and co-expressed miRNAs in the regulation of endothelial dysfunction, we found that among the genes targeted by the 14q32-located miRNAs, those with functional implications related to modulation of immune system processes and to extracellular matrix organization were significantly enriched. In fact, interactions between inflammatory activation and endothelial dysfunction have been previously described in patients with BAV (Ali et al., 2014). In addition, we also found that the 14q32-located miRNAs present in our co-expression network targeted genes that were related to the TGF-β signaling pathway. The TGF-β family is composed of several cytokines with diverse functions, including the regulation of tissue repair and fibrosis, extracellular matrix remodeling, and inflammation as well as cell proliferation and migration (Bobik, 2006). Previous studies have implicated the impairment of TGF-β signaling in BAV pathology and the development of BAV-associated aortopathy (Forte et al., 2016). Additionally, functional interactions between TGF-β and NO have been demonstrated in endothelial cells (Saura et al., 2005). All these data suggest that the 14q32 miRNA cluster may play a pivotal role in the induction of BAV-associated endothelial damage.

Furthermore, in addition to studying the post-transcriptional implications of the regulatory functions of the 14q32 miRNA cluster, we thought it would be interesting to understand the regulatory mechanisms that could affect the activation or repression of the expression of this miRNA cluster. The imprinted status of the maternally expressed RNAs of the *DLK1-MEG3* locus, including the 14q32 miRNA cluster, is regulated by epigenetic mechanisms, specifically by the methylation of two differentially methylated regions (DMRs) located upstream of the transcription activation site of *MEG3* (Murphy et al., 2003; Kameswaran et al., 2014). The hypermethylation of either of these two DMRs has been associated with decreased expression of the maternal transcript (Kagami et al., 2010). In various models, such as in human type 2 diabetic islets, repression of the 14q32 miRNA cluster is strongly correlated with hypermethylation of the *MEG3*-DMR, and modifications at this region increase susceptibility to disease (Kameswaran et al., 2014). Interestingly, Boon et al. (2016) proposed that aging induces the expression of *MEG3* and that *MEG3*-mediated changes in the epigenetic regulation of gene expression contributes to aging-related endothelial dysfunction. Moreover, Gordon et al. (2010) suggested that *MEG3* may regulate the expression of *VEGF*; they showed that loss of *MEG3* leads to up-regulation of the expression of genes in the VEGF and Notch signaling pathways in mouse brains. Furthermore, DNA methylation mechanisms are responsive to disturbed flow (Dunn et al., 2014); in fact, endothelial gene expression can be regulated by flow-dependent epigenetic mechanisms (Jiang et al., 2015). Therefore, the disturbed flow associated with BAV may promote not only the secretion of EMPs but also the *MEG3*-mediated epigenetic regulation of the 14q32 miRNA cluster and thus may play a key role in the regulation of endothelial damage in BAV disease. On the other hand, DLK1 is the best-studied non-canonical Notch ligand and acts as an inhibitor of Notch signaling *in vitro* (Baladrón et al., 2005). In this manner, regulation of the expression of genes located in the 14q32 locus could also modulate the crosstalk between TGF-β and the VEGF and Notch signaling pathways, which have been previously described to act co-ordinately in space and time in the regulation of vascular morphogenesis (Holderfield and Hughes, 2008).

LIMITATIONS

We studied the miRNAs associated with the secretion of PECAM$^+$ EMPs in the context of BAV-induced endothelial damage, but we did not determine if this pattern of expression of PECAM$^+$ EMPs-associated miRNAs is also deregulated when the endothelial damage is caused by other conditions.

In summary, we propose that the changes in hemodynamic forces in the vascular system that are caused by the bicuspid morphology of the aortic valve might result in the expression of a specific pattern of PECAM$^+$ EMP-associated miRNAs that regulates a potent post-transcriptional network that might be involved in the regulation of endothelial damage. We reported that the highly co-expressed and PECAM$^+$ EMP-associated miRNAs clustered within the 14q32 locus might modulate a functional regulatory miRNA co-expression network that targets functionally related genes, which could be the molecular effectors linking the impairment of various signaling pathways (VEGFA, TGF-β, NOTCH) involved in the pathophysiology of BAV disease. Thus, we propose that the 14q32 miRNAs may act as master switches for endothelial damage and that inhibition of

either individual or a combination of 14q32 miRNAs might offer a new therapeutic approach for BAV disease.

AUTHOR CONTRIBUTIONS

NM: Performed the experiments, analyzed the data, and wrote the manuscript; RB and GA: Performed the experiments; MF: Contributed in sample collection and writing the manuscript; JA: Conceived and designed the study, analyzed the data and revised the manuscript. All authors read and approved the final manuscript.

FUNDING

This study received funding through a grant for clinical investigation from the *Sociedad Española de Cardiología.*

SUPPLEMENTARY MATERIAL

The Supplementary Material for this article can be found online at: http://journal.frontiersin.org/article/10.3389/fphys.2017.00648/full#supplementary-material

REFERENCES

Agarwal, V., Bell, G. W., Nam, J.-W., and Bartel, D. P. (2015). Predicting effective microRNA target sites in mammalian mRNAs. *Elife* 4:e05005. doi: 10.7554/eLife.05005

Aicher, D., Urbich, C., Zeiher, A., Dimmeler, S., and Schäfers, H.-J. (2007). Endothelial nitric oxide synthase in bicuspid aortic valve disease. *Ann. Thorac. Surg.* 83, 1290–1294. doi: 10.1016/j.athoracsur.2006.11.086

Alegret, J. M., Ligero, C., Vernis, J. M., Beltrán-Debón, R., Aragonés, G., Duran, I., et al. (2013). Factors related to the need for surgery after the diagnosis of bicuspid aortic valve: one center's experience under a conservative approach. *Int. J. Med. Sci.* 10, 176–182. doi: 10.7150/ijms.5399

Alegret, J. M., Martínez-Micaelo, N., Aragonès, G., and Beltrán-Debón, R. (2016). Circulating endothelial microparticles are elevated in bicuspid aortic valve disease and related to aortic dilation. *Int. J. Cardiol.* 217, 35–41. doi: 10.1016/j.ijcard.2016.04.184

Alegret, J. M., Palazón, O., Duran, I., and Vernis, J. M. (2005). Aortic valve morphology definition with transthoracic combined with transesophageal echocardiography in a population with high prevalence of bicuspid aortic valve. *Int. J. Cardiovasc. Imaging* 21, 213–217. doi: 10.1007/s10554-004-3901-9

Ali, O. A., Chapman, M., Nguyen, T. H., Chirkov, Y. Y., Heresztyn, T., Mundisugih, J., et al. (2014). Interactions between inflammatory activation and endothelial dysfunction selectively modulate valve disease progression in patients with bicuspid aortic valve. *Heart* 100, 800–805. doi: 10.1136/heartjnl-2014-305509

Amabile, N., Guérin, A. P., Leroyer, A., Mallat, Z., Nguyen, C., Boddaert, J., et al. (2005). Circulating endothelial microparticles are associated with vascular dysfunction in patients with end-stage renal failure. *J. Am. Soc. Nephrol.* 16, 3381–3388. doi: 10.1681/ASN.2005050535

Baladrón, V., Ruiz-Hidalgo, M. J., Nueda, M. L., Díaz-Guerra, M. J. M., García-Ramírez, J. J., Bonvini, E., et al. (2005). dlk acts as a negative regulator of Notch1 activation through interactions with specific EGF-like repeats. *Exp. Cell Res.* 303, 343–359. doi: 10.1016/j.yexcr.2004.10.001

Baskerville, S. (2005). Microarray profiling of microRNAs reveals frequent coexpression with neighboring miRNAs and host genes. *RNA* 11, 241–247. doi: 10.1261/rna.7240905

Benetatos, L., Hatzimichael, E., Londin, E., Vartholomatos, G., Loher, P., Rigoutsos, I., et al. (2013). The microRNAs within the DLK1-DIO3 genomic region: involvement in disease pathogenesis. *Cell. Mol. Life Sci.* 70, 795–814. doi: 10.1007/s00018-012-1080-8

Benjamini, Y., and Hochberg, Y. (1995). Controlling the false discovery rate: a practical and powerful approach to multiple testing. *J. R. Stat. Soc. Ser. B* 57, 289–300.

Biner, S., Rafique, A. M., Ray, I., Cuk, O., Siegel, R. J., and Tolstrup, K. (2009). Aortopathy is prevalent in relatives of bicuspid aortic valve patients. *J. Am. Coll. Cardiol.* 53, 2288–2295. doi: 10.1016/j.jacc.2009.03.027

Bissell, M. M., Hess, A. T., Biasiolli, L., Glaze, S. J., Loudon, M., Pitcher, A., et al. (2013). Aortic dilation in bicuspid aortic valve disease: flow pattern is a major contributor and differs with valve fusion type. *Circ. Cardiovasc. Imaging* 6, 499–507. doi: 10.1161/CIRCIMAGING.113.000528

Bobik, A. (2006). Transforming growth factor-betas and vascular disorders. *Arterioscler. Thromb. Vasc. Biol.* 26, 1712–1720. doi: 10.1161/01.ATV.0000225287.20034.2c

Boon, R. A., Hofmann, P., Michalik, K. M., Lozano-Vidal, N., Berghäuser, D., Fischer, A., et al. (2016). Long noncoding RNA Meg3 controls endothelial cell aging and function. *J. Am. Coll. Cardiol.* 68, 2589–2591. doi: 10.1016/j.jacc.2016.09.949

Braverman, A. C., Güven, H., Beardslee, M. A., Makan, M., Kates, A. M., Moon, M. R., et al. (2005). The bicuspid aortic valve. *Curr. Probl. Cardiol.* 30, 470–522. doi: 10.1016/j.cpcardiol.2005.06.002

Ci, H.-B., Ou, Z.-J., Chang, F.-J., Liu, D.-H., He, G.-W., Xu, Z., et al. (2013). Endothelial microparticles increase in mitral valve disease and impair mitral valve endothelial function. *Am. J. Physiol. Endocrinol. Metab.* 304, E695–E702. doi: 10.1152/ajpendo.00016.2013

Cline, M. S., Smoot, M., Cerami, E., Kuchinsky, A., Landys, N., Workman, C., et al. (2007). Integration of biological networks and gene expression data using cytoscape. *Nat. Protoc.* 2, 2366–2382. doi: 10.1038/nprot.2007.324

Davignon, J., and Ganz, P. (2004). Role of endothelial dysfunction in atherosclerosis. *Circulation* 109, III27–III32. doi: 10.1161/01.CIR.0000131515.03336.f8

Diehl, P., Fricke, A., Sander, L., Stamm, J., Bassler, N., Htun, N., et al. (2012). Microparticles: major transport vehicles for distinct microRNAs in circulation. *Cardiovasc. Res.* 93, 633–644. doi: 10.1093/cvr/cvs007

Dignat-George, F., and Boulanger, C. M. (2011). The many faces of endothelial microparticles. *Arterioscler. Thromb. Vasc. Biol.* 31, 27–33. doi: 10.1161/ATVBAHA.110.218123

Dunn, J., Qiu, H., Kim, S., Jjingo, D., Hoffman, R., Kim, C. W., et al. (2014). Flow-dependent epigenetic DNA methylation regulates endothelial gene expression and atherosclerosis. *J. Clin. Invest.* 124, 3187–3199. doi: 10.1172/JCI74792

Forte, A., Galderisi, U., Cipollaro, M., De Feo, M., and Corte, A. D. (2016). Epigenetic regulation of TGF- 1 signalling in dilative aortopathy of the thoracic ascending aorta. *Clin. Sci.* 130, 1389–1405. doi: 10.1042/CS20160222

Gleeson, T. G., Mwangi, I., Horgan, S. J., Cradock, A., Fitzpatrick, P., and Murray, J. G. (2008). Steady-state free-precession (SSFP) cine MRI in distinguishing normal and bicuspid aortic valves. *J. Magn. Reson. Imaging* 28, 873–878. doi: 10.1002/jmri.21547

Gordon, F. E., Nutt, C. L., Cheunsuchon, P., Nakayama, Y., Provencher, K. A., Rice, K. A., et al. (2010). Increased expression of angiogenic genes in the brains of mouse meg3-null embryos. *Endocrinology* 151, 2443–2452. doi: 10.1210/en.2009-1151

Holderfield, M. T., and Hughes, C. C. W. (2008). Crosstalk between vascular endothelial growth factor, notch, and transforming growth factor-beta in vascular morphogenesis. *Circ. Res.* 102, 637–652. doi: 10.1161/CIRCRESAHA.107.167171

Irizarry, R. A., Hobbs, B., Collin, F., Beazer-Barclay, Y. D., Antonellis, K. J., Scherf, U., et al. (2003). Exploration, normalization, and summaries of high density oligonucleotide array probe level data. *Biostatistics* 4, 249–264. doi: 10.1093/biostatistics/4.2.249

Jiang, Y.-Z., Manduchi, E., Stoeckert, C. J., and Davies, P. F. (2015). Arterial endothelial methylome: differential DNA methylation in athero-susceptible disturbed flow regions *in vivo*. *BMC Genomics* 16:506. doi: 10.1186/s12864-015-1656-4

Jimenez, J. J., Jy, W., Mauro, L. M., Soderland, C., Horstman, L. L., and Ahn, Y. S. (2003). Endothelial cells release phenotypically and quantitatively

distinct microparticles in activation and apoptosis. *Thromb. Res.* 109, 175–180. doi: 10.1016/S0049-3848(03)00064-1

Kagami, M., O'Sullivan, M. J., Green, A. J., Watabe, Y., Arisaka, O., Masawa, N., et al. (2010). The IG-DMR and the MEG3-DMR at Human Chromosome 14q32.2: Hierarchical interaction and distinct functional properties as imprinting control centers. *PLoS Genet.* 6:e1000992. doi: 10.1371/journal.pgen.1000992

Kameswaran, V., Bramswig, N. C., McKenna, L. B., Penn, M., Schug, J., Hand, N. J., et al. (2014). Epigenetic regulation of the DLK1-MEG3 microRNA cluster in human type 2 diabetic islets. *Cell Metab.* 19, 135–145.

Kim, V. N., and Nam, J.-W. (2006). Genomics of microRNA. *Trends Genet.* 22, 165–173. doi: 10.1016/j.tig.2006.01.003

Kim, Y.-G., Sun, B. J., Park, G.-M., Han, S., Kim, D.-H., Song, J.-M., et al. (2012). Aortopathy and bicuspid aortic valve: haemodynamic burden is main contributor to aortic dilatation. *Heart* 98, 1822–1827. doi: 10.1136/heartjnl-2012-302828

Kim, Y.-K., Yu, J., Han, T. S., Park, S.-Y., Namkoong, B., Kim, D. H., et al. (2009). Functional links between clustered microRNAs: suppression of cell-cycle inhibitors by microRNA clusters in gastric cancer. *Nucleic Acids Res.* 37, 1672–1681. doi: 10.1093/nar/gkp002

Lau, N. C. (2001). An abundant class of tiny RNAs with probable regulatory roles in caenorhabditis elegans. *Science* 294, 858–862. doi: 10.1126/science.1065062

Marin, T., Gongol, B., Chen, Z., Woo, B., Subramaniam, S., Chien, S., et al. (2013). Mechanosensitive microRNAs—role in endothelial responses to shear stress and redox state. *Free Radic. Biol. Med.* 64, 61–68. doi: 10.1016/j.freeradbiomed.2013.05.034

Martínez-Micaelo, N., Beltrán-Debón, R., Baiges, I., Faiges, M., and Alegret, J. M. (2017). Specific circulating microRNA signature of bicuspid aortic valve disease. *J. Transl. Med.* 15:76. doi: 10.1186/s12967-017-1176-x

Mourelatos, Z., Dostie, J., Paushkin, S., Sharma, A., Charroux, B., Abel, L., et al. (2002). miRNPs: a novel class of ribonucleoproteins containing numerous microRNAs. *Genes Dev.* 16, 720–728. doi: 10.1101/gad.974702

Murphy, S. K., Wylie, A. A., Coveler, K. J., Cotter, P. D., Papenhausen, P. R., Sutton, V. R., et al. (2003). Epigenetic detection of human chromosome 14 uniparental disomy. *Hum. Mutat.* 22, 92–97. doi: 10.1002/humu.10237

Okamoto, K., Koda, M., Okamoto, T., Onoyama, T., Miyoshi, K., Kishina, M., et al. (2016). A series of microRNA in the Chromosome 14q32.2 Maternally imprinted region related to progression of non-alcoholic fatty liver disease in a mouse model. *PLoS ONE* 11:e0154676. doi: 10.1371/journal.pone.0154676

Opgen-Rhein, R., and Strimmer, K. (2007). From correlation to causation networks: a simple approximate learning algorithm and its application to high-dimensional plant gene expression data. *BMC Syst. Biol.* 1:37. doi: 10.1186/1752-0509-1-37

Padang, R., Bannon, P. G., Jeremy, R., Richmond, D. R., Semsarian, C., Vallely, M., et al. (2013). The genetic and molecular basis of bicuspid aortic valve associated thoracic aortopathy: a link to phenotype heterogeneity. *Ann. Cardiothorac. Surg.* 2, 83–91. doi: 10.3978/j.issn.2225-319X.2012.11.17

Paraskevopoulou, M. D., Georgakilas, G., Kostoulas, N., Vlachos, I. S., Vergoulis, T., Reczko, M., et al. (2013). DIANA-microT web server v5.0: service integration into miRNA functional analysis workflows. *Nucleic Acids Res.* 41, W169–W173. doi: 10.1093/nar/gkt393

Pepe, G., Nistri, S., Giusti, B., Sticchi, E., Attanasio, M., Porciani, C., et al. (2014). Identification of fibrillin 1 gene mutations in patients with bicuspid aortic valve (BAV) without Marfan syndrome. *BMC Med. Genet.* 15:23. doi: 10.1186/1471-2350-15-23

Pirro, M., Schillaci, G., Paltriccia, R., Bagaglia, F., Menecali, C., Mannarino, M. R., et al. (2006). Increased ratio of CD31+/CD42- microparticles to endothelial progenitors as a novel marker of atherosclerosis in hypercholesterolemia. *Arterioscler. Thromb. Vasc. Biol.* 26, 2530–2535. doi: 10.1161/01.ATV.0000243941.72375.15

Ranjan, V., Xiao, Z., and Diamond, S. L. (1995). Constitutive NOS expression in cultured endothelial cells is elevated by fluid shear stress. *Am. J. Physiol.* 269, H550–H555.

Ritchie, M. E., Phipson, B., Wu, D., Hu, Y., Law, C. W., Shi, W., et al. (2015). Limma powers differential expression analyses for RNA-sequencing and microarray studies. *Nucleic Acids Res.* 43:e47. doi: 10.1093/nar/gkv007

Saura, M., Zaragoza, C., Herranz, B., Griera, M., Diez-Marqués, L., Rodriguez-Puyol, D., et al. (2005). Nitric oxide regulates transforming growth factor-β signaling in endothelial cells. *Circ. Res.* 97, 115–123. doi: 10.1161/01.RES.0000191538.76771.66

Schäfer, J., and Strimmer, K. (2005). An empirical bayes approach to inferring large-scale gene association networks. *Bioinformatics* 21, 754–764. doi: 10.1093/bioinformatics/bti062

Sutherland, W. H. F., de Jong, S. A., Hessian, P. A., and Williams, M. J. A. (2010). Ingestion of native and thermally oxidized polyunsaturated fats acutely increases circulating numbers of endothelial microparticles. *Metab. Clin. Exp.* 59, 446–453. doi: 10.1016/j.metabol.2009.07.033

Tzemos, N., Therrien, J., Yip, J., Thanassoulis, G., Tremblay, S., Jamorski, M. T., et al. (2008). Outcomes in adults with bicuspid aortic valves. *JAMA* 300, 1317–1325. doi: 10.1001/jama.300.11.1317

Vion, A.-C., Ramkhelawon, B., Loyer, X., Chironi, G., Devue, C., Loirand, G., et al. (2013). Shear stress regulates endothelial microparticle release. *Circ. Res.* 112, 1323–1333. doi: 10.1161/CIRCRESAHA.112.300818

Vlachos, I. S., Paraskevopoulou, M. D., Karagkouni, D., Georgakilas, G., Vergoulis, T., Kanellos, I., et al. (2015a). DIANA-TarBase v7.0: indexing more than half a million experimentally supported miRNA:mRNA interactions. *Nucleic Acids Res.* 43, D153–D159. doi: 10.1093/nar/gku1215

Vlachos, I. S., Zagganas, K., Paraskevopoulou, M. D., Georgakilas, G., Karagkouni, D., Vergoulis, T., et al. (2015b). DIANA-miRPath v3.0: deciphering microRNA function with experimental support. *Nucleic Acids Res.* 43, W460–W466. doi: 10.1093/nar/gkv403

Wang, J., Haubrock, M., Cao, K.-M., Hua, X., Zhang, C.-Y., Wingender, E., et al. (2011). Regulatory coordination of clustered microRNAs based on microRNA-transcription factor regulatory network. *BMC Syst. Biol.* 5:199. doi: 10.1186/1752-0509-5-199

Wang, Y., Luo, J., Zhang, H., and Lu, J. (2016). microRNAs in the Same clusters evolve to coordinately regulate functionally related genes. *Mol. Biol. Evol.* 33, 2232–2247. doi: 10.1093/molbev/msw089

Wolfe, D., Dudek, S., Ritchie, M. D., Pendergrass, S. A., Ramos, P., Criswell, L., et al. (2013). Visualizing genomic information across chromosomes with PhenoGram. *BioData Min.* 6:18. doi: 10.1186/1756-0381-6-18

Conflict of Interest Statement: The authors declare that the research was conducted in the absence of any commercial or financial relationships that could be construed as a potential conflict of interest.

frontiers in Physiology

REVIEW
published: 16 June 2017
doi: 10.3389/fphys.2017.00429

Non-coding RNA Contribution to Thoracic and Abdominal Aortic Aneurysm Disease Development and Progression

Yuhuang Li[1] *and Lars Maegdefessel*[1,2]*

[1] Vascular Biology Unit, Department of Vascular and Endovascular Surgery, Klinikum rechts der Isar der Technical University of Munich, Munich, Germany, [2] Department of Medicine, Karolinska Institutet, Stockholm, Sweden

Multiple research groups have started to uncover the complex genetic and epigenetic machinery necessary to maintain cardiovascular homeostasis. In particular, the key contribution of non-coding RNAs (ncRNAs) in regulating gene expression has recently received great attention. Aneurysms in varying locations of the aorta are defined as permanent dilations, predisposing to the fatal consequence of rupture. The characteristic pathology of an aneurysm is characterized by progressive vessel wall dilation, promoted by dying vascular smooth muscle cells and limited proliferation, as well as impaired synthesis and degradation of extracellular matrix components, which at least partially is the result of transmural inflammation and its disruptive effect on vessel wall homeostasis. Currently no conservative pharmacological approach exists that could slow down aneurysm progression and protect from the risk of acute rupture. In the recent past, several non-coding RNAs (mainly microRNAs) have been discovered as being involved in aneurysm progression throughout varying locations of the aorta. Exploring ncRNAs as key regulators and potential therapeutic targets by using antisense oligonucleotide strategies could open up promising opportunities for patients in the near future. Purpose of this current review is to summarize current findings and novel concepts of perspectivly utilizing ncRNAs for future therapeutic and biomarker applications.

Keywords: aortic aneurysm, non-coding RNA (ncRNA), MicroRNA (miRNA), gene expression regulation, vascular diseases, long non-coding RNA (lncRNA)

OPEN ACCESS

Edited by:
Amalia Forte,
Università degli Studi della Campania "Luigi Vanvitelli" Caserta, Italy

Reviewed by:
Anna Zampetaki,
King's College School, United Kingdom
Daniela Carnevale,
Sapienza Università di Roma, Italy

***Correspondence:**
Lars Maegdefessel
lars.maegdefessel@tum.de

Specialty section:
This article was submitted to Vascular Physiology, a section of the journal Frontiers in Physiology

Received: *28 April 2017*
Accepted: *02 June 2017*
Published: *16 June 2017*

Citation:
Li Y and Maegdefessel L (2017) Non-coding RNA Contribution to Thoracic and Abdominal Aortic Aneurysm Disease Development and Progression. Front. Physiol. 8:429. doi: 10.3389/fphys.2017.00429

INTRODUCTION

Aortic aneurysms (AAs) are asymmetrical dilations of the aorta with diameters >1.5 times the normal size (Kent, 2014). They are most commonly located in the infrarenal abdominal aorta but can also be found in the thoracic aorta. The overall prevalence of abdominal AAs (AAAs) is 6% in men and 1.6% in women (Li et al., 2013); the incidence for thoracic AAs (TAAs) is roughly 10/10,000 in our population (Elefteriades et al., 2015). Fatal outcomes due to aortic rupture occur when intraluminal pressures exceed the capacity of the arterial wall, with mortality rates as high as 80% (Golledge and Norman, 2011). It is estimated that aneurysm ruptures account for nearly 15,000 deaths in the United States annually (Lloyd-Jones et al., 2009). Most of these fatalities are due to abdominal aneurysms, with thoracic and thoracoabdominal aneurysms accounting for 1 to 4% of all aneurysm-related deaths (Lindsay and Dietz, 2011). The asymptomatic characteristic of

aneurysms makes their assessment challenging. Unless AAs rapidly increase or acutely rupture, or thrombi embolize into the distal arterial system, AAs behave as a silent disease (Kent, 2014).

Currently, the only available treatment of AAs is surgical intervention, such as prosthetic replacement (open surgery) or strengthening (endoprosthesis) of the aorta (Golledge et al., 2006). The latter endovascular repair has become the preferable option in the past decade, accounting for ∼70% of AA procedures performed in Europe and North America (Schanzer et al., 2017; Williams and Brooke, 2017). However, clinically surgical intervention is only recommended when aneurysms are prone to rupture, since both interventional procedures carry surgical risks (Kent, 2014). Unfortunately, no effective pharmacological approaches have been approved to limit the progression or risk of aneurysm rupture in humans (Golledge et al., 2006). Obtaining a better understanding of the cellular mechanisms driving aneurysm development and progression is not only essential to fill this gap but is also important to identify new biomarkers and therapeutic targets.

This review focuses on the contribution of non-coding RNAs (ncRNAs) to AA development and progression, and discusses their potential therapeutic value in this context. With the completion of human genome project in 2003, the "protein-centered" dogma of molecular biology was challenged with the discovery that while >98% of our genome is "non-coding," it is still transcribed (Esteller, 2011). Accumulating evidence has shown that this refined orechstrating system of ncRNA mediators are powerful regulators of various aspects of cellular function and disease progression (Vidigal and Ventura, 2015; Engreitz et al., 2016; **Figure 1**). In general, ncRNAs are classified, based on an arbitrary cut-off size of 200 nucleotides (nt), into separate groups of small ncRNAs and long non-coding RNAs (lncRNAs). MicroRNAs (miRNAs) are the most well-studied group of small ncRNAs, and ∼22 nt in length, whereas lncRNAs are larger than 200 nt and their distinct functions being largely unexplored (Cech and Steitz, 2014).

CELLULAR MECHANISMS BEHIND AORTIC ANEURYSM DEVELOPMENT AND PROGRESSION

The lack of pharmacological approaches to limit aneurysm progression and rupture mandates a better understanding of the pathogenesis and cellular mechanisms of aneurysm development. New mechanistic insights may identify potential therapeutic targets. Here, we summarize the pathologic mechanisms and related molecular characteristics behind thoracic and abdominal aneurysm development and progression.

THORACIC AORTIC ANEURYSM

Despite the common phenotypic manifestations with AAAs (discussed below), TAAs exhibit a strong heritable pattern, with different pathophysiologies, risk factors, and evolutionary progression. For example, the known risk factors most associated with AAAs include cigarette smoking, increasing age, hypertension, hyperlipidemia, and atherosclerosis, whereas TAAs are primarily associated with connective tissue diseases, bicuspid aortic valve disease, and familial thoracic aneurysm syndrome. Nevertheless, perturbed extracellular matrix (ECM) homeostasis, transforming growth factor-β (TGF-β) signaling, and vascular smooth muscle cell (SMC) plasticity and survival have been proposed as important processes in TAA pathogenesis (Verstraeten et al., 2017). Recently, a genetic predisposition to TAAs has been identified, highlighting the dominant role of gene mutations in the TGF-β signaling cascade and SMC contractile apparatus (Isselbacher et al., 2016). Additionally, research in experimental aneurysms has revealed hyperstimulation of the TGF-β pathway in TAAs (Neptune et al., 2003; Habashi et al., 2006), likely the result of genetic perturbations. Mutations of TGF-β signaling molecules are proposed to upregulate counter-regulatory pathways, such as those involving mitogen-activated protein kinase (MAPK), which can directly drive aneurysm development (Holm et al., 2011). Interestingly, TGF-β is poorly expressed in human AAAs and appears to play a protective role in their development. The modulation of TGF-β signaling prevents AAA formation in both elastase infusion and angiotensin II (AngII) perfusion animal models of AAA (Wang et al., 2010, 2013). On the other hand, mutations in the SMC contractile apparatus result in a loss of contractile structure, which is essential for the maintenance of an intact focal adhesion complex and the integrity of the ECM (Milewicz et al., 2008). It is currently unclear whether the relationship between such a contraction vasculopathy and TGF-β dysregulation correlates with - or is a precipitating cause of TAAs (Isselbacher et al., 2016), considering that TGF-β can both induce a phenotypic switch in SMCs and stimulate the secretion of matrix-degrading enzymes, such as matrix metalloproteinases (MMPs), from these cells(Renard et al., 2013).

ABDOMINAL AORTIC ANEURYSM

The defined mechanisms underlying AAAs are as well incompletely understood. AAA formation is thought to be a complex process, involving all vascular cell subtypes (Maegdefessel et al., 2013). The pathological features are characterized by endothelial dysfunction, chronic adventitial and medial inflammatory cell infiltration, ECM degradation, elastin fragmentation and medial devitalization, as well as SMC phenotype alterations (early stages) and apoptosis (late stages; Shimizu et al., 2006). Work in both common small animal models and humans has indicated that AAA development involves local inflammation and the infiltration of monocytes/macrophages, neutrophils, mast cells, and T and B lymphocytes (Sun et al., 2007). These infiltrating cells secrete various inflammatory cytokines and chemokines, such as interleukin (IL)-1β, IL-6, tumor necrosis factor (TNF)-α, and monocyte chemoattractant protein-1 (MCP-1), which can induce the activation of MMPs, particularly MMP-2 and MMP-9 (Golledge et al., 2006). These events contribute to ECM degradation and SMC depletion, leading to AAA progression and rupture.

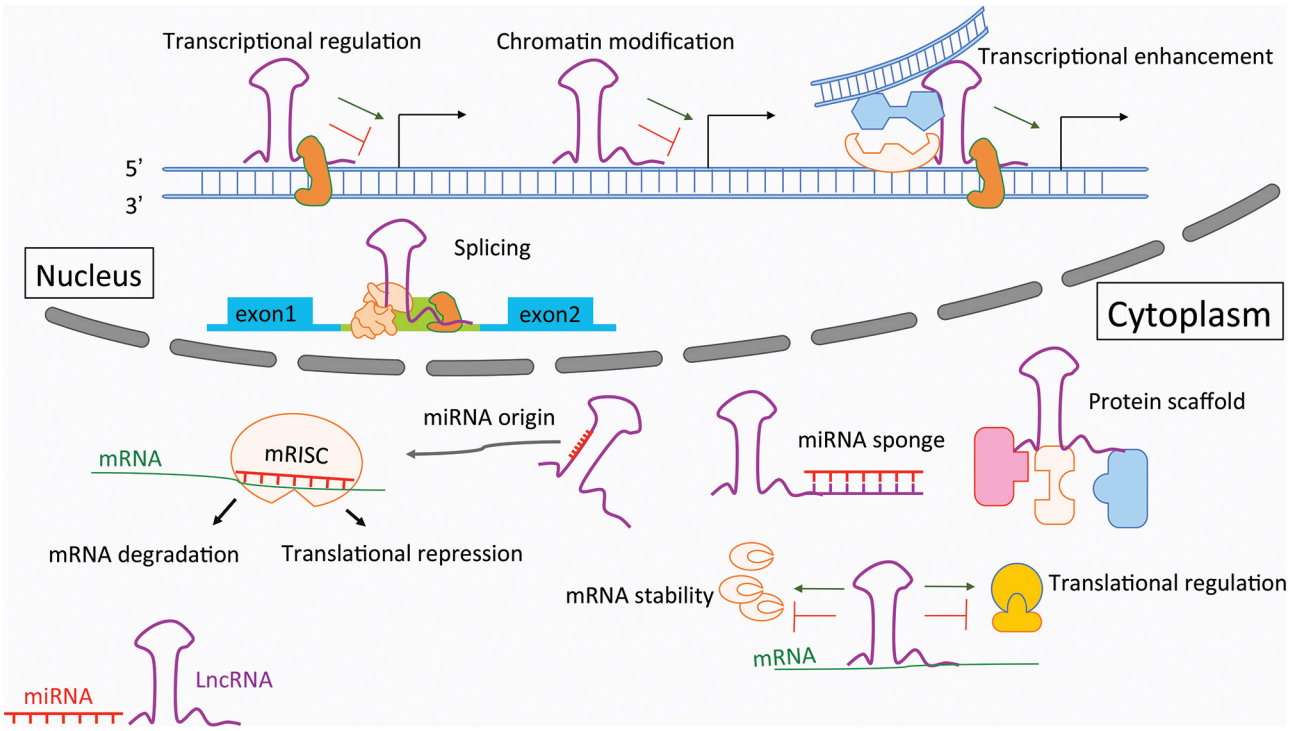

FIGURE 1 | Mechanisms of action for non-coding RNAs during disease development and progression. Long non-coding RNAs (lncRNAs) regulate DNA processing via transcriptional regulation, chromatin modification, trsncriptional enhancement, as well as by affecting splicing mechanisms in the nucleus. Within the cytoplasm lncRNAs are involved by sponging microRNAs (miRNAs) or by sesrving as miRNA host transcripts (miRNA origin), as well as via playing an important role as protein scaffolds and affectors of mRNA stability and transcription. Mature, single-stranded miRNAs get processed into the messenger RNA induced silencing complex (mRISC) where they bind to messenger RNA (mRNA), augmenting gene expression either via translational repression, or mRNA degradation.

NON-CODING RNAS

ncRNAs are RNA molecules that are not translated into protein products. They can be functionally classified into the following subgroups: gene expression regulation (miRNAs, piRNAs, lncRNAs), RNA maturation (snRNAs, snoRNAs), and protein synthesis (rRNAs, tRNAs; Fu, 2014). In this section, we will review some important aspects of miRNAs and lncRNAs, and highlight their regulatory roles in AA development and progression.

MICRORNAS

MicroRNAs (miRNAs) are endogenous RNAs of ∼22 nt that post-transcriptionally repress the expression of target genes, usually by binding to the 3′ untranslated region (UTR) of messenger RNA (mRNA). The stepwise progression of miRNA maturation has already been established (Lee et al., 2002, 2003). The first step is nuclear cleavage of primary-miRNA (pri-miRNA) by Drosha RNase III endonuclease, resulting in a 60–70-nt stem-loop intermediate known as miRNA precursor (pre-miRNA), which is then actively transported from the nucleus to the cytoplasm by guanosine triphosphate (GTP)-binding nuclear protein Ran (RAs-related Nuclear protein Ran-GTP) and the export receptor exportin-5. In the cytoplasm, pre-miRNA is further processed by the enzyme Dicer, producing an imperfect siRNA-like duplex that composes the mature miRNA. Fully processed miRNAs associate with, and serve as specificity determinants for, the Argonaute (Ago) family of proteins within the RNA-induced silencing complex (RISC; Hutvagner and Zamore, 2002). At sites with extensive pairing complementarity, miRNAs can direct Ago-catalyzed mRNA cleavage. More commonly, though, they direct translational repression, mRNA destabilization, or a combination of these two processes (Bartel, 2009; Djuranovic et al., 2011).

MiRNAs have emerged as key post-transcriptional regulators of gene expression in the past decade, playing important roles in various biological processes and in disease development and progression(Bartel, 2004; Ebert and Sharp, 2012; Mendell and Olson, 2012). For AAs in particular, several miRNAs have been identified as crucial regulators, orchestrating the functions of all subtypes of vascular cells (**Table 1**). Endothelial cell (EC) dysfunction and leukocyte infiltration, degradation of the ECM, and SMC depletion are regarded as three pathological hallmarks of AAAs (Guo et al., 2006). As the aneurysm miRNA signature may differ depending on disease localization and morphology (Busch et al., 2016), one should act with caution when elucidating and comparing deregulations examined in human aneurysms, animal models, or cultured cells *in vitro*.

TABLE 1 | MicroRNAs involoved in aortic aneurysms.

miRNAs	Type	Sample studied	Cellular origin	Regulation	Target genes	Related Functions	References
miR-15a	AAA	Human whole aorta, HAoSMCs	VSMC	↑	CDKN2B	Promotes proliferation and decreases apoptosis of VSMC	Gao et al., 2017
miR-17 cluster	TAD	Human dilated aorta, HAoSMCs from BAV	VSMC	↑	TIMP1, TIMP2	Downregulates ECM	Wu et al., 2016
miR-21	AAA	Human and mouse whole aorta, HAoSMCs	VSMC	↑	PTEN	Promotes proliferation and decreases apoptosis of VSMC	Maegdefessel et al., 2012a
miR-24	AAA	Human and mouse whole aorta and plasma, HAoSMCs, macrophage	VSMC, macrophage	↓	CHI3L1	Inhibits vascular inflammation	Maegdefessel et al., 2014
miR-26a	AAA	Mouse whole aorta, HAoSMCs	VSMC	↓	SMAD1, SMAD4	Promotes proliferation and inhibits differentiation, apoptosis of VSMC, alters TGF-β signaling	Leeper et al., 2011
miR-29	AAA, TAA	Human and mouse whole aorta, HAoSMCs	Fibroblast, VSMC	↓	COL1A1, COL3A1, COL5A1, ELN, MMP2, MMP9	Downregulates ECM and reulates fibrosis	Boon et al., 2011; Maegdefessel et al., 2012b
miR-29a	TAD	Human aorta, HAoSMCs	VSMC	↓	MMP2, MMP9	Downregulates ECM	Jones et al., 2011
miR-29b	TAA	Fbn1(C1039G/+) aorta, HAoSMCs	VSMC	↑	ELN, MMP2	Upregulates ECM and promotes apoptosis of VSMC	Merk et al., 2012
miR-29c	AAA	Human serum, HUVEs	EC	↑	ELN, COL4A1, PTEN, VEGFA	Regulates ECM	Licholai et al., 2016
miR-98	AAA	THP-1, HAoSMCs	Macrophage, VSMC	-	-	MCP-1/miR-98/IL-6/p38 regulatory loop, induce VSMC apoptosis	Wang et al., 2015b
miR-129	AAA	Mouse whole aorta, HAoSMCs	VSMC	↓	Wnt5a	Inhibits proliferation and induce apoptosis of VSMC	Zhang et al., 2016
miR-143/145	TAD	Human TAD aorta, mouse aorta, HAoSMCs	VSMC	↓	Klf4, myocardin, Elk-1, SRF	Promotes differentiation and represses proliferation of VSMC	Lesauskaite et al., 2001; Elia et al., 2009; Liao et al., 2011
miR-155	AAA	Human and mouse whole aorta, human plasma, HAoSMCs	TC	↑ in tissue, ↓ in plama	CTLA4, SMAD2	Promotes vascular inflammation	Biros et al., 2014
miR-181b	AAA, TAA	Human and mouse whole aorta, HAoSMCs	Macrophage, VSMC	↑	TIMP3, ELN	Downregulates ECM	Di Gregoli et al., 2017
miR-195	AAA	Human and mouse whole aorta, HAoSMCs	VSMC	↑	COL1A1, COL1A2, COL3A1, FBN1, ELN, MMP2, MMP9	Regulates ECM	Zampetaki et al., 2014
miR-221/222	AAA	Human whole aorta, Rat SMCs and Ecs	VSMC, EC	↑	kip1, kip2, c-kit	Pro-proliferative, pro-migration, and anti-apoptotic effects, Promote a synthetic phenotype in VSMCs	Davis et al., 2009; Liu et al., 2012

(Continued)

TABLE 1 | Continued

miRNAs	Type	Sample studied	Cellular origin	Regulation	Target genes	Related Functions	References
miR-223	AAA	Human aorta and plasma, Rat Cerebral Aneurysms	Macrophage	↑ in tissue, ↓ in plama	MMP12	Inhibits vascular inflammation	Kanematsu et al., 2011; Kin et al., 2012; Lee et al., 2013
miR-516a	AAA	HAoSMCs	VSMC	↑	MTHFR, MMP2, TIMP1	Regulates ECM	Tung Chan et al., 2017
miR-712/205	AAA	Mouse whole aorta, HAoSMCs	EC, leukocytes	↑	TIMP3, RECK	Induces inflammation, regulate ECM	Kim et al., 2014

AAA, abdominal aortic aneurysm; TAA, thoracic aortic aneurysm; TAD, thoracic aortic dissection; HAoSMCs, human aortic smooth muscle cells; HUVEs, human umbilical vein endothelial cells; VSMC, vascular smooth muscle cell, EC, endothelial cell; TC, T lymphocytes; COL1A1/2, collagen type 1 alpha 1/2; COL3A1/2, collagen type 3 alpha 1; FBN, fibrillin; ELN, elastin; kip1/CDKN1B, Cyclin-dependent kinase inhibitor 1B; kip2/CDKN1C, Cyclin-dependent kinase inhibitor 1B; c-kit/SCFR, Mast/stem cell growth factor receptor; ELK1, ETS domain-containing protein; KLF4, Kruppel-like factor 4; CTLA4, cytotoxic T-lymphocyte associated protein 4; MCL1, myeloid cell leukemia 1; MMP, matrix metalloproteinase; TIMP3, metalloproteinase inhibitor 3; PTEN, phosphatase and tensin homolog; CHI3L1, chitinase 3 Like 1; Wnt Wnt5a, Family Member 5A; SMAD, mothers against decapentaplegic homolog; RECK, reversion-inducing-cysteine-rich protein with kazal motifs; VEGFA, Vascular endothelial growth factor A; MTHFR, methylenetetrahydrofolate reductase. ECM, extracellular matrix; TGF-β, transforming growth factor-β.

MIRNAS, ENDOTHELIAL DYSFUNCTION, AND VASCULAR INFLAMMATION

ECs are the first cell sensors exposed to pathologic factors, such as hyperlipidemia and turbulent flow shear stress, in the lumen of the aorta. To address the role of endothelial miRNAs in AAA development, Kim et al. (2014) utilized the mouse AngII infusion model of AAAs, one of the most important experimental platforms to study the pathophysiology of AAAs. Using an miRNA microarray platform, the authors experimentally confirmed the upregulation of miR-712/205 in ECs as well as in the medial layer of the aorta. Of note, the two key inhibitors of MMPs, tissue inhibitor of metalloproteinase 3 (TIMP3) and reversion-inducing-cysteine-rich protein with kazal motifs (RECK), which lead to both the activation of MMPs in the aortic wall and the development of AAAs in the mouse AngII infusion model, were validated as direct targets of miR-712. In addition, the manipulation of both AngII and miR-712/205 affected the adhesion of circulating leukocytes, further highlighting the therapeutic potential of targeting this pathway, while implying that other mechanisms are involved. Furthermore, in human vascular ECs, other genes related to ECM synthesis and maintenance of ECM integrity, such as elastin (ELN), collagen type 4 alpha 1 (COL4A1), phosphatase and tensin homolo (PTEN), and vascular endothelial growth factor A (VEGFA), were recently identified as targets of miR-29c and are significantly elevated in the sera of AAA patients (Licholai et al., 2016).

Subsequent inflammatory cell infiltration may be facilitated by miR-155, whose levels were found to be highly increased in AAA biopsies and circulating sera in AAA patients (Biros et al., 2014). It is believed that miR-155 not only promotes chronic inflammation by enhancing T cell development via the downregulation of cytotoxic T-lymphocyte associated protein 4 (CTLA4), but also blocks mothers against decapentaplegic homolog (SMAD2) translation and protein synthesis during the regulation of TGF-β signaling, leading to AAA development. Similarly, miR-181b was shown to endow macrophages with more invasive and proliferative capabilities to control aneurysm progression via the negative regulation of tissue inhibitor of MMP-3 expression (TIMP3; Di Gregoli et al., 2017). Moreover, miR-223, a novel regulator of inflammation that inhibits proinflammatory pathways and enhances anti-inflammatory responses, was dysregulated in AAAs (Kin et al., 2012) and negatively correlated with MCP-1, TNF-α, and TGF-β expression in diseased aortic tissues(Kanematsu et al., 2011; Lee et al., 2013). Recently, miR-103a (Jiao et al., 2017) was reported as an "anti-aneurysmal" miRNA that suppresses inflammation within the aortic wall, limiting AAA formation and progression by downregulating the protease ADAM Metallopeptidase Domain 10 (ADAM10).

Our lab discovered miR-24 as a key regulator of vascular inflammation and AAA pathology (Maegdefessel et al., 2014). Before elucidating the highly conserved miR-23b-24-27b cluster in AAA diseases, others have shown that this miRNA family is involved in postinfarction cardiac angiogenesis (Fiedler et al., 2011), cardiomyocyte survival (Qian et al., 2011), cancer

(Hatziapostolou et al., 2011; Qian et al., 2011), and atherosclerosis (Geng et al., 2016). The miR-23b-24-27b cluster has been further linked to inflammation by its ability to modulate the nuclear factor kappa-light-chain-enhancer of activated B cells (NF-κB) pathway in macrophages (Thulasingam et al., 2011). In addition, Hatziapostolou et al. (2011) demonstrated an miRNA-inflammatory feedback loop, consisting of miR-124, IL-6R, signal transducer and activator of transcription 3 (STAT3), miR-24, and miR-629, in which the systemic administration of miRNAs prevented and suppressed hepatocellular carcinogenesis by the induction of tumor-specific apoptosis without toxic side effects.

In our own study (Maegdefessel et al., 2014), we profiled miRNA expression and validated the downregulation of the miR-23b-24-27b cluster in murine AAA models, finding that miR-24 displayed the most significant inverse regulation with its predicted targets. Human AAAs also show evidence of miR-24 downregulation, which correlates inversely with aneurysm size. Further analysis suggested "chitinase 3-like 1′ (Chi3l1), a mediator/marker of inflammation, as an intriguing miR-24 target. Chi3l1 is secreted by differentiated macrophages in early stage atherosclerotic lesions and modulates SMC proliferation and migration (Rehli et al., 2003). In the context of AAAs, miR-24-Chi3l1 interactions appear to have broad effects on all cells present in the aortic wall, such as the regulation of macrophage survival and cytokine synthesis, promotion of aortic SMC migration and cytokine production, and stimulation of adhesion molecule expression in vascular ECs. Furthermore, overexpression of miR-24 in murine models was able to significantly decrease Chi3l1 levels, leading to arrested AAA development and reduced immune responses and cytokine activities, suggesting that miR-24 downregulation contributes to aneurysm growth. In contrast, the inhibition of miR-24 was shown to accelerate AAA progression by augmentation of the degree of inflammatory and apoptosis-related responses.

Consistent with findings related to miR-24 and the inflammation loop, Pua et al. (2016) provided evidence that miR-24 and miR-27 suppress allergic inflammation and target regulators of T helper 2 cell-associated cytokine production. These data suggest that miR-24 may be involved in leukocyte infiltration during aneurysm development. Another study from Geng et al. (2016) examined the pathological consequences of subclinical endotoxemia during both the low-grade inflammatory polarization of monocytes and the progression of atherosclerosis. These authors observed that subclinical endotoxemia was able to shift monocytes into a nonresolving inflammatory state, with elevated levels of lymphocyte antigen 6 complex locus C (Ly6C), chemokine (C-C motif) receptor 5 (CCR5), and MCP-1, and reduced levels of scavenger receptor class B member 1 (SR-B1), due to the disruption of homeostatic tolerance by elevated miR-24 levels and reduced levels of the key negative-feedback regulator interleukin-1 receptor-associated kinase (IRAK)-M. MiR-24 targets SMAD4, which is required for the expression of IRAK-M and the key lipid-processing molecule SR-B1. IRAK-M deficiency in turn leads to elevated miR-24 levels, sustaining the disruption of monocyte homeostasis and aggravating atherosclerosis. Another study recently confirmed the role of miR-24-Chi3l1 interactions in Staphylococcus aureus-stimulated macrophages (Jingjing et al., 2017). MiR-24 was found to decrease both M1 macrophage polarization and production of proinflammatory cytokines, and induce both M2 macrophage polarization and secretion of anti-inflammatory factors. These actions are mediated by the direct suppression of Chi3l1 and the inhibition of the MAPK pathway.

MIRNAS AND SMOOTH MUSCLE CELL HOMEOSTASIS

SMCs are the predominant cells in the tunica media of the aorta and are essential for the maintenance of aortic structure and function. The phenotype of SMCs can change from a contractile (differentiated) to a synthetic (dedifferentiated) state, and vice versa, in response to changing environmental conditions. The differentiated phenotype is characterized by high levels of contractile gene expression, with low rates of proliferation, migration, and ECM synthesis; the dedifferentiated phenotype has the opposite features. Dysregulation of both phenotype switching and SMC apoptosis contributes to the development and progression of AAs (Henderson et al., 1999; Ailawadi et al., 2009). Previous studies have revealed that SMC homeostasis is intensively regulated by a vast array of miRNAs (**Table 1**).

Leeper and collaborators (Leeper et al., 2011) were able to prove that miR-26a is an important regulator of the SMC phenotype. They performed a microarray-based study during human aortic SMC differentiation *in vitro* and showed that miR-26a was the highest-ranked significant miRNA present. SMC behavior was evaluated by the modulation of miR-26 via the transfection of either pre-miR or anti-miR. The decreased level of miR-26a was associated with a reduction in SMC proliferation and migration, and a significant increase in H_2O_2-induced apoptosis. Mechanistically, miR-26a targeted the expression of SMAD1 and SMAD4, members of the TGF-β signaling cascade, and thus affected AAA development. Moreover, the expression of miR-26a was found to be progressively downregulated in two murine AAA models, suggesting that miR-26a may represent a novel therapeutic target in conditions of pathologic aneurysmal dilation.

MiR-221/222, which are highly expressed in SMCs and ECs, seem to have a cell-specific effect on the aorta. Liu et al. (2012) isolated SMCs and ECs from the aortas of male Sprague-Dawley rats and assessed the cellular responses to miR-221/222. Interestingly, these miRNAs had pro-proliferative, pro-migratory, and anti-apoptotic effects on SMCs - but the completely opposite effect on ECs. MiR-221/222 appears to directly target and downregulate p27 (Kip1), p57 (Kip2), and c-Kit, three proteins that are involved in key processes of cell differentiation, proliferation, migration, and apoptosis, and are also differentially expressed in SMCs and ECs. Consistent with these data, Davis et al. (2009). identified that miR-221 was critical for the platelet-derived growth factor (PDGF)-mediated induction of cell proliferation by downregulating the expression of p27 (Kip1) and c-Kit.

In our previous work (Maegdefessel et al., 2012a), we discovered the essential role of miR-21 in SMC homeostasis during AAA development. MiR-21 is highly expressed in SMCs and is known to be involved in the regulation of SMC biology by targeting several cell fate-determination genes, such as PTEN (Horita et al., 2011), programmed cell death 4 (PDCD4; Liu et al., 2010), and B cell lymphoma 2 (BCL2; Ji et al., 2007). Ji et al. (2007) found that miR-21 was one of the most upregulated miRNAs in the vascular wall after balloon injury, and that miR-21 depletion significantly decreased neointima formation, suggesting that miR-21 serves as an important regulator of neointimal hyperplasia, which results from an imbalance between SMC proliferation and apoptosis. Indeed, these authors confirmed that PTEN and BCL2, two important signaling molecules associated with SMC growth and apoptosis, were miR-21 targets. In addition, evidence from the study of Davis et al. (2008) showed that miR-21 mediated the TGF-β- and bone morphogenetic protein (BMP)-induced contractile phenotype switch in human SMCs. Meanwhile, miR-21 downregulated PDCD4, which in turn acts as a negative-feedback regulator of smooth muscle contractile genes (Davis et al., 2008). These data together indicate that miR-21 regulates SMC contractile function, proliferation, and apoptosis.

We found that miR-21 expression was substantially increased as AAAs developed in both the porcine pancreatic elastase perfusion and AngII infusion AAA models. PTEN, a key negative regulator of the phosphoinositide 3-kinase pathway, was the only target significantly downregulated and was inversely correlated with miR-21 expression during AAA development and progression. Lentiviral overexpression of miR-21 limited AAA growth, which was associated with increased SMC proliferation and decreased levels of PTEN expression and apoptosis in the aortic wall. In contrast, systemic injections of a locked nucleic acid (LNA)-modified antagomir targeting miR-21 diminished the pro-proliferative impact of downregulated PTEN, leading to a marked increase in AAA size. Our *in vitro* studies also identified the transcription factor NF-κB as a crucial positive regulator of miR-21 expression in vascular cells. Nicotine, IL-6, and AngII were each able to induce miR-21 via the upregulation of NF-κB.

For translational purposes, the utilization of local delivery tools has been discussed previously and is under current investigation by our lab and others (Maegdefessel, 2014). Local delivery into the vasculature and diseased aorta appears feasible by using drug eluting stents and balloons, enabling miRNA-based therapies to avoid off-target effects in the respiratory, renal and cardiovascular system, as well as the liver and the spleen. For miR-21 inhibition, and its effects on SMC proliferation we have utilized an anti-miR-21-eluting stent to effectively prevent experimental in-stent restenosis without significant observable side effects (Wang et al., 2015a). However, to make balloon and/or stent- delivered miRNA modulators a real option for the future, additional obstacles have to taken, including optimal patient selection and timing of the intervention, as well as strategies how to handle disease-related barriers, such as intraluminal thrombi and the varying anatomy of different AAA. In relation to this, the development of novel (ideally patient-like) pre-clinical models of AAA, utilizing large animal models (e.g., landrace pigs and/or Yucatan mini-pigs), which based on their dimension and physiological properties (circulating blood volume, size of the aorta, blood pressure, etc.) are better suited for translational approaches to test novel therapies in aortic diseases.

MIRNAS AND EXTRACELLULAR MATRIX FORMATION

The aortic wall is composed of three layers: the intima, the media, and the adventitia. Medial SMCs and an arrangement of ECM structural proteins, primarily collagen and elastin, are essential for the maintenance of the structure and function of the aorta. During AA development, the integrity of these layers and protein components are disrupted. Degradation of the ECM is one of the characteristics of AAs, yet the mechanisms underlying this process are incompletely understood. It has been suggested that TGF-β signaling plays a key role in ECM dysregulation and AAA development.

Among the miR-15 family members, miR-195 levels were shown to be significantly increased in the aortas of Apo E-deficient mice after AngII infusion. Consistent with the increased levels of miR-195 in dissected human aortas, the direct binding of miR-195 to several ECM transcripts was detected. Based on these findings, Zampetaki et al. (2014) conducted a proteomics analysis of the secretome of murine aortic SMCs after miR-195 manipulation and revealed that miR-195 targets a group of ECM proteins, including collagens, proteoglycans, elastin, and proteins associated with elastic microfibrils. The inhibition of miR-195 *in vivo* led to higher expression levels of aortic elastin, being related to increases in levels of both MMP-2 and MMP-9.

In human plasma, miR-195 expression was shown to lead to an inverse correlation between the presence of AAAs and aortic diameter (Zampetaki et al., 2014). These data indicated that miR-195 may contribute to the pathogenesis of AAAs via ECM dysregulation.

In addition to miR-195, previous data from our lab has illustrated a crucial role for miR-29b in ECM homeostasis and AAA development (Maegdefessel et al., 2012b). The miR-29 family of miRNAs (miR-29a, miR-29b, and miR-29c) have been reported to target various genes that encode ECM proteins involved in fibrotic responses, including several collagen isoforms (e.g., collagen types I and III), fibrillin-1, and elastin (van Rooij et al., 2006). A profibrotic response is usually considered a pathological feature, accompanied by significant malfunctions of affected organs, including the respiratory and renal system, as well as the heart and the liver. However, fibrotic responses and ECM deposition appear essentially beneficial for patients with AAs, based on the fact that one of the hallmarks of AAs is the constant degradation of the ECM.

Our data indicated that miR-29b was the only member of the miR-29 family whose levels were substantially decreased at three different time points during murine AAA development and progression. Anti-miR-29b treatment mainly increased the expression of genes encoding collagen (Col1a1, Col2a1, Col3a1, and Col5a1) and elastin, which accounted for limited aneurysm expansion. In contrast, the overexpression of miR-29b using a

lentiviral vector led to rapid AAA expansion and an increased rate of aortic rupture. Furthermore, human AAA tissue samples displayed a similar pattern of reduced miR-29b expression with increased collagen gene expression in comparison to tissue samples from non-aneurysmal organ donor controls. Furthermore, cell culture studies identified aortic fibroblasts as the likely cell type mediating the profibrotic effects of miR-29b. Interestingly, TGF-β, a validated regulator of tissue fibrosis, can repress miR-29b expression, which suggests a protective role of TGF-β in limiting AAA development. A more detailed discussion of the miR-29 family in relation to aging and TAAs can be found below.

MIRNAS IN TAAS

The miR-143/145 cluster is highly expressed in SMCs; it is one of the most studied miRNAs in the regulation of SMC phenotype switching and vascular disease pathogenesis (Boettger et al., 2009). MiR-145 has been repeatedly shown to promote SMC differentiation and to inhibit SMC proliferation (Cheng et al., 2009; Cordes et al., 2009). Tunica media SMCs have been observed to transform from a contractile phenotype to a synthetic phenotype during thoracic aortic dissection (TAD; Lesauskaite et al., 2001). Elia et al. (2009) also found decreased miR-143 and miR-145 expression levels in human AAs, which subsequently induced structural changes in the aorta, due to the incomplete differentiation of SMCs. In addition, Liao et al. (2011) reported that miR-143 and miR-145 were downregulated in TAD, which may account for the underdifferentiation of SMCs and aortic remodeling.

Apart from the proinflammatory effects elicited by activated macrophages, miR-181b was also shown to be involved in ECM dysregulation during TAA development and progression. Prominent fragmentation of the elastic lamellae, a key feature of TAAs, was abrogated by the inhibition of miR-181b compared with control animals; increased TIMP3 expression and collagen accumulation were also observed (Di Gregoli et al., 2017).

As mentioned above, miR-29 family members have also been shown to participate in TAA development and progression. Boon et al. (2011) managed to link miRNA regulation to aortic dilatation and aging. The authors discovered that elevated expression levels of miR-29 family members were associated with a profound downregulation of numerous ECM components in the aortas of aged mice, as well as in two experimental models of aortic dilation (i.e., AngII perfusion and Fibulin4$^{R/R}$ mice). Consistent with our results in AAAs (Maegdefessel et al., 2012b), LNA-modified antisense oligonucleotide-mediated silencing of miR-29 was found to induce collagen gene isoform expression and inhibit AngII-stimulated dilation of aortas in mice.

In a similar context, Merk and collaborators (Merk et al., 2012) further revealed that miR-29b participates in early aneurysm development in Marfan/Fbn1$^{C1039G/+}$ mice. Blockade of miR-29b prevented early aneurysm development, cell apoptosis, and ECM deficiencies in the aortic root. These data suggest that miR-29 may represent a novel molecular target to augment matrix synthesis and maintain the structural integrity of the vascular wall.

A study from Jones et al. (2011) identified the role of miR-29a in TAA development. A significant inverse relationship between miR-29a and MMP-2 was identified in clinical TAA specimens, indicating that miR-29a may regulate ECM production by targeting MMP-2 during TAA development.

Recently, a new cluster of miRNAs (miR-17-associated miRNAs) was identified in progressive aortic dilation (Wu et al., 2016). Patients with a bicuspid aortic valve (BAV) are at increased risk for progressive aortic dilation associated with ECM degradation, relating to the increased activity of MMPs. In the heart, MMP activity is regulated via miR-17-enforced repression of TIMP, a mechanism the investigators were able to establish for the ascending aorta as well. MiRNA profiling of samples from dilated sections of ascending aortas indicated significantly increased miR-17 cluster expression levels in less dilated aortic segments compared to severely dilated segments. Both TIMP-1 and TIMP-2 were validated as miR-17 targets, and their expression levels were substantially decreased in the less dilated samples. As expected, the subsequent increased activity of MMPs was found to contribute to ECM disruption and aortic dilation. In addition, an miR-17 mimic decreased TIMP-1 and TIMP-2 expression and increased MMP2 activity in SMCs isolated from normal and BAV aortas, whereas the opposite effects were seen with an miR-17 inhibitor, suggesting that the miR-17-TIMP-MMP pathway mediates matrix degradation in progressive aortic dilation in BAV-associated AAs.

LONG NON-CODING RNAS

Long non-coding RNAs (lncRNAs) are generally defined as RNA transcripts with lengths >200 nt that do not encode proteins. They are involved in numerous biological events, such as signaling via scaffolding proteins, shaping nuclear architecture, imprinting genomic loci, and regulating enzymatic activity (Engreitz et al., 2016; **Figure 1**). The aberrant expression or mutation of lncRNA genes has been implicated in various human diseases (Batista and Chang, 2013). However, the functional roles and mechanisms of most lncRNAs remain elusive (Cech and Steitz, 2014).

Particularly in cardiovascular development and diseases, very few lncRNAs have been functionally characterized. Braveheart was the first lncRNA described in the heart, being required for cardiac development (Klattenhoff et al., 2013). Similarly, the lncRNA Fendrr regulates the transcriptional network required for cardiac development via interactions with histone-modifying complexes (polycomb Repressive Complex 2, PRC2 and trithorax group/myeloid/lymphoid or mixed-lineage Leukemia, TrxG/MLL) (Grote et al., 2013). There are other lncRNAs related to the differentiation of human embryonic stem cells, including TERMINATOR, ALIEN, and PUNISHER (Kurian et al., 2015).

During the development of cardiovascular diseases, lncRNAs seem to either serve as potential indicators (biomarkers) or regulators of cell function and disease progression. For instance, Novlnc6 was found to be differentially expressed

in patients with dilated cardiomyopathy (Ounzain et al., 2015), and Hotair levels were reduced in patients with BAV and related valve calcifications (Carrion et al., 2014). The expression levels of the lncRNAs HIF1A antisense RNA (aHIF), antisense non-coding RNA in the INK4 Locus (ANRIL), KCNQ1 opposite strand/antisense transcript 1 (KCNQ1OT1), myocardial infarction associated transcrip (MIAT), and metastasis associated lung adenocarcinoma transcript 1 (MALAT1) may be associated with acute myocardial infarction(Vausort et al., 2014). MALAT1 regulates EC function and vascular inflammation in patients with diabetes-induced vascular complications (Michalik et al., 2014), while MIAT was identified as a competing endogenous RNA, that forms a feedback loop with VEGF and miR-150-5p and controls EC function in diabetic retinopathies (Yan et al., 2015). The long intergenic non-coding RNA (lincRNA)-p21 was shown to repress proliferation and induce apoptosis of SMCs in atherosclerotic plaques (Wu et al., 2014).

One particular lncRNA, H19, appears to have a universal effect on the cardiovascular system. The downregulation of H19 was shown to promote cell proliferation and inhibit cell apoptosis during late-stage cardiac differentiation by regulating the negative role of miR-19b in Sox6 expression (Han et al., 2016). H19 was also shown to mediate the inhibition of melatonin by inducing the premature senescence of c-kit+ cardiac progenitor cells via miR-675 stimulation (Cai et al., 2016). In addition, H19 inhibition was found to decrease human umbilical vein endothelial cells (HUVEC) growth and capillary formation, while the H19-miR-675 axis targets calcium/calmodulin dependent protein kinase II Delta (CaMKIIδ), thus serving as a negative regulator of cardiac hypertrophy (Liu et al., 2016). H19-derived miR-675 was found to aggravate restenosis by targeting PTEN in VSMCs (Lv et al., 2017). These data indicate that H19 participates in cardiac development and related cardiovascular disease processes. The altered DNA methylation of H19 in calcified aortic valve disease was shown to promote mineralization by silencing NOTCH1 (Hadji et al., 2016). LncRNAs that have been studied for their implications in SMC plasticity and AA development and dilation are summarized in **Table 2**.

LNCRNAS AND SMOOTH MUSCLE CELL FATE

The lncRNA ANRIL was identified as a transcript within the chromosome 9p21 locus, in which genetic variants are believed to contribute to the risk of cardiovascular disease (Broadbent et al., 2008). The genomic region (9p21) also contains the cyclin-dependent kinase Inhibitor 2A (CDKN2A) and CDKN2B genes, which encode for the cell cycle regulators p16 (INK4a), p14 (ARF), and p15 (INK4b). Two independent studies by Congrains et al. (2012) and Motterle et al. (2012) demonstrated that the alleles linked to atherosclerosis-related phenotypes and risk of common carotid artery stenosis were consistently associated with lower expression levels of ANRIL. Knockdown of ANRIL

TABLE 2 | LncRNAs involoved in VSMCs and aortic aneurysms.

LncRNAs	Sample studied	Regulation	Related genes	Related Functions	References
ANRIL	human blood, mouse atherosclerotic plaque, HAoSMCs	↓	CDKN2A, CDKN2B, DAB2IP, LRP1, LRPR, CNTN3	Influences CDKN2A/B expression and promotes proliferation of VSMC	Congrains et al., 2012; Motterle et al., 2012
RNCR3	Human blood, mouse atherosclerotic plaque, HAoSMCs, ECs	↑	KLF-2, miR-185-5p	Acts as a ceRNAs, decreases EC and VSMC proliferation	Shan et al., 2016
H19	Balloon-injured artery, HAoSMCs	↑	miR-675	Generates miRNA, Promotes VSMC proliferation	Lv et al., 2017
Lnc-Ang362	mVSMCs	↑	miR-221/222	Produces miRs and promotes VSMC proliferation	Leung et al., 2016
SENCR	HAoSMCs	-	FLI1	Inhibits migration of VSMC	Bell et al., 2014
Lnc-GAS5	mouse ocular vessels, SHR rat artery, HUVECs, HAoSMCs	↓	β-Catenin	Regulates ECs activation and proliferation, VSMC phenotypic conversion, and EC-VSMC communication	Wang et al., 2016
Lnc-MEG3	HAoSMCs	-	p53, MMP-2	Promotes proliferation and migration and decrease apoptosis of VSMC	Liu et al., 2017
MYOSLID	HCASMC	-	MYOCD/serum response factor and TGF-β/SMAD	Regulates VSMC phenotype	Zhao et al., 2016
HIF1A-AS1	Human TAAs serum, HAoSMCs	-	BRG1, Casp3/8, BCL2	Inhibits proliferation and induced apoptosis of VSMC	He et al., 2015; Wang et al., 2015c

ANRIL, antisense non-coding RNA in the INK4 locus; SENCR, smooth muscle and endothelial cell-enriched migration/differentiation-associated lncRNA; GAS5, long noncoding RNA–growth arrest–specific 5; Lnc-MEG3, long noncoding RNA–Maternally expressed gene 3; MYOSLID, MYOcardin-induced smooth muscle lncRNA; HIF1A-AS1, antisense hypoxia inducible factor 1 alpha anti sense RNA; mVSMC, mouse vascular smooth muscle cells; HAoSMCs, human aorta smooth muscle cells; HUVEs, human umbilical vein endothelial cells; HCASMC, human coronary smooth muscle cells; LRP1, low density lipoprotein receptor-related protein 1; LRPR, low density lipoprotein receptor; CDKN, cyclin-dependent kinase inhibitors; DAB2IP, DAB2 interacting protein; CNTN3, contactin-3; KLF-2, Kruppel-like factor 2; FLI1, friend leukemia integration 1 transcription factor; ceRNAs, competing endogenous RNAs; BCL2, B-cell lymphoma 2; BRG1, Brahma-related gene 1; TGF-β, transforming growth factor-β; SMAD, mothers against decapentaplegic homolog.

in SMCs was shown to cause significant variations in the expression of CDKN2A/B and reduced cell growth, suggesting that ANRIL may have pro-proliferation effects on SMCs. Leeper and colleagues have shown that loss of CDKN2B is crucial for aneurysm development via promoting p53-dependent SMC apoptosis (Leeper et al., 2013). The role of ANRIL itself in AA development needs to be investigated further.

LncRNA-RNCR3 is another lncRNA that has been linked to atherosclerosis-related vascular dysfunction (Shan et al., 2016). RNCR3 expression is significantly upregulated in mouse and human aortic atherosclerotic lesions, and inhibition of RNCR3 was shown to be sufficient to accelerate the development of atherosclerosis, aggravate hypercholesterolemia and inflammatory factor releases, and decrease EC and VSMC proliferation. Mechanistically, RNCR3 acts as a competing endogenous RNA (ceRNA) and forms a feedback loop with Kruppel-like factor 2 and miR-185-5p to regulate cell function. This study illuminated one of the most common mechanisms by which lncRNAs can act as ceRNAs to decrease the targeting concentration of miRNA, ultimately resulting in the derepression of other mRNAs with common miRNA response elements (Tay et al., 2014).

Another proposed mechanism of action for lncRNAs describes how these molecules serve as hosts for miRNA transcription. Lv et al. (2017) found that lncRNA H19 and H19-derived miR-675 are overexpressed in the neointima of balloon-injured arteries. In principal, they were able to show that lncRNA H19 promoted the proliferation of SMCs in an miR-675/PTEN-dependent manner. Similar roles were detected for the lnc-Ang362, which is substantially increased in response to AngII treatment (Leung et al., 2016). Knockdown of lnc-Ang362 reduces the expression of miR-222 and miR-221, suggesting its function as a miRNA host transcript. In addition, a reduction in the transcript levels of lnc-Ang362 was associated with a decrease in cell proliferation, suggesting that it plays a role in cell growth. These data evoke tremendous interest, considering that one of the most popular murine models of AAA development is AngII infusion in Apo $E^{-/-}$ mice.

Smooth muscle and endothelial cell enriched migration/differentiation-associated long non-coding RNA (SENCR) was identified from the RNA sequencing of human coronary artery SMCs (Bell et al., 2014). SENCR is transcribed in the cytoplasm from the 5′ end of the friend leukemia integration 1 (FLI1) gene and exists as two splice variants. Experimental knockdown of SENCR has been shown to result in the decreased expression of myocardin and numerous smooth muscle contractile genes, and the increased expression of a number of promigratory genes. Results from loss-of-function studies support the role of Sencr as an inhibitor of SMC migration. Whether this property of phenotype regulation plays a role in AA development awaits further investigation.

In terms of SMC phenotypic switching, lncRNA-growth arrest-specific 5 (GAS5) was reported to be involved in hypertension-related vascular remodeling via changes in endothelial activation and proliferation, SMC phenotype

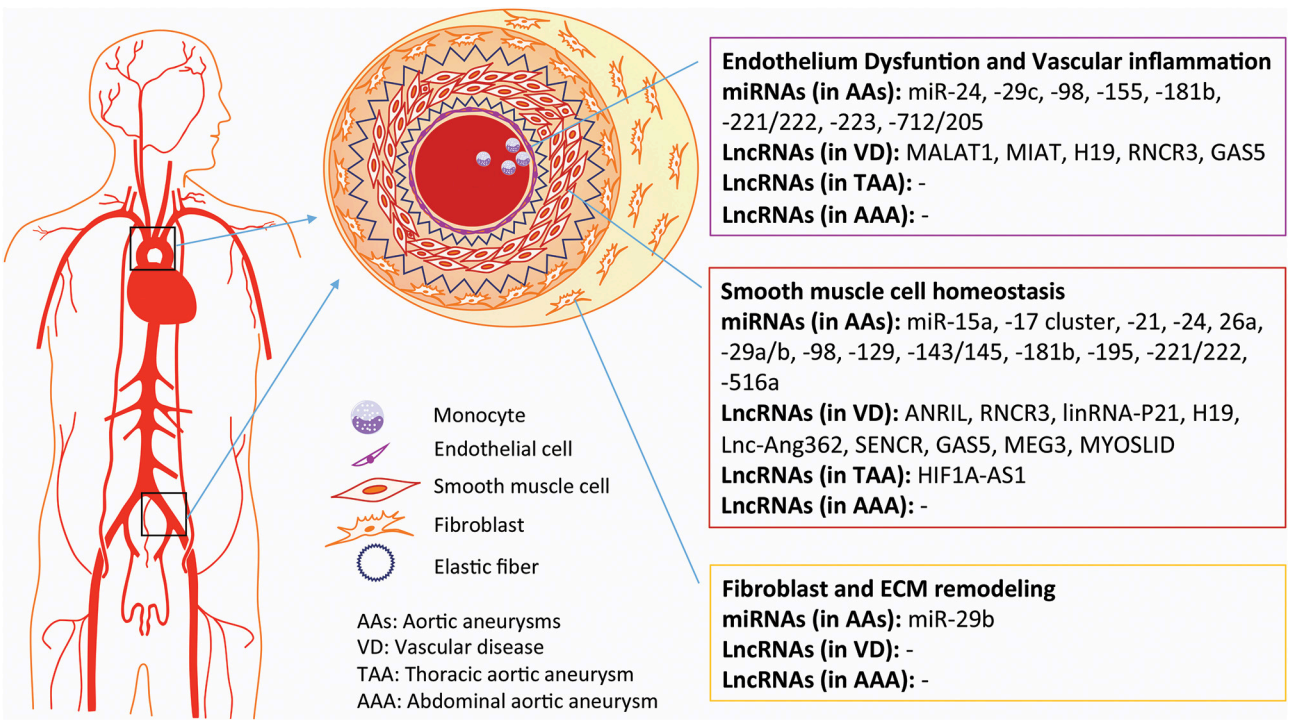

FIGURE 2 | Non-coding RNAs involved in vascular disease and aortic aneurysms.

conversion, and EC-VSMC communication, primarily through β-catenin signaling (Wang et al., 2016).

Recently, Zhao et al. (2016) described a novel lncRNA, named myocardin-induced smooth muscle lncRNA (MYOSLID), which is related to SMC phenotype regulation. MYOSLID, a direct transcriptional target of both the MYOCD/serum response factor (SRF) and TGF-β/SMAD pathways, promotes SMC differentiation and inhibits SMC proliferation. Depletion of MYOSLID in SMCs was shown to not only disrupt actin stress fiber formation and block nuclear translocation of MYOCD-related transcription factor A (MKL1), but was also found to abrogate TGF-β1-induced SMAD2 phosphorylation. These data suggest that MYOSLID may play a role in AA development via the crosstalk between the dysregulation of the VSMC phenotype and TGF-β signaling.

LNCRNAS AND AAS

HIF1 alpha-antisense RNA 1 (HIF1A-AS1) was the first reported lncRNA that was found to play a role in TAA pathogenesis (Wang et al., 2015c). The expression of HIF1A-AS1 was shown to be regulated by Brahma-related gene 1, whose levels are elevated in TAAs. Suppression of HIF1A-AS1 was found to result in reduced apoptosis and increased proliferation of VSMCs. Furthermore, the expression of HIF1a-AS1 was reported to be significantly increased in sera from TAA patients (He et al., 2015). Knockdown of HIF1A-AS1 was shown to decrease the expression of caspase-3 and caspase-8, increase the expression of BCL2, and attenuate palmitic acid (PA)-induced cell apoptosis in SMCs. Loeys-Dietz syndrome (LDS) is an autosomal dominant genetic connective tissue disorder, and most LDS patients will commonly develop an aneurysm in the aortic root. Yu et al. (2015) found that the lncRNA AK056155 was up-regulated in LDS specimen, which correlated with an activation of the AKT/PI3K and TGF-β1 signaling.

Currently, there are no available publications of the roles of lncRNAs in AAAs. One paper from Falak et al. (2014) suggested that a putative lincRNA within the linkage region of protease inhibitor 15 (Pi15), a candidate gene marker for the risk of abdominal aortic internal elastic laminal ruptures in rats, may be involved in the regulation of Pi15 expression, providing some clues about the roles of lncRNAs in the initiation of human AAAs.

SUMMARY AND PERSPECTIVE

Today, undiscovered asymptomatic AAs are still considered to be ticking time bombs, owing to their incredibly high rates of mortality (∼80%) when ruptured. Current clinical management of AAs, based only on size, is not satisfactory. Thus, extraordinary efforts have been launched to determine the pathophysiological characteristics and molecular events of the diseased aorta. Increasing evidence suggests that ncRNAs play crucial roles throughout AA development and might serve as therapeutic targets (**Figure 2**). As mentioned above, the pathogenesis and molecular mechanisms of TAAs and AAAs are distinguishable, suggesting that the roles of ncRNAs will be as well. As the field of miRNAs gradually matures, some promising candidates, such as miR-122, miR-21, miR-15, and miR-34 (Janssen et al., 2013; Christopher et al., 2016), may be further investigated in preclinical and clinical trials. The combined modulation of miRNAs in specific cell subtypes, like increasing SMC survival by miR-21 and inducing adventitial fibrosis by inbibiting miR-29b, would be worthwhile investments in AAA therapy.

The field of lncRNAs is still in its infancy and faces many challenges. First, the conservation of lncRNAs among species is not as high as that of miRNAs, and humanized models or organoid cultures will be necessary to study primate-specific lncRNAs. Second, mechanisms of action of lncRNAs are complicated and may be organ- or cell-specific. Third, the molecular mechanisms may be broadly diverse, based on the subcellular localization of lncRNAs and the existence of disparate transcriptional variants. Single-cell profiling and single-molecule imaging techniques are crucial to the detailed identification of components of these processes and machineries. Finally, a more efficient and specific delivery system is required for the modulation of lncRNAs *in vivo* to minimize off-targets and translate findings into clinical practice.

AUTHOR CONTRIBUTIONS

Both authors listed contributed to this manuscript by conceptually designing and drafting the manuscript. Both authors have seen and approved the article for submission to Frontiers in Physiology.

ACKNOWLEDGMENTS

Research in the Maegdefessel laboratory on non-coding RNAs in cardiovascular disease is supported by the Swedish Heart-Lung-Foundation (20120615, 20130664, and 20140186), the Ragnar Söderberg Foundation (M55/14), the Swedish Research Council (2015-03140), the European Research Council (ERC-StG NORVAS), and a DZHK Junior Research Group (JRG_LM_MRI).

REFERENCES

Ailawadi, G., Moehle, C. W., Pei, H., Walton, S. P., Yang, Z., Kron, I. L. et al. (2009). Smooth muscle phenotypic modulation is an early event in aortic aneurysms. *J. Thorac. Cardiovasc. Surg.* 138, 1392–1399. doi: 10.1016/j.jtcvs.2009.07.075

Bartel, D. P. (2004). MicroRNAs, genomics, biogenesis, mechanism, and function. *Cell* 116, 281–297. doi: 10.1016/S0092-8674(04)00045-5

Bartel, D. P. (2009). MicroRNAs, target recognition and regulatory functions. *Cell* 136, 215–233. doi: 10.1016/j.cell.2009.01.002

Batista, P. J., and Chang, H. Y. (2013). Long noncoding RNAs, cellular address codes in development and disease. *Cell* 152, 1298–1307. doi: 10.1016/j.cell.2013.02.012

Bell, R. D., Long, X., Lin, M., Bergmann, J. H., Nanda, V. Cowan, S. L., et al. (2014). Identification and initial functional characterization of a human vascular cell-enriched long noncoding RNA. *Arterioscler Thromb. Vasc. Biol.* 34, 1249–1259. doi: 10.1161/ATVBAHA.114.303240

Biros, E., Moran, C. S., Wang, Y., Walker, P. J., Cardinal, J., and Golledge, J. (2014). microRNA profiling in patients with abdominal aortic aneurysms,

the significance of miR-155. *Clin. Sci.* 126, 795–803. doi: 10.1042/CS20130599

Boettger, T., Beetz, N., Kostin, S., Schneider, J., Kruger, M., Hein, L., et al. (2009). Acquisition of the contractile phenotype by murine arterial smooth muscle cells depends on the Mir143/145 gene cluster. *J. Clin. Invest.* 119, 2634–2647. doi: 10.1172/JCI38864

Boon, R. A., Seeger, T., Heydt, S., Fischer, A., Hergenreider, E., Vinciguerra, M., et al. (2011). MicroRNA-29 in aortic dilation, implications for aneurysm formation. *Circ. Res.* 109, 1115–1119. doi: 10.1161/CIRCRESAHA.111.255737

Broadbent, H. M., Peden, J. F., Lorkowski, S., Goel, A., Ongen, H., Green, F., et al. (2008). Susceptibility to coronary artery disease and diabetes is encoded by distinct, tightly linked SNPs in the ANRIL locus on chromosome 9p. *Hum. Mol. Genet.* 17, 806–814. doi: 10.1093/hmg/ddm352

Busch, A., Busch, M., Scholz, C. J., Kellersmann, R., Otto, C., Chernogubova, E., et al. (2016). Aneurysm miRNA Signature Differs, Depending on Disease Localization and Morphology. *Int. J. Mol. Sci.* 17. doi: 10.3390/ijms17010081

Cai, B., Ma, W., Bi, C., Yang, F., Zhang, L., Han, Z., et al. (2016). Long noncoding RNA H19 mediates melatonin inhibition of premature senescence of c-kit(+) cardiac progenitor cells by promoting miR-675. *J. Pineal Res.* 61, 82–95. doi: 10.1111/jpi.12331

Carrion, K., Dyo, J., Patel, V., Sasik, R., Mohamed, S. A., Hardiman, G., et al. (2014). The long non-coding HOTAIR is modulated by cyclic stretch and WNT/beta-CATENIN in human aortic valve cells and is a novel repressor of calcification genes. *PLoS ONE* 9:e96577. doi: 10.1371/journal.pone.0096577

Cech, T. R., and Steitz, J. A. (2014). The noncoding RNA revolution-trashing old rules to forge new ones. *Cell* 157, 77–94. doi: 10.1016/j.cell.2014.03.008

Cheng, Y., Liu, X., Yang, J., Lin, Y., Xu, D. Z., Lu, Q., et al. (2009). MicroRNA-145, a novel smooth muscle cell phenotypic marker and modulator, controls vascular neointimal lesion formation. *Circ. Res.* 105, 158–166. doi: 10.1161/CIRCRESAHA.109.197517

Christopher, A. F., Kaur, R. P., Kaur, G., Kaur, A., Gupta, V., and Bansal, P. (2016). MicroRNA therapeutics, Discovering novel targets and developing specific therapy. *Perspect. Clin. Res.* 7, 68–74. doi: 10.4103/2229-3485.179431

Congrains, A., Kamide, K., Oguro, R., Yasuda, O., Miyata, K., Yamamoto, E., et al. (2012). Genetic variants at the 9p21 locus contribute to atherosclerosis through modulation of ANRIL and CDKN2A/B. *Atherosclerosis* 220, 449–455. doi: 10.1016/j.atherosclerosis.2011.11.017

Cordes, K. R., Sheehy, N. T., White, M. P., Berry, E. C., Morton, S. U., Muth, A. N., et al. (2009). miR-145 and miR-143 regulate smooth muscle cell fate and plasticity. *Nature* 460, 705–710. doi: 10.1038/nature08195

Davis, B. N., Hilyard, A. C., Lagna, G., and Hata, A. (2008). SMAD proteins control DROSHA-mediated microRNA maturation. *Nature* 454, 56–61. doi: 10.1038/nature07086

Davis, B. N., Hilyard, A. C., Nguyen, P. H., Lagna, G., and Hata, A. (2009). Induction of microRNA-221 by platelet-derived growth factor signaling is critical for modulation of vascular smooth muscle phenotype. *J. Biol. Chem.* 284, 3728–3738. doi: 10.1074/jbc.M808788200

Di Gregoli, K., Mohamad Anuar, N. N., Bianco, R., White, S. J., Newby, A. C., Muth, A. N., et al. (2017). MicroRNA-181b Controls Atherosclerosis and Aneurysms Through Regulation of TIMP-3 and Elastin. *Circ. Res.* 120, 49–65. doi: 10.1161/CIRCRESAHA.116.309321

Djuranovic, S., Nahvi, A., and Green, R. (2011). A parsimonious model for gene regulation by miRNAs. *Science* 331, 550–553. doi: 10.1126/science.1191138

Ebert, M. S., and Sharp, P. A. (2012). Roles for microRNAs in conferring robustness to biological processes. *Cell* 149, 515–524. doi: 10.1016/j.cell.2012.04.005

Elefteriades, J. A., Sang, A., Kuzmik, G., and Hornick, M. (2015). Guilt by association, paradigm for detecting a silent killer (thoracic aortic aneurysm). *OpenHeart* 2:e000169. doi: 10.1136/openhrt-2014-000169

Elia, L., Quintavalle, M., Zhang, J., Contu, R., Cossu, L., Latronico, M. V., et al. (2009). The knockout of miR-143 and -145 alters smooth muscle cell maintenance and vascular homeostasis in mice, correlates with human disease. *Cell Death Differ.* 16, 1590–1598. doi: 10.1038/cdd.2009.153

Engreitz, J. M., Ollikainen, N., and Guttman, M. (2016). Long non-coding RNAs, spatial amplifiers that control nuclear structure and gene expression. *Nat. Rev. Mol. Cell Biol.* 17, 756–770. doi: 10.1038/nrm.2016.126

Esteller, M. (2011). Non-coding RNAs in human disease. *Nat. Rev. Genet.* 12, 861–874. doi: 10.1038/nrg3074

Falak, S., Schafer, S., Baud, A., Hummel, O., Schulz, H., Gauguier, D., et al. (2014). Protease inhibitor 15, a candidate gene for abdominal aortic internal elastic lamina ruptures in the rat. *Physiol. Genomics* 46, 418–428. doi: 10.1152/physiolgenomics.00004.2014

Fiedler, J., Jazbutyte, V., Kirchmaier, B. C., Gupta, S. K., Lorenzen, J., Hartmann, D., et al. (2011). MicroRNA-24 regulates vascularity after myocardial infarction. *Circulation* 124, 720–730. doi: 10.1161/CIRCULATIONAHA.111.039008

Fu, X. D. (2014). Non-coding RNA, a new frontier in regulatory biology. *Natl. Sci. Rev.* 1, 190–204. doi: 10.1093/nsr/nwu008

Gao, P., Si, J., Yang, B., and Yu, J. (2017). Upregulation of MicroRNA-15a Contributes to Pathogenesis of Abdominal Aortic Aneurysm (AAA) by Modulating the Expression of Cyclin-Dependent Kinase Inhibitor 2B (CDKN2B). *Med. Sci. Monit.* 23, 881–888. doi: 10.12659/MSM.898233

Geng, S., Chen, K., Yuan, R., Peng, L., Maitra, U., Diao, N., et al. (2016). The persistence of low-grade inflammatory monocytes contributes to aggravated atherosclerosis. *Nat. Commun.* 7:13436. doi: 10.1038/ncomms13436

Golledge, J., Muller, J., Daugherty, A., and Norman, P. (2006). Abdominal aortic aneurysm, pathogenesis and implications for management. *Arterioscler. Thromb. Vasc. Biol.* 26, 2605–2613. doi: 10.1161/01.ATV.0000245819.32762.cb

Golledge, J., and Norman, P. E. (2011). Current status of medical management for abdominal aortic aneurysm. *Atherosclerosis* 217, 57–63. doi: 10.1016/j.atherosclerosis.2011.03.006

Grote, P., Wittler, L., Hendrix, D., Koch, F., Wahrisch, S., Beisaw, A., et al. (2013). The tissue-specific lncRNA Fendrr is an essential regulator of heart and body wall development in the mouse. *Dev. Cell* 24, 206–214. doi: 10.1016/j.devcel.2012.12.012

Guo, D. C., Papke, C. L., He, R., and Milewicz, D. M. (2006). Pathogenesis of thoracic and abdominal aortic aneurysms. *Ann. N. Y. Acad. Sci.* 1085, 339–352. doi: 10.1196/annals.1383.013

Habashi, J. P., Judge, D. P., Holm, T. M., Cohn, R. D., Loeys, B. L., Cooper, T. K., et al. (2006). Losartan, an AT1 antagonist, prevents aortic aneurysm in a mouse model of Marfan syndrome. *Science* 312, 117–121. doi: 10.1126/science.1124287

Hadji, F., Boulanger, M. C., Guay, S. P., Gaudreault, N., Amellah, S., Mkannez, G., et al. (2016). Altered DNA Methylation of Long Noncoding RNA H19 in Calcific Aortic Valve Disease Promotes Mineralization by Silencing NOTCH1. *Circulation* 134, 1848–1862. doi: 10.1161/CIRCULATIONAHA.116.023116

Han, Y., Xu, H., Cheng, J., Zhang, Y., Gao, C., et al. (2016). Downregulation of long non-coding RNA H19 promotes P19CL6 cells proliferation and inhibits apoptosis during late-stage cardiac differentiation via miR-19b-modulated Sox6. *Cell Biosci.* 6:58. doi: 10.1186/s13578-016-0123-5

Hatziapostolou, M., Polytarchou, C., Aggelidou, E., Drakaki, A., Poultsides, G. A., Jaeger, S. A., et al. (2011). An HNF4α-miRNA inflammatory feedback circuit regulates hepatocellular oncogenesis. *Cell* 147, 1233–1247. doi: 10.1016/j.cell.2011.10.043

He, Q., Tan, J., Yu, B., Shi, W., and Liang, K. (2015). Long noncoding RNA HIF1A-AS1A reduces apoptosis of vascular smooth muscle cells, implications for the pathogenesis of thoracoabdominal aorta aneurysm. *Pharmazie* 70, 310–315.

Henderson, E. L., Geng, Y. J., Sukhova, G. K., Whittemore, A. D., Knox, J., and Libby, P. (1999). Death of smooth muscle cells and expression of mediators of apoptosis by T lymphocytes in human abdominal aortic aneurysms. *Circulation* 99, 96–104. doi: 10.1161/01.CIR.99.1.96

Holm, T. M., Habashi, J. P., Doyle, J. J., Bedja, D., Chen, Y., van Erp, C., et al. (2011). Noncanonical TGFbeta signaling contributes to aortic aneurysm progression in Marfan syndrome mice. *Science* 332, 358–361. doi: 10.1126/science.1192149

Horita, H. N., Simpson, P. A., Ostriker, A., Furgeson, S., Van Putten, V., Weiser-Evans, M. C., et al. (2011). Serum response factor regulates expression of phosphatase and tensin homolog through a microRNA network in vascular smooth muscle cells. *Arterioscler. Thromb. Vasc. Biol.* 31, 2909–2919. doi: 10.1161/ATVBAHA.111.233585

Hutvagner, G., and Zamore, P. D. (2002). A microRNA in a multiple-turnover RNAi enzyme complex. *Science* 297, 2056–2060. doi: 10.1126/science.1073827

Isselbacher, E. M., Lino Cardenas, C. L., and Lindsay, M. E. (2016). Hereditary Influence in Thoracic Aortic Aneurysm and Dissection. *Circulation* 133, 2516–2528. doi: 10.1161/CIRCULATIONAHA.116.009762

Janssen, H. L., Reesink, H. W., Lawitz, E. J., Zeuzem, S., Rodriguez-Torres, M., Patel, K., et al. (2013). Treatment of HCV infection by targeting microRNA. *N. Engl. J. Med.* 368, 1685–1694. doi: 10.1056/NEJMoa1209026

Ji, R., Cheng, Y., Yue, J., Yang, J., Liu, X., Chen, H., et al. (2007). MicroRNA expression signature and antisense-mediated depletion reveal an essential role of MicroRNA in vascular neointimal lesion formation. *Circ. Res.* 100, 1579–1588. doi: 10.1161/CIRCRESAHA.106.141986

Jiao, T., Yao, Y., Zhang, B., Hao, D. C., Sun, Q. F., Li, J. B., et al. (2017). Role of MicroRNA-103a Targeting ADAM10 in Abdominal Aortic Aneurysm. *Biomed. Res. Int.* 2017:9645874. doi: 10.1155/2017/9645874

Jingjing, Z., Nan, Z., Wei, W., Qinghe, G., Weijuan, W., Peng, W., et al. (2017). MicroRNA-24 Modulates *Staphylococcus aureus*-Induced Macrophage Polarization by Suppressing CHI3L1. *Inflammation* 40, 995–1005. doi: 10.1007/s10753-017-0543-3

Jones, J. A., Stroud, R. E., O'Quinn, E. C., Black, L. E., Barth, J. L., Elefteriades, J. A., et al. (2011). Selective microRNA suppression in human thoracic aneurysms, relationship of miR-29a to aortic size and proteolytic induction. *Circ. Cardiovasc. Genet.* 4, 605–613. doi: 10.1161/CIRCGENETICS.111.960419

Kanematsu, Y., Kanematsu, M., Kurihara, C., Tada, Y., Tsou, T. L., van Rooijen, N., et al. (2011). Critical roles of macrophages in the formation of intracranial aneurysm. *Stroke* 42, 173–178. doi: 10.1161/STROKEAHA.110.590976

Kent, K. C. (2014). Clinical practice. Abdominal aortic aneurysms. *N. Engl. J. Med.* 371, 2101–2108. doi: 10.1056/NEJMcp1401430

Kim, C. W., Kumar, S., Son, D. J., Jang, I. H., Griendling, K. K., and Jo, H. (2014). Prevention of abdominal aortic aneurysm by anti-microRNA-712 or anti-microRNA-205 in angiotensin II-infused mice. *Arterioscler. Thromb. Vasc. Biol.* 34, 1412–1421. doi: 10.1161/ATVBAHA.113.303134

Kin, K., Miyagawa, S., Fukushima, S., Shirakawa, Y., Torikai, K., Shimamura, K., et al. (2012). Tissue- and plasma-specific MicroRNA signatures for atherosclerotic abdominal aortic aneurysm. *J. Am. Heart Assoc.* 1:e000745. doi: 10.1161/jaha.112.000745

Klattenhoff, C. A., Scheuermann, J. C., Surface, L. E., Bradley, R. K., Fields, P. A., Steinhauser, M. L., et al. (2013). Braveheart, a long noncoding RNA required for cardiovascular lineage commitment. *Cell* 152, 570–583. doi: 10.1016/j.cell.2013.01.003

Kurian, L., Aguirre, A., Sancho-Martinez, I., Benner, C., Hishida, T., et al. (2015). Identification of novel long noncoding RNAs underlying vertebrate cardiovascular development. *Circulation* 131, 1278–1290. doi: 10.1161/CIRCULATIONAHA.114.013303

Lee, H. J., Yi, J. S., Lee, H. J., Lee, I. W., Park, K. C., and Yang, J. H. (2013). Dysregulated expression profiles of MicroRNAs of experimentally induced cerebral aneurysms in rats. *J. Korean Neurosurg. Soc.* 53, 72–76. doi: 10.3340/jkns.2013.53.2.72

Lee, Y., Ahn, C., Han, J., Choi, H., Kim, J., Yim, J., et al. (2003). The nuclear RNase III Drosha initiates microRNA processing. *Nature* 425, 415–419. doi: 10.1038/nature01957

Lee, Y., Jeon, K., Lee, J. T., Kim, S., and Kim, V. N. (2002). MicroRNA maturation, stepwise processing and subcellular localization. *EMBO J.* 21, 4663–4670. doi: 10.1093/emboj/cdf476

Leeper, N. J., Raiesdana, A., Kojima, Y., Chun, H. J., Azuma, J., Maegdefessel, L., et al. (2011). MicroRNA-26a is a novel regulator of vascular smooth muscle cell function. *J. Cell. Physiol.* 226, 1035–1043. doi: 10.1002/jcp.22422

Leeper, N. J., Raiesdana, A., Kojima, Y., Kundu, R. K., Cheng, H., Maegdefessel, L., et al. (2013). Loss of CDKN2B promotes p53-dependent smooth muscle cell apoptosis and aneurysm formation. *Arterioscler. Thromb. Vasc. Biol.* 33, e1–e10. doi: 10.1161/ATVBAHA.112.300399

Lesauskaite, V., Tanganelli, P., Sassi, C., Neri, E., Diciolla, F., Ivanoviene, L., et al. (2001). Smooth muscle cells of the media in the dilatative pathology of ascending thoracic aorta, morphology, immunoreactivity for osteopontin, matrix metalloproteinases, and their inhibitors. *Hum. Pathol.* 32, 1003–1011. doi: 10.1053/hupa.2001.27107

Leung, A., Stapleton, K., and Natarajan, R. (2016). Functional Long Non-coding RNAs in Vascular Smooth Muscle Cells. *Curr. Top. Microbiol. Immunol.* 394, 127–141. doi: 10.1007/82_2015_441

Li, X., Zhao, G., Zhang, J., Duan, Z., and Xin, S. (2013). Prevalence and trends of the abdominal aortic aneurysms epidemic in general population–a meta-analysis. *PLoS ONE* 8:e81260. doi: 10.1371/journal.pone.0081260

Liao, M., Zou, S., Weng, J., Hou, L., Yang, L., Zhao, Z., et al. (2011). A microRNA profile comparison between thoracic aortic dissection and normal thoracic aorta indicates the potential role of microRNAs in contributing to thoracic aortic dissection pathogenesis. *J. Vasc. Surg.* 53, 1341–1349 e3. doi: 10.1016/j.jvs.2010.11.113

Licholai, S., Szczeklik, W., and Sanak, M. (2016). miR-29c-3p is an effective biomarker of abdominal aortic aneurysm in patients undergoing elective surgery. *Microrna* 5, 124–131. doi: 10.2174/2211536605666160901103754

Lindsay, M. E., and Dietz, H. C. (2011). Lessons on the pathogenesis of aneurysm from heritable conditions. *Nature* 473, 308–316. doi: 10.1038/nature10145

Liu, L., An, X., Li, Z., Song, Y., Li, L., Zuo, S., et al. (2016). The H19 long noncoding RNA is a novel negative regulator of cardiomyocyte hypertrophy. *Cardiovasc. Res.* 111, 56–65. doi: 10.1093/cvr/cvw078

Liu, W., Liu, X., Luo, M., Liu, X., Luo, Q., Tao, H., et al. (2017). dNK derived IFN-gamma mediates VSMC migration and apoptosis via the induction of LncRNA MEG3, A role in uterovascular transformation. *Placenta* 50, 32–39. doi: 10.1016/j.placenta.2016.12.023

Liu, X., Cheng, Y., Yang, J., Krall, T. J., Huo, Y., and Zhang, C. (2010). An essential role of PDCD4 in vascular smooth muscle cell apoptosis and proliferation, implications for vascular disease. *Am. J. Physiol. Cell Physiol.* 298, C1481–C1488. doi: 10.1152/ajpcell.00413.2009

Liu, X., Cheng, Y., Yang, J., Xu, L., and Zhang, C. (2012). Cell-specific effects of miR-221/222 in vessels, molecular mechanism and therapeutic application. *J. Mol. Cell. Cardiol.* 52, 245–255. doi: 10.1016/j.yjmcc.2011.11.008

Lloyd-Jones, D., Adams, R., Carnethon, M., De Simone, G., Ferguson, T. B., Flegal, K., et al. (2009). Heart disease and stroke statistics–2009 update, a report from the American Heart Association Statistics Committee and Stroke Statistics Subcommittee. *Circulation* 119, 480–486. doi: 10.1161/CIRCULATIONAHA.108.191259

Lv, J., Wang, L., Zhang, J., Lin, R., Wang, L., Sun, W., et al. (2017). Long noncoding RNA H19-derived miR-675 aggravates restenosis by targeting PTEN. *Biochem. Biophys. Res. Commun.* doi: 10.1016/j.bbrc.2017.01.011. [Epub ahead of print].

Maegdefessel, L. (2014). The emerging role of microRNAs in cardiovascular disease. *J. Intern. Med.* 276, 633–644. doi: 10.1111/joim.12298

Maegdefessel, L., Azuma, J., Toh, R., Deng, A., Merk, D. R., Raiesdana, A., et al. (2012a). MicroRNA-21 blocks abdominal aortic aneurysm development and nicotine-augmented expansion. *Sci. Transl. Med.* 4:122ra22. doi: 10.1126/scitranslmed.3003441

Maegdefessel, L., Azuma, J., Toh, R., Merk, D. R., Deng, A., Chin, J. T., et al. (2012b). Inhibition of microRNA-29b reduces murine abdominal aortic aneurysm development. *J. Clin. Invest.* 122, 497–506. doi: 10.1172/JCI61598

Maegdefessel, L., Spin, J. M., Adam, M., Raaz, U., Toh, R., Nakagami, F., et al. (2013). Micromanaging abdominal aortic aneurysms. *Int. J. Mol. Sci.* 14, 14374–14394. doi: 10.3390/ijms140714374

Maegdefessel, L., Spin, J. M., Raaz, U., Eken, S. M., Toh, R., et al. (2014). miR-24 limits aortic vascular inflammation and murine abdominal aneurysm development. *Nat. Commun.* 5:5214. doi: 10.1038/ncomms6214

Mendell, J. T., and Olson, E. N. (2012). MicroRNAs in stress signaling and human disease. *Cell* 148, 1172–1187. doi: 10.1016/j.cell.2012.02.005

Merk, D. R., Chin, J. T., Dake, B. A., Maegdefessel, L., Miller, M. O., et al. (2012). miR-29b participates in early aneurysm development in Marfan syndrome. *Circ. Res.* 110, 312–324. doi: 10.1161/CIRCRESAHA.111.253740

Michalik, K. M., You, X., Manavski, Y., Doddaballapur, A., Zornig, M., et al. (2014). Long noncoding RNA MALAT1 regulates endothelial cell function and vessel growth. *Circ. Res.* 114, 1389–1397. doi: 10.1161/CIRCRESAHA.114.303265

Milewicz, D. M., Guo, D. C., Tran-Fadulu, V., Lafont, A. L., Papke, C. L., Inamoto, S., et al. (2008). Genetic basis of thoracic aortic aneurysms and dissections, focus on smooth muscle cell contractile dysfunction. *Annu. Rev. Genomics Hum. Genet.* 9, 283–302. doi: 10.1146/annurev.genom.8.080706.092303

Motterle, A., Pu, X., Wood, H., Xiao, Q., Gor, S., Ng, F. L., et al. (2012). Functional analyses of coronary artery disease associated variation on chromosome 9p21 in vascular smooth muscle cells. *Hum. Mol. Genet.* 21, 4021–4029. doi: 10.1093/hmg/dds224

Neptune, E. R., Frischmeyer, P. A., Arking, D. E., Myers, L., Bunton, T. E., Gayraud, B., et al. (2003). Dysregulation of TGF-beta activation contributes to pathogenesis in Marfan syndrome. *Nat. Genet.* 33, 407–411. doi: 10.1038/ng1116

Ounzain, S., Micheletti, R., Beckmann, T., Schroen, B., Alexanian, M., Pezzuto, I., et al. (2015). Genome-wide profiling of the cardiac transcriptome after myocardial infarction identifies novel heart-specific long non-coding RNAs. *Eur. Heart J.* 36, 353–368a. doi: 10.1093/eurheartj/ehu180

Pua, H. H., Steiner, D. F., Patel, S., Gonzalez, J. R., Ortiz-Carpena, J. F., Kageyama, R., et al. (2016). MicroRNAs 24 and 27 suppress allergic inflammation and target a network of regulators of T Helper 2 cell-associated cytokine production. *Immunity* 44, 821–832. doi: 10.1016/j.immuni.2016.01.003

Qian, L., Van Laake, L. W., Huang, Y., Liu, S., Wendland, M. F., and Srivastava, D. (2011). miR-24 inhibits apoptosis and represses Bim in mouse cardiomyocytes. *J. Exp. Med.* 208, 549–560. doi: 10.1084/jem.20101547

Rehli, M., Niller, H. H., Ammon, C., Langmann, S., Schwarzfischer, L., Andreesen, R., et al. (2003). Transcriptional regulation of CHI3L1, a marker gene for late stages of macrophage differentiation. *J. Biol. Chem.* 278, 44058–44067. doi: 10.1074/jbc.M306792200

Renard, M., Callewaert, B., Baetens, M., Campens, L., MacDermot, K., Fryns, J. P., et al. (2013). Novel MYH11 and ACTA2 mutations reveal a role for enhanced TGFbeta signaling in FTAAD. *Int. J. Cardiol.* 165, 314–321. doi: 10.1016/j.ijcard.2011.08.079

Schanzer, A., Simons, J. P., Flahive, J., Durgin, J., Aiello, F. A., Doucet, D., et al. (2017). Outcomes of fenestrated and branched endovascular repair of complex abdominal and thoracoabdominal aortic aneurysms. *J. Vasc. Surg.* S0741-5214(17)30101-5. doi: 10.1016/j.jvs.2016.12.111

Shan, K., Jiang, Q., Wang, X. Q., Wang, Y. N., Yang, H., Yao, M. D., et al. (2016). Role of long non-coding RNA-RNCR3 in atherosclerosis-related vascular dysfunction. *Cell Death Dis.* 7, e2248. doi: 10.1038/cddis.2016.145

Shimizu, K., Mitchell, R. N., and Libby, P. (2006). Inflammation and cellular immune responses in abdominal aortic aneurysms. *Arterioscler. Thromb. Vasc. Biol.* 26, 987–994. doi: 10.1161/01.ATV.0000214999.12921.4f

Sun, J., Sukhova, G. K., Yang, M., Wolters, P. J., MacFarlane, L. A., Libby, P., et al. (2007). Mast cells modulate the pathogenesis of elastase-induced abdominal aortic aneurysms in mice. *J. Clin. Invest.* 117, 3359–3368. doi: 10.1172/JCI 31311

Tay, Y., Rinn, J., and Pandolfi, P. P. (2014). The multilayered complexity of ceRNA crosstalk and competition. *Nature* 505, 344–352. doi: 10.1038/nature12986

Thulasingam, S., Massilamany, C., Gangaplara, A., Dai, H., Yarbaeva, S., Subramaniam, S., et al. (2011). miR-27b*, an oxidative stress-responsive microRNA modulates nuclear factor-kB pathway in RAW 264.7 cells. *Mol. Cell. Biochem.* 352, 181–188. doi: 10.1007/s11010-011-0752-2

Tung Chan, C. Y., Yee Cheuk, B. L., and Keung Cheng, S. W. (2017). Abdominal aortic aneurysm-associated microRNA-516a-5p regulates expressions of methylenetetrahydrofolate reductase, matrix metalloproteinase-2 and tissue inhibitor of matrix metalloproteinase-1 in human abdominal aortic vascular smooth muscle cells. *Ann. Vasc. Surg.* S0890-5096(17)30377-1. doi: 10.1016/j.avsg.2016.10.062

van Rooij, E., Sutherland, L. B., Liu, N., Williams, A. H., McAnally, J., Gerard, R. D., et al. (2006). A signature pattern of stress-responsive microRNAs that can evoke cardiac hypertrophy and heart failure. *Proc. Natl. Acad. Sci. U.S.A.* 103, 18255–18260. doi: 10.1073/pnas.0608791103

Vausort, M., Wagner, D. R., and Devaux, Y. (2014). Long noncoding RNAs in patients with acute myocardial infarction. *Circ. Res.* 115, 668–677. doi: 10.1161/CIRCRESAHA.115.303836

Verstraeten, A., Luyckx, I., and Loeys, B. (2017). Aetiology and management of hereditary aortopathy. *Nat. Rev. Cardiol.* 14, 197–208. doi: 10.1038/nrcardio.2016.211

Vidigal, J. A., and Ventura, A. (2015). The biological functions of miRNAs, lessons from *in vivo* studies. *Trends Cell Biol.* 25, 137–147. doi: 10.1016/j.tcb.2014.11.004

Wang, D., Deuse, T., Stubbendorff, M., Chernogubova, E., Erben, R. G., Eken, S. M., et al. (2015a). Local MicroRNA Modulation Using a Novel Anti-miR-21-Eluting Stent effectively prevents experimental in-stent restenosis. *Arterioscler. Thromb. Vasc. Biol.* 35, 1945–1953. doi: 10.1161/ATVBAHA.115. 305597

Wang, Q., Shu, C., Su, J., and Li, X. (2015b). A crosstalk triggered by hypoxia and maintained by MCP-1/miR-98/IL-6/p38 regulatory loop between human aortic smooth muscle cells and macrophages leads to aortic smooth muscle cells apoptosis via Stat1 activation. *Int. J. Clin. Exp. Pathol.* 8, 2670–2679.

Wang, S., Zhang, X., Yuan, Y., Tan, M., Zhang, L., Xue, X., et al. (2015c). BRG1 expression is increased in thoracic aortic aneurysms and regulates proliferation and apoptosis of vascular smooth muscle cells through the long non-coding RNA HIF1A-AS1 *in vitro*. *Eur. J. Cardiothorac. Surg.* 47, 439–446. doi: 10.1093/ejcts/ezu215

Wang, Y., Ait-Oufella, H., Herbin, O., Bonnin, P., Ramkhelawon, B., Taleb, S., et al. (2010). TGF-beta activity protects against inflammatory aortic aneurysm progression and complications in angiotensin II-infused mice. *J. Clin. Invest.* 120, 422–432. doi: 10.1172/JCI38136

Wang, Y., Krishna, S., Walker, P. J., Norman, P., and Golledge, J. (2013). Transforming growth factor-beta and abdominal aortic aneurysms. *Cardiovasc. Pathol.* 22, 126–132. doi: 10.1016/j.carpath.2012.07.005

Wang, Y. N., Shan, K., Yao, M. D., Yao, J., Wang, J. J., Li, X., et al. (2016). Long Noncoding RNA-GAS5, a novel regulator of hypertension-induced vascular remodeling. *Hypertension* 68, 736–748. doi: 10.1161/HYPERTENSIONAHA.116.07259

Williams, C. R., and Brooke, B. S. (2017). Effectiveness of open versus endovascular abdominal aortic aneurysm repair in population settings, A systematic review of statewide databases. *Surgery* S0039-6060(17)30075-2. doi: 10.1016/j.surg.2017.01.014

Wu, G., Cai, J., Han, Y., Chen, J., Huang, Z. P., Chen, C., et al. (2014). LincRNA-p21 regulates neointima formation, vascular smooth muscle cell proliferation, apoptosis, and atherosclerosis by enhancing p53 activity. *Circulation* 130, 1452–1465. doi: 10.1161/CIRCULATIONAHA.114.011675

Wu, J., Song, H. F., Li, S. H., Guo, J., Tsang, K., Tumiati, L., et al. (2016). Progressive aortic dilation is regulated by miR-17-Associated miRNAs. *J. Am. Coll. Cardiol.* 67, 2965–2977. doi: 10.1016/j.jacc.2016.04.027

Yan, B., Yao, J., Liu, J. Y., Li, X. M., Wang, X. Q., Li, Y. J., et al. (2015). lncRNA-MIAT regulates microvascular dysfunction by functioning as a competing endogenous RNA. *Circ. Res.* 116, 1143–1156. doi: 10.1161/CIRCRESAHA.116.305510

Yu, B., Liu, L., Sun, H., and Chen, Y. (2015). Long noncoding RNA AK056155 involved in the development of Loeys-Dietz syndrome through AKT/PI3K signaling pathway. *Int. J. Clin. Exp. Pathol.* 8, 10768–10775.

Zampetaki, A., Attia, R., Mayr, U., Gomes, R. S., Phinikaridou, A., Yin, X., et al. (2014). Role of miR-195 in aortic aneurysmal disease. *Circ. Res.* 115, 857–866. doi: 10.1161/CIRCRESAHA.115.304361

Zhang, Y., Liu, Z., Zhou, M., and Liu, C. (2016). MicroRNA-129-5p inhibits vascular smooth muscle cell proliferation by targeting Wnt5a. *Exp. Ther. Med.* 12, 2651–2656. doi: 10.3892/etm.2016.3672

Zhao, J., Zhang, W., Lin, M., Wu, W., Jiang, P., Tou, E., et al. (2016). MYOSLID is a novel serum response factor-dependent long noncoding RNA that amplifies the vascular smooth muscle differentiation program. *Arterioscler. Thromb. Vasc. Biol.* 36, 2088–2099. doi: 10.1161/ATVBAHA.116.307879

Conflict of Interest Statement: The authors declare that the research was conducted in the absence of any commercial or financial relationships that could be construed as a potential conflict of interest.

frontiers in Physiology

ORIGINAL RESEARCH
published: 25 July 2017
doi: 10.3389/fphys.2017.00536

Mechanisms of Smooth Muscle Cell Differentiation Are Distinctly Altered in Thoracic Aortic Aneurysms Associated with Bicuspid or Tricuspid Aortic Valves

*Elena Ignatieva[1], Daria Kostina[1,2], Olga Irtyuga[1], Vladimir Uspensky[1], Alexey Golovkin[1], Natalia Gavriliuk[1], Olga Moiseeva[1], Anna Kostareva[1,3] and Anna Malashicheva[1,3,4]**

[1] Laboratory of Molecular Cardiology, Almazov Federal Medical Research Centre, Saint Petersburg, Russia, [2] Department of Medical Physics, Peter the Great Saint-Petersburg Polytechnic University, Saint Petersburg, Russia, [3] Laboratory of Bioinformatics and Genomics, Institute of Translational Medicine, ITMO University, Saint Petersburg, Russia, [4] Faculty of Biology, Saint-Petersburg State University, Saint Petersburg, Russia

OPEN ACCESS

Edited by:
Amalia Forte,
Università degli Studi della Campania "Luigi Vanvitelli" Caserta, Italy

Reviewed by:
Per Hellstrand,
Lund University, Sweden
David Anthony Tulis,
Brody School of Medicine at East Carolina University, United States

***Correspondence:**
Anna Malashicheva
malashicheva_ab@almazovcentre.ru;
amalashicheva@gmail.com

Specialty section:
This article was submitted to Vascular Physiology, a section of the journal Frontiers in Physiology

Received: *01 May 2017*
Accepted: *10 July 2017*
Published: *25 July 2017*

Citation:
Ignatieva E, Kostina D, Irtyuga O, Uspensky V, Golovkin A, Gavriliuk N, Moiseeva O, Kostareva A and Malashicheva A (2017) Mechanisms of Smooth Muscle Cell Differentiation Are Distinctly Altered in Thoracic Aortic Aneurysms Associated with Bicuspid or Tricuspid Aortic Valves. Front. Physiol. 8:536. doi: 10.3389/fphys.2017.00536

Cellular and molecular mechanisms of thoracic aortic aneurysm are not clear and therapeutic approaches are mostly absent. Thoracic aortic aneurysm is associated with defective differentiation of smooth muscle cells (SMC) of aortic wall. Bicuspid aortic valve (BAV) comparing to tricuspid aortic valve (TAV) significantly predisposes to a risk of thoracic aortic aneurysms. It has been suggested recently that BAV-associated aortopathies represent a separate pathology comparing to TAV-associated dilations. The only proven candidate gene that has been associated with BAV remains *NOTCH1.* In this study we tested the hypothesis that Notch-dependent and related TGF-β and BMP differentiation pathways are differently altered in aortic SMC of BAV- vs. TAV-associated aortic aneurysms. SMC were isolated from aortic tissues of the patients with BAV- or TAV-associated aortic aneurysms and from healthy donors used as controls. Gene expression was verified by qPCR and Western blotting. For TGF-β induced differentiation SMC were treated with the medium containing TGF-β1. To induce proosteogenic signaling we cultured SMC in the presence of specific osteogenic factors. Notch-dependent differentiation was induced via lentiviral transduction of SMC with activated Notch1 domain. *MYOCD* expression, a master gene of SMC differentiation, was down regulated in SMC of both BAV and TAV patients. Discriminant analysis of gene expression patterns included a set of contractile genes specific for SMC, Notch-related genes and proosteogenic genes and revealed that control cells form a separate cluster from both BAV and TAV group, while BAV- and TAV-derived SMC are partially distinct with some overlapping. In differentiation experiments TGF-β caused similar patterns of target gene expression for BAV- and TAV derived cells while the induction was higher in the diseased cells than in control ones. Osteogenic induction caused significant change in *RUNX2* expression exclusively in BAV group. Notch activation induced significant

ACTA2 expression also exclusively in BAV group. We show that Notch acts synergistically with proosteogenic factors to induce *ACTA2* transcription and osteogenic differentiation. In conclusion we have found differences in responsiveness of SMC to Notch and to proosteogenic induction between BAV- and TAV-associated aortic aneurysms.

Keywords: thoracic aortic aneurysms, bicuspid aortic valves, tricuspid aortic valves, smooth muscle cells, differentiation

INTRODUCTION

Thoracic aortic aneurysm (TAA) is a life threatening condition, which is manifested by progressive enlargement of the thoracic aorta due to destructive changes in the aortic wall. Therapeutic agents that may influence the process are absent to date and the only therapeutic decision is a surgical intervention (Davis et al., 2014). Up to 20% of patients with TAA have a positive family history, confirming the autosomal-dominant nature of this disease. The genetic basis of TAA is heterogeneous and involves most importantly genes coding for components of the vascular smooth muscle contractile apparatus, the extracellular matrix of connective tissue and key molecules of the transforming growth factor-β signaling (Luyckx and Loeys, 2015).

TAAs are characterized by extensive loss of smooth muscle cells (SMC) and changes in their functionality (Della Corte et al., 2008; Forte et al., 2013; Phillippi et al., 2014; Malashicheva et al., 2016). At the same time, the role of SMC during development and progression of aortic aneurysms is not well defined. Vascular SMC are characterized by specific molecular markers and contractile functions. Unlike other terminally differentiated muscle cells, vascular SMC have a unique ability to reversibly modify their contractile phenotype to a dedifferentiated state in response to changes in local environmental cues (Owens, 1995; Owens et al., 2004). The molecular basis of SMC differentiation in response to pro-differentiation signals is the expression of several highly specific contractile proteins, including smooth muscle α-actin (SMA), SM22α, and calponin. Abnormal control of the SMC phenotype leads to progression of vascular pathologies, including aneurysms (Ailawadi et al., 2009).

Myocardin (*MYOCD*) is an essential factor for the SMC differentiated phenotype. This transcription cofactor is both necessary and sufficient for the development and differentiation of most SMC (Wang et al., 2003; Long et al., 2008; Miano, 2015). Myocardin is a cardiac and smooth muscle–specific coactivator of serum response factor (SRF) that is able to transcriptionally activate CArG box–containing cardiac and smooth muscle target genes, such as smooth muscle α-actin, or SMA (*ACTA2*), SM22α (*TAGLN*), and calponin (*CNN1*) (Wang et al., 2003; Qiu et al., 2005; Huang et al., 2008; Long et al., 2008).

TGF-beta has been for a long time considered as a key participant of driving SMC differentiation state in the aorta by activating the genetic program that includes a set of SMC differentiation marker genes (Guo and Chen, 2012).

TAA may occur in the presence of a tricuspid or a bicuspid aortic valve (TAV and BAV), respectively. Several lines of evidence suggest that the mechanism of aneurysm development is distinct between the two patient groups (Folkersen et al., 2011; Balistreri et al., 2013; Kjellqvist et al., 2013; Maleki et al., 2013; Phillippi et al., 2014; Paloschi et al., 2015). The genetic background underlying BAV/TAA is clearly not monogenic and complex. So far, a few genes such as *NOTCH1* (Garg et al., 2005; Mohamed et al., 2006; Mckellar et al., 2007; Mcbride et al., 2008; Andreassi and Della Corte, 2016; Forte et al., 2016; Koenig et al., 2017) and *GATA5* (Padang et al., 2012) have been associated with non-syndromic forms of BAV/TAA.

In the vascular system, Notch receptors (Notch1–4) and ligands (Jag1 and 2 and Dll1, 3, and 4) are expressed. Activation of Notch receptors requires binding to a transmembrane ligand presented by neighbor cells. This binding enables a series of cleavage events in the receptor, resulting in the release of the intracellular region of Notch protein (Notch intracellular domain, NICD). NICD, the transcriptionally active form of Notch, translocates to the nucleus where it regulates a broad range of target genes (Andersson et al., 2011). The outcome of Notch activation is cell type and context dependent with multiple combinations of receptors and ligands that transduce different biological effect (Mašek and Andersson, 2017).

Controversy exists regarding the effect of Notch signaling on vascular SMC phenotype. Notch signaling has been linked to smooth muscle differentiation both *in vitro* and *in vivo* (Doi et al., 2006; Noseda et al., 2006; Boucher et al., 2012). At the same time, some data are consistent with a model wherein Notch signaling represses SMC differentiation and maintenance of the contractile SMC phenotype (Sweeney et al., 2004; Morrow et al., 2005; Proweller et al., 2005).

Although, the role of Notch has been extensively studied in the context of development and cancer (Briot et al., 2016) recent experiments using *in vitro* assays and mouse models also showed that changes in Notch activity can impact organ homeostasis in adults (Rostama et al., 2014, 2015; Briot et al., 2015). A recent research established a molecular framework coupling angiogenesis, angiocrine signals and osteogenesis via Notch signaling (Ramasamy et al., 2014).

SMC have high plasticity and are able to convert from the differentiated contractile phenotype to a variety of synthetic dedifferentiated states exhibiting in some cases chondrogenesis and osteogenesis during the pathogenesis of vascular diseases (Hilaire et al., 2016). The mechanisms of bone and vascular calcification seem to be similar and are connected through Notch/BMP/TGF-β crosstalk (Hilaire et al., 2016; Towler, 2017). It is known also that aortic tissues of BAV-patients are predisposed to progressive calcification and thus proosteogenic mechanisms might be involved in the pathogenesis of BAV-associated aortopathies.

Thus, it is obvious that functionality of SMC associated with their differentiation state is attenuated in the cells deriving from the TAA patients of both BAV and TAV groups. Myocardin, TGF-β, Notch and BMP are the main pathways responsible for the functional state of SMC in the aortic wall. The objective of the present study was to elucidate more precisely the mechanisms that attenuate differentiation state of the diseased SMC and to reveal possible differences between BAV- and TAV-derived SMC. For this we stimulated TGF-β, osteogenic and Notch differentiation pathways and compared control and diseased cells from the BAV and TAV group. We show that myocardin, TGF-β, BMP and Notch–related mechanisms of SMC differentiation are attenuated in the smooth muscle cells of the patients with thoracic aortic aneurys; Notch-dependent and proosteogenic genes show distinct expression in smooth muscle cells of BAV- vs. TAV-related aortic aneurysms.

MATERIALS AND METHODS

Patients

The clinical research protocol was approved by the local Ethics Committee of the Almazov Federal Medical Research Center and was in accordance with the principle of the Declaration of Helsinki. All patients gave signed informed consent.

Samples of the aneurysmal wall of the thoracic aorta were harvested during aortic surgery at the Almazov Federal Medical Research Center. Eleven specimens were sampled from patients with thoracic aortic aneurysm with tricuspid aortic valve (TAV) ($n = 11$) (**Table 1**). Fourteen specimens were sampled from patients with thoracic aortic aneurysm with bicuspid aortic valve (BAV) ($n = 14$). Patients with connective tissue disorders were excluded. Control aortic specimens were obtained from organ transplant donors ($n = 13$) and all had TAV. All tissues were sampled from the outer curvature of the thoracic aorta.

TABLE 1 | Clinical characteristics of the study groups.

	TAV ($n = 11$)	BAV ($n = 14$)	C ($n = 13$)
Male gender (%)	46	59	60
Age (years)	64 ± 6	62 ± 4	40 ± 5
Aortic diameter (cm)	5.6 ± 0.18	5.9 ± 0.16	<3
Aortic CSA/h (cm^2/m)	6.6 ± 0.6	7.6 ± 0.6	
Peak valve gradient (mmHg)	83 ± 9	86 ± 11	
Mean valve gradient (mmHg)	55 ± 7	59 ± 9	
Aortic valve area index (cm^2/m^2)	0.39 ± 0.02	0.38 ± 0.02	
Hypertension (%)	84	81	
Medication			
Angiotensin receptor blockers (%)	38	18	
Statins (%)	0	41	
Aspirin (%)	31	14	

Values are means ± S.E.M.

Primary Cultures

To obtain SMC cultures the cells were isolated from the aortic wall by collagenase digestion as described previously (Malashicheva et al., 2016). SMC were cultured in growth medium containing DMEM (Invitrogen) supplemented with 20% fetal bovine serum (FBS, Invitrogen), 2 mM L-glutamine, sodium pyruvate and penicillin/streptomycin (100 mg/l) (Invitrogen). The cells were used in experiments at passages 2–7.

Osteogenic Differentiation

To induce osteogenic differentiation SMC were seeded at 80% confluency in growth medium and after 24 h the medium was changed to osteogenic differentiation media containing DMEM/F12 (Invitrogen) with 1% penicillin/streptomycin, 10 mM β-glycerolphosphate, 200 μM L-ascorbic acid and 100 nM dexamethasone (Sigma). Gene expression was analyzed 5 days after the induction of differentiation.

TGF-β Induced Differentiation

SMC were seeded in the growth medium and after they were attached to the culture plate the medium was changed to serum-free DMEM/F12 (Invitrogen) with 1% penicillin/streptomycin. After 24 h 2,5 ng/ml of human recombinant TGF-β1 (Peprotech) was added. The cells were harvested 96 h after the addition of TGF-β1 for either qPCR or Westernblotting analyses.

Genetic Construct and Lentiviruses

Lentiviral packaging plasmids were a generous gift of D. Trono (École Polytechnique Fédérale de Lausanne, Switzerland); pLVTHM was modified to bear Notch1 intracellular domain of Notch1 (Kostina et al., 2016). Lentiviral particles were produced using 293 packaging line as described previously (Malashicheva et al., 2007).

The efficiency of transgene expression with NICD-bearing virus was verified by Westernblotting with the antibodies to Notch1 (SC6014, Santa Cruz) and by qPCR with primers to Notch1 target gene *HEY1*.

Control transductions were performed using GFP-bearing lentiviral vector.

Alkaline-Phosphatase Staining

In vitro calcification was determined by alkaline-phosphatase (ALP) activity, which is an early marker of osteogenic differentiation. ALP staining was performed using Sigma BCIP®/NBT kit 14 days after the initiation of differentiation. Cells were washed with PBS and incubated with alkaline-phosphatase working solution for 10-15 min at room temperature. ALP activity appeared as blue deposition and plates were photographed with digital camera.

qPCR Analysis

Total RNA was extracted from SMCs using Extract RNA reagent (Eurogen, Russia) according to the instructions of the manufacturer. Total RNA (1 μg) was reverse transcribed with MMLV RT kit (Eurogen, Russia). Real-time PCR was performed with 1 μL cDNA and SYBRGreen PCR Mastermix (Eurogen, Russia) in the Light Cycler system using specific forward and reverse primers for target genes. Primer sequences are available

upon request. Changes in target genes expression levels were calculated using the comparative ΔΔCT method. The mRNA levels were normalized to *GAPDH* mRNA.

Westernblotting

Proteins were extracted from SMC as follows. The cells were treated with lysis buffer containing 50 mM Tris (pH 8), 150 mM NaCl, 1% Triton X-100, 1% sodium deoxycholate, and 5 mM EDTA (Sigma) and protease inhibitor cocktail (Roche). Extracts were separated by 10% sodium dodecyl sulfate-polyacrylamide gel electrophoresis (SDS-PAGE). Primary antibodies used for Westernblotting were the following: Notch1 (SC6014, Santa Cruz), SM22α (ab14106, Abcam), SMA (sc-32251, Santa Cruz), vimentin (M072529, DAKO), beta-actin (ab6276, Abcam), pSMAD (Abcam), calponin (SantaCruz), tubulin (Sigma).

Statistics

Discriminant analysis was used to investigate what parameters in gene expression could divide groups of patients. Also discriminant analysis gives an opportunity to predict what parameters are mostly common for each group.

Linear discriminant function analysis was performed to determine which continuous variables discriminate between groups of BAV, TAV and controls. Continuous variables were qPCR gene expression data from ΔΔCT estimation. A stepwise analysis enumerating steps, *p*-value significance level, and *F*-test were performed. A discrimination level was evaluated by assessing Wilks' lambda. Significance of an identifying criterion was determined after drawing scatterplots of canonical values and calculating classification value and Mahalanobis squared distance. Discriminant function analysis was performed with Statistica 7.0 software.

Correlation analysis was performed using R software (version 2.12.0; R Foundation for Statistical Computing, Vienna, Austria). Spearman correlation coefficient was used. The significance of correlations was evaluated by a two-tailed Mann–Whitney test.

qPCR data on gene expression was analyzed using Graph Pad Prizm. Values are expressed as means ± SEM. Groups were compared using the Mann–Whitney non-parametric test. A value of $P \leq 0.05$ was considered significant.

RESULTS

BAV- and TAV-Derived SMC Demonstrate Distinct Correlation Profiles for Expression of Myocardin

We measured the expression level of *MYOCD* gene encoding myocardin in smooth muscle cells (SMC) derived from aortic wall of the patients with thoracic aortic aneurysm (TAA) associated with either tricuspid- or bicuspid aortic valve (TAV- and BAV- correspondingly) and healthy controls. *MYOCD* expression level was significantly down regulated in the SMC of both groups of the patents (**Figure 1A**). To explore the relationships between myocardin and smooth muscle-specific contractile proteins we assessed correlations between mRNA transcript levels of *MYOCD* and SMC differentiation marker genes *ACTA2* (SMA), *TAGLN* (SM22), *CNN1* (calponin), and *VIM* (vimentin) using the Spearman correlation coefficient (**Figure 1B**). MYOCD expression level positively and statistically significantly correlated with *ACTA2*, *TAGLN,* and *VIM* expression levels in control group. In contrary, in the BAV group we observed statistically significant positive correlation only between *MYOCD* and *VIM* expression levels and negative correlation between *MYOCD* and *CNN1*. In the TAV group no correlations were observed. Thus, the patterns of correlations of *MYOCD* expression with contractile proteins expression were distinct in all three groups of SMC: BAV- and TAV-derived ad controls.

Expression Analysis of Contractile, BMP- and Notch and Related Gene in SMC of BAV and TAV Patients

To identify if the SMC from BAV- and TAV-patients and control group form clusters by gene expression we used multivariate discriminant function analysis. In addition to *MYOCD*, *ACTA2*, *CNN*, *TAGLN*, *VIM* expression data from above section we measured the expression of Notch-related genes known to be expressed in SMC (*NOTCH1*, *NOTCH2*, *NOTCH3, JAG1*, *HES1, HEY, SNAIL,* and *SLUG*) and proosteogenic genes known to be involved in calcification (*BMP2*, *RUNX2*, *POSTIN*, *CTNNB1*, SOX9, *OPN*, and *OPG*; Rutkovskiy et al., 2016). In the course of discriminant analysis we identified 11 genes with high prognostic and discriminant value (**Table 2**). These genes were used to examine if the SMC from BAV, TAV, and control groups form independent clusters. Graphical result of the examined groups based on the discriminant analysis (**Figure 2**) demonstrates that control SMC form a separate cluster from both BAV- and TAV groups by expression of Notch-related and proosteogenic genes, while BAV- and TAV-derived SMC clusters demonstrate distinct patterns with partial overlap.

TGF-Beta Induces Similar Response in BAV and TAV-Derived SMC

In order to define whether there was a difference in TGF-β responsiveness between BAV- and TAV-derived SMC and controls, we measured the expression of phenotypic markers of the contractile SMC after treatment with human recombinant TGF-β1 (**Figure 3**). *ACTA2*, *CNN1*, *TAGLN*, *MYOCD*, *POSTN* mRNA were up regulated after TGF-β treatment in all three groups (**Figure 3A**, upper panel). We correspondingly observed elevation of protein level of SMA, calponin, SM22α in all three groups of SMC as well (**Figure 3B**). However, when compared to SMC from healthy aortas, aneurysm-derived SMC exhibited a more pronounced TGF-β induced response, which could be counted more precisely by qPCR data. In the lower panel of **Figure 3A**, we presented data as fold change mRNA i.e., the ratio of mRNA level after TGF-β treatment to the initial mRNA level before the treatment. The transcriptional upregulation was more pronounced in BAV- and TAV-derived SMC, respectively, in comparison with control: *ACTA2* (6.1- and 8.1-fold, vs. 2.7-fold), *TAGLN* (3.7- and 7.2-fold, vs. 1.4-fold), *CNN1* (5.7- and 7-fold, vs. 2.2-fold), *POSTN* (2.7- and 2.4-fold vs. 1.4-fold). Although the data on *MYOCD* mRNA expression did not

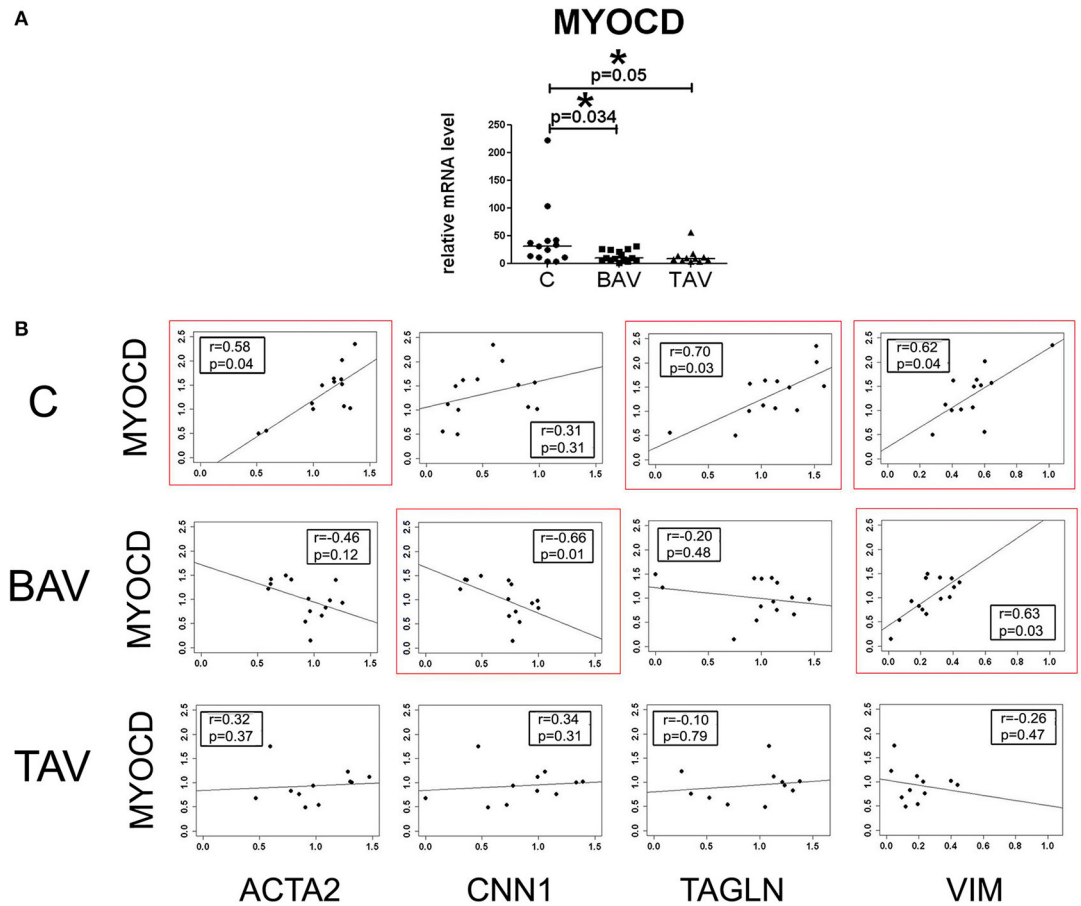

FIGURE 1 | Myocardin expression in aortic smooth muscle cells (SMC) from patients with thoracic aortic aneurysm with tricuspid aortic valve (TAV) or bicuspid aortic valve (BAV) and controls (C). **(A)** Relative mRNA levels for *MYOCD* (myocardin) in SMC from patients with aortic aneurysm (TAV, $n = 11$; BAV, $n = 14$), and control cells (C, $n = 13$). The significance of gene expression differences between groups was evaluated by a two-tailed Mann–Whitney test; line represents the median; $^*p < 0.05$. **(B)** Scatter plots showing correlations of *MYOCD* and SMC marker genes *ACTA2*, *TAGLN, CNN1, VIM* expression levels in SMC of patients with aortic aneurysm with BAV, TAV, and healthy controls. mRNA levels were analyzed by qPCR and normalized to *GAPDH*. The x- and y-axis show log RQ (relative quantification $= 2^{-\Delta\Delta Ct}$). *r*, Spearman correlation coefficient; p, *p*-value. *P*-values less than 0.05 were considered to be statistically significant. Statistically significant correlations are highlighted by red rectangles.

achieve statistical significance, there was a trend toward more powerful induction of its mRNA in SMC from TAV patients comparing to the control group ($p = 0.055$). Thus, TGF-beta induces similar pattern of responsive gene activation for BAV and TAV-derived cells, and this activation is higher in the cells of BAV and TAV patients compared to the cells of healthy donors.

BAV- and TAV-Derived Smooth Muscle Cells Differ in Their Differentiation Properties in Osteogenic Conditions

We induced osteogenic differentiation in SMC by addition of specific osteogenic factors to culture medium (**Figure 4**). Protein levels for SMA and SM22 were elevated in all three groups, by Westernblotting staining (**Figure 4C**). More precise estimation of corresponding gene transcription levels revealed statistically significant elevation of *ACTA2* and *TAGLN* transcript levels in both groups of diseased cells, but not in control group (**Figure 4A**). Osteogenic medium induced significant induction of *RUNX2* transcription in BAV-derived SMC after 5 days of osteogenic induction (**Figure 4A**). To verify if osteogenic medium indeed caused change in SMC phenotype, we cultured the cells under osteogenic conditions for 14 days and then stained them for alkaline phosphatase activity (ALP), a marker of osteogenic differentiation. Correspondingly we observed the most intensive alkaline phosphatase activity (ALP), for the SMC from BAV-patients (**Figure 4B**) suggesting that BAV-derived aortic SMC are more prone to osteogenic differentiation compared to TAV-derived SMC and SMC from healthy controls.

Notch Differently Induces Differentiation in BAV-Derived SMC

To look how responsive to Notch activation are the SMC derived from BAV- and TAV-patients compared to control cells we activated Notch signaling in SMC via transduction

TABLE 2 | Genes included in the model for discriminant analysis.

	Wilks' Lambda	Partial Lambda	F-remove (2.71)	*p*-level
VIM	0.293439	0.787751	3.367953	0.050683
BMP2	0.258843	0.893039	1.497141	0.243155
SNAIL	0.308272	0.749846	4.170081	0.027362
NOTCH1	0.231626	0.997973	0.025387	0.974958
HEY1	0.238413	0.969564	0.392391	0.679527
TAGLN	0.258818	0.893125	1.495798	0.243447
ACTA2	0.374827	0.616702	7.769094	0.002377
CNN1	0.376774	0.613516	7.874362	0.002228
MYOCD	0.284798	0.811652	2.900690	0.073642
SLUG	0.271318	0.851977	2.171758	0.135005
OPG	0.270577	0.854312	2.131650	0.139704

with the lentivirus bearing Notch1-intracellular domain (NICD) (**Figure 5**). For control GFP-bearing virus was used. Notch-activation induced *ACTA2* transcription and corresponding SMA protein accumulation, which was observed in all three groups, but statistically significant *ACTA2* up regulation was observed only in BAV group. The data suggests that BAV-derived cells are more responsive to Notch activation of *ACTA2* transcription comparing to TAV and control cells.

Notch Signaling Is Coupling Osteogenic and Myofibroblast Induction in SMC

Participation of Notch signaling in osteogenic differentiation is rather controversial as this signaling has been shown both to promote and to prevent proosteogenic gene expression (Acharya et al., 2011; Yip et al., 2011; Zeng et al., 2013; Theodoris et al., 2015). Therefore, we induced osteogenic differentiation in aortic SMC and activated Notch signaling via lentivitral transduction with NICD-bearing virus (**Figure 6**). ALP staining after 14 days of culture in osteogenic conditions showed that NICD increased calcification of SMC in the presence of osteogenic medium comparing to the osteogenic medium without NICD. NICD induced up regulation of proosteogenic *RUNX2* transcription and Notch target gene transcription *HEY1* in both normal and osteogenic medium. In contrary *ACTA2* transcription was significantly induced by NICD only in osteogenic conditions (**Figure 6**).

DISCUSSION

In this study we show that smooth muscle cell differentiation pathways that are dependent on myocardin and TGF-β are attenuated in the patients with thoracic aortic aneurysm associated with bicuspid or tricuspid aortic valve. BAV-derived SMC differ from TAV-derived SMC in sensitivity to Notch-activation and to proosteogenic signals.

Consistent with the previous study that smooth muscle cells from thoracic aneurysms are characterized by decreased expression of SMC contractile proteins (Malashicheva et al., 2016), both BAV- and TAV-derived smooth muscle cells also demonstrated reduced *MYOCD expression level* compared to the

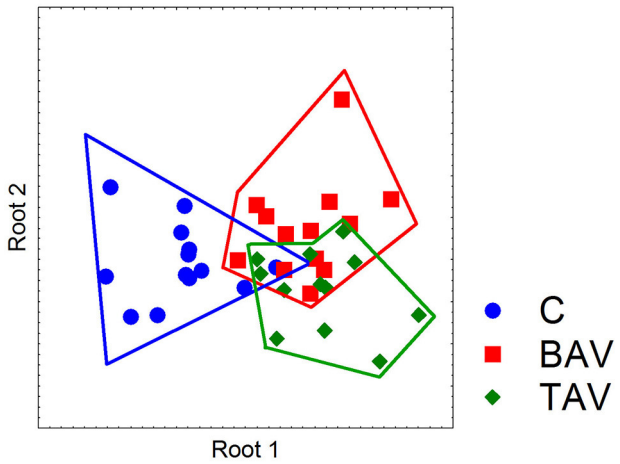

FIGURE 2 | Partition of the examined groups based on the results of discriminant analysis. Discriminant analysis was used to investigate what parameters in gene expression could divide groups of patients. Expression data on SMC differentiation markers (*MYOCD*, *ACTA2*, *CNN*, *TAGLN*, and *VIM*), Notch-related genes (*NOTCH1*, *NOTCH2*, *NOTCH3, JAG1*, *HES1, HEY, SNAIL,* and *SLUG*) and proosteogenic genes (*BMP2*, *RUNX2*, *POSTIN*, *CTNNB1*, *SOX9*, *OPN*, and *OPG*) were used. In the course of discriminant analysis 11 genes with high prognostic and discriminant value were identified (**Table 2**) and these genes were used to examine if the SMC from BAV, TAV, and control groups form independent clusters. Dot plot demonstrates that control SMC form a separate cluster from both BAV- and TAV groups by expression of Notch-related and proosteogenic genes, while BAV- and TAV-derived SMC clusters partially overlap.

cells from healthy individuals. Moreover, in SMC from healthy aortas *MYOCD* level positively correlated with the levels of *ACTA2* and *TAGLN*, which are early SMC markers, but not with later marker *CNN1*, which is activated in the middle stage of the SMC differentiation (Owens et al., 2004). At the same time, BAV-derived SMC demonstrated a strong negative correlation between *MYOCD* and *CNN1* expression, while in TAV-derived SMC we did not observe any correlation between MYOCD and other transcripts.

Myocardin is important in maintaining the normal SMC contractile phenotype (Long et al., 2008; Miano, 2015). The exact relation of myocardin upregulation to the heart and vascular diseases remains unclear. Remarkably, mutations in the *MYH11* (smooth muscle myosin heavy chain) and *ACTA2* (smooth muscle actin) genes (Zhu et al., 2006; Guo et al., 2007) were shown to cause familial thoracic aneurysms and dissections. Each of these genes is regulated directly by myocardin in the postnatal vasculature confirming that dysregulated myocardin-dependent transcription can be directly involved in aneurysm formation in humans (Huang et al., 2008).

To our surprise, we revealed a direct correlation of myocardin mRNA with vimentin mRNA (VIM) in control and BAV-derived SMC (**Figure 1**), but not in TAV-derived cells. Vimentin is a cytoskeletal protein of the intermediate filaments. Increased expression of vimentin in the vascular SMC has been associated with vascular injury and used as a marker of SMC synthetic, dedifferentiated phenotype (Owens et al., 2004). However, it is

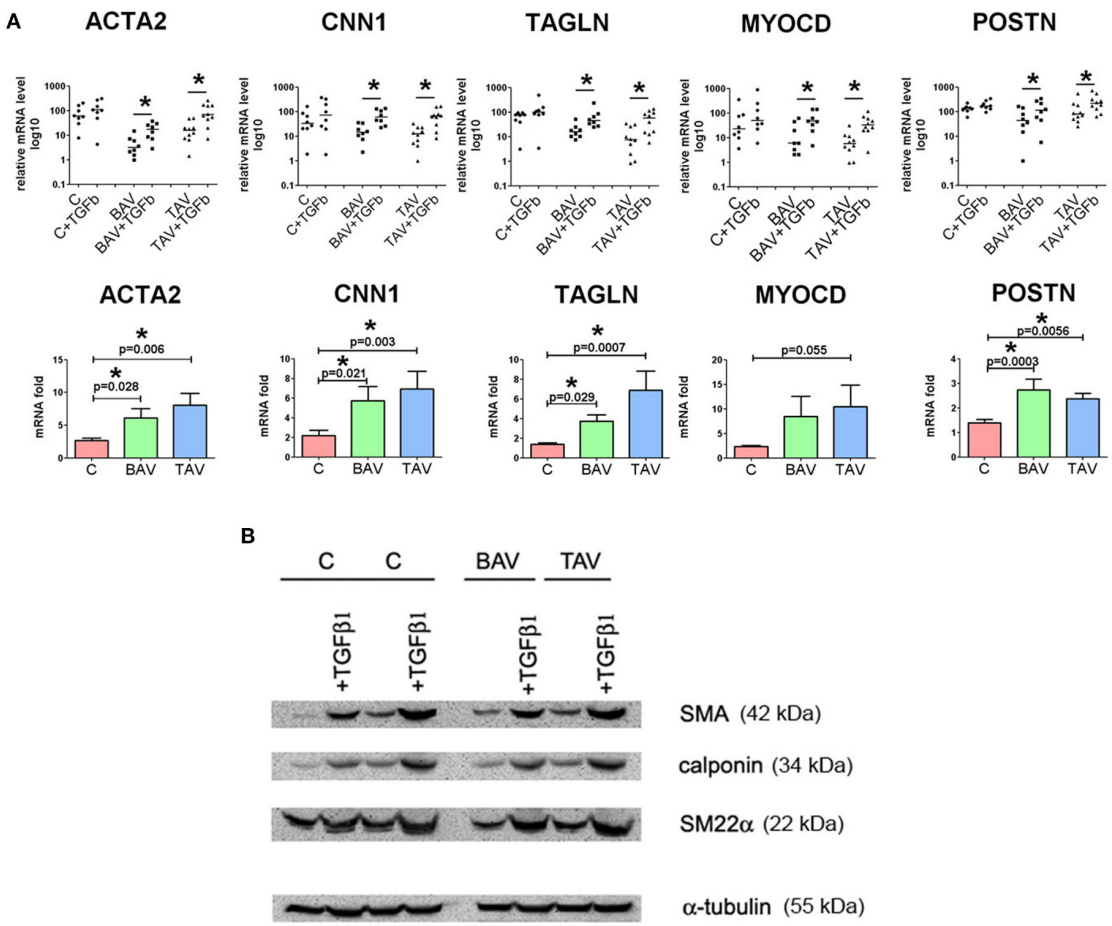

FIGURE 3 | Effects of transforming growth factor TGFβ1 stimulation on the expression of differentiation marker genes in primary human aortic smooth muscle cells (SMC) from healthy donors (C) and patients with thoracic aortic aneurysm with either tricuspid aortic valve (TAV) or bicuspid aortic valve (BAV). SMC were grown to postconfluence, serum-starved for 96 h, and then TGFβ1 (2,5 ng/ml) was added for 96 h. **(A)** Upper panel: as confirmed statistically, TGF-β1 treatment significantly increased mRNA expression for SMC differentiation marker genes *ACTA2* (α-smooth muscle actin), *TAGLN* (transgelin, or SM22α), *CNN1* (calponin), *MYOCD* and *POSTN* in SMC from the patients with thoracic aortic aneurysm. Line represents the median; $^*p < 0.05$. Lower panel: fold change gene expression for *ACTA2*, *TAGLN, CNN1, MYOCD,* and *POSTN* in SMC from controls and patients with thoracic aortic aneurysm after treatment with TGF-β1. Data are presented as fold change mRNA i.e., the ratio of mRNA level after TGF-β1 treatment to the initial mRNA level before the treatment. Bar represents the mean with SD. mRNA level was determined by qPCR and gene expression was equalized by *GAPDH* expression. C, $n = 8$; TAV, $n = 10$; BAV, $n = 8$. Groups were compared using Mann-Whitney nonparametric test. **(B)** Westernblotting analysis for detection of smooth muscle actin (SMA), calponin, SM22α in SMC after treatment with TGF-β1. α-Tubulin was used as a control to verify total amount of protein.

apparent, that functions of vimentin are more complex, and vimentin is a necessary component of fully functional contractile apparatus in smooth muscle cells.

Our data suggest that the observed "imbalance" between myocardin and smooth muscle-specific genes expression in aortic SMC from BAV and TAV-associated aneurysms is likely to depend on additional still unknown signals that can modulate a role of myocardin in directing an endogenous SMC differentiation program in aneurysm and this requires further research.

TGF-β is among the most potent factors that promote and maintain the vascular SMC contractile phenotype by upregulating smooth muscle structural genes. We revealed that aortic SMC from BAV- and TAV-related aneurysms are more responsive to pro-differentiation effect of the exogenous TGF-β1 than SMC from healthy aortas. However, we did not observe any difference in the response to TGF-β1 between BAV- and TAV-derived SMC. TGF-β pathway is apparently involved in TAA progression. Accumulating evidences are associated with increased TGF-β signaling in aneurysms (Forte et al., 2013; Gomez et al., 2013; Nataatmadja et al., 2013). Recently increased TGF-β activity during TAA formation has been reported in patients with TAV, but not BAV, presumably as a result of an increased sequestration of TGF-β in the extracellular matrix in aortas of BAV patients (Paloschi et al., 2015). Evidently, TGF-β signaling in aneurysm progression is very complex and is also influenced by epigenetic mechanisms such as histone modifications, microRNA

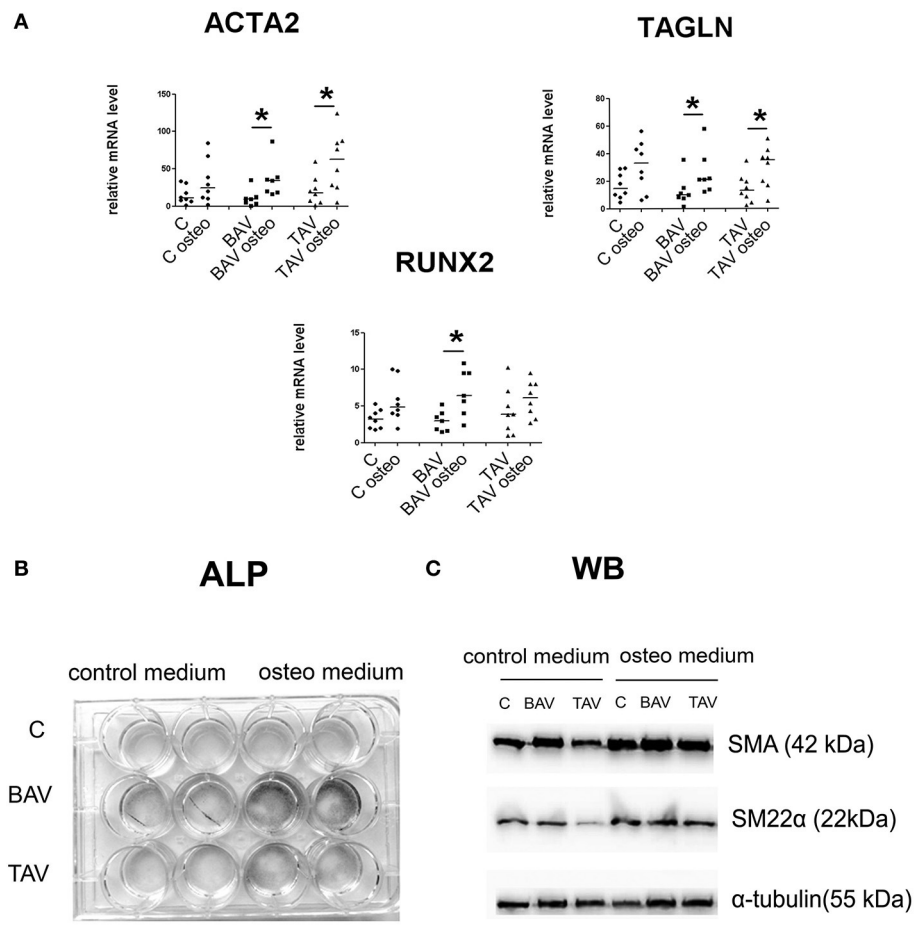

FIGURE 4 | BAV- and TAV-derived smooth muscle cells (SMC) differ in their differentiation properties in osteogenic conditions. SMC from patients with thoracic aortic aneurysm with either tricuspid aortic valve (TAV) or bicuspid aortic valve (BAV) and controls (C) were cultured with control or osteogenic [in the presence of 10 mM β-glycerolphosphate, 200 μM L-ascorbic acid and 100 nM dexamethasone (Sigma)] medium for 5 days. At day 5, total RNA and protein were extracted for qPCR analysis **(A)** and Westernblotting **(B)**, respectively. TAV, $n = 8$, BAV, $n = 7$, C, $n = 8$. **(A)** Culture in osteogenic conditions was accompanied by SMC-marker gene activation, which is stronger in aneurysm-derived cells, and also by statistically significant increase in *RUNX2* expression only in BAV-derived cells. Relative mRNA levels for *ACTA2, TAGLN,* and *RUNX2* in human aortic SMC were determined by qPCR and normalized to *GAPDH.* Groups were compared using Mann-Whitney nonparametric test; line represents the median; $^*p < 0.05$. **(B)** *In vitro* induced calcification. SMC were cultured in osteogenic conditions, and ALP activity was visualized with BCIP/NBT at day 14. **(C)** Representative Western blots for detection of smooth muscle actin (SMA), and SM22α, in human aortic SMC after culture in osteogenic conditions. α-Tubulin was used as a control to verify total amount of protein.

expression and possibly others (Forte et al., 2016; Albinsson et al., 2017).

The discriminant analysis of expression of genes responsible for SMC differentiation state and genes related to Notch and proosteogenic regulation (**Figure 2**) suggested that SMC from BAV and TAV patients have distinct gene expression profile of these groups of genes from the cells of healthy donors.

Notch is an important regulator of SMC (Boucher et al., 2012). Among all Notch receptors and ligands Notch2 and Notch3 appear to be the most important for SMC. These two receptors influence the phenotype and functions of SMC (Baeten and Lilly, 2015; Liu et al., 2015). Notch is a key signaling pathway in development, ensuring cross talk between different types of cells and their physiological differentiation (Andersson et al., 2011). Notch signaling in the endothelium of the vessel is positioned to mediate differentiation of underlying SMC ensuring integrity of the vessel wall (Pedrosa et al., 2015). We have shown recently that Notch signaling is attenuated in aortic endothelial cells of BAV patients (Kostina et al., 2016). In the present work we show alteration in Notch responsiveness in BAV-derived SMC. We suggest that the initial process of the vessel formation as well as further healing in response to constant shear stress in the aorta could be impaired in the BAV patients via Notch-dependent events in particular through inactive feedback loop connecting endothelial and smooth muscle cells and their mutual influence on cellular functional state.

Cardiovascular calcification is gaining an increased attention nowadays as it seems to be a "default" state of various pathologies (Hilaire et al., 2016). Osteogenic medium induced more elevated *RUNX2* expression and more prominent calcification

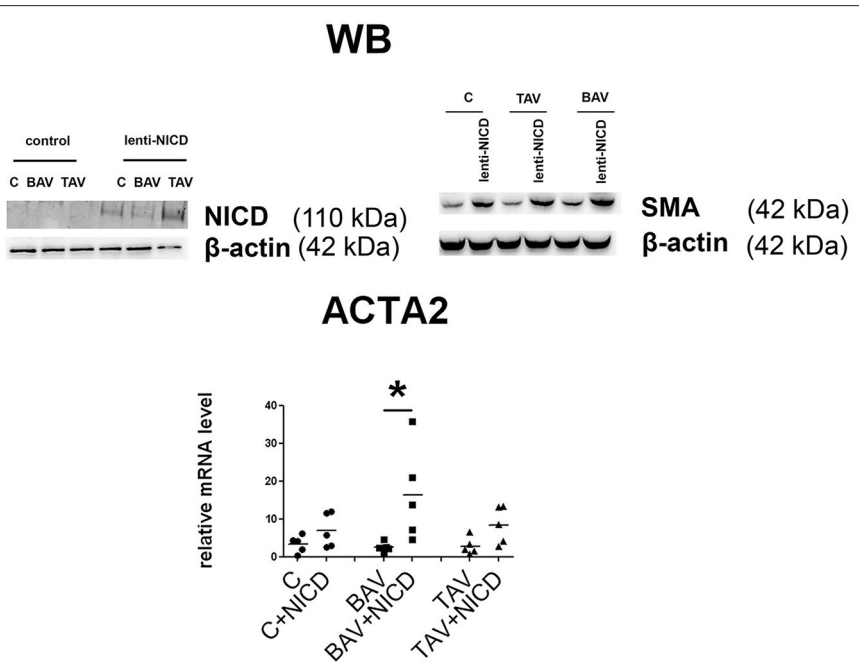

FIGURE 5 | Induction of smooth muscle differentiation in primary aortic smooth muscle cells (SMC) from healthy donors (C) and patients with thoracic aortic aneurysm either tricuspid aortic valve (TAV) or bicuspid aortic valve (BAV) by introduction of Notch-intracellular domain (NICD). C, $n = 5$; BAV, $n = 5$; TAV, $n = 5$. Upper panel represents Western blots for detection of Notch1-activated intracellular domain (NICD) and SMA accumulation after lenrivirial transduction with NICD. Lower panel represents analysis of *ACTA2* induction. mRNA level was determined by qPCR and gene expression was equalized by *GAPDH* expression. Groups are compared using Mann-Whitney nonparametric test; line represents the median; $*p < 0.05$.

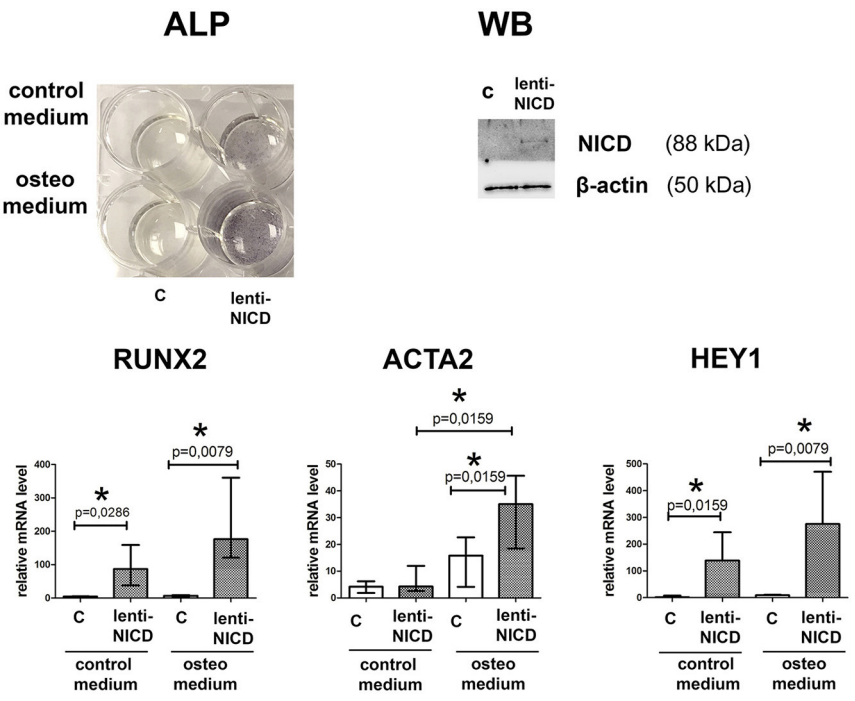

FIGURE 6 | Notch activation in smooth muscle cells (SMC) causes proosteogenic response. SMC were cultured in the presence of growth medium or osteogenic medium and with absence or presence of NICD (c and lenti-NICD, respectively). **Upper panel** represents ALP activity revealed in SMC 14 days after the induction of osteogenic differentiation. Western blot (WB) represents detection of Notch1-activated intracellular domain (NICD) in the transduced SMC. **Lower panel** represent analysis of *RUNX2*, *ACTA2,* and *HEY1* induction by NICD. Level of mRNA was determined by qPCR and gene expression was equalized by *GAPDH* expression. Groups are compared using Mann-Whitney nonparametric test; bars represent SEM, $*p < 0.05$.

in BAV-derived SMC. These results suggest a dysregulation of proosteogenic pathways in the BAV-derived cells. Notch activation induced significant elevation of *ACTA2* expression and corresponding SMA protein accumulation in BAV-derived cells. It has been shown previously that the cross-talk between BMP2 and Notch signaling pathways induces osteogenic differentiation of vascular SMC (Shimizu et al., 2011). At the same time increased expression of *ACTA2* has been shown to directly reduce the clonal potential of human mesenchymal stem cells and to guide their differentiation toward osteoblasts. Hence, SMA not only identifies osteoprogenitors in mesenchymal populations as shown by others before (Kalajzic et al., 2008; Grcevic et al., 2012), but may be part of the mechanism driving differentiation (Talele et al., 2015). Our data are in line with this as we observed that only BAV-derived cells are able to elevate the level of *ACTA2* in response to Notch stimulation. In addition we show that simultaneous action of osteogenic medium and Notch activation leads to elevated *ACTA2* expression and to an increase in osteogenic differentiation in SMC. Thus, this Notch-dependent elevation of *ACTA2* might be a direct prerequisite to calcification. Synergy between attenuated Notch and proosteogenic sensitivity could cause the final predisposition to osteogenic phenotype in BAV-derived SMC.

This study has some important limitations. First, the groups of the patients were not quite large. Second, we worked *in vitro* with isolated smooth muscle cells, but in aortic wall there is a community of SMC and endothelial cells and the communication between these different type of cells now is gaining more attention to understand proper function of the whole vessel (Lilly, 2014). Nevertheless, we suggest that our findings are relevant for searching potential targets to ameliorate aortic wall integrity.

AUTHOR CONTRIBUTIONS

EI and DK made experiments, analyzed data and wrote the manuscript. OI, VU, NG, and OM analyzed data of the patients and collected patient samples. AG and AK analyzed data. AM designed research, analyzed data, and wrote the manuscript.

FUNDING

This work was supported by Government of Russian Federation, Grant 074-U01, Russian Foundation of Basic Research grant 17-04-01318.

REFERENCES

Acharya, A., Hans, C. P., Koenig, S. N., Nichols, H. A., Galindo, C. L., Garner, H. R., et al. (2011). Inhibitory role of Notch1 in calcific aortic valve disease. *PloS ONE* 6:e27743. doi: 10.1371/journal.pone.0027743

Ailawadi, G., Moehle, C. W., Pei, H., Walton, S. P., Yang, Z., Kron, I. L., et al. (2009). Smooth muscle phenotypic modulation is an early event in aortic aneurysms. *J. Thorac. Cardiovasc. Surg.* 138, 1392–1399. doi: 10.1016/j.jtcvs.2009.07.075

Albinsson, S., Della Corte, A., Alajbegovic, A., Krawczyk, K. K., Bancone, C., Galderisi, U., et al. (2017). Patients with bicuspid and tricuspid aortic valve exhibit distinct regional microrna signatures in mildly dilated ascending aorta. *Heart Vessels* 32, 750–767. doi: 10.1007/s00380-016-0942-7

Andersson, E. R., Sandberg, R., and Lendahl, U. (2011). Notch signaling: simplicity in design, versatility in function. *Development* 138, 3593–3612. doi: 10.1242/dev.063610

Andreassi, M. G., and Della Corte, A. (2016). Genetics of bicuspid aortic valve aortopathy. *Curr. Opin. Cardiol.* 31, 585–592. doi: 10.1097/HCO.0000000000000328

Baeten, J. T., and Lilly, B. (2015). Differential regulation of NOTCH2 and NOTCH3 contribute to their unique functions in vascular smooth muscle cells. *J. Biol. Chem.* 290, 16226–16237. doi: 10.1074/jbc.M115.655548

Balistreri, C. R., Pisano, C., Candore, G., Maresi, E., Codispoti, M., and Ruvolo, G. (2013). Focus on the unique mechanisms involved in thoracic aortic aneurysm formation in bicuspid aortic valve versus tricuspid aortic valve patients: clinical implications of a pilot study. *Eur. J. Cardio Thorac. Surg.* 43, e180–e186. doi: 10.1093/ejcts/ezs630

Boucher, J. M., Gridley, T., and Liaw, L. (2012). Molecular pathways of notch signaling in vascular smooth muscle cells. *Front. Physiol.* 3:81. doi: 10.3389/fphys.2012.00081

Briot, A., Bouloumié, A., and Iruela-Arispe, M. L. (2016). Notch, lipids, and endothelial cells. *Curr. Opin. Lipidol.* 27, 513–520. doi: 10.1097/MOL.0000000000000337

Briot, A., Civelek, M., Seki, A., Hoi, K., Mack, J. J., Lee, S. D., et al. (2015). Endothelial NOTCH1 is suppressed by circulating lipids and antagonizes inflammation during atherosclerosis. *J. Exp. Med.* 212, 2147–2163. doi: 10.1084/jem.20150603

Davis, F. M., Rateri, D. L., and Daugherty, A. (2014). Mechanisms of aortic aneurysm formation: translating preclinical studies into clinical therapies. *Heart* 100, 1498–1505. doi: 10.1136/heartjnl-2014-305648

Della Corte, A., Quarto, C., Bancone, C., Castaldo, C., Di Meglio, F., Nurzynska, D., et al. (2008). Spatiotemporal patterns of smooth muscle cell changes in ascending aortic dilatation with bicuspid and tricuspid aortic valve stenosis: focus on cell–matrix signaling. *J. Thorac. Cardiovasc. Surg.* 135:e12. doi: 10.1016/j.jtcvs.2007.09.009

Doi, H., Iso, T., Sato, H., Yamazaki, M., Matsui, H., Tanaka, T., et al. (2006). Jagged1-selective notch signaling induces smooth muscle differentiation via a RBP-Jκ-dependent pathway. *J. Biol. Chem.* 281, 28555–28564. doi: 10.1074/jbc.M602749200

Folkersen, L., Wågsäter, D., Paloschi, V., Jackson, V., Petrini, J., Kurtovic, S., et al. (2011). Unraveling divergent gene expression profiles in bicuspid and tricuspid aortic valve patients with thoracic aortic dilatation: the ASAP study. *Mol. Med.* 17:1365. doi: 10.2119/molmed.2011.00286

Forte, A., Della Corte, A., Grossi, M., Bancone, C., Provenzano, R., Finicelli, M., et al. (2013). Early cell changes and TGFβ pathway alterations in the aortopathy associated with bicuspid aortic valve stenosis. *Clin. Sci.* 124, 97–108. doi: 10.1042/CS20120324

Forte, A., Galderisi, U., Cipollaro, M., De Feo, M., and Della Corte, A. (2016). Epigenetic regulation of TGF-β1 signalling in dilative aortopathy of the thoracic ascending aorta. *Clin. Sci.* 130, 1389–1405. doi: 10.1042/CS20160222

Garg, V., Muth, A. N., Ransom, J. F., Schluterman, M. K., Barnes, R., King, I. N., et al. (2005). Mutations in NOTCH1 cause aortic valve disease. *Nature* 437, 270–274. doi: 10.1038/nature03940

Gomez, D., Kessler, K., Michel, J.-B., and Vranckx, R. (2013). Modifications of chromatin dynamics control smad2 pathway activation in aneurysmal smooth muscle cellsnovelty and significance. *Circ. Res.* 113, 881–890. doi: 10.1161/CIRCRESAHA.113.301989

Grcevic, D., Pejda, S., Matthews, B. G., Repic, D., Wang, L., Li, H., et al. (2012). *In vivo* fate mapping identifies mesenchymal progenitor cells. *Stem cells* 30, 187–196. doi: 10.1002/stem.780

Guo, D.-C., Pannu, H., Tran-Fadulu, V., Papke, C. L., Robert, K. Y., Avidan, N., et al. (2007). Mutations in smooth muscle α-actin (ACTA2) lead to thoracic aortic aneurysms and dissections. *Nature Genet.* 39, 1488–1493. doi: 10.1038/ng.2007.6

Guo, X., and Chen, S.-Y. (2012). Transforming growth factor-β and smooth muscle differentiation. *World J. Biol. Chem.* 3, 41–52. doi: 10.4331/wjbc.v3.i3.41

Hilaire, C. S., Liberman, M., and Miller, J. D. (2016). Bidirectional translation in cardiovascular calcification. *Arterioscler. Thromb. Vasc. Biol.* 36, e19–e24. doi: 10.1161/atvbaha.115.307056

Huang, J., Cheng, L., Li, J., Chen, M., Zhou, D., Lu, M. M., et al. (2008). Myocardin regulates expression of contractile genes in smooth muscle cells and is required for closure of the ductus arteriosus in mice. *J. Clin. Invest.* 118, 515–525. doi: 10.1172/jci33304

Kalajzic, Z., Li, H., Wang, L.-P., Jiang, X., Lamothe, K., Adams, D. J., et al. (2008). Use of an alpha-smooth muscle actin GFP reporter to identify an osteoprogenitor population. *Bone* 43, 501–510. doi: 10.1016/j.bone.2008.04.023

Kjellqvist, S., Maleki, S., Olsson, T., Chwastyniak, M., Branca, R., Lehtiö, J., et al. (2013). A combined proteomic and transcriptomic approach shows diverging molecular mechanisms in thoracic aortic aneurysm development in patients with tricuspid-and bicuspid aortic valve. *Mol. Cell. Proteomics* 12, 407–425. doi: 10.1074/mcp.M112.021873

Koenig, S. N., Lincoln, J., and Garg, V. (2017). Genetic basis of aortic valvular disease. *Curr. Opin. Cardiol.* 32, 239–245. doi: 10.1097/HCO.0000000000000384

Kostina, A. S., Uspensky, V. E., Irtyuga, O. B., Ignatieva, E. V., Freylikhman, O., Gavriliuk, N. D., et al. (2016). Notch-dependent EMT is attenuated in patients with aortic aneurysm and bicuspid aortic valve. *Biochim. Biophys. Acta* 1862, 733–740. doi: 10.1016/j.bbadis.2016.02.006

Lilly, B. (2014). We have contact: endothelial cell-smooth muscle cell interactions. *Physiology* 29, 234–241. doi: 10.1152/physiol.00047.2013

Liu, N., Li, Y., Chen, H., Wei, W., An, Y., and Zhu, G. (2015). RNA interference-mediated NOTCH3 knockdown induces phenotype switching of vascular smooth muscle cells *in vitro*. *Int. J. Clin. Exp. Med.* 8:12674. Available online at: www.ijcem.com/files/ijcem0011005.pdf

Long, X., Bell, R. D., Gerthoffer, W. T., Zlokovic, B. V., and Miano, J. M. (2008). Myocardin is sufficient for a smooth muscle-like contractile phenotype. *Arterioscler. Thromb. Vasc. Biol.* 28, 1505–1510. doi: 10.1161/ATVBAHA.108.166066

Luyckx, I., and Loeys, B. L. (2015). The genetic architecture of non-syndromic thoracic aortic aneurysm. *Heart* 101, 1678–1684. doi: 10.1136/heartjnl-2014-306381

Malashicheva, A., Kanzler, B., Tolkunova, E., Trono, D., and Tomilin, A. (2007). Lentivirus as a tool for lineage-specific gene manipulations. *Genesis* 45, 456–459. doi: 10.1002/dvg.20313

Malashicheva, A., Kostina, D., Kostina, A., Irtyuga, O., Voronkina, I., Smagina, L., et al. (2016). Phenotypic and functional changes of endothelial and smooth muscle cells in thoracic aortic aneurysms. *Int. J. Vasc. Med.* 2016, 1–11. doi: 10.1155/2016/3107879

Maleki, S., Björck, H. M., Paloschi, V., Kjellqvist, S., Folkersen, L., Jackson, V., et al. (2013). Aneurysm development in patients with Bicuspid Aortic Valve (BAV): possible connection to repair deficiency? *AORTA* 1, 13–22. doi: 10.12945/j.aorta.2013.12.011

Mašek, J., and Andersson, E. R. (2017). The developmental biology of genetic Notch disorders. *Development* 144, 1743–1763. doi: 10.1242/dev.148007

Mcbride, K. L., Riley, M. F., Zender, G. A., Fitzgerald-Butt, S. M., Towbin, J. A., Belmont, J. W., et al. (2008). NOTCH1 mutations in individuals with left ventricular outflow tract malformations reduce ligand-induced signaling. *Hum. Mol. Genet.* 17, 2886–2893. doi: 10.1093/hmg/ddn187

Mckellar, S. H., Tester, D. J., Yagubyan, M., Majumdar, R., Ackerman, M. J., and Sundt, T. M. (2007). Novel NOTCH1 mutations in patients with bicuspid aortic valve disease and thoracic aortic aneurysms. *J. Thorac. Cardiovasc. Surg.* 134, 290–296. doi: 10.1016/j.jtcvs.2007.02.041

Miano, J. M. (2015). Myocardin in biology and disease. *J. Biomed. Res.* 29, 3–19. doi: 10.7555/JBR.29.20140151

Mohamed, S. A., Aherrahrou, Z., Liptau, H., Erasmi, A. W., Hagemann, C., Wrobel, S., et al. (2006). Novel missense mutations (p. T596M and p. P1797H) in NOTCH1 in patients with bicuspid aortic valve. *Biochem. Biophys. Res. Commun.* 345, 1460–1465. doi: 10.1016/j.bbrc.2006.05.046

Morrow, D., Scheller, A., Birney, Y. A., Sweeney, C., Guha, S., Cummins, P. M., et al. (2005). Notch-mediated CBF-1/RBP-Jκ-dependent regulation of human vascular smooth muscle cell phenotype *in vitro*. *Am. J. Physiol.* 289, C1188–C1196. doi: 10.1152/ajpcell.00198.2005

Nataatmadja, M., West, J., Prabowo, S., and West, M. (2013). Angiotensin II receptor antagonism reduces transforming growth factor beta and smad signaling in thoracic aortic aneurysm. *Ochsner. J.* 13, 42–48. Available online at: http://www.ochsnerjournal.org/doi/pdf/10.1043/1524-5012-13.1.42

Noseda, M., Fu, Y., Niessen, K., Wong, F., Chang, L., Mclean, G., et al. (2006). Smooth muscle α-actin is a direct target of Notch/CSL. *Circ. Res.* 98, 1468–1470. doi: 10.1161/01.RES.0000229683.81357.26

Owens, G. K. (1995). Regulation of differentiation of vascular smooth muscle cells. *Physiol. Rev.* 75, 487–517.

Owens, G. K., Kumar, M. S., and Wamhoff, B. R. (2004). Molecular regulation of vascular smooth muscle cell differentiation in development and disease. *Physiol. Rev.* 84, 767–801. doi: 10.1152/physrev.00041.2003

Padang, R., Bagnall, R. D., Richmond, D. R., Bannon, P. G., and Semsarian, C. (2012). Rare non-synonymous variations in the transcriptional activation domains of GATA5 in bicuspid aortic valve disease. *J. Mol. Cell. Cardiol.* 53, 277–281. doi: 10.1016/j.yjmcc.2012.05.009

Paloschi, V., Gådin, J. R., Khan, S., Björck, H. M., Du, L., Maleki, S., et al. (2015). Aneurysm development in patients with a bicuspid aortic valve is not associated with transforming growth factor-β activation. *Arterioscler. Thromb. Vasc. Biol.* 35, 973–980. doi: 10.1161/ATVBAHA.114.304996

Pedrosa, A.-R., Trindade, A., Fernandes, A.-C., Carvalho, C., Gigante, J., Tavares, A. T., et al. (2015). Endothelial Jagged1 antagonizes Dll4 regulation of endothelial branching and promotes vascular maturation downstream of Dll4/Notch1. *Arterioscler. Thromb. Vasc. Biol.* 35, 1134–1146. doi: 10.1161/ATVBAHA.114.304741

Phillippi, J. A., Green, B. R., Eskay, M. A., Kotlarczyk, M. P., Hill, M. R., Robertson, A. M., et al. (2014). Mechanism of aortic medial matrix remodeling is distinct in patients with bicuspid aortic valve. *J. Thorac. Cardiovasc. Surg.* 147, 1056–1064. doi: 10.1016/j.jtcvs.2013.04.028

Proweller, A., Pear, W. S., and Parmacek, M. S. (2005). Notch signaling represses myocardin-induced smooth muscle cell differentiation. *J. Biol. Chem.* 280, 8994–9004. doi: 10.1074/jbc.M413316200

Qiu, P., Ritchie, R. P., Fu, Z., Cao, D., Cumming, J., Miano, J. M., et al. (2005). Myocardin enhances Smad3-mediated transforming growth factor-β1 signaling in a CArG box-independent manner. *Circ. Res.* 97, 983–991. doi: 10.1161/01.RES.0000190604.90049.71

Ramasamy, S. K., Kusumbe, A. P., Wang, L., and Adams, R. H. (2014). Endothelial Notch activity promotes angiogenesis and osteogenesis in bone. *Nature* 507, 376–380. doi: 10.1038/nature13146

Rostama, B., Peterson, S. M., Vary, C. P., and Liaw, L. (2014). Notch signal integration in the vasculature during remodeling. *Vascul. Pharmacol.* 63, 97–104. doi: 10.1016/j.vph.2014.10.003

Rostama, B., Turner, J. E., Seavey, G. T., Norton, C. R., Gridley, T., Vary, C. P., et al. (2015). DLL4/Notch1 and BMP9 interdependent signaling induces human endothelial cell quiescence via P27KIP1 and thrombospondin-1. *Arterioscler. Thromb. Vasc. Biol.* 35, 2626–2637. doi: 10.1161/ATVBAHA.115.306541

Rutkovskiy, A., Stensløkken, K. O., and Vaage, I. (2016). Osteoblast differentiation at a glance. *Med. Sci. Monit. Basic Res.* 22, 95–106. doi: 10.12659/MSMBR.901142

Shimizu, T., Tanaka, T., Iso, T., Matsui, H., Ooyama, Y., Kawai-Kowase, K., et al. (2011). Notch signaling pathway enhances bone morphogenetic protein 2 (BMP2) responsiveness of Msx2 gene to induce osteogenic differentiation and mineralization of vascular smooth muscle cells. *J. Biol. Chem.* 286, 19138–19148. doi: 10.12659/MSMBR.901142

Sweeney, C., Morrow, D., Birney, Y. A., Coyle, S., Hennessy, C., Scheller, A., et al. (2004). Notch 1 and 3 receptor signaling modulates vascular smooth muscle cell growth, apoptosis, and migration via a CBF-1/RBP-Jk dependent pathway. *FASEB J.* 18, 1421–1423. doi: 10.1096/fj.04-1700fje

Talele, N. P., Fradette, J., Davies, J. E., Kapus, A., and Hinz, B. (2015). Expression of α-smooth muscle actin determines the fate of mesenchymal stromal cells. *Stem Cell Rep.* 4, 1016–1030. doi: 10.1016/j.stemcr.2015.05.004

Theodoris, C. V., Li, M., White, M. P., Liu, L., He, D., Pollard, K. S., et al. (2015). Human disease modeling reveals integrated transcriptional and epigenetic mechanisms of NOTCH1 haploinsufficiency. *Cell* 160, 1072–1086. doi: 10.1016/j.cell.2015.02.035

Towler, D. A. (2017). Commonalities between vasculature and bone. *Circulation* 135, 320–322. doi: 10.1161/CIRCULATIONAHA.116.022562

Wang, Z., Wang, D.-Z., Pipes, G. T., and Olson, E. N. (2003). Myocardin is a master regulator of smooth muscle gene expression. *Proce. Natl. Acad. Sci. U.S.A.* 100, 7129–7134. doi: 10.1073/pnas.1232341100

Yip, C. Y., Blaser, M. C., Mirzaei, Z., Zhong, X., and Simmons, C. A. (2011). Inhibition of pathological differentiation of valvular interstitial cells by C-type natriuretic peptide. *Arterioscler. Thromb. Vasc. Biol.* 31, 1881–1889. doi: 10.1161/ATVBAHA.111.223974

Zeng, Q., Song, R., Ao, L., Weyant, M. J., Lee, J., Xu, D., et al. (2013). Notch1 promotes the pro-osteogenic response of human aortic valve interstitial cells via modulation of ERK1/2 and nuclear factor-κB activation. *Arterioscler. Thromb. Vasc. Biol.* 33, 1580–1590. doi: 10.1161/ATVBAHA.112.300912

Zhu, L., Vranckx, R., Van Kien, P. K., Lalande, A., Boisset, N., Mathieu, F., et al. (2006). Mutations in myosin heavy chain 11 cause a syndrome associating thoracic aortic aneurysm/aortic dissection and patent ductus arteriosus. *Nat. Genet.* 38, 343–349. doi: 10.1038/ng1721

Conflict of Interest Statement: The authors declare that the research was conducted in the absence of any commercial or financial relationships that could be construed as a potential conflict of interest.

frontiers in Physiology

MINI REVIEW
published: 10 August 2017
doi: 10.3389/fphys.2017.00569

Molecular Regulation of Arterial Aneurysms: Role of Actin Dynamics and microRNAs in Vascular Smooth Muscle

*Azra Alajbegovic†, Johan Holmberg† and Sebastian Albinsson *†*

Department of Experimental Medical Science, Lund University, Lund, Sweden

Aortic aneurysms are defined as an irreversible increase in arterial diameter by more than 50% relative to the normal vessel diameter. The incidence of aneurysm rupture is about 10 in 100,000 persons per year and ruptured arterial aneurysms inevitably results in serious complications, which are fatal in about 40% of cases. There is also a hereditary component of the disease and dilation of the ascending thoracic aorta is often associated with congenital heart disease such as bicuspid aortic valves (BAV). Furthermore, specific mutations that have been linked to aneurysm affect polymerization of actin filaments. Polymerization of actin is important to maintain a contractile phenotype of smooth muscle cells enabling these cells to resist mechanical stress on the vascular wall caused by the blood pressure according to the law of Laplace. Interestingly, polymerization of actin also promotes smooth muscle specific gene expression via the transcriptional co-activator MRTF, which is translocated to the nucleus when released from monomeric actin. In addition to genes encoding for proteins involved in the contractile machinery, recent studies have revealed that several non-coding microRNAs (miRNAs) are regulated by this mechanism. The importance of these miRNAs for aneurysm development is only beginning to be understood. This review will summarize our current understanding about the influence of smooth muscle miRNAs and actin polymerization for the development of arterial aneurysms.

Keywords: microRNA, aneurysm, BAV, actin polymerization, myocardin related transcription factors

OPEN ACCESS

Edited by:
Luis A. Martinez-Lemus, University of Missouri, United States

Reviewed by:
Shuangtao Ma, Michigan State University, United States
Lakshmidevi Pulakat, University of Missouri, United States

***Correspondence:**
Sebastian Albinsson
sebastian.albinsson@med.lu.se

† These authors have contributed equally to this work.

Specialty section:
This article was submitted to Vascular Physiology, a section of the journal Frontiers in Physiology

Received: *28 April 2017*
Accepted: *21 July 2017*
Published: *10 August 2017*

Citation:
Alajbegovic A, Holmberg J and Albinsson S (2017) Molecular Regulation of Arterial Aneurysms: Role of Actin Dynamics and microRNAs in Vascular Smooth Muscle. Front. Physiol. 8:569. doi: 10.3389/fphys.2017.00569

INTRODUCTION

Aneurysms are caused by a weakening in the arterial wall resulting in a local distension of the affected vessel. Although aneurysms can occur at various sites of the vasculature, aortic aneurysms are the most common and typically classified in terms of their anatomical location: thoracic aortic aneurysms (TAA) and abdominal aortic aneurysms (AAA). A study from the Global Burden of Disease lists aortic aneurysm among the 10 most common causes of cardiovascular disease-related death (Roth et al., 2015).

Aneurysm pathology is characterized by endothelial dysfunction, reduced contractile function due to altered actin dynamics and/or changes in smooth muscle phenotype, and degradation of elastic fibers and collagen. Although the etiology of aneurysms may differ depending on the affected site, certain mechanisms involved in the progressive weakening of the vascular wall are likely general for multiple forms of aneurysms. In most cases, aneurysms develop slowly and cause

no noticeable symptoms until rupture occurs, hampering early intervention. There are currently no therapeutic drugs available and current treatment options are limited to open surgery or endovascular repair. Consequently, there is an acute need for additional therapeutic approaches.

According to the National Heart, Lung, and Blood Institute, environmental risk factors for aortic aneurysms include age, male gender, smoking, and high blood pressure. In addition, genetic factors play a role in the cause of aortic aneurysms, albeit stronger for TAA than AAA (Biddinger et al., 1997; Morisaki and Morisaki, 2016). TAA is a common finding in conditions such as Marfan and Loeys-Dietz syndrome (Dietz et al., 1991; Loeys et al., 2006), and bicuspid aortic valve (BAV) (Prakash et al., 2014). BAV is present in 0.5–2% of the population and is the most common congenital heart anomaly although symptoms, including TAA, typically develop in adulthood (Hoffman and Kaplan, 2002; Siu and Silversides, 2010). It is clinically heterogenous and the exact cause is unclear. Unlike Marfan syndrome and Loeys-Dietz syndrome, which is caused by mutations in the *FBN1* and *TGFBR1*/*TGFBR2* genes, respectively, no gene causing BAV has been identified.

Inherited predisposition to thoracic aortic disease in the absence of syndromic features has also been reported. Recent studies demonstrate that mutations in *ACTA2* and *MYH11,* encoding the contractile proteins smooth muscle cell α-actin and β-myosin heavy chain, respectively, can cause thoracic aortic aneurysms and dissections (TAAD) (Zhu et al., 2006; Guo et al., 2007). Importantly, mutations in *ACTA2* are the most prevalent genetic cause of TAAD and to date more than 40 *ACTA2* mutations have been identified (Guo et al., 2007; Morisaki et al., 2009; Regalado et al., 2015). Some of the *ACTA2* mutations have been shown to interfere with actin polymerization (Guo et al., 2007; Malloy et al., 2012; Lu et al., 2015). As such, *ACTA2* mutations may lead to a defective contractile function and reduced ability of vascular smooth muscle cells (SMCs) to resist mechanical stress on the arterial wall and consequently increasing the susceptibility for aneurysm and dissection. The first part of this Review focuses on actin polymerization in formation of aneurysms and its potential role for the regulation of gene expression via the myocardin related transcription factor, MRTF.

Recently, microRNAs (miRNAs) have been associated with the formation of both aortic and intracranial aneurysms. MiRNAs are small, single-stranded non-coding RNAs. They are ∼22 nucleotides in length and regulate gene expression post-transcriptionally by binding to complementary target sites in mRNA molecules. A number of miRNAs are differentially expressed in aortic aneurysms, including miR-29 (Boon et al., 2011), members of the miR-15 family (Zampetaki et al., 2014), miR-21 (Maegdefessel et al., 2012a), miR-26 (Leeper et al., 2011), and miR-143/145 (Elia et al., 2009). Moreover, we have identified a group of miRNAs regulated by actin polymerization and MRTF. Several of these miRNAs are downregulated in dilated aorta suggesting that they may play a role in the development of aneurysms (Alajbegovic et al., 2016). In the second part of this Review, we focus on the importance of miRNAs for the formation of arterial aneurysms. Taken together, identification and characterization of both coding and non-coding genes associated with actin polymerization may aid in the development of much needed new therapeutic strategies against aneurysms formation. These may not be specifically involved in BAV-associated aortopathy, but it is clear that common mechanisms are involved in various forms of arterial aneurysms, which can improve our understanding of the cause of this disease.

THE ROLE OF ACTIN POLYMERIZATION IN THE DEVELOPMENT OF ARTERIAL ANEURYSM

Mutations that have been linked to arterial aneurysm involve dynamic changes in polymerization of actin filaments (Guo et al., 2009; Lu et al., 2015). Actins constitute a family of highly conserved proteins that polymerizes into filaments and play a number of important roles in various biological processes including force generation, cellular mechanosensing, regulation of cell differentiation, and in the maintenance of vascular wall integrity. In mammals, actin exists in six isoforms expressed in a tissue-specific manner (Perrin and Ervasti, 2010). In vascular SMCs, α-actin (ACTA2) is the predominantly expressed actin isoform and the most abundant protein accounting for ∼40% of the total cellular protein load (Fatigati and Murphy, 1984).

In humans, heterozygous *ACTA2* mutations predispose individuals to aortic aneurysm (**Table 1**). To date, ∼40 mutations have been identified in the *ACTA2* gene. Missense mutations in *ACTA2* are the predominant genetic component of familial TAAD, accounting for 12–21% of all cases (Guo et al., 2007; Morisaki et al., 2009; Disabella et al., 2011; Renard et al., 2013). In most families the disease segregates as an autosomal dominant trait with variable penetrance and high clinical heterogeneity. Aortic tissue from patients carrying *ACTA2* mutations show an abnormal medial layer of the vessel wall with a disorganized structure indicating actin filament instability and/or abnormal filament assembly (Regalado et al., 2015) (Guo et al., 2007; Morisaki et al., 2009). Several studies have addressed these mutations to get an insight into how *ACTA2* mutations can cause TAAD. Carriers of R258C mutation show high penetrance and poor prognosis with a median life expectancy of ∼35 years of age (Regalado et al., 2015). Using a baculoviral system Lu et al. could show that the R285C mutation in α-actin resulted in a less stable filament with increased sensitivity to cleavage by cofilin, a decreased rate of polymerization and a slower interaction with smooth muscle myosin leading to reduced force generation (Lu et al., 2015). In a later study by the same group, similar biochemical properties on actin function were obtained studying ACTA2 mutation R179H (Lu et al., 2016). Carriers of this mutation show early onset of disease with high penetrance and poor patient prognosis causing multisystemic smooth muscle dysfunction (Milewicz et al., 2010b; Munot et al., 2012; Georgescu et al., 2015; Regalado et al., 2015). More recently, Liu et al. developed a model system to study R258C-induced effects in a cellular context. Using patient-derived dermal fibroblasts the authors could demonstrate that mutated smooth muscle α-actin abrogated multiple cytoskeletal functions attributed to induction of wild type smooth muscle α-actin, including stress

TABLE 1 | List of identified ACTA2 mutations with clinical and pathological characteristics.

ACTA2 gene mutation	Actin polymerization	Vascular pathology	Clinical characteristics
p.R149C		Aortic tissue: proteoglycan accumulation, loss and fragmentation of elastic fibers, focal loss of SMCs, SMC disarray, SMC hyperplasia in vasa vasorum (Guo et al., 2007; Disabella et al., 2011)	TAAD, Stroke, premature CAD (Guo et al., 2009), Livedo reticularis (Guo et al., 2007), iris cysts (Morisaki et al., 2009), iris flocculi (Guo et al., 2007; Disabella et al., 2011; Chamney et al., 2015)
p.R118Q	Perturbs ACTA2 filament assembly or stability (Guo et al., 2007), causes filament instability with faster disassembly rates and increased critical concentrations, hypersensitive to cofilin severing (Bergeron et al., 2011)	Coronary and epicardial artery: Stenosis of the vessel with increased SMC proliferation (Guo et al., 2009)	TAAD, Stroke, premature CAD (Guo et al., 2007, 2009)
p.T353N	Perturbs ACTA2 filament assembly or stability (Guo et al., 2007)	Aortic tissue: SMC hyperplasia in vasa vasorum (Guo et al., 2007)	TAAD (Guo et al., 2007, 2009)
p.R258C/H	Causes actin filament instability, increased susceptibility to severing by cofilin, higher affinity binding to profilin, perturbed interaction with smooth muscle myosin, decreased rate of polymerization (Malloy et al., 2012; Lu et al., 2015)	Aortic tissue: proteoglycan accumulation, loss and fragmentation of elastic fibers, areas with SMC loss, SMC disarray (Guo et al., 2007)	TAAD, premature stroke including Moyamoya disease (Guo et al., 2009), PDA (Guo et al., 2007)
p.R39H			TAAD, premature stroke, CAD (Guo et al., 2009)
p.R39C			TAAD (Hoffjan et al., 2011; Renard et al., 2013)
p.P72Q			TAAD (Guo et al., 2009)
p.N117T	Causes filament instability, with faster disassembly rates and increased critical concentrations, hyposensitive to severing by cofilin (Bergeron et al., 2011)		TAAD, Stroke (Guo et al., 2009)
p.Y135H			TAAD (Guo et al., 2009)
p.V154A			TAAD (Guo et al., 2009)
p.G160D			TAAD (Guo et al., 2009)
p.R185Q			TAAD, CAD (Guo et al., 2009)
p.R212Q			TAAD (Guo et al., 2009; Morisaki et al., 2009), premature stroke, CAD (Guo et al., 2009)
p.P245H			TAAD, Stroke (Guo et al., 2009)
p.I250L			TAAD, Stroke (Guo et al., 2009)
p.R292G		Stenosis of epicardial arteries, increased SMC proliferation (Guo et al., 2009)	TAAD (Guo et al., 2009)
p.T326N			TAAD, Stroke, CAD (Guo et al., 2009)
p.T353N			TAAD, Stroke, CAD (Guo et al., 2009)
p.R179H	Increased susceptibility to severing by cofilin, higher affinity binding to profilin, perturbed interaction with smooth muscle myosin, increased disassembly rate, binds less cooperatively to MRTFA (Lu et al., 2016)	Aortic tissue: fibroproliferative lesions in the intima, medial SMC proliferation and fragmentation of elastic fiber, proteoglycan accumulation, stenosis of vasa vasorum (Milewicz et al., 2010a) (Georgescu et al., 2015) Cerebral arteries: Intimal thickening, medial fibrosis, fragmented and thickened elastic laminae, SMC proliferation (Munot et al., 2012) (Georgescu et al., 2015)	Ascending aortic aneurysm, PDA cerebrovascular disease, fixed dilated pupils, hypotonic bladder, malrotation, hypoperistalsis of the gut and pulmonary hypertension,congenital mydriasis (Milewicz et al., 2010a; Al-Mohaissen et al., 2012; Munot et al., 2012; Logeswaran et al., 2017)
p.D82E		Aortic wall: Loss of SMCs (Disabella et al., 2011)	TAAD, Myopia ($n = 2/2$) (Disabella et al., 2011)
p.E243K		Aortic wall: Loss of SMCs (Disabella et al., 2011)	TAAD, Myopia ($n = 2/2$) (Disabella et al., 2011)
p.V45L			TAAD (Disabella et al., 2011)
IVS4+1G>A		Aortic wall: SMC hyperplasia in vasa vasorum, disarray of medial SMC (Disabella et al., 2011)	TAAD, Scoliosis ($n = 5/8$), Pes planus ($n = 5/8$), Livedo reticularis ($n = 1/8$), Iris flocculi ($n = 1/8$), Myopia ($n = 2/8$) (Disabella et al., 2011)

(Continued)

TABLE 1 | Continued

ACTA2 gene mutation	Actin polymerization	Vascular pathology	Clinical characteristics
p.M49V			TAAD (Hoffjan et al., 2011; Renard et al., 2013)
p.G340R			TAAD (Hoffjan et al., 2011)
p.G152_T205del			TAAD (Morisaki et al., 2009)
p.Y145C (sporadic case)			TAAD (Morisaki et al., 2009)
p.D26Y		Aortic tissue: medial degeneration with loss and fragmentation of elastic fibers, disarray and loss of SMCs, accumulation of proteoglycan, SMCs hyperplasia of vasa vasorum ($n = 2$) (Yoo et al., 2010)	TAAD (Yoo et al., 2010)
p.R314X			TAAD (Renard et al., 2013)
p.S340CfxX25			TAAD (Renard et al., 2013)
p.G38R			TAAD (Renard et al., 2013)
p.H42N			TAAD (Renard et al., 2013)
p.Q61R			TAAD (Renard et al., 2013)
p.N117I			TAAD (Ke et al., 2016)
p.L348R			TAAD (Ke et al., 2016)
p.Y168N (sporadic case)			TAAD, BAV ($n = 1/1$) (Ke et al., 2016)
p.K328N		Aortic tissue: elastic fiber fragmentation, SMC disarray, adventitial fibrosis (Ware et al., 2014)	TAAD, congenital mydriasis ($n = 2/2$) (Ware et al., 2014)

CAD, coronary artery disease; BAV, bicuspid valve; PDA, patent ductus arteriosus; p, protein reference sequence.

fiber formation, focal adhesions, matrix contraction, cellular migration, and filamentous to soluble actin ratio (Liu et al., 2017). Similar findings have been obtained by mutating the same arginine residue to a histidine, R285H. Using budding yeast as a model system, Malloy et al. showed that the yeast R258H actin produced abnormal cytoskeletal morphology and filament instability (Malloy et al., 2012). Moreover, a study on human ACTA2 mutations N117T and R118Q revealed mutation-specific effects on actin behavior suggesting that several individual mechanisms may contribute to the pathogenesis of familial TAAD (Bergeron et al., 2011).

It seems that various types of arteries respond differently to the underlying mutation contributing to a diverse pathology (Guo et al., 2009). ACTA2 mutations lead to dilation of larger vessels such as the aorta but occlusion of smaller arteries. The different response arteries display to a single gene mutation has been attributed to several factors including vascular SMCs lineage diversity, elastic vs. muscular arteries, and differences in mechanical forces on the vascular wall (Guo et al., 2009; Milewicz et al., 2010a).

In addition to aortic aneurysms, other features associated with subset of families with *ACTA2* mutations include cases with BAV and a predisposition for occlusive vascular diseases, including thrombotic stroke and coronary artery disease (Guo et al., 2007, 2009; Ke et al., 2016). The association of BAV with TAAD has been reported frequently suggesting that a common gene defect underlies this association (Edwards et al., 1978; Loscalzo et al., 2007). Included in the occlusive vascular diseases were cases with livedo reticularis, a skin rash caused by occlusion of dermal arteries and Moyamoya, a cerebrovascular disease characterized by progressive stenosis (Guo et al., 2007, 2009; Bergeron et al., 2011). Studies on tissue from affected individuals demonstrate an excessive proliferation of SMCs and myofibroblasts contributing to vascular occlusion (Guo et al., 2009; Milewicz et al., 2010a). This increase in SMC proliferation has been attributed to the role α-actin plays in regulating smooth muscle phenotype by shifting the F/G-actin ratio. It is well-established that when F-actin polymerization is inhibited the monomeric pool of G-actin is increased. The downstream effects of an increased pool of G-actin include retention of the actin-binding transcription factor, myocardin-related transcription factor (MRTF-A/B), in the cytosol. MRTF is a transcriptional co-factor that complexes with serum response factor (SRF) to drive expression of SMC-specific genes. As a consequence, an increase in G-actin may alter the phenotype of SMCs, from a highly contractile phenotype to a more proliferative phenotype. In a recent study, we have demonstrated that polymerization of actin filaments, and MRTF-dependent gene expression, is reduced in mildly dilated aortas from patients with stenotic tricuspid aortic valve (TAV) or BAV (Alajbegovic et al., 2016). This result suggests that altered actin polymerization may be an early event in the development of ascending aortic aneurysm and that the effect is not specific for BAV-associated disease.

Knockout of MRTF-B results in embryonic lethality associated with a spectrum of cardiovascular defects including aortic aneurysms (Oh et al., 2005; Li et al., 2012). The importance of MRTF-A/B for aneurysm formation in adult mice using smooth muscle-specific inducible double knockout has to our knowledge not been investigated. However, tamoxifen inducible, SMC-specific deletion of myocardin in mice leads to dilation of the thoracic aorta, dissection and rupture mimicking the pathology seen in TAAD patients (Huang et al., 2015). Myocardin

is a muscle-restricted transcription factor, part of the myocardin family of transcriptional coactivators that, similar to MRTFs, promotes the expression of smooth muscle specific genes.

Further support of an important role of myocardin family co-activators for aneurysm formation is suggested by studies using smooth muscle specific knockout mice of intergrin-linked kinase (ILK) (Shen et al., 2011). ILK is a serine/threonine kinase with the main function to link extracellular matrix (ECM) via integrins to the actin cytoskeleton (Qian et al., 2005). SMC-conditional ILK mutant mice die around the perinatal period exhibiting defective morphogenetic development of the greater arteries including aneurysmal dilation of the thoracic aorta. Histological analysis revealed a profound vascular pathology of the arterial tunica media with changes in SMC phenotype, disruption of elastic lamellae, and a decreased actin polymerization (Shen et al., 2011). In agreement with a role of actin for nuclear translocation of MRTF, ILK deletion caused cytoplasmic retention of MRTF-A in aortic SMCs. In support of this study, conditional deletion of *Ilk* in neural crest cells results in aortic aneurysm and embryonic lethality (Arnold et al., 2013). *Ilk* mutant mice show defective differentiation of neural crest cells into SMCs and disorganization of actin stress fibers. Thus, these studies suggest that ILK regulates a signaling pathway involving actin polymerization that protects against aortic aneurysm. As such, *Ilk* mutant mice may prove helpful as animal models for additional insight into the pathogenesis of arterial aneurysms.

ROLE OF MICRORNAS IN ANEURYSM DEVELOPMENT

MicroRNAs (miRNAs) are small (∼22 nt) non-coding RNAs that are involved in post-transcriptional regulation of protein synthesis (Bartel, 2004). The biogenesis of miRNAs involve transcription by RNA polymerases, cleavage by endoribonucleases Drosha and Dicer, and incorporation into the RNA-induced silencing complex (RISC). The miRNAs then target 3′-UTR of mRNAs by binding with partial complementarity to the mRNA sequence. Perfect base pairing of the seed region (nucleotides 2–7 of the miRNA) to the mRNA is necessary for miRNA-dependent regulation. Binding of the RISC complex to mRNAs results in translational inhibition and in some cases mRNA degradation. In recent years, several miRNAs have been shown to be involved in the development of vascular disease states including aneurysms (Albinsson and Sward, 2013; Duggirala et al., 2015). Altered composition of ECM proteins in the vascular wall is one of the hallmarks of aortic aneurysms. Both fibroblasts and SMCs play important roles in matrix deposition and several studies have focused on the potential involvement of miRNAs in the regulation of ECM synthesis in these cell types.

The miR-29 family (miR-29a/b/c) stands out in its ability to target mRNAs encoding for ECM proteins, including collagens, elastin, and fibrillin-1 (van Rooij et al., 2008; Ekman et al., 2013; Maegdefessel et al., 2014). Pioneering work by Boon et al. demonstrated increased expression of miR-29b in two mouse models of aortic aneurysm (AngII-treated aged mice and Fibulin4(R/R) mice) and in early aortic dilation associated with BAV and TAV in humans (Boon et al., 2011). Importantly, AngII mediated dilation of mouse aorta was prevented using LNA-modified antisense oligonucleotide-mediated silencing of miR-29 (Boon et al., 2011). The therapeutic effect of miR-29 inhibition is consistent in other animal models of aneurysm formation (Maegdefessel et al., 2012b) (Zampetaki et al., 2014). However, in contrast with the study by Boon et al., additional studies have demonstrated reduced expression of miR-29 family members in human aortic aneurysms (Jones et al., 2011; Maegdefessel et al., 2012b). This discrepancy may depend on several factors including differences in tissue sampling (as discussed below) and the characteristics of the aortic dilation (Maegdefessel et al., 2014).

In a recently published study, we investigated differential miRNA expression in the convexity and concavity of the aortic arch of patients with mildly dilated aortae associated with either BAV or TAV. These samples were compared with biopsies from healthy donors. The convexity of the aortic wall is more disease-prone than the concavity, which may depend on differences in wall shear stress on the endothelial cells (Atkins et al., 2014). Comparison of these two regions may thus be important to understand the role of flow dynamics for the development of ascending aortic wall remodeling. We found that miR-29a/c was upregulated in the aortic concavity of dilated aorta associated with BAV (Albinsson et al., 2017). Further analysis revealed that miR-29a/c expression was reduced in the convexity compared to the concavity in BAV. A two-fold threshold was used which excluded minor changes in miRNA expression. However, it is interesting to note that both miR-29a (fold change: −1.96) and miR-29c (fold change: −1.43) were reduced in the convexity of BAV aorta compared to donor controls. Only minor differences were observed in miR-29b expression in either setting. These results propose that the discrepancy in miR-29 expression in biopsies from patients with BAV associated aortic dilation may depend on the localization of the obtained tissue sample. Similar to miR-29, miR-15 family members (miR-15, miR-16, miR-195, and miR-497) targets several ECM components (Ott et al., 2011). However, while *in vivo* administration of miR-195 inhibitor increases ECM production, this effect is not sufficient to prevent aneurysm formation (Zampetaki et al., 2014).

Although miR-29 appears to be particularly promising for therapeutic intervention, additional miRNAs have been demonstrated to be dysregulated in aortic aneurysms, including miR-21 (Maegdefessel et al., 2012a), miR-26 (Leeper et al., 2011), and the miR-143/145 cluster (Elia et al., 2009). In a recent study, we demonstrated that a group of smooth muscle miRNAs, including miR-143/145, miR-1, miR-378a, and miR-22, are regulated by actin dynamics via the actin sensitive transcription factor MRTF-A (Alajbegovic et al., 2016). With the exception of miR-22, these miRNAs were found to be highly enriched in muscle-containing tissues and downregulated in phenotypically modified SMCs. Interestingly, the levels of polymerized actin were reduced in biopsies of mildly dilated aorta (<4.5 cm) from patients with either stenotic TAV or BAV. Accordingly, the expression of the actin-regulated miRNAs was reduced in dilated aorta. These results point toward a role of actin polymerization

and actin-sensitive transcription factors for the transcriptional control of miRNA expression in aortic aneurysm development (**Figure 1**). In support of this notion, miR-145 overexpression reduces the formation of AngII-induced AAA (Wu et al., 2016). The study by Wu et al. suggests that the effect of miR-145 involves reduced MMP2 activation. However, it is interesting to note that miR-145 has been shown to promote actin polymerization in smooth muscle cells (Xin et al., 2009; Albinsson et al., 2010), which may offer additional protection against aortic dilation.

Downregulation of miR-143/145 in the vascular wall has also been demonstrated in intracranial aneurysms (Jiang et al., 2013; Liu et al., 2014; Bekelis et al., 2016), suggesting that down-regulation of this miRNA cluster may be a general mechanism of aneurysm formation. Moreover, miR-21 is upregulated in both aortic (Maegdefessel et al., 2012a) and cerebral aneurysms (Bekelis et al., 2016). The increase in miR-21 and decrease in miR-143/145 clearly indicates reduced contractile differentiation of SMCs in the aneurysmal vascular wall. Although, phenotypic modulation of SMCs is likely to contribute to various vascular disease states, it is primarily an evolutionary conserved repair mechanism in response to vascular injury. Therefore, reversing this process can result in loss of endogenous protection against factors that promote aneurysm development. This is evident from results demonstrating that inhibition of miR-21 augments aortic dilation, while overexpression of miR-21 significantly reduced aortic dilation in an elastase-induced model of aortic aneurysm (Maegdefessel et al., 2012a). The effect of miR-21 overexpression is likely due to increased smooth muscle proliferation via decreased PTEN and increased Akt activation. This effect increases wall thickness and maintains wall stress at relatively low levels according to the Law of Laplace.

In summary, miRNAs are promising therapeutic targets against aneurysm formation. A common mechanism for the therapeutic effect of miRNAs appears to be to strengthen

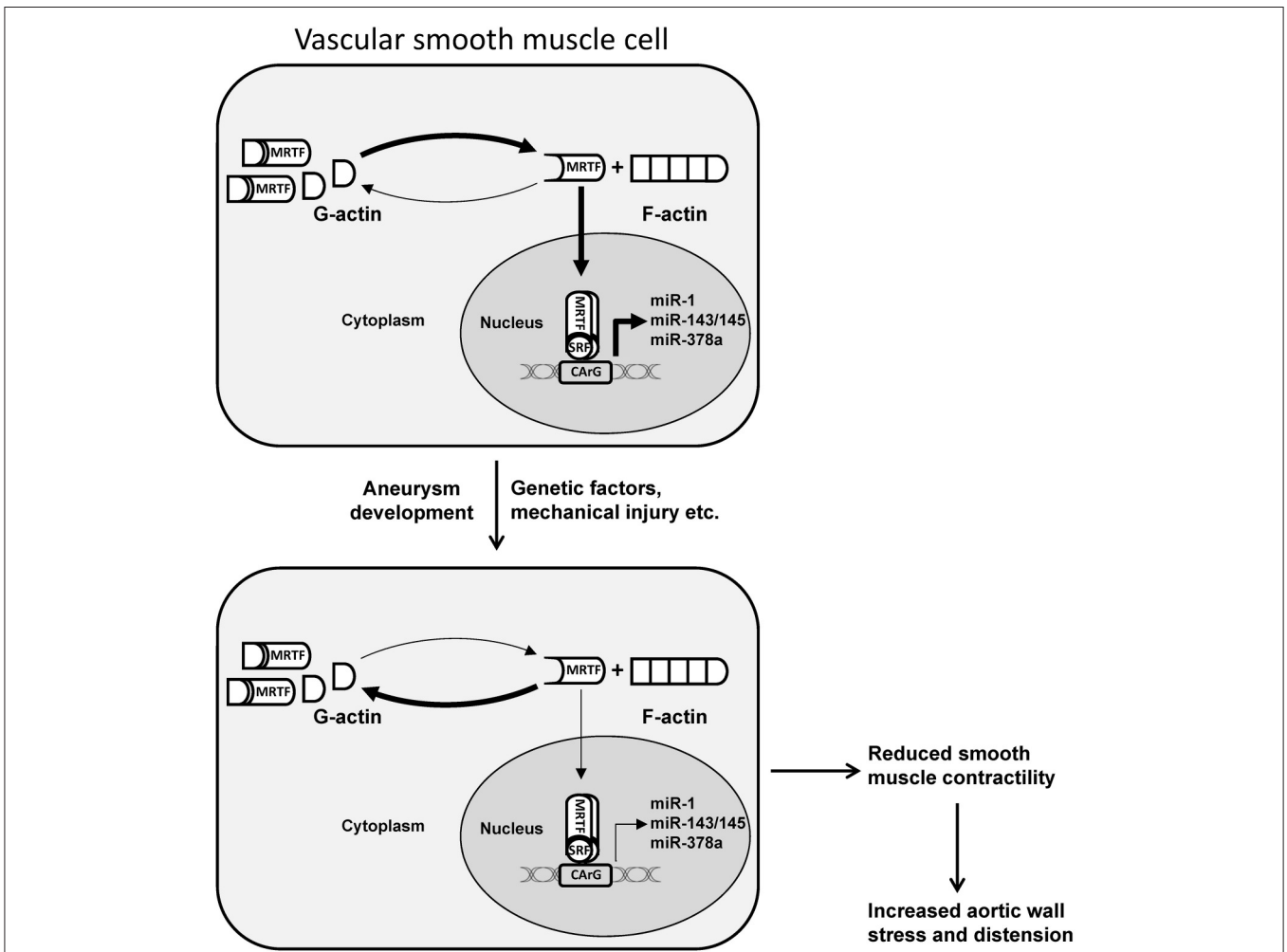

FIGURE 1 | Schematic illustration of MRTF-dependent transcriptional regulation of miRNAs in dilated aorta**.** An increase in cytosolic or nuclear G-actin due to mutations in actin, mechanical injury, or other factors involved in aneurysm formation, results in decreased nuclear accumulation of MRTF and reduced transcription of miRNAs associated with contractile smooth muscle cells. In addition to other mechanisms, this can result in reduced smooth muscle contractility and increased aortic wall stress and distension. MRTF, myocardin related transcription factor; SRF, serum response factor. Adapted from Alajbegovic et al. (2016).

the vascular wall to better withstand mechanical forces of the blood pressure. This is accomplished by either increasing ECM production (miR-29 inhibitor), increasing smooth muscle growth (miR-21 mimic), or increasing smooth muscle contractile differentiation (miR-145 mimic).

SUMMARY

In summary, several lines of evidence support a role of actin polymerization in the development of aortic aneurysms. The effects of altered actin polymerization may be mediated directly, via loss of structural integrity, and/or via reduced contractility resulting in hampered resistance to tensile stretch exerted by the blood pressure. Furthermore, increasing evidence suggests that the regulation of myocardin family co-activators by actin polymerization is essential for protection against aneurysm development. This effect may be mediated in part via small non-coding RNAs. Further studies are warranted to elucidate the importance of actin regulated miRNAs for the development of arterial aneurysms. In addition, although changes in the expression of some miRNAs appear to be general for several types of aneurysms, our detailed analysis of miRNA expression in BAV vs. TAV-associated aortopathy has revealed differential miRNA signatures in these conditions. These findings need to be further explored to understand the importance of the specific differences in miRNA expression in BAV-associated aortic dilation.

AUTHOR CONTRIBUTIONS

JH wrote introduction; AA wrote section on actin polymerization; SA wrote section on miRNAs, and summary. All authors contributed equally to this work.

ACKNOWLEDGMENTS

This work was supported by the Swedish Research Council, the Swedish Heart and Lung Foundation, the Novo Nordisk Foundation, the Crafoord Foundation, the Royal Physiographic Society, and the Magnus Bergvall Foundation.

REFERENCES

Alajbegovic, A., Turczynska, K. M., Hien, T. T., Cidad, P., Sward, K., Hellstrand, P., et al. (2016). Regulation of microRNA expression in vascular smooth muscle by mrtf-a and actin polymerization. *Biochim. Biophys. Acta* 1864, 1088–1098. doi: 10.1016/j.bbamcr.2016.12.00

Albinsson, S., and Sward, K. (2013). Targeting smooth muscle microRNAs for therapeutic benefit in vascular disease. *Pharmacol. Res.* 75, 28–36. doi: 10.1016/j.phrs.2013.04.003

Albinsson, S., Della Corte, A., Alajbegovic, A., Krawczyk, K. K., Bancone, C., Galderisi, U., et al. (2017). Patients with bicuspid and tricuspid aortic valve exhibit distinct regional microRNA signatures in mildly dilated ascending aorta. *Heart Vessels* 32, 750–767. doi: 10.1007/s00380-016-0942-7

Albinsson, S., Suarez, Y., Skoura, A., Offermanns, S., Miano, J. M., and Sessa, W. C. (2010). MicroRNAs are necessary for vascular smooth muscle growth, differentiation, and function. *Arterioscler. Thromb. Vasc. Biol.* 30, 1118–1126. doi: 10.1161/ATVBAHA.109.200873

Al-Mohaissen, M., Allanson, J. E., O'Connor, M. D., Veinot, J. P., Brandys, T. M., Maharajh, G., et al. (2012). Brachial artery occlusion in a young adult with an *ACTA2* thoracic aortic aneurysm. *Vasc. Med.* 17, 326–329. doi: 10.1177/1358863X12453973

Arnold, T. D., Zang, K., and Vallejo-Illarramendi, A. (2013). Deletion of integrin-linked kinase from neural crest cells in mice results in aortic aneurysms and embryonic lethality. *Dis. Model. Mech.* 6, 1205–1212. doi: 10.1242/dmm.011866

Atkins, S. K., Cao, K., Rajamannan, N. M., and Sucosky, P. (2014). Bicuspid aortic valve hemodynamics induces abnormal medial remodeling in the convexity of porcine ascending aortas. *Biomech. Model. Mechanobiol.* 13, 1209–1225. doi: 10.1007/s10237-014-0567-7

Bartel, D. P. (2004). MicroRNAs: genomics, biogenesis, mechanism, and function. *Cell* 116, 281–297. doi: 10.1016/S0092-8674(04)00045-5

Bekelis, K., Kerley-Hamilton, J. S., Teegarden, A., Tomlinson, C. R., Kuintzle, R., Simmons, N., et al. (2016). MicroRNA and gene expression changes in unruptured human cerebral aneurysms. *J. Neurosurg.* 125, 1390–1399. doi: 10.3171/2015.11.JNS151841

Bergeron, S. E., Wedemeyer, E. W., Lee, R., Wen, K. K., McKane, M., Pierick, A. R., et al. (2011). Allele-specific effects of thoracic aortic aneurysm and dissection alpha-smooth muscle actin mutations on actin function. *J. Biol. Chem.* 286, 11356–11369. doi: 10.1074/jbc.M110.203174

Biddinger, A., Rocklin, M., Coselli, J., and Milewicz, D. M. (1997). Familial thoracic aortic dilatations and dissections: a case control study. *J. Vasc. Surg.* 25, 506–511. doi: 10.1016/S0741-5214(97)70261-1

Boon, R. A., Seeger, T., Heydt, S., Fischer, A., Hergenreider, E., Horrevoets, A. J., et al. (2011). MicroRNA-29 in aortic dilation: implications for aneurysm formation. *Circ. Res.* 109, 1115–1119. doi: 10.1161/CIRCRESAHA.111.255737

Chamney, S., McGimpsey, S., McConnell, V., and Willoughby, C. E. (2015). Iris flocculi as an ocular marker of *ACTA2* mutation in familial thoracic aortic aneurysms and dissections. *Ophthalmic Genet.* 36, 86–88. doi: 10.3109/13816810.2013.833634

Dietz, H. C., Cutting, G. R., Pyeritz, R. E., Maslen, C. L., Sakai, L. Y., Corson, G. M., et al. (1991). Marfan syndrome caused by a recurrent de novo missense mutation in the fibrillin gene. *Nature* 352, 337–339. doi: 10.1038/352337a0

Disabella, E., Grasso, M., Gambarin, F. I., Narula, N., Dore, R., Favalli, V., et al. (2011). Risk of dissection in thoracic aneurysms associated with mutations of smooth muscle alpha-actin 2 (*ACTA2*). *Heart* 97, 321–326. doi: 10.1136/hrt.2010.204388

Duggirala, A., Delogu, F., Angelini, T. G., Smith, T., Caputo, M., Rajakaruna, C., et al. (2015). Non coding rnas in aortic aneurysmal disease. *Front. Genet.* 6:125. doi: 10.3389/fgene.2015.00125

Edwards, W. D., Leaf, D. S., and Edwards, J. E. (1978). Dissecting aortic aneurysm associated with congenital bicuspid aortic valve. *Circulation* 57, 1022–1025. doi: 10.1161/01.CIR.57.5.1022

Ekman, M., Bhattachariya, A., Dahan, D., Uvelius, B., Albinsson, S., and Sward, K. (2013). miR-29 repression in bladder outlet obstruction contributes to matrix remodeling and altered stiffness. *PLoS ONE* 8:e82308. doi: 10.1371/journal.pone.0082308

Elia, L., Quintavalle, M., Zhang, J., Contu, R., Cossu, L., Latronico, M. V., et al. (2009). The knockout of mir-143 and -145 alters smooth muscle cell maintenance and vascular homeostasis in mice: correlates with human disease. *Cell Death Differ.* 16, 1590–1598. doi: 10.1038/cdd.2009.153

Fatigati, V., and Murphy, R. A. (1984). Actin and tropomyosin variants in smooth muscles. Dependence on tissue type. *J. Biol. Chem.* 259, 14383–14388.

Georgescu, M. M., Pinho Mda, C., Richardson, T. E., Torrealba, J., Buja, L. M., Milewicz, D. M., et al. (2015). The defining pathology of the new clinical and histopathologic entity *ACTA2*-related cerebrovascular disease. *Acta Neuropathol. Commun.* 3:81 doi: 10.1186/s40478-015-0262-7

Guo, D. C., Pannu, H., Tran-Fadulu, V., Papke, C. L., Yu, R. K., Avidan, N., et al. (2007). Mutations in smooth muscle alpha-actin (*ACTA2*) lead to thoracic aortic aneurysms and dissections. *Nat. Genet.* 39, 1488–1493. doi: 10.1038/ng.2007.6

Guo, D. C., Papke, C. L., Tran-Fadulu, V., Regalado, E. S., Avidan, N., Johnson, R. J., et al. (2009). Mutations in smooth muscle alpha-actin (*ACTA2*) cause

coronary artery disease, stroke, and moyamoya disease, along with thoracic aortic disease. *Am. J. Hum. Genet.* 84, 617–627. doi: 10.1016/j.ajhg.2009.04.007

Hoffjan, S., Waldmuller, S., Blankenfeldt, W., Kotting, J., Gehle, P., Binner, P., et al. (2011). Three novel mutations in the *ACTA2* gene in german patients with thoracic aortic aneurysms and dissections. *Eur. J. Hum. Genet.* 19, 520–524. doi: 10.1038/ejhg.2010.239

Hoffman, J. I., and Kaplan, S. (2002). The incidence of congenital heart disease. *J. Am. Coll. Cardiol.* 39, 1890–1900. doi: 10.1016/S0735-1097(02)01886-7

Huang, J., Wang, T., Wright, A. C., Yang, J., Zhou, S., Li, L., et al. (2015). Myocardin is required for maintenance of vascular and visceral smooth muscle homeostasis during postnatal development. *Proc. Natl. Acad. Sci. U.S.A.* 112, 4447–4452. doi: 10.1073/pnas.1420363112

Jiang, Y., Zhang, M., He, H., Chen, J., Zeng, H., Li, J., et al. (2013). MicroRNA/mrna profiling and regulatory network of intracranial aneurysm. *BMC Med. Genomics* 6:36. doi: 10.1186/1755-8794-6-36

Jones, J. A., Stroud, R. E., O'Quinn, E. C., Black, L. E., Barth, J. L., Elefteriades, J. A., et al. (2011). Selective microRNA suppression in human thoracic aneurysms: relationship of miR-29a to aortic size and proteolytic induction. *Circ. Cardiovasc. Genet.* 4, 605–613. doi: 10.1161/CIRCGENETICS.111.960419

Ke, T., Han, M., Zhao, M., Wang, Q. K., Zhang, H., Zhao, Y., et al. (2016). Alpha-actin-2 mutations in chinese patients with a non-syndromatic thoracic aortic aneurysm. *BMC Med. Genet.* 17:45. doi: 10.1186/s12881-016-0310-6

Leeper, N. J., Raiesdana, A., Kojima, Y., Chun, H. J., Azuma, J., Maegdefessel, L., et al. (2011). MicroRNA-26a is a novel regulator of vascular smooth muscle cell function. *J. Cell. Physiol.* 226, 1035–1043. doi: 10.1002/jcp.22422

Li, J., Bowens, N., Cheng, L., Zhu, X., Chen, M., Hannenhalli, S., et al. (2012). Myocardin-like protein 2 regulates tgfbeta signaling in embryonic stem cells and the developing vasculature. *Development* 139, 3531–3542. doi: 10.1242/dev.082222

Liu, D., Han, L., Wu, X., Yang, X., Zhang, Q., and Jiang, F. (2014). Genome-wide microRNA changes in human intracranial aneurysms. *BMC Neurol.* 14:188. doi: 10.1186/s12883-014-0188-x

Liu, Z., Chang, A. N., Grinnell, F., Trybus, K. M., Milewicz, D. M., Stull, J. T., et al. (2017). Vascular disease-causing mutation, smooth muscle alpha-actin r258c, dominantly suppresses functions of alpha-actin in human patient fibroblasts. *Proc. Natl. Acad. Sci. U.S.A.*114, E5569–E5578. doi: 10.1073/pnas.1703506114

Loeys, B. L., Schwarze, U., Holm, T., Callewaert, B. L., Thomas, G. H., Pannu, H., et al. (2006). Aneurysm syndromes caused by mutations in the tgf-beta receptor. *N. Engl. J. Med.* 355, 788–798. doi: 10.1056/NEJMoa055695

Logeswaran, T., Friedburg, C., Hofmann, K., Akintuerk, H., Biskup, S., Graef, M., et al. (2017). Two patients with the heterozygous r189h mutation in *ACTA2* and complex congenital heart defects expands the cardiac phenotype of multisystemic smooth muscle dysfunction syndrome. *Am. J. Med. Genet. A* 173, 959–965. doi: 10.1002/ajmg.a.38102

Loscalzo, M. L., Goh, D. L., Loeys, B., Kent, K. C., Spevak, P. J., and Dietz, H. C. (2007). Familial thoracic aortic dilation and bicommissural aortic valve: a prospective analysis of natural history and inheritance. *Am. J. Med. Genet. A* 143A, 1960–1967. doi: 10.1002/ajmg.a.31872

Lu, H., Fagnant, P. M., Bookwalter, C. S., Joel, P., and Trybus, K. M. (2015). Vascular disease-causing mutation r258c in *ACTA2* disrupts actin dynamics and interaction with myosin. *Proc. Natl. Acad. Sci. U.S.A.* 112, E4168–E4177. doi: 10.1073/pnas.1507587112

Lu, H., Fagnant, P. M., Krementsova, E. B., and Trybus, K. M. (2016). Severe molecular defects exhibited by the r179h mutation in human vascular smooth muscle alpha-actin. *J. Biol. Chem.* 291, 21729–21739. doi: 10.1074/jbc.M116.744011

Maegdefessel, L., Azuma, J., and Tsao, P. S. (2014). MicroRNA-29b regulation of abdominal aortic aneurysm development. *Trends Cardiovasc. Med.* 24, 1–6. doi: 10.1016/j.tcm.2013.05.002

Maegdefessel, L., Azuma, J., Toh, R., Deng, A., Merk, D. R., Raiesdana, A., et al. (2012a). MicroRNA-21 blocks abdominal aortic aneurysm development and nicotine-augmented expansion. *Sci. Transl. Med.* 4:122ra122. doi: 10.1126/scitranslmed.3003441

Maegdefessel, L., Azuma, J., Toh, R., Merk, D. R., Deng, A., Chin, J. T., et al. (2012b). Inhibition of microRNA-29b reduces murine abdominal aortic aneurysm development. *J. Clin. Invest.* 122, 497–506. doi: 10.1172/JCI61598

Malloy, L. E., Wen, K. K., Pierick, A. R., Wedemeyer, E. W., Bergeron, S. E., Vanderpool, N. D., et al. (2012). Thoracic aortic aneurysm (taad)-causing mutation in actin affects formin regulation of polymerization. *J. Biol. Chem.* 287, 28398–28408. doi: 10.1074/jbc.M112.371914

Milewicz, D. M., Kwartler, C. S., Papke, C. L., Regalado, E. S., Cao, J., and Reid, A. J. (2010a). Genetic variants promoting smooth muscle cell proliferation can result in diffuse and diverse vascular diseases: evidence for a hyperplastic vasculomyopathy. *Genet. Med.* 12, 196–203. doi: 10.1097/GIM.0b013e3181cdd687

Milewicz, D. M., Ostergaard, J. R., Ala-Kokko, L. M., Khan, N., Grange, D. K., Mendoza-Londono, R., et al. (2010b). *De novo ACTA2* mutation causes a novel syndrome of multisystemic smooth muscle dysfunction. *Am. J. Med. Genet. A* 152A, 2437–2443. doi: 10.1002/ajmg.a.33657

Morisaki, H., Akutsu, K., Ogino, H., Kondo, N., Yamanaka, I., Tsutsumi, Y., et al. (2009). Mutation of *ACTA2* gene as an important cause of familial and nonfamilial nonsyndromatic thoracic aortic aneurysm and/or dissection (taad). *Hum. Mutat.* 30, 1406–1411. doi: 10.1002/humu.21081

Morisaki, T., and Morisaki, H. (2016). Genetics of hereditary large vessel diseases. *J. Hum. Genet.* 61, 21–26. doi: 10.1038/jhg.2015.119

Munot, P., Saunders, D. E., Milewicz, D. M., Regalado, E. S., Ostergaard, J. R., Braun, K. P., et al. (2012). A novel distinctive cerebrovascular phenotype is associated with heterozygous arg179 *ACTA2* mutations. *Brain* 135, 2506–2514. doi: 10.1093/brain/aws172

Oh, J., Richardson, J. A., and Olson, E. N. (2005). Requirement of myocardin-related transcription factor-b for remodeling of branchial arch arteries and smooth muscle differentiation. *Proc. Natl. Acad. Sci. U.S.A.* 102, 15122–15127. doi: 10.1073/pnas.0507346102

Ott, C. E., Grunhagen, J., Jager, M., Horbelt, D., Schwill, S., Kallenbach, K., et al. (2011). MicroRNAs differentially expressed in postnatal aortic development downregulate elastin via 3′ utr and coding-sequence binding sites. *PLoS ONE* 6:e16250. doi: 10.1371/journal.pone.0016250

Perrin, B. J., and Ervasti, J. M. (2010). The actin gene family: function follows isoform. *Cytoskeleton* 67, 630–634. doi: 10.1002/cm.20475

Prakash, S. K., Bosse, Y., Muehlschlegel, J. D., Michelena, H. I., Limongelli, G., Della Corte, A., et al. (2014). A roadmap to investigate the genetic basis of bicuspid aortic valve and its complications: insights from the international bavcon (bicuspid aortic valve consortium). *J. Am. Coll. Cardiol.* 64, 832–839. doi: 10.1016/j.jacc.2014.04.073

Qian, Y., Zhong, X., Flynn, D. C., Zheng, J. Z., Qiao, M., Wu, C., et al. (2005). Ilk mediates actin filament rearrangements and cell migration and invasion through pi3k/akt/rac1 signaling. *Oncogene* 24, 3154–3165. doi: 10.1038/sj.onc.1208525

Regalado, E. S., Guo, D. C., Prakash, S., Bensend, T. A., Flynn, K., Estrera, A., et al. (2015). Aortic disease presentation and outcome associated with *ACTA2* mutations. *Circ. Cardiovasc. Genet.* 8, 457–464. doi: 10.1161/CIRCGENETICS.114.000943

Renard, M., Callewaert, B., Baetens, M., Campens, L., MacDermot, K., Fryns, J. P., et al. (2013). Novel myh11 and *ACTA2* mutations reveal a role for enhanced tgfbeta signaling in ftaad. *Int. J. Cardiol.* 165, 314–321. doi: 10.1016/j.ijcard.2011.08.079

Roth, G. A., Huffman, M. D., Moran, A. E., Feigin, V., Mensah, G. A., Naghavi, M., et al. (2015). Global and regional patterns in cardiovascular mortality from 1990 to 2013. *Circulation* 132, 1667–1678. doi: 10.1161/CIRCULATIONAHA.114.008720

Shen, D., Li, J., Lepore, J. J., Anderson, T. J., Sinha, S., Lin, A. Y., et al. (2011). Aortic aneurysm generation in mice with targeted deletion of integrin-linked kinase in vascular smooth muscle cells. *Circ. Res.* 109, 616–628. doi: 10.1161/CIRCRESAHA.110.239343

Siu, S. C., and Silversides, C. K. (2010). Bicuspid aortic valve disease. *J. Am. Coll. Cardiol.* 55, 2789–2800. doi: 10.1016/j.jacc.2009.12.068

van Rooij, E., Sutherland, L. B., Thatcher, J. E., DiMaio, J. M., Naseem, R. H., Marshall, W. S., et al. (2008). Dysregulation of microRNAs after myocardial infarction reveals a role of miR-29 in cardiac fibrosis. *Proc. Natl. Acad. Sci. U.S.A.* 105, 13027–13032. doi: 10.1073/pnas.0805038105

Ware, S. M., Shikany, A., Landis, B. J., James, J. F., and Hinton, R. B. (2014). Twins with progressive thoracic aortic aneurysm, recurrent dissection and *ACTA2* mutation. *Pediatrics* 134, e1218–e1223. doi: 10.1542/peds.2013-2503

Wu, J., Wang, J., Li, X., Liu, X., Yu, X., and Tian, Y. (2016). MicroRNA-145 mediates the formation of angiotensin ii-induced murine abdominal aortic aneurysm. *Heart Lung Circ.* 6, 619–626. doi: 10.1016/j.hlc.2016.10.009

Xin, M., Small, E. M., Sutherland, L. B., Qi, X., McAnally, J., Plato, C. F., et al. (2009). MicroRNAs miR-143 and miR-145 modulate cytoskeletal dynamics and responsiveness of smooth muscle cells to injury. *Genes Dev.* 23, 2166–2178. doi: 10.1101/gad.1842409

Yoo, E. H., Choi, S. H., Jang, S. Y., Suh, Y. L., Lee, I., Song, J. K., et al. (2010). Clinical, pathological, and genetic analysis of a korean family with thoracic aortic aneurysms and dissections carrying a novel asp26tyr mutation. *Ann. Clin. Lab. Sci.* 40, 278–284.

Zampetaki, A., Attia, R., Mayr, U., Gomes, R. S., Phinikaridou, A., Yin, X., et al. (2014). Role of miR-195 in aortic aneurysmal disease. *Circ. Res.* 115, 857–866. doi: 10.1161/CIRCRESAHA.115.304361

Zhu, L., Vranckx, R., Khau Van Kien, P., Lalande, A., Boisset, N., Mathieu, F., et al. (2006). Mutations in myosin heavy chain 11 cause a syndrome associating thoracic aortic aneurysm/aortic dissection and patent ductus arteriosus. *Nat. Genet.* 38, 343–349. doi: 10.1038/ng1721

Conflict of Interest Statement: The authors declare that the research was conducted in the absence of any commercial or financial relationships that could be construed as a potential conflict of interest.

The reviewer LP and handling Editor declared their shared affiliation, and the handling Editor states that the process met the standards of a fair and objective review.

frontiers in Physiology

REVIEW
published: 30 November 2017
doi: 10.3389/fphys.2017.00938

Thoracic Aortic Aneurysm Development in Patients with Bicuspid Aortic Valve: What Is the Role of Endothelial Cells?

*Vera van de Pol[1], Kondababu Kurakula[1], Marco C. DeRuiter[2] and Marie-José Goumans[1]**

[1] Department of Molecular Cell Biology, Leiden University Medical Center, Leiden, Netherlands, [2] Department of Anatomy and Embryology, Leiden University Medical Center, Leiden, Netherlands

Bicuspid aortic valve (BAV) is the most common type of congenital cardiac malformation. Patients with a BAV have a predisposition for the development of thoracic aortic aneurysm (TAA). This pathological aortic dilation may result in aortic rupture, which is fatal in most cases. The abnormal aortic morphology of TAAs results from a complex series of events that alter the cellular structure and extracellular matrix (ECM) composition of the aortic wall. Because the major degeneration is located in the media of the aorta, most studies aim to unravel impaired smooth muscle cell (SMC) function in BAV TAA. However, recent studies suggest that endothelial cells play a key role in both the initiation and progression of TAAs by influencing the medial layer. Aortic endothelial cells are activated in BAV mediated TAAs and have a substantial influence on ECM composition and SMC phenotype, by secreting several key growth factors and matrix modulating enzymes. In recent years there have been significant advances in the genetic and molecular understanding of endothelial cells in BAV associated TAAs. In this review, the involvement of the endothelial cells in BAV TAA pathogenesis is discussed. Endothelial cell functioning in vessel homeostasis, flow response and signaling will be highlighted to give an overview of the importance and the under investigated potential of endothelial cells in BAV-associated TAA.

Keywords: bicuspid aortic valve, thoracic aortic aneurysm, endothelial cells, endothelial-to-mesenchymal transformation, transforming growth factor beta, angiotensin II, nitric oxide, notch1

OPEN ACCESS

Edited by:
Amalia Forte,
Università degli Studi della Campania "Luigi Vanvitelli" Caserta, Italy

Reviewed by:
Salah A. Mohamed,
University Hospital Schleswig-Holstein, Germany
Per Hellstrand,
Lund University, Sweden

***Correspondence:**
Marie-José Goumans
m.j.goumans@lumc.nl

Specialty section:
This article was submitted to Vascular Physiology, a section of the journal Frontiers in Physiology

Received: *23 June 2017*
Accepted: *06 November 2017*
Published: *30 November 2017*

Citation:
van de Pol V, Kurakula K, DeRuiter MC and Goumans M-J (2017) Thoracic Aortic Aneurysm Development in Patients with Bicuspid Aortic Valve: What Is the Role of Endothelial Cells? Front. Physiol. 8:938. doi: 10.3389/fphys.2017.00938

Bicuspid aortic valve (BAV) is the most common congenital cardiovascular malformation with a prevalence of 0.5–1.5% in the general population and a male predominance of about 3:1 (Roberts, 1970; Basso et al., 2004). In this anomaly, the aortic valve consists of 2 leaflets instead of the regular 3 leaflets. The BAV usually exhibits normal function at birth and during early life, however in adulthood BAV patients can develop several serious complications such as valvular stenosis and/or regurgitation, aortic dilation, and thoracic aortic aneurysms (TAA). Although TAAs occur both in tricuspid aortic valves (TAV) and BAV, it has been estimated that 50–70% of BAV patients develop aortic dilation and ∼40% of BAV patients develop TAAs (Yuan et al., 2010; Saliba and Sia, 2015). Moreover, patients with a BAV have a 9-fold higher risk for aortic dissection compared to the

general population (Lewin and Otto, 2005). To monitor dilation progression in BAV patients the aortic diameter is regularly measured using echocardiography. However, no treatment options are available to prevent dilation or impact on the remodeling aortic wall. Surgical intervention with the aim to prevent rupture is therefore currently the only therapy for TAAs.

THORACIC AORTIC ANEURYSM

While smooth muscle cells (SMCs) in the healthy media have a contractile phenotype, they are not terminally differentiated. This ensures the ability to regenerate the vessel wall after injury. This flexible change between cellular phenotypes is called "phenotypic switching," with the contractile and synthetic SMCs on opposite sides of the spectrum. After phenotypic switching the synthetic SMCs can migrate towards a wounded area by secreting proteinases to break down the ECM. Synthetic SMCs also proliferate and produce ECM to repair the wall. When the vessel wall is repaired, synthetic SMCs will re-differentiate toward a contractile phenotype. TAA is characterized by phenotypic switching of contractile to synthetic SMCs and fragmentation of elastic lamellae (**Figure 1**). The BAV aorta is more prone to TAA development, possibly due to differences in vascular homeostasis. For example, it has been shown that non-dilated BAV aorta, like the dilated TAV aorta, has an increased collagen turnover (Wågsäter et al., 2013). Moreover, orientation, fiber thickness, and collagen crosslinking is altered in the dilated BAV aorta compared to the TAV aorta (Tsamis et al., 2016). Additionally, decreased expression levels of lamin A/C, α-smooth muscle actin (α-SMA), calponin, and smoothelin were not only found in dilated, but also in non-dilated BAV aorta (Grewal et al., 2014). Abdominal aortic aneurysms (AAA) share some common features with TAA, but differ in that atherosclerosis plays a major role in AAA, whereas medial degeneration is characteristic of TAA (Guo et al., 2006).

The mechanism initiating thoracic aortic dilation is thus far unknown, however, the two main hypotheses are that either an altered flow greatly impacts vessel wall homeostasis (flow hypothesis) or that an intrinsic cellular defect contributes to the formation of BAV as well as to the dilation of the aorta in these patients (genetic hypothesis; Girdauskas et al., 2011a). Several genes related to structural proteins have been found mutated in BAV patients, such as *ACTA2, MYH11.* Furthermore, in BAV patients multiple mutations have also been found in genes related to signaling proteins such as *NOTCH1* and genes related to the TGFβ signaling pathway (Girdauskas et al., 2011b; Tan et al., 2012; Andelfinger et al., 2016). In addition to isolated cases, BAV has also been demonstrated to occur within families (Huntington et al., 1997; Calloway et al., 2011). Interestingly, 32% of the first-degree relatives of BAV patients with a TAV also develop aortic root dilation, suggesting that the genetic predisposition for BAV and TAA overlap or may be identical in these families (Biner et al., 2009). However, a clear inheritance pattern remains to be found. TAAs are also observed in patients with other syndromes such as Marfan, Loeys–Dietz, and Ehler–Danlos, but contrastingly, BAV seldom occurs in these syndromes (El-Hamamsy and Yacoub, 2009; Ruddy et al., 2013). For an overview of genetic variation associated with BAV and the effect on endothelial functioning see **Table 1**.

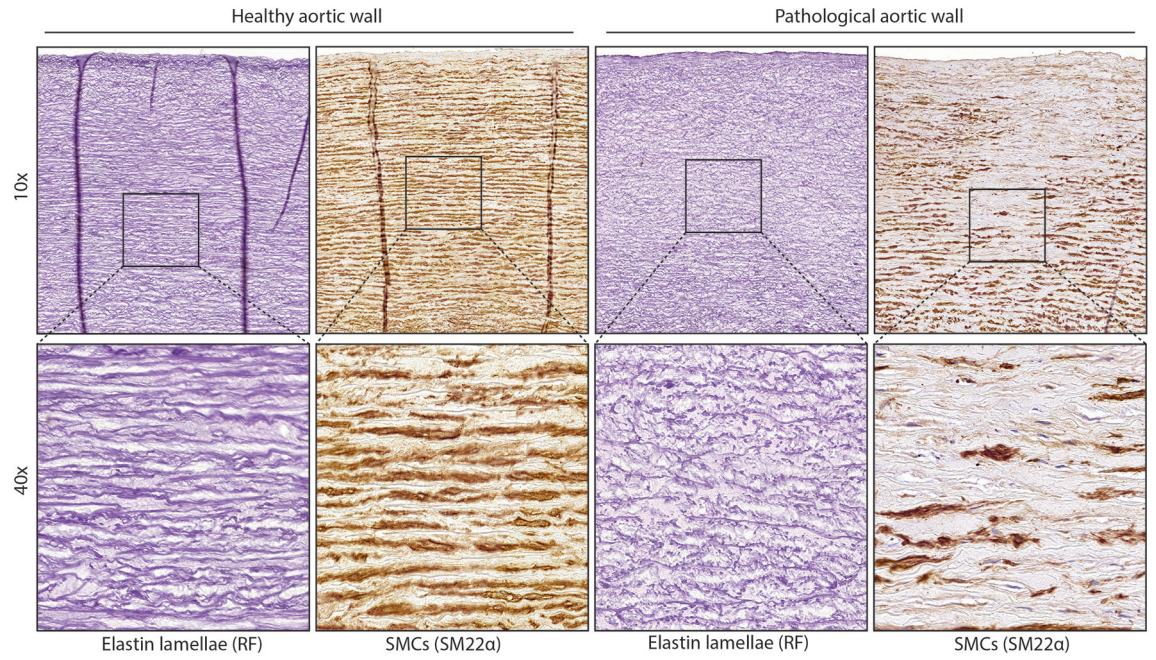

FIGURE 1 | Structure of normal and diseased aortic wall. Images of aortic tissue showing elastic lamellae (stained with RF) or smooth muscle cells (SM22 staining) On the left is normal aortic tissue, the right image shows aortic tissue with fragmentation of the lamellae or loss of contractile SMCs.

TABLE 1 | Consequences of genetics associated with BAV on cardiac malformations and endothelial cell functioning.

Pathway	Mutation	Effect	Other cardiovascular malformations	BAV occurrence	Effect of mutation on endothelial function
TGFb	*Gata5*^{cre}*Alk2*$^{fl/fl}$ [b] (Thomas et al., 2012)	ALK2 deletion in cushion mesenchyme	not/under developed non-coronary leaflet	78–83%	Constitutively active ALK2 induces EndoMT and is required for HDL induced EC survival and protection from calcification (Yao et al., 2008; Medici et al., 2010)
	ENG[a] (Wooten et al., 2010)	Conservative peptide shift	HHT	Increased haplotype in BAV with an OR of 2.79	Flow and ligand induced EC migration is disrupted increased proliferation and responsiveness to TGFβ1 (Pece-Barbara et al., 2005; Jin et al., 2017)
	TGFBR2[a] (Attias et al., 2009; Girdauskas et al., 2011b)	Missense/nonsense/splicing mutations	LDS, Marfan, TAA	7% of the cohort	Maintenance of vascular integrity (Allinson et al., 2012)
	SMAD6[a] (Tan et al., 2012)	Loss of function	AoS, AoC, and aortic calcification	3/436 patients, 0/829 controls	Increases SMAD6, inhibits TGFβ signaling (Topper et al., 1997)
	Adamts5$^{-/-}$*Smad2*$^{+/-}$ [b] (Dupuis et al., 2013)	Loss of function for Adamts5 and SMAD2	Myxomatous valves, BPV	75% Non-coronary with either left or right coronary cusp	Embryonic vascular instability, SMAD2 increases eNOS expression (Itoh et al., 2012)
Other	*Ift88*$^{fl/fl}$*Nfatc*^{Cre} [b] (Toomer et al., 2017)	Endothelial specific loss of primary cillia	–	68% BAV right/non-coronary fusion	ECs without primary cilia undergo EndoMT upon shear stress (Egorova et al., 2011)
	eNOS$^{-/-}$ [b] (Lee et al., 2000)	No functional eNOS	–	42% BAV right/non-coronary fusion	Decreased EndoMT (Förstermann and Münzel, 2006)
	Gata5[a] */Tie2*^{cre}*Gata5*$^{fl/fl}$ [b] (Laforest and Nemer, 2012; Bonachea et al., 2014; Shi et al., 2014)	Reduced Gata5 activity Gata5[a]/Gata5 deletion in ECs[b]	VSD, aortic stenosis[a] / LV hypertrophy, AS[b]	autosomal dominant BAV inheritance[a] / 25%[b]	Altered PKA and NO signaling (Messaoudi et al., 2015)
	NOTCH1[a] (Garg et al., 2005)	Autosomal dominant mutant notch1	CAVD and other cardiac malformations	Autosomal dominant inheritance with complete penetrance	NOTCH1 increases calcification, oxidative stress and inflammation, when exposed to shear stress (Theodoris et al., 2015)
	NKX2.5[a] (Qu et al., 2014)	Loss of function	ASD, PFO, AS and conduction defects	One family with an autosomal dominant inheritance	–
	ACTA2[a] (Guo et al., 2007)	Missense mutation	Family with FTAAD	3/18 patients with TAAD and mutation	–
	FBN1[a] (Attias et al., 2009)	Diverse	Marfan, TAA	4% of the cohort	–

[a] *Found in human.*
[b] *Found in mice.*
OR, Odds ratio; AoC, Aortic coarctation; AoS, Aortic valve stenosis; AS, Aortic stenosis; ASD, Atrial septal defect; BPV, Bicuspid pulmonary valve; CAVD, calcific aortic valve disease; HHT, Hereditary hemorrhagic telangiectasia; LDS, Loeys-Dietz syndrome; LV, Left ventricle; PFO, Patent foramen ovale.

ENDOTHELIAL CELLS IN VESSEL HOMEOSTASIS

Due to the obvious medial degeneration in the aortic wall, research in the past decades has focussed on characterizing the organization and SMC phenotype of the aortic media during dilation and aneurysm (Wolinsky, 1970; Halloran et al., 1995; Ruddy et al., 2013). Therefore, despite their main regulatory function, endothelial cells have so far taken the back seat in research toward understanding and treating aortic dilation. However, there is growing evidence that endothelial cells play an important role in the development and progression of aortic dilation.

Endothelial cells line the lumen of the aorta which, together with some ECM and the internal elastic lamella, form the intima. As the layer between the blood (flow) and the main structural component of the aorta (the media) the function of endothelial cells is to communicate the signal between these two

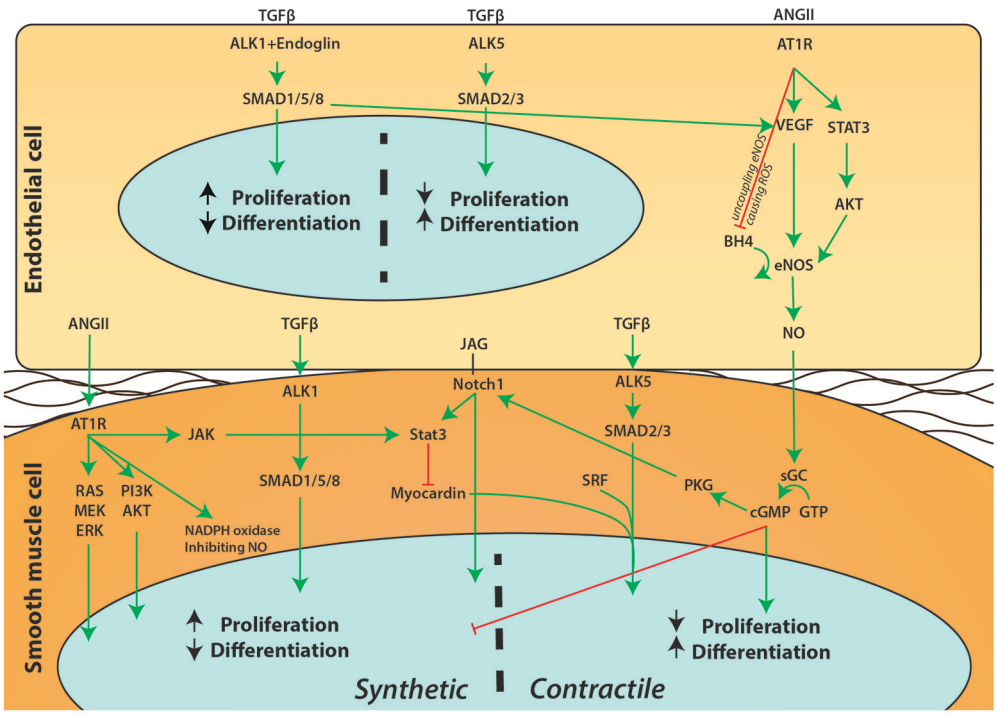

FIGURE 2 | Schematic overview of signaling pathways between endothelial cells and SMCs. A simplified overview on the communication between endothelial cells and SMCs is depicted. Extensive crosstalk between pathways such as Notch1, ANGII, TGFβ, and NO can influence proliferation and differentiation of SMCs and affect the phenotypic switch of SMCs.

layers. Upon flow and stimuli such as inflammatory cytokines, signaling pathways like TGFβ, angiotensin, and nitric oxide (NO) allow endothelial cells to directly target the contraction status of SMCs or indirectly target the SMC contractile phenotype to influence vessel wall functioning (**Figure 2**). Primary cilia on the luminal surface of the endothelial cells enable mechanosensing and signaling (Egorova et al., 2012). Endothelial cells lacking cilia change toward a mesenchymal phenotype, a process called endothelial to mesenchymal transformation (EndoMT) in which endothelial specific genes such as VE-cadherin and PECAM1 are down-regulated, whereas mesenchymal genes such as αSMA and fibronectin are up-regulated (Egorova et al., 2011). Intriguingly, a recent study demonstrated that *Ift88*$^{fl-fl}$ mice crossed with *Nfatc*^{Cre}, thereby lacking a primary cilium specifically in endothelial cells, display a highly penetrant BAV (Toomer et al., 2017; **Table 1**).

THE INFLUENCE OF FLOW ON ENDOTHELIAL FUNCTIONING AND VESSEL HOMEOSTASIS

The flow pattern of blood from the heart into the aorta is altered by a BAV (Barker et al., 2012). This difference between TAV and BAV hemodynamics in the aorta can be beautifully demonstrated using 4D MRI. Compared to a TAV, BAV generate a high velocity "jet" propelling at an angle against the wall in the BAV aorta. This jet stream also causes an increase in peak shear stress on the endothelial cells (Barker et al., 2012). As mentioned above, aside from the genetic hypothesis, the altered flow is also hypothesized to cause the aortic dilation in BAV.

It has been long known that adjusting flow induces remodeling of the vessel wall. Already, more than 30 years ago it was published that by decreasing blood flow in the carotid artery of rabbits by 70%, the lumen size of the vessel was decreased by 21% to compensate for the decreased blood flow (Langille and O'Donnell, 1986). Vascular remodeling is induced by increased shear stress on endothelial cells to restore original shear forces on the wall (Baeyens et al., 2016a). That flow greatly impacts endothelial functioning is also portrayed by the localization of fatty streaks and atherosclerosis at branch points and curves of arteries (Baeyens et al., 2016a). The turbulent flow at these locations causes dysfunctional endothelium: endothelial cells undergo apoptosis or exhibit increased proliferation. Moreover, permeability is increased, allowing LDL penetration into the intima. In addition, inflammatory cell adhesion and infiltration is increased. Laminar flow induces the opposing quiescent endothelial phenotype characterized by a low turnover, alignment in the direction of the flow, decreased expression of inflammatory adhesion molecules like I-CAM and a low permeability caused by increased cell-cell adhesion molecules such as N-CAM and E-cadherin (Chistiakov et al., 2017). Experiments using co-culture of endothelial cells and SMCs revealed that flow on endothelial cells can also impact the phenotype of the underlying SMCs. Laminar shear stress on endothelial cells induces a contractile phenotype in synthetic SMCs, shown with both co-culture experiments of endothelial

cells under flow with SMCs, as by adding conditioned medium from flow exposed endothelial cells to SMCs (Tsai et al., 2009; Zhou et al., 2013). Upon laminar flow, endothelial cells signal toward SMCs using, for example, microRNA (miR)-126, prostacyclin, TGFβ3, and NO (Noris et al., 1995; Tsai et al., 2009; Walshe et al., 2013; Zhou et al., 2013) MiR-126 in endothelial microparticles (EMPs) decreases SMC proliferation and neointima formation (Jansen et al., 2017). Interestingly, EMP secretion is elevated in BAV associated TAA (Alegret et al., 2016). It is believed that EMPs are formed when endothelial cells are trying to avoid undergoing apoptosis, possibly explaining the association of elevated levels of EMPs with vascular diseases such as diabetes, congestive heart failure and acute coronary syndrome (Rössig et al., 2000; Bernal-Mizrachi et al., 2003; Tramontano et al., 2010).

MiR-126 is only one means by which endothelial cells can impact on the vascular homeostasis. The main signaling pathways involved in BAV TAA and endothelial cells will be discussed in the next paragraphs.

ANGIOTENSIN II SIGNALING IN TAA

One of the major signaling pathways disturbed in aortic dilation is the Renin-Angiotensin-Aldosterone-System (RAAS), which is important for maintaining blood pressure. By constriction/relaxation of blood vessels and adjusting water retention of the kidneys, the blood pressure is regulated. The juxtaglomerular cells in the kidney and baroreceptors in vessel wall can sense arterial blood pressure. Upon a drop in pressure, renin is released by the juxtaglomerular cells and renin then converts angiotensinogen into angiotensin I (ANGI), which in turn is converted by angiotensin converting enzyme (ACE) into angiotensin II (ANGII). Amongst others, ANGII can cause contraction of the SMCs to increase blood pressure. This contraction is caused by the binding of ANGII to the angiotensin II type 1 receptor (AT1) on the SMCs, resulting in activation of the Ca^{2+}/calmodulin pathway, activating the myosin ligh chain kinase followed by rapid phosphorylation of MLC, causing contraction of SMCs. In addition, ANGII stimulates the cortex of the adrenal gland to secrete aldosterone, which increases water resorption in the kidney.

Aside from this direct vasoconstrictive effect, prolonged RAAS activation has diverse pathological effects. Aldosterone has been shown to cause endothelial dysregulation as well as a synthetic phenotype in SMCs (Hashikabe et al., 2006). Chronic infusion of ANGII in *ApoE*$^{-/-}$ mice demonstrated to cause progressive TAAs and AAAs (Daugherty et al., 2000, 2010). The administration of ANGII in these mice decreased αSMA and calponin expression in the mouse aortas (Leibovitz et al., 2009; Chou et al., 2015). Moreover, ACE2 expression was increased in mouse aortas after ANGII infusion as well as in dilated aortas of BAV patients (Patel et al., 2014). ACE insertion/deletion polymorphisms were also identified as risk factor for the development of TAA in BAV patients (Foffa et al., 2012). Furthermore, a correlation was found between chronic elevated levels of ANGII and endothelial cell dysfunction in patients with hyperaldosteronism, underlining the importance of the RAAS system and endothelial functioning (Matsumoto et al., 2015).

A seminal study performed by Rateri and colleagues, displayed the importance of endothelial cell functioning in the ANGII aneurysm model (Rateri et al., 2011). Interestingly, mice with specific deletion of *AT1* in SMCs or monocytes still developed aortic aneurysms following a chronic ANGII infusion, while mice with an endothelial specific knock-out of *AT1* did not exhibit dilation of the thoracic aorta. This study indicates that the primary target cell for ANGII in this model is the endothelial cell, which in turn influences the SMCs, causing the aortic structure to break down. How exactly this ANGII-endothelial cell signaling affects the SMC phenotype remains a crucial and intriguing question to be investigated. The same group 1 year later showed that AAA are not inhibited in the endothelial cell specific *AT1* knock-out, elegantly demonstrating that indeed there is a difference in pathogenesis between TAA and AAA (Rateri et al., 2012). This difference might be explained by a more prominent role for the adventitia than the intima in AAA development, or the developmentally different origin of SMCs in different parts of the aorta (Police et al., 2009; Tieu et al., 2009; Tanaka et al., 2015; Sawada et al., 2017).

Aside from studies to understand the pathogenesis of TAA, ANGII treatment to model aortic aneurysm in mice is also used in the search of new treatment options. A recent study reported that treating ANGII infused mice with a combination therapy of Rosuvastatin and Bexarotene (retinoid X receptor-a ligand) inhibited aneurysm formation (Escudero et al., 2015). Moreover, they showed that this combination therapy affected endothelial cell proliferation, migration and signaling. In addition, upon ANGII treatment the VEGF secretion by endothelial cells *in vitro* was decreased (Escudero et al., 2015). SMCs from BAV patients exhibited an increased AT1R expression *in vitro,* which was reduced to the levels of control SMCs after treatment with losartan (Nataatmadja et al., 2013). Interestingly, antagonizing TGFβ by blocking the AT1 receptor using Losartan in a Marfan disease model mouse (*FBN1* mutation) demonstrated promising results for preventing and even reversing aortic dilation (Habashi et al., 2006). Furthermore, several clinical studies in Marfan patients reveal similar exciting results. However, a meta-analysis of clinical studies toward Losartan in Marfan patients did not show a reduction of aortic dilation in Losartan treated patients (Gao et al., 2016). Losartan treatment in BAV patients has not been investigated yet. A clinical study was initiated, but recently terminated due to low enrolment[1]. Therefore, the effect of Losartan on BAV TAA still needs to be determined.

NOTCH1 SIGNALING IN TAA

Notch signaling plays an important role in cardiovascular development (Niessen and Karsan, 2008). In contrast to many signaling pathways, Notch signaling is cell-cell contact

[1] Clinicaltrials.Gov (consulted 15-09-2017). *Identifier NCT01390181.*

dependent. There are 4 Notch homologs of which Notch1 is the best known. Binding of Notch1 ligands Jagged1, Jagged2, and/or Delta expressed in one cell induces cleavage of the receptor and nuclear translocation of the intracellular domain in the other cell causing transcription of, amongst others, the HES/HEY gene family, key regulators in EndoMT (Noseda et al., 2004). Notch1 signaling induces EndoMT in endothelial cells and promotes a contractile phenotype in SMCs (Tang et al., 2010). Moreover, Notch1 signaling is required for angiogenesis (Krebs et al., 2000).

Notch1 signaling was displayed to be crucial for normal development of the aortic valve and outflow tract amongst others, as determined in *Notch1*$^{-/-}$ mice (High et al., 2009). Specifically in the neural crest cells, Notch1 signaling is important. It was found that disruption of endothelial Jagged1 signaling to Notch1 on neural crest cells, inhibits SMC differentiation (High et al., 2008). The Notch1 signaling pathway, as well as the TGFβ signaling pathway, is involved in EndoMT occurring in the outflow tract cushions, where endothelial cells assume a mesenchymal cell phenotype to populate the developing cardiac valves (Niessen et al., 2008). Thereby EndoMT is a crucial part of aortic valve development. Previous studies hypothesized that EndoMT may also play a role in the pathogenesis of BAV. Additionally, genes involved in this process such as *NOTCH1, TGFBR2,* and *SMAD6*, have been found to cause BAV in mouse models, as well as being linked to BAV in human studies (Garg et al., 2005; Girdauskas et al., 2011b; Tan et al., 2012; Andelfinger et al., 2016; Gillis et al., 2017; Koenig et al., 2017). Mice with *Notch1* missense alleles have been characterized with multiple outflow tract and EndoMT defects (Koenig et al., 2015). Recently, it was demonstrated that specifically endothelial Notch1 signaling is required for normal outflow tract and valve development (Koenig et al., 2016). Moreover, a *Notch1* mutation was found in a family with BAV, underscoring Notch1 as an important signaling pathway in BAV (Garg et al., 2005). These mutations have been associated with an increased risk of calcific aortic valve disease (CAVD), explained by the normally repressive function of Notch1 on calcification in valvular cells (Garg et al., 2005; Nigam and Srivastava, 2009; Kent et al., 2013). Additionally, one study reported severely calcified valves in BAV patients with Cornelia de Lange syndrome, a disease caused by dysfunctional Notch1 signaling (Oudit et al., 2006).

Aside from the role of Notch1 signaling in valve formation, proper Notch1 signaling is also important for the homeostasis of the aorta, as illustrated by several studies. The non-dilated aorta of BAV patients showed increased Notch1 signaling and EndoMT marker expression based on proteomic analysis (Maleki et al., 2016). Furthermore, a study using endothelial cells isolated from BAV-TAA aorta demonstrated decreased *Notch1*, *Notch4,* and *Dll4* mRNA levels compared to TAV non-aneurysmal tissue (Kostina et al., 2016). Moreover, upon TGFβ stimulation, there was a defective Notch1 dependent EndoMT response. Endothelial marker proteins such as VWF and PECAM, were unchanged between BAV and TAV endothelial cells. However, EndoMT markers HES1 and SLUG were significantly less upregulated in BAV endothelial cells compared to TAV endothelial cells. In addition, *JAG1* expression is normally upregulated upon Notch1 signaling and acts as a positive feedback-loop. This upregulation of Jagged1 was decreased in BAV endothelial cells, explaining at least part of the dysfunctional Notch1 signaling in BAV patients with TAA (Kostina et al., 2016).

Interestingly, Notch1 plasma levels in combination with TNFα-converting enzyme were shown to correlate highly with the presence of AAA (Wang et al., 2015). Furthermore, studies demonstrated that *NOTCH1* haploinsufficiency or Notch1 inhibition can prevent or reduce the formation of AAA in ANGII infused mice (Hans et al., 2012; Cheng et al., 2014). However, the similarity in Notch signaling between AAA and TAA is debatable, as it has been displayed that in descending TAA tissue, in contrast to the ascending TAA, the SMCs exhibit a decreased Notch1 signaling, emphasizing the importance of the local environment in the aortic aneurysm formation (Zou et al., 2012).

ENOS SIGNALING IN TAA

Nitric oxide (NO) is produced when NO synthase (NOS) converts arginine into citrulline, releasing NO in the process. NOS was originally discovered in neurons (nNOS/NOS1), after which inducible NOS (iNOS/NOS2) and endothelial NOS (eNOS/NOS3) were found. eNOS phosphorylation increases NO production and is induced by factors such as shear stress, acetylcholine and histamine. NO has a very short half-life of a few seconds, making it a local and timely signal transducer. Endothelial secreted NO diffuses into the SMC where it relaxes the cell by increasing the calcium uptake into the sarcoplasmic reticulum: NO stimulates the sarco/endoplasmic reticulum ATPase (SERCA), and thereby decreases cytoplasmic Ca^{+} levels (Van Hove et al., 2009). Additionally, NO has also been revealed to regulate gene transcription by reacting with NO sensitive transcription factors (Bogdan, 2001). Finally NO has been shown to impact the SMC inflammatory status, however more research is required to fully understand the effect of NO on SMC phenotype (Shin et al., 1996). Uncoupled eNOS causes free oxygen radicals to be formed, which damages proteins and DNA.

Multiple studies have identified an important role for dysregulated endothelial NO signaling in aneurysm development. For example, it has been demonstrated that the oxidative stress is increased in the media of the aortas of BAV patients compared to TAV aortas (Billaud et al., 2017). Interestingly, a mouse model with uncoupled eNOS (HPH-1 mice) rapidly developed AAA and aortic rupture upon ANGII infusion, whereas wild-type (WT) mice did not display this phenotype (Gao et al., 2012). Re-coupling of eNOS by infusion of folic acid, inhibited AAA formation (Gao et al., 2012). A study investigating the effect of iNOS deletion in an elastase infusion mouse model of experimentally induced AAA did not demonstrate any substantial exacerbation of the aneurysm phenotype, indicating the importance of endothelial NO in aneurysm formation (Lee et al., 2001). Intriguingly, a later study identified plasma and tissue levels of the eNOS co-factor tetrahydrobiopterin, necessary for coupling of eNOS, correlate

with aneurysm development in *ApoE*$^{-/-}$ mice and HPH-1 mice (Siu and Cai, 2014). In line with these studies, it was shown that endothelial specific expression of reactive oxygen species, by an endothelial specific overexpression of NOX2, can cause aortic dissection in WT mice upon ANGII infusion (Fan et al., 2014). Moreover, eNOS knockout mice develop BAV, underlining the importance of endothelial dysfunction in the formation of BAV and the related TAA (Lee et al., 2000).

In patients with a TAV and TAA, profiling of the aortic tissue revealed that eNOS phosphorylation was increased via a miR-21 dependent mechanism (Licholai et al., 2016). MiR-21 is specifically upregulated by shear stress and causes PTEN mRNA degradation, allowing an increase in eNOS phosphorylation (Weber et al., 2010). Furthermore, BAV TAA patient aortic samples displayed increased eNOS expression and activation compared to TAV TAA controls (Kotlarczyk et al., 2016). These studies indicate an increased eNOS activity in TAA formation in BAV patients. Contrastingly, decreased eNOS expression has been found in 72.7% aortic samples of BAV patients ($N = 22$; Kim et al., 2016). In addition, a negative correlation between eNOS expression levels and aortic dilation in BAV patients was reported (Aicher et al., 2007).

In conclusion, multiple studies have investigated eNOS in the BAV aorta, with contrasting outcomes (Aicher et al., 2007; Mohamed et al., 2012; Kim et al., 2016; Kotlarczyk et al., 2016). These discrepancies may be caused by differences between patient populations, location of the aortic sample used, stage of aortic aneurysm formation and the use of different control samples for comparison. Nonetheless, all these studies indicate that normal levels of coupled eNOS are necessary to maintain a healthy aortic wall.

TGFβ SIGNALING IN TAA

TGFβ signaling is mediated by binding of the ligand TGFβ to the TGFβ type 2 receptor, which recruits and phosphorylates a TGFβ type 1 receptor. While there is only one type 2 receptor, TGFβ can signal via two TGFβ type 1 receptors, Activin-like kinase (ALK)1 and ALK5. Upon ligand binding, ALK5 can phosphorylate SMAD2 or SMAD3 and ALK1 can phosphorylate SMAD1, SMAD5 or SMAD8. The phosphorylated SMADs translocate into the nucleus with SMAD4 to induce the canonical signaling pathway. TGFβ can also signal via non-canonical pathways by activating PI3K/AKT, MAPK, or NF-kB. Via the canonical and non-canonical pathways, TGFβ influences cell cycle arrest, apoptosis, inflammation, proliferation, and more.

In endothelial cells, TGFβ signaling can either inhibit or stimulate the cell growth and function depending on the context (Goumans and Ten Dijke, 2017). TGFβ signaling via ALK1 induces proliferation and migration, whereas ALK5 signaling promotes plasminogen activator inhibitor 1 (PAI1) expression, decreasing breakdown of ECM which is necessary for maturation of the vessel wall (Goumans et al., 2002; Watabe et al., 2003). The two opposing effects of TGFβ signaling enable the initial growth of vessels followed by stabilization of the ECM and attraction of SMCs. Moreover, endothelial TGFβ signaling in concert with platelet derived growth factor-BB is crucial for attracting and differentiating pre-SMCs during vasculogenesis (Hirschi et al., 1998). Because of these crucial functions of TGFβ during embryonic development, loss of TGFβ signaling in the vascular system, either total knockout, SMC or endothelial cell specific deletion is embryonically lethal (Goumans and Ten Dijke, 2017). In SMCs TGFβ induces a contractile phenotype, and dysregulation of TGFβ therefore can have a major impact on SMC phenotype (Guo and Chen, 2012). The importance of endothelial TGFβ signaling on SMC differentiation is illustrated by co-culture of endothelial cells and SMCs. Cultured alone, the SMCs have a synthetic phenotype, but when co-cultured with endothelial cells, they differentiate into contractile SMCs via the PI3K/AKT signaling pathway (Brown et al., 2005).

The TGFβ Type III receptor endoglin (*ENG*) is highly expressed by endothelial cells and plays a role in the ALK1 and ALK5 signaling balance (Goumans et al., 2003). In fact, without endoglin, endothelial cells stop proliferating as a result of decreased ALK1 signaling (Lebrin et al., 2004). In addition, knock-out of *ENG* in mice causes embryonic lethality due to impaired angiogenesis, whereas vasculogenesis remains intact (Li et al., 1999; Arthur et al., 2000). This exemplifies the pivotal role for TGFβ signaling in endothelial cells for proper angiogenesis. As mentioned above, TGFβ signaling, like Notch1 signaling, is important for the process of EndoMT necessary for the developing cardiac valves. Chimera research using *ENG*$^{-/-}$ mice embryonic stem cells, added to WT mice morulae highlighted the indispensable role of endoglin for EndoMT in the developing cardiac valves (Nomura-Kitabayashi et al., 2009). These chimeric mice showed contribution of the *ENG*$^{-/-}$ cells to the endothelium. However, no *ENG*$^{-/-}$ cells participated in populating the atrio-ventricular (AV) mesenchyme of the developing AV cushions. Intriguingly, a single-nucleotide polymorphism in *ENG* was found in BAV patients, indicating that in BAV patients endothelial TGFβ signaling might be altered, potentially promoting a phenotypic switch in the underlying SMCs (Wooten et al., 2010).

Many studies using *in vitro*, *ex vivo* and histological methods, also indicate a role for TGFβ signaling in TAA formation in BAV. Unstimulated, cultured BAV and TAV SMCs did not demonstrate any difference in gene expression in basal conditions, however after TGFβ stimulation, 217 genes were found differentially expressed between BAV and TAV SMCs demonstrating a difference in TGFβ signaling (Paloschi et al., 2015). Moreover, induced pluripotent stem cells (iPSCs) derived from BAV patients with a dilated aorta exhibited decreased TGFβ signaling compared with iPSCs from TAV controls without aortic dilation (Jiao et al., 2016). Conversely, a hypothesis-free analysis of the secretome of BAV TAA indicated a highly activated TGFβ signaling pathway in the aortic wall of BAV patients when compared to the secretome of TAV aneurysmal aortic tissue (Rocchiccioli et al., 2017). This study showed, using mass spectrometry on all proteins in conditioned medium of the aortic samples, a 10-fold increase of latent TGFβ binding protein 4 (LTBP4) in the BAV samples (Rocchiccioli et al., 2017). Histological analysis identified that, compared to normal aortic tissue, BAV dilated aortic tissue had increased levels of SMAD3

and TGFβ protein in the tunica media (Nataatmadja et al., 2013). However, when compared to dilated TAV aorta, the expression of SMAD 2/3 was higher in the TAV dilated aorta than the BAV dilated aorta (Rocchiccioli et al., 2017). Furthermore, it has been shown that the circulating TGFβ levels in BAV patient are elevated, which is in agreement with studies showing increased TGFβ signaling (Hillebrand et al., 2014; Rueda-Martínez et al., 2017).

Multiple studies have demonstrated that antagonizing TGFβ signaling in aneurysm mouse models prevents and even reverses aneurysm formation (Habashi et al., 2006; Ramnath et al., 2015; Chen et al., 2016). The positive effects of TGFβ antagonism on aneurysm formation were shown in using a neutralizing TGFβ-antibody or by blocking the AT1 receptor using Losartan, which also decreases TGFβ signaling. In different mice models, Fibrillin-1 deficient, Fibulin-4 deficient and ANGII treated mice, the TGFβ inhibition prevented and reversed aortic aneurysm, making it a promising target for therapy (Habashi et al., 2006; Ramnath et al., 2015; Chen et al., 2016). A study using cultured SMCs revealed that Losartan treatment decreased intracellular TGFβ protein levels and nuclear SMAD3 localization (Nataatmadja et al., 2013). BAV derived SMCs displayed a decrease in endoglin expression upon Losartan treatment (Lazar-Karsten et al., 2016). Furthermore, serum TGFβ levels decreased when mice were treated with Losartan. The same was also seen in Marfan patients treated with Losartan, validating the study results obtained in mice (Habashi et al., 2006; Matt et al., 2009). However, as mentioned above, so far Losartan treatment does not seem to decrease or prevent aneurysm formation in a clinical setting. Given the recent success of specific TGFβ blockers in other vascular disorders such as pulmonary arterial hypertension (PAH) and restenosis, targeting the TGFβ pathway more directly could be a strategy for developing new treatment modalities for TAA (Yao et al., 2009; Yung et al., 2016).

ENDOTHELIAL DYSFUNCTION IN OTHER DISEASES: IMPLICATIONS FOR BAV-TAA?

Many cardiovascular disorders have highlighted the importance of normal endothelial functioning for maintaining homeostasis across the vessel wall, such as atherosclerosis, brain aneurysms, PAH, and hereditary haemorrhagic telangiectasia (HHT). PAH and HHT are 2 major genetic diseases in which the role of the endothelial cells is well recognized. Two recent advances in these research fields worth mentioning for future perspectives in BAV TAA research, will be discussed in the next paragraphs.

PAH is an incurable fatal disease caused by remodeling of the pulmonary arteries. Proliferation of the pulmonary artery smooth muscle cells (PASMCs) causes narrowing and occlusion of the lumen, leading to an increased pressure in the lungs and increased load of the right ventricle (Morrell et al., 2009). While originally defined as a SMC disorder, over the past years dysfunction of the endothelial cells has become of interest in the pathogenesis of PAH (Morrell et al., 2009; Sakao et al., 2009; Xu and Erzurum, 2011). The application of conditioned medium from normal endothelial cells to PASMCs resulted in an increase in PASMC proliferation rate (Eddahibi et al., 2006). This effect is exaggerated when adding conditioned medium of endothelial cells from PAH patients. Complementary, PASMCs from PAH patients showed an increased proliferation to both endothelial cell conditioned media, compared with control PASMCs. Two of the major players identified within the conditioned medium are miR-143 and miR-145. These miRs have been demonstrated to highly impact the SMC phenotypic switch, inducing a contractile phenotype (Boettger et al., 2009). Expression of these two miRs is regulated by TGFβ and they have been shown to be secreted in exosomes (Climent et al., 2015; Deng et al., 2015). Intriguingly, in PAH mouse models as well as patient lung tissue and cultured SMCs, miR-143-3p expression is increased. Furthermore, miR-$143^{-/-}$ mice developed pulmonary hypertension, a phenotype that was rescued by restoring miR-143 levels (Deng et al., 2015).

Interestingly, signaling from endothelial cells to SMCs concerning miR-143 and miR-145 has also been investigated in atherosclerosis research (Hergenreider et al., 2012). Transduction of HUVECs with the shear-responsive transcription factor KLF2, or exposure of HUVECs to flow caused an increase in miR-143 and miR-145, indicating a flow responsiveness of the miR-143 and miR-145 expression (Hergenreider et al., 2012). Additionally, endothelial cells secrete miR-143 and miR-145 in microvesicles which alter gene expression in SMCs. Moreover, when treating *ApoE*$^{-/-}$ mice with endothelial secreted vesicles containing, amongst others, miR-143 and miR-145, the mice developed less atherosclerosis (Hergenreider et al., 2012). SMCs of miR143 and miR-145 knockout mice displayed increased migration and proliferation. In addition, analyses of the mouse aortas showed ECM degradation in the miR-143 and miR-145 deficient mice. These results support the findings of a role for miR-143 and miR-145 in inducing a contractile SMC phenotype (Elia et al., 2009). Furthermore, in TAA miR-143 and miR-145 were found to be decreased compared to non-dilated samples (Elia et al., 2009). The impact these miRs have on SMC phenotype, the expression regulation by flow and their secretion by endothelial cells as well as the decrease in TAA, makes them relevant and interesting for BAV TAA research. The first study toward BAV and miR-143 and miR-145 was recently published, describing a local decrease of miR-143 and miR-145 in the inner curve of the BAV aorta compared to the outer curve. Moreover, they also found altered miR expression affecting mechanotransduction (Albinsson et al., 2017).

Intriguingly, mechanotransduction has also been of interest in HHT research. HHT is a vascular disease characterized by frequent severe bleedings due to fragile and tortuous blood vessels. Disturbed TGFβ signaling plays a major role in the development of these malformed blood vessels. Eighty percent of HHT patients have a mutation in *ENG* (HHT1) or *ALK1* (HHT2; McDonald et al., 2015). The endothelial cell-SMC communication is disrupted in HHT, and recruiting and differentiation of SMCs falters causing improperly formed vessels. Disturbed mechanotransduction in endothelial cells has been shown to impact BMP/SMAD1/5 signaling as well as vessel stabilization in HHT (Baeyens et al., 2016b). By subjecting endothelial cells to shear stress, SMAD1 was activated. Moreover, decreasing either ALK1 or endoglin both inhibited

the SMAD1 activation in response to flow. Interestingly, when co-cultured with pericytes, both ALK1 and endoglin were found to be crucial for endothelial shear stress induced migration and proliferation of these pericytes (Baeyens et al., 2016b). It would be highly interesting to investigate if BAV endothelial cells also have an intrinsic mechanotransduction defect causing the aorta to be prone to TAA development. The study by Albinsson and colleagues showing the altered miR related to mechanotransduction in BAV aorta samples is an important first step to lead the BAV TAA research field toward relevant studies on mechanotransduction defects possibly explaining (part of the) BAV TAA pathogenesis.

CONCLUSIONS AND FUTURE PERSPECTIVES

BAV is a common congenital cardiac malformation and the majority of BAV patients develop TAA over time. Although the last decade has witnessed the discovery of several key findings in the field of BAV-associated TAAs, the cellular and molecular mechanisms in BAV-associated TAAs that drive the degeneration of media of the vessel wall are still largely unknown. Many studies have focussed on changes in the signaling pathways in SMCs, however the importance of endothelial cells and their contribution to the initiation and progression of BAV-associated TAAs has not been appreciated in detail.

Under normal physiological conditions, endothelial cells and SMCs communicate with each other for optimal function of the vessel wall in order to maintain homeostasis in the circulatory system. Dysregulation of this communication can lead to medial degeneration and aortic aneurysm, clearly demonstrated in animal models using ANGII infusion or eNOS uncoupling. Interestingly, blocking TGFβ signaling is a possible treatment option to prevent TAA formation, as evidenced by multiple animal studies mentioned before. Patient samples also indicate a pivotal role for these pathways as revealed by the dysregulation of eNOS, Notch1 and TGFβ signaling proteins in the BAV aortic tissue. The involvement of these pathways is validated by the mutations that have been shown to cause BAV and/or TAA in mouse models and the finding of mutations in these genes in patients with BAV and TAA. In addition to these observations made *in vivo*, *in vitro* studies using patient derived endothelial cells indicate an EndoMT defect in cultured cells from BAV patients. In conclusion, all studies to date indicate great potential of an underexplored research field concerning the endothelial-smooth muscle cell communication in the BAV TAA formation.

While hardly studied in BAV, the importance of endothelial functioning for vessel homeostasis has been elucidated in other vascular disorders such as PAH, HHT, and atherosclerosis. In line with the latest research in these fields, it would be very interesting to investigate if the mechanotransduction and/or microvesicle secretion is altered in endothelial cells of BAV TAA patients. Unfortunately, research toward endothelial cell

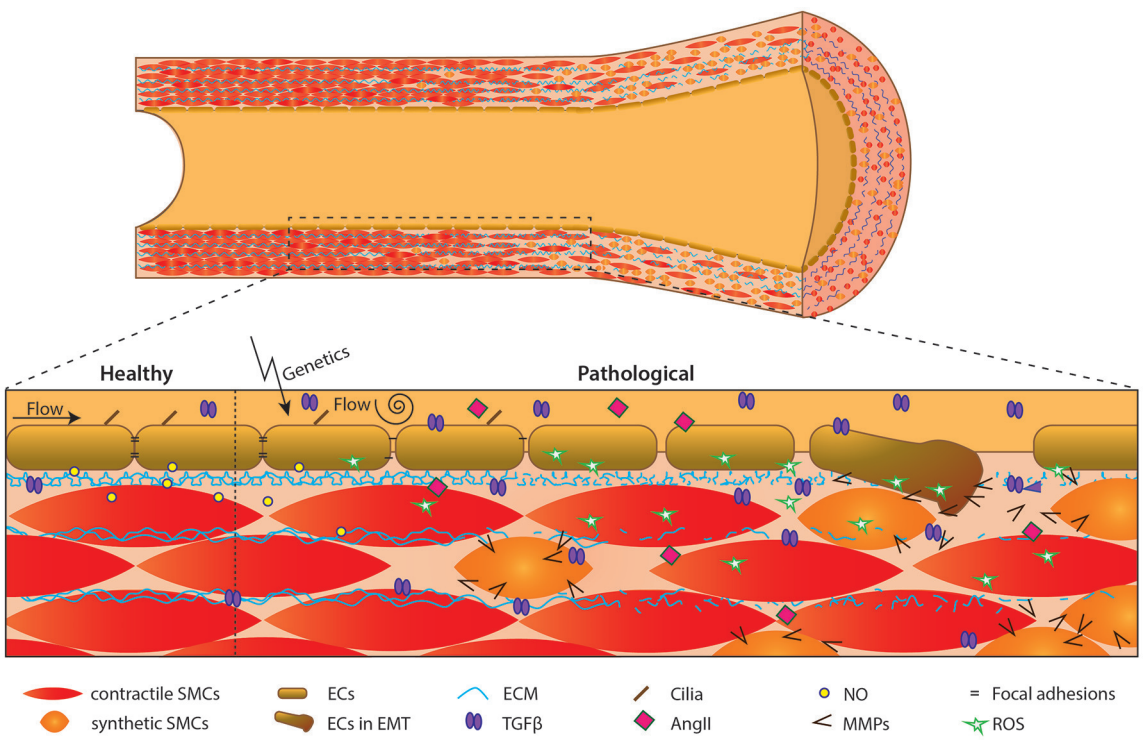

FIGURE 3 | Schematic overview of events in development of aortic dilation. Schematic overview of an aorta over time. Initiation by flow and/or genetics causes endothelial cell dysfunction, affecting the aortic structure i.e., causing synthetic SMCs and lamellar fragmentation.

contribution in BAV TAA pathogenesis has been hampered by the difficulty of obtaining non-end stage study material. The discovery of circulating endothelial progenitor cells (EPCs) and endothelial colony forming cells (ECFCs) will provide a new study model, facilitating patient specific analysis of the endothelial contribution to the disease (Asahara et al., 1997; Ingram et al., 2004). Thus far, one study was published using these circulatory cells from BAV patients. An impaired EPC migration and colony formation potential was shown when the cells were isolated from BAV patients with a dysfunctional valve compared to BAV patients with a normal functioning valve (Vaturi et al., 2011). Currently, the cause and effect of impaired EPCs is unknown, and more research is required to understand the full potential of circulating EPCs and ECFCs in BAV TAA pathogenesis and their use as a biomarker for patient stratification.

Although few studies on the role of endothelium in BAV disease and its associated TAAs have been performed in the last decade, some seminal papers have been published. In this review we have created an overview of the recent studies implicating endothelial cells as a pivotal player of vascular homeostasis, and their underappreciated role in TAA pathogenesis in patients with a BAV. **Figure 3** schematically depicts the different factors and processes involved in BAV TAA development as discussed throughout this review. Up to date, we are still unable to stratify and cure BAV patients with TAA patients. Therefore, further research is required to understand the role of endothelial cells and comprehend the interplay between endothelial cells and SMCs in BAV-associated TAA. In conclusion, appreciation of the role of endothelium is crucial for a better understanding of BAV TAA pathogenesis, which is necessary in development of new therapeutic strategies for the BAV-associated TAAs.

AUTHOR CONTRIBUTIONS

VvdP, KK, and M-JG conceptualized the review. All authors listed have made a substantial, direct and intellectual contribution to the work, and approved it for publication.

ACKNOWLEDGMENTS

We acknowledge support from the Netherlands CardioVascular Research Initiative: the Dutch Heart Foundation, Dutch Federation of University Medical Centers, the Netherlands Organization for Health Research and Development, and the Royal Netherlands Academy of Sciences Grant CVON-PHAEDRA (CVON 2012-08) and the Dutch Heart Foundation grant number 2013T093 awarded to the BAV consortium.

REFERENCES

Aicher, D., Urbich, C., Zeiher, A., Dimmeler, S., and Schäfers, H. J. (2007). Endothelial nitric oxide synthase in bicuspid aortic valve disease. *Ann. Thorac. Surg.* 83, 1290–1294. doi: 10.1016/j.athoracsur.2006.11.086

Albinsson, S., Della Corte, A., Alajbegovic, A., Krawczyk, K. K., Bancone, C., Galderisi, U., et al. (2017). Patients with bicuspid and tricuspid aortic valve exhibit distinct regional microrna signatures in mildly dilated ascending aorta. *Heart Vessels* 32, 750–767. doi: 10.1007/s00380-016-0942-7

Alegret, J. M., Martínez-Micaelo, N., Aragonès, G., and Beltrán-Debón, R. (2016). Circulating endothelial microparticles are elevated in bicuspid aortic valve disease and related to aortic dilation. *Int. J. Cardiol.* 217, 35–41. doi: 10.1016/j.ijcard.2016.04.184

Allinson, K. R., Lee, H. S., Fruttiger, M., Mccarty, J. H., and Arthur, H. M. (2012). Endothelial expression of TGFbeta type II receptor is required to maintain vascular integrity during postnatal development of the central nervous system. *PLoS ONE* 7:e39336. doi: 10.1371/annotation/8d859757-284b-406d-9cb9-a8776ad32fb1

Andelfinger, G., Loeys, B., and Dietz, H. (2016). A decade of discovery in the genetic understanding of thoracic aortic disease. *Can. J. Cardiol.* 32, 13–25. doi: 10.1016/j.cjca.2015.10.017

Arthur, H. M., Ure, J., Smith, A. J., Renforth, G., Wilson, D. I., Torsney, E., et al. (2000). Endoglin, an ancillary TGFbeta receptor, is required for extraembryonic angiogenesis and plays a key role in heart development. *Dev. Biol.* 217, 42–53. doi: 10.1006/dbio.1999.9534

Asahara, T., Murohara, T., Sullivan, A., Silver, M., Van der Zee, R., Li, T., et al. (1997). Isolation of putative progenitor endothelial cells for angiogenesis. *Science* 275, 964–967. doi: 10.1126/science.275.5302.964

Attias, D., Stheneur, C., Roy, C., Collod-Béroud, G., Detaint, D., Faivre, L., et al. (2009). Comparison of clinical presentations and outcomes between patients with TGFBR2 and FBN1 mutations in Marfan syndrome and related disorders. *Circulation* 120, 2541–2549. doi: 10.1161/CIRCULATIONAHA.109.887042

Baeyens, N., Bandyopadhyay, C., Coon, B. G., Yun, S., and Schwartz, M. A. (2016a). Endothelial fluid shear stress sensing in vascular health and disease. *J. Clin. Invest.* 126, 821–828. doi: 10.1172/JCI83083

Baeyens, N., Larrivée, B., Ola, R., Hayward-Piatkowskyi, B., Dubrac, A., Huang, B., et al. (2016b). Defective fluid shear stress mechanotransduction mediates hereditary hemorrhagic telangiectasia. *J. Cell Biol.* 214, 807–816. doi: 10.1083/jcb.201603106

Barker, A. J., Markl, M., Bürk, J., Lorenz, R., Bock, J., Bauer, S., et al. (2012). Bicuspid aortic valve is associated with altered wall shear stress in the ascending aorta. *Circ. Cardiovasc. Imaging* 5, 457–466. doi: 10.1161/CIRCIMAGING.112.973370

Basso, C., Boschello, M., Perrone, C., Mecenero, A., Cera, A., Bicego, D., et al. (2004). An echocardiographic survey of primary school children for bicuspid aortic valve. *Am. J. Cardiol.* 93, 661–663. doi: 10.1016/j.amjcard.2003.11.031

Bernal-Mizrachi, L., Jy, W., Jimenez, J. J., Pastor, J., Mauro, L. M., Horstman, L. L., et al. (2003). High levels of circulating endothelial microparticles in patients with acute coronary syndromes. *Am. Heart J.* 145, 962–970. doi: 10.1016/S0002-8703(03)00103-0

Billaud, M., Phillippi, J. A., Kotlarczyk, M. P., Hill, J. C., Ellis, B. W., St Croix, C. M., et al. (2017). Elevated oxidative stress in the aortic media of patients with bicuspid aortic valve. *J. Thorac. Cardiovasc. Surg.* 154, 1756–1762. doi: 10.1016/j.jtcvs.2017.05.065

Biner, S., Rafique, A. M., Ray, I., Cuk, O., Siegel, R. J., and Tolstrup, K. (2009). Aortopathy is prevalent in relatives of bicuspid aortic valve patients. *J. Am. Coll. Cardiol.* 53, 2288–2295. doi: 10.1016/j.jacc.2009.03.027

Boettger, T., Beetz, N., Kostin, S., Schneider, J., Krüger, M., Hein, L., et al. (2009). Acquisition of the contractile phenotype by murine arterial smooth muscle cells depends on the Mir143/145 gene cluster. *J. Clin. Invest.* 119, 2634–2647. doi: 10.1172/JCI38864

Bogdan, C. (2001). Nitric oxide and the regulation of gene expression. *Trends Cell Biol.* 11, 66–75. doi: 10.1016/S0962-8924(00)01900-0

Bonachea, E. M., Chang, S. W., Zender, G., Lahaye, S., Fitzgerald-Butt, S., Mcbride, K. L., et al. (2014). Rare GATA5 sequence variants identified in individuals with bicuspid aortic valve. *Pediatr. Res.* 76, 211–216. doi: 10.1038/pr.2014.67

Brown, D. J., Rzucidlo, E. M., Merenick, B. L., Wagner, R. J., Martin, K. A., and Powell, R. J. (2005). Endothelial cell activation of the smooth muscle cell phosphoinositide 3-kinase/Akt pathway promotes differentiation. *J. Vasc. Surg.* 41, 509–516. doi: 10.1016/j.jvs.2004.12.024

Calloway, T. J., Martin, L. J., Zhang, X., Tandon, A., Benson, D. W., and Hinton, R. B. (2011). Risk factors for aortic valve disease in bicuspid aortic valve: a family-based study. *Am. J. Med. Genet. A* 155a, 1015–1020. doi: 10.1002/ajmg.a.33974

Chen, X., Rateri, D. L., Howatt, D. A., Balakrishnan, A., Moorleghen, J. J., Cassis, L. A., et al. (2016). TGF-beta neutralization enhances AngII-induced aortic rupture and aneurysm in both thoracic and abdominal regions. *PLoS ONE* 11:e0153811. doi: 10.1371/journal.pone.0153811

Cheng, J., Koenig, S. N., Kuivaniemi, H. S., Garg, V., and Hans, C. P. (2014). Pharmacological inhibitor of notch signaling stabilizes the progression of small abdominal aortic aneurysm in a mouse model. *J. Am. Heart Assoc.* 3:e001064. doi: 10.1161/JAHA.114.001064

Chistiakov, D. A., Orekhov, A. N., and Bobryshev, Y. V. (2017). Effects of shear stress on endothelial cells: go with the flow. *Acta Physiol.* 219, 382–408. doi: 10.1111/apha.12725

Chou, C. H., Chen, Y. H., Hung, C. S., Chang, Y. Y., Tzeng, Y. L., Wu, X. M., et al. (2015). Aldosterone impairs vascular smooth muscle function: from clinical to bench research. *J. Clin. Endocrinol. Metab.* 100, 4339–4347. doi: 10.1210/jc.2015-2752

Climent, M., Quintavalle, M., Miragoli, M., Chen, J., Condorelli, G., and Elia, L. (2015). TGFbeta triggers miR-143/145 transfer from smooth muscle cells to endothelial cells, thereby modulating vessel stabilization. *Circ. Res.* 116, 1753–1764. doi: 10.1161/CIRCRESAHA.116.305178

Daugherty, A., Manning, M. W., and Cassis, L. A. (2000). Angiotensin II promotes atherosclerotic lesions and aneurysms in apolipoprotein E-deficient mice. *J. Clin. Invest.* 105, 1605–1612. doi: 10.1172/JCI7818

Daugherty, A., Rateri, D. L., Charo, I. F., Owens, A. P., Howatt, D. A., and Cassis, L. A. (2010). Angiotensin II infusion promotes ascending aortic aneurysms: attenuation by CCR2 deficiency in apoE-/- mice. *Clin. Sci.* 118, 681–689. doi: 10.1042/CS20090372

Deng, L., Blanco, F. J., Stevens, H., Lu, R., Caudrillier, A., Mcbride, M., et al. (2015). MicroRNA-143 activation regulates smooth muscle and endothelial cell crosstalk in pulmonary arterial hypertension. *Circ. Res.* 117, 870–883. doi: 10.1161/CIRCRESAHA.115.306806

Dupuis, L. E., Osinska, H., Weinstein, M. B., Hinton, R. B., and Kern, C. B. (2013). Insufficient versican cleavage and Smad2 phosphorylation results in bicuspid aortic and pulmonary valves. *J. Mol. Cell. Cardiol.* 60, 50–59. doi: 10.1016/j.yjmcc.2013.03.010

Eddahibi, S., Guignabert, C., Barlier-Mur, A. M., Dewachter, L., Fadel, E., Dartevelle, P., et al. (2006). Cross talk between endothelial and smooth muscle cells in pulmonary hypertension: critical role for serotonin-induced smooth muscle hyperplasia. *Circulation* 113, 1857–1864. doi: 10.1161/CIRCULATIONAHA.105.591321

Egorova, A. D., Khedoe, P. P., Goumans, M. J., Yoder, B. K., Nauli, S. M., Ten Dijke, P., et al. (2011). Lack of primary cilia primes shear-induced endothelial-to-mesenchymal transition. *Circ. Res.* 108, 1093–1101. doi: 10.1161/CIRCRESAHA.110.231860

Egorova, A. D., Van der Heiden, K., Poelmann, R. E., and Hierck, B. P. (2012). Primary cilia as biomechanical sensors in regulating endothelial function. *Differentiation* 83, S56–61. doi: 10.1016/j.diff.2011.11.007

El-Hamamsy, I., and Yacoub, M. H. (2009). Cellular and molecular mechanisms of thoracic aortic aneurysms. *Nat. Rev. Cardiol.* 6, 771–786. doi: 10.1038/nrcardio.2009.191

Elia, L., Quintavalle, M., Zhang, J., Contu, R., Cossu, L., Latronico, M. V., et al. (2009). The knockout of miR-143 and−145 alters smooth muscle cell maintenance and vascular homeostasis in mice: correlates with human disease. *Cell Death Differ.* 16, 1590–1598. doi: 10.1038/cdd.2009.153

Escudero, P., Navarro, A., Ferrando, C., Furio, E., Gonzalez-Navarro, H., Juez, M., et al. (2015). Combined treatment with bexarotene and rosuvastatin reduces angiotensin-II-induced abdominal aortic aneurysm in apoE(-/-) mice and angiogenesis. *Br. J. Pharmacol.* 172, 2946–2960. doi: 10.1111/bph.13098

Fan, L. M., Douglas, G., Bendall, J. K., Mcneill, E., Crabtree, M. J., Hale, A. B., et al. (2014). Endothelial cell-specific reactive oxygen species production increases susceptibility to aortic dissection. *Circulation* 129, 2661–2672. doi: 10.1161/CIRCULATIONAHA.113.005062

Foffa, I., Murzi, M., Mariani, M., Mazzone, A. M., Glauber, M., Ait Ali, L., et al. (2012). Angiotensin-converting enzyme insertion/deletion polymorphism is a risk factor for thoracic aortic aneurysm in patients with bicuspid or tricuspid aortic valves. *J. Thorac. Cardiovasc. Surg.* 144, 390–395. doi: 10.1016/j.jtcvs.2011.12.038

Förstermann, U., and Münzel, T. (2006). Endothelial nitric oxide synthase in vascular disease: from marvel to menace. *Circulation* 113, 1708–1714. doi: 10.1161/CIRCULATIONAHA.105.602532

Gao, L., Chen, L., Fan, L., Gao, D., Liang, Z., Wang, R., et al. (2016). The effect of losartan on progressive aortic dilatation in patients with Marfan's syndrome: a meta-analysis of prospective randomized clinical trials. *Int. J. Cardiol.* 217, 190–194. doi: 10.1016/j.ijcard.2016.04.186

Gao, L., Siu, K. L., Chalupsky, K., Nguyen, A., Chen, P., Weintraub, N. L., et al. (2012). Role of uncoupled endothelial nitric oxide synthase in abdominal aortic aneurysm formation: treatment with folic acid. *Hypertension* 59, 158–166. doi: 10.1161/HYPERTENSIONAHA.111.181644

Garg, V., Muth, A. N., Ransom, J. F., Schluterman, M. K., Barnes, R., King, I. N., et al. (2005). Mutations in NOTCH1 cause aortic valve disease. *Nature* 437, 270–274. doi: 10.1038/nature03940

Gillis, E., Kumar, A. A., Luyckx, I., Preuss, C., Cannaerts, E., Van De Beek, G., et al. (2017). Candidate gene resequencing in a large bicuspid aortic valve-associated thoracic aortic aneurysm cohort: SMAD6 as an important contributor. *Front. Physiol.* 8:400. doi: 10.3389/fphys.2017.00400

Girdauskas, E., Borger, M. A., Secknus, M. A., Girdauskas, G., and Kuntze, T. (2011a). Is aortopathy in bicuspid aortic valve disease a congenital defect or a result of abnormal hemodynamics? A critical reappraisal of a one-sided argument. *Eur. J. Cardiothorac. Surg.* 39, 809–814. doi: 10.1016/j.ejcts.2011.01.001

Girdauskas, E., Schulz, S., Borger, M. A., Mierzwa, M., and Kuntze, T. (2011b). Transforming growth factor-beta receptor type II mutation in a patient with bicuspid aortic valve disease and intraoperative aortic dissection. *Ann. Thorac. Surg.* 91, e70–71. doi: 10.1016/j.athoracsur.2010.12.060

Goumans, M. J., and Ten Dijke, P. (2017). TGF-β signaling in control of cardiovascular function. *Cold Spring Harb. Perspect. Biol.* 767–805. doi: 10.1101/cshperspect.a022210

Goumans, M. J., Valdimarsdottir, G., Itoh, S., Lebrin, F., Larsson, J., Mummery, C., et al. (2003). Activin receptor-like kinase (ALK)1 is an antagonistic mediator of lateral TGFbeta/ALK5 signaling. *Mol. Cell* 12, 817–828. doi: 10.1016/S1097-2765(03)00386-1

Goumans, M. J., Valdimarsdottir, G., Itoh, S., Rosendahl, A., Sideras, P., and Ten Dijke, P. (2002). Balancing the activation state of the endothelium via two distinct TGF-beta type I receptors. *EMBO J.* 21, 1743–1753. doi: 10.1093/emboj/21.7.1743

Grewal, N., Gittenberger-De Groot, A. C., Poelmann, R. E., Klautz, R. J., Lindeman, J. H., Goumans, M. J., et al. (2014). Ascending aorta dilation in association with bicuspid aortic valve: a maturation defect of the aortic wall. *J. Thorac. Cardiovasc. Surg.* 148, 1583–1590. doi: 10.1016/j.jtcvs.2014.01.027

Guo, D. C., Pannu, H., Tran-Fadulu, V., Papke, C. L., Yu, R. K., Avidan, N., et al. (2007). Mutations in smooth muscle alpha-actin (ACTA2) lead to thoracic aortic aneurysms and dissections. *Nat. Genet.* 39, 1488–1493. doi: 10.1038/ng.2007.6

Guo, D. C., Papke, C. L., He, R., and Milewicz, D. M. (2006). Pathogenesis of thoracic and abdominal aortic aneurysms. *Ann. N. Y. Acad. Sci.* 1085, 339–352. doi: 10.1196/annals.1383.013

Guo, X., and Chen, S. Y. (2012). Transforming growth factor-beta and smooth muscle differentiation. *World J. Biol. Chem.* 3, 41–52. doi: 10.4331/wjbc.v3.i3.41

Habashi, J. P., Judge, D. P., Holm, T. M., Cohn, R. D., Loeys, B. L., Cooper, T. K., et al. (2006). Losartan, an AT1 antagonist, prevents aortic aneurysm in a mouse model of Marfan syndrome. *Science* 312, 117–121. doi: 10.1126/science.1124287

Halloran, B. G., Davis, V. A., Mcmanus, B. M., Lynch, T. G., and Baxter, B. T. (1995). Localization of aortic disease is associated with intrinsic differences in aortic structure. *J. Surg. Res.* 59, 17–22. doi: 10.1006/jsre.1995.1126

Hans, C. P., Koenig, S. N., Huang, N., Cheng, J., Beceiro, S., Guggilam, A., et al. (2012). Inhibition of Notch1 signaling reduces abdominal aortic aneurysm

in mice by attenuating macrophage-mediated inflammation. *Arterioscler. Thromb. Vasc. Biol.* 32, 3012–3023. doi: 10.1161/ATVBAHA.112.254219

Hashikabe, Y., Suzuki, K., Jojima, T., Uchida, K., and Hattori, Y. (2006). Aldosterone impairs vascular endothelial cell function. *J. Cardiovasc. Pharmacol.* 47, 609–613. doi: 10.1097/01.fjc.0000211738.63207.c3

Hergenreider, E., Heydt, S., Tréguer', K., Boettger, T., Horrevoets, A. J., Zeiher, A. M., et al. (2012). Atheroprotective communication between endothelial cells and smooth muscle cells through miRNAs. *Nat. Cell Biol.* 14, 249–256. doi: 10.1038/ncb2441

High, F. A., Jain, R., Stoller, J. Z., Antonucci, N. B., Lu, M. M., Loomes, K. M., et al. (2009). Murine Jagged1/Notch signaling in the second heart field orchestrates Fgf8 expression and tissue-tissue interactions during outflow tract development. *J. Clin. Invest.* 119, 1986–1996. doi: 10.1172/JCI38922

High, F. A., Lu, M. M., Pear, W. S., Loomes, K. M., Kaestner, K. H., and Epstein, J. A. (2008). Endothelial expression of the Notch ligand Jagged1 is required for vascular smooth muscle development. *Proc. Natl. Acad. Sci. U.S.A.* 105, 1955–1959. doi: 10.1073/pnas.0709663105

Hillebrand, M., Millot, N., Sheikhzadeh, S., Rybczynski, M., Gerth, S., Kölbel, T., et al. (2014). Total serum transforming growth factor-beta1 is elevated in the entire spectrum of genetic aortic syndromes. *Clin. Cardiol.* 37, 672–679. doi: 10.1002/clc.22320

Hirschi, K. K., Rohovsky, S. A., and D'Amore, P. A. (1998). PDGF, TGF-beta, and heterotypic cell-cell interactions mediate endothelial cell-induced recruitment of 10T1/2 cells and their differentiation to a smooth muscle fate. *J. Cell Biol.* 141, 805–814. doi: 10.1083/jcb.141.3.805

Huntington, K., Hunter, A. G., and Chan, K. L. (1997). A prospective study to assess the frequency of familial clustering of congenital bicuspid aortic valve. *J. Am. Coll. Cardiol.* 30, 1809–1812. doi: 10.1016/S0735-1097(97)00372-0

Ingram, D. A., Mead, L. E., Tanaka, H., Meade, V., Fenoglio, A., Mortell, K., et al. (2004). Identification of a novel hierarchy of endothelial progenitor cells using human peripheral and umbilical cord blood. *Blood* 104, 2752–2760. doi: 10.1182/blood-2004-04-1396

Itoh, F., Itoh, S., Adachi, T., Ichikawa, K., Matsumura, Y., Takagi, T., et al. (2012). Smad2/Smad3 in endothelium is indispensable for vascular stability via S1PR1 and N-cadherin expressions. *Blood* 119, 5320–5328. doi: 10.1182/blood-2011-12-395772

Jansen, F., Stumpf, T., Proebsting, S., Franklin, B. S., Wenzel, D., Pfeifer, P., et al. (2017). Intercellular transfer of miR-126-3p by endothelial microparticles reduces vascular smooth muscle cell proliferation and limits neointima formation by inhibiting LRP6. *J. Mol. Cell. Cardiol.* 104, 43–52. doi: 10.1016/j.yjmcc.2016.12.005

Jiao, J., Xiong, W., Wang, L., Yang, J., Qiu, P., Hirai, H., et al. (2016). Differentiation defect in neural crest-derived smooth muscle cells in patients with aortopathy associated with bicuspid aortic valves. *EBioMedicine* 10, 282–290. doi: 10.1016/j.ebiom.2016.06.045

Jin, Y., Muhl, L., Burmakin, M., Wang, Y., Duchez, A. C., Betsholtz, C., et al. (2017). Endoglin prevents vascular malformation by regulating flow-induced cell migration and specification through VEGFR2 signalling. *Nat. Cell Biol.* 19, 639–652. doi: 10.1038/ncb3534

Kent, K. C., Crenshaw, M. L., Goh, D. L., and Dietz, H. C. (2013). Genotype-phenotype correlation in patients with bicuspid aortic valve and aneurysm. *J. Thorac. Cardiovasc. Surg.* 146, 158–165.e151. doi: 10.1016/j.jtcvs.2012.09.060

Kim, Y. H., Kim, J. S., Choi, J. W., Chang, H. W., Na, K. J., Kim, J. S., et al. (2016). Clinical implication of aortic wall biopsy in aortic valve disease with bicuspid valve pathology. *Korean J. Thorac. Cardiovasc. Surg.* 49, 443–450. doi: 10.5090/kjtcs.2016.49.6.443

Koenig, S. N., Bosse, K. M., Nadorlik, H. A., Lilly, B., and Garg, V. (2015). Evidence of aortopathy in mice with haploinsufficiency of Notch1 in Nos3-null background. *J Cardiovasc Dev Dis* 2, 17–30. doi: 10.3390/jcdd2010017

Koenig, S. N., Bosse, K., Majumdar, U., Bonachea, E. M., Radtke, F., and Garg, V. (2016). Endothelial notch1 is required for proper development of the semilunar valves and cardiac outflow tract. *J. Am. Heart Assoc.* 5:e003075. doi: 10.1161/JAHA.115.003075

Koenig, S. N., Lincoln, J., and Garg, V. (2017). Genetic basis of aortic valvular disease. *Curr. Opin. Cardiol.*. doi: 10.1097/HCO.0000000000000384

Kostina, A. S., Uspensky Vcapital Ie, C., Irtyuga, O. B., Ignatieva, E. V., Freylikhman, O., Gavriliuk, N. D., et al. (2016). Notch-dependent EMT is attenuated in patients with aortic aneurysm and bicuspid aortic valve. *Biochim. Biophys. Acta* 1862, 733–740. doi: 10.1016/j.bbadis.2016.02.006

Kotlarczyk, M. P., Billaud, M., Green, B. R., Hill, J. C., Shiva, S., Kelley, E. E., et al. (2016). Regional disruptions in endothelial nitric oxide pathway associated with bicuspid aortic valve. *Ann. Thorac. Surg.* 102, 1274–1281. doi: 10.1016/j.athoracsur.2016.04.001

Krebs, L. T., Xue, Y., Norton, C. R., Shutter, J. R., Maguire, M., Sundberg, J. P., et al. (2000). Notch signaling is essential for vascular morphogenesis in mice. *Genes Dev.* 14, 1343–1352.

Laforest, B., and Nemer, M. (2012). Genetic insights into bicuspid aortic valve formation. *Cardiol. Res. Pract.* 2012:180297. doi: 10.1155/2012/180297

Langille, B. L., and O'donnell, F. (1986). Reductions in arterial diameter produced by chronic decreases in blood flow are endothelium-dependent. *Science* 231, 405–407. doi: 10.1126/science.3941904

Lazar-Karsten, P., Belge, G., Schult-Badusche, D., Focken, T., Radtke, A., Yan, J., et al. (2016). Generation and characterization of vascular smooth muscle cell lines derived from a patient with a bicuspid aortic valve. *Cells* 5:E19. doi: 10.3390/cells5020019

Lebrin, F., Goumans, M. J., Jonker, L., Carvalho, R. L., Valdimarsdottir, G., Thorikay, M., et al. (2004). Endoglin promotes endothelial cell proliferation and TGF-beta/ALK1 signal transduction. *EMBO J.* 23, 4018–4028. doi: 10.1038/sj.emboj.7600386

Lee, J. K., Borhani, M., Ennis, T. L., Upchurch, G. R. Jr., and Thompson, R. W. (2001). Experimental abdominal aortic aneurysms in mice lacking expression of inducible nitric oxide synthase. *Arterioscler. Thromb. Vasc. Biol.* 21, 1393–1401. doi: 10.1161/hq0901.095750

Lee, T. C., Zhao, Y. D., Courtman, D. W., and Stewart, D. J. (2000). Abnormal aortic valve development in mice lacking endothelial nitric oxide synthase. *Circulation* 101, 2345–2348. doi: 10.1161/01.CIR.101.20.2345

Leibovitz, E., Ebrahimian, T., Paradis, P., and Schiffrin, E. L. (2009). Aldosterone induces arterial stiffness in absence of oxidative stress and endothelial dysfunction. *J. Hypertens.* 27, 2192–2200. doi: 10.1097/HJH.0b013e328330a963

Lewin, M. B., and Otto, C. M. (2005). The bicuspid aortic valve: adverse outcomes from infancy to old age. *Circulation* 111, 832–834. doi: 10.1161/01.CIR.0000157137.59691.0B

Li, D. Y., Sorensen, L. K., Brooke, B. S., Urness, L. D., Davis, E. C., Taylor, D. G., et al. (1999). Defective angiogenesis in mice lacking endoglin. *Science* 284, 1534–1537. doi: 10.1126/science.284.5419.1534

Licholai, S., Blaz, M., Kapelak, B., and Sanak, M. (2016). Unbiased profile of MicroRNA expression in ascending aortic aneurysm tissue appoints molecular pathways contributing to the pathology. *Ann. Thorac. Surg.* 102, 1245–1252. doi: 10.1016/j.athoracsur.2016.03.061

Maleki, S., Kjellqvist, S., Paloschi, V., Magné, J., Branca, R. M., Du, L., et al. (2016). Mesenchymal state of intimal cells may explain higher propensity to ascending aortic aneurysm in bicuspid aortic valves. *Sci. Rep.* 6:35712. doi: 10.1038/srep35712

Matsumoto, T., Oki, K., Kajikawa, M., Nakashima, A., Maruhashi, T., Iwamoto, Y., et al. (2015). Effect of aldosterone-producing adenoma on endothelial function and Rho-associated kinase activity in patients with primary aldosteronism. *Hypertension* 65, 841–848. doi: 10.1161/HYPERTENSIONAHA.114.05001

Matt, P., Schoenhoff, F., Habashi, J., Holm, T., Van Erp, C., Loch, D., et al. (2009). Circulating transforming growth factor-beta in Marfan syndrome. *Circulation* 120, 526–532. doi: 10.1161/CIRCULATIONAHA.108.841981

McDonald, J., Wooderchak-Donahue, W., Vansant Webb, C., Whitehead, K., Stevenson, D. A., and Bayrak-Toydemir, P. (2015). Hereditary hemorrhagic telangiectasia: genetics and molecular diagnostics in a new era. *Front. Genet.* 6:1. doi: 10.3389/fgene.2015.00001

Medici, D., Shore, E. M., Lounev, V. Y., Kaplan, F. S., Kalluri, R., and Olsen, B. R. (2010). Conversion of vascular endothelial cells into multipotent stem-like cells. *Nat. Med.* 16, 1400–1406. doi: 10.1038/nm.2252

Messaoudi, S., He, Y., Gutsol, A., Wight, A., Hébert, R. L., Vilmundarson, R. O., et al. (2015). Endothelial Gata5 transcription factor regulates blood pressure. *Nat. Commun.* 6, 8835. doi: 10.1038/ncomms9835

Mohamed, S. A., Radtke, A., Saraei, R., Bullerdiek, J., Sorani, H., Nimzyk, R., et al. (2012). Locally different endothelial nitric oxide synthase protein levels in ascending aortic aneurysms of bicuspid and tricuspid aortic valve. *Cardiol. Res. Pract.* 2012:165957. doi: 10.1155/2012/165957

Morrell, N. W., Adnot, S., Archer, S. L., Dupuis, J., Jones, P. L., Maclean, M. R., et al. (2009). Cellular and molecular basis of pulmonary arterial hypertension. *J. Am. Coll. Cardiol.* 54, S20–S31. doi: 10.1016/j.jacc.2009.04.018

Nataatmadja, M., West, J., Prabowo, S., and West, M. (2013). Angiotensin II receptor antagonism reduces transforming growth factor beta and smad signaling in thoracic aortic aneurysm. *Ochsner J.* 13, 42–48.

Niessen, K., and Karsan, A. (2008). Notch signaling in cardiac development. *Circ. Res.* 102, 1169–1181. doi: 10.1161/CIRCRESAHA.108.174318

Niessen, K., Fu, Y., Chang, L., Hoodless, P. A., Mcfadden, D., and Karsan, A. (2008). Slug is a direct Notch target required for initiation of cardiac cushion cellularization. *J. Cell Biol.* 182, 315–325. doi: 10.1083/jcb.200710067

Nigam, V., and Srivastava, D. (2009). Notch1 represses osteogenic pathways in aortic valve cells. *J. Mol. Cell. Cardiol.* 47, 828–834. doi: 10.1016/j.yjmcc.2009.08.008

Nomura-Kitabayashi, A., Anderson, G. A., Sleep, G., Mena, J., Karabegovic, A., Karamath, S., et al. (2009). Endoglin is dispensable for angiogenesis, but required for endocardial cushion formation in the midgestation mouse embryo. *Dev. Biol.* 335, 66–77. doi: 10.1016/j.ydbio.2009.08.016

Noris, M., Morigi, M., Donadelli, R., Aiello, S., Foppolo, M., Todeschini, M., et al. (1995). Nitric oxide synthesis by cultured endothelial cells is modulated by flow conditions. *Circ. Res.* 76, 536–543. doi: 10.1161/01.RES.76.4.536

Noseda, M., Mclean, G., Niessen, K., Chang, L., Pollet, I., Montpetit, R., et al. (2004). Notch activation results in phenotypic and functional changes consistent with endothelial-to-mesenchymal transformation. *Circ. Res.* 94, 910–917. doi: 10.1161/01.RES.0000124300.76171.C9

Oudit, G. Y., Chow, C. M., and Cantor, W. J. (2006). Calcific bicuspid aortic valve disease in a patient with Cornelia de Lange syndrome: linking altered Notch signaling to aortic valve disease. *Cardiovasc. Pathol.* 15, 165–167. doi: 10.1016/j.carpath.2006.02.002

Paloschi, V., Gadin, J. R., Khan, S., Bjorck, H. M., Du, L., Maleki, S., et al. (2015). Aneurysm development in patients with a bicuspid aortic valve is not associated with transforming growth factor-beta activation. *Arterioscler. Thromb. Vasc. Biol.* 35, 973–980. doi: 10.1161/ATVBAHA.114.304996

Patel, V. B., Zhong, J. C., Fan, D., Basu, R., Morton, J. S., Parajuli, N., et al. (2014). Angiotensin-converting enzyme 2 is a critical determinant of angiotensin II-induced loss of vascular smooth muscle cells and adverse vascular remodeling. *Hypertension* 64, 157–164. doi: 10.1161/HYPERTENSIONAHA.114.03388

Pece-Barbara, N., Vera, S., Kathirkamathamby, K., Liebner, S., Di Guglielmo, G. M., Dejana, E., et al. (2005). Endoglin null endothelial cells proliferate faster and are more responsive to transforming growth factor beta1 with higher affinity receptors and an activated Alk1 pathway. *J. Biol. Chem.* 280, 27800–27808. doi: 10.1074/jbc.M503471200

Police, S. B., Thatcher, S. E., Charnigo, R., Daugherty, A., and Cassis, L. A. (2009). Obesity promotes inflammation in periaortic adipose tissue and angiotensin II-induced abdominal aortic aneurysm formation. *Arterioscler. Thromb. Vasc. Biol.* 29, 1458–1464. doi: 10.1161/ATVBAHA.109.192658

Qu, X. K., Qiu, X. B., Yuan, F., Wang, J., Zhao, C. M., Liu, X. Y., et al. (2014). A novel NKX2.5 loss-of-function mutation associated with congenital bicuspid aortic valve. *Am. J. Cardiol.* 114, 1891–1895. doi: 10.1016/j.amjcard.2014.09.028

Ramnath, N. W., Hawinkels, L. J., Van Heijningen, P. M., Te Riet, L., Paauwe, M., Vermeij, M., et al. (2015). Fibulin-4 deficiency increases TGF-beta signalling in aortic smooth muscle cells due to elevated TGF-beta2 levels. *Sci. Rep.* 5:16872. doi: 10.1038/srep16872

Rateri, D. L., Moorleghen, J. J., Balakrishnan, A., Owens, A. P. 3rd, Howatt, D. A., Subramanian, V., et al. (2011). Endothelial cell-specific deficiency of Ang II type 1a receptors attenuates Ang II-induced ascending aortic aneurysms in LDL receptor-/- mice. *Circ. Res.* 108, 574–581. doi: 10.1161/CIRCRESAHA.110.222844

Rateri, D. L., Moorleghen, J. J., Knight, V., Balakrishnan, A., Howatt, D. A., Cassis, L. A., et al. (2012). Depletion of endothelial or smooth muscle cell-specific angiotensin II type 1a receptors does not influence aortic aneurysms or atherosclerosis in LDL receptor deficient mice. *PLoS ONE* 7:e51483. doi: 10.1371/journal.pone.0051483

Roberts, W. C. (1970). The congenitally bicuspid aortic valve. A study of 85 autopsy cases. *Am. J. Cardiol.* 26, 72–83. doi: 10.1016/0002-9149(70)90761-7

Rocchiccioli, S., Cecchettini, A., Panesi, P., Farneti, P. A., Mariani, M., Ucciferri, N., et al. (2017). Hypothesis-free secretome analysis of thoracic aortic aneurysm reinforces the central role of TGF-beta cascade in patients with bicuspid aortic valve. *J. Cardiol.* 69, 570–576. doi: 10.1016/j.jjcc.2016.05.007

Rössig, L., Haendeler, J., Mallat, Z., Hugel, B., Freyssinet, J. M., Tedgui, A., et al. (2000). Congestive heart failure induces endothelial cell apoptosis: protective role of carvedilol. *J. Am. Coll. Cardiol.* 36, 2081–2089. doi: 10.1016/S0735-1097(00)01002-0

Ruddy, J. M., Jones, J. A., and Ikonomidis, J. S. (2013). Pathophysiology of thoracic aortic aneurysm (TAA): is it not one uniform aorta? Role of embryologic origin. *Prog. Cardiovasc. Dis.* 56, 68–73. doi: 10.1016/j.pcad.2013.04.002

Rueda-Martínez, C., Lamas, O., Carrasco-Chinchilla, F., Robledo-Carmona, J., Porras, C., Sánchez-Espín, G., et al. (2017). Increased blood levels of transforming growth factor beta in patients with aortic dilatation. *Interact. Cardiovasc. Thorac. Surg.* 25, 571–574. doi: 10.1093/icvts/ivx153

Sakao, S., Tatsumi, K., and Voelkel, N. F. (2009). Endothelial cells and pulmonary arterial hypertension: apoptosis, proliferation, interaction and transdifferentiation. *Respir. Res.* 10:95. doi: 10.1186/1465-9921-10-95

Saliba, E., and Sia, Y. (2015). The ascending aortic aneurysm: when to intervene? *IJC Heart Vasc.* 6, 91–100. doi: 10.1016/j.ijcha.2015.01.009

Sawada, H., Rateri, D. L., Moorleghen, J. J., Majesky, M. W., and Daugherty, A. (2017). Smooth muscle cells derived from second heart field and cardiac neural crest reside in spatially distinct domains in the media of the ascending aorta-brief report. *Arterioscler. Thromb. Vasc. Biol.* 37, 1722–1726. doi: 10.1161/ATVBAHA.117.309599

Shi, L. M., Tao, J. W., Qiu, X. B., Wang, J., Yuan, F., Xu, L., et al. (2014). GATA5 loss-of-function mutations associated with congenital bicuspid aortic valve. *Int. J. Mol. Med.* 33, 1219–1226. doi: 10.3892/ijmm.2014.1700

Shin, W. S., Hong, Y. H., Peng, H. B., De Caterina, R., Libby, P., and Liao, J. K. (1996). Nitric oxide attenuates vascular smooth muscle cell activation by interferon-gamma. The role of constitutive NF-kappa B activity. *J. Biol. Chem.* 271, 11317–11324. doi: 10.1074/jbc.271.19.11317

Siu, K. L., and Cai, H. (2014). Circulating tetrahydrobiopterin as a novel biomarker for abdominal aortic aneurysm. *Am. J. Physiol. Heart Circ. Physiol.* 307, H1559–H1564. doi: 10.1152/ajpheart.00444.2014

Tan, H. L., Glen, E., Töpf, A., Hall, D., O'sullivan, J. J., Sneddon, L., et al. (2012). Nonsynonymous variants in the SMAD6 gene predispose to congenital cardiovascular malformation. *Hum. Mutat.* 33, 720–727. doi: 10.1002/humu.22030

Tanaka, H., Zaima, N., Sasaki, T., Sano, M., Yamamoto, N., Saito, T., et al. (2015). Hypoperfusion of the adventitial vasa vasorum develops an abdominal aortic aneurysm. *PLoS ONE* 10:e0134386. doi: 10.1371/journal.pone.0134386

Tang, Y., Urs, S., Boucher, J., Bernaiche, T., Venkatesh, D., Spicer, D. B., et al. (2010). Notch and transforming growth factor-beta (TGFbeta) signaling pathways cooperatively regulate vascular smooth muscle cell differentiation. *J. Biol. Chem.* 285, 17556–17563. doi: 10.1074/jbc.M109.076414

Theodoris, C. V., Li, M., White, M. P., Liu, L., He, D., Pollard, K. S., et al. (2015). Human disease modeling reveals integrated transcriptional and epigenetic mechanisms of NOTCH1 haploinsufficiency. *Cell* 160, 1072–1086. doi: 10.1016/j.cell.2015.02.035

Thomas, P. S., Sridurongrit, S., Ruiz-Lozano, P., and Kaartinen, V. (2012). Deficient signaling via Alk2 (Acvr1) leads to bicuspid aortic valve development. *PLoS ONE* 7:e35539. doi: 10.1371/journal.pone.0035539

Tieu, B. C., Lee, C., Sun, H., Lejeune, W., Recinos, A. III., Ju, X., et al. (2009). An adventitial IL-6/MCP1 amplification loop accelerates macrophage-mediated vascular inflammation leading to aortic dissection in mice. *J. Clin. Invest.* 119, 3637–3651. doi: 10.1172/JCI38308

Toomer, K. A., Fulmer, D., Guo, L., Drohan, A., Peterson, N., Swanson, P., et al. (2017). A role for primary cilia in aortic valve development and disease. *Dev. Dyn.* 246, 625–634. doi: 10.1002/dvdy.24524

Topper, J. N., Cai, J., Qiu, Y., Anderson, K. R., Xu, Y. Y., Deeds, J. D., et al. (1997). Vascular MADs: two novel MAD-related genes selectively inducible by flow in human vascular endothelium. *Proc. Natl. Acad. Sci. U.S.A.* 94, 9314–9319. doi: 10.1073/pnas.94.17.9314

Tramontano, A. F., Lyubarova, R., Tsiakos, J., Palaia, T., Deleon, J. R., and Ragolia, L. (2010). Circulating endothelial microparticles in diabetes mellitus. *Mediators Inflamm.* 2010:250476. doi: 10.1155/2010/250476

Tsai, M. C., Chen, L., Zhou, J., Tang, Z., Hsu, T. F., Wang, Y., et al. (2009). Shear stress induces synthetic-to-contractile phenotypic modulation in smooth muscle cells via peroxisome proliferator-activated receptor alpha/delta

activations by prostacyclin released by sheared endothelial cells. *Circ. Res.* 105, 471–480. doi: 10.1161/CIRCRESAHA.109.193656

Tsamis, A., Phillippi, J. A., Koch, R. G., Chan, P. G., Krawiec, J. T., D'amore, A., et al. (2016). Extracellular matrix fiber microarchitecture is region-specific in bicuspid aortic valve-associated ascending aortopathy. *J. Thorac. Cardiovasc. Surg.* 151, 1718–1728.e1715. doi: 10.1016/j.jtcvs.2016.02.019

Van Hove, C. E., Van Der Donckt, C., Herman, A. G., Bult, H., and Fransen, P. (2009). Vasodilator efficacy of nitric oxide depends on mechanisms of intracellular calcium mobilization in mouse aortic smooth muscle cells. *Br. J. Pharmacol.* 158, 920–930. doi: 10.1111/j.1476-5381.2009.00396.x

Vaturi, M., Perl, L., Leshem-Lev, D., Dadush, O., Bental, T., Shapira, Y., et al. (2011). Circulating endothelial progenitor cells in patients with dysfunctional versus normally functioning congenitally bicuspid aortic valves. *Am. J. Cardiol.* 108, 272–276. doi: 10.1016/j.amjcard.2011.03.039

Wågsäter, D., Paloschi, V., Hanemaaijer, R., Hultenby, K., Bank, R. A., Franco-Cereceda, A., et al. (2013). Impaired collagen biosynthesis and cross-linking in aorta of patients with bicuspid aortic valve. *J. Am. Heart Assoc.* 2:e000034. doi: 10.1161/JAHA.112.000034

Walshe, T. E., Dela Paz, N. G., and D'amore, P. A. (2013). The role of shear-induced transforming growth factor-beta signaling in the endothelium. *Arterioscler. Thromb. Vasc. Biol.* 33, 2608–2617. doi: 10.1161/ATVBAHA.113.302161

Wang, Y. W., Ren, H. L., Wang, H. F., Li, F. D., Li, H. H., and Zheng, Y. H. (2015). Combining detection of Notch1 and tumor necrosis factor-alpha converting enzyme is a reliable biomarker for the diagnosis of abdominal aortic aneurysms. *Life Sci.* 127, 39–45. doi: 10.1016/j.lfs.2015.02.009

Watabe, T., Nishihara, A., Mishima, K., Yamashita, J., Shimizu, K., Miyazawa, K., et al. (2003). TGF-beta receptor kinase inhibitor enhances growth and integrity of embryonic stem cell-derived endothelial cells. *J. Cell Biol.* 163, 1303–1311. doi: 10.1083/jcb.200305147

Weber, M., Baker, M. B., Moore, J. P., and Searles, C. D. (2010). MiR-21 is induced in endothelial cells by shear stress and modulates apoptosis and eNOS activity. *Biochem. Biophys. Res. Commun.* 393, 643–648. doi: 10.1016/j.bbrc.2010.02.045

Wolinsky, H. (1970). Comparison of medial growth of human thoracic and abdominal aortas. *Circ. Res.* 27, 531–538. doi: 10.1161/01.RES.27.4.531

Wooten, E. C., Iyer, L. K., Montefusco, M. C., Hedgepeth, A. K., Payne, D. D., Kapur, N. K., et al. (2010). Application of gene network analysis techniques identifies AXIN1/PDIA2 and endoglin haplotypes associated with bicuspid aortic valve. *PLoS ONE* 5:e8830. doi: 10.1371/journal.pone.0008830

Xu, W., and Erzurum, S. C. (2011). Endothelial cell energy metabolism, proliferation, and apoptosis in pulmonary hypertension. *Compr. Physiol.* 1, 357–372. doi: 10.1002/cphy.c090005

Yao, E. H., Fukuda, N., Ueno, T., Matsuda, H., Nagase, H., Matsumoto, Y., et al. (2009). A pyrrole-imidazole polyamide targeting transforming growth factor-beta1 inhibits restenosis and preserves endothelialization in the injured artery. *Cardiovasc. Res.* 81, 797–804. doi: 10.1093/cvr/cvn355

Yao, Y., Shao, E. S., Jumabay, M., Shahbazian, A., Ji, S., and Boström, K. I. (2008). High-density lipoproteins affect endothelial BMP-signaling by modulating expression of the activin-like kinase receptor 1 and 2. *Arterioscler. Thromb. Vasc. Biol.* 28, 2266–2274. doi: 10.1161/ATVBAHA.108.176958

Yuan, S. M., Jing, H., and Lavee, J. (2010). The bicuspid aortic valve and its relation to aortic dilation. *Clinics* 65, 497–505. doi: 10.1590/S1807-59322010000500007

Yung, L. M., Nikolic, I., Paskin-Flerlage, S. D., Pearsall, R. S., Kumar, R., and Yu, P. B. (2016). A selective transforming growth factor-beta ligand trap attenuates pulmonary. *Hypertension*. 194, 1140–1151. doi: 10.1164/rccm.201510-1955OC

Zhou, J., Li, Y. S., Nguyen, P., Wang, K. C., Weiss, A., Kuo, Y. C., et al. (2013). Regulation of vascular smooth muscle cell turnover by endothelial cell-secreted microRNA-126: role of shear stress. *Circ. Res.* 113, 40–51. doi: 10.1161/CIRCRESAHA.113.280883

Zou, S., Ren, P., Nguyen, M., Coselli, J. S., Shen, Y. H., and Lemaire, S. A. (2012). Notch signaling in descending thoracic aortic aneurysm and dissection. *PLoS ONE* 7:e52833. doi: 10.1371/journal.pone.0052833

Conflict of Interest Statement: The authors declare that the research was conducted in the absence of any commercial or financial relationships that could be construed as a potential conflict of interest.

frontiers in Physiology

REVIEW
published: 25 September 2017
doi: 10.3389/fphys.2017.00687

Pathogenic Mechanisms of Bicuspid Aortic Valve Aortopathy

*Noor M. Yassine, Jasmine T. Shahram and Simon C. Body**

Department of Anesthesiology, Perioperative and Pain Medicine, Brigham and Women's Hospital, Boston, MA, United States

Bicuspid aortic valve (BAV) is the most common congenital valvular defect and is associated with ascending aortic dilation (AAD) in a quarter of patients. AAD has been ascribed both to the hemodynamic consequences of normally functioning and abnormal BAV morphology, and to the effect of rare and common genetic variation upon function of the ascending aortic media. AAD manifests in two overall and sometimes overlapping phenotypes: that of aortic root aneurysm, similar to the AAD of Marfan syndrome; and that of tubular AAD, similar to the AAD seen with tricuspid aortic valves (TAVs). These aortic phenotypes appear to be independent of BAV phenotype, have different embryologic origins and have unique etiologic factors, notably, regarding the role of hemodynamic changes inherent to the BAV phenotype. Further, in contrast to Marfan syndrome, the AAD seen with BAV is infrequently present as a strongly inherited syndromic phenotype; rather, it appears to be a less-penetrant, milder phenotype. Both reduced levels of normally functioning transcriptional proteins and structurally abnormal proteins have been observed in aneurysmal aortic media. We provide evidence that aortic root AAD has a stronger genetic etiology, sometimes related to identified common non-coding fibrillin-1 (*FBN1*) variants and other aortic wall protein variants in patients with BAV. In patients with BAV having tubular AAD, we propose a stronger hemodynamic influence, but with pathology still based on a functional deficit of the aortic media, of genetic or epigenetic etiology. Although it is an attractive hypothesis to ascribe common mechanisms to BAV and AAD, thus far the genetic etiologies of AAD have not been associated to the genetic etiologies of BAV, notably, not including BAV variants in *NOTCH1* and *GATA4*.

Keywords: bicuspid aortic valve, genetics, thoracic aortic aneurysm, fibrillin, GATA4, transforming growth factor-β

OPEN ACCESS

Edited by:
Amalia Forte,
Università degli Studi della Campania "Luigi Vanvitelli" Caserta, Italy

Reviewed by:
Yongshi Wang,
Fudan University, China
Cynthia St. Hilaire,
University of Pittsburgh, United States

****Correspondence:***
Simon C. Body
sbody@bwh.harvard.edu

Specialty section:
This article was submitted to Vascular Physiology, a section of the journal Frontiers in Physiology

Received: *31 May 2017*
Accepted: *28 August 2017*
Published: *25 September 2017*

Citation:
Yassine NM, Shahram JT and Body SC (2017) Pathogenic Mechanisms of Bicuspid Aortic Valve Aortopathy. Front. Physiol. 8:687. doi: 10.3389/fphys.2017.00687

INTRODUCTION

Bicuspid aortic valve (BAV) disease is the most common congenital valvular abnormality, with an incidence in male Caucasians of ∼1.5% and lower incidence in female and non-Caucasian individuals (Michelena et al., 2014). A spectrum of other infrequent congenital abnormalities, such as coarctation of the aorta, has been described with BAV (Michelena et al., 2014; Prakash et al., 2014). There is moderate heritability of BAV, but the vast majority of affected patients do not possess other syndromic features and have indeterminate inheritance (Prakash et al., 2014). Unlike the majority of congenital cardiac disease, BAV is most frequently diagnosed in adulthood, notably, with the onset of aortic valvular dysfunction, ascending aortic dilation (AAD; Michelena et al., 2008, 2011; McKellar et al., 2010) or endocarditis (Kiyota et al., 2017). More than 50%, and perhaps as high as 75%, of patients with BAV undergo aortic valve replacement during their lifetime

(Michelena et al., 2011). Similarly, more than 25% of patients with BAV undergo aortic surgery, often concurrent with aortic valve replacement (Michelena et al., 2011), with most aortic surgery performed for dilation of the aortic root or ascending aorta, and rarely for aortic dissection.

CLINICAL PHENOTYPING OF BAV-RELATED AORTOPATHY

BAV aortopathy is not a single clinical phenotype (Cotrufo and Della Corte, 2009; Della Corte and Bancone, 2012; Della Corte, 2014; Della Corte et al., 2014a,b). There is marked variability of AAD dimensional phenotypes with aortic dilation observed heterogeneously from the aortic annulus to the aortic arch (Girdauskas and Borger, 2013; Della Corte, 2014). Although several classification systems for AAD exist, the simplest divides the spectrum into two classes: aortic root AAD vs. tubular AAD (**Figure 1**). Although simplistic, it provides an attractive distinction that can be used for initial work and is perhaps justified based on embryonic origin of the tissue and functional characterization of valve morphology and disease (Della Corte et al., 2007). Evidence supporting this classification comes from three sources: longitudinal follow-up of patients with BAV and AAD notably after aortic valve replacement; imaging of aortic blood flow to define areas of increased wall stress; and histologic studies that are consistent with the natural history of the disease and imaging findings.

Tubular Ascending Aortic Phenotype

The most frequent clinical presentation of BAV is a murmur or incidental finding of calcific aortic valve disease (CAVD) after the age of 50 years, occurring on average 15 years before symptoms of tricuspid aortic valve (TAV)-related aortic stenosis typically occur. Commonly, there is a concurrent AAD above the sinotubular junction with high-velocity and turbulent flow eccentricity from the stenotic BAV, toward the convex aortic surface. This eccentricity has been described to cause altered shear stresses from increased velocities through the stenotic valve (Della Corte et al., 2007), but it is apparent that abnormal flow patterns exist in the absence of stenosis, merely from the presence of the bicuspid valve (Entezari et al., 2014). Fusion of the right and non-coronary cusps has been more frequently associated with dilation of the tubular ascending aorta, but not exclusively so (Della Corte et al., 2014a; Girdauskas et al., 2016b). However, it is not clear that hemodynamic forces are the only etiologic factor. The supporting clinical data tend to be anecdotal, including a low incidence of aortic events such as surgery or AAD after resection of the stenotic aortic valve (Girdauskas et al., 2012, 2014). However, dilation of the aorta continues after curative aortic valve replacement (Girdauskas et al., 2016a; Regeer et al., 2016; Naito et al., 2017). To date, there is no valid prediction index for aortic dilation (Abdulkareem et al., 2013; Geisbusch et al., 2014; Gagne-Loranger et al., 2016).

Imaging data are more robust and support a hemodynamic component to tubular AAD. Using magnetic resonance imaging to measure 3-dimensional blood flow through the valve and aorta over time creates 4-dimensional maps of blood flow within the aorta. This technology provides the most detailed hemodynamic assessment and should be integrated into future investigation of the aortic wall cell biology. But phenotypic imaging still has significant issues of measurement classification and of comparison of data from different imaging modalities (Park et al., 2017), between pediatric and adult clinical imaging methods, and across the spectra of body habitus and age. These issues have previously limited our ability to identify biological mechanisms of AAD across a wide phenotypic spectrum such as root aneurysm vs. ascending aortic aneurysm, and dilated vs. normal aorta. Marked improvements in genetics, genomics, epigenetics and molecular biology over the last two decades have overcome limitations in imaging phenotypes, enabling phenotyping based instead on the disease biology.

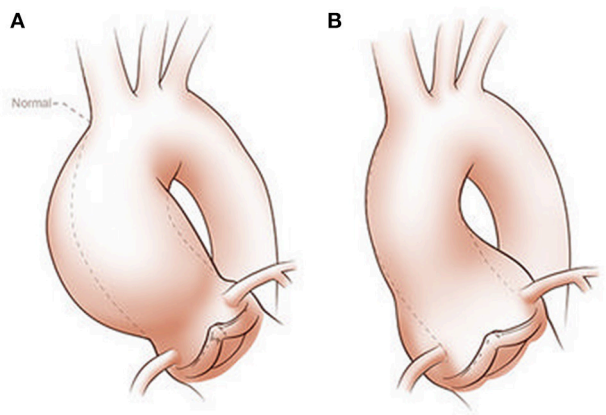

FIGURE 1 | Classification of ascending aortic dilation phenotypes. Ascending aortic dilations (aneurysms) can be classified into a tubular phenotype **(A)** located above the sinotubular junction (STJ) and an aortic root phenotype **(B)** located below the STJ. This classification is neither explanatory nor complete, as ascending aortic dilations frequently extend above or below the STJ and may extend into the aortic arch or beyond. However, it provides a functional distinction based on embryogenic origins of the aorta and surgical approaches. Copyright: Glen Oomen, M.Sc. (http://www.glenoomen.com/medical-illustration/b2mswldypmppf644fjbm1k9kc3w472)

Aortic Root Dilation Phenotype

About 15% of patients with AAD have a dilated aortic root characterized by dilated sinuses and annulus, often including the sinotubular junction; these patients present at a younger age because of the severity of aortic incompetence, occurring in the absence of CAVD. This phenotype has been more frequently associated with right-left cusp fusion (Jassal et al., 2010; Della Corte et al., 2014a), but not reliably so (Girdauskas et al., 2016b; Habchi et al., 2017). In contrast to the accelerated CAVD seen in patients with BAV having the tubular ascending aortic phenotype, which perhaps results from abnormal aortic shear stress, this phenotype probably results from a primary structural lesion of the aortic root and annulus rather than occurring secondarily to altered aortic wall stresses, with the aortic incompetence directly resulting from the aortic annulus and root lesion.

This simplistic classification of AAD emphasizes limitations in our understanding. Some patients with a seemingly normally functioning BAV exhibit early and marked tubular AAD, while conversely, many patients with long-standing BAV and CAVD do not have AAD. The association between BAV morphotype (right-left vs. right-non-coronary fusion) and aortic phenotype (root vs. tubular) is weak (Habchi et al., 2017), and mechanistic studies still do not explain the overall phenotypes. It is recognized that merely accounting for the severity of valve disease, the configuration of the valve, the presence or absence of a raphe, or aortic dimensions does not describe the severity of aortic wall disease, or risk of future adverse events (Fedak et al., 2016). More likely, approaches that make use of molecular markers of aortic wall dysfunction, specific imaging phenotypes using 4-dimensional flow MRI and genetic risk factors will have greater precision.

EMBRYOLOGY OF THE AORTIC ROOT AND ASCENDING AORTA

The two broad root and tubular phenotypes of AAD, and their dissimilarity to descending thoracic aortic disease, reflect the embryonic origin of aortic cell lineage. These have been recently reviewed (Martin et al., 2015; Anderson et al., 2016). The aortic root and ascending aortic phenotypes match embryologic dissemination of ectodermal and mesenchymal cells from the cardiac neural crest (CNC) and second heart field (SHF), respectively, into the truncal outflow tract (Jiang et al., 2000).

The embryonic heart and aorta are developed from three precursor cell populations: proepicardial cells, cardiogenic mesodermal cells, and CNC cells. Proepicardial progenitors principally form the epicardium and coronary vessels (**Figure 2**). Cardiogenic mesodermal cells contribute to the first and second heart fields. The first heart field (created first in embryogenesis) forms the early embryonic heart tube that contributes to the left ventricle and portions of the right ventricle and atria. The SHF (created second in embryogenesis) is the primary source of the outflow tract (conus cordis and truncus arteriosus) as well as the majority of the right ventricle and the venous pole of the heart (Dyer and Kirby, 2009). The SHF contributes both myocardium to the outflow tract and smooth muscle to the truncus arteriosus. CNC cells arise from the ectodermal dorsal neural tube and migrate through the pharyngeal arches to the anterior domain of the SHF. CNC mesenchymal cells contribute to the aortopulmonary valves and outflow tracts, ascending aorta and arch, and proximal pulmonary artery (Snarr et al., 2008; Plein et al., 2015; Jiao et al., 2016).

SHF and CNC cells are not randomly intermixed in the outflow tract and ascending aorta. Cell lineage tracking, principally in mouse embryos, reveals that SHF mesenchymal cells are dominantly located in the aortic root. Above the aortic root, SHF cells are more localized to the adventitial side of the aortic media until they are no longer present in the developing structures (Waldo et al., 2005; Harmon and Nakano, 2013). In contrast, CNC cells populate the intimal edge of the ascending aorta, occupying the whole media as far as the left subclavian artery (Pfaltzgraff et al., 2014; **Figure 3**). The transition from SHF to CNC predominance occurs closer to the root on the dorsal (posterior) side of the aorta than on the ventral (anterior) side (Sawada et al., 2017). Yet, CNC cells are required for embryonic development of the aortic and pulmonary valves, and for outflow tract development and septation (Phillips et al., 2013). Although debated, in the developing aortic valve CNC cells populate the aortic surface (fibrosa) of the valve, while SHF cells populate the ventricular surface (ventricularis) of the valve (**Figure 4**). The fibrosa has a high type I and III collagen content arranged in a concentric fashion and is notable for its propensity to develop CAVD, while the ventricularis is notable for its high elastin content arranged in a radial fashion and is spared from development of CAVD. These histologic differences that have a vital functional role in aortic valve biomechanics may reflect embryologic origins from SHF and CNC, but embryogenesis of the CNC and SHF into the aortopulmonary valves and aorta are more complex than merely "filling in their assigned cellular spaces" and deleting unnecessary pharyngeal arteries (**Figure 5**). These cellular populations have complementary roles in signaling each other, notably, using various proteins—canonical Wnt, non-canonical Wnt, transforming growth factor (TGF)-β, sonic hedgehog (Shh), fibroblast growth factor (Fgf), bone morphogenetic protein (BMP), and Notch—that determine spatial and functional relationships with other cell types during embryogenesis. These pathways also have vital functional roles in adulthood; thus, errors in embryonic signaling that potentially cause outflow tract structural abnormalities such as BAV may also result in AAD in adulthood. An attractive hypothesis is that a lineage-specific cell defect causes the aortic disease that occurs in association with BAV (Jiang et al., 2000; Jiao et al., 2016). In summary, although it has been postulated that the root and tubular phenotypes of AAD may indicate distinct genetic origins (Girdauskas and Borger, 2013), there is still a need for direct supporting evidence (Girdauskas et al., 2011).

HISTOPATHOLOGY OF THE AORTA IN TAV AND BAV

The aorta and large vessels are composed of the intima, a layer of endothelial cells that sit directly on the internal elastic lamina; the media, consisting of concentric layers of smooth muscle cells (SMCs) and their extracellular matrix (ECM); and the adventitia, principally made up of myofibroblasts that produce collagen, able to deal with stresses above physiological pressures (**Figure 6**). The main mechanical function of the aortic media is providing elastic recoil for pulsatile aortic pressure, enabled by its organized composition of SMCs and ECM.

Smooth Muscle Cells

SMCs are the majority cell type within the aortic wall. They are not terminally differentiated but rather have the ability to express proteins involved in contraction and ECM synthesis during development and in response to mechanical and chemical stimuli (**Figure 7**). This plasticity, allows transition along a continuum between a fibroblast-like, proliferative, ECM-producing phenotype and a quiescent contractile phenotype.

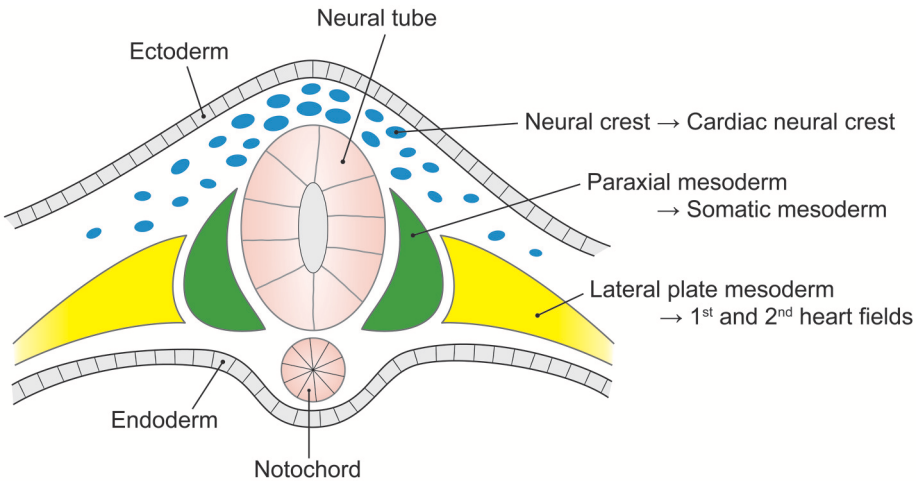

FIGURE 2 | The embryological origins of the thoracic vasculature and outflow tract. The embryonic first and second heart fields are derived from the lateral plate mesoderm. The first heart field forms the early heart tube, into which second heart field cells migrate to form the convoluting heart. The cardiac neural crest is derived from a clone of neural crest cells that migrate along the third and fourth pharyngeal arches to form the head and upper limb arteries along with the ascending aorta and aortic arch. The pulmonary artery is formed from neural crest cells that migrate along the sixth pharyngeal arch.

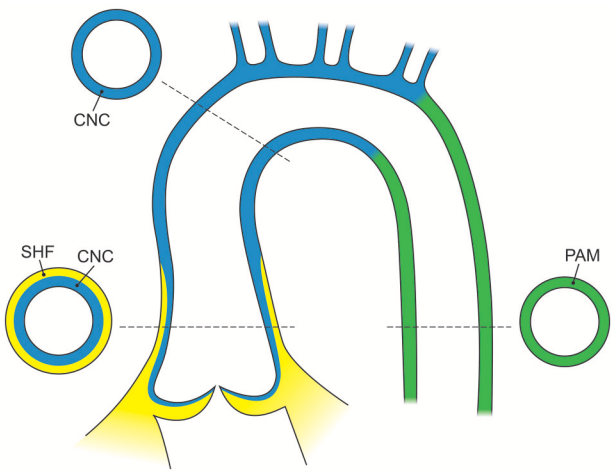

FIGURE 3 | The embryological origins of smooth muscle cells of the aorta. The adult aortic root is principally derived from the second heart field (yellow), whereas the ascending aorta and arch are derived from the cardiac neural crest (blue) and the descending aorta is derived from the paraxial mesoderm (green). In the adult aorta, smooth muscle cells of both the second heart field and neural crest form the aortic root and ascending aorta, while the descending aorta below the ductus arteriosus is composed of cells from the lateral mesoderm. CNC, cardiac neural crest; SHF, second heart field; PAM, paraxial mesoderm.

Quiescent contractile SMCs have low production of ECM proteins but express contractile proteins including smooth muscle alpha-actin and myosin heavy chains (Humphrey et al., 2015).

SMCs are bound to elastic fibers, Fbn-1 and collagen type VI, with basal lamina connections linking them to each other and providing a template structure for lamellar (or laminar) organization (Perrucci et al., 2017). Arteries therefore have multiple lamellae (fish scale-like plates) comprising the media, with the number seemingly set during embryogenesis and related to the diameter and stress upon the vessel; thus, the aorta has the greatest number of lamellae. When activated to an immature phenotype, SMCs proliferate and migrate, while producing greater amounts of ECM proteins, thereby regulating the aorta's mechanical properties in response to physiological wall stresses.

At the cell surface, tyrosine kinase, integrin and G-protein receptor-mediated factors (including basic fibroblast, platelet-derived, epidermal, and insulin-like growth factors) favor a proliferative SMC phenotype. Importantly, angiotensin (AT) II mediates both contractile and proliferative phenotypes through its type I and type II receptors, ATR-I and ATR-II, respectively; the former seem to mediate increased TGF-β levels, leading to a proliferative phenotype and ECM remodeling, whereas the latter favor a contractile phenotype.

Extracellular Matrix

The ECM is principally composed of elastin, along with collagen types I, III, IV, V, and VI; fibronectin; Fbn-1; fibulin-4; and proteoglycans of dermatan, chondroitin, and heparin, along with other proteins; these proteins are interspersed with SMCs and form lamellar plates (Wagenseil and Mecham, 2009). The number of lamellae is greater in larger vessels facing greater wall tension and seems to remain stable after birth. Elastic microfibrils are linked to SMCs of adjacent lamellae via integrins $\sigma_5\beta_1$ and $\sigma v\beta_3$, creating an oblique capacitor for vascular stress. Each lamella is oriented obliquely to adjacent lamellae, creating an even distribution of stress across the aortic wall. Apparently, in the normal aorta, SMCs have little active role in managing wall tension and the microfibrillar structure is the major passive contributor.

Essential to the function of the aortic media, microfibrils provide the structural integrity and organization of the aortic

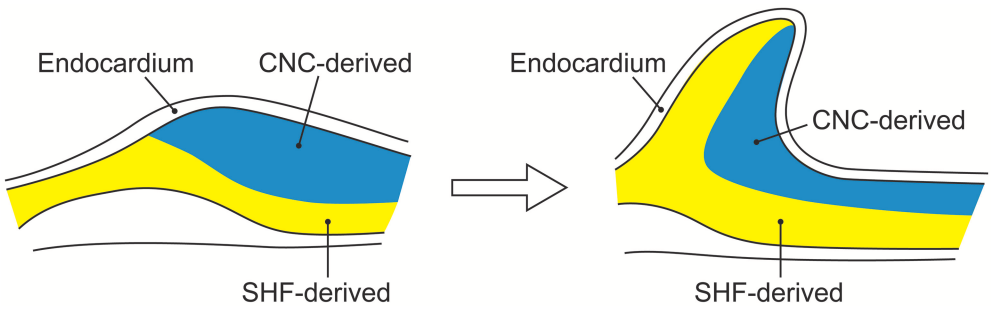

FIGURE 4 | The embryological origins of smooth muscle cells of the aortic valve. Embryonic development of the aorta valve incorporates smooth muscle cells derived from both the second heart field and cardiac neural crest. Although, portrayed as two layers of distinct cellular origins with cardiac neural crest-derived cells occupying the fibrosal side (left side of each figure) of the valve and second heart field-derived cells occupying the ventricular side of the valve (left side of each figure), there is evidence for endocardial-to-mesenchymal transformation in the endocardial cushions that develop into the valve, along with considerable plasticity of all elements of the developing valve.

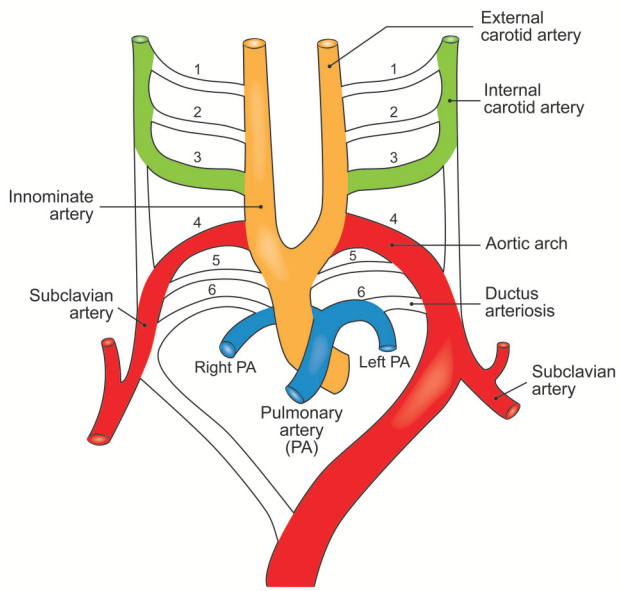

FIGURE 5 | The embryological destinations of the intrathoracic vasculature. Development of the upper body arterial tree is predicated on expansion, migration, and apoptosis of cell populations in the branchial arteries to yield its neonatal structure. The branchial arteries are numbered 1–6.

wall, forming a folding, compliant 10–12 nm structure at physiological wall tensions. Structurally, the microfibril is composed of polymeric fibrillin wrapped around an amorphous elastin core, which in turn is formed from monomers of tropoelastin produced by SMCs and covalently cross-linked by lysyl oxidase (Wagenseil and Mecham, 2009; **Figure 8**). In addition to Fbn-1 and elastin, other proteins including TGF-β binding proteins (LTBP 1–4), emilins, microfibril-associated glycoproteins (MAGP-1 and -2), and members of the fibulin 1–4 family are present in the microfibril (Wu et al., 2013). Fibrillin is notable for its many protein- and integrin-binding sites and its ability to sequester growth factors, notably TGF-β, BMPs and epidermal growth factors (Robertson et al., 2011). In addition to providing a compliant structure, the microfibril serves a cell adhesion function for SMCs, the intima and the adventitia. Collagens I, III, and V are fibril-forming collagens, with types I and III providing high-tensile strength to the vessel wall, in contrast to elastin in the media, which manages physiological tensions.

TAV vs. BAV Aortopathy

AAD unrelated to BAV is characterized by severe elastin degeneration with fibrosis and cystic degeneration of the media in concert with inflammatory histologic changes, along with adventitial and intimal thickening (Balistreri et al., 2013; Forte et al., 2013). However, BAV aortopathy has distinct differences from TAV aortopathy (**Table 1**); the ascending aorta of patients with BAV generally shows non-inflammatory loss of SMCs, with multifocal apoptosis and medial degeneration (Balistreri et al., 2013) but a fiber architecture similar to that of the normal aorta (Phillippi et al., 2014). Similar to the histologic and molecular perturbations reported in Marfan syndrome, BAV aortic tissues have lower fibrillin content and an increase tissue TGF-β1 levels that is due to the disease (Doyle et al., 2012; Nataatmadja et al., 2013).

In the absence of aortic aneurysm, the aorta in BAV often appears macroscopically and histologically normal, or nearly so. But phenotypic variation is seen among patients with BAV undergoing non-aortic surgery, and histologic diversity is evident across different portions of the ascending aorta within the same patient for those with aortic aneurysm. Both the intima and adventitia are thickened (Forte et al., 2013). The convex (outer curve) of the aorta is more frequently dilated in patients with BAV, a change often ascribed to greater shear stress from asymmetric flow across the valve, and has been reported to exhibit greater elastic fiber fragmentation, reduced collagen types I and III expression, and SMC apoptosis (Cotrufo et al., 2005; Della Corte et al., 2008). Matrix metalloproteases (MMP) are also differentially expressed across different aortic sites in BAV, with higher levels of MMP-2 and tissue inhibitor of metalloprotease (TIMP)-3 seen in the concavity of the ascending aorta (Mohamed et al., 2012). These differences are

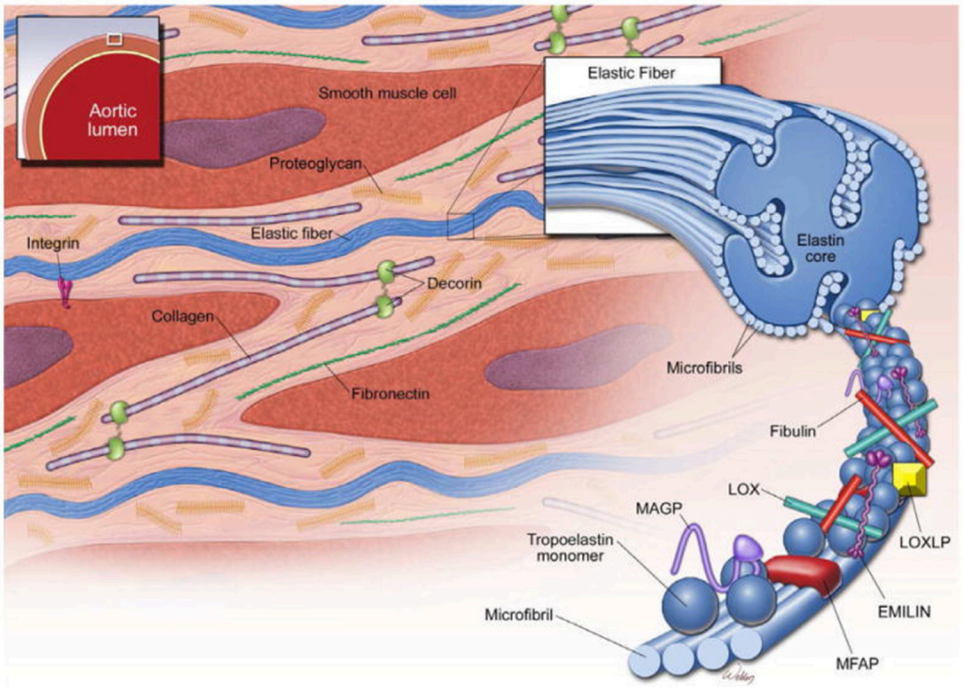

FIGURE 6 | Structure of the ascending aortic media. The media of the aortic wall is composed of vascular smooth muscle cells (SMCs) and an extracellular matrix (ECM) of elastic fibers, collagen fibers, and proteoglycans. Elastic fibers are the major ECM component and provide extensibility to the aortic wall. Cross-linking of tropoelastin monomers by lysyl oxidase (LOX) forms elastin molecules, which in turn cross-link with microfibrils to form elastic fibers. Microfibrils are composed of fibrillin and several microfibril-associated proteins (MFAPs), such as elastin microfibril interface-located protein 1 (EMILIN-1), microfibril-associated glycoproteins (MAGP-1 and -2), and fibulins. Notably, microfibrils provide a substrate for the large latent complex and transforming growth factor-β sequestration. Modified from Wu et al. (2013).

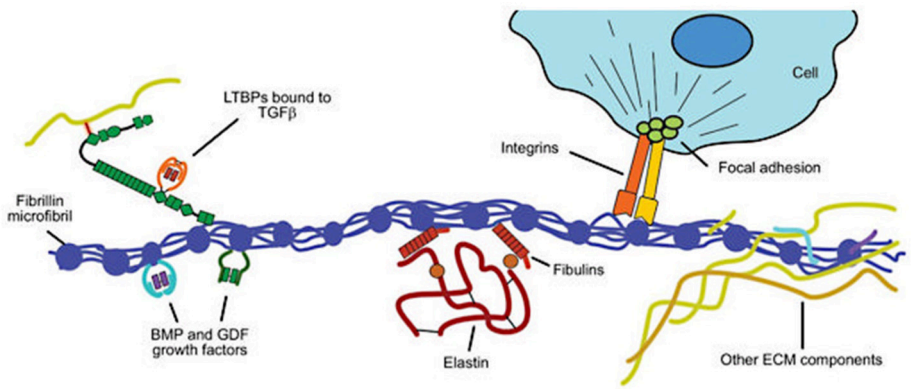

FIGURE 7 | Structural and functional roles of fibrillin in the extracellular matrix. Fibrillin microfibrils associate with elastin to form elastic fibers in the aortic media (see **Figure 2**). Key functional roles are (i) binding to elastin *via* the fibulins and other extracellular matrix (ECM) glycoproteins; (ii) sequestering transforming growth factor-β (TGF-β) via the large latent complex, bone morphogenetic protein (BMP) and growth and differentiation factors (GDFs); and (iii) linking to smooth muscle cells of the media via integrins. Modified from Robertson et al. (2011).

also seen in microRNA expression when comparing convex and concave portions of dilated aortas in BAV (Albinsson et al., 2017). Taken together, these findings strongly support a thesis that active cellular processes are involved in development of bicuspid aortopathy, perhaps or even probably, mediated by hemodynamic forces. But regional histologic findings often do not match expected hemodynamic stresses (Cotrufo et al., 2005; Leone et al., 2012), and many studies have failed to account for the clinical phenotype, notably making little distinction between the dilated aortic root and the dilated tubular aorta.

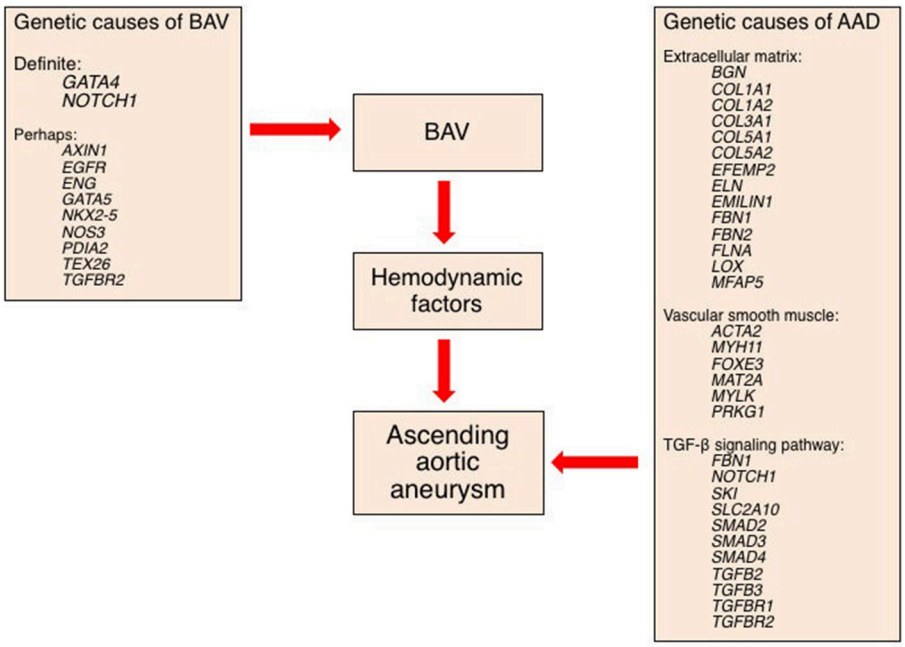

FIGURE 8 | Schematic of a mechanistic approach to the development of thoracic ascending aortic dilation (AAD) ultimately leading to aneurysm. This schematic assumes three groups of AAD etiologic factors: genes causing a bicuspid aortic valve (BAV) that may also be causing AAD; genes causing AAD but not BAV; and hemodynamic factors that contribute to AAD.

HEMODYNAMIC AND GENETIC MECHANISMS OF BAV-RELATED AORTOPATHY

Much of what we believe about the etiology of AAD and thoracic aortic dissection observed in association with BAV is based on two competing, or more likely complementary, etiologic hypotheses of increased wall stress and pathologic structural or functional deficits of the aortic wall. Yet, the evidence for each is neither strong nor specific to BAV-related aortopathy. Much is derived from aortopathy observed in association with TAV and comes exclusively from end-stage disease tissue obtained at surgery because tissue is rarely obtained earlier in disease, when aortic dimensions are smaller. This is understandable but limits insight into mechanisms that may be specific to BAV or aortic phenotype, and biological mechanisms of early-stage aortopathy.

Hemodynamic Mechanisms of BAV-Related Aortopathy

There is extensive evidence that blood flow and shear stress in the tubular ascending aorta are markedly altered by a BAV, even in the absence of significant flow obstruction (Entezari et al., 2014; Garcia et al., 2016; Cao et al., 2017; Raghav et al., 2017; Shan et al., 2017; **Figure 9**). However, fused-leaflet morphology is not a sole determinant of helicity of blood flow or region of maximal wall stress in the tubular ascending aorta (Raghav et al., 2017; Shan et al., 2017), as age and clinical characteristics are important (Burris et al., 2016; Girdauskas et al., 2016b; van Ooij et al., 2016; Shan et al., 2017).

TABLE 1 | TAV vs. BAV aortopathy.

Tricuspid aortopathy	Bicuspid aortopathy
EPIDEMIOLOGY	
Rare	Frequent in BAV population
Onset later in life (>70 years)	Onset earlier in life (<70 years)
Association with hypertension and other risk factors for aortopathy	Reduced association with risk factors for aortopathy
Lower correlation with severity of aortic stenosis	Moderate correlation with severity of aortic stenosis
MACROSCOPIC AORTOPATHY	
Commonly symmetric dilation of the tubular ascending aorta	Higher prevalence of aortic root aneurysm
Lower prevalence of aortic stenosis	Higher prevalence of aortic dilation
Aortopathy and dissection rarely occurs after AVR	Higher prevalence of dilation of the outer curve of the ascending aorta
	Associated with coarctation of the aorta
	Reported association with type of cusp fusion
	Common transverse aortic stenosis jet
	Aortopathy and dissection occasionally occurs after AVR
MICROSCOPIC AORTOPATHY	
Severe elastin degeneration	Normal fiber architecture
Cystic degeneration of the media	Loss of smooth muscle cells with apoptosis
Inflammatory response often present	Medial degeneration and lower fibrillin content

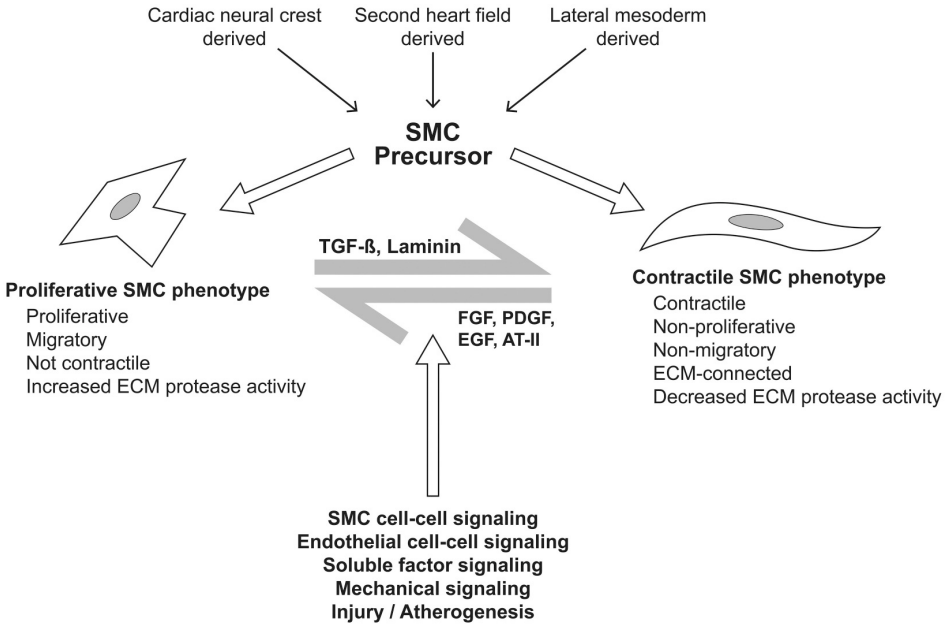

FIGURE 9 | Plasticity of smooth muscle cell phenotype. The spectrum of smooth muscle cell (SMC) phenotype from proliferative to contractile phenotypes is dependent upon signaling from multiple sources. The sources include adjacent SMCs and vascular endothelial cells, mediated by cell-cell interaction and soluble factors including transforming growth factor-β (TGF-β), laminin, fibroblast growth factor, platelet derived growth factor, epidermal growth factor, and angiotensin II, amongst others. Mechanical signaling *via* the extracellular matrix, cell-cell mechanical sensing, and the intracellular cytoskeleton and primary cilium are propagated through the intracellular dense plaques. These signals yield changes in cytoskeletal architecture and drive plasticity across the spectrum of SMC phenotype.

Abnormal flow characteristics from the BAV impose abnormal mechanical stresses upon portions of the aortic wall, leading to alterations of cell-mediated processes (Atkins and Sucosky, 2014; Shan et al., 2017). In general, these processes include dysregulation of ECM and medial elastin fiber degeneration (Guzzardi et al., 2015), at least in part mediated by MMP-dependent pathways. Comparing regions of the tubular ascending aorta having 4-dimensional flow MRI-assessed high vs. normal wall shear stress, the former areas exhibit thinner elastin fibers and less total elastin content, indicating increased medial elastin degradation (Guzzardi et al., 2015). Likewise, evidence of ECM dysregulation has been found in regions of high wall shear stress in the form of increased expression of *TGFB1*; *MMP* types 1, 3 and perhaps 2; and *TIMP1*. However, there is marked inter-individual variation, implying that the pathways may be important as a response mechanism for aortic wall shear stress that leads to reduced elasticity of the aorta, although their value as a prediction tool is limited. Importantly, they may also merely reflect end-stage disease, with mechanosensors in the aortic wall initiating earlier transcriptional and post-transcriptional pathways mediated by microRNA expression (Albinsson et al., 2017). There are several mechanisms of mechanotransduction, including the endothelial glycocalyx layer on the luminal surface of the aorta, basal integrins, primary cilia, and platelet endothelial adhesion molecule-1 (Russell-Puleri et al., 2017), amongst others. Notably, the complex of polycystin-1 (derived from the *PKD1* gene) and polycystin-2 forms a mechanosensitive cation channel of the primary cilia, which serve as mechanosensors by interacting with filament-A bound to cytoskeletal actin (Patel and Honore, 2010).

Direct comparison of multiple murine elastase and genetic aortic aneurysm models has provided useful insights (Bellini et al., 2017). Aneurysmal development was found to correlate with increased wall stiffness as distensibility was lost, as perhaps adventitial collagen became the principal controller of wall stiffness. The inability of intramural SMCs and myofibroblasts to maintain nearly normal circumferential wall stiffness in these models is consistent with a compromised ability to mechanoregulate the ECM. Mechanistically, SMCs and myofibroblasts secrete TGF-β1, platelet-derived growth factor, and AT II, amongst other factors that regulate their own function and cell fate, as well as that of nearby cells, creating a local environment sensitive to local hemodynamic forces.

The absence thus far of identified variants in genes coding for mechanosensing proteins that play a human AAD implies either that these variants are embryonic lethal or that mechanosensing is not a primary lesion in AAD, despite views otherwise (Humphrey et al., 2014, 2015). However, downstream effectors have a comprehensive role in AAD, especially proteins involved in generation and maintenance of the ECM, vascular SMC contraction or metabolism, and mediation by the TGF-β signaling pathway.

Genetic Mechanisms of BAV-Related Aortopathy

It is reasonable to hypothesize several possible genetic mechanisms of increased risk of BAV-AAD or TAV-AAD (**Figure 9**). These likely include (i) one or more genes responsible for BAV that also are mechanistically responsible for AAD (pleiotropy); (ii) the independent actions of one or more genes upon a phenotype such as BAV (polygenic influence), while other genes act upon the AAD phenotype; (iii) two or more genes that mechanistically interact to produce a single phenotype (epistasis); and (iv) genetic variants that interact with hemodynamic factors to produce AAD (gene-by-environment interaction). Given the complexity of the disease, clinical factors that alter disease progression, the mixed inheritance pattern and association of numerous genes with AAD in animal models and the general population, it is reasonable to investigate individual and combined contributions of all four mechanisms.

Numerically, few cases of BAV-AAD are associated with extra-cardiac manifestations. A small proportion of patients with BAV have coarctation of the aorta, while an even smaller proportion have Turner, Marfan, Loeys-Dietz, and other even rarer syndromes resulting from *FBN1*, *COL3A1*, *SMAD3,* and *TGFBR1/2* genetic variants, amongst others. The majority of AAD in both TAV and BAV is non-syndromic, although at least a third of patients have identified genetic variants for familial AAD including variants of *ACTA2, MYH11, MYLK, FBN1,* and *TGFB2*, amongst others. These imperfect associations are noteworthy in that they emphasize the complexity of embryonic development, the adult onset of genetic AAD disease, and, for syndromic AAD, the importance of specific proteins across a wide variety of organ systems. The other lesson is that variants in or near a single gene lead to a spectrum of severity and manifestations of AAD, akin to pleiotropy; a notable example is *FBN1* variants, for which clinical phenotype can range from severe forms of Marfan syndrome to merely an increased risk of AAD in adulthood.

Human BAV has been associated with rare, but highly penetrant, exonal variants in *NOTCH1* (Garg et al., 2005; Mohamed et al., 2006; Foffa et al., 2013; Dargis et al., 2016), *AXIN1* (Wooten et al., 2010), *EGFR* (Dargis et al., 2016), *ENG* (Wooten et al., 2010), *GATA5* (Padang et al., 2012; Bonachea et al., 2014a; Shi et al., 2014), *NKX2–5* (Qu et al., 2014; Dargis et al., 2016), *NOS3* (Girdauskas et al., 2017), *PDIA2* (Wooten et al., 2010), *TEX26* (Dargis et al., 2016), and *TGFBR2* (Dargis et al., 2016). Furthermore, BAV presenting together with AAD has been associated with rare variants in *NOTCH1* (McKellar et al., 2007; Girdauskas et al., 2017), *AXIN1* (Girdauskas et al., 2017), *TGFBR2* (Martin et al., 2011; Girdauskas et al., 2017), *FBN1* (Pepe et al., 2014), *SMAD2* (Prapa et al., 2014), *NOS3* (Girdauskas et al., 2017), *ACTA2* (Guo et al., 2007), *TGFB2* (Lindsay et al., 2012), and other genes (Girdauskas et al., 2017). To date, the only locus containing common variants associated with BAV is *GATA4* (Yang et al., 2017), but this locus has not been associated with AAD. More than 40 genes have been linked to BAV in mice or hamsters (Wu et al., 2017).

Approximately 30 genes are associated with AAD in the general population, but many of these are rare exonal variants identified in only a few families or individuals (Brownstein et al., 2017). The majority encode proteins involved in generation and maintenance of the ECM *(BGN, COL1A1, COL1A2, COL3A1, COL5A1, COL5A2, EFEMP2, ELN, EMILIN1, FBN1, FBN2, FLNA, LOX, MFAP5*); vascular SMC contraction or metabolism (*ACTA2, MYH11, FOXE3, MAT2A, MYLK, PRKG1*); or TGF-β signaling (*FBN1*, *NOTCH1*, *SKI*, *SLC2A10*, *SMAD2*, *SMAD3*, *SMAD4*, *TGFB2, TGFB3, TGFBR1, TGFBR2*). Almost one-quarter of patients with AAD possess a mutation in one of these genes. Rare or uncommon mutations in six of these genes [*AXIN1* (Girdauskas et al., 2017), *ELN* (Girdauskas et al., 2017), *FN1* (Girdauskas et al., 2017), *NOS3* (Girdauskas et al., 2017), *NOTCH1* (Garg et al., 2005; McKellar et al., 2007; Foffa et al., 2013; Bonachea et al., 2014b; Kerstjens-Frederikse et al., 2016) and *TGFBR2* (Dargis et al., 2016)] have been associated with AAD in patients with BAV. Thus, it is unlikely that these genes are responsible for a significant proportion of the AAD seen in this valvular disorder. However, *FBN1* has been shown to have common variants that are associated with AAD in patients with BAV, and it is therefore a leading mechanistic candidate, especially given its dual structural and TGF-β signaling roles (LeMaire et al., 2011; Pepe et al., 2014; Guo et al., 2016; Girdauskas et al., 2017).

INTEGRATED MECHANISM(S) OF BAV ANEURYSM AND DISSECTION

Over the last decade of genetic studies that have identified highly penetrant coding variants in a set of interrelated genes that are associated with aortic disease, it has become apparent that the ECM and SMCs are the important factors in aortic integrity and function. The predominance of identified genetic causes of AAD coming from ECM, vascular SMC contraction or metabolism, or the TGF-β signaling pathway points to avenues for investigating aortopathy and allows prioritization of candidate pathways, especially for a role of common variants in *FBN1*.

Why Bicuspid Aortopathy May be Two or More Diseases

As previously mentioned, there is reasonable evidence that AAD phenotypes mirror distribution of embryonic SHF and CNC cells. Clinical similarity of the BAV aortic root phenotype to the aortic aneurysm phenotype of Marfan syndrome further implies common mechanisms and cellular pathways. This similarity is reinforced by the observation of decreased tissue fibrillin and increased TGF-β content in both (Nataatmadja et al., 2013). But surprisingly, if we expected the root aneurysm phenotype of both Marfan syndrome and BAV to mirror the distribution of CNC migration, BAV morphotype is not well-correlated with aortic aneurysm morphotype (Jackson et al., 2011; Habchi et al., 2017).

Characteristics of tubular AAD differ between bicuspid and tricuspid aortopathy. There is extensive evidence that the hemodynamic forces on the aortic wall seen in both non-stenotic and stenotic BAV differ between the vessel's concave and convex aspects and also differ from those seen in the non-stenotic TAV

(Shan et al., 2017). These differences probably, but not certainly, drive the difference in gross morphology and histopathology across the aorta's axial plane. Further, numerous studies have identified biochemical differences between BAV and TAV that drive, or occur in response to, histopathological differences. For BAV, these include SMC apoptosis and increased MMP secretion, whereas for TAV, these include elastic fiber fragmentation, cystic medial necrosis and fibrosis (Boyum et al., 2004; Balistreri et al., 2013).

If we postulate a genetic background to BAV aortopathy, it would be reasonable to assume that *FBN1* variants would dominate the genetic cause of aortic root aneurysm, as common *FBN1* variants have been associated with non-syndromic bicuspid aortic aneurysm, independent to the position of the aneurysm (LeMaire et al., 2011). This has not been shown, however; deleterious variants in *NOTCH1*, *AXIN1* and *NOS3* have been found to be more common than deleterious *FBN1* variants, at least in one cohort (Girdauskas et al., 2017). However, common *FBN1* variants have not yet been associated with non-syndromic bicuspid aortic aneurysm, without reference to the position of the aneurysm (LeMaire et al., 2011). To date, *FBN1* variants have not been associated with BAV in the absence of aortopathy.

For tubular AAD, it is reasonable to postulate that hemodynamic factors including predominant jet direction, along with several genetic factors may have a role in bicuspid aortopathy. It could also be argued that the genetic variant associated with BAV, especially the *NOTCH1* variant, might also be causal for aortopathy, but supporting data are lacking at this time.

Fbn-1 and the TGF-β Pathway

Fbn-1 is a backbone microfibrillar protein with structural and signaling functions. When abnormal Fbn-1 was first identified as the cause of Marfan syndrome in 1991 (Dietz et al., 1991), it was believed that the coding mutations resulted in a structural weakness of microfibrils (Matt et al., 2008), leading to arterial wall "weakness" and the syndrome's vascular manifestations. Supporting this assertion, more severe or earlier aortic disease had been associated with *FBN1* truncating or splicing variants (Schrijver et al., 2002; Baudhuin et al., 2015) and with variants in exons 24–32 (Faivre et al., 2007). But this is a vastly simplistic overview.

The ∼3,000 currently identified phenotypically important *FBN1* mutations fall into two classes. The more common class of dominant mutations (with a single coding variant on one chromosomal copy of *FBN1*) results in a mixture of mutated and normal, non-mutated Fbn-1 protein in the ECM, a pattern called a dominant negative (DN) mutation. The result is aberrant Fbn-1 folding, which in turn leads to a disorganized ECM and weakened microfibrillar structure. Alternatively, the less common class of haploinsufficiency (decreased protein production from the mutated *FBN1* gene on one, or rarely two, chromosomes) results in decreased amounts of normal Fbn-1 protein present in the ECM; compared with DN mutations, this class of defects carries greater risk of aortic aneurysm or vascular dissection (Franken et al., 2017). To date, it is not readily apparent whether the DN mutation class or haploinsufficiency class of *FBN1* variants, or their combination, plays an important role in BAV aortopathy.

Fbn-1's principal signaling functions are mediated by TGF-β1, BMP, and epidermal growth factor. Both mutated and decreased Fbn-1 protein lead to impaired ability to sequester TGF-β1 on the latent TGF-β binding protein, resulting in increased tissue and circulating levels of this growth factor (Mathieu et al., 2015). TGF-β1 is activated by proteolytic cleavage from its inactive form on the latent TGF-β binding protein, a process that is governed by both wall stress and integrin activation by MMP and other mechanisms (Wipff and Hinz, 2008; Forte et al., 2016; Perrucci et al., 2017). Once released, TGF-β1 binds to cell surface TGF-β1 receptor complexes (TGFRB1/2). This process in turn activates the canonical Smad 2/3 and the Smad 1/5/8 transcription factors by phosphorylation, leading to a contractile SMC phenotype under normal developmental circumstances (**Figure 10**). In contrast, TGF-β1 mediated non-canonical Smad-independent pathways can induce increased MMP activity and ECM degradation. Complicating this relationship, AT II may

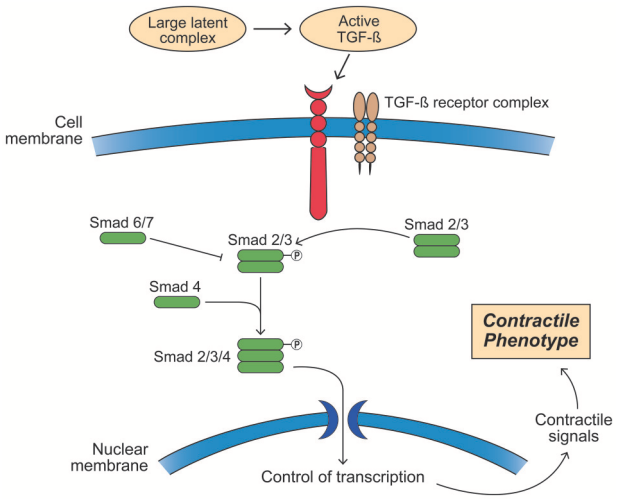

FIGURE 10 | Activation of the transforming growth factor-β (TGF-β) signaling pathway leading to a smooth muscle cell contractile phenotype. Members of the TGF-β superfamily that include TGF-βs, bone morphogenetic proteins (BMPs), and growth and differentiation factors (GDFs) have similar functional properties regulating cell growth, differentiation, apoptosis, and extracellular matrix synthesis in vascular smooth muscle cells (SMCs). TGF-β ligands are synthesized as latent precursor molecules (LTGF-β), which are activated via proteolytic cleavage. Active TGF-β signaling is transmitted through two types of transmembrane serine/threonine protein kinase receptors: TGF-β type I (TGFβRI) and principally type II (TGFβRII) and mediated by a sequence of phosphorylated Smad proteins. In addition to the canonical Smad signaling pathway that directly regulates the transcription of Smad-dependent target genes, TGF-β function can also be mediated by Smad-independent pathways including MAPK signaling pathways, such as p38 MAPK and c-Jun NH2-terminal kinase, phosphatidylinositol 3-kinase/Akt pathway, and Wnt signaling. TGF-β signaling via TGFβRII plays a pivotal role in both second heart field and cardiac neural crest derived SMC phenotype differentiation during vascular development as well as SMC phenotypic switching in disease states. TGF-β signaling induces SMCs to change shape into elongated SMC shape accompanied by an up-regulation of SMC contractile proteins.

also be able to activate the Smad2 pathway either indirectly by increasing tissue TGF-β1 or directly via activation of the ATR-I (Nagashima et al., 2001; Franken et al., 2015). Furthermore, emerging evidence suggests that there may be epigenetic control of TGF-β1 in aortic aneurysm and vascular disease that adds yet an additional layer to this already complex picture (Leeper et al., 2011; Shah et al., 2015; Forte et al., 2016). Thus, TGF-β1 has important roles in tissue fibrosis, cellular differentiation and proliferation, and ECM remodeling through several pathways (Forte et al., 2010).

The strength of the association between *FBN1* variants and aortic disease in BAV is similar to that in Marfan syndrome. LeMaire and colleagues have identified a ∼250-kbp locus in *FBN1* that is associated with thoracic aortic aneurysm and dissection in both patients with non-bicuspid and patients with BAVs (LeMaire et al., 2011). This is an important finding as it provides the first identification of common variant(s) in a gene having a role in aneurysmal disease in Marfan syndrome, in the general population and in BAV, for which a pathogenic mechanism had already been established.

Manipulation of TGF-β1 function is an attractive therapeutic approach implemented in several high-quality, relatively short-term clinical trials of the angiotensin receptor blocker (ARB) losartan with promising, but not definitive results. The distinction between qualitative and quantitative *FBN1* mutations is important as this drug decreases TGF-β1 production, offsetting the increased circulating levels of this growth factor seen in Marfan syndrome and BAV (Nataatmadja et al., 2013). In a sub-study of the COMPARE trial examining the effect of losartan upon on-going aortic root dilation in patients with Marfan syndrome, the drug was more effective in slowing progression in patients with haploinsufficient variants than in those with protein mutational variants, implying that Fbn-1's role in modifying TGF-β1 is an important mechanism of aortic root dilation (Franken et al., 2017). This finding does not necessarily imply that structural weakness of microfibrils is unimportant, however.

NOTCH1

Rare but highly penetrant *NOTCH1* variants in two syndromic pedigrees (Garg et al., 2005) were the first definitive genetic associations with BAV and have been further identified in specific BAV root aneurysm and other phenotypes (McKellar et al., 2007; Dargis et al., 2016; Girdauskas et al., 2017). In addition, rare *NOTCH1* variants have been associated with left and right heart structural lesions and with other, non-cardiac phenotypes (Luxan et al., 2013). Notch 1–4 proteins are heterodimeric transmembrane receptors for Jag1/2 and Dll1/3/4, and they promote endothelial-to-mesenchymal transformation of SHF cells to form the outflow tract valves. The strongest evidence thus far for a role for Notch proteins in AAD is the presence of proximal aortic disease in Notch1$^{+/-}$; NOS3$^{-/-}$ mice (Koenig et al., 2015) and a possible association with decreased endothelial-to-mesenchymal transition in human BAV endothelium (Kostina et al., 2016). Although, Notch1 is essential for outflow tract development and may contribute to development of some BAV, its role in thoracic aortic aneurysm, if any, is uncertain.

GATA4

The important role of the GATA sequence binding proteins in embryonic cardiac development is well-recognized (Martin et al., 2015) and is reinforced by presence of BAV in mouse *GATA* knockouts (Laforest and Nemer, 2011; Laforest et al., 2011), by association of uncommon variants with BAV (Bonachea et al., 2014a; Shi et al., 2014), and recently by identification of common *GATA4* variants in human BAV (Yang et al., 2017). However, although some patients with BAV having GATA variants were found to have thoracic aortic disease, there is currently no evidence that these variants play a role in AAD.

IS THERE A BIOMARKER FOR AORTIC DISSECTION?

There may be some value to having a circulating biomarker that can identify future aortic aneurysm in young people in order to direct anti-hypertensive or other preventive therapy for AAD. Perhaps value also could come from identifying a highly *predictive* risk index of aortic dissection in a cohort at perceived higher risk, such as patients with aortic aneurysm. The biomarker would need to predict risk over a reasonable length of time between pragmatic assessments. Aortic dimension has been the most used marker of aortic dissection risk, yet it provides little prognostic information over the clinically important range of 40–55 mm (2010 ACCF/AHA/AATS/ACR/ASA/SCA/SCAI/SIR/STS/SVM Guidelines For the Diagnosis and Management of Patients with Thoracic Aortic Disease Representative, Erbel et al., 2014; 2010 ACCF/AHA/AATS/ACR/ASA/SCA/SCAI/SIR/STS/SVM Guidelines For the Diagnosis and Management of Patients with Thoracic Aortic Disease Representative Members et al., 2016), while the majority of aortic dissections occur at dimensions less than these (Pape et al., 2007). This limitation has led to other approaches such as examining morphometry (Biaggi et al., 2009; Habchi et al., 2017), hemodynamic factors (Atkins et al., 2016; DeCampli, 2017; Raghav et al., 2017), the position and shape of the aneurysm (Schaefer et al., 2008; Della Corte et al., 2014b), aortic growth rate (Elefteriades and Farkas, 2010), and aortic distensibility parameters (Benedik et al., 2013). To date, observed population-based associations are weak and are unlikely to provide any predictive value for the individual patient.

However, as we learn more about aortic disease, it is possible that circulating tissue markers will reflect the biology of the aortic wall. Overall, the fundamental weakness of this approach is that an aortic dissection signal could be diluted by other, much larger tissue signals. In addition, because dissection is likely a phenomenon having varied risk factors (hemodynamic, genetic, aortic size, and others), it would be reasonable to assume that multiple markers would be required. Based on known biology, candidate biomarkers can potentially include (i) structural proteins of the smooth muscle contractile network such as actin, myosin, and fibrillin; (ii) regulatory and structural proteins of the aortic ECM such as collagen, elastin, MMPs and their inhibitors; and (iii) ligands and receptors of the TGF-β pathway.

MMPs and Their Inhibitors

MMPs, notably MMP-1, 2, 8, and 9, control degradation of the ECM and other cell processes. Tissue and circulating levels of MMP-2 and 9 are the best examined and have been reported to be elevated (Koullias et al., 2004; Schmoker et al., 2007) or not (Tscheuschler et al., 2016; Wang et al., 2016) in patients with thoracic aortic aneurysm, and higher in patients with BAV than in patients with TAV (Boyum et al., 2004; LeMaire et al., 2005; Ikonomidis et al., 2012; Wang et al., 2016). On their own, these data don't provide a complete picture as TIMPs modify the actions of MMPs. Circulating and tissue TIMP levels have been shown to be elevated (Mohamed et al., 2012) or not (Boyum et al., 2004; LeMaire et al., 2005; Ikonomidis et al., 2013; Wang et al., 2016) in patients with BAV and in patients with a thoracic aortic aneurysm. It is very likely that circulating levels of MMPs and TIMPs do not accurately reflect aortic wall tissue levels, comparable to the case for other biomarkers, and therefore do not have a prognostic role in aortic dissection, especially over the range of aortic diseases.

Transforming Growth Factor-β

TGF-β has a well-established causal role in the vascular complications of Marfan syndrome (Matt et al., 2008; Hillebrand et al., 2014). Variants in its receptors *TGFBR1, TGFBR2, TGFB2, and TGFB3* are responsible for Loeys-Dietz syndrome types 1, 2, 4, and 5, respectively, along with arterial tortuosity, thoracic aortic aneurysm and BAV disease (Brownstein et al., 2017). As a biomarker, circulating TGF-β1 is elevated in patients with Marfan syndrome, NOTCH1-associated aneurysm and BAV-associated aneurysm (Hillebrand et al., 2014). In seminal work, Forte and colleagues examined mRNA expression of a range of TGF-β pathway genes (*TGF-β1*, *MMP-2/14*, *ENG,* and others) from non-dilated and dilated aortas of patients with BAV, identifying complex relationships between gene and protein expression in the aorta, and aortic size (Forte et al., 2017). *TGF-β1* mRNA was elevated in non-dilated aortas but less so in dilated ones. In contrast, serum levels of TGF-β1 were lower in non-dilated aortas and not significantly elevated in dilated ones. These conflicting data underscore the need for further investigation.

To date, there is no circulating biomarker that can yet provide prospective information for either aortic aneurysm or dissection. There is also no reasonable and safe method for physical biopsy of the ascending aorta. A pragmatic approach of allowing targeted drug or other therapy for a high-risk cohort to prevent an event some 10–60 years in the future may include assessment of genetic markers, along with conventional and molecular imaging.

CONCLUSION

AAD has been ascribed to both the hemodynamic consequences of normal and abnormal BAV morphology and to the effect of rare and common genetic variation upon function of the ascending aortic media. We propose an overall thesis that compared with tubular AAD, aortic root AAD has a stronger genetic etiology, perhaps related to identified common non-coding *FBN1* variants that are associated with AAD in patients with tricuspid and BAVs. In patients with BAV having tubular AAD, we propose a stronger hemodynamic influence, but one that is still based on a functional deficit of the aortic media of genetic or epigenetic etiology. The pathogenesis of AAD likely involves both structural coding variants and non-coding variants, and thus far has not been related to identified genetic etiologies of BAV, notably, variants in *NOTCH1* and *GATA4*.

AUTHOR CONTRIBUTIONS

All the authors substantially contributed to (1) the conception or design of the work, acquisition a revision of literature data; (2) drafting the work or revising it critically for important intellectual content; (3) final approval of the version to be published; and All authors agree to be accountable for all aspects of the work in ensuring that questions related to the accuracy or integrity of any part of the work are appropriately investigated and resolved.

FUNDING

This work was supported by NIH grant R01HL114823 (SB).

REFERENCES

2010 ACCF/AHA/AATS/ACR/ASA/SCA/SCAI/SIR/STS/SVM Guidelines For the Diagnosis and Management of Patients with Thoracic Aortic Disease Representative Members, Hiratzka, L. F., Creager, M. A., Isselbacher, E. M., Svensson, L. G., 2014 AHA/ACC Guideline for the Management of Patients With Valvular Heart Disease Representative Members, Nishimura, R. A., et al. (2016). Surgery for aortic dilatation in patients with bicuspid aortic valves: a statement of clarification from the American College of Cardiology/American Heart Association Task Force on Clinical Practice Guidelines. *Circulation* 133, 680–686. doi: 10.1161/CIR.0000000000000331

Abdulkareem, N., Soppa, G., Jones, S., Valencia, O., Smelt, J., and Jahangiri, M. (2013). Dilatation of the remaining aorta after aortic valve or aortic root replacement in patients with bicuspid aortic valve: a 5-year follow-up. *Ann. Thorac. Surg.* 96, 43–49. doi: 10.1016/j.athoracsur.2013.03.086

Albinsson, S., Della Corte, A., Alajbegovic, A., Krawczyk, K. K., Bancone, C., Galderisi, U., et al. (2017). Patients with bicuspid and tricuspid aortic valve exhibit distinct regional microrna signatures in mildly dilated ascending aorta. *Heart Vessels* 32, 750–767. doi: 10.1007/s00380-016-0942-7

Anderson, R. H., Mori, S., Spicer, D. E., Brown, N. A., and Mohun, T. J. (2016). Development and morphology of the ventricular outflow tracts. *World J. Pediatr. Congenit. Heart Surg.* 7, 561–577. doi: 10.1177/2150135116651114

Atkins, S. K., and Sucosky, P. (2014). Etiology of bicuspid aortic valve disease: focus on hemodynamics. *World J. Cardiol.* 6, 1227–1233. doi: 10.4330/wjc.v6.i12.1227

Atkins, S. K., Moore, A. N., and Sucosky, P. (2016). Bicuspid aortic valve hemodynamics does not promote remodeling in porcine aortic wall concavity. *World J. Cardiol.* 8, 89–97. doi: 10.4330/wjc.v8.i1.89

Balistreri, C. R., Pisano, C., Candore, G., Maresi, E., Codispoti, M., and Ruvolo, G. (2013). Focus on the unique mechanisms involved in thoracic aortic aneurysm formation in bicuspid aortic valve vs. tricuspid aortic valve patients: clinical implications of a pilot study. *Eur. J. Cardiothorac. Surg.* 43, e180–e186. doi: 10.1093/ejcts/ezs630

Baudhuin, L. M., Kotzer, K. E., and Lagerstedt, S. A. (2015). Increased frequency of FBN1 truncating and splicing variants in Marfan syndrome patients with aortic events. *Genet. Med.* 17, 177–187. doi: 10.1038/gim.2014.91

Bellini, C., Bersi, M. R., Caulk, A. W., Ferruzzi, J., Milewicz, D. M., Ramirez, F., et al. (2017). Comparison of 10 murine models reveals a distinct biomechanical phenotype in thoracic aortic aneurysms. *J. R. Soc. Interface* 14:20161036. doi: 10.1098/rsif.2016.1036

Benedik, J., Pilarzcyk, K., Wendt, D., Price, V., Tsagakis, K., Perrey, M., et al. (2013). Is there any difference in aortic wall quality between patients with aortic stenosis and those with regurgitation? *Eur. J. Cardiothorac. Surg.* 44, 754–759. doi: 10.1093/ejcts/ezt123

Biaggi, P., Matthews, F., Braun, J., Rousson, V., Kaufmann, P. A., and Jenni, R. (2009). Gender, age, and body surface area are the major determinants of ascending aorta dimensions in subjects with apparently normal echocardiograms. *J. Am. Soc. Echocardiogr.* 22, 720–725. doi: 10.1016/j.echo.2009.03.012

Bonachea, E. M., Chang, S. W., Zender, G., LaHaye, S., Fitzgerald-Butt, S., McBride, K. L., et al. (2014a). Rare GATA5 sequence variants identified in individuals with bicuspid aortic valve. *Pediatr. Res.* 76, 211–216. doi: 10.1038/pr.2014.67

Bonachea, E. M., Zender, G., White, P., Corsmeier, D., Newsom, D., Fitzgerald-Butt, S., et al. (2014b). Use of a targeted, combinatorial next-generation sequencing approach for the study of bicuspid aortic valve. *BMC Med. Genomics* 7:56. doi: 10.1186/1755-8794-7-56

Boyum, J., Fellinger, E. K., Schmoker, J. D., Trombley, L., McPartland, K., Ittleman, F. P., et al. (2004). Matrix metalloproteinase activity in thoracic aortic aneurysms associated with bicuspid and tricuspid aortic valves. *J. Thorac. Cardiovasc. Surg.* 127, 686–691. doi: 10.1016/j.jtcvs.2003.11.049

Brownstein, A. J., Ziganshin, B. A., Kuivaniemi, H., Body, S. C., Bale, A. E., and Elefteriades, J. A. (2017). Genes associated with thoracic aortic aneurysm and dissection: an update and clinical implications. *Aorta* 5, 11–20. doi: 10.12945/j.aorta.2017.17.003

Burris, N. S., Dyverfeldt, P., and Hope, M. D. (2016). Ascending aortic stiffness with bicuspid aortic valve is variable and not predicted by conventional parameters in young patients. *J. Heart Valve Dis.* 25, 270–280. doi: 10.1186/1532-429X-17-S1-Q80

Cao, K., Atkins, S. K., McNally, A., Liu, J., and Sucosky, P. (2017). Simulations of morphotype-dependent hemodynamics in non-dilated bicuspid aortic valve aortas. *J. Biomech.* 50, 63–70. doi: 10.1016/j.jbiomech.2016.11.024

Cotrufo, M., and Della Corte, A. (2009). The association of bicuspid aortic valve disease with asymmetric dilatation of the tubular ascending aorta: identification of a definite syndrome. *J. Cardiovasc. Med.* 10, 291–297. doi: 10.2459/JCM.0b013e3283217e29

Cotrufo, M., Della Corte, A., De Santo, L. S., Quarto, C., De Feo, M., Romano, G., et al. (2005). Different patterns of extracellular matrix protein expression in the convexity and the concavity of the dilated aorta with bicuspid aortic valve: preliminary results. *J. Thorac. Cardiovasc. Surg.* 130, 504–511. doi: 10.1016/j.jtcvs.2005.01.016

Dargis, N., Lamontagne, M., Gaudreault, N., Sbarra, L., Henry, C., Pibarot, P., et al. (2016). Identification of gender-specific genetic variants in patients with bicuspid aortic valve. *Am. J. Cardiol.* 117, 420–426. doi: 10.1016/j.amjcard.2015.10.058

DeCampli, W. M. (2017). Ascending aortopathy with bicuspid aortic valve: more, but not enough, evidence for the hemodynamic theory. *J. Thorac. Cardiovasc. Surg.* 153, 6–7. doi: 10.1016/j.jtcvs.2016.10.033

Della Corte, A. (2014). Phenotypic heterogeneity of bicuspid aortopathy: a potential key to decode the prognosis? *Heart* 100, 96–97. doi: 10.1136/heartjnl-2013-305004

Della Corte, A., and Bancone, C. (2012). Multiple aortopathy phenotypes with bicuspid aortic valve: the importance of terminology and definition criteria. *Eur. J. Cardiothorac. Surg.* 41, 1404; Author reply: 1405. doi: 10.1093/ejcts/ezr216

Della Corte, A., Bancone, C., Dialetto, G., Covino, F. E., Manduca, S., D'Oria, V., et al. (2014a). Towards an individualized approach to bicuspid aortopathy: different valve types have unique determinants of aortic dilatation. *Eur. J. Cardiothorac. Surg.* 45, e118–e124; discussion: e124. doi: 10.1093/ejcts/ezt601

Della Corte, A., Bancone, C., Dialetto, G., Covino, F. E., Manduca, S., Montibello, M. V., et al. (2014b). The ascending aorta with bicuspid aortic valve: a phenotypic classification with potential prognostic significance. *Eur. J. Cardiothorac. Surg.* 46(2), 240–247; discussion 247. doi: 10.1093/ejcts/ezt621

Della Corte, A., Bancone, C., Quarto, C., Dialetto, G., Covino, F. E., Scardone, M., et al. (2007). Predictors of ascending aortic dilatation with bicuspid aortic valve: a wide spectrum of disease expression. *Eur. J. Cardiothorac. Surg.* 31, 397–404; discussion 404–405. doi: 10.1016/j.ejcts.2006.12.006

Della Corte, A., Quarto, C., Bancone, C., Castaldo, C., Di Meglio, F., Nurzynska, D., et al. (2008). Spatiotemporal patterns of smooth muscle cell changes in ascending aortic dilatation with bicuspid and tricuspid aortic valve stenosis: focus on cell-matrix signaling. *J. Thorac. Cardiovasc. Surg.* 135(1), 8–18, 18.e1–2. doi: 10.1016/j.jtcvs.2007.09.009

Dietz, H. C., Cutting, G. R., Pyeritz, R. E., Maslen, C. L., Sakai, L. Y., Corson, G. M., et al. (1991). Marfan syndrome caused by a recurrent *de novo* missense mutation in the fibrillin gene. *Nature* 352, 337–339. doi: 10.1038/352337a0

Doyle, J. J., Gerber, E. E., and Dietz, H. C. (2012). Matrix-dependent perturbation of TGFbeta signaling and disease. *FEBS Lett.* 586, 2003–2015. doi: 10.1016/j.febslet.2012.05.027

Dyer, L. A., and Kirby, M. L. (2009). The role of secondary heart field in cardiac development. *Dev. Biol.* 336, 137–144. doi: 10.1016/j.ydbio.2009.10.009

Elefteriades, J. A., and Farkas, E. A. (2010). Thoracic aortic aneurysm clinically pertinent controversies and uncertainties. *J. Am. Coll. Cardiol.* 55, 841–857. doi: 10.1016/j.jacc.2009.08.084

Entezari, P., Schnell, S., Mahadevia, R., Malaisrie, C., McCarthy, P., Mendelson, M., Collins, J., et al. (2014). From unicuspid to quadricuspid: influence of aortic valve morphology on aortic three-dimensional hemodynamics. *J. Magn. Reson. Imaging* 40, 1342–1346. doi: 10.1002/jmri.24498

Erbel, R., Aboyans, V., Boileau, C., Bossone, E., Bartolomeo, R. D., et al. (2014). 2014 ESC Guidelines on the diagnosis and treatment of aortic diseases: document covering acute and chronic aortic diseases of the thoracic and abdominal aorta of the adult. The Task Force for the Diagnosis and Treatment of Aortic Diseases of the European Society of Cardiology (ESC). *Eur. Heart J.* 35, 2873–2926. doi: 10.1093/eurheartj/ehu281

Faivre, L., Collod-Beroud, G., Loeys, B. L., Child, A., Binquet, C., Gautier, E., et al. (2007). Effect of mutation type and location on clinical outcome in 1,013 probands with Marfan syndrome or related phenotypes and FBN1 mutations: an international study. *Am. J. Hum. Genet.* 81, 454–466. doi: 10.1086/520125

Fedak, P. W., Barker, A. J., and Verma, S. (2016). Year in review: bicuspid aortopathy. *Curr. Opin. Cardiol.* 31, 132–138. doi: 10.1097/HCO.0000000000000258

Foffa, I., Ait Ali, L., Panesi, P., Mariani, M., Festa, P., Botto, N., et al. (2013). Sequencing of NOTCH1, GATA5, TGFBR1 and TGFBR2 genes in familial cases of bicuspid aortic valve. *BMC Med. Genet.* 14:44. doi: 10.1186/1471-2350-14-44

Forte, A., Bancone, C., Cobellis, G., Buonocore, M., Santarpino, G., Fischlein, T. J., et al. (2017). A possible early biomarker for bicuspid aortopathy: circulating transforming growth factor β-1 to soluble endoglin ratio. *Circ. Res.* 120, 1800–1811. doi: 10.1161/CIRCRESAHA.117.310833

Forte, A., Della Corte, A., De Feo, M., Cerasuolo, F., and Cipollaro, M. (2010). Role of myofibroblasts in vascular remodelling: focus on restenosis and aneurysm. *Cardiovasc. Res.* 88, 395–405. doi: 10.1093/cvr/cvq224

Forte, A., Della Corte, A., Grossi, M., Bancone, C., Maiello, C., Galderisi, U., et al. (2013). Differential expression of proteins related to smooth muscle cells and myofibroblasts in human thoracic aortic aneurysm. *Histol. Histopathol.* 28, 795–803. doi: 10.14670/HH-28.795

Forte, A., Galderisi, U., Cipollaro, M., De Feo, M., and Della Corte, A. (2016). Epigenetic regulation of TGF-beta1 signalling in dilative aortopathy of the thoracic ascending aorta. *Clin. Sci.* 130, 1389–1405. doi: 10.1042/CS20160222

Franken, R., Radonic, T., den Hartog, A. W., Groenink, M., Pals, G., van Eijk, M. et al. (2015). The revised role of TGF-beta in aortic aneurysms in Marfan syndrome. *Neth. Heart J.* 23, 116–121. doi: 10.1007/s12471-014-0622-0

Franken, R., Teixido-Tura, G., Brion, M., Forteza, A., Rodriguez-Palomares, J., Gutierrez, L., et al. (2017). Relationship between fibrillin-1 genotype and severity of cardiovascular involvement in Marfan syndrome. *Heart* doi: 10.1136/heartjnl-2016-310631. [Epub ahead of print].

Gagne-Loranger, M., Dumont, E., Voisine, P., Mohammadi, S., and Dagenais, F. (2016). Natural history of 40-50 mm root/ascending aortic aneurysms in the current era of dedicated thoracic aortic clinics. *Eur. J. Cardiothorac. Surg.* 50, 562–566. doi: 10.1093/ejcts/ezw123

Garcia, J., Barker, A. J., Murphy, I., Jarvis, K., Schnell, S., Collins, J. D., et al. (2016). Four-dimensional flow magnetic resonance imaging-based characterization of aortic morphometry and haemodynamics: impact of age, aortic diameter, and valve morphology. *Eur. Heart J. Cardiovasc. Imaging* 17, 877–884. doi: 10.1093/ehjci/jev228

Garg, V., Muth, A. N., Ransom, J. F., Schluterman, M. K., Barnes, R., King. I. N., et al. (2005). Mutations in NOTCH1 cause aortic valve disease. *Nature* 437, 270–274. doi: 10.1038/nature03940

Geisbusch, S., Stefanovic, A., Schray, D., Oyfe, I., Lin, H. M., Di Luozzo, G., et al. (2014). A prospective study of growth and rupture risk of small-to-moderate size ascending aortic aneurysms. *J. Thorac. Cardiovasc. Surg.* 147, 68–74. doi: 10.1016/j.jtcvs.2013.06.030

Girdauskas, E., and Borger, M. A. (2013). Bicuspid aortic valve and associated aortopathy: an update. *Semin. Thorac. Cardiovasc. Surg.* 25, 310–316. doi: 10.1053/j.semtcvs.2014.01.004

Girdauskas, E., Disha, K., Borger, M. A., and Kuntze, T. (2014). Long-term prognosis of ascending aortic aneurysm after aortic valve replacement for bicuspid vs. tricuspid aortic valve stenosis. *J. Thorac. Cardiovasc. Surg.* 147, 276–282. doi: 10.1016/j.jtcvs.2012.11.004

Girdauskas, E., Disha, K., Raisin, H. H., Secknus, M. A., Borger, M. A., and Kuntze, T. (2012). Risk of late aortic events after an isolated aortic valve replacement for bicuspid aortic valve stenosis with concomitant ascending aortic dilation. *Eur. J. Cardiothorac. Surg.* 42, 832–837; discussion: 837–838. doi: 10.1093/ejcts/ezs137

Girdauskas, E., Geist, L., Disha, K., Kazakbaev, I., Gross, T., Schulz, S., et al. (2017). Genetic abnormalities in bicuspid aortic valve root phenotype: preliminary resultsdagger. *Eur. J. Cardiothorac. Surg.* 52, 156–162. doi: 10.1093/ejcts/ezx065

Girdauskas, E., Rouman, M., Disha, K., Dubslaff, G., Fey, B., Misfeld, M., et al. (2016a). The fate of mild-to-moderate proximal aortic dilatation after isolated aortic valve replacement for bicuspid aortic valve stenosis: a magnetic resonance imaging follow-up studydagger. *Eur. J. Cardiothorac. Surg.* 49, e80–e86; discussion: e86–e87. doi: 10.1093/ejcts/ezv472

Girdauskas, E., Rouman, M., Disha, K., Dubslaff, G., Fey, B., Theis, B., et al. (2016b). Aortopathy in bicuspid aortic valve stenosis with fusion of right-left vs. right-non-coronary cusps: are these different diseases? *J. Heart Valve Dis.* 25, 262–269.

Girdauskas, E., Schulz, S., Borger, M. A., Mierzwa, M., and Kuntze, T. (2011). Transforming growth factor-beta receptor type II mutation in a patient with bicuspid aortic valve disease and intraoperative aortic dissection. *Ann. Thorac. Surg.* 91, e70–e71. doi: 10.1016/j.athoracsur.2010.12.060

Guo, D. C., Grove, M. L., Prakash, S. K., Eriksson, P., Hostetler, E. M., LeMaire, S. A., et al. (2016). Genetic variants in LRP1 and ULK4 are associated with acute aortic dissections. *Am. J. Hum. Genet.* 99, 762–769. doi: 10.1016/j.ajhg.2016.06.034

Guo, D. C., Pannu, H., Tran-Fadulu, V., Papke, C. L., Yu, R. K., Avidan, N., et al. (2007). Mutations in smooth muscle alpha-actin (ACTA2) lead to thoracic aortic aneurysms and dissections. *Nat. Genet.* 39, 1488–1493. doi: 10.1038/ng.2007.6

Guzzardi, D. G., Barker, A. J., van Ooij, P., Malaisrie, S. C., Puthumana, J. J., Belke, D. D., et al. (2015). Valve-related hemodynamics mediate human bicuspid aortopathy: insights from wall shear stress mapping. *J. Am. Coll. Cardiol.* 66, 892–900. doi: 10.1016/j.jacc.2015.06.1310

Habchi, K. M., Ashikhmina, E., Vieira, V. M., Shahram, J. T., Isselbacher, E. M., Sundt, T. M., III., et al. (2017). Association between bicuspid aortic valve morphotype and regional dilatation of the aortic root and trunk. *Int. J. Cardiovasc. Imaging* 33, 341–349. doi: 10.1007/s10554-016-1016-8

Harmon, A. W., and Nakano, A. (2013). Nkx2-5 lineage tracing visualizes the distribution of second heart field-derived aortic smooth muscle. *Genesis* 51, 862–869. doi: 10.1002/dvg.22721

Hillebrand, M., Millot, N., Sheikhzadeh, S., Rybczynski, M., Gerth, S., Kolbel, T., et al. (2014). Total serum transforming growth factor-beta1 is elevated in the entire spectrum of genetic aortic syndromes. *Clin. Cardiol.* 37, 672–679. doi: 10.1002/clc.22320

Humphrey, J. D., Milewicz, D. M., Tellides, G., and Schwartz, M. A. (2014). Cell biology. Dysfunctional mechanosensing in aneurysms. *Science* 344, 477–479. doi: 10.1126/science.1253026

Humphrey, J. D., Schwartz, M. A., Tellides, G., and Milewicz, D. M. (2015). Role of mechanotransduction in vascular biology: focus on thoracic aortic aneurysms and dissections. *Circ. Res.* 116, 1448–1461. doi: 10.1161/CIRCRESAHA.114.304936

Ikonomidis, J. S., Ivey, C. R., Wheeler, J. B., Akerman, A. W., Rice, A., Patel, R. K., et al. (2013). Plasma biomarkers for distinguishing etiologic subtypes of thoracic aortic aneurysm disease. *J. Thorac. Cardiovasc. Surg.* 145, 1326–1333. doi: 10.1016/j.jtcvs.2012.12.027

Ikonomidis, J. S., Ruddy, J. M., Benton, S. M. Jr., Arroyo, J., Brinsa, T., Stroud, R. E., et al. (2012). Aortic dilatation with bicuspid aortic valves: cusp fusion correlates to matrix metalloproteinases and inhibitors. *Ann. Thorac. Surg.* 93, 457–463. doi: 10.1016/j.athoracsur.2011.09.057

Jackson, V., Petrini, J., Caidahl, K., Eriksson, M. J., Liska, J., Eriksson, P., et al. (2011). Bicuspid aortic valve leaflet morphology in relation to aortic root morphology: a study of 300 patients undergoing open-heart surgery. *Eur. J. Cardiothorac. Surg.* 40, e118–e124. doi: 10.1016/j.ejcts.2011.04.014

Jassal, D. S., Bhagirath, K. M., Tam, J. W., Sochowski, R. A., Dumesnil, J. G., Giannoccaro, P. J., et al. (2010). Association of Bicuspid aortic valve morphology and aortic root dimensions: a substudy of the aortic stenosis progression observation measuring effects of rosuvastatin (ASTRONOMER) study. *Echocardiography* 27, 174–179. doi: 10.1111/j.1540-8175.2009.00993.x

Jiang, X., Rowitch, D. H., Soriano, P., McMahon, A. P., and Sucov, H. M. (2000). Fate of the mammalian cardiac neural crest. *Development* 127, 1607–1616.

Jiao, J., Xiong, W., Wang, L., Yang, J., Qiu, P., Hirai, H., et al. (2016). Differentiation defect in neural crest-derived smooth muscle cells in patients with aortopathy associated with bicuspid aortic valves. *EBioMedicine* 10, 282–290. doi: 10.1016/j.ebiom.2016.06.045

Kerstjens-Frederikse, W. S., van de Laar, I. M., Vos, Y. J., Verhagen, J. M., Berger, R. M., Lichtenbelt, K. D., et al. (2016). Cardiovascular malformations caused by NOTCH1 mutations do not keep left: data on 428 probands with left-sided CHD and their families. *Genet. Med.* 18, 914–923. doi: 10.1038/gim.2015.193

Kiyota, Y., Della Corte, A., Montiero Vieira, V., Habchi, K., Huang, C.-C., Della Ratta, E. E., et al. (2017). Risk and outcomes of aortic valve endocarditis among patients with bicuspid and tricuspid aortic valves. *Open Heart* 4:e000545. doi: 10.1136/openhrt-2016-000545

Koenig, S. N., Bosse, K. M., Nadorlik, H. A., Lilly, B., and Garg, V. (2015). Evidence of aortopathy in mice with haploinsufficiency of Notch1 in Nos3-null background. *J. Cardiovasc. Dev. Dis.* 2, 17–30. doi: 10.3390/jcdd2010017

Kostina, A. S., Uspensky, V. E., Irtyuga, O. B., Ignatieva, E. V., Freylikhman, O., Gavriliuk, N. D. et al. (2016). Notch-dependent EMT is attenuated in patients with aortic aneurysm and bicuspid aortic valve. *Biochim. Biophys. Acta* 1862, 733–740. doi: 10.1016/j.bbadis.2016.02.006

Koullias, G. J., Ravichandran, P., Korkolis, D. P., Rimm, D. L., and Elefteriades, J. A. (2004). Increased tissue microarray matrix metalloproteinase expression favors proteolysis in thoracic aortic aneurysms and dissections. *Ann. Thorac. Surg.* 78, 2106–2110; discussion: 2110–2111. doi: 10.1016/j.athoracsur.2004.05.088

Laforest, B., and Nemer, M. (2011). GATA5 interacts with GATA4 and GATA6 in outflow tract development. *Dev. Biol.* 358, 368–378. doi: 10.1016/j.ydbio.2011.07.037

Laforest, B., Andelfinger, G., and Nemer, M. (2011). Loss of Gata5 in mice leads to bicuspid aortic valve. *J. Clin. Invest.* 121, 2876–2887. doi: 10.1172/JCI44555

Leeper, N. J., Raiesdana, A., Kojima, Y., Chun, H. J., Azuma, J., Maegdefessel, L., et al. (2011). MicroRNA-26a is a novel regulator of vascular smooth muscle cell function. *J. Cell. Physiol.* 226, 1035–1043. doi: 10.1002/jcp.22422

LeMaire, S. A., McDonald, M. L., Guo, D. C., Russell, L., Miller, C. C. III, Johnson, R., et al. (2011). Genome-wide association study identifies a susceptibility locus for thoracic aortic aneurysms and aortic dissections spanning FBN1 at 15q21.1. *Nat. Genet.* 43, 996–1000. doi: 10.1038/ng.934

LeMaire, S. A., Wang, X., Wilks, J. A., Carter, S. A., Wen, S., Won, T., et al. (2005). Matrix metalloproteinases in ascending aortic aneurysms: bicuspid vs. trileaflet aortic valves. *J. Surg. Res.* 123, 40–48. doi: 10.1016/j.jss.2004.06.007

Leone, O., Biagini, E., Pacini, D., Zagnoni, S., Ferlito, M., Graziosi, M., et al. (2012). The elusive link between aortic wall histology and echocardiographic anatomy in bicuspid aortic valve: implications for prophylactic surgery. *Eur. J. Cardiothorac. Surg.* 41, 322–327. doi: 10.1016/j.ejcts.2011.05.064

Lindsay, M. E., Schepers, D., Bolar, N. A., Doyle, J. J., Gallo, E., Fert-Bober, J., et al. (2012). Loss-of-function mutations in TGFB2 cause a syndromic presentation of thoracic aortic aneurysm. *Nat. Genet.* 44, 922–927. doi: 10.1038/ng.2349

Luxan, G., Casanova, J. C., Martinez-Poveda, B., Prados, B., D'Amato, G., MacGrogan, D., et al. (2013). Mutations in the NOTCH pathway regulator

MIB1 cause left ventricular noncompaction cardiomyopathy. *Nat. Med.* 19, 193–201. doi: 10.1038/nm.3046

Martin, M., Rodriguez, I., Palacin, M., Rios-Gomez, E., and Coto, E. (2011). TGFBR2 gene mutational spectrum in aortic pathology. *J. Am. Coll. Cardiol.* 57, 518–519; author reply: 519. doi: 10.1016/j.jacc.2010.07.052

Martin, P. S., Kloesel, B., Norris, R. A., Lindsay, M., Milan, D., and Body, S. C. (2015). Embryonic development of the bicuspid aortic valve. *J. Cardiovasc. Dev. Dis.* 2, 248–272. doi: 10.3390/jcdd2040248

Mathieu, P., Bosse, Y., Huggins, G. S., Corte, A. D., Pibarot, P., Michelena, H. J., et al. (2015). The pathology and pathobiology of bicuspid aortic valve: state of the art and novel research perspectives. *J. Pathol. Clin. Res.* 1, 195–206. doi: 10.1002/cjp2.21

Matt, P., Habashi, J., Carrel, T., Cameron, D. E., Van Eyk, J. E., and Dietz, H. C. (2008). Recent advances in understanding Marfan syndrome: should we now treat surgical patients with losartan? *J. Thorac. Cardiovasc. Surg.* 135, 389–394. doi: 10.1016/j.jtcvs.2007.08.047

McKellar, S. H., Michelena, H. I., Li, Z., Schaff, H. V., and Sundt, T. M. III. (2010). Long-term risk of aortic events following aortic valve replacement in patients with bicuspid aortic valves. *Am. J. Cardiol.* 106, 1626–1633. doi: 10.1016/j.amjcard.2010.07.043

McKellar, S. H., Tester, D. J., Yagubyan, M., Majumdar, R., Ackerman, M. J., and Sundt, T. M. III. (2007). Novel NOTCH1 mutations in patients with bicuspid aortic valve disease and thoracic aortic aneurysms. *J. Thorac. Cardiovasc. Surg.* 134, 290–296. doi: 10.1016/j.jtcvs.2007.02.041

Michelena, H. I., Desjardins, V. A., Avierinos, J. F., Russo, A., Nkomo, V. T., Sundt. T. M., et al. (2008). Natural history of asymptomatic patients with normally functioning or minimally dysfunctional bicuspid aortic valve in the community. *Circulation* 117, 2776–2784. doi: 10.1161/CIRCULATIONAHA.107.740878

Michelena, H. I., Khanna, A. D., Mahoney, D., Margaryan, E., Topilsky, Y., Suri, R. M., et al. (2011). Incidence of aortic complications in patients with bicuspid aortic valves. *JAMA* 306, 1104–1112. doi: 10.1001/jama.2011.1286

Michelena, H. I., Prakash, S. K., Della Corte, A., Bissell, M. M., Anavekar, N., Mathieu, P., et al. (2014). Bicuspid aortic valve: identifying knowledge gaps and rising to the challenge from the International Bicuspid Aortic Valve Consortium (BAVCon). *Circulation* 129, 2691–2704. doi: 10.1161/CIRCULATIONAHA.113.007851

Mohamed, S. A., Aherrahrou, Z., Liptau, H., Erasmi, A. W., Hagemann, C., Wrobel, S., et al. (2006). Novel missense mutations (p.T596M and p.P1797H) in NOTCH1 in patients with bicuspid aortic valve. *Biochem. Biophys. Res. Commun.* 345, 1460–1465. doi: 10.1016/j.bbrc.2006.05.046

Mohamed, S. A., Noack, F., Schoellermann, K., Karluss, A., Radtke, A., Schult-Badusche, D., et al. (2012). Elevation of matrix metalloproteinases in different areas of ascending aortic aneurysms in patients with bicuspid and tricuspid aortic valves. *ScientificWorldJournal* 2012, 806261. doi: 10.1100/2012/806261

Nagashima, H., Sakomura, Y., Aoka, Y., Uto, K., Kameyama, K., Ogawa, M., et al. (2001). Angiotensin II type 2 receptor mediates vascular smooth muscle cell apoptosis in cystic medial degeneration associated with Marfan's syndrome. *Circulation* 104(12 Suppl. 1), I282–I287. doi: 10.1161/hc37t1.094856

Naito, S., Gross, T., Disha, K., von Kodolitsch, Y., Reichenspurner, H., and Girdauskas, E. (2017). Late post-AVR progression of bicuspid aortopathy: link to hemodynamics. *Gen. Thorac. Cardiovasc. Surg.* 65, 252–258. doi: 10.1007/s11748-017-0746-4

Nataatmadja, M., West, J., Prabowo, S., and West, M. (2013). Angiotensin II receptor antagonism reduces transforming growth factor beta and smad signaling in thoracic aortic aneurysm. *Ochsner J.* 13, 42–48.

Padang, R., Bagnall, R. D., Richmond, D. R., Bannon, P. G., and Semsarian, C. (2012). Rare non-synonymous variations in the transcriptional activation domains of GATA5 in bicuspid aortic valve disease. *J. Mol. Cell. Cardiol.* 53, 277–281. doi: 10.1016/j.yjmcc.2012.05.009

Pape, L. A., Tsai, T. T., Isselbacher, E. M., Oh, J. K., O'Gara, P. T., Evangelista, A., et al. (2007). Aortic diameter >or = 5.5 cm is not a good predictor of type A aortic dissection: observations from the International Registry of Acute Aortic Dissection (IRAD). *Circulation* 116, 1120–1127. doi: 10.1161/CIRCULATIONAHA.107.702720

Park, J. Y., Foley, T. A., Bonnichsen, C. R., Maurer, M. J., Goergen, K. M., Nkomo, V. T., et al. (2017). Transthoracic echocardiography vs. computed tomography for ascending aortic measurements in patients with bicuspid aortic valve. *J. Am. Soc. Echocardiogr.* 30, 625–635. doi: 10.1016/j.echo.2017.03.006

Patel, A., and Honore, E. (2010). Polycystins and renovascular mechanosensory transduction. *Nat. Rev. Nephrol.* 6, 530–538. doi: 10.1038/nrneph.2010.97

Pepe, G., Nistri, S., Giusti, B., Sticchi, E., Attanasio, M., Porciani, C., et al. (2014). Identification of fibrillin 1 gene mutations in patients with bicuspid aortic valve (BAV) without Marfan syndrome. *BMC Med. Genet.* 15:23. doi: 10.1186/1471-2350-15-23

Perrucci, G. L., Rurali, E., Gowran, A., Pini, A., Antona, C., Chiesa, R., et al. (2017). Vascular smooth muscle cells in Marfan syndrome aneurysm: the broken bricks in the aortic wall. *Cell. Mol. Life Sci.* 74, 267–277. doi: 10.1007/s00018-016-2324-9

Pfaltzgraff, E. R., Shelton, E. L., Galindo, C. L., Nelms, B. L., Hooper, C. W., Poole, S. D., et al. (2014). Embryonic domains of the aorta derived from diverse origins exhibit distinct properties that converge into a common phenotype in the adult. *J. Mol. Cell. Cardiol.* 69, 88–96. doi: 10.1016/j.yjmcc.2014.01.016

Phillippi, J. A., Green, B. R., Eskay, M. A., Kotlarczyk, M. P., Hill, M. R., Robertson, A. M., et al. (2014). Mechanism of aortic medial matrix remodeling is distinct in patients with bicuspid aortic valve. *J. Thorac. Cardiovasc. Surg.* 147, 1056–1064. doi: 10.1016/j.jtcvs.2013.04.028

Phillips, H. M., Mahendran, P., Singh, E., Anderson, R. H., Chaudhry, B., and Henderson, D. J. (2013). Neural crest cells are required for correct positioning of the developing outflow cushions and pattern the arterial valve leaflets. *Cardiovasc. Res.* 99, 452–460. doi: 10.1093/cvr/cvt132

Plein, A., Fantin, A., and Ruhrberg, C. (2015). Neural crest cells in cardiovascular development. *Curr. Top. Dev. Biol.* 111, 183–200. doi: 10.1016/bs.ctdb.2014.11.006

Prakash, S. K., Bosse, Y., Muehlschlegel, J. D., Michelena, H. I., Limongelli, G., Della Corte, A., et al. (2014). A roadmap to investigate the genetic basis of bicuspid aortic valve and its complications: insights from the International BAVCon (Bicuspid Aortic Valve Consortium). *J. Am. Coll. Cardiol.* 64, 832–839. doi: 10.1016/j.jacc.2014.04.073

Prapa, S., Mccarthy, K., Krexi, D., Gatzoulis, M., and Ho, S. (2014). The aortic root phenotype in bicuspid aortic valve disease: evidence of shared Smad2 activation in aortic regions of distinct embryologic origin. *Cardiovasc. Res.* 103, S16. doi: 10.1093/cvr/cvu082.38

Qu, X. K., Qiu, X. B., Yuan, F., Wang, J., Zhao, C. M., Liu, X. Y., et al. (2014). A novel NKX2.5 loss-of-function mutation associated with congenital bicuspid aortic valve. *Am. J. Cardiol.* 114, 1891–1895. doi: 10.1016/j.amjcard.2014.09.028

Raghav, V., Barker, A. J., Mangiameli, D., Mirabella, L., Markl, M., and Yoganathan, A. P. (2017). Valve mediated hemodynamics and their association with distal ascending aortic diameter in bicuspid aortic valve subjects. *J. Magn. Reson. Imaging.* doi: 10.1002/jmri.25719. [Epub ahead of print].

Regeer, M. V., Versteegh, M. I., Klautz, R. J., Schalij, M. J., Bax, J. J., Marsan, N. A., et al. (2016). Effect of aortic valve replacement on aortic root dilatation rate in patients with bicuspid and tricuspid aortic valves. *Ann. Thorac. Surg.* 102, 1981–1987. doi: 10.1016/j.athoracsur.2016.05.038

Robertson, I., Jensen, S., and Handford, P. (2011). TB domain proteins: evolutionary insights into the multifaceted roles of fibrillins and LTBPs. *Biochem. J.* 433, 263–276. doi: 10.1042/BJ20101320

Russell-Puleri, S., Dela Paz, N. G., Adams, D., Chattopadhyay, M., Cancel, L., Ebong, E., et al. (2017). Fluid shear stress induces upregulation of COX-2 and PGI2 release in endothelial cells via a pathway involving PECAM-1, PI3K, FAK, and p38. *Am. J. Physiol. Heart Circ. Physiol.* 312, H485–H500. doi: 10.1152/ajpheart.00035.2016

Sawada, H., Rateri, D. L., Moorleghen, J. J., Majesky, M. W., and Daugherty, A. (2017). Smooth muscle cells derived from second heart field and cardiac neural crest reside in spatially distinct domains in the media of the ascending aorta. *Arterioscler. Thromb. Vasc. Biol.* 37, 1722–1726. doi: 10.1161/ATVBAHA.117.309599

Schaefer, B. M., Lewin, M. B., Stout, K. K., Gill, E., Prueitt, A., Byers, P. H., et al. (2008). The bicuspid aortic valve: an integrated phenotypic classification of leaflet morphology and aortic root shape. *Heart* 94, 1634–1638. doi: 10.1136/hrt.2007.132092

Schmoker, J. D., McPartland, K. J., Fellinger, E. K., Boyum, J., Trombley, L., Ittleman, F. P., et al. (2007). Matrix metalloproteinase and tissue inhibitor expression in atherosclerotic and nonatherosclerotic thoracic aortic aneurysms. *J. Thorac. Cardiovasc. Surg.* 133, 155–161. doi: 10.1016/j.jtcvs.2006.07.036

Schrijver, I., Liu, W., Odom, R., Brenn, T., Oefner, P., Furthmayr, H., et al. (2002). Premature termination mutations in FBN1: distinct effects on differential allelic expression and on protein and clinical phenotypes. *Am. J. Hum. Genet.* 71, 223–237. doi: 10.1086/341581

Shah, A. A., Gregory, S. G., Krupp, D., Feng, S., Dorogi, A., Haynes, C., et al. (2015). Epigenetic profiling identifies novel genes for ascending aortic aneurysm formation with bicuspid aortic valves. *Heart Surg. Forum* 18, E134–E139. doi: 10.1532/hsf.1247

Shan, Y., Li, J., Wang, Y., Wu, B., Barker, A. J., Markl, M., et al. (2017). Aortic shear stress in patients with bicuspid aortic valve with stenosis and insufficiency. *J. Thorac. Cardiovasc. Surg.* 153, 1263.e1–1272.e1. doi: 10.1016/j.jtcvs.2016.12.059

Shi, L. M., Tao, J. W., Qiu, X. B., Wang, J., Yuan, F., Xu, L., et al. (2014). GATA5 loss-of-function mutations associated with congenital bicuspid aortic valve. *Int. J. Mol. Med.* 33, 1219–1226. doi: 10.3892/ijmm.2014.1700

Snarr, B. S., Kern, C. B., and Wessels, A. (2008). Origin and fate of cardiac mesenchyme. *Dev. Dyn.* 237, 2804–2819. doi: 10.1002/dvdy.21725

Tscheuschler, A., Meffert, P., Beyersdorf, F., Heilmann, C., Kocher, N., Uffelmann, X., et al. (2016). MMP-2 isoforms in aortic tissue and serum of patients with ascending aortic aneurysms and aortic root aneurysms. *PLoS ONE* 11:e0164308. doi: 10.1371/journal.pone.0164308

van Ooij, P., Garcia, J., Potters, W. V., Malaisrie, S. C., Collins, J. D., Carr, J. C., et al. (2016). Age-related changes in aortic 3D blood flow velocities and wall shear stress: implications for the identification of altered hemodynamics in patients with aortic valve disease. *J. Magn. Reson. Imaging* 43, 1239–1249. doi: 10.1002/jmri.25081

Wagenseil, J. E., and Mecham, R. P. (2009). Vascular extracellular matrix and arterial mechanics. *Physiol. Rev.* 89, 957–989. doi: 10.1152/physrev.00041.2008

Waldo, K. L., Hutson, M. R., Ward, C. C., Zdanowicz, M., Stadt, H. A., Kumiski, D., et al. (2005). Secondary heart field contributes myocardium and smooth muscle to the arterial pole of the developing heart. *Dev. Biol.* 281, 78–90. doi: 10.1016/j.ydbio.2005.02.012

Wang, Y., Wu, B., Dong, L., Wang, C., Wang, X., and Shu, X. (2016). Circulating matrix metalloproteinase patterns in association with aortic dilatation in bicuspid aortic valve patients with isolated severe aortic stenosis. *Heart Vessels* 31, 189–197. doi: 10.1007/s00380-014-0593-5

Wipff, P. J., and Hinz, B. (2008). Integrins and the activation of latent transforming growth factor beta1 - an intimate relationship. *Eur. J. Cell Biol.* 87, 601–615. doi: 10.1016/j.ejcb.2008.01.012

Wooten, E. C., Iyer, L. K., Montefusco, M. C., Hedgepeth, A. K., Payne, D. D., Kapur, N. K., et al. (2010). Application of gene network analysis techniques identifies AXIN1/PDIA2 and endoglin haplotypes associated with bicuspid aortic valve. *PLoS ONE* 5:e8830. doi: 10.1371/journal.pone.0008830

Wu, B., Wang, Y., Xiao, F., Butcher, J. T., Yutzey, K. E., and Zhou, B. (2017). Developmental mechanisms of aortic valve malformation and disease. *Annu. Rev. Physiol.* 79, 21–41. doi: 10.1146/annurev-physiol-022516-034001

Wu, D., Shen, Y. H., Russell, L., Coselli, J. S., and LeMaire, S. A. (2013). Molecular mechanisms of thoracic aortic dissection. *J. Surg. Res.* 184, 907–924. doi: 10.1016/j.jss.2013.06.007

Yang, B., Zhou, W., Jiao, J., Nielsen, J. B., Mathis, M. R., Heydarpour, M., et al. (2017). Protein-altering and regulatory genetic variants near GATA4 implicated in bicuspid aortic valve. *Nat. Commun.* 8, 15481. doi: 10.1038/ncomms15481

Conflict of Interest Statement: The authors declare that the research was conducted in the absence of any commercial or financial relationships that could be construed as a potential conflict of interest.

frontiers in Physiology

ORIGINAL RESEARCH
published: 26 June 2017
doi: 10.3389/fphys.2017.00441

4D Flow Analysis of BAV-Related Fluid-Dynamic Alterations: Evidences of Wall Shear Stress Alterations in Absence of Clinically-Relevant Aortic Anatomical Remodeling

*Filippo Piatti[1], Francesco Sturla[1], Malenka M. Bissell[2], Selene Pirola[3], Massimo Lombardi[4], Igor Nesteruk[5], Alessandro Della Corte[6], Alberto C. L. Redaelli[1] and Emiliano Votta[1]**

[1] Department of Electronics, Information and Bioengineering, Politecnico di Milano, Milan, Italy, [2] Division of Cardiovascular Medicine, Radcliffe Department of Medicine, University of Oxford, Oxford, United Kingdom, [3] Department of Chemical Engineering, Imperial College London, London, United Kingdom, [4] Multimodality Cardiac Imaging Section, IRCCS Policlinico San Donato, San Donato Milanese, Milan, Italy, [5] Department of Free Boundary Flows, Institute of Hydromechanics, National Academy of Sciences of Ukraine, Kyiv, Ukraine, [6] Department of Cardiothoracic and Respiratory Sciences, Università Degli Studi Della Campania 'L. Vanvitelli' Naples, Naples, Italy

OPEN ACCESS

Edited by:
Yi Zhu,
Tianjin Medical University, China

Reviewed by:
Philippe Sucosky,
Wright State University, United States
Julie A. Phillippi,
University of Pittsburgh, United States

***Correspondence:**
Emiliano Votta
emiliano.votta@polimi.it

Specialty section:
This article was submitted to Vascular Physiology, a section of the journal Frontiers in Physiology

Received: *31 March 2017*
Accepted: *09 June 2017*
Published: *26 June 2017*

Citation:
Piatti F, Sturla F, Bissell MM, Pirola S, Lombardi M, Nesteruk I, Della Corte A, Redaelli ACL and Votta E (2017) 4D Flow Analysis of BAV-Related Fluid-Dynamic Alterations: Evidences of Wall Shear Stress Alterations in Absence of Clinically-Relevant Aortic Anatomical Remodeling. Front. Physiol. 8:441. doi: 10.3389/fphys.2017.00441

Bicuspid aortic valve (BAV) is the most common congenital cardiac disease and is a foremost risk factor for aortopathies. Despite the genetic basis of BAV and of the associated aortopathies, BAV-related alterations in aortic fluid-dynamics, and particularly in wall shear stresses (WSSs), likely play a role in the progression of aortopathy, and may contribute to its pathogenesis. To test whether WSS may trigger aortopathy, in this study we used 4D Flow sequences of phase-contrast cardiac magnetic resonance imaging (CMR) to quantitatively compare the *in vivo* fluid dynamics in the thoracic aorta of two groups of subjects: (i) five prospectively enrolled young patients with normo-functional BAV and with no aortic dilation and (ii) ten age-matched healthy volunteers. Through the semi-automated processing of 4D Flow data, the aortic bulk flow at peak systole was quantified, and WSSs acting on the endothelium of the ascending aorta were characterized throughout the systolic phase in terms of magnitude and time-dependency through a method recently developed by our group. Variables computed for each BAV patient were compared vs. the corresponding distribution of values obtained for healthy controls. In BAV patients, ascending aorta diameter was measured on cine-CMR images at baseline and at 3-year follow-up. As compared to controls, normo-functional BAV patients were characterized by minor bulk flow disturbances at peak systole. However, they were characterized by evident alterations of WSS distribution and peak values in the ascending aorta. In particular, in four BAV patients, who were characterized by right-left leaflet fusion, WSS peak values exceeded by 27–46% the 90th percentile of the distribution obtained for healthy volunteers. Only in the BAV patient with right-non-coronary leaflet fusion the same threshold was exceeded by 132%. Also, evident alterations in the time-dependency of WSS magnitude and direction were observed. Despite, these fluid-dynamic alterations, no clinically relevant anatomical remodeling was

observed in the BAV patients at 3-year follow-up. In light of previous evidence from the literature, our results suggest that WSS alterations may precede the onset of aortopathy and may contribute to its triggering, but WSS-driven anatomical remodeling, if any, is a very slow process.

Keywords: bicuspid aortic valve, aortopathy, fluid dynamics, wall shear stress, magnetic resonance imaging, 4D flow

INTRODUCTION

Bicuspid aortic valve (BAV) is the most common congenital cardiac disease and affects about 2% of newborns (Michelena et al., 2014). BAV is a recognized risk factor for aortopathies, with more than 50% of BAV patients developing aneurysm of the ascending aorta (Nistri et al., 1999; Fedak et al., 2002).

The development of BAV-related aortopathies has been attributed to genetic and hemodynamic bases (Verma and Siu, 2014), with several studies focusing on their relative contribution (Fedak et al., 2002; Siu and Silversides, 2010; Girdauskas et al., 2011; Wendell et al., 2013; Guzzardi et al., 2015).

In regard to fluid dynamics, the velocity jet during systole has been shown to be deflected in the BAV aorta (Robicsek et al., 2004; Della Corte et al., 2012). This alteration causes different nested helical flow patterns in the ascending aorta depending on the BAV fusion phenotype (Hope et al., 2010), as well as a regional abnormal distribution of wall shear stress (WSS) stimuli on the aortic wall (Bissell et al., 2013). Through mechanotransduction pathways, these alterations may trigger altered gene and protein expression, inflammatory processes, and altered regulation of endothelial and smooth muscle cells (Chien, 2006; Chiu and Chien, 2011; Wang et al., 2013; McCormick et al., 2017). Indeed, increased WSS stimuli are associated with extracellular matrix (ECM) dysregulation and elastic fiber degeneration (Guzzardi et al., 2015; Albinsson et al., 2017). Regions with elevated WSS revealed an increase in the concentration of transforming growth factor (TGF)-β1 and activation of aortic wall matrix metalloproteinase (MMP): TGF-β1 is strongly implicated in the mechanotransduction of WSS upstream of flow-induced vascular remodeling (Ohno et al., 1995), while MMP is highly implicated in degradation of elastic ECM components (Chung et al., 2007). Interestingly, differential expression of MicroRNAs, which can modulate mechanotransduction pathways, was detected in the convexity and concavity of the ascending aorta of BAV patients with mild aortic dilation, suggesting a potential role of fluid-dynamics already at the early stage of aortopathy (Albinsson et al., 2017).

To better clarify the potential role of BAV-related aortic flow alterations in the onset and development of aortopathies, recent studies isolated the effects of such alterations in non-dilated aortas through computational fluid dynamics (CFD) and *in vitro* experiments. Cao et al. (2017) used CFD to quantify the WSS acting on the wall of a non-dilated aorta in presence of healthy aortic valve and of BAV with different fusion patterns. That analysis highlighted the alterations in terms of WSS magnitude and time-oscillations induced by the different BAV morphotypes. McNally et al. (2017) achieved similar results through *in vitro* experiments, in which two-dimensional particle image velocimetry (PIV) was used to quantify the velocity distribution and the shear stress distribution in the non-dilated ascending aorta associated to different BAV fusion patterns. In an elegant study (Atkins et al., 2014), integrated the numerical and *in vitro* approaches. Through CFD, the authors computed the highly space- and time-resolved distribution of WSS over the convexity of the aorta in presence of healthy aortic valve and BAV, respectively, and extracted the time-course of WSS at relevant spots. Based on those data, samples of healthy tissue from the extrados of porcine aortas were stimulated for 48 h in highly controlled conditions with healthy and BAV-related WSS histories. In the latter case, the authors observed an increase in the expression of MMPs involved in the degradation of the aortic wall *tunica media*. Although these studies provided relevant evidences, they suffered from some limitations. As BAV-related fluid-dynamics was quantified through CFD, the simplifying assumptions typically characterizing this approach were adopted (e.g., rigid aortic wall and idealized velocity profiles used as inlet boundary conditions). Also, computations were performed with paradigmatic configurations of the thoracic aorta and of the aortic valve.

Recently, 3D time-resolved phase-contrast cardiac magnetic resonance pulse sequences with three-directional velocity-encoding (4D Flow) have been used to direct quantify the *in vivo* fluid dynamics in the aorta, and proved to be a valuable technique to elucidate the role of BAV-related WSS alterations (Bissell et al., 2013; Hope et al., 2014) on a patient-specific basis. In principle, this approach could allow for overcoming the limitations of computational and *in vitro* modeling approaches. Yet, from a technical standpoint, the reliability of WSS computation is challenged by technical limits of 4D Flow sequences, specifically in terms of spatial and temporal resolution of the measured discrete velocity data (Markl et al., 2014). State of the art sequences typically obtain isotropic voxels with a characteristic dimension ranging from 1.5 to 2 mm, while the cardiac cycle is sampled in 20–30 phases, resulting in a temporal resolution of 30–50 ms (Dyverfeldt et al., 2015). Indeed, reliable descriptions of WSS spatial distributions and good reproducibility in WSS estimations were found when comparing BAV patients against control groups (Barker et al., 2012a; Bissell et al., 2013; Van Ooij et al., 2014a), supporting the fact that WSS estimation may have a role as a tool to grade the level of aortopathy progression. Nevertheless, the aforementioned limitations of 4D Flow sequences hamper the accuracy of WSS computations, which have been proved to underestimate expected *in vivo* values up to one order of magnitude (Petersson et al., 2012; Piatti et al., 2016). To reduce the impact of these limitations,

we recently developed a novel method for the quantification of WSSs that was proved to be more accurate as compared to the previous state of the art (Piatti et al., 2016). Also, from a clinical standpoint, published studies typically focused on BAV patients with pre-existing aortic remodeling and aortic valve stenosis (Barker et al., 2012b; Hope et al., 2014; Van Ooij et al., 2014b). These derangements may impact on the quantified fluid dynamic features, making them unsuitable to gain insight on the specific role of WSS in the onset of BAV-related aortopathies.

To test the possible role of WSS alterations as triggers of aortopathy, in the present work we used 4D Flow data to quantify the *in vivo* fluid dynamics and WSS distributions in the thoracic aorta of young normo-functional BAV patients with no clinical evidence of aortic stenosis or aortic wall remodeling, and we quantitatively compared results vs. a cohort of healthy controls.

MATERIALS AND METHODS

Clinical Population and Follow-Up

Five patients with a normo-functional BAV were recruited prospectively at a single university hospital from cardiology clinics, cardiac MRI, and echocardiography sessions. Detailed demographics of the enrolled patients are reported in **Table 1**. 2D cine-MRI images were used to analyze valve function and measure aortic diameters on double oblique planes positioned along the aortic root. Aortic diameter was measured next to the right pulmonary artery. This measurement was repeated at 3-year follow-up to assess potential aortic remodeling. Ten age-matched healthy volunteers (HV, female males, age of 23 ± 7) were enrolled as control group and were free from any known significant medical problem. Both BAV patients and HVs underwent 4D Flow acquisitions. The outcome of follow-up measurements on BAV patients was not known when 4D Flow data were processed. The study complies with the declaration of Helsinki and was approved by the West Berkshire ethics committee, United Kingdom. All participants gave written informed consent.

TABLE 1 | Demographics of BAV patients.

	BAV patients ($n = 5$)
Age [years]	25 ± 10
Sex (Male:Female)	4:1
BSA [m^2]	1.83 ± 0.123
Lesion Cusps (RL:RN:LN)	4:1:0
AI (Mild:Moderate:Severe)	1:0:0
AS (Mild:Moderate:Severe)	4:1:0
AAo [mm]	24.2 ± 2.7
AAo/BSA [mm/m^2]	13.3 ± 2.1
Hear rate [bpm]	61 ± 5
Cardiac Output [l/min]	5.2 ± 1.0
Peripheral Diastolic Blood Pressure [mmHg]	58 ± 7
Peripheral Systolic Blood Pressure [mmHg]	113 ± 8
Mean Arterial Pressure [mmHg]	76 ± 9
COMORBIDITIES	
Cardiovascular problems	none
Hay fever	2
Heart burn	1
Gastritis	1

BAV, Bicuspid aortic valve; BSA, body surface area; RL, right-left fusion; RN, right and non-coronary fusion; LN, left and non-coronary fusion; AI, aortic insufficiency; AS, aortic stenosis; AAo, ascending aorta diameter. Values are displayed as mean ± SD.

4D Flow Acquisitions

4D flow acquisitions were performed at John Radcliffe Hospital (Oxford, United Kingdom) on a 3.0 T MR system (Trio, Siemens, Erlangen, Germany). Flow-sensitive gradient-echo pulse sequence MRI was used to characterize and quantify blood flow in the thoracic aorta. Datasets were acquired with prospective ECG-gating during free-breathing, using a respiratory navigator. The volume of acquisition was oriented along an oblique-sagittal plane encompassing the ascending aorta, the aortic arch, and the thoracic aorta. 4D Flow sequences were performed with the following parameters: echo time = 2.29–2.63 ms, repetition time = 38.4–41.6 ms, flip angle = 7°, voxel size = 1.46–1.67 × 1.46–1.67 × 1.8–2.2 mm^3, temporal resolution = 50.72–76.91 ms. The velocity-encoding range (VENC) was properly determined using the lowest non-aliasing velocity on scout measurements, resulting in 1.3–1.5 m/s and 1.5–1.9 m/s for HVs and BAV patients, respectively.

4D Flow Data Processing

Through *ad-hoc* in-house software implemented in MATLAB (The MathWorks Inc., Natick, MA, United States), 4D Flow data were analyzed through a semi-automated pipeline that consisted of five steps.

The first step consisted of 4D flow velocity data encoding and pre-filtering. Phase-contrast images of each encoded flow direction (**Figure 1A**) were scaled by the corresponding VENC value to obtain the Cartesian velocity components (Markl et al., 2011). Velocity components were automatically processed to correct from eddy current errors, velocity aliasing and to decrease MR noise through median filtering (Bock et al., 2007). The Euclidean norm of the 3D velocity vectors was then computed based on the Cartesian components for all acquired time frames to obtain the magnitude intensity of the velocity vector (**Figure 1B**).

In the second step, through visual inspection of the dataset, the time-frame with the highest velocity-to-noise ratio was identified as the most representative of peak systole. At the selected time-frame, four landmarks were manually positioned inside the acquired volume at locations corresponding to the left ventricle outflow tract (LVOT), right pulmonary artery (PA), brachiocephalic artery (BrA), and the most distal visible point of the descending aorta (DeA; **Figure 1C**). Moreover, the 3D geometry of the aortic lumen was defined. The boundaries of the lumen were manually traced to define the region of interest (ROI) on each para-sagittal slice of the 4D Flow volume (**Figure 1D**). Tracing resulted in a 2D binary mask associating a value equal to 1 to the voxels inside the traced boundary, and equal to 0 otherwise. A 3D binary mask was obtained merging the 2D masks (**Figure 1E**). Subsequently, the aortic wall and the

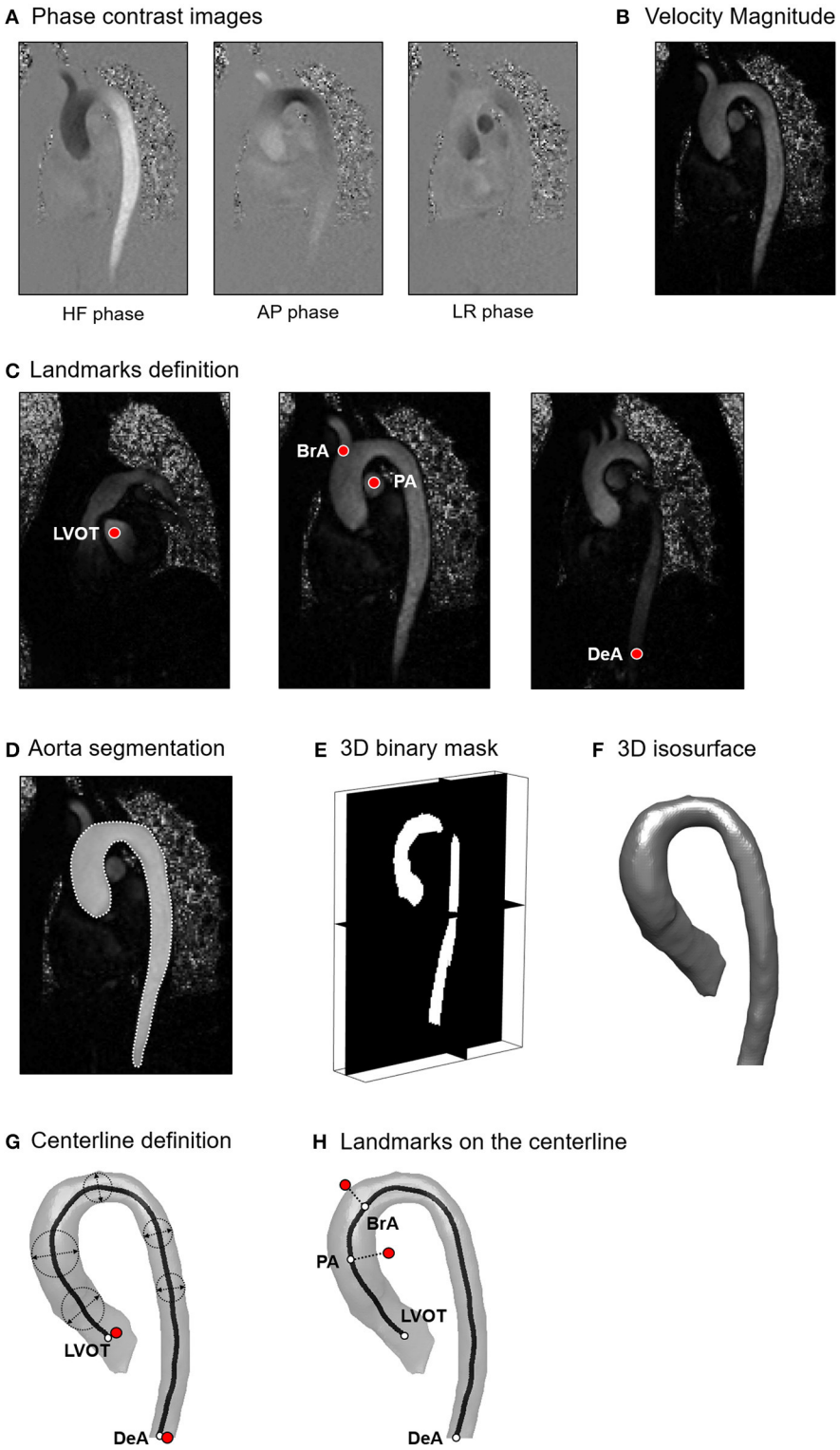

FIGURE 1 | (A) Phase contrast images encoded for Head-Foot (HF), Antero-Posterior (AP) and Left-Right (LR) directions; **(B)** Magnitude intensity of the velocity vector computed as the Euclidean norm of the 3D velocity vectors. **(C)** Definition of anatomically relevant landmarks of the aortic lumen: left ventricle outflow tract (LVOT), brachiocephalic artery (BrA), right pulmonary artery (PA), distal point of the descending aorta (DeA); **(D)** Tracing of the aortic lumen boundaries; **(E)** 3D binary mask obtained from the stack of manually traced slices; **(F)** 3D isosurface of the aortic lumen; **(G)** Computation of the vessel centerline; **(H)** Projection of the identified landmarks on the centerline.

centerline of the aorta were automatically defined. The wall was identified as the closed iso-surface encompassing the borders of the 3D binary ROI, and it was smoothed through Laplacian diffusion filtering (Desbrun et al., 1999) to obtain a regularized surface mesh (**Figure 1F**). The centerline of the vessel wall was obtained through skeletonization of the ROI (Shih, 2010); the points defining the skeleton were ordered end-to-end via Dijkstra algorithm (Dijkstra, 1959), specifying the projections of LVOT and DeA landmarks on the skeleton as starting and ending points, respectively (**Figure 1G**). The resulting ordered points were fitted with non-uniform rational bi-cubic spline (NURBS) curve interpolation that was smoothed via 5th order moving average filtering to obtain the centerline of the vessel wall. PA and BrA landmarks were finally projected to the closest points on the centerline (**Figure 1H**).

In the third step, aorta cross-sections were defined along the vessel's centerline. Starting from LVOT, a set of equally spaced points $\mathbf{P}_i$ was automatically generated on the vessel centerline, prescribing a distance Δx between consecutive points $\mathbf{P}_i$ and $\mathbf{P}_{i+1}$ equal to the average voxel dimension of the dataset (**Figure 2A**). Each point $\mathbf{P}_i$ and its corresponding unit vector $\mathbf{x'}_3$ locally tangent to the centerline were used to automatically define a cross-section π_i passing through $\mathbf{P}_i$ and normal to $\mathbf{x'}_3$ (**Figure 2B**). For each voxel whose center $\mathbf{C}_j$ was located within $0.5^*\Delta x$ from π_i, the projection ($\mathbf{C'}_j$) of $\mathbf{C}_j$ was computed (**Figure 2B**), and the three velocity components ($\mathbf{u}_{1j}$, $\mathbf{u}_{2j}$, $\mathbf{u}_{3j}$) measured at $\mathbf{C}_j$ were associated to $\mathbf{C'}_j$. The discrete velocity values obtained over π_i were interpolated through cubic splines to increase the spatial resolution of data, and velocity components were transformed into the local reference system ($\mathbf{x'}_1$, $\mathbf{x'}_2$, $\mathbf{x'}_3$; **Figure 2C**). In addition, for each point $\mathbf{C'}_{B,l}$ of π_i belonging to the boundary of the vessel wall Γ_π, a second local reference system was defined, which consisted of the local inward normal to the wall surface, assumed as the radial direction $\mathbf{x'}_{r,l}$, the normal to the cross section $\mathbf{x'}_3$, assumed as the longitudinal direction, and the cross product of $\mathbf{x'}_{r,l}$ by $\mathbf{x'}_3$, assumed as the circumferential direction $\mathbf{x'}_{t,l}$ (**Figure 2D**).

In the fourth step, the aortic bulk flow was automatically quantified. Velocity data of each cross-section were processed to compute the variables of interest:

(i) Vessel cross-sectional area A_i, as the surface of the piecewise linear polygon defined by the boundary points $\mathbf{C'_{B,l}}$;
(ii) Equivalent diameter $D_i = 2 \cdot \sqrt{A_i}/\pi$;
(iii) Net flow rate waveform $Q_i(t)$. At each time-frame t_k, $Q_i(t_k) = \frac{A_i}{N_i}\sum_1^N v'_3(t_k)$, where N_i is the number of data points over the i-th cross section. The time-frames corresponding to peak systole (T_{Ps}) and to the end of systole (T_{Es}) were automatically identified based on $Q_i(t)$, as the maximum point and as the last point of the descending phase of $Q_i(t)$, respectively. The mid time-frame in the $T_{Ps} - T_{Es}$ transitory was considered as the mid-deceleration time point (T_{dec});
(iv) Peak flow rate $\left(Q_{max}^{LVOT}\right)$ and stroke volume (SV) at the level of the LVOT. SV was estimated as the area under $Q_i(t)$, via trapezoidal method between the first time-frame, i.e., the onset of systole, and T_{Es};
(v) Peak and mean values of velocity magnitudes ($\mathbf{|V|_{i\_max}}$ and $\mathbf{|V|_{i\_mean}}$, respectively);
(vi) Flow jet angle ($\alpha_{\pi i}$), defined as the angle between the mean positive velocity vector, i.e., the average of vectors with positive component v'_3, and $\mathbf{x'}_3$ (Sigovan et al., 2011);
(Vii) Normalized flow displacement ($\mathbf{d}_{\pi i}$), defined as the distance between the center of velocity and the center of the lumen $\mathbf{P}_i$ (Sigovan et al., 2011).

$\mathbf{|V|_{i\_max}}$, $\mathbf{|V|_{i\_mean}}$, $\alpha_{\pi i}$ and $\mathbf{d}_{\pi i}$ were computed at three consecutive time-frames centered in T_{ps}. The analysis was focused on two specific sectors of the ascending aorta: the proximal tract, running from LVOT to PA landmarks, and the distal tract, running from PA to BrA.

The values of the listed hemodynamic variables computed in BAV patients were compared off-line vs. those computed for HVs with non-parametric Mann–Whitney t-test, adopting a $p = 0.05$ as statistically significant, using GraphPad Prism 7 (GraphPad Software, Inc., La Jolla, CA, USA).

In the fifth step, the distribution of WSS vectors ($\overrightarrow{WSS}$) acting on the aortic endothelium was quantified. To this aim, the stresses tensor τ_{ij} was computed at the boundary of the fluid domain under the assumption of Newtonian blood rheological

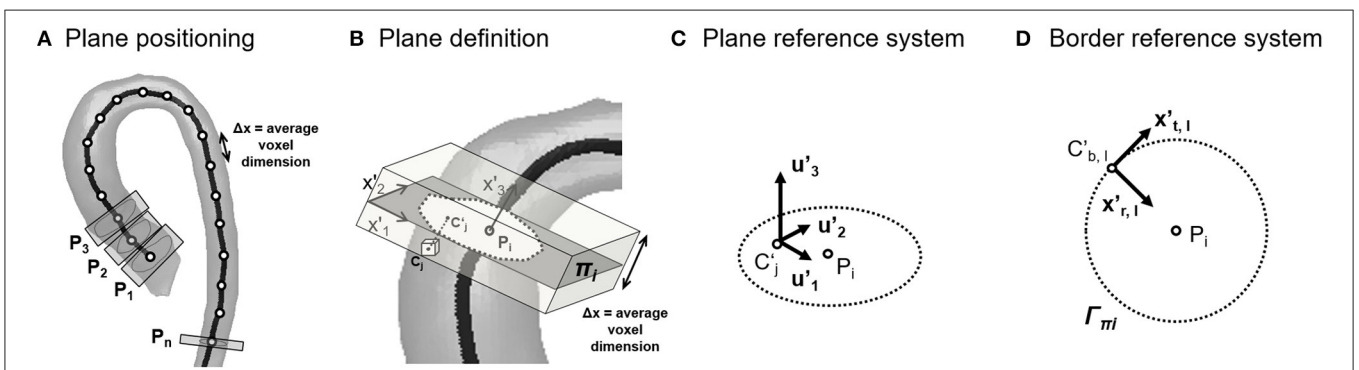

FIGURE 2 | (A) Position along the centerline of the points (P_i) used to define the cross-sections of the aortic lumen; **(B)** On each cross-section, original discrete velocity points (C_j) enclosed by the segmentation and within a tolerance (0.51 of a voxel) were projected as (C'_j) on the plane (π_i) and interpolated. According to the orientation of the cross-section, local reference systems were defined inside the vessel lumen **(C)** and on the vessel's wall **(D)**.

behavior (Baskurt and Meiselman, 2003):

$$\tau_{ij} = \mu \left(\frac{\partial u_i}{\partial x_j} + \frac{\partial u_j}{\partial x_i} \right) \quad with\ i \neq j$$

where viscosity μ was set to 3.7cP (Baskurt and Meiselman, 2003), and spatial derivatives of velocities were computed numerically. In the local reference system $\mathbf{x'}_{r,l}$, $\mathbf{x'}_{t,l}$, $\mathbf{x'}_3$, where $\mathbf{x'}_{r,l}$ is the local inward normal to the aortic wall, the 3D vector $\mathbf{T}$ was computed as:

$$\boldsymbol{T} = \tau \cdot \boldsymbol{x'_{r,l}}$$

The 3D shear stress vector $\overrightarrow{WSS}$ was then computed as:

$$\overrightarrow{WSS} = \boldsymbol{x'_{r,l}} \times \left(\boldsymbol{T} \times \boldsymbol{x'_{r,l}} \right)$$

The axial ($\overrightarrow{WSS}_{Axial}$) and circumferential ($\overrightarrow{WSS}_{Circ}$) components of $\overrightarrow{WSS}$ were finally obtained by projecting $\overrightarrow{WSS}$ on the local axes $\mathbf{x'_3}$ and $\mathbf{x'_{t,l}}$, respectively.

$\overrightarrow{WSS}$ was computed throughout the systolic phase, i.e., from the first time-frame to $\mathbf{T_{Es}}$. As in a recent work of our group (Piatti et al., 2016), the numerical computation of the spatial derivatives of velocity was performed through two novel methods.

The first method, named Global Volumetric (GV), is based on the use of 3D Sobel filters to compute voxelwise the components of the strain rate tensor and yielded the distribution of $\overrightarrow{WSS}_{GV}$ for each point of the triangular elements of the surface representing the aortic wall. We showed previously that this method correctly captures the spatial trends in $\overrightarrow{WSS}$, despite underestimating pointwise values (Piatti et al., 2016). Additionally, the oscillations in time of $\overrightarrow{WSS}_{GV}$ were computed by means of the Oscillatory Shear Index (OSI), of the Relative Residence Time (RRT), and of the Transversal WSS (TransWSS), as defined in **Table 2** (Soulis et al., 2011; Jahangiri et al., 2015; Mohamied et al., 2017). Specifically, the OSI quantifies changes in $\overrightarrow{WSS}$ direction during time, and ranges from 0.0 to 0.5 as $\overrightarrow{WSS}$ rotates by 0° to 180°. The OSI was computed also for the single components $\overrightarrow{WSS}_{Axial}$ and $\overrightarrow{WSS}_{Circ}$, obtaining the two indexes OSI_{Ax} and OSI_{Circ} (Supplementary Material). RRT combines the effect of time-averaged WSS vector magnitude at a given region of the endothelium with its corresponding OSI value: RRT gets lower as $\overrightarrow{WSS}$ increases and OSI decreases, i.e., when locally the wall is loaded by fast and constant flow jets, and it gets greater as $\overrightarrow{WSS}$ decreases and OSI increases, i.e., when the wall is loaded by slow and highly time-dependent flow jets. TransWSS measures the component of the $\overrightarrow{WSS}$ that is perpendicular to the time-averaged $\overrightarrow{WSS}$, representative of the average direction of the flow. This metric is hence defined in a reference frame based on the flow direction and not on the geometry of the vessel wall.

The second method, named Local Planar (LP), was adopted to obtain the distribution of $\overrightarrow{WSS}_{LP}$ for specific locations of the vessel wall based on the velocity values over a single vessel cross-section. As demonstrated in Piatti et al. (2016), this approach allows for improving the pointwise quantification of $\overrightarrow{WSS}$. It is based on the application of 2D derivative filters; in Piatti et al. (2016), 2D Sobel filters were exploited to compute the components of the strain rate tensor, while in the present study B-Spline based filters (Hast, 2014) were used, owing to the improved results verified through preliminary benchmarking (unpublished data). $\overrightarrow{WSS}_{LP}$ was characterized in terms of magnitude and angle that quantifies the deviation of $\overrightarrow{WSS}_{LP}$ from the longitudinal, i.e., axial, direction of the vessel (for a 0° angle, the WSS vector is purely axial and points downstream from the considered cross-section; for 90° angle, the WSS vector is purely circumferential; for a 180° angle, the WSS vector is again purely axial, but points upstream of the considered cross-section).

TABLE 2 | Definition of time-averaged WSS magnitude (AWSS), time-averaged WSS vector (AWSSV), Oscillatory Shear Index (OSI), Relative Residence Time (RRT), and Transversal WSS (TransWSS).

Variable	Definition
AWSS [Pa]	$\frac{1}{T}\int_0^T \left\lvert \overrightarrow{WSS} \right\rvert dt$
AWSSV [Pa]	$\frac{1}{T}\left\lvert \int_0^T \overrightarrow{WSS} dt \right\rvert$
OSI [–]	$0.5 \cdot \left(1 - \frac{AWSSV}{AWSS}\right)$
RRT [Pa^{-1}]	$\left[(1 - 2.0 \cdot OSI) \cdot AWSS\right]^{-1}$
TransWSS [Pa]	$\left\lvert \overrightarrow{WSS} \right\rvert \cdot \left(\vec{n} \wedge \frac{\int_0^T \overrightarrow{WSS} dt}{\left\lvert \int_0^T \overrightarrow{WSS} dt \right\rvert} \right)$

Representation of Results at the Aortic Wall

The analysis of $\overrightarrow{WSS}_{GV}$, OSI and RRT data was focused on the ascending aorta, i.e., on the tract of the vessel running from LVOT to BrA. $\overrightarrow{WSS}_{GV}$ values were averaged over three time-frames centered in $\mathbf{T_{ps}}$. To rule out the effects of inter-subject anatomical variability when comparing different aortas, $\overrightarrow{WSS}_{GV}$, OSI and RRT data were represented in terms of heat maps over a normalized 2D template (**Figure 3A**). The position of points in the relevant tract of the aortic wall was expressed in terms of: (i) normalized longitudinal position s along the centerline with $s = 0$ at LVOT and $s = 1$ at BrA; (ii) given a cross section at $s = \hat{s}$, normalized circumferential position $r(\hat{s})$ along the boundary of the cross-section ($r = 0$ at the most anterior point, and increases when moving counterclockwise over the boundary). The 2D template was sub-divided into 8 sectors with respect to LVOT, PA and BrA landmarks and anatomical short axis orientations (Antero: A; Posterior: P; Right: R; Left: L; **Figure 3B**).

RESULTS

Aortic Growth at 3-Year Follow Up

No clinically relevant increase in diameter was measured at 3-year follow-up. On patients BAV02-BAV05, an increase in diameter by <1.5 mm was measured, which is below the threshold indicated by guidelines as symptom of disease progression (0.5 mm/year, Della Corte et al., 2013). On patient BAV01, an increase in diameter by 1.8 mm was measured, which

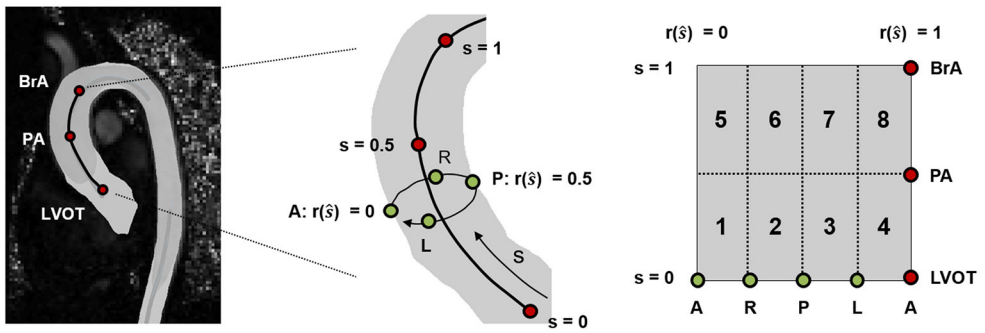

FIGURE 3 | (A) Definition of the normalized reference system used to map on a 2D template the spatial localization of points on the 3D aortic wall. The longitudinal position of points is represented by s ($s = 0$ at LVOT and $s = 1$ at BrA). For a given cross section at $s = \hat{s}$, the circumferential position is represented by r($\hat{s}$). **(B)** Sub-division of the 2D template into 8 sectors based on the anatomical landmarks (LVOT, PA, BrA) and orientation points (Antero: A, Posterior: P, Left: L, Right: R).

was equivalent to a yearly growth rate of 0.6 mm/year, only slightly above the threshold. However, 1.8 mm is comparable to the in-plane resolution of the cine-MRI images used to perform the measurements, and indeed no macroscopic remodeling of the aorta could be observed.

Aorta Bulk Flow

For all the analyzed datasets, streamlines over the whole acquired domain within the ROI were computed and visualized using ParaView (Sandia Corporation, Kitware Inc., Albuquerque, NM, USA) at $t = T_{ps}$ and $t = T_{dec}$ (**Figure 4**).

Qualitatively, HVs were systematically characterized by a centered and nearly laminar flow in the entire ROI, as exemplified by dataset HV02 (**Figure 4**). At T_{ps}, macroscopic secondary flows were absent, but were observed at T_{dec} close to the intrados of the ascending aorta. All normo-BAV patients presented altered secondary flows at T_{ps}, owing to the BAV deflected jet (**Figure 4**, white asterisks). The jet was directed anteriorly, toward the extrados of the aorta, in patients characterized by RL leaflet fusion (BAV01-BAV04). The jet was directed posteriorly, toward the intrados, in case of RN fusion (BAV05). Also, aberrant flows were observed in the distal curvature of the aortic arch in BAV01 and BAV05 patients. At T_{dec}, the same pattern of secondary flows observed in HVs was observed also in BAV01, BAV03, and BAV04. The pattern was somewhat complementary, with disturbances displaced toward the extrados of the ascending aorta, in the only case of RN fusion (BAV05). More evident flow disturbances represented by helicoidal structures were observed all over the ascending aorta and arch in BAV02.

In BAV patients Q_{max}^{LVOT} and SV values ranged from 12.6 to 26.3 l/min and from 80 to 156 ml/beat, respectively. These values were slightly higher as compared to those obtained for HVs, which ranged from 18.4 to 30.3 l/min and from 62 to 135 ml/beat, respectively. However, these differences were not statistically significant ($p = 0.44$ and $p = 0.68$, respectively).

For HVs and BAV patients, the peak value of $|\mathbf{V}|_{\mathbf{i\_max}}$ and D_i and the average value of $|\mathbf{V}|_{\mathbf{i\_mean}}$, $\boldsymbol{\alpha}_{\pi i}$ and $\mathbf{d}_{\pi i}$ over the centerline of the ascending aorta were considered for the two tracts LVOT-PA and PA-BrA (**Table 3**). No statistically significant differences were observed between the two groups in terms of peak D_i in the LVOT–PA tract ($p = 0.31$) nor in the PA–BrA tract ($p = 0.25$). Statistically significant differences between HVs and BAVs ($p = 0.04$) were found only for the peak values of $|\mathbf{V}|_{\mathbf{i\_max}}$ in the LVOT–PA tract, and for the average value of $\boldsymbol{\alpha}_{\pi i}$ in the PA–BrA tract. Non-negligible though not statistically significant differences were observed for the average value of $|\mathbf{V}|_{\mathbf{i\_mean}}$ in both tracts ($p = 0.05$ in the LVOT-PA tract, $p = 0.07$ in the PA-BrA tract), and for the peak value of $|\mathbf{V}|_{\mathbf{i\_max}}$ ($p = 0.05$) in the PA–BrA tract.

Fluid-Dynamic Stimuli on the Aortic Wall

For HVs, the heat maps of the 10th, 50th, and 90th percentiles of the $|\overrightarrow{WSS}_{GV}|$, OSI and RRT distribution in this group (**Figures 5A**, **6A**, **7A**) were used as term of comparison for the heat maps obtained for each BAV patient (**Figures 5B**, **6B**, **7B**).

In the HVs population, $|\overrightarrow{WSS}_{GV}|$ values were higher in the posterior and anterior sides of the wall of the distal ascending aorta, i.e., from PA up to BrA (posterior: 1.08 ÷ 1.13 Pa, anterior 0.90 ÷ 1.22 Pa), while lower values were detected in the lateral sides (right: 0.58 ÷ 0.80 Pa, left: 0.40 ÷ 0.56 Pa (**Figure 5A**). In the proximal ascending aorta (i.e., sectors immediately downstream of LVOT), $\left|\overrightarrow{WSS}_{GV}\right|$ was uniformly redistributed over the circumferential extent of the vessel wall, but with a high inter-subject variability (range: 0.20 ÷ 1.19 Pa), as underscored by the differences between 10th and 90th percentile heat maps. In BAV patients, a high inter-subject variability of $|\overrightarrow{WSS}_{GV}|$ distribution was evident all over the wall of the ascending aorta, with different patient-specific localizations and extent of high and low $|\overrightarrow{WSS}_{GV}|$ regions (**Figure 5B**).

For both HVs and BAV patients, the distribution of OSI was consistent with the one of $|\overrightarrow{WSS}_{GV}|$. For instance, in HVs the 50th percentile heat map showed regions of high OSI at the right and left side of the distal ascending aorta (right: 0.24 ÷ 0.38, left: 0.21 ÷ 0.28; **Figure 6A**), which corresponded to low WSS regions. A similar correspondence between low $|\overrightarrow{WSS}_{GV}|$ regions and high

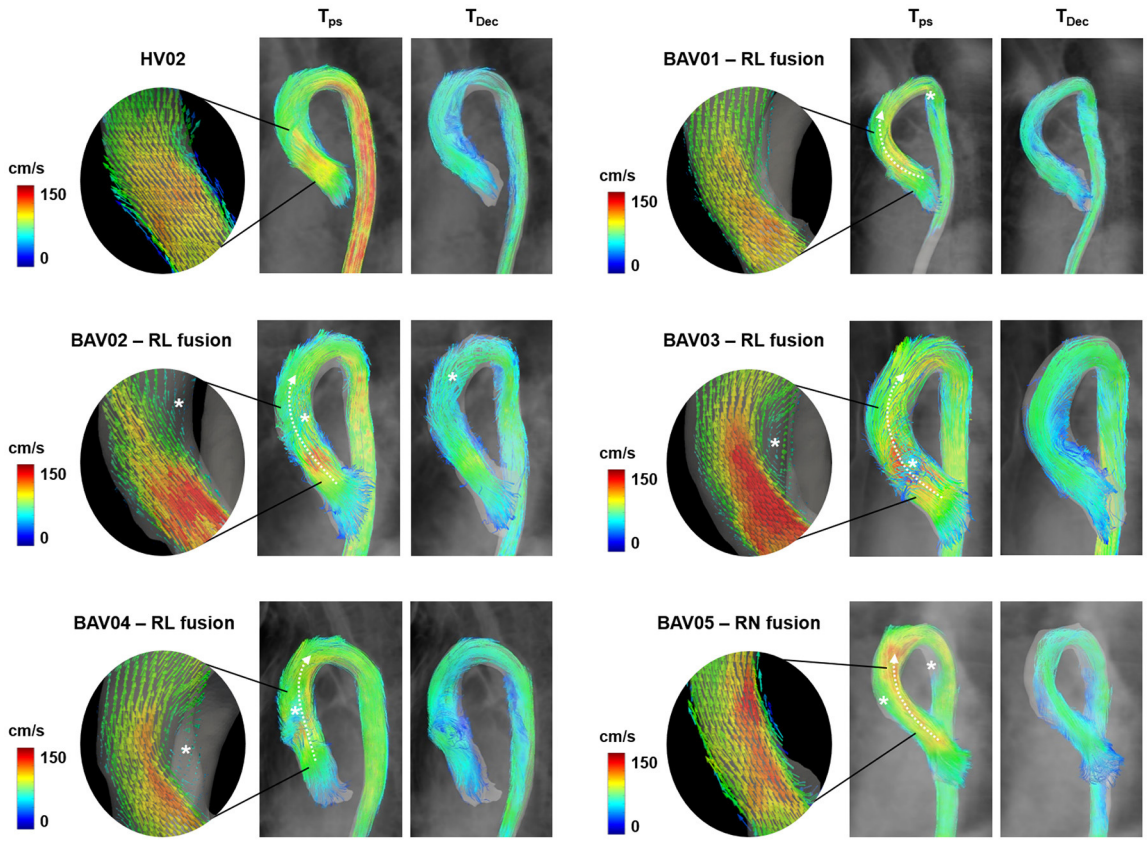

FIGURE 4 | Visualization of 3D blood flow streamlines within the aortic lumen at the time-frames corresponding to peak-systole (T_{ps}) and to mid-deceleration phase (T_{Dec}). In rounded panels, the features of blood flow jet across the aortic valve during systolic ejection are highlighted through vectors projected on a long-axis view of the left ventricle outflow tract. White asterisks are reported in presence of macroscopic altered secondary flows.

TABLE 3 | Hemodynamic variables computed along the centerline for HV and BAV patients, from LVOT to PA and from PA to BrA landmarks.

	LVOT-PA			PA-BrA		
	HV	**BAV**	***p***	**HV**	**BAV**	***p***
D_{max} [mm]	29.9 ÷ 20.5	28.8 ÷ 23.4	0.31	28.9 ÷ 20.4	29.0 ÷ 19.4	0.25
$\|V\|_{max}$ [cm/s]	179.7 ÷ 116.4	204.6 ÷ 137.0	**0.04**	146.1 ÷ 84.6	205.5 ÷ 117.6	0.05
$\|V\|_{mean}$ [cm/s]	97.1 ÷ 56.5	117.8 ÷ 77.9	0.05	82.1 ÷ 53.6	107.9 ÷ 64.0	0.07
d_π [–]	0.12 ÷ 0.04	0.07 ÷ 0.06	0.79	0.08 ÷ 0.03	0.09 ÷ 0.03	0.91
α_π [°]	12.8 ÷ 6.7	14.3 ÷ 7.4	0.77	21.8 ÷ 9.2	13.0 ÷ 7.6	**0.04**

Statistically significant differences ($p < 0.05$) are reported in bold.

OSI values could be observed for most locations of the heat maps obtained for BAV patients, thus preserving a high inter-subject variability in the distribution of OSI values (**Figure 6B**). The decomposition of the OSI along the circumferential and axial directions of the vessel showed that in BAV patients extended regions of the aortic wall were characterized by OSI_{Ax} values exceeding the 90th percentile of the distribution observed in HVs (Supplementary Figure 1). These regions were consistent with those characterized by extremely high value of the OSI computed for the full WSS vector (**Figure 6B**). By contrast, in BAV patients wide regions of the aortic wall were characterized by OSI_{Circ} values that were below the 10th percentile of the distribution observed in HVs (Supplementary Figure 2).

RRT heat maps consistently combined the features observed for OSI and $|\overrightarrow{WSS}_{GV}|$ (**Figure 7**).

Differently from the previously reported metrics, the TransWSS was characterized by a lower inter-subject variability over the HVs: the only exception consisted in the posterior-left region, where TransWSS ranged from 0.06 to 0.39 Pa (**Figure 8**). Also, all BAV patients were characterized by spread regions with abnormally high or low TransWSSs. These differences were observed particularly in the distal ascending aorta, i.e.,

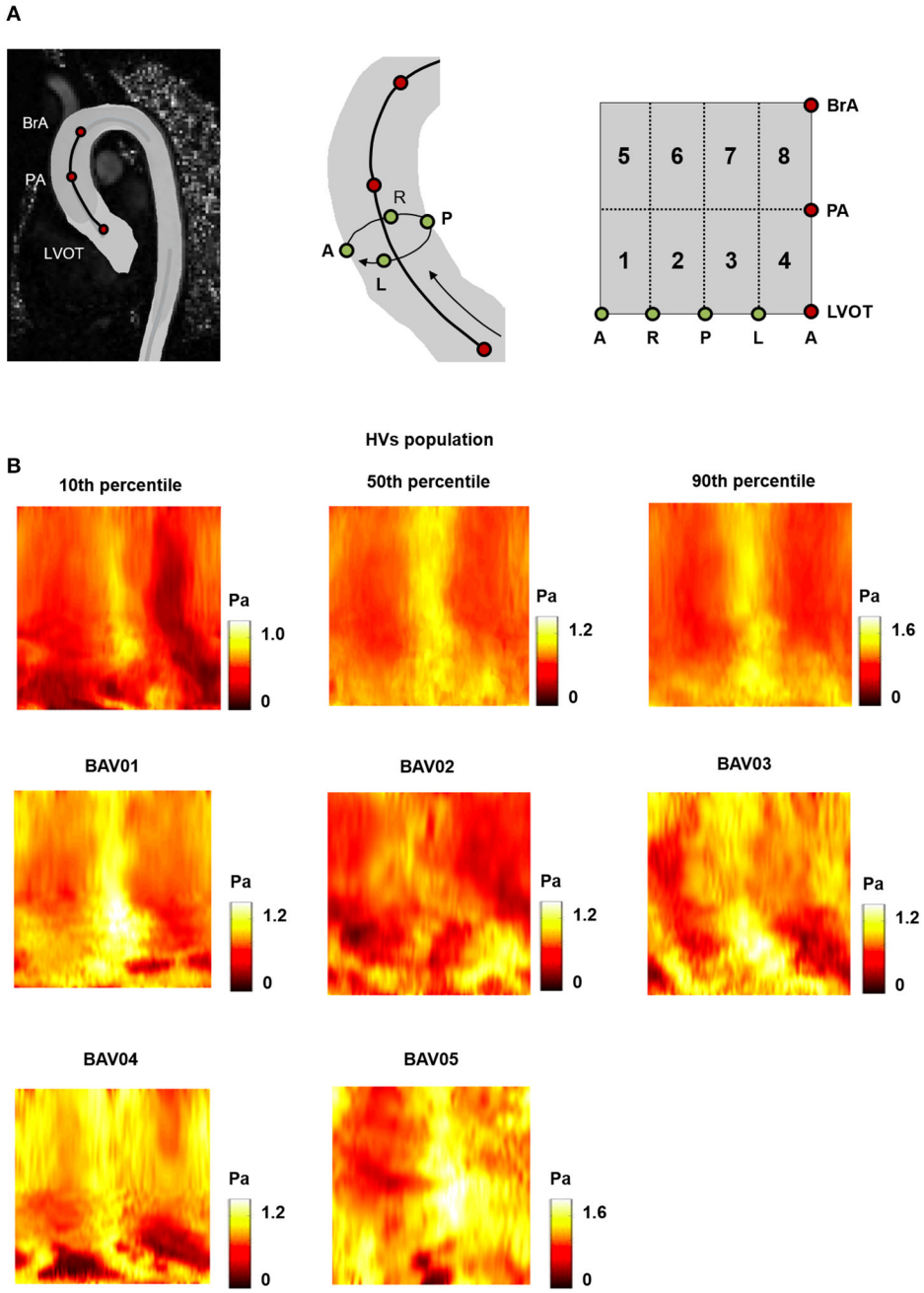

FIGURE 5 | (A) The 2D template detailed in **Figure 3** is reported for the sake of clarity. **(B)** Wall Shear Stress (WSS) heat maps for HVs (represented as 10th, 50th, and 90th percentiles) and for each BAV patient obtained at peak systole.

from PA up to BrA, with values ranging from 0.03 Pa to 0.51 Pa (**Figure 8**).

To better highlight the patient-specific deviations of BAV patients from the HVs distribution, HV-relative heat maps were also obtained and represented on the same 2D template for each wall-related variable, with an approach resembling the one used in Van Ooij et al. (2014b). Specifically, each point on the wall of the ascending aorta was classified based on whether the corresponding value of the relevant variable was (i) abnormally high, i.e., higher than HVs 90th percentile, (ii) abnormally low, i.e., lower than HVs 10th percentile, (iii) between HVs 50th and 90th percentiles, (iv) between HVs 10th and 50th percentiles (**Figure 9**).

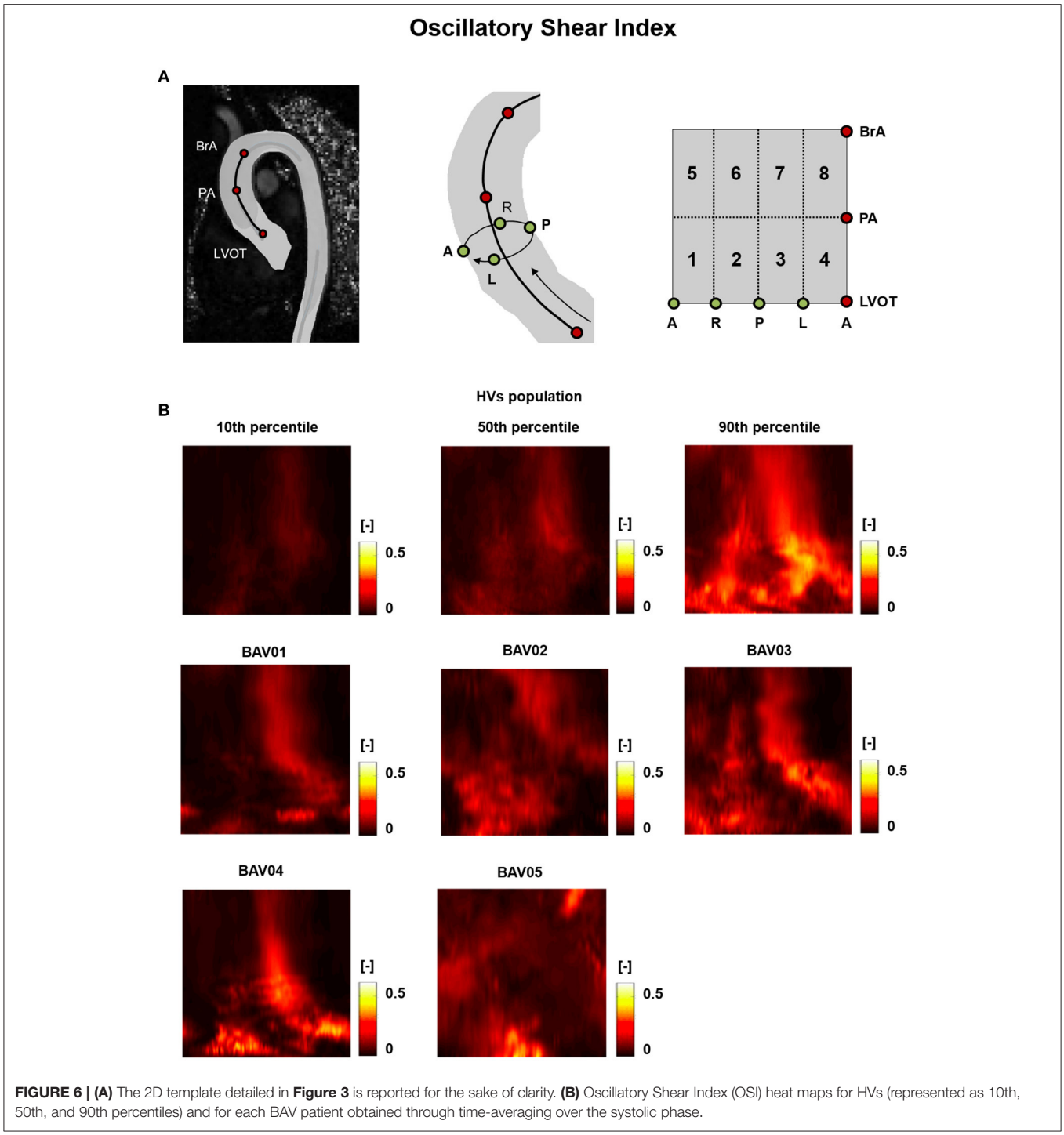

FIGURE 6 | (A) The 2D template detailed in **Figure 3** is reported for the sake of clarity. **(B)** Oscillatory Shear Index (OSI) heat maps for HVs (represented as 10th, 50th, and 90th percentiles) and for each BAV patient obtained through time-averaging over the systolic phase.

When considering BAV patients with RL fusion (BAV01-BAV04), localized regions with abnormally high $|\overrightarrow{WSS}_{GV}|$ values were detected for patient BAV02. Wide regions with abnormally high $|\overrightarrow{WSS}_{GV}|$ were detected on the distal ascending aorta of BAV03 and BAV04, and on the proximal ascending aorta of BAV01. Detected values exceeded the HV 90th percentile by up to 27.3, 27.3, 30.5, 45.8% for BAV01-BAV04, respectively. Regions of abnormally low $|\overrightarrow{WSS}_{GV}|$ were localized distally in BAV03 or proximally in BAV04, as well as in large portions of the anterior and posterior ascending aorta of BAV02. For patient BAV05, characterized by RN fusion, a pervasive abnormal increase in $|\overrightarrow{WSS}_{GV}|$ was evident: around 72% of the wall of the ascending aorta was subject to abnormally high $|\overrightarrow{WSS}_{GV}|$ values, which exceeded the HV 90th percentile by up to 131.7% (**Figure 9A**).

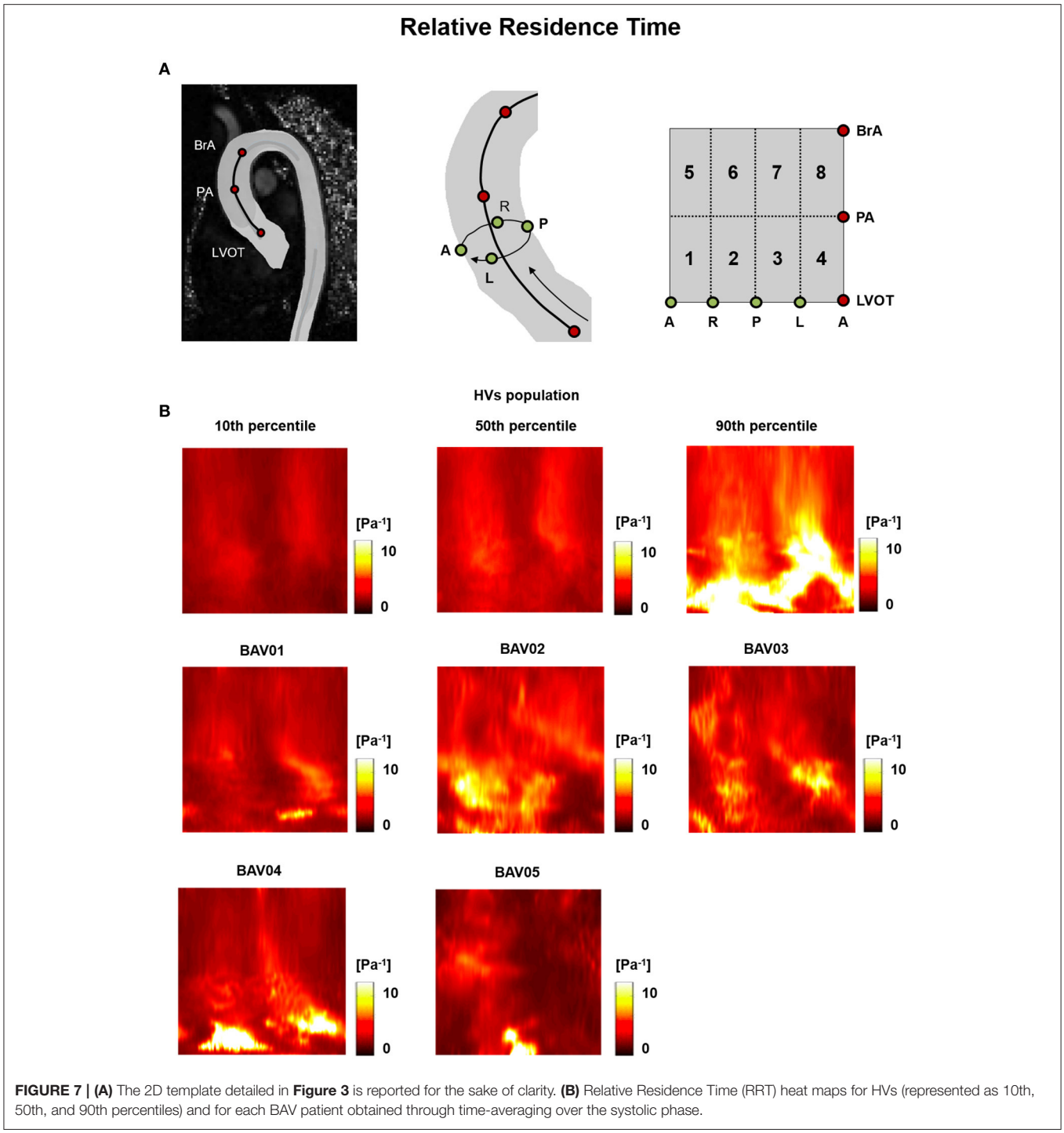

FIGURE 7 | (A) The 2D template detailed in **Figure 3** is reported for the sake of clarity. **(B)** Relative Residence Time (RRT) heat maps for HVs (represented as 10th, 50th, and 90th percentiles) and for each BAV patient obtained through time-averaging over the systolic phase.

Regions characterized by abnormally high OSI values were found in the anterior sectors of the ascending aorta of patients from the RL fusion cohort (BAV02, BAV03) and for the patient with RN fusion (BAV05). In BAV04, few regions of abnormally high OSI values were found proximally, while abnormally low OSI values were computed in the distal left-extrados of the aortic wall. Of note, BAV01 was free from abnormally high OSI values, but was characterized by abnormally low OSI values over 22% of the ascending aorta wall (**Figure 9B**). Overall, RRT HV-relative heat maps showed a complementary pattern as compared to the obtained for $|\overrightarrow{WSS}_{GV}|$ values, thus confirming the prevalent contribution of $|\overrightarrow{WSS}_{GV}|$ over OSI in determining the value of RRT. This predominant behavior of $|\overrightarrow{WSS}_{GV}|$ was particularly evident in the anterior regions of the ascending aorta of BAV05 characterized by high values of both $|\overrightarrow{WSS}_{GV}|$ and OSI

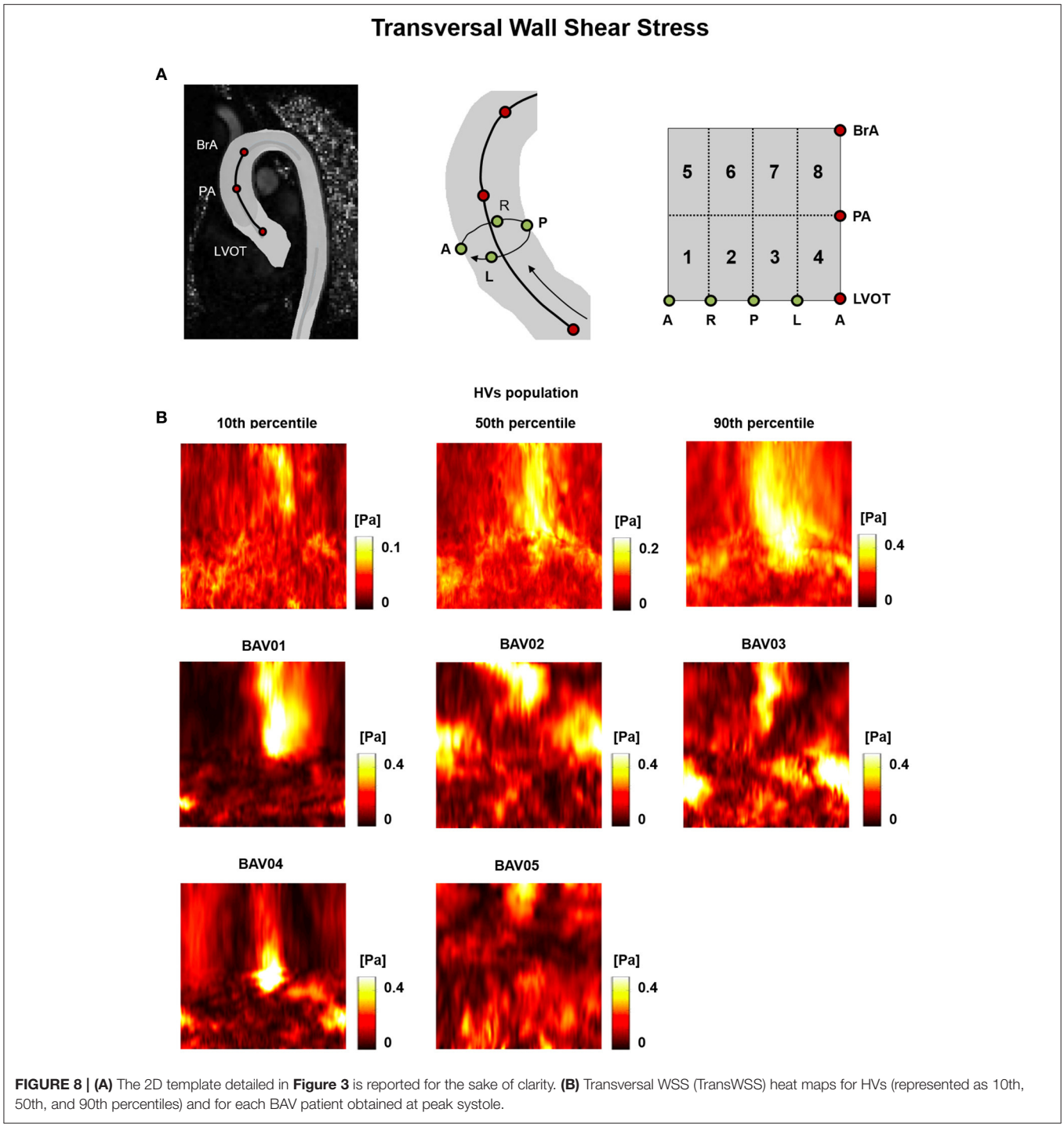

FIGURE 8 | (A) The 2D template detailed in **Figure 3** is reported for the sake of clarity. **(B)** Transversal WSS (TransWSS) heat maps for HVs (represented as 10th, 50th, and 90th percentiles) and for each BAV patient obtained at peak systole.

(**Figure 9C**). Considering the HV-relative maps of TransWSS computed at peak systole, BAV patients were characterized by ubiquitous differences with respect to the HVs population, both in regions above HV 90th percentile and below HV 10th percentile. These differences appeared more widely spread on the aortic wall for all BAV patients as compared to the patterns obtained for the other computed indexes (**Figure 9D**).

Furthermore, six different hot-spots were selected (**Figure 9A**) on HV-relative $|\overrightarrow{WSS}_{GV}|$ heat maps of different BAV patients. These hot spots were selected because they were characterized by different combinations of $|\overrightarrow{WSS}_{GV}|$, OSI and RRT HV-relative classifications. At each selected hot spot, the time-course of magnitude and orientation of $\overrightarrow{WSS}_{LP}$ was computed. For both features, the time-course was compared to the time dependent

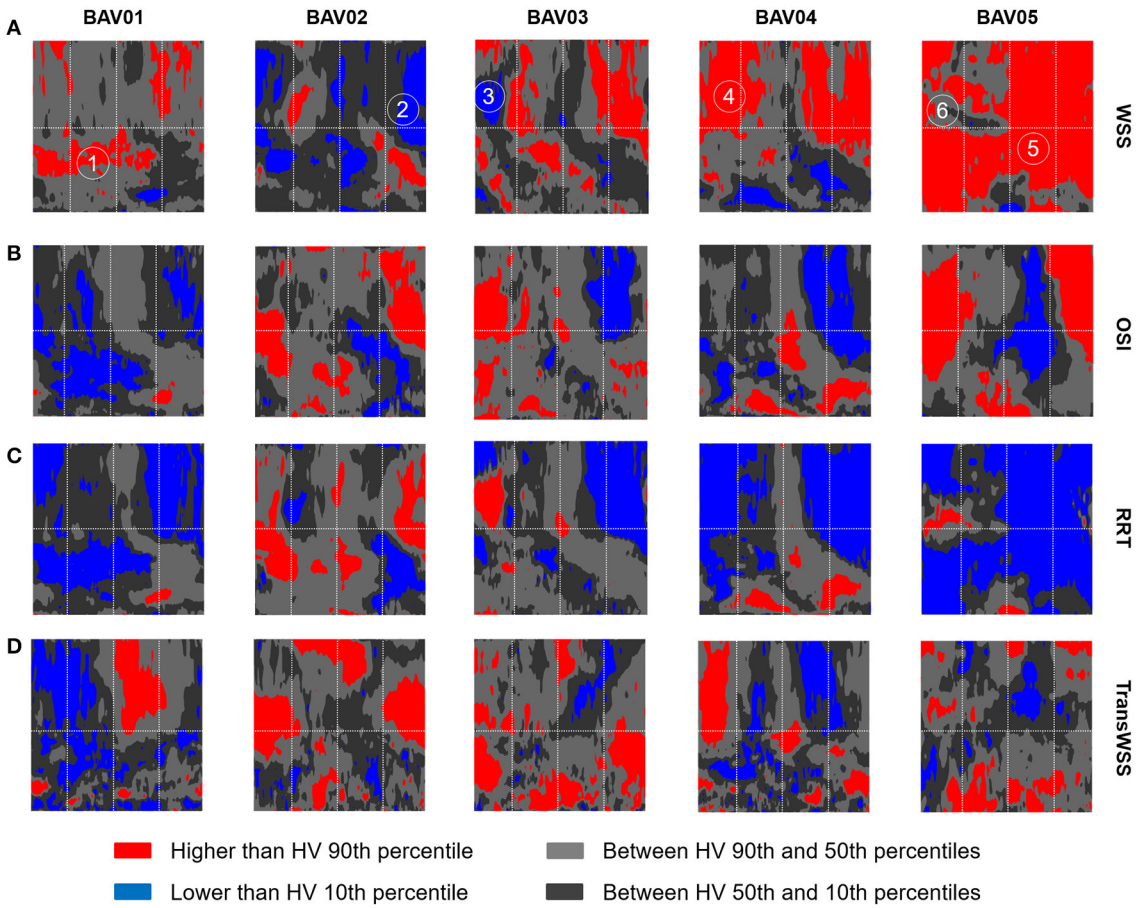

FIGURE 9 | Representation on the 2D template detailed in **Figure 3** of the HV-relative heat maps of WSS **(A)**, OSI **(B)**, RRT **(C)**, and TransWSS **(D)** computed for each BAV patient. The HV-relative heat maps are obtained from point-wise comparison of each BAV patient against HVs population and color-coded accordingly: higher than 90th percentile (red), lower than 10th percentile (blue), between 90th and 10th percentiles (light gray, dark gray). On the HV-relative heat maps, six hot-spots were labeled and identified.

range (10th–90th percentile) obtained in HVs at the same normalized location (**Figure 10**). Of note, computed $|\overrightarrow{WSS}_{LP}|$ values were approximately one order of magnitude higher than the $|\overrightarrow{WSS}_{GV}|$ computed over the aortic wall. This result is consistent with the much better capability of the LP approach, as compared to the GV one, to realistically capture $|\overrightarrow{WSS}|$ values, as demonstrated in Piatti et al. (2016). The analysis of the different time-courses of $|\overrightarrow{WSS}_{LP}|$ showed that regions of abnormally high values can be subject to overloading throughout the whole systolic phase (hot spots 4 and 5) or only for a part of it (hot spots 1 and 6). Considering the time-dependent courses of $\overrightarrow{WSS}_{LP}$ angle, similar ranges were found in BAV patients with respect to the corresponding hot-spots in HVs, especially considering the first part of the systole. However, the dynamics of angle variations showed altered patterns when associated either with high (hot spots 2, 3, and 6) or low (hot spot 1) OSI values. Also, hot spots characterized by abnormally high OSI values were systematically characterized also by time-oscillations of $|\overrightarrow{WSS}_{LP}|$ only during the systolic deceleration phase (hot spots 2, 3, and 6).

DISCUSSION

Novelty of the Study

In this work, we exploited the *in vivo* measurements yielded by 4D Flow sequences to analyze blood fluid dynamics and $\overrightarrow{WSS}$ -related indexes in young normo-functional BAV patients (age 25 ± 10 years) without aortic stenosis or aortic dilation and to compare them vs. age-matched healthy controls. To the best of our knowledge, this is the first study of this kind specifically focused on a cohort of BAV-affected patients without any anatomical derangement of the aorta at the organ length-scale. From this standpoint, the present study differs from previous studies based on 4D Flow imaging, which were run on very heterogeneous cohorts of BAV patients that included elder patients and subjects already affected by aortic dilation or aortic stenosis (Barker et al., 2012a; Hope et al., 2014). Consequently, those studies typically aimed to testing possible correlations between the altered fluid-dynamic stimuli on the aortic wall and its microstructural/anatomical derangements (Barker et al., 2012a; Bissell et al., 2013; Hope et al., 2014; Mahadevia et al.,

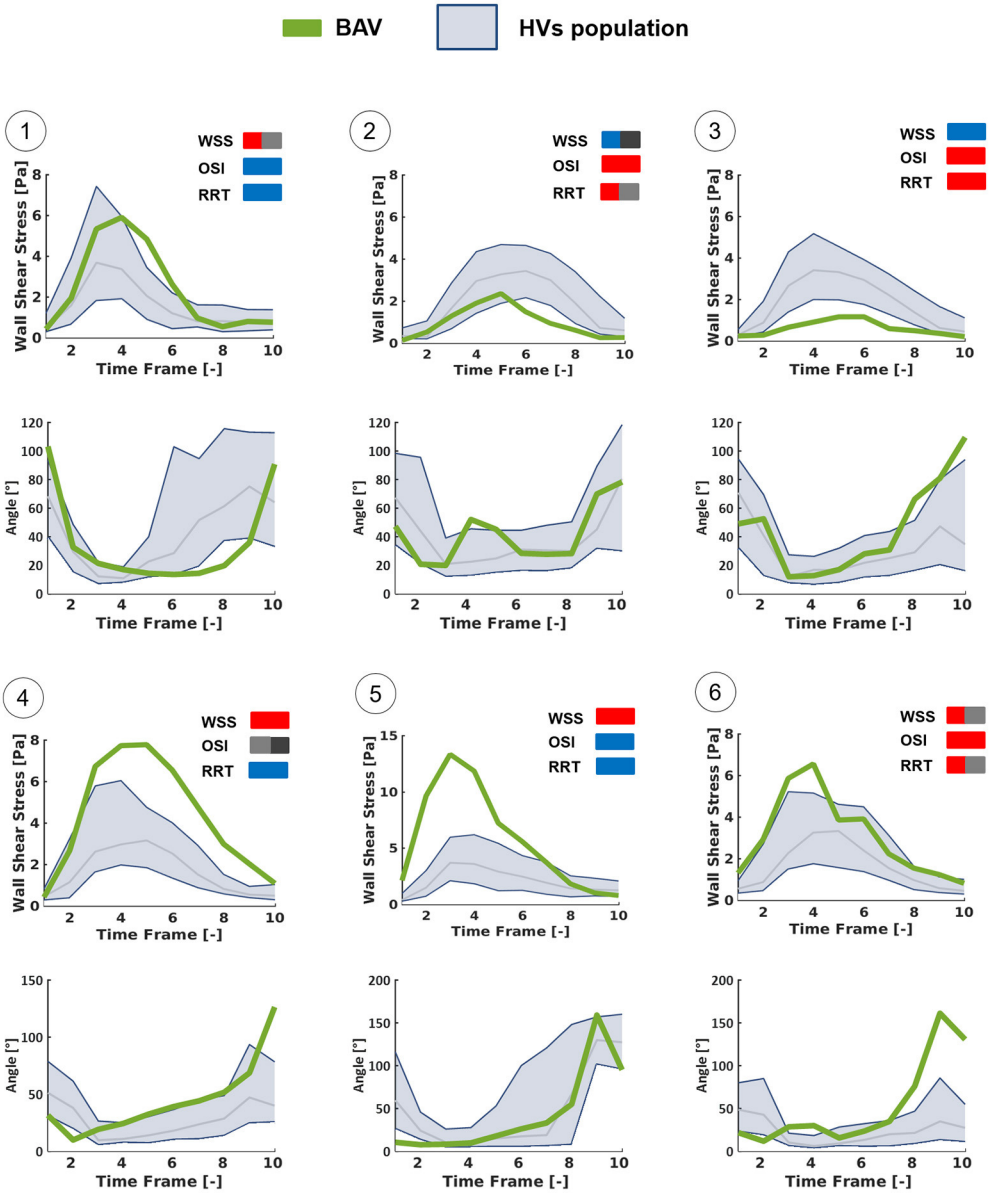

FIGURE 10 | Time-dependent WSS waveforms computed at the selected hot-spots detailed in **Figure 9** using the LP method, throughout the systolic phase. Each BAV patient-specific case (green line) was compared with HVs population (blue zone: from 10th to 90th percentiles) in terms of the magnitude of WSS vector and of the angle between it and the axial direction of the vessel.

2014) following the onset of aortopathy: differently, the present study aims at gaining insight into the possible role of such altered fluid-dynamic stimuli as trigger of the response pathways that ultimately lead to aortopathy.

A second novel aspect of the study resides in the computation of $\overrightarrow{WSS}$ and of the related metrics. Regarding the computation of $\overrightarrow{WSS}$, we obtained the 3D vector based on the calculation of the strain rate tensor through derivative filters. To the best of our knowledge, this method is not used by other research groups in the context of 4D Flow data processing. As expected from our previous benchmarking (Piatti et al., 2016), this method, and namely its implementation on 2D cross-sections, yielded values of $\overrightarrow{WSS}$ magnitude that are greater than those reported in the literature by approximately one order of magnitude. For instance, in Barker et al. (2012a) systolic values of 0.3 ± 0.1 Pa are reported for the ascending aorta of healthy subjects with a cardiac output of 5.2 ± 1.2 l/min, and values ranging from 0.4 ± 0.2 Pa to 0.8 ± 0.3 Pa, depending on the aortic side, are reported for BAV patients with non-stenotic valve, moderate aortic dilation, and cardiac output of 6.3 ± 1.7 l/min. Similarly, in Hope et al. (2011), even when considering the wall region impacted by highly eccentric systolic jets, peak $\overrightarrow{WSS}$ magnitude values of 1.67 Pa were

reported in BAV patients. Regarding the $\overrightarrow{WSS}$ -related metrics, we provided for the first time such a broad spectrum of indexes, in the attempt to test whether some indexes may be more relevant in the context of BAV-related aortopathies.

$\overrightarrow{WSS}$-Related Indexes as a Mean to Detect Altered Fluid Dynamics

In the present study, we could find remarkable abnormalities in the space distribution, in the peak magnitude values, and in the time-course of $\overrightarrow{WSS}$ acting on the ascending aorta of the considered cohort of BAV patients characterized by normo-functional valves and non-dilated aortas. These abnormalities were even more evident when considering $\overrightarrow{WSS}$ -derived indexes; in particular, every considered BAV patient was characterized by pervasive alterations of the TransWSS and by broad regions with extremely low values of OSI_{Circ}, indicating that alterations affect not only peak $\left|\overrightarrow{WSS}\right|$, but also the time-course and the directionality of $\overrightarrow{WSS}$. Of note, the computed $\overrightarrow{WSS}$ -related alterations vs. healthy controls were remarkable and more evident than those appearing from the qualitative and quantitative analysis of the bulk flow. Also, within the sub-group of RL fusion patients, the flow field pattern appeared repeatable, in particular at peak systole. Instead, $\left|\overrightarrow{WSS}\right|$, OSI and RRT heatmaps highlighted a non-negligible inter-subject variability. These evidences should be cautiously evaluated owing to the small number of considered BAV patients, however they suggest that the quantitative analysis of $\overrightarrow{WSS}$ -derived indexes may have a greater potential to discriminate between healthy and aberrant fluid dynamics, and possibly to grade the severity of the BAV-related fluid-dynamic alterations on a patient-specific basis as compared to the analysis of the bulk flow field.

Relevance of Our Results to the Understanding of the Progression of BAV-Related Aortopathy

Even though we computed far greater values of $\left|\overrightarrow{WSS}\right|$ as compared to previous studies focused on the ascending aorta and based on the processing of 4D Flow data, the alterations we found in our BAV patients vs. HVs were consistent, in terms of percentage variations, with those obtained on more heterogenous cohorts of BAV patients (Hope et al., 2010; Bissell et al., 2013), as well as on BAV patients characterized by severe aortic dilation and selected for immediate aortic resection (Van Ooij et al., 2014a). Yet, measurements of ascending aorta diameter at 3-year follow-up did not reveal any clinically relevant aortic anatomical remodeling at the organ length scale, despite the anomalies in $\overrightarrow{WSS}$ detected at baseline on the endothelium of the aortic wall. This evidence was true not only when abnormally high $\left|\overrightarrow{WSS}\right|$ values affected limited regions and exceeded HVs values by up to 46% (BAV01-BAV04), but also when abnormally high $\left|\overrightarrow{WSS}\right|$ values affected the entire ascending aorta and were characterized by a striking 132% increase as compared to HVs values (BAV05).

Hence, in the context of BAV-related aortopathy our results, if analyzed *per-se*, may suggest two mutually exclusive interpretations. On the one hand, one may conclude that there is no cause-effect relationship between altered fluid-dynamic stimuli and onset of aortopathy. On the other hand, one may conclude that the anatomical remodeling of the aortic wall due to altered fluid-dynamic stimuli is a slow process that develops over decades and may not be detected in young patients.

However, the analysis of our results in light of the evidences of previous studies from the literature suggests that the first interpretation is extremely unlikely, whereas the second one might be realistic. Indeed, recent studies investigated the effects of BAV-related fluid-dynamic alterations in non-dilated and initially healthy aortas, isolating these alterations from possible concomitant pathophysiological factors (Atkins et al., 2014; Atkins, 2016; Cao et al., 2017; McNally et al., 2017). Morphotype-dependent flow alterations in the aorta proved to generate different mechanical stimuli on the aortic wall in terms of $\overrightarrow{WSS}$ magnitude and directionality (Cao et al., 2017). These BAV-specific mechanical stimuli were different on the convexity and on the concavity of the ascending aorta. Interestingly, when applied *in vitro* to fresh specimens of healthy porcine aortas, these two region-dependent stimuli induced different responses: only when reproducing the $\overrightarrow{WSS}$ pattern computed at the convexity significant alterations in the expression of MMP-2 and MMP-9, which are involved in medial degradation, were detected already after 48 h (Atkins et al., 2014; Atkins, 2016). Similar evidences of dysregulations in gene expression and metalloproteinase concentration were also reported at the sites of highest $\left|\overrightarrow{WSS}\right|$ in BAV patients undergoing aortic resection, thus in presence of clinically-relevant aortopathy at the organ-scale length (Guzzardi et al., 2015).

Combining these previous evidences with the ones we obtained in the study herein presented we may speculate that $\overrightarrow{WSS}$ alterations precede the onset of aortopathy, that their short-term effect is detectable only at the cell level or at the microscale, and that the subsequent anatomical remodeling occurs only on the very long term. Should this speculation be correct, its practical implication would be that any follow-up study aimed at assessing the prognostic potential of fluid-dynamic alterations should be planned over a time-frame of decades.

LIMITATIONS

The present study has some technical and clinical limitations that should be considered prior to drawing any strong conclusion based on our results.

As for the methods adopted to process 4D Flow, it is worth noticing that the definition of the ROI was based on manual tracings. As such, it was inherently affected by operator-dependent uncertainty. Such uncertainty impacts the definition of the local position of the aortic wall. Moreover, the ROI was defined only at the time-point with the highest signal-to-noise ratio, assumed as peak systole, and it was subsequently used to process velocity data at each systolic time-point of the dataset. The practical implication of this approach is that the real motion of the aortic wall was not accounted for. Of course, both the abovementioned aspects impact the reliability of computed

$\left|\overrightarrow{WSS}\right|$ results, even though our values likely represent a better approximation of the friction actually exerted by the fluid on the vessel wall, as compared to the estimations obtained by alternative methods (Piatti et al., 2016).

Moreover, the spatial and temporal resolution of the datasets, even if compliant with the indications from the Consensum Statement (Dyverfeldt et al., 2015), inherently introduce limitations in the computation of space- and time-derivatives. The latter aspect in particular impacts the computation of OSI and of RRT.

From a clinical standpoint, the main limitation consists in the small number of subjects considered in the study. A larger number of healthy controls would allow for a more robust statistical distribution of data to be used as term of comparison for BAV data. Also, a larger cohort of BAV patients would allow to include relevant sub-populations with different fusion patterns and to verify the presence of fusion-specific features.

Follow-up was limited to a 3-year time-frame and did not include further 4D Flow acquisitions allowing for the evaluation of the changes in fluid dynamics occurring over time in the single patient. Extending the follow-up time-frame and performing such further acquisitions may yield relevant information on the role of fluid dynamics in the evolution toward the onset of the aortopathy or in the progression of the aortopathy itself following its onset.

ETHICS STATEMENT

Human subjects were enrolled and underwent clinical imaging acquisitions at John Radcliffe Hospital, Oxford, UK. The Institutional Review Board approved the study and informed consent was obtained from each participant.

AUTHOR CONTRIBUTIONS

FP, SP, IN, and EV defined and implemented the algorithms to process 4D flow datasets and quantify the fluid-dynamic indexes of interest. MB performed the 4D flow acquisitions on the subjects enrolled in the study. FP and FS processed the datasets and performed the fluid-dynamic quantifications. MB, AD, and ML provided the clinical interpretation of results. AR provided the engineering interpretation of results. All authors contributed to conceiving the study and to writing the manuscript.

FUNDING

This study received funding from the Italian Ministry of Health—(Young Researchers 2009 Program, Grant number GR-2009-1580434), the British Heart Foundation, the H2020 EU Project AMMODIT—Approximation Methods for Molecular Modeling and Diagnosis Tools, Project ID 645672, and the H2020 EU Project MUSICARE—Multisectoral Integrative Approaches To Cardiac Care, Project ID MSCA-ITN 642458.

SUPPLEMENTARY MATERIAL

The Supplementary Material for this article can be found online at: http://journal.frontiersin.org/article/10.3389/fphys.2017.00441/full#supplementary-material

REFERENCES

Albinsson, S., Della Corte, A., Alajbegovic, A., Krawczyk, K. K., Bancone, C., Galderisi, U., et al. (2017). Patients with bicuspid and tricuspid aortic valve exhibit distinct regional microrna signatures in mildly dilated ascending aorta. *Heart Vessels* 32, 750–767. doi: 10.1007/s00380-016-0942-7

Atkins, S. K. (2016). Bicuspid aortic valve hemodynamics does not promote remodeling in porcine aortic wall concavity. *World J. Cardiol.* 8, 89–97. doi: 10.4330/wjc.v8.i1.89

Atkins, S. K., Cao, K., Rajamannan, N. M., and Sucosky, P. (2014). Bicuspid aortic valve hemodynamics induces abnormal medial remodeling in the convexity of porcine ascending aortas. *Biomech. Model. Mechanobiol.* 13, 1209–1225. doi: 10.1007/s10237-014-0567-7

Barker, A. J., Markl, M., Bürk, J., Lorenz, R., Bock, J., Bauer, S., et al. (2012a). Bicuspid aortic valve is associated with altered wall shear stress in the ascending aorta. *Circ. Cardiovasc. Imaging* 5, 457–466. doi: 10.1161/CIRCIMAGING.112.973370

Barker, A. J., Staehle, F., Bock, J., Jung, B. A., and Markl, M. (2012b). Analysis of complex cardiovascular flow with three-component acceleration-encoded MRI. *Magn. Reson. Med.* 67, 50–61. doi: 10.1002/mrm.22974

Baskurt, O. K., and Meiselman, H. J. (2003). Blood rheology and hemodynamics. *Semin. Thromb. Hemost.* 29, 435–450. doi: 10.1055/s-2003-44551

Bissell, M. M., Hess, A. T., Biasiolli, L., Glaze, S. J., Loudon, M., Pitcher, A., et al. (2013). Aortic dilation in bicuspid aortic valve disease: flow pattern is a major contributor and differs with valve fusion type. *Circ. Cardiovasc. Imaging* 6, 499–507. doi: 10.1161/CIRCIMAGING.113.000528

Bock, J., Kreher, B., Hennig, J., and Markl, M. (2007). "Optimized pre-processing of time-resolved 2D and 3D phase contrast MRI data," in *Proceedings International Society for Magnetic Resonanc Medicine.* Available online at: http://cds.ismrm.org/ismrm-2007/files/1_program.pdf

Cao, K., Atkins, S. K., McNally, A., Liu, J., and Sucosky, P. (2017). Simulations of morphotype-dependent hemodynamics in non-dilated bicuspid aortic valve aortas. *J. Biomech.* 50, 63–70. doi: 10.1016/j.jbiomech.2016.11.024

Chien, S. (2006). Mechanotransduction and endothelial cell homeostasis: the wisdom of the cell. *AJP Hear. Circ. Physiol.* 292, H1209–H1224. doi: 10.1152/ajpheart.01047.2006

Chiu, J.-J., and Chien, S. (2011). Effects of disturbed flow on vascular endothelium: pathophysiological basis and clinical perspectives. *Physiol. Rev.* 91, 327–387. doi: 10.1152/physrev.00047.2009

Chung, A. W. Y., Au Yeung, K., Sandor, G. G. S., Judge, D. P., Dietz, H. C., and Van Breemen, C. (2007). Loss of elastic fiber integrity and reduction of vascular smooth muscle contraction resulting from the upregulated activities of matrix metalloproteinase-2 and -9 in the thoracic aortic aneurysm in Marfan syndrome. *Circ. Res.* 101, 512–522. doi: 10.1161/CIRCRESAHA.107.157776

Della Corte, A., Bancone, C., Buonocore, M., Dialetto, G., Covino, F. E., Manduca, S., et al. (2013). Pattern of ascending aortic dimensions predicts the growth rate of the aorta in patients with bicuspid aortic valve. *JACC Cardiovasc. Imaging* 6, 1301–1310. doi: 10.1016/j.jcmg.2013.07.009

Della Corte, A., Bancone, C., Conti, C. A., Votta, E., Redaelli, A., Del Viscovo, L., et al. (2012). Restricted cusp motion in right-left type of bicuspid aortic valves: a new risk marker for aortopathy. *J. Thorac. Cardiovasc. Surg.* 144, 360.e1–369.e1. doi: 10.1016/j.jtcvs.2011.10.014

Desbrun, M., Meyer, M., Schröder, P., and Barr, A. H. (1999). "Implicit fairing of irregular meshes using diffusion and curvature flow," in *SIGGRAPH' 99*

Proceedings of the 26th Annual Conference on Computer Graphics and Interactive Techniques, (New York, NY: ACM Press/Addison-Wesley Publishing Co.), 317–324.

Dijkstra, E. W. (1959). A note on two problems in connexion with graphs. *Numer. Math.* 1, 269–271. doi: 10.1007/BF01386390

Dyverfeldt, P., Bissell, M., Barker, A. J., Bolger, A. F., Carlhäll, C.-J., Ebbers, T., et al. (2015). 4D flow cardiovascular magnetic resonance consensus statement. *J. Cardiovasc. Magn. Reson.* 17:72. doi: 10.1186/s12968-015-0174-5

Fedak, P. W. M., Verma, S., David, T. E., Leask, R. L., Weisel, R. D., and Butany, J. (2002). Clinical and pathophysiological implications of a bicuspid aortic valve. *Circulation* 106, 900–904. doi: 10.1161/01.CIR.0000027905.26586.E8

Girdauskas, E., Borger, M. A., Secknus, M. A., Girdauskas, G., and Kuntze, T. (2011). Is aortopathy in bicuspid aortic valve disease a congenital defect or a result of abnormal hemodynamics? A critical reappraisal of a one-sided argument. *Eur. J. Cardio Thoracic Surg.* 39, 809–814. doi: 10.1016/j.ejcts.2011.01.001

Guzzardi, D. G., Barker, A. J., Van Ooij, P., Malaisrie, S. C., Puthumana, J. J., Belke, D. D., et al. (2015). Valve-related hemodynamics mediate human bicuspid aortopathy: insights from wall shear stress mapping. *J. Am. Coll. Cardiol.* 66, 892–900. doi: 10.1016/j.jacc.2015.06.1310

Hast, A. (2014). Simple filter design for first and second order derivatives by a double filtering approach. *Pattern Recogn. Lett.* 42, 65–71. doi: 10.1016/j.patrec.2014.01.014

Hope, M. D., Hope, T. A., Meadows, A. K., Ordovas, K. G., Urbania, T. H., Alley, M. T., et al. (2010). Bicuspid aortic valve : four-dimensional MR evaluation of ascending aortic systolic flow patterns. *Radiology* 255, 53–61. doi: 10.1148/radiol.09091437

Hope, M. D., Hope, T. A., Crook, S. E. S., Ordovas, K. G., Urbania, T. H., Alley, M. T., et al. (2011). 4D flow CMR in assessment of valve-related ascending aortic disease. *JACC Cardiovasc. Imaging* 4, 781–787. doi: 10.1016/j.jcmg.2011.05.004

Hope, M. D., Sigovan, M., Wrenn, S. J., Saloner, D., and Dyverfeldt, P. (2014). MRI hemodynamic markers of progressive bicuspid aortic valve-related aortic disease. *J. Magn. Reson. Imaging* 40, 140–145. doi: 10.1002/jmri.24362

Jahangiri, M., Saghafian, M., and Sadeghi, M. R. (2015). Numerical study of turbulent pulsatile blood flow through stenosed artery using fluid-solid interaction. *Comput. Math. Methods Med.* 2015:515613. doi: 10.1155/2015/515613

Mahadevia, R., Barker, A. J., Schnell, S., Entezari, P., Kansal, P., Fedak, P. W. M., et al. (2014). Bicuspid aortic cusp fusion morphology alters aortic three-dimensional outflow patterns, wall shear stress, and expression of aortopathy. *Circulation* 129, 673–682. doi: 10.1161/CIRCULATIONAHA.113.003026

Markl, M., Kilner, P. J., and Ebbers, T. (2011). Comprehensive 4D velocity mapping of the heart and great vessels by cardiovascular magnetic resonance. *J. Cardiovasc. Magn. Reson.* 13:7. doi: 10.1186/1532-429X-13-7

Markl, M., Schnell, S., and Barker, A. J. (2014). 4D flow imaging: current status to future clinical applications. *Curr. Cardiol. Rep.* 16:481. doi: 10.1007/s11886-014-0481-8

McCormick, M. E., Manduchi, E., Witschey, W. R. T., Gorman, R. C., Gorman, J. H., Jiang, Y.-Z., et al. (2017). Spatial phenotyping of the endocardial endothelium as a function of intracardiac hemodynamic shear stress. *J. Biomech.* 50, 11–19. doi: 10.1016/j.jbiomech.2016.11.018

McNally, A., Madan, A., and Sucosky, P. (2017). Morphotype-dependent flow characteristics in bicuspid aortic valve ascending aortas: a benchtop particle image velocimetry study. *Front. Physiol.* 8:44. doi: 10.3389/fphys.2017.00044

Michelena, H. I., Prakash, S. K., Della Corte, A., Bissell, M. M., Anavekar, N., Mathieu, P., et al. (2014). Bicuspid aortic valve identifying knowledge gaps and rising to the challenge from the international bicuspid aortic valve consortium (BAVCON). *Circulation* 129, 2691–2704. doi: 10.1161/CIRCULATIONAHA.113.007851

Mohamied, Y., Sherwin, S. J., and Weinberg, P. D. (2017). Understanding the fluid mechanics behind transverse wall shear stress. *J. Biomech.* 50, 102–109. doi: 10.1016/j.jbiomech.2016.11.035

Nistri, S., Sorbo, M. D., Marin, M., Palisi, M., Scognamiglio, R., and Thiene, G. (1999). Aortic root dilatation in young men with normally functioning bicuspid aortic valves. *Heart* 82, 19–22. doi: 10.1136/hrt.82.1.19

Ohno, M., Cooke, J. P., Dzau, V. J., and Gibbons, G. H. (1995). Fluid shear stress induces endothelial transforming growth factor beta-1 transcription and production. Modulation by potassium channel blockade. *J. Clin. Invest.* 95, 1363–1369. doi: 10.1172/JCI117787

Petersson, S., Dyverfeldt, P., and Ebbers, T. (2012). Assessment of the accuracy of MRI wall shear stress estimation using numerical simulations. *J. Magn. Reson. Imaging* 36, 128–138. doi: 10.1002/jmri.23610

Piatti, F., Pirola, S., Bissell, M., Nesteruk, I., Sturla, F., Della Corte, A., et al. (2016). Towards the improved quantification of *in vivo* abnormal wall shear stresses in BAV-affected patients from 4D-flow imaging: Benchmarking and application to real data. *J. Biomech.* 50, 93–101. doi: 10.1016/j.jbiomech.2016.11.044

Robicsek, F., Thubrikar, M. J., Cook, J. W., and Fowler, B. (2004). The congenitally bicuspid aortic valve: how does it function? Why does it fail? *Ann. Thorac. Surg.* 77, 177–185. doi: 10.1016/S0003-4975(03)01249-9

Shih, F. Y. (2010). *Image Processing and Pattern Recognition*. Hoboken, NJ: John Wiley & Sons, Inc. doi: 10.1002/9780470590416

Sigovan, M., Hope, M. D., Dyverfeldt, P., and Saloner, D. (2011). Comparison of four-dimensional flow parameters for quantification of flow eccentricity in the ascending aorta. *J. Magn. Reson. Imaging* 34, 1226–1230. doi: 10.1002/jmri.22800

Siu, S. C., and Silversides, C. K. (2010). Bicuspid Aortic Valve Disease. *J. Am. Coll. Cardiol.* 55, 2789–2800. doi: 10.1016/j.jacc.2009.12.068

Soulis, J. V., Lampri, O. P., Fytanidis, D. K., and Giannoglou, G. D. (2011). "Relative residence time and oscillatory shear index of non-Newtonian flow models in aorta," in *10th International Workshop on Biomedical Engineering*. (Kos: IEEE). doi: 10.1109/IWBE.2011.6079011. Available online at: http://ieeexplore.ieee.org/document/6079011/

Van Ooij, P., Potters, W. V., Collins, J., Carr, M., Carr, J., Malaisrie, S. C., et al. (2014a). Characterization of abnormal wall shear stress using 4D flow MRI in human bicuspid aortopathy. *Ann. Biomed. Eng.* 43, 1385–1397. doi: 10.1007/s10439-014-1092-7

Van Ooij, P., Potters, W. V., Nederveen, A. J., Allen, B. D., Collins, J., Carr, J., et al. (2014b). A methodology to detect abnormal relative wall shear stress on the full surface of the thoracic aorta using four-dimensional flow MRI. *Magn. Reson. Med.* 1227, 1216–1227. doi: 10.1002/mrm.25224

Verma, S., and Siu, S. C. (2014). Aortic Dilatation in patients with bicuspid aortic valve. *N. Engl. J. Med.* 370, 1920–1929. doi: 10.1056/NEJMra1207059

Wang, C., Baker, B. M., Chen, C. S., and Schwartz, M. A. (2013). Endothelial cell sensing of flow direction. *Arterioscler. Thromb. Vasc. Biol.* 33, 2130–2136. doi: 10.1161/ATVBAHA.113.301826

Wendell, D. C., Samyn, M. M., Cava, J. R., Ellwein, L. M., Krolikowski, M. M., Gandy, K. L., et al. (2013). Including aortic valve morphology in computational fluid dynamics simulations: initial findings and application to aortic coarctation. *Med. Eng. Phys.* 35, 723–735. doi: 10.1016/j.medengphy.2012.07.015

Conflict of Interest Statement: The authors declare that the research was conducted in the absence of any commercial or financial relationships that could be construed as a potential conflict of interest.

frontiers in Physiology

ORIGINAL RESEARCH
published: 31 May 2017
doi: 10.3389/fphys.2017.00374

Abnormal Haemodynamic Flow Patterns in Bicuspid *Pulmonary* Valve Disease

*Malenka M. Bissell *, Margaret Loudon, Stefan Neubauer and Saul G. Myerson*

Division of Cardiovascular Medicine, Radcliffe Department of Medicine, University of Oxford Centre for Clinical Magnetic Resonance Research, Oxford, United Kingdom

Abnormal flow patterns in the aortas of those with bicuspid aortic valves (BAVs) are increasingly recognized as important in the pathogenesis of aortic dilatation but pulmonary flow patterns in bicuspid *pulmonary* valves have not been studied. Bicuspid *pulmonary* valve disease is rare and a small numbers of case reports describe concomitant pulmonary artery dilation similar to the dilation of the ascending aorta, which is often seen in BAVs disease. We examined three cases of bicuspid *pulmonary* valve disease, 10 healthy volunteers and 10 patients with BAV disease but a tricuspid *pulmonary* valve. All participants underwent anatomical and functional imaging of the pulmonary valve, pulmonary artery, and right ventricle as well as advanced time-resolved 3-dimensional cardiac magnetic resonance imaging (4D flow) to assess the flow pattern in the pulmonary artery. All patients with a bicuspid *pulmonary* valve had pulmonary artery dilation and showed distinct helical flow abnormalities with increased rotational flow and increased flow displacement compared to a mild left-handed flow pattern in the healthy volunteers. Additionally, there was marked asymmetry seen in the systolic wall shear stress (WSS) pattern, with the highest values in the anterior wall of the pulmonary artery. In comparison, patients with a BAV but a tricuspid *pulmonary* valve had normal flow patterns in the pulmonary artery. These haemodynamic findings are similar to recent studies in bicuspid *aortic* disease, and suggest the importance of flow patterns in the pathophysiology of vessel dilation in both aortic and pulmonary bicuspid valve disease.

Keywords: helical flow, 4D flow MRI, bicuspid valve disease, dilation, humans

OPEN ACCESS

Edited by:
Amalia Forte,
Università degli Studi della Campania "Luigi Vanvitelli" Caserta, Italy

Reviewed by:
Jacopo Biasetti,
Johns Hopkins University, United States
Xin Wu,
Texas A&M University, United States

****Correspondence:***
Malenka M. Bissell
malenka.bissell@cardiov.ox.ac.uk

Specialty section:
This article was submitted to Vascular Physiology, a section of the journal Frontiers in Physiology

Received: *07 March 2017*
Accepted: *19 May 2017*
Published: *31 May 2017*

Citation:
Bissell MM, Loudon M, Neubauer S and Myerson SG (2017) Abnormal Haemodynamic Flow Patterns in Bicuspid Pulmonary Valve Disease. Front. Physiol. 8:374. doi: 10.3389/fphys.2017.00374

INTRODUCTION

Recent advances in cardiovascular magnetic resonance imaging have altered the understanding of the pathophysiology of aortic dilation in bicuspid *aortic* valve (BAV) disease. 4D flow magnetic resonance imaging (4D flow MRI) allows visualization and quantification in all major blood vessels in a 3D image, time resolved over the cardiac cycle. The acquisition slab over the area of interest includes time resolved velocity encoding images in three directions and a time resolved magnitude image per slice. These images are then corrected for Maxwell effects, aliasing and eddy currents and then reconstructed for visualization. For analysis, analysis planes are placed perpendicular to the vessel of interest and hemodynamic flow changes are quantified, such as flow angle and flow displacement, calculating how much the flow jet deviates from the midline of the vessel, rotational flow (circulation, an integral of vorticity), and wall shear stress (WSS) estimations based on the interpolation of local velocity derivatives. These visualization and quantification methods have

been applied to BAV disease and shown, that the majority of patients exhibit a marked right-handed helical flow pattern (Hope et al., 2011; Barker et al., 2012; Bissell et al., 2013; Meierhofer et al., 2013). There findings have led to the hypothesis that haemodynamic flow disturbances, in the form of increased flow angle and flow displacement (leading to increased helical flow and thereby increased asymmetrical WSS, play a major part in the development of aortic dilation (Hope et al., 2011; Barker et al., 2012; Bissell et al., 2013; Meierhofer et al., 2013). The concept that increased WSS contributes to an aortopathy is further supported by a recent study examining histopathological changes in excised BAV aortas. Changes such as reduced elastin were only present in areas with increased WSS, but not in areas with normal WSS as assessed with 4D flow MRI prior to aortic resection (Guzzardi et al., 2015).

If the observed flow changes are indeed caused by a bicuspid valve, we hypothesized that these flow changes may also be present in bicuspid *pulmonary* valve disease. However, isolated bicuspid *pulmonary* valve disease is rare with only few case reports in the literature. In 1955, Ford et al. reviewed the literature and found as few as 15 cases with a confirmed bicuspid *pulmonary* valve (Ford et al., 1956). Autopsy findings in the case described by Ford et al. already documented a markedly dilated pulmonary artery with normal arterial wall structure, a finding confirmed in later case reports (Jodocy et al., 2009; Vedanthan et al., 2009; Goda et al., 2012; Krauss et al., 2014). To date nothing is known about flow pattern in the pulmonary arteries in these isolated cases. The aim of this study was two-fold:

(1) To assess whether helical flow patterns were present in the pulmonary artery in patients with a bicuspid *pulmonary* valve suggesting it is the bicuspid valve itself contributing to flow patterns. This would be done using 4D flow MRI to examine flow patterns in the pulmonary artery in patients with a bicuspid *pulmonary* valve compared to healthy volunteers.
(2) To assess if BAV patients with morphological normal pulmonary valves also exhibit helical flow patterns in the pulmonary artery, suggesting other factors may be involved in the generation of helical flow patterns. Again, 4D flow MRI flow patterns in patients with a BAV compared to healthy volunteers will be compared.

MATERIALS AND METHODS

Twenty-three prospectively enrolled participants underwent 4D flow MRI assessment including the assessment of flow patterns in the main pulmonary artery. This included three patients with a bicuspid *pulmonary* valve with a normal aortic valve, 10 age- and sex matched healthy volunteers (male, mean age 61 $\pm$ 9 years) and 10 age- and sex-matched patients with a BAV but normal tricuspid *pulmonary* valve (male, mean age 61 $\pm$ 8 years).

Cardiovascular Magnetic Resonance (CMR) Acquisition

Each subject underwent two CMR scans—one on a 1.5 Tesla system (Avanto, Siemens, Erlangen, Germany) for anatomical imaging; the second on a 3.0 Tesla system (Trio, Siemens, Erlangen, Germany) for 4D flow assessment, both using a 32-channel cardiac coil. All images were electrocardiogram (ECG)-gated. Steady-state free-precession (SSFP) cine sequences acquired during a single breath-hold were used for pulmonary artery dimension measurements, right ventricular volume assessment and pulmonary valve morphology. The velocity across the pulmonary valve was measured using through-plane phase contrast velocity mapping in an image slice placed perpendicular to the pulmonary artery, just above the valve tips. CMR42 (Circle Cardiovascular Imaging Inc., Calgary, Canada) was used for analysis of standard anatomical and velocity parameters.

4D Flow MRI Assessment

Flow-sensitive gradient-echo pulse sequence CMR datasets were acquired with prospective ECG-gating during free-breathing, using a respiratory navigator. The image acquisition volume was in an oblique sagittal plane encompassing the thoracic aorta, main pulmonary artery and the proximal pulmonary branch arteries. Sequence parameters: echo time 2.5 ms, repetition time 5.1 ms, flip angle 7°, voxel size 2.0 $\times$ 1.7 $\times$ 2.2 mm^3, temporal resolution 40 ms. The velocity encoding range was determined using the lowest non-aliasing velocity on scout measurements. Data acquisition lasted 10–15 min and the data was therefore collected from and averaged over hundreds of cardiac cycles. Dataset processing and WSS calculation were conducted with customized Matlab software Version R2010a (The MathWorks Inc., Natick, Massachusetts, USA) and EnSight Version 9.1.2 (CEI Inc., Apex, North Carolina, USA), as described previously (Frydrychowicz et al., 2007; Markl et al., 2007; Stalder et al., 2008; Barker et al., 2012). The 3-dimensional flow patterns were measured in a short axis slice through the main pulmonary artery (**Figure 1**). Measurements were averaged over systole in the acquired cardiac cycle (one time frame before and three after peak systolic flow) to mitigate measurement noise (Barker et al., 2012).

4D Flow MRI Quantification

Flow through a BAV has been shown to be highly abnormal with markedly accentuated helical flow (Hope et al., 2010). Helical flow is composed of a forward component (along the long axis of the aorta) and a rotational component (rotating around the long axis in a circumferential direction). The rotational component of helical flow can be quantified using the circulation measure, which is the integral of vorticity with respect to the cross-sectional area of the aorta (Farthing and Peronneau, 1979; Hess et al., 2013).

WSS was calculated using the 3-dimensional flow vector and magnitude data using the published analysis method by Stalder et al. (2008). WSS quantifies the shearing force of the moving blood against the vessel lumen using the viscosity of the blood, deformation tensor (which includes the velocity components and spatial dimensions as part of the three-directional velocity field of the acquired CMR data) and inward unit normal (which describes the direction toward the center of the vessel; Stalder et al., 2008). In the analysis plane, the vessel wall was manually

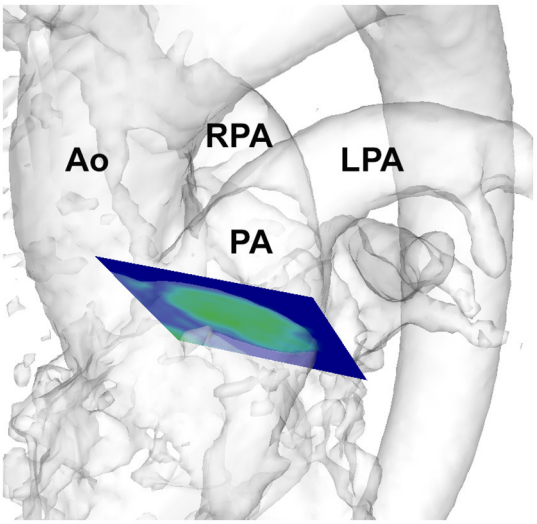

FIGURE 1 | Depiction of analysis plane placement in the pulmonary artery in a healthy volunteer. Ao, aorta; PA, pulmonary artery; RPA, right pulmonary artery; LPA, left pulmonary artery.

traced for each time frame within the cardiac cycle to define the area for analysis.. Systolic WSS was measured in eight anatomical positions within the pulmonary artery lumen.

The systolic flow angle was also calculated—this is defined as the angle between the line perpendicular to the short axis analysis plane and the instantaneous mean flow vector at peak systole (Entezari et al., 2013). Flow displacement was defined as the distance (in millimeters) from the vessel centroid to the velocity-weighted centroid (Mahadevia et al., 2014).

Student *t*-test was used for statistical comparison where appropriate. A $p < 0.05$ was considered significant. Mean values were reported ± one standard deviation. For comparison with the individual bicuspid *pulmonary* valve patients, we also reported the minimum and maximum values of healthy volunteers to indicate the range of these values normally seen in a healthy population sample.

This study was carried out in accordance with the recommendations of the West Berkshire ethics committee with written informed consent from all subjects. All subjects gave written informed consent in accordance with the Declaration of Helsinki. The protocol was approved by the West Berkshire ethics committee.

Patient Characteristics

Of the three patients with bicuspid *pulmonary* valves, patient 1 (69 years) was one of the first "blue" babies that underwent catheter balloon valvotomy of his *pulmonary* valve in London in 1949. He has not needed any intervention since. He was a non-smoker, overweight (BMI 35) and on no cardiovascular medications but hypertensive during the study visit (169/69 mmHg). He also suffered from gout.

Patient 2 (73 years) was diagnosed incidentally with a bicuspid *pulmonary* valve during a recent cardiovascular magnetic resonance exam. He was an ex-smoker, normotensive and on no cardiovascular medications.

Patient 3 (47 years) had more complex heart disease with a double outlet right ventricle and marked pulmonary stenosis. He was an ex-smoker, normotensive, and on no cardiovascular medications. He also suffered from gout.

BAV disease patients had isolated valve disease with no other cardiovascular problems such as coronary artery disease or coarctation of the aorta. The age range was 47–72 years. The patients were normotensive, 4 patients were on blood pressure lowering agents, 1 participants still smoked, and 4 participants were ex-smokers. All participants had normal left ventricular function (ejection fraction 57–70%). Two patients suffered from gastroesophageal reflux.

All healthy volunteers were free from cardiovascular disease or any other non-cardiac disease. The age range was 47–75 years. They were normotensive and not actively smoking.

RESULTS

Bicuspid *Pulmonary* Valve Disease

Pulmonary Valve and Right Ventricular Function

Patient 1 had a well-functioning bicuspid *pulmonary* valve (peak velocity across the pulmonary valve was 1.3 m/s with no regurgitation) and he had normal right ventricular (RV) function [ejection fraction 52%, RV end diastolic volume (RVEDD) 130 ml]. Patient 2 also had a well-functioning bicuspid *pulmonary* valve (peak velocity across the *pulmonary* valve was 1.6 m/s with no regurgitation) with normal right ventricular function (ejection fraction 56%, RVEDD 138 ml). Patient 3 had more complex heart disease with a double outlet right ventricle and marked pulmonary stenosis (narrowing of the valve, peak velocity 3.6 m/s with no regurgitation). All three patients were male and had a normal aortic valve with normal ascending aortic measurements. However, they all had a dilated pulmonary artery (4.5, 3.6, and 3.1 cm) compared with 2.6 ± 0.3 cm in the healthy volunteers.

4D Flow MRI Quantification

When assessing the flow pattern in the pulmonary artery, patients 1 and 2 had a marked right-handed helical flow (rotational flow value 5.2 and 2.1 mm/m^2; **Figure 2**) compared to a mild left-handed helical flow in healthy volunteers with a mean rotational flow of -1.2 ± 1.7 mm/m^2. The 3rd patient had a marked left-handed helical flow (rotational flow value -9.5 mm/m^2; **Table 1**). The flow angle with which the blood jet leaves the pulmonary valve was increased in 2 of the 3 patients (24.6, 9.2, and 17.4° vs. 9.8 ± 7.2° in healthy volunteers). Flow displacement was markedly increased in all 3 patients (15.1, 8.2, and 5.8 mm vs. 1.6 ± 0.7 mm in healthy volunteers). Comparing the WSS averaged over systole, the maximum WSS was lower in patient 1 and 2 (0.59 and 0.73 N/m^2) than the healthy volunteers (0.88 ± 0.25 N/m^2) and only elevated in patient 3 with a stenotic (narrowed) pulmonary valve (1.39 N/m^2). However, there was a marked asymmetry seen in all three patients with highest WSS values in the anterior section with a marked anterior-posterior asymmetry (0.44, 0.48, and 1.18 N/m^2) compared to healthy volunteers with negligible asymmetry (0.06 ± 0.12 N/m^2; **Figure 3**).

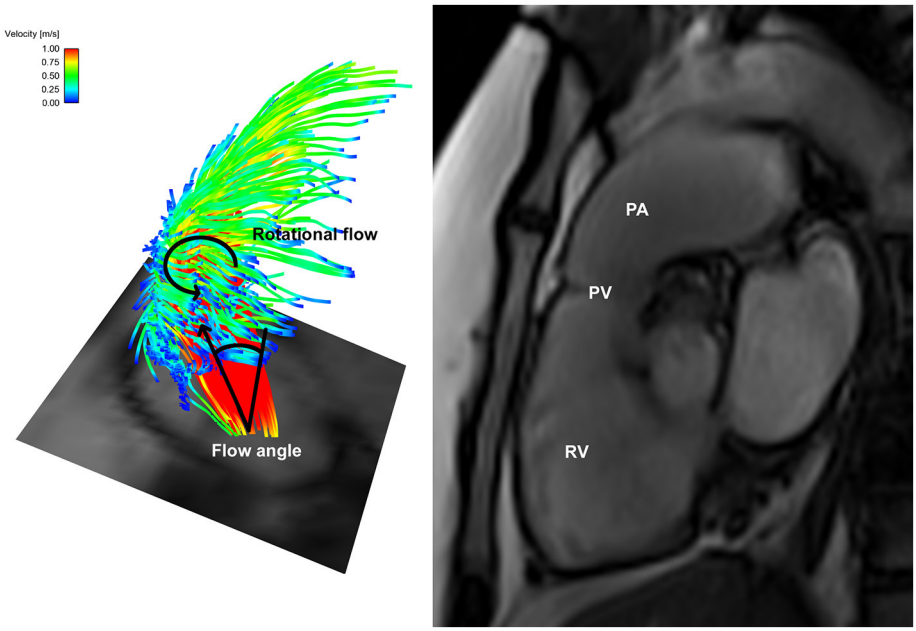

FIGURE 2 | Helical flow pattern in bicuspid *pulmonary* valve disease patient 1—**Left**: Flow particle traces depiction showing marked right-handed helical flow pattern arising from the bicuspid pulmonary valve with an increased flow angle; **Right**: Dilated pulmonary artery in the same patient. RV, right ventricle; PV, pulmonary valve; PA, pulmonary artery.

TABLE 1 | Wall shear stress quantification in bicuspid *pulmonary* valve disease compared to healthy volunteers.

	Healthy volunteers			Bicuspid *pulmonary* valve		
	Mean	**Minimum**	**Maximum**	**Patient 1**	**Patient 2**	**Patient 3**
Age in years	60.5	47	75	69	73	47
Rotational flow in mm/m^2	−1.2	−4.1	1.4	**5.2**	**2.1**	**-9.5**
Flow angle in °	9.8	1.49	26.3	24.6	9.2	17.4
Displacement in mm	1.6	0.4	2.6	**15.1**	**8.2**	**5.8**
Pulmonary artery diameter in cm	2.6	2.2	3.1	**4.5**	**3.6**	3.1
Maximum Wall shear stress in N/m^2	0.88	0.46	1.44	0.59	0.73	1.39
Wall shear stress ant-post asymmetry in N/m^2	0.06	−0.09	0.29	**0.44**	**0.48**	**1.18**

In bold are the patient values which are outside the healthy volunteer range.

The Pulmonary Artery in Bicuspid *Aortic* Valve Disease

A recent echocardiographic publication suggested that the pulmonary artery may also be enlarged in patients with a BAV but normal trileaflet *pulmonary* valve (Kutty et al., 2010). We therefore also assessed the pulmonary artery in a sex- and age matched subgroup of our recently published BAV cohort (Bissell et al., 2013). There were no statistically significant differences however compared to healthy volunteers in pulmonary artery size (2.6 ± 0.2 cm vs. 2.6 ± 0.3 cm; $p = 0.5$), rotational flow (−0.6 ± 1.6 mm/m^2 vs. −1.2 ± 1.7 mm/m^2; $p = 0.48$), flow angle (9.4 ± 6.5° vs. 9.8 ± 7.2°; $p = 0.39$), displacement (1.9 ± 1.1 mm vs. 1.6 ± 0.7 mm; $p = 0.41$) and mean systolic WSS (0.61 ± 0.11 N/m^2 vs. 0.88 ± 0.25 N/m^2; $p = 0.75$; **Figure 4**).

DISCUSSION

We believe our study is the first to describe flow abnormalities in bicuspid *pulmonary* disease. Small numbers of case reports have described a dilated pulmonary artery in association with bicuspid *pulmonary* valves, raising the possibility of a similar underlying pathophysiology to that of BAV disease.

The advent of 4D flow imaging has shown abnormalities of flow patterns and WSS in the ascending aorta of patients with BAV disease. Several research units have described characteristic findings of increased wall shear in the anterior ascending aortic wall. It is not clear whether patients also have underlying aortic wall architectural abnormalities but a recent study demonstrated that changes in the aortic wall composition occur at sites of highest shear stress, suggesting flow

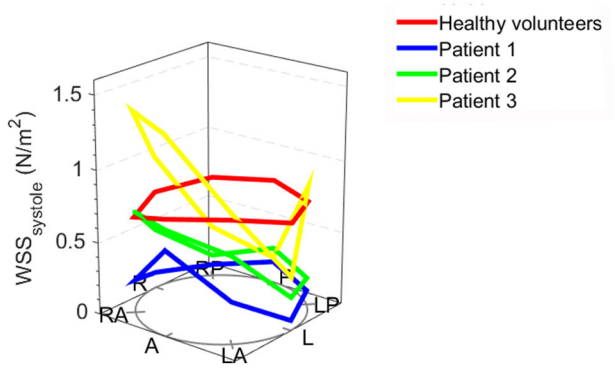

FIGURE 3 | Systolic wall shear stress (WSS) in individual bicuspid *pulmonary* valve patients and the mean WSS values of healthy volunteers: the anatomical positions are shown at the bottom of the figure. A, anterior (outer curvature); LA, left anterior; L, left; LP, left posterior; P, posterior; RP, right posterior; R, right; RA, right anterior; the height of the dots indicates the WSS value.

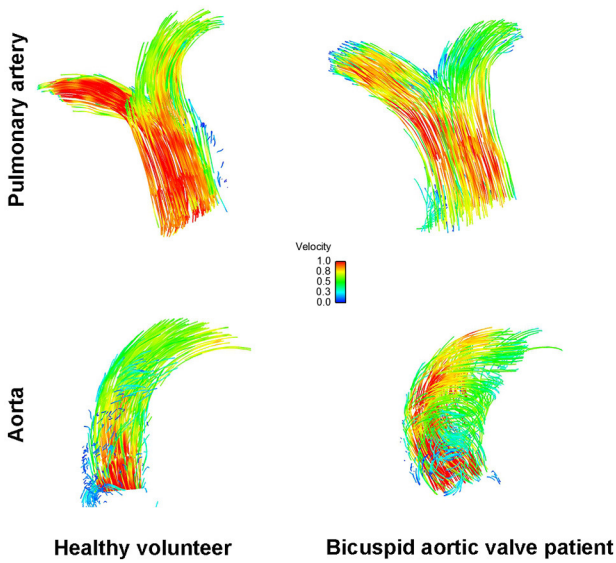

FIGURE 4 | Flow particle traces depiction showing normal flow pattern in the pulmonary artery (top) and the aorta (bottom) in healthy volunteers (left) and in bicuspid *aortic* valve disease (right).

is implicated in aortic dilatation and changes to the aortic wall composition may be a secondary phenomenon (Guzzardi et al., 2015).

In this study all three patients with a bicuspid *pulmonary* valve had a dilated pulmonary artery; furthermore all three patients also had rotational flow and flow displacement values outside the range seen in healthy volunteers. The observed WSS asymmetry, with increased values in the anterior pulmonary artery wall, are similar to these observed in the aorta of patients with a BAV (Bissell et al., 2013). These findings suggest the flow disturbances downstream of a bicuspid *pulmonary* valve are similar to those seen in BAV disease.

The morphology of the valve appears to be central to the development of abnormal flow patterns. In patients with a BAV but a tricuspid *pulmonary* valve these flow disturbances were seen only in the aorta but not the *pulmonary* arteries. The lack of flow abnormalities in the pulmonary arteries suggests it less likely that an intrinsic vessel wall abnormality (affecting the aorta and pulmonary artery) is the underlying cause for the observed abnormalities alone.

Blood into the pulmonary artery is ejected at much lower pressures than into the aorta which may explain the only mild effects of the helical flow pattern on WSS and wall dilation. While a bicuspid *pulmonary* valve may be clinically rare, these novel findings further underline the importance of haemodynamic flow disturbances in the pathophysiology of vessel dilation in bicuspid valve disease. To assess the prognostic value of 4D flow MRI and the clinical implication of our findings, longitudinal cohort studies of both bicuspid aortic and pulmonary valve disease are necessary to understand the degree of involvement haemodynamic changes have in vessel dilation and whether 4D flow MRI is a clinically useful imaging biomarker for predicting aortic growth rate.

Limitations

As bicuspid *pulmonary* valve disease is rare, patient numbers were small. 4D flow MRI is a new imaging technique but measures such as WSS have been validated, even though the true WSS is likely to be higher than the measured value, due to limited spatial resolution and partial volume effects, as discussed previously (Markl et al., 2011). Furthermore, 4D flow MRI acquisition is averaged over hundreds of cycles. Therefore, we are unable to assess beat-to-beat variability. As patients are lying supine and are at rest during the imaging, the beat-to-beat variability is likely to be low.

AUTHOR CONTRIBUTIONS

MB designed the work, completed the acquisition, analysis and interpretation of the work, drafted the work, approved the final version and agree to be accountable for all aspects of the work in ensuring that questions related to the accuracy or integrity of any part of the work are appropriately investigated and resolved. ML contributed to the design and acquisition of the work, revisited the work critically for important intellectual content, approved the final version and agree to be accountable for all aspects of the work in ensuring that questions related to the accuracy or integrity of any part of the work are appropriately investigated and resolved. SN and SM supervised the design of the study and interpretation of the work, revisited the work critically for important intellectual content, approved the final version and agree to be accountable for all aspects of the work in ensuring that questions related to the accuracy or integrity of any part of the work are appropriately investigated and resolved.

FUNDING

MB was supported by the British Heart Foundation Clinical Research Training Fellowship FS/10/043/28415. ML, SM, and SN receive funding from the National Institute for Health Research (NIHR) Oxford Biomedical Research Centre Program. SN acknowledges support of the Oxford British Heart Foundation Centre of Research Excellence.

REFERENCES

Barker, A. J., Markl, M., Burk, J., Lorenz, R., Bock, J., Bauer, S., et al. (2012). Bicuspid aortic valve is associated with altered wall shear stress in the ascending aorta. *Circ. Cardiovasc. Imaging* 5, 457–466. doi: 10.1161/CIRCIMAGING.112.973370

Bissell, M. M., Hess, A. T., Biasiolli, L., Glaze, S. J., Loudon, M., Pitcher, A., et al. (2013). Aortic dilation in bicuspid aortic valve disease: flow pattern is a major contributor and differs with valve fusion type. *Circ. Cardiovasc. Imaging* 6, 499–507. doi: 10.1161/CIRCIMAGING.113.000528

Entezari, P., Schnell, S., Mahadevia, R., Rinewalt, D., Malaisrie, C., McCarthy, P., et al. (2013). From unicuspid to quadricuspid: the impact of aortic valve morphology on 3D hemodynamics. *J. Cardiovasc. Magn. Reson.* 15, O79. doi: 10.1186/1532-429X-15-S1-E36

Farthing, S., and Peronneau, P. (1979). Flow in the thoracic aorta. *Cardiovasc. Res.* 13, 607–620. doi: 10.1093/cvr/13.11.607

Ford, A. B., Hellerstein, H. K., Wood, C., and Kelly, H. B. (1956). Isolated congenital bicuspid pulmonary valve; clinical and pathologic study. *Am. J. Med.* 20, 474–486. doi: 10.1016/0002-9343(56)90131-0

Frydrychowicz, A., Harloff, A., Jung, B., Zaitsev, M., Weigang, E., Bley, T. A., et al. (2007). Time-resolved, 3-dimensional magnetic resonance flow analysis at 3 T: visualization of normal and pathological aortic vascular hemodynamics. *J. Comput. Assist. Tomogr.* 31, 9–15. doi: 10.1097/01.rct.0000232918.45158.c9

Goda, M., Budts, W., Troost, E., and Meyns, B. (2012). Bicuspid pulmonary valve with atrial septal defect leading to pulmonary aneurysm. *Ann. Thorac. Surg.* 93, 1706–1708. doi: 10.1016/j.athoracsur.2011.09.063

Guzzardi, D. G., Barker, A. J., van Ooij, P., Malaisrie, S. C., Puthumana, J. J., Belke, D. D., et al. (2015). Valve-related hemodynamics mediate human bicuspid aortopathy: insights from wall shear stress mapping. *J. Am. Coll. Cardiol.* 66, 892–900. doi: 10.1016/j.jacc.2015.06.1310

Hess, A. T., Bissell, M. M., Glaze, S. J., Pitcher, A., Myerson, S. G., Neubauer, S., et al. (2013). Evaluation of Circulation as a quantifying metric in 4D flow MRI. *J. Cardiovasc. Magn. Reson.* 15:E36. doi: 10.1186/1532-429X-15-S1-E36

Hope, M. D., Hope, T. A., Crook, S. E., Ordovas, K. G., Urbania, T. H., Alley, M. T., et al. (2011). 4D flow CMR in assessment of valve-related ascending aortic disease. *JACC Cardiovasc. Imaging* 4, 781–787. doi: 10.1016/j.jcmg.2011.05.004

Hope, M. D., Hope, T. A., Meadows, A. K., Ordovas, K. G., Urbania, T. H., Alley, M. T., et al. (2010). Bicuspid aortic valve: four-dimensional MR evaluation of ascending aortic systolic flow patterns. *Radiology* 255, 53–61. doi: 10.1148/radiol.09091437

Jodocy, D., Friedrich, G. J., Bonatti, J. O., Muller, S., Laufer, G., Pachinger, O., et al. (2009). Left main compression syndrome by idiopathic pulmonary artery aneurysm caused by medial necrosis Erdheim-Gsell combined with bicuspid pulmonary valve. *J. Thorac. Cardiovasc. Surg.* 138, 234–236. doi: 10.1016/j.jtcvs.2008.02.076

Krauss, T., Berchem, L., Blanke, P., Zeh, W., and Pache, G. (2014). 4D-cine CT imaging of a bicuspid pulmonary valve. *J. Cardiovasc. Comput. Tomogr.* 8, 170–171. doi: 10.1016/j.jcct.2013.12.018

Kutty, S., Kaul, S., Danford, C. J., and Danford, D. A. (2010). Main pulmonary artery dilation in association with congenital bicuspid aortic valve in the absence of pulmonary valve abnormality. *Heart* 96, 1756–1761. doi: 10.1136/hrt.2010.199109

Mahadevia, R., Barker, A. J., Schnell, S., Entezari, P., Kansal, P., Fedak, P. W., et al. (2014). Bicuspid aortic cusp fusion morphology alters aortic three-dimensional outflow patterns, wall shear stress, and expression of aortopathy. *Circulation* 129, 673–682. doi: 10.1161/CIRCULATIONAHA.113.003026

Markl, M., Harloff, A., Bley, T. A., Zaitsev, M., Jung, B., Weigang, E., et al. (2007). Time-resolved 3D MR velocity mapping at 3T: improved navigator-gated assessment of vascular anatomy and blood flow. *J. Magn. Reson. Imaging* 25, 824–831. doi: 10.1002/jmri.20871

Markl, M., Wallis, W., and Harloff, A. (2011). Reproducibility of flow and wall shear stress analysis using flow-sensitive four-dimensional MRI. *J. Magn. Reson. Imaging* 33, 988–994. doi: 10.1002/jmri.22519

Meierhofer, C., Schneider, E. P., Lyko, C., Hutter, A., Martinoff, S., Markl, M., et al. (2013). Wall shear stress and flow patterns in the ascending aorta in patients with bicuspid aortic valves differ significantly from tricuspid aortic valves: a prospective study. *Eur. Heart J. Cardiovasc. Imaging* 14, 797–804. doi: 10.1093/ehjci/jes273

Stalder, A. F., Russe, M. F., Frydrychowicz, A., Bock, J., Hennig, J., and Markl, M. (2008). Quantitative 2D and 3D phase contrast MRI: optimized analysis of blood flow and vessel wall parameters. *Magn. Reson. Med.* 60, 1218–1231. doi: 10.1002/mrm.21778

Vedanthan, R., Sanz, J., and Halperin, J. (2009). Bicuspid pulmonic valve. *J. Am. Coll. Cardiol.* 54, e5. doi: 10.1016/j.jacc.2009.05.027

Conflict of Interest Statement: The authors declare that the research was conducted in the absence of any commercial or financial relationships that could be construed as a potential conflict of interest.

frontiers in Physiology

ORIGINAL RESEARCH
published: 01 February 2017
doi: 10.3389/fphys.2017.00044

Morphotype-Dependent Flow Characteristics in Bicuspid Aortic Valve Ascending Aortas: A Benchtop Particle Image Velocimetry Study

Andrew McNally[1], *Ashish Madan*[2] *and Philippe Sucosky*[2]*

[1] *Department of Aerospace and Mechanical Engineering, University of Notre Dame, Notre Dame, IN, USA,* [2] *Department of Mechanical and Materials Engineering, Wright State University, Dayton, OH, USA*

The bicuspid aortic valve (BAV) is a major risk factor for secondary aortopathy such as aortic dilation. The heterogeneous BAV morphotypes [left-right-coronary cusp fusion (LR), right-non-coronary cusp fusion (RN), and left-non-coronary cusp fusion (LN)] are associated with different dilation patterns, suggesting a role for hemodynamics in BAV aortopathogenesis. However, assessment of this theory is still hampered by the limited knowledge of the hemodynamic abnormalities generated by the distinct BAV morphotypes. The objective of this study was to compare experimentally the hemodynamics of a normal (i.e., non-dilated) ascending aorta (AA) subjected to tricuspid aortic valve (TAV), LR-BAV, RN-BAV, and NL-BAV flow. Tissue BAVs reconstructed from porcine TAVs were subjected to physiologic pulsatile flow conditions in a left-heart simulator featuring a realistic aortic root and compliant aorta. Phase-locked particle image velocimetry experiments were carried out to characterize the flow in the aortic root and in the tubular AA in terms of jet skewness and displacement, as well as mean velocity, viscous shear stress and Reynolds shear stress fields. While all three BAVs generated skewed and asymmetrical orifice jets (up to 1.7- and 4.0-fold increase in flow angle and displacement, respectively, relative to the TAV at the sinotubular junction), the RN-BAV jet was out of the plane of observation. The LR- and NL-BAV exhibited a 71% increase in peak-systolic orifice jet velocity relative to the TAV, suggesting an inherent degree of stenosis in BAVs. While these two BAV morphotypes subjected the convexity of the aortic wall to viscous shear stress overloads (1.7-fold increase in maximum peak-systolic viscous shear stress relative to the TAV-AA), the affected sites were morphotype-dependent (LR-BAV: proximal AA, NL-BAV: distal AA). Lastly, the LR- and NL-BAV generated high degrees of turbulence in the AA (up to 2.3-fold increase in peak-systolic Reynolds shear stress relative to the TAV) that were sustained from peak systole throughout the deceleration phase. This *in vitro* study reveals substantial flow abnormalities (increased jet skewness, asymmetry, jet velocity, turbulence, and shear stress overloads) in non-dilated BAV aortas, which differ from those observed in dilated aortas but still coincide with aortic wall regions prone to dilation.

Keywords: hemodynamics, bicuspid aortic valve, aorta, aortopathy, particle image velocimetry

OPEN ACCESS

Edited by:
Alessandro Della Corte,
Second University of Naples, Italy

Reviewed by:
Irena Levitan,
University of Illinois at Chicago, USA
Emiliano Votta,
Polytechnic University of Milan, Italy

***Correspondence:**
Philippe Sucosky
philippe.sucosky@wright.edu

Specialty section:
This article was submitted to Vascular Physiology, a section of the journal Frontiers in Physiology

Received: *15 November 2016*
Accepted: *17 January 2017*
Published: *01 February 2017*

Citation:
McNally A, Madan A and Sucosky P (2017) Morphotype-Dependent Flow Characteristics in Bicuspid Aortic Valve Ascending Aortas: A Benchtop Particle Image Velocimetry Study. Front. Physiol. 8:44. doi: 10.3389/fphys.2017.00044

INTRODUCTION

With an incidence rate between 0.5 and 2.0%, the bicuspid aortic valve (BAV) is the most common congenital heart defect and is characterized by the presence of two functional leaflets instead of three in the normal tricuspid aortic valve (TAV) (Roberts, 1970; Ward, 2000). The most common type-I BAV phenotype features two unequally sized cusps and a raphe along the site of fusion on the larger cusp but covers three distinct anatomies, each associated with a different raphe location. While the most prevalent left-right (LR) type-I BAV subtype results from the fusion between the left- and right-coronary leaflets, fusion can also occur between the non- and left-coronary leaflets (NL subtype), or between the right- and non-coronary leaflets (RN subtype) (Sievers and Schmidtke, 2007).

The BAV is a major risk factor for secondary valvular and vascular disease such as calcific aortic valve disease and aortic dilation. Although the susceptibility of BAV patients to such disorders has been described historically as genetic, there is increasing support for a hemodynamic pathway (Barker and Markl, 2011; Girdauskas et al., 2011; Sucosky and Rajamannan, 2013; Atkins and Sucosky, 2014; Sucosky, 2014; Della Corte, 2015). The demonstration of the skewness of the BAV orifice jet (Robicsek et al., 2004; Della Corte et al., 2011) and of its impingement on the anterolateral aortic wall (Robicsek et al., 2004; Hope et al., 2008, 2010), which correlate with the asymmetric formation of calcific nodules on BAV leaflets (Thubrikar et al., 1986; Sabet et al., 1999) and the asymmetric dilation patterns in BAV ascending aortas (AAs) (Fazel et al., 2008; Schaefer et al., 2008), has generated renewed support for the involvement of hemodynamic stresses in BAV disease and for the investigation of the flow in BAV aortas.

Phase contrast magnetic resonance imaging (PC-MRI) and echocardiography have revealed the existence of stress overloads in BAV aortic wall regions prone to dilation (van Ooij et al., 2015), their association with extracellular matrix dysfunction (Girdauskas et al., 2014) and their dependence on the BAV morphotype (Bissell et al., 2013). While those studies have been instrumental in providing evidence for a hemodynamic root of BAV disease, the reliability of those *in vivo* flow characterizations is challenged by the inherent lack of spatial resolution of the imaging technique and the possible hemodynamic impact of pre-existing anatomical abnormalities (e.g., dilated aorta, stenotic valve). Computational models have been designed to circumvent those limitations. Spatially resolved fluid-structure interaction simulations in intact valve-aorta geometries have demonstrated the existence of contrasted abnormalities in fluid shear stress directionality and magnitude on type-I BAV leaflets (Chandra et al., 2012), the existence of stress overloads in BAV AAs (Gilmanov and Sotiropoulos, 2016) and their ability to mediate aortic wall degeneration (Atkins et al., 2014), and the influence of the BAV cusp fusion on aortic flow abnormalities (Cao and Sucosky, 2015; Cao et al., 2017). However, the complexity of the native tissue mechanical characteristics and the native turbulent flow regime combined with the computationally demanding coupling of the fluid and structural problems are still hampering those models. On this basis, the *in vitro* approach, which aims at measuring the flow in realistic anatomies using high-resolution flow diagnostic techniques, poses as a legitimate alternative to the *in vivo* and *in silico* approaches. Particle image velocimetry (PIV) measurements in TAV and BAV tissue models have reported increased energy loss, flow turbulence and unsteadiness in BAVs as well as increased wall shear stress in BAV AAs (Saikrishnan et al., 2012; Yap et al., 2012; Seaman and Sucosky, 2014; Seaman et al., 2014). Laser Doppler velocimetry measurements performed in a physiologic flow loop have revealed increased fluid shear stress frequency on BAV leaflets relative to TAV leaflets (Yap et al., 2012). Lastly, PIV experiments in simulated calcified valve models have indicated the dependence of BAV flow abnormalities on the degree of calcification (Seaman et al., 2014). Although these flow measurements have provided a reasonable compromise between accuracy and fidelity to the native configuration, they have often implemented chemically fixed valves and rigid or simplified aorta geometries, which resulted in an approximation of the native hemodynamics.

The review of the current literature on BAV hemodynamics reveals several knowledge shortcomings, which can be articulated by the following questions: (1) *What is the initial impact of the BAV anatomy on the large-scale flow structures and wall shear stress in the native AA?* (2) *What is the influence of the BAV cusp fusion on those flow characteristics?* Therefore, the objective of the present study was to quantify and compare experimentally the pulsatile flow characteristics generated in the aortic root and AA by a TAV and the three type-I BAV morphotypes (i.e., LR-BAV, RN-BAV, NL-BAV) using PIV.

METHODS

Valve Models

Four tissue valve models were constructed to replicate a TAV anatomy and the three type-I BAV morphotypes (i.e., LR-, RN- and NL-BAV). These anatomies were selected based on their high prevalence and their common association with aortopathy (Sievers and Schmidtke, 2007). Each model was created from a normal TAV excised from a porcine heart obtained from a local abattoir. Following slaughter, the whole aortic root (i.e., aortic sinus and leaflets) was transported to the laboratory in ice-cold phosphate buffer saline (PBS). Upon arrival in the laboratory, all subsequent procedures were conducted within an hour and by frequently dipping the aortic root in PBS to keep it moist at all times. The aortic root was first trimmed to remove excess muscle and connective tissue, while preserving the narrow strip of aortic tissue along which each leaflet attaches to the wall. The resulting valve was then sutured to a circular supporting plate following our previously published protocol (Seaman et al., 2014, 2015). The BAV models were created by suturing two leaflets (left- and right-coronary leaflets for LR-BAV, non- and left-coronary leaflets for NL-BAV, and right- and non-coronary leaflets for RN-BAV) along their common free edge (**Figure 1**). In an effort to maintain the native mechanical properties of the leaflets, no fixative agent was used during the valve preparation or during the measurements.

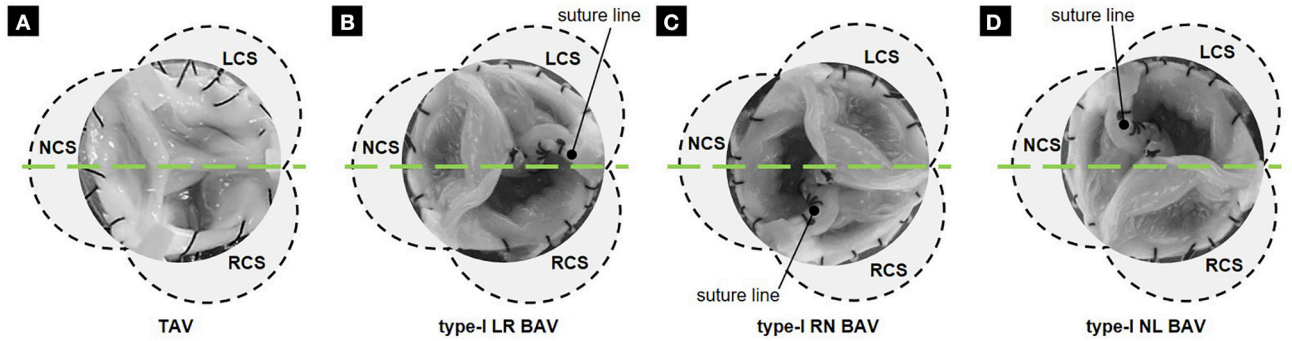

FIGURE 1 | Tissue valve models: (A) TAV; **(B)** LR BAV; **(C)** RN BAV; and **(D)** NL BAV (RCS, right-coronary sinus; NCS, non-coronary sinus; LCS, left-coronary sinus; green line, laser sheet position 1).

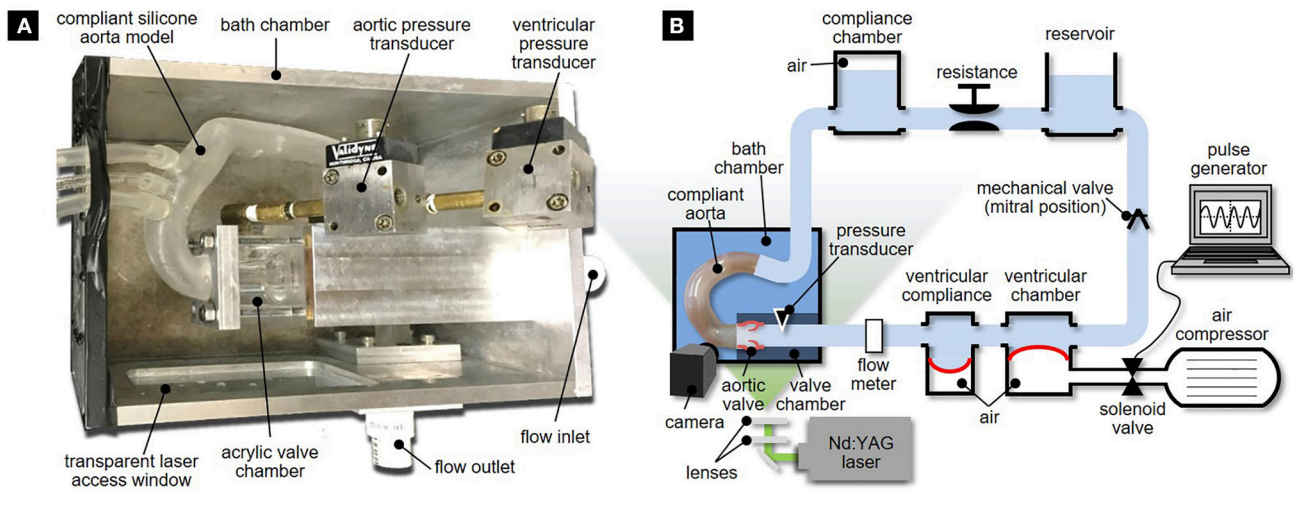

FIGURE 2 | Experimental setup: (A) bath chamber with valve chamber and compliant aorta phantom; and **(B)** left-heart simulator.

Valve and Aorta Chamber

The valve sutured on its mounting plate was placed in a valve chamber made of acrylic and constructed with flat external walls to minimize refraction of the incident laser sheet (**Figure 2A**). The chamber consists of an idealized three-lobed sinus geometry (Swanson and Clark, 1974; Angelini et al., 1989) and a straight cylindrical conduit (inner diameter: 24 mm; length: 20 mm) mimicking the proximal segment of the tubular AA. The valve chamber was designed to allow control over the angular position of the circular mounting plate relative to the aortic sinuses, which permitted the precise positioning of the fused leaflet for each morphotype.

The valve chamber was connected to a realistic compliant aortic arch model. The aorta geometry was reconstructed based on computed tomography images of a human aorta obtained from the Visible Human Project. This model matched the one used in our previous computational study on the effects of BAV flow on AA hemodynamics (Cao and Sucosky, 2015). The optically accessible silicone compliant model was fabricated using three-dimensional printing (Medisim Corp. Inc., Alton, ON) and featured a uniform wall thickness (2.0 ± 0.2 mm).

To enhance optical access and limit optical distortion, the aorta phantom and the valve chamber were submerged in a rectangular bath chamber filled with an index matching solution of water and glycerol (55 and 45% by volume, respectively). The properties of this mixture (density: 1060 kg/m^3, dynamic viscosity: 3.8 cP) approximated blood properties while providing partial index matching (refractive index: 1.40) with the silicone and acrylic materials (refractive index: 1.41 and 1.49, respectively). The bath chamber features an inlet and outflow ports that connect to the inlet section of the valve chamber and the outlet section of the aorta phantom, respectively.

Pulsatile Flow Loop Setup

The bath chamber was mounted in a modified version of our left-heart simulator (Seaman et al., 2015). The flow loop (**Figure 2B**) was driven by a pulse generator consisting of an air compressor (1NNE5, Grainger, Lake Forest, IL) delivering

pressurized air (35 psi) to a ventricular chamber (6NZK3 diaphragm accumulator, Parker Hannifin, Cleveland, OH) mimicking ventricular function. The filling of the ventricular chamber was controlled by a 2-position 3-way solenoid valve (56C-13-111CA, Mac Valves, Wixom, MI) whose timing was regulated by a square wave signal generated in Labview (National Instruments Corp., Austin, TX). Ventricular compliance was introduced by the inclusion of a second diaphragm accumulator (6NZK2, Parker Hannifin) just downstream of the ventricular chamber.

A fluid reservoir (volume: 4 L) fed the ventricular chamber during diastole to replicate atrial function, while enabling control over the hydrostatic pressure generated in the loop. A gate valve and a compliance chamber (volume: 1.5 L) connected downstream of the bath chamber were used to adjust vascular resistance and compliance. The instantaneous flow rate delivered by the left-heart simulator was measured downstream of the ventricular compliance chamber by an in-line ultrasonic flow meter (ME-XPN-19, Transonic, Ithaca, NY). Two pressure ports located 24 mm upstream and 24 mm downstream of the valve annulus were connected to two pressure transducers (DP15-34, Validyne Engineering Corp., Northridge, CA) to provide ventricular and aortic pressure measurements. The flow loop was tuned to generate a near physiologic aortic pressure of 135/70 mmHg at 70 beats per minutes. This condition resulted in a cardiac output of 3.1 L/min in the TAV and a smaller cardiac output between 2.8 and 3.0 L/min in the BAVs, due to their intrinsic degree of stenosis and higher resistance to the flow (**Figure 3**). Those levels are within the physiologic ranges reported for BAV patients (average cardiac output: 3.5 ± 1.3 L/min) (Barker et al., 2010; Mirabella et al., 2015).

PIV Setup

PIV was used to investigate the flow fields in the aortic root and the AA. The flow was seeded with neutrally buoyant hollow glass microspheres (Sphericel 110P8, Potters Industries LLC., Malvern, PA) with a mean diameter of 11.7 μm and a density of 1100 kg/m^3. The PIV system (Flowmaster, LaVision, Goettingen, Germany) consisted of a double-head Nd:YAG laser (New Wave Research Solo II) generating a pulsed output beam (wavelength: 532 nm; energy: 30 mJ; pulse duration: 3–5 ns). Optical mirrors and lenses were used to form the beam into a 200 μm thick laser sheet. For each valve model, the laser sheet was positioned to illuminate two sections of the flow through a laser access window located on the side of the bath chamber. The first laser position illuminated the middle horizontal cross section of the valve chamber, while the second position illuminated the middle cross section intersecting the centerline of the silicone AA model. This setup enabled the capture of the flow characteristics in the middle cross sections of the aortic root and proximal tubular AA, as well as in the middle cross section of the distal tubular AA (**Figure 4**; see **Figure 1** for laser position relative to each valve model). The two resulting fields of view were separated by a 10-mm long stainless steel connector plate, which blocked optical access to the flow over that region. For each laser position, a charge-coupled device camera (Imager Pro X 2M) fitted with a 60-mm lens (Micro Nikkor, Nikon Inc., Melville, NY) and narrow band pass filter (532 ± 10 nm) was placed above the bath chamber perpendicular to the laser sheet to image a 62 × 46 mm section of the flow at a resolution of 1648 × 1214 pixels. Image acquisition was performed by a 64-bit, dual channel frame grabber coupled to a dual-core, dual-processor computer. For each valve model and each laser position, image sets were collected at 20 phases of the cardiac cycle. At each phase, 415 image pairs were captured by the camera in phase-locked mode. Briefly, for the first phase, image acquisition and laser pulsing were synchronized with the opening of the solenoid valve regulating the filling of the ventricular chamber. For all other phases, a delay was imposed to capture the image pairs at the desired phase of the cardiac cycle. The image pairs were cross-correlated in Davis 7.2 (LaVision) using a multi-pass scheme with an initial interrogation window of 64 × 64 pixels with a 50% overlap and a final interrogation window of 8 × 8 pixels with a 50% overlap, which permitted to achieve a spatial resolution of 300 μm.

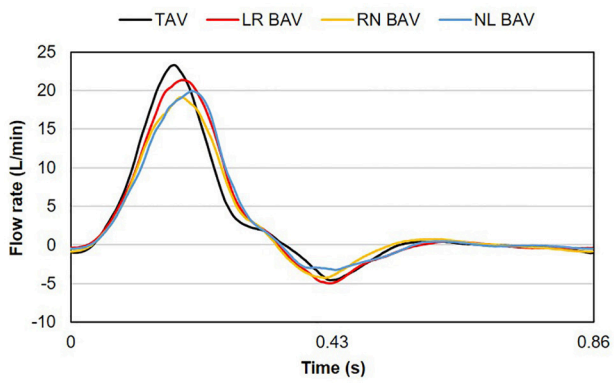

FIGURE 3 | Flow rate waveforms generated by the left-heart simulator with the four valve models.

Hemodynamic Characterization

The in-plane instantaneous velocity fields $\mathbf{u}(\mathbf{x}, t)$ obtained by cross-correlation were first filtered to eliminate erroneous velocity vectors and then ensemble-averaged over 415 realizations to yield an average velocity field $\overline{\mathbf{u}}(\mathbf{x}, t)$ at each phase. All subsequent analyses were performed in Tecplot 360 (Tecplot Inc., Bellevue, WA). The velocity fluctuations $\mathbf{u}'(\mathbf{x}, t)$ were obtained by Reynolds decomposition:

$$\mathbf{u}'(\mathbf{x}, t) = \mathbf{u}(\mathbf{x}, t) - \overline{\mathbf{u}}(\mathbf{x}, t). \quad (1)$$

The viscous shear stress $\bar{\tau}(\mathbf{x}, t)$ was calculated in Tecplot as

$$\bar{\tau}(\mathbf{x}, t) = \mu \left(\frac{\partial \bar{u}_1(\mathbf{x}, t)}{\partial x_2} + \frac{\partial \bar{u}_2(\mathbf{x}, t)}{\partial x_1} \right), \quad (2)$$

where μ is the fluid dynamic viscosity. Turbulence characteristics were quantified in terms of the Reynolds shear stress $\tau'(\mathbf{x}, t)$ defined as

$$\tau' = \rho \overline{u'_1(\mathbf{x}, t) u'_2(\mathbf{x}, t)}, \quad (3)$$

where ρ is the fluid density. In addition, consistent with previous flow analyses on patient MRI data, flow skewness and eccentricity

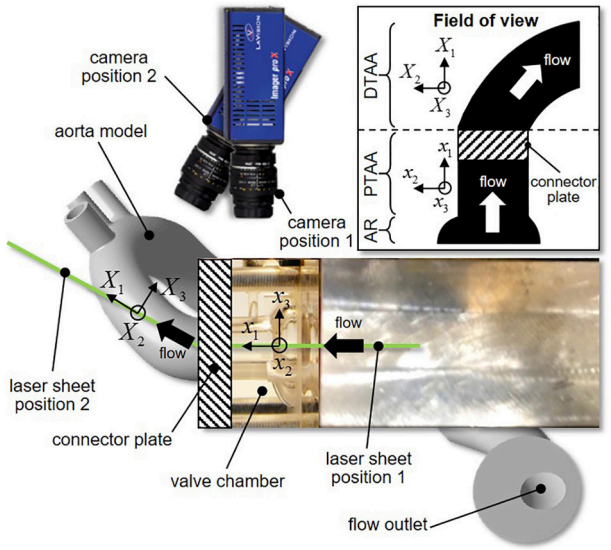

FIGURE 4 | Laser sheet and camera configurations (inset, reconstructed field of view; AR, aortic root; PTAA, proximal tubular ascending aorta; DTAA, distal tubular ascending aorta).

were measured in three sections located 4 mm downstream of the sinotubular junction (section 1 in **Figure 5**), in the middle AA (section 2 in **Figure 5**), and in the distal section of the tubular AA (section 3 in **Figure 5**). The skewness of the systolic valvular jet was assessed in terms of the valve flow angle (θ) defined as

$$\theta = \cos^{-1}(\mathbf{n} \cdot \mathbf{Q}), \tag{4}$$

where $\mathbf{Q}$ is the mean flow vector and $\mathbf{n}$ is the unit vector normal to the aortic section of interest (Mahadevia et al., 2014). The eccentricity of the systolic valvular jet was characterized in terms of the flow displacement (d), i.e., the distance between the center of the aortic section of interest and the centroid of the top 15% of velocities in the same section (Sigovan et al., 2011). These two metrics were calculated on the peak-systolic flow field.

RESULTS

Jet Skewness, Eccentricity and Mean Velocity Field

The mean velocity fields $\bar{\mathbf{u}}(\mathbf{x}, t)$ measured at peak systole and early diastole for all valve models are shown in **Figure 5**. Peak-systolic flow angle and flow displacement values for each valve are reported in **Table 1**. At peak-systole, the TAV generates an orifice jet essentially aligned along the axis of the aorta. Further downstream, the flow patterns and velocity vectors follow the curvature of the tubular AA smoothly. These observations are supported by the moderate flow angle and flow displacement ($6.3 < \theta < 14.1^\circ$, $0.6 < d < 1.4$ mm) measured throughout the geometry. In contrast, the BAVs generate orifice jets skewed toward the convexity of the tubular AA. While this phenomenon is obvious for the LR-BAV, it is less pronounced in the RN- and NL-BAV cases, due to the orientation of the RN- and NL-BAV jets out of the plane of observation. The apparent skewness of the NL-BAV jet toward the wall convexity is a technical artifact due to the inability of the two-dimensional PIV plane to capture the full three-dimensional helical flow characteristics generated by this morphotype in the aorta. The combination of the larger flow angles and displacements generated by the BAVs ($3.2 < \theta < 37.1^\circ$, $0.3 < d < 8.2$ mm) forces the jet to impinge the AA wall at locations proximal to the TAV jet impingement site. In addition, the initial flow asymmetry observed in the three BAVs generates a recirculation zone near the concavity of the proximal tubular AA, whose direction depends on the morphotype (LR-BAV and RN-BAV: clockwise; TAV and NL-BAV: counterclockwise).

While the three morphotypes generate a jet-like flow structure characterized by a high-velocity core and a low-velocity mixing zone near the valve orifice, some interesting variations can be observed downstream. In the RN-BAV and NL-BAV, the skewed orifice jet formed in the aortic root separates into two branches near the inlet of the distal tubular AA before remerging near the outlet, suggesting the existence of recirculation and out-of-plane motion. In contrast, the LR-BAV flow maintains a jet-like structure up to the distal section of the tubular AA. The progressive development of the flow along the axis of the aorta tends to normalize the flow and eliminate the differences observed upstream as suggested by the nearly similar velocity profiles, low flow angles ($\theta < 1.8^\circ$, $d < 5.8$ mm) and displacements measured at the outlet section. Lastly, the analysis of the in-plane peak-systolic velocity magnitude also reveals important differences between the valves. While the TAV maintains a normal peak-systolic velocity (1.7 m/s), the LR-BAV and NL-BAV peak velocities (2.9 and 3.9 m/s, respectively) fall in the stenotic range.

Viscous Shear Stress

The peak-systolic and early diastolic viscous shear stress fields $\bar{\tau}(\mathbf{x}, t)$ are shown in **Figure 6**. At peak systole, the shear stresses are concentrated in the shear layers that extend from the tip of the leaflets. The skewness of the LR- and NL-BAV jets toward the convexity of the proximal tubular AA subjects the aortic wall to a 1.7-fold increase in shear stress magnitude relative to the TAV. However, while the region of wall shear stress overload remains constrained in the proximal tubular AA in the LR-BAV case, it localizes in the distal tubular AA in the NL-BAV case. During the deceleration phase, the convexity of the TAV proximal aorta experiences a substantial reduction in wall shear stress (72% reduction relative to peak-systole). This is not the case with the LR- and NL-BAV aortas, in which the complex rotational flow structures subject the wall to sustained wall shear stress overloads (2.0-fold increase relative to the TAV) despite the reduction in forward flow momentum. The RN-BAV, which generates an orifice jet outside the measurement plane, subjects the convexity of the aortic wall to milder viscous shear stresses in the plane of observation.

Reynolds Shear Stress

The peak-systolic and early diastolic Reynolds shear stress fields $\tau'(\mathbf{x}, t)$ are shown in **Figure 7**. Regardless of the valve anatomy,

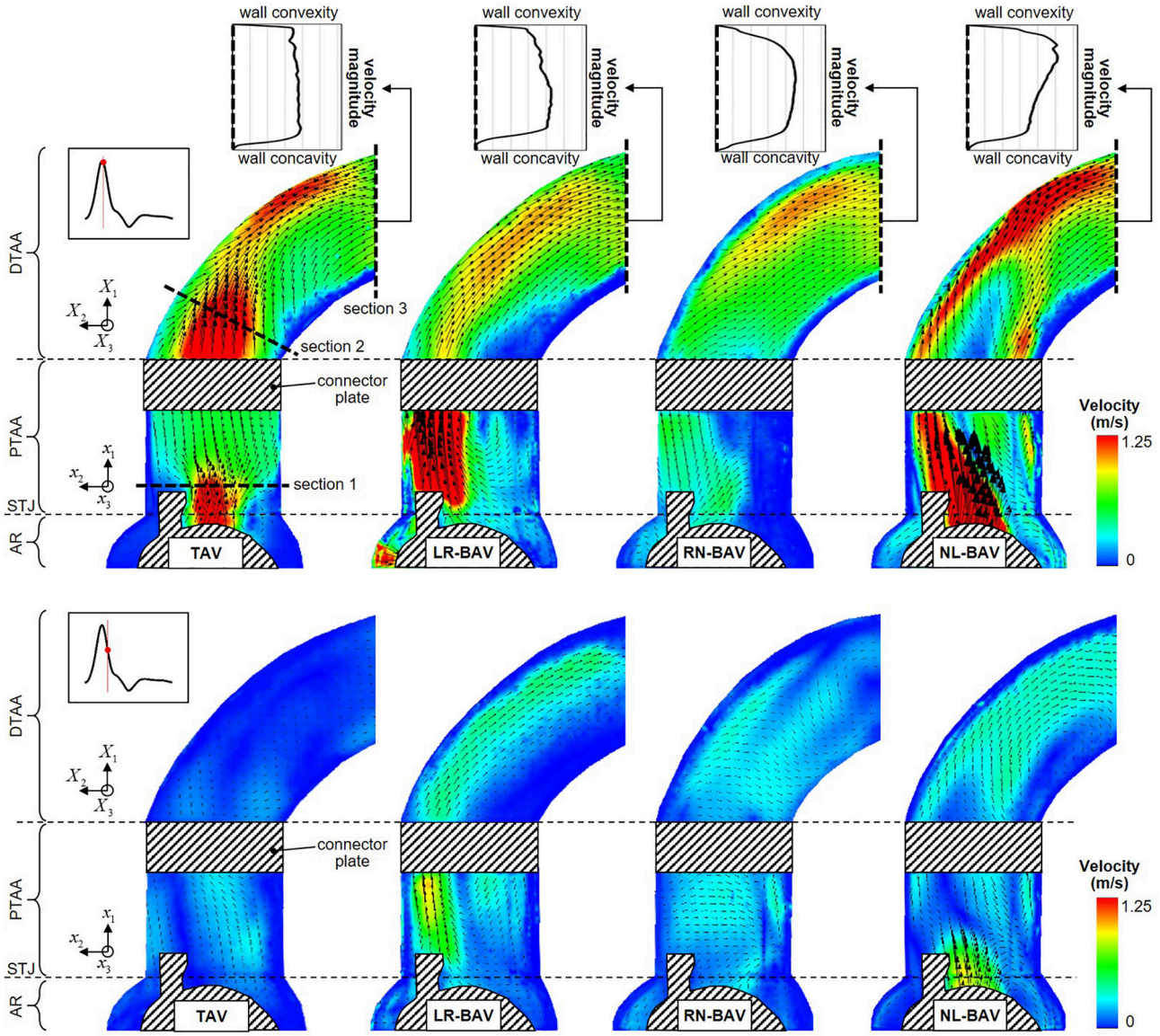

FIGURE 5 | Snapshots of the mean velocity fields generated by the four valve models at peak systole (top) and late systole (bottom), and peak-systolic velocity profiles measured across the outlet section of the aorta phantom (AR, aortic root; STJ, sinotubular junction; PTAA, proximal tubular ascending aorta; DTAA, distal tubular ascending aorta).

the peak Reynolds shear stress is two-orders-of-magnitude larger than the peak viscous shear stress, indicating the domination of the flow by the turbulent stresses. As expected, those effects are the most apparent in the wake of the leaflets, where turbulence effects and velocity fluctuations attain their maximum. The only exception to this observation is for the RN-BAV due to the orientation of the jet out of the plane of observation. Turbulent stress levels are substantially more moderate in the distal section of the AA, which suggests the possible relaminarization of the flow in this region. Consistent with the viscous shear stress measurements, the comparison of the Reynolds shear stress fields at peak systole and during deceleration reveals that turbulence dominates the flow only at peak systole in the TAV aorta (49% reduction in maximum Reynolds shear stress between peak systole and deceleration), while it is sustained over a longer period in the LR-BAV and NL-BAV aortas (24% difference in maximum Reynolds shear stress between peak systole and deceleration).

DISCUSSION

This *in vitro* study implemented PIV to characterize morphotype-dependent flow abnormalities in BAV aortas, prior to dilation. The results complement previous demonstrations of the existence of flow abnormalities in BAV aortas by revealing: (1) the existence of different degrees of flow abnormalities in

dilated and non-dilated BAV aortas, and (2) the existence of viscous shear stress overloads in non-dilated BAV aorta regions prone to aortopathy.

Summary of Morphotype-Dependent Flow Abnormalities

The use of the same aorta geometry and flow conditions in all our experiments permits to isolate the critical impact of the BAV morphotype on hemodynamics. First, at least two BAV morphotypes (LR- and NL-BAV) generated some degree of hemodynamic stenosis as quantified by jet velocity. While the RN-BAV jet velocity was in the normal range, measurements of the three velocity components in multiple planes would be needed to determine whether this morphotype was normo-functional or stenotic like the two other morphotypes. Nevertheless, the existence of intrinsic stenosis in BAVs is consistent with clinical reports that have estimated that nearly 50% of all BAVs exhibit some level of stenosis, without the presence of calcification (Keane et al., 2000; Sievers and Schmidtke, 2007; Hope et al., 2010). Second, the type of leaflet fusion was shown to affect primarily the site of impingement of the valve orifice jet on the aortic wall, with the LR-BAV jet impinging on the proximal convexity and the NL-BAV jet impinging further downstream in the distal proximity of the aortic wall. This morphotype-dependence resulted in different sites of viscous shear stress overload. Third, the different BAV morphotypes affected both flow eccentricity and skewness to different extents and in different regions of the AA. The results suggest that the RN-BAV generated the most pronounced abnormality in flow angle throughout the AA, although this conclusion should be considered carefully since RN-BAV flow was mostly out of the plane of observation in the experiments. In contrast, the LR- and NL-BAV morphotypes had a greater impact on flow eccentricity, with the LR-BAV generating abnormalities in the proximal and middle AA and the NL-BAV in the middle and distal AA. Lastly, the type of leaflet fusion also affected the extent and spread of flow abnormalities in the AA. In fact, while LR-BAV flow abnormalities were mostly contained within the proximal AA and progressively attenuated as the flow developed in the distal AA (16% and 12% reduction in flow angle and displacement, respectively), RN- and NL-BAV flow abnormalities amplified as the flow developed from the proximal to the distal section (up to 97 and 555% increase in flow angle and displacement, respectively). These morphotype-dependent flow features, which essentially coincide with the morphotype-dependent expression of aortopathy, may play a role in BAV aortopathy initiation and development.

Implications for BAV Aortopathy

The viscous shear stress levels measured in this study are in agreement with those from previous experimental and computational studies (Weston et al., 1999; Barker et al., 2012; Chandra et al., 2012; Meierhofer et al., 2013; Seaman et al., 2014, 2015) and have been suggested as a possible driver of aortopathy (Barker et al., 2012; Atkins and Sucosky, 2014; Atkins et al., 2014, 2016b). The present experimental results confirm the existence of shear stress overloads in aortic wall regions prone to dilation, even in normal non-dilated aortas. While this observation only suggests the potential involvement of hemodynamics in the pathogenesis of BAV aortopathy, it provides a more solid evidence of the existence of a hemodynamic pathway of BAV aortopathy when the results are put in the perspective of previous *ex vivo* and clinical studies. In fact, it is well known that 1) BAVs are associated with morphotype-dependent dilation patterns (Fazel et al., 2008; Schaefer et al., 2008); and 2) BAVs generate morphotype-dependent flow abnormalities in regions prone to dilation (as shown in the present study and in Hope et al., 2014; Cao and Sucosky, 2015; van Ooij et al., 2015; Fedak et al., 2016; Cao et al., 2017). The possible causality between these two facts has been partially but rigorously provided by *ex vivo* studies conducted in our laboratory, which have demonstrated the ability of the stress abnormalities generated in the disease-prone convexity of the LR-BAV aorta to trigger aortic medial remodeling via MMP-dependent pathways and the absence of any significant remodeling in response to the hemodynamics of the disease-protected concavity (Atkins and Sucosky, 2014; Atkins et al., 2014, 2016b; Sucosky, 2014). In this context, the data presented in this study suggests that the elucidation of the shear stress environment in BAV AAs might be critical toward the development of improved clinical guidelines for the management of BAV patients (Atkins et al., 2016a).

TABLE 1 | Peak-systolic flow angle and displacement.

	Measurement site	TAV	LR-BAV	RN-BAV	NL-BAV
θ (°)	Section 1	14.1	18.4	23.4	3.2
	Section 2	6.3	15.6	37.1	6.3
	Section 3	13.7	12.4	14.8	12.7
d (mm)	Section 1	1.4	6.8	1.1	4.0
	Section 2	0.6	6.0	7.2	8.2
	Section 3	1.2	−0.4	−0.3	5.8

Impact of Aortic Dilation on BAV Hemodynamics

An important novelty of the present study is its particular focus on the impact of BAV flow in non-dilated aortas. The rationale for this investigation is supported by the need to determine whether the flow abnormalities typically present in BAV aortas are the consequence of the abnormal valve anatomy or a dilated aorta. Similarly to previous *in vivo* results, which may have included dilated BAV aortas (Bissell et al., 2013; Mahadevia et al., 2014), the present experimental study confirms the skewness of the BAV orifice jet toward the convexity of the aortic wall, the dependence of the degree of jet skewness on the BAV morphotype and the existence of viscous shear stress overloads in the convexity of BAV aortas. Interestingly, the absence of dilation in the present study did not systematically attenuate the degree of hemodynamic abnormality captured *in vivo* in dilated BAV aortas. This is particularly apparent for the in-plane flow skewness, which was 38% smaller in the non-dilated LR-BAV aorta but 69% larger in the non-dilated RN-BAV aorta as compared to their dilated counterparts (Mahadevia et al., 2014).

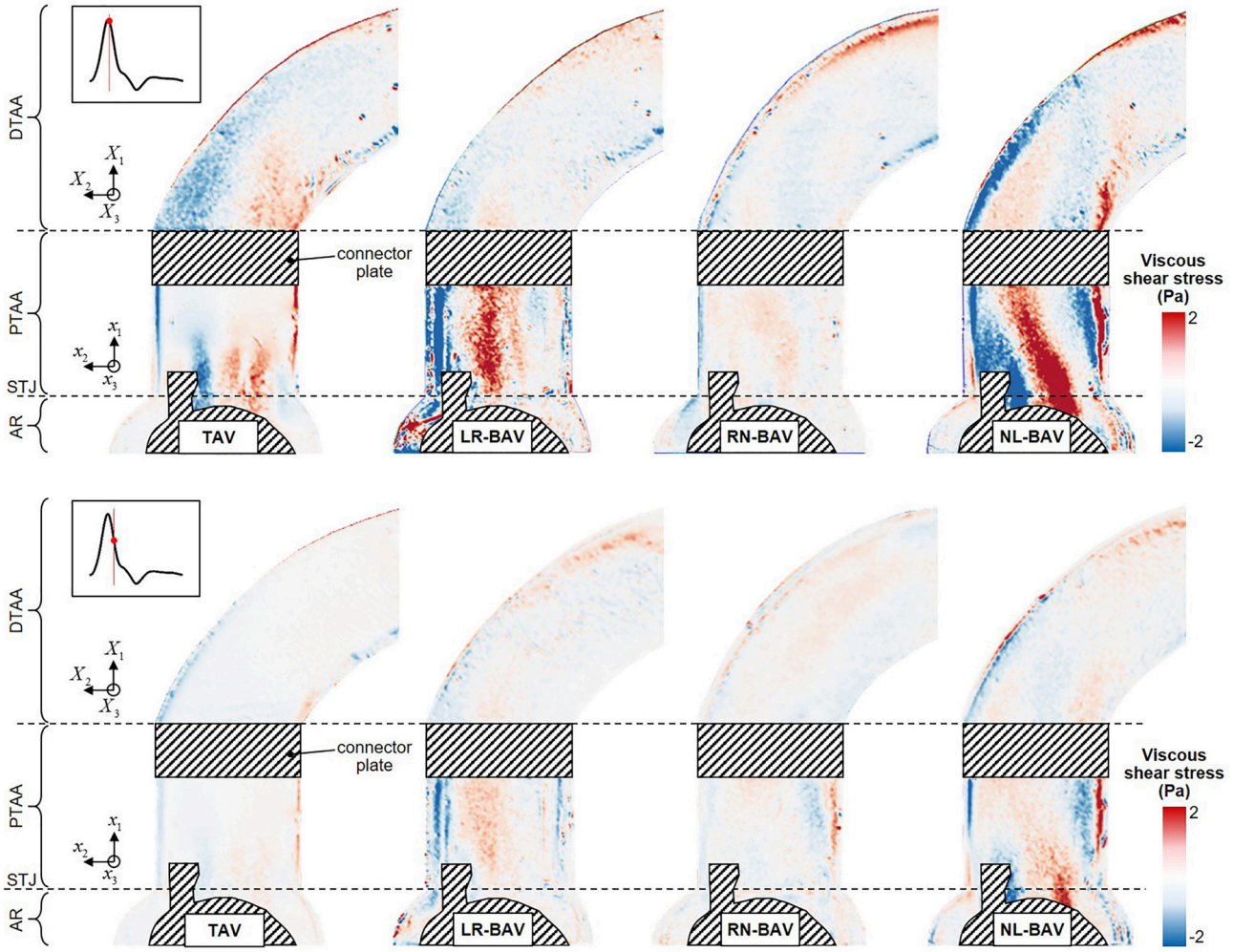

FIGURE 6 | Snapshots of the viscous shear stress fields generated by the four valve models at peak systole (top) and late systole (bottom) (AR, aortic root; STJ, sinotubular junction; PTAA, proximal tubular ascending aorta; DTAA, distal tubular ascending aorta).

Lastly, the present experimental results confirm the existence of shear stress overloads in BAV aortic wall regions prone to dilation, but also demonstrate that those abnormalities exist prior to dilation. These observations are supported by previous computational results suggesting the possible impact of aortic dilation on aortic flow (Cao et al., 2017). Therefore, while the present results confirm the morphotype-dependence of flow abnormalities in BAV aortas, they also suggest the alteration of this dependence throughout the course of the disease and the synergistic effects of BAV anatomy and aorta anatomy on aortic flow.

Limitations

Although the experiments were carried out with the upmost rigor, the experimental technique and methodology include a few limitations. First, PIV only permitted to capture the flow in a two-dimensional section and was not able to provide more insights into the three-dimensional flow structures. While this is a known limitation of the PIV technique, it did not prevent the demonstration of flow differences between the different valve models investigated. However, this limitation combined with the relatively poor performance of PIV in quantifiying near-wall flow regions may explain some of the differences in flow and viscous shear stress between the present study in a normal aorta and previous *in vivo* studies in potentially dilated BAV aortas (Piatti et al., 2017). Second, the pressure conditions generated within the flow loop only approximated physiologic levels due to the partial replication of the native systemic compliance and resistance. However, the resulting cardiac outputs remained within the physiologic range. More importantly, all valve models were tested under the same pressure conditions in order to allow for the direct comparison of the flow results and the effective isolation of the impact of the valve morphotype. Third, the flow characterization was based on one specimen for each valve anatomy. Therefore, the flow results reported in the present study may not be fully representative of the hemodynamic abnormalities generated by each valve type. While a larger sample size would enable the production of statistically

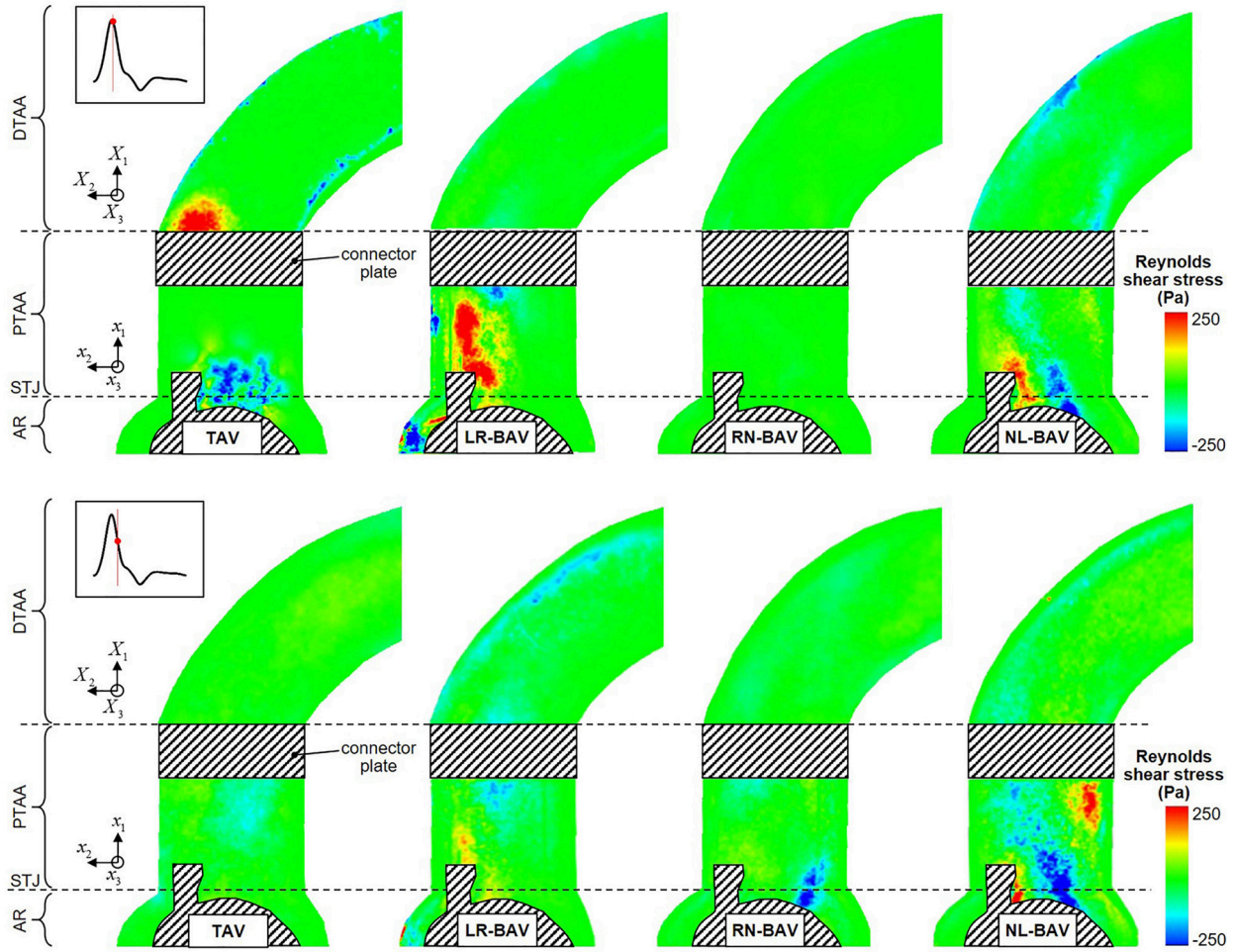

FIGURE 7 | Snapshots of the Reynolds shear stress fields generated by the four valve models at peak systole (top) and late systole (bottom) (AR, aortic root; STJ, sinotubular junction; PTAA, proximal tubular ascending aorta; DTAA, distal tubular ascending aorta).

meaningful data, the use of a single specimen per valve was motivated by the requirement to obtain spatially and temporally resolved flow measurements while limiting processing time (192 h for each valve) and data storage requirements (1.5 TB for all raw images and processed velocity fields). Lastly, although the benchtop flow loop was able to generate near-physiologic pulsatile flow conditions, it included some geometrical and functional idealization (e.g., non-compliant three-lobed aortic sinus, uniaxial left-ventricular contraction) that did not replicate exactly the native anatomical characteristics of the aortic sinus and the native deformation of the left ventricle. However, the use of approximated but similar left ventricular outflow condition and sinus geometry in all experiments permitted to achieve our central objective to isolate the impact of valvular anatomy on aorta hemodynamics.

CONCLUSION

This experimental study isolated for the first time the impact of the BAV morphotype on aortic flow in a compliant and realistic aorta geometry. The results demonstrate the impact of leaflet fusion on downstream hemodynamics and reveal substantial differences with respect to *in vivo* studies on dilated aortas. Most significantly, all BAV morphotypes subject the aortic wall to shear stress overloads at locations prone to dilation, providing more support for the existence of a hemodynamic etiology in BAV aortopathy.

AUTHOR CONTRIBUTIONS

AMN and AM performed the experiments, analyzed the data and wrote the paper. PS analyzed the data, wrote the paper and conceived the work.

FUNDING

Research described in this paper has been funded by the National Science Foundation (CAREER CMMI-1148558), the American Heart Association (17GRNT3350028, 11SDG7600103, and 14PRE18940010).

REFERENCES

Angelini, A., Ho, S. Y., Anderson, R. H., Devine, W. A., Zuberbuhler, J. R., Becker, A. E., et al. (1989). The morphology of the normal aortic valve as compared with the aortic valve having two leaflets. *J. Thorac. Cardiovasc. Surg.* 98, 362–367.

Atkins, S. K., Cao, K., Rajamannan, N. M., and Sucosky, P. (2014). Bicuspid aortic valve hemodynamics induces abnormal medial remodeling in the convexity of porcine ascending aortas. *Biomech. Model. Mechanobiol.* 13, 1209–1225. doi: 10.1007/s10237-014-0567-7

Atkins, S. K., McNally, A., and Sucosky, P. (2016a). Mechanobiology in cardiovascular disease management: potential strategies and current needs. *Front. Bioeng. Biotechnol.* 4:79. doi: 10.3389/fbioe.2016.00079

Atkins, S. K., Moore, A., and Sucosky, P. (2016b). Bicuspid aortic valve hemodynamics does not promote remodeling in porcine aortic wall concavity. *World J. Cardiol.* 8, 89–97. doi: 10.4330/wjc.v8.i1.89

Atkins, S. K., and Sucosky, P. (2014). The etiology of bicuspid aortic valve disease: focus on hemodynamics. *World J. Cardiol.* 12, 1227–1233. doi: 10.4330/wjc.v6.i12.1227

Barker, A. J., Lanning, C., and Shandas, R. (2010). Quantification of hemodynamic wall shear stress in patients with bicuspid aortic valve using phase-contrast MRI. *Ann. Biomed. Eng.* 38, 788–800. doi: 10.1007/s10439-009-9854-3

Barker, A. J., and Markl, M. (2011). The role of hemodynamics in bicuspid aortic valve disease. *Eur. J. Cardiothorac. Surg.* 39, 805–806. doi: 10.1016/j.ejcts.2011.01.006

Barker, A. J., Markl, M., Bürk, J., Lorenz, R., Bock, J., Bauer, S., et al. (2012). Bicuspid aortic valve is associated with altered wall shear stress in the ascending aorta. *Circ. Cardiovasc. Imaging* 5, 457–466. doi: 10.1161/CIRCIMAGING.112.973370

Bissell, M. M., Hess, A. T., Biasiolli, L., Glaze, S. J., Loudon, M., Pitcher, A., et al. (2013). Aortic dilation in bicuspid aortic valve disease: flow pattern is a major contributor and differs with valve fusion type. *Circ. Cardiovasc. Imaging* 6, 499–507. doi: 10.1161/CIRCIMAGING.113.000528

Cao, K., Atkins, S. K., McNally, A., Liu, J., and Sucosky, P. (2017). Simulations of morphotype-dependent hemodynamics in non-dilated bicuspid aortic valve aortas. *J. Biomech*. 50, 63–70. doi: 10.1016/j.jbiomech.2016.11.024

Cao, K., and Sucosky, P. (2015). Effect of bicuspid aortic valve cusp fusion on aorta wall shear stress: preliminary computational assessment and implication for aortic dilation. *World J. Cardiovasc. Dis.* 5, 129–140. doi: 10.4236/wjcd.2015.56016

Chandra, S., Rajamannan, N. M., and Sucosky, P. (2012). Computational assessment of bicuspid aortic valve wall-shear stress: implications for calcific aortic valve disease. *Biomech. Model. Mechanobiol.* 11, 1085–1096. doi: 10.1007/s10237-012-0375-x

Della Corte, A. (2015). The conundrum of aortic dissection in patients with bicuspid aortic valve: the tissue, the mechanics and the mathematics. *Eur. J. Cardiothorac. Surg.* 48, 150–151. doi: 10.1093/ejcts/ezu418

Della Corte, A., Bancone, C., Conti, C. A., Votta, E., Redaelli, A., Del Viscovo, L., et al. (2011). Restricted cusp motion in right-left type of bicuspid aortic valves: A new risk marker for aortopathy. *J. Thorac. Cardiovasc. Surg*. 144, 360–369. doi: 10.1016/j.jtcvs.2011.10.014

Fazel, S. S., Mallidi, H. R., Lee, R. S., Sheehan, M. P., Liang, D., Fleischman, D., et al. (2008). The aortopathy of bicuspid aortic valve disease has distinctive patterns and usually involves the transverse aortic arch. *J. Thorac. Cardiovasc. Surg.* 135, 901–907. doi: 10.1016/j.jtcvs.2008.01.022

Fedak, P. W., Barker, A. J., and Verma, S. (2016). Year in review: bicuspid aortopathy. *Curr. Opin. Cardiol.* 31, 132–138. doi: 10.1097/HCO.0000000000000258

Gilmanov, A., and Sotiropoulos, F. (2016). Comparative hemodynamics in an aorta with bicuspid and trileaflet valves. *Theor. Comput. Fluid Dyn*. 30 67–85. doi: 10.1007/s00162-015-0364-7

Girdauskas, E., Borger, M. A., Secknus, M. A., Girdauskas, G., and Kuntze, T. (2011). Is aortopathy in bicuspid aortic valve disease a congenital defect or a result of abnormal hemodynamics? A critical reappraisal of a one-sided argument. *Eur. J. Cardiothorac. Surg.* 39, 809–814. doi: 10.1016/j.ejcts.2011.01.001

Girdauskas, E., Rouman, M., Disha, K., Scholle, T., Fey, B., Theis, B., et al. (2014). Correlation between systolic transvalvular flow and proximal aortic wall changes in bicuspid aortic valve stenosis. *Eur. J. Cardiothorac. Surg.* 46, 234–239; discussion 239. doi: 10.1093/ejcts/ezt610

Hope, M. D., Hope, T. A., Meadows, A. K., Ordovas, K. G., Urbania, T. H., Alley, M. T., et al. (2010). Bicuspid aortic valve: four-dimensional MR evaluation of ascending aortic systolic flow patterns. *Radiology* 255, 53–61. doi: 10.1148/radiol.09091437

Hope, M. D., Meadows, A. K., Hope, T. A., Ordovas, K. G., Reddy, G. P., Alley, M. T., et al. (2008). Images in cardiovascular medicine. Evaluation of bicuspid aortic valve and aortic coarctation with 4D flow magnetic resonance imaging. *Circulation* 117, 2818–2819. doi: 10.1161/CIRCULATIONAHA.107.760124

Hope, M. D., Sigovan, M., Wrenn, S. J., Saloner, D., and Dyverfeldt, P. (2014). MRI hemodynamic markers of progressive bicuspid aortic valve-related aortic disease. *J. Magn. Reson. Imaging* 40, 140–145. doi: 10.1002/jmri.24362

Keane, M. G., Wiegers, S. E., Plappert, T., Pochettino, A., Bavaria, J. E., and Sutton, M. G. (2000). Bicuspid aortic valves are associated with aortic dilatation out of proportion to coexistent valvular lesions. *Circulation* 102, 35–39. doi: 10.1161/01.CIR.102.suppl_3.III-35

Mahadevia, R., Barker, A. J., Schnell, S., Entezari, P., Kansal, P., Fedak, P. W. M., et al. (2014). Bicuspid aortic cusp fusion morphology alters aortic 3D Outflow patterns, wall shear stress and expression of aortopathy. *Circulation* 129, 673–682. doi: 10.1161/CIRCULATIONAHA.113.003026

Meierhofer, C., Schneider, E. P., Lyko, C., Hutter, A., Martinoff, S., Markl, M., et al. (2013). Wall shear stress and flow patterns in the ascending aorta in patients with bicuspid aortic valves differ significantly from tricuspid aortic valves: a prospective study. *Eur. Heart J. Cardiovasc. Imaging* 14, 797–804. doi: 10.1093/ehjci/jes273

Mirabella, L., Barker, A. J., Saikrishnan, N., Coco, E. R., Mangiameli, D. J., Markl, M., et al. (2015). MRI-based protocol to characterize the relationship between bicuspid aortic valve morphology and hemodynamics. *Ann. Biomed. Eng.* 43, 1815–1827. doi: 10.1007/s10439-014-1214-2

Piatti, F., Pirola, S., Bissell, M., Nesteruk, I., Sturla, F., Della Corte, A., et al. (2017). Towards the improved quantification of *in vivo* abnormal wall shear stresses in BAV-affected patients from 4D-flow imaging: benchmarking and application to real data. *J. Biomech.* 50, 93–101. doi: 10.1016/j.jbiomech.2016.11.044

Roberts, W. C. (1970). The congenitally bicuspid aortic valve. A study of 85 autopsy cases. *Am. J. Cardiol.* 26, 72–83. doi: 10.1016/0002-9149(70)90761-7

Robicsek, F., Thubrikar, M. J., Cook, J. W., and Fowler, B. (2004). The congenitally bicuspid aortic valve: how does it function? Why does it fail? *Ann. Thorac. Surg.* 77, 177–185. doi: 10.1016/S0003-4975(03)01249-9

Sabet, H. Y., Edwards, W. D., Tazelaar, H. D., and Daly, R. C. (1999). Congenitally bicuspid aortic valves: a surgical pathology study of 542 cases (1991 through 1996) and a literature review of 2,715 additional cases. *Mayo Clin. Proc.* 74, 14–26. doi: 10.4065/74.1.14

Saikrishnan, N., Yap, C.-H., Milligan, N. C., Vasilyev, N. V., and Yoganathan, A. P. (2012). *In vitro* characterization of bicuspid aortic valve hemodynamics using particle image velocimetry. *Ann. Biomed. Eng.* 40, 1760–1775. doi: 10.1007/s10439-012-0527-2

Schaefer, B. M., Lewin, M. B., Stout, K. K., Gill, E., Prueitt, A., Byers, P. H., et al. (2008). The bicuspid aortic valve: an integrated phenotypic classification of leaflet morphology and aortic root shape. *Heart* 94, 1634–1638. doi: 10.1136/hrt.2007.132092

Seaman, C., Akingba, A. G., and Sucosky, P. (2014). Steady flow hemodynamic and energy loss measurements in normal and simulated calcified tricuspid and bicuspid aortic valves. *J. Biomech. Eng.* 136, 1–11. doi: 10.1115/1.4026575

Seaman, C., McNally, A., Biddle, S., Jankowski, L., and Sucosky, P. (2015). generation of simulated calcific lesions in valve leaflets for flow studies. *J. Heart Valve Dis.* 24, 1–11.

Seaman, C., and Sucosky, P. (2014). Anatomic versus effective orifice area in a bicuspid aortic valve. *Echocardiography* 31:1028. doi: 10.1111/echo.12720

Sievers, H. H., and Schmidtke, C. (2007). A classification system for the bicuspid aortic valve from 304 surgical specimens. *J. Thorac. Cardiovasc. Surg.* 133, 1226–1233. doi: 10.1016/j.jtcvs.2007.01.039

Sigovan, M., Hope, M. D., Dyverfeldt, P., and Saloner, D. (2011). Comparison of four-dimensional flow parameters for quantification of flow eccentricity in the ascending aorta. *J. Magn. Reson. Imaging* 34, 1226–1230. doi: 10.1002/jmri.22800

Sucosky, P. (2014). "Hemodynamic mechanisms of bicuspid aortic valve calcification and aortopathy," in *Molecular Biology of Valvular Heart Disease*, ed N. Rajamannan (London: Springer), 81–94.

Sucosky, P., and Rajamannan, N. M. (2013). "Bicuspid aortic valve disease: from bench to bedside," in *Cardiac Valvular Medicine*, ed N. Rajamannan (London: Springer), 17–21.

Swanson, M., and Clark, R. E. (1974). Dimensions and geometric relationships of the human aortic value as a function of pressure. *Circulation* 35, 871–882. doi: 10.1161/01.RES.35.6.871

Thubrikar, M. J., Aouad, J., and Nolan, S. P. (1986). Patterns of calcific deposits in operatively excised stenotic or purely regurgitant aortic valves and their relation to mechanical stress. *Am. J. Cardiol.* 58, 304–308. doi: 10.1016/0002-9149(86)90067-6

van Ooij, P., Potters, W. V., Collins, J., Carr, M., Carr, J., Malaisrie, S. C., et al. (2015). Characterization of abnormal wall shear stress using 4D flow MRI in human bicuspid aortopathy. *Ann. Biomed. Eng.* 43, 1385–1397. doi: 10.1007/s10439-014-1092-7

Ward, C. (2000). Clinical significance of the bicuspid aortic valve. *Heart* 83, 81–85. doi: 10.1136/heart.83.1.81

Weston, M. W., LaBorde, D. V., and Yoganathan, A. P. (1999). Estimation of the shear stress on the surface of an aortic valve leaflet. *Ann. Biomed. Eng.* 27, 572–579. doi: 10.1114/1.199

Yap, C. H., Saikrishnan, N., Tamilselvan, G., Vasilyev, N., Yoganathan, A. P., and Vasiliyev, N. (2012). The congenital bicuspid aortic valve can experience high frequency unsteady shear stresses on its leaflet surface. *Am. J. Physiol. Heart Circ. Physiol.* 303, H721–H731. doi: 10.1152/ajpheart.00829.2011a

Conflict of Interest Statement: The authors declare that the research was conducted in the absence of any commercial or financial relationships that could be construed as a potential conflict of interest.

frontiers in Physiology

ORIGINAL RESEARCH
published: 28 August 2017
doi: 10.3389/fphys.2017.00622

Characteristics of Carotid Artery Structure and Mechanical Function and Their Relationships with Aortopathy in Patients with Bicuspid Aortic Valves

*Mihyun Kim, Chi Young Shim *, Seong-Chan You, In-Jeong Cho, Geu-Ru Hong, Jong-Won Ha and Namsik Chung*

Division of Cardiology, Severance Cardiovascular Hospital, Yonsei University College of Medicine, Seoul, South Korea

Patients with a bicuspid aortic valve (BAV) often have proximal aortic dilatation and systemic vascular dysfunction. We hypothesized that BAV patients would have different carotid artery structural and functional characteristics compared to tricuspid aortic valve (TAV) patients. In 28 patients with surgically confirmed BAV and 27 patients with TAV, intima media thickness (IMT), number of plaques, fractional area change (FAC), global circumferential strain (GCS), and standard deviation of CS (SD-CS) in both common carotid arteries were assessed using duplex ultrasound and velocity vector imaging (VVI). Patients with BAV were younger and had less co-morbidity, but showed a significantly larger ascending aorta (43.3 ± 7.5 vs. 37.0 ± 6.2 mm, $p < 0.001$) and a higher prevalence of aortopathy (61 vs. 30%, $p = 0.021$) than those with TAV. BAV patients showed a significantly lower IMT and fewer plaques. Although FAC and GCS were not significantly different between the two groups, they tended to be lower in the BAV group when each group was divided into three subgroups according to age. There was a significant age-dependent increase in IMT and decreases in FAC and GCS in the TAV group ($p = 0.005$, $p = 0.001$, $p = 0.002$, respectively), but this phenomenon was not evident in the BAV group ($p = 0.074$, $p = 0.248$, $p = 0.394$, respectively). BAV patients with aortopathy showed a higher SD-CS than those without aortopathy ($p = 0.040$), reflecting disordered mechanical function. In conclusion, BAV patients have different carotid artery structure and function compared with TAV patients, suggesting intrinsic vascular abnormalities that are less affected by established cardiovascular risk factors and more strongly related to the presence of aortopathy.

Keywords: bicuspid aortic valve, aortopathy, ultrasound, velocity vector imaging, carotid artery

OPEN ACCESS

Edited by:
Alessandro Della Corte, Monaldi Hospital, Italy

Reviewed by:
Soo Youn Lee, Sejong General Hospital, South Korea
Vincenzo Lionetti, Sant'Anna School of Advanced Studies, Italy
Samantha K. Atkins, University of Notre Dame, United States

****Correspondence:***
Chi Young Shim
cysprs@yuhs.ac

Specialty section:
This article was submitted to Vascular Physiology, a section of the journal Frontiers in Physiology

Received: *31 March 2017*
Accepted: *11 August 2017*
Published: *28 August 2017*

Citation:
Kim M, Shim CY, You S-C, Cho I-J, Hong G-R, Ha J-W and Chung N (2017) Characteristics of Carotid Artery Structure and Mechanical Function and Their Relationships with Aortopathy in Patients with Bicuspid Aortic Valves. Front. Physiol. 8:622. doi: 10.3389/fphys.2017.00622

INTRODUCTION

Bicuspid aortic valve (BAV) is the most common congenital heart valve disease (Verma and Siu, 2014). Patients with BAV are more likely to have proximal aortic dilation and systemic vascular dysfunction such as endothelial dysfunction or arterial stiffness than patients with a tricuspid aortic valve (TAV; Ferencik and Pape, 2003; Tadros et al., 2009). Intrinsic pathology of accelerated

degeneration of the aortic media and combined hemodynamic factors are considered to be the main contributors to aortic dilation (Fedak et al., 2002; Wilton and Jahangiri, 2006). Reduced arterial elasticity in any site of the aorta or carotid artery has been proven in patients with BAV because the intrinsic pathologic alterations are not confined to the proximal part of aorta but extend into the entire aorta (Grotenhuis et al., 2007; Bilen et al., 2012).

Assessment of carotid artery structure and function has been highlighted in patients with aortic valve (AV) disease because carotid atherosclerosis and degenerative AV disease have common risk factors and pathogenesis. However, the structural and functional characteristics of the carotid artery in patients with BAV compared to those with TAV have not been comprehensively demonstrated. Also, the association between carotid mechanical dysfunction and the presence of aortopathy is uncertain (Petrini et al., 2014). Recently, lower carotid strain and a higher carotid stiffness index were shown in patients with BAV than in healthy controls, especially when the patients have dilation of the aorta (Li et al., 2016). In another study examining IMT of the descending aorta, IMT of the descending aorta was not directly influenced by the presence of BAV. Age was the main determinant of the aortic IMT (Petrini et al., 2016).

In this study, we hypothesized that: (1) patients with BAV would present less atherosclerotic structural change in the carotid arteries than those with TAV, (2) patients with BAV would have a different carotid mechanical function reflecting intrinsic wall abnormalities, and (3) the presence of aortopathy in patients with BAV would affect the carotid artery mechanical function. To support our hypotheses, we comprehensively evaluated carotid arterial structure and function using either carotid artery Duplex ultrasound or velocity vector imaging (VVI) in patients with BAV, compared the findings with those in patients with TAV, and analyzed the data according to the presence of aortopathy.

METHODS

Study Subjects

Twenty-eight patients with BAV disease and 27 patients with TAV were performed carotid artery Duplex ultrasound as part of preoperative evaluation before AV surgery at Severance Cardiovascular Hospital in Yonsei University (Seoul, South Korea) from January 2015 to January 2016. Patients with left ventricular systolic dysfunction (left ventricular ejection fraction <40%), rheumatic AV disease, arrhythmia, systemic inflammatory disease, and those who were not suitable for analysis by carotid VVI were excluded from the study. The patients' medical records were comprehensively reviewed regarding the following demographic and clinical risk factors: age, sex, hypertension, diabetes mellitus, dyslipidemia, and coronary artery disease (diagnosed as greater than 50% angiographic narrowing). According to valve dysfunction, the subjects were analyzed separately either in patients with severe AS or in patients with severe AR. Also, we divided the subjects into subgroups according to age: group 1 (<59 years), group 2 (60–69 years), and group 3 (≥70 years). Patients with BAV and those with TAV were also each categorized into two subgroups according to the presence of aortopathy (ascending aorta diameter >40 mm). This study was approved by our institutional ethics committee and complied with the Declaration of Helsinki. Written informed consent was exempt by the board as this study was a research involving the existing noninvasive images. Patient records/information was anonymized and de-identified prior to analysis.

Echocardiography

Standard two-dimensional and Doppler measurements were performed at least 1 month before the AV surgery following current recommendations for the assessment of valvular stenosis or regurgitation (Baumgartner et al., 2009; Lancellotti et al., 2010). Congenital BAV was diagnosed when only two cusps were unequivocally identified in systole and diastole in the short-axis view, with a clear "fish mouth" appearance during systole, as described in a previous study (Lee et al., 2015). BAV morphology was classified into the following four types according to position and pattern of raphe and cusps: Type 1, one raphe with fusion of the left coronary and right coronary cusps; type 2, one raphe with fusion of the right coronary and non-coronary cusps; type 3, one raphe with fusion of the left coronary and non-coronary cusps; type 0, no raphe with two developed cusps. The severity of aortic stenosis (AS) or aortic regurgitation (AR) was assessed using an integrated approach. All measurements of the aorta were performed according to recommendations on the QRS complex of the electrocardiogram (Lang et al., 2005). The dimension of the sinus of Valsalva was measured perpendicular to the right and left (or none) aortic sinuses. The sinotubular junction was measured where the aortic sinuses meet the tubular aorta. The ascending aorta (AA) was measured ∼2 cm distal to the sinotubular junction. Continuous-wave Doppler was used to measure the aortic transvalvular maximal velocities, and peak and mean gradients were calculated using the simplified Bernoulli equation. AV area was calculated using the continuity equation (velocity-time integral method). Stroke volume was calculated using the Doppler method as follows: $0.785 \times$ (left ventricular outflow track diameter) $^2 \times$ left ventricular outflow track velocity-time integral (Lang et al., 2005).

Carotid Artery Duplex Ultrasound

Both carotid arteries were assessed using a high-resolution, real-time, 8-MHz linear scanner (Acuson SC2000^{TM} Ultrasound System, Siemens Medical Solutions, USA Inc. Mountain View, CA). Optimal longitudinal and cross-sectional B-mode images of the common carotid arteries (CCAs) proximal to the bifurcation were obtained and stored digitally. A preliminary scan of internal, external, and common carotid arteries was performed to evaluate the presence of plaques and/or stenosis. Plaque was defined as either intima-media thickness (IMT) >1.3 mm or the presence of focal thickening at least 50% greater than the neighboring site on initial ultrasound examination. The IMT was calculated from manual measurements at the far wall of the carotid artery 1 cm proximal to the carotid bulb of both CCAs from leading edge (lumen-intima) to leading edge (media-adventitia) during end diastole (Sillesen et al., 2012).

Carotid Artery Velocity Vector Imaging

VVI measurements were performed on cross-sectional, two-dimensional ultrasound images of carotid arteries using an offline VVI workstation (Syngo US Workplace, Siemens). To obtain the optimal image for VVI analysis the images were stored at a rate of 60–120 frames/s using acoustic capture. Cross-sectional images of the CCA proximal to the bifurcation were scanned at the site without plaques. Cross-sectional images of the CCA either on the left or on the right from proximal to the bifurcation were divided into six segments. All segments were plotted by manually locating the endpoints of each segment on media–adventitia borders. The carotid artery borders were then identified and outlined according to the locations of the endpoints computed by the workstation (Cho et al., 2010; Yang et al., 2010, 2011). The fractional area change (FAC) was defined as the percentage change in cross-sectional area (CSA) between systole and diastole: FAC (%) = (largest CSA − smallest CSA)/(largest CSA) × 100. Global circumferential strain (GCS) was calculated as the average of peak circumferential strain of the six segments from each CCA (Kim et al., 2013). The GCS values from both CCAs were then averaged. The standard deviations of CS (SD-CS) of the six segments were analyzed on each CCA, and then the values from both CCAs were averaged. The inter-observer and intra-observer variability values for the VVI analyses were previously evaluated using 20 random carotid images in our laboratory (Cho et al., 2010; Yang et al., 2010). Representative images are shown in **Figure 1**.

Statistical Analyses

Data are expressed as mean ± standard deviation or as frequency and percentage. Continuous variables were compared using Student's *t*-test or analysis of variance (ANOVA), and categorical variables were compared with Fisher's exact test or Chi-squared test. To evaluate the relationships between aging and various carotid arterial measurements, participants were divided into subgroups according to age followed by evaluation of age-related changes in arterial measurements by analysis of variance. $P < 0.05$ were considered statistically significant. Statistical analysis was performed using standard software (SPSS 22.0, SPSS Inc., Chicago, IL).

RESULTS

Baseline Characteristics

Table 1 displays baseline characteristics of the two groups. Patients with BAV were significantly younger than those with TAV. The BAV subjects had fewer co-morbidities such as hypertension, dyslipidemia, and coronary artery disease, but gender proportion, prevalence of diabetes mellitus, history of smoking, average blood pressure, heart rate and systemic vascular resistance were comparable between the two groups. There were no significant differences in medication histories.

Table 2 shows echocardiographic characteristic of the two groups. In terms of AV dysfunction, about two-thirds of patients in each group had severe AS, and the remainder showed severe AR, without any differences between the two groups. According to the classification of BAV morphology, type 1 morphology was the most prevalent ($n = 13$, 45%). Patients with BAV had a significantly larger ascending aorta (43.3 ± 7.5 vs. 37.0 ± 6.2 mm, $p < 0.001$) and a higher prevalence of aortopathy (61 vs. 30%, $p = 0.021$) than those with TAV. The LV dimensions, ejection fraction, and stroke volume on echocardiography were comparable between the two groups. Regarding LV diastolic function, TAV patients had a higher E/e' and more enlarged left atrium than BAV patients.

Carotid Artery Structure and Function

Table 3 shows the data from duplex ultrasound and VVI in the two groups. Patients with BAV showed a significantly lower IMT, fewer plaques, and a lower incidence of carotid artery stenosis. These structural differences probably reflect the younger age and lower prevalence of common cardiovascular risk factors and coronary artery disease in patients with BAV. In VVI with speckle tracking method, FAC and GCS, which reflect arterial distensibility and mechanical function, respectively, tended to be lower in patients with BAV compared to those with TAV even though the patients with BAV were younger.

Table 4 presents the comparisons of carotid structure and function between BAV patients and TAV patients according to valve dysfunction. In patients with severe AS, number of carotid plaques tended to be lower in BAV patients than in TAV patients

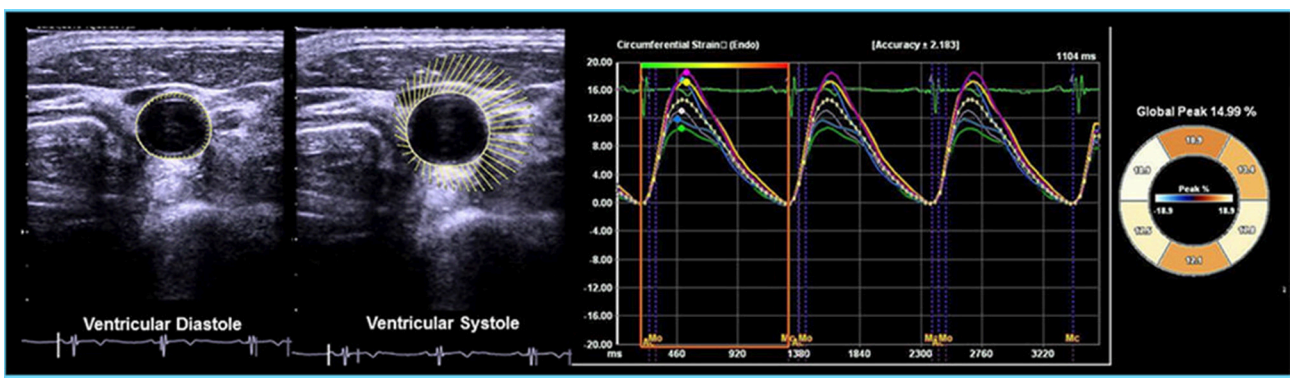

FIGURE 1 | Representative example of VVI analysis of the carotid artery.

TABLE 1 | Baseline characteristics of the study population.

	BAV ($n = 28$)	TAV ($n = 27$)	p-value
Age, year	58.2 ± 11.1	70.2 ± 11.3	< 0.001
Men, *n* (%)	20 (71)	16 (59)	0.343
Body mass index, g/m^2	24.0 ± 3.3	24.0 ± 2.6	0.962
Hypertension, *n* (%)	9 (32)	18 (67)	0.010
Diabetes mellitus, *n* (%)	1 (4)	4 (15)	0.147
Dyslipidemia, *n* (%)	12 (43)	18 (67)	0.038
Smoking, *n* (%)	12 (43)	7 (26)	0.187
CAD, *n* (%)	9 (33)	19 (70)	0.006
Systolic blood pressure, mmHg	120.4 ± 15.1	123.3 ± 12.8	0.445
Diastolic blood pressure, mmHg	73.6 ± 13.8	68.5 ± 8.5	0.103
Heart rate, bpm	67 ± 8	69 ± 12	0.475
Systemic vascular resistance, dyne-sec-cm^{-5}	1416 ± 600	1354 ± 466	0.686
MEDICATION			
RAAS blocker, *n* (%)	13 (46)	18 (67)	0.250
ß-blocker, *n* (%)	8 (28)	12 (44)	0.316
Calcium channel blocker, *n* (%)	7 (25)	8 (30)	0.823
Diuretics, *n* (%)	11 (39)	19 (70)	0.055
Statin, *n* (%)	11 (39)	12 (44)	0.878

BAV, bicuspid aortic valve; TAV, tricuspid aortic valve; CAD, coronary artery disease; bpm, beats per minute; RAAS, renin angiotensin aldosterone system.

TABLE 2 | Echocardiographic characteristics of the study population.

	BAV ($n = 28$)	TAV ($n = 27$)	p-value
AORTIC VALVE DYSFUNCTION			
Severe AS, *n* (%)	20 (71)	18 (67)	0.702
Severe AR, *n* (%)	8 (29)	9 (33)	
Mean systolic PG, mmHg	46.4 ± 23.6	50.1 ± 22.2	0.599
BAV PHENOTYPES			
Type 1 (RCC+LCC)	13 (45)	–	–
Type 2 (RCC+NCC)	5 (17)	–	–
Type 3 (LCC+NCC)	0 (0)	–	–
Type 0 (No raphe)	10 (34)	–	–
AORTA CHARACTERISTICS			
Valsalva sinus, mm	35.8 ± 8.1	33.9 ± 5.7	0.320
Ascending aorta, mm	43.3 ± 7.5	37.0 ± 6.2	< 0.001
Presence of aortopathy, n (%)	17 (61)	8 (30)	0.021
LEFT VENTRICULAR FUNCTION			
LVEDD, mm	53.3 ± 10.2	56.5 ± 11.7	0.275
LVESD, mm	36.1 ± 8.7	37.9 ± 10.4	0.495
LVEF, %	63.2 ± 7.8	64.4 ± 10.2	0.639
Stroke volume, ml	87.6 ± 28.9	86.2 ± 33.4	0.877
E/e'	13.1 ± 5.3	19.1 ± 9.8	0.026
LA volume index, ml/m^2	38.9 ± 14.0	49.9 ± 17.5	0.008

AS, aortic stenosis; AR, aortic regurgitation; PG, pressure gradient; LVEDD, left ventricular end-diastolic dimension; LVESD, left ventricular end-systolic dimension; LVEF, left ventricular ejection fraction; LA, left atrium.

TABLE 3 | Carotid artery structure and function of the study population.

	BAV ($n = 28$)	TAV ($n = 27$)	p-value
DUPLEX ULTRASOUND			
Carotid intima-media thickness			
Average, mm	0.77 ± 0.17	0.92 ± 0.16	0.003
Left, mm	0.79 ± 0.20	0.94 ± 0.20	0.005
Right, mm	0.76 ± 0.18	0.89 ± 0.19	0.012
Carotid plaque			
Total number	1.8 ± 2.0	3.2 ± 2.3	0.017
No plaque, *n* (%)	9 (32)	4 (15)	0.130
Single, *n* (%)	7 (25)	1 (4)	0.029
Multiple, *n* (%)	12 (43)	21 (81)	0.004
Carotid artery stenosis, *n* (%)	3 (11)	6 (22)	0.045
VELOCITY VECTOR IMAGING			
Fractional area change			
Average, %	8.52 ± 5.96	9.86 ± 6.25	0.421
Left, %	8.15 ± 6.12	9.36 ± 6.77	0.487
Right, %	8.90 ± 6.25	10.36 ± 6.26	0.392
Peak circumferential strain, %			
Average, %	3.67 ± 3.59	4.52 ± 3.52	0.380
Left, %	3.46 ± 3.71	4.22 ± 3.67	0.451
Right, %	3.88 ± 3.70	4.81 ± 3.77	0.354
***SD* of peak circumferential strain**			
Average, %	2.76 ± 1.90	3.21 ± 1.90	0.384
Left, %	2.27 ± 1.46	2.49 ± 1.27	0.553
Right, %	3.25 ± 3.06	3.93 ± 3.20	0.424

BAV, bicuspid aortic valve; TAV, tricuspid aortic valve; SD, standard deviation.

TABLE 4 | Carotid artery structure and function in the subgroups according to valve dysfunction.

	BAV	TAV	p-value
With severe AS	**($n = 20$)**	**($n = 18$)**	
Carotid intima-media thickness, mm	0.82 ± 0.17	0.89 ± 0.16	0.246
Carotid plaque, *n*	2.1 ± 2.1	3.5 ± 2.6	0.086
Carotid artery stenosis, *n* (%)	2 (10)	3 (17)	0.789
Fractional area change, %	6.17 ± 2.83	6.45 ± 2.44	0.731
Peak circumferential strain, %	2.39 ± 1.54	2.66 ± 1.13	0.567
SD of peak circumferential strain, %	3.57 ± 2.90	3.83 ± 2.14	0.696
With severe AR	**($n = 8$)**	**($n = 9$)**	
Carotid intima-media thickness, mm	0.68 ± 0.17	0.92 ±0.16	0.019
Carotid plaque, *n*	0.6 ± 0.8	2.5 ± 2.3	0.017
Carotid artery stenosis, *n* (%)	1 (13)	3 (33)	0.056
Fractional area change, %	13.79 ± 8.80	16.52 ±5.87	0.450
Peak circumferential strain, %	6.75 ± 5.29	4.52 ± 3.70	0.560
SD of peak circumferential strain, %	3.57 ± 2.90	3.83 ± 2.14	0.550

BAV, bicuspid aortic valve; TAV, tricuspid aortic valve; AS, aortic stenosis; AR, aortic regurgitation; SD, standard deviation

($p = 0.086$). In the subgroup of severe AR, carotid IMT, number of carotid plaques and incidence of carotid artery stenosis were significantly lower in BAV patients compared to TAV patients ($p = 0.019$, $p = 0.017$, and $p = 0.056$, respectively). Although, the subgroups had a small number of patients, the main findings are consistent with the results from overall patients.

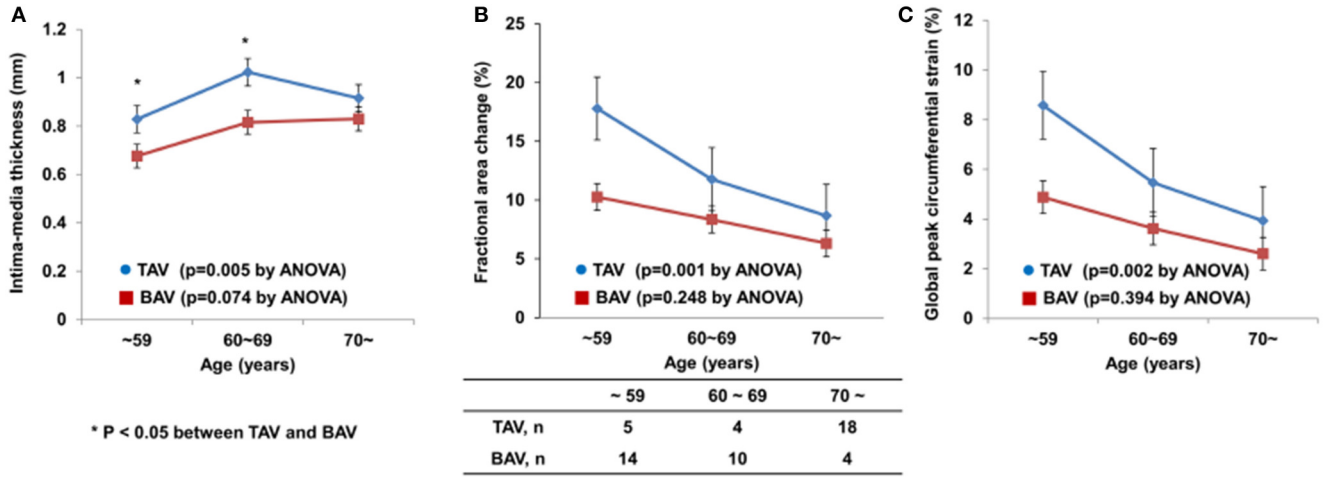

	~ 59	60 ~ 69	70 ~
TAV, n	5	4	18
BAV, n	14	10	4

FIGURE 2 | Age-dependent changes in carotid IMT **(A)**, FAC **(B)**, and GCS **(C)** in patients with BAV or TAV.

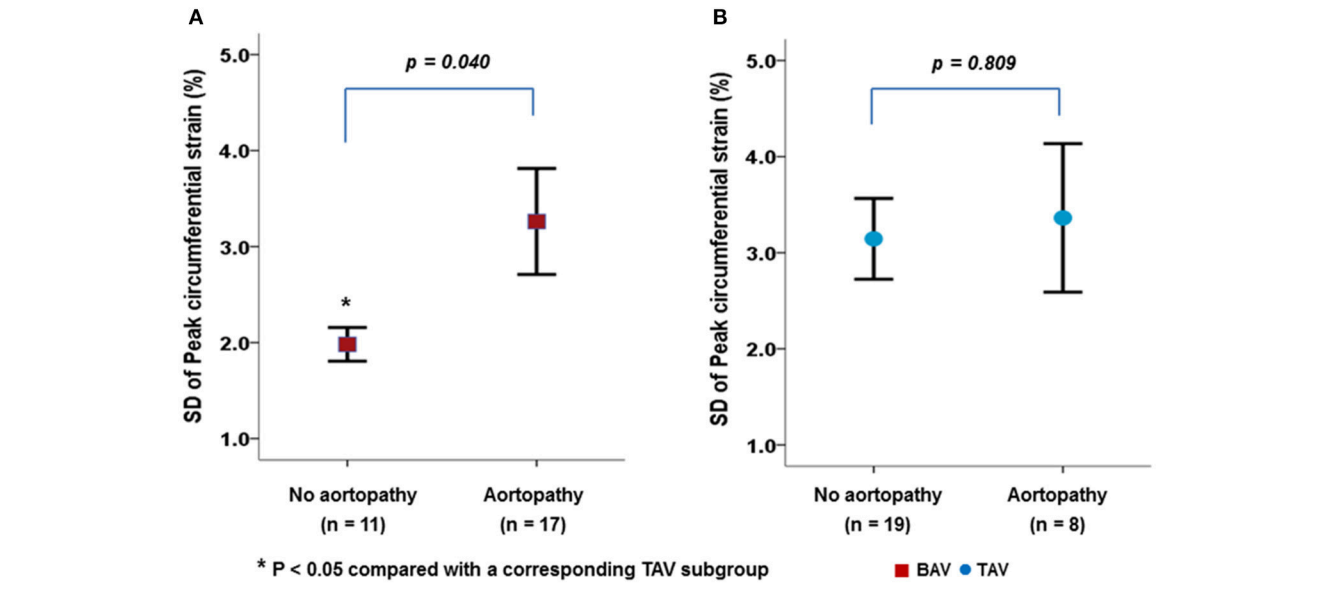

FIGURE 3 | Differences in carotid mechanical function between BAV **(A)** and TAV **(B)** according to the presence of aortopathy.

The patients in each group were classified into three subgroups according to age. **Figure 2** shows carotid IMT, FAC, and GCS according to age group. Interestingly, there was a significant age-dependent increase in carotid IMT and decreases in FAC and GCS of CCAs in the TAV group ($p = 0.005$, $p = 0.001$, $p = 0.002$, respectively), but this phenomenon was not evident in the BAV group ($p = 0.074$, $p = 0.248$, $p = 0.394$, respectively). The average carotid IMT in patients with BAV who were <70 years old was significantly lower than that in patients with TAV of corresponding age. In addition, FAC and GCS were consistently lower in patients with BAV than in patients with TAV in each subgroup based on age.

Figure 3 presents the VVI parameters according to the presence of aortopathy in patients with BAV or TAV. BAV patients with aortopathy showed a significantly higher SD-CS than those without aortopathy (**Figure 3A**, $p = 0.040$). However, the presence of aortopathy had no apparent influence on carotid mechanical function in patients with TAV (**Figure 3B**, $p = 0.809$).

Table 5 presents the comparisons of aortic valve, aorta and carotid artery characteristics and function according to the BAV phenotypes. The number of carotid plaques was the highest in patients with type 0 phenotype probably due to the relatively higher prevalence of severe AS in the type 0 phenotype. The averages in FAC and GCS in patients with type 0 phenotype

TABLE 5 | Aortic valve, aorta and carotid artery characteristics according to BAV phenotypes.

	Type 1 RCC+LCC (*n* = 13)	Type 2 RCC+NCC (*n* = 5)	Type 0 No raphe (*n* = 10)	*p*-value
Age, year	54.9±11.5	62.0 ± 9.4	61.0 ± 11.4	0.316
Severe AS, *n* (%)	8 (62)	3 (60)	9 (90)	0.051
Presence of aortopathy, *n* (%)	8 (62)	4 (80)	5 (50)	0.535
Carotid intima-media thickness, mm	0.73 ± 0.18	0.84 ± 0.20	0.83 ± 0.15	0.515
Carotid plaque, *n*	0.60 ± 0.91	2.20 ± 1.09	2.89 ± 2.66	0.009
Carotid artery stenosis, *n* (%)	1 (10)	2 (40)	1 (10)	0.689
Fractional area change, %	10.03 ± 7.88	7.67 ± 4.85	6.02 ±2.98	0.731
Peak circumferential strain, %	4.70 ± 4.69	3.04 ± 2.25	2.30 ± 1.62	0.277
SD of peak circumferential strain,%	3.51 ± 2.82	2.54 ± 0.65	2.31 ± 1.93	0.202

BAV, bicuspid aortic valve; TAV, tricuspid aortic valve; AS, aortic stenosis; SD, standard deviation.

tended to be lower compared to those with other phenotypes without statistical significance.

DISCUSSION

The principal findings of this study are as follows: (1) Patients with BAV show fewer structural changes in carotid arteries related to atherosclerosis than patients with TAV, and (2) patients with BAV manifest greater mechanical dysfunction as assessed by VVI, probably related to arterial intrinsic pathology, compared to patients with TAV. Furthermore, our study reveals an important pathophysiological linkage between bicuspid aortopathy and vascular dysfunction by presenting the attenuated age-dependent changes in carotid arterial function and the relationship with the presence of aortopathy. To the best of our knowledge, this study is the first to demonstrate the characteristics of carotid artery structure and function in BAV patients with VVI.

Histologic and Functional Changes of Vasculature in Patients with BAV

The BAV population has been reported to manifest increased degradation of elastin and collagen in the aortic wall mediated by matrix metalloproteinase-2, which is strongly expressed in tissue excised from the proximal aorta of patients with BAV (de Sa et al., 1999; Niwa et al., 2001). Overexpression of matrix metalloproteinase-2 is not only confined to the proximal aorta, but is also evident in the pulmonary trunk and thoracic aorta in patients with BAV (Fedak et al., 2005; Rabkin, 2014). In addition, a higher plasma level of matrix metalloproteinase-2 has been demonstrated in patients with BAV (Tzemos et al., 2010). The histological and serologic evidence of matrix metalloproteinase-2 overexpression in patients with BAV suggests a widespread pathology in systemic vasculature (Tzemos et al., 2010; Wang et al., 2014). On the other hand, BAV hemodynamics and flow abnormalities may initiate the aortopathy as a compensatory response to maintain constant wall shear stress. Abnormal hemodynamics in the ascending aorta may drive the production of circulating matrix metalloproteinase-2, and then affect the entire arterial system (Bissell et al., 2013).

Regarding systemic vascular function, increased central aortic stiffness in patients with BAV has been reported in previous studies (Nistri et al., 2008; Shim et al., 2011; Warner et al., 2013). Central aortic stiffness was positively correlated with the degree of aortic dilation in subjects with BAV (Shim et al., 2011). Interestingly, increased central aortic stiffness was found even in patients with non-dilated proximal aortas (Shim et al., 2011; Warner et al., 2013). Therefore, the functional changes of systemic arteries probably precede apparent structural changes. Recently, a few investigators have evaluated carotid elasticity using two dimensional and M-mode echocardiography (Li et al., 2016). The lower carotid strain and a higher carotid stiffness index in BAV patients with or without proximal aorta dilation than in healthy controls (Li et al., 2016). In another study examining IMT of the descending aorta, IMT of the descending aorta was not influenced by the presence of BAV but determined by aging (Petrini et al., 2016). Furthermore, the clinical implications of functional and structural abnormalities of the aorta have been highlighted in patients with BAV. In subjects with a normally functioning BAV, increased aortic stiffness and dilated ascending aorta were well correlated with left ventricular diastolic function (Lee et al., 2015). Moreover, in patients with moderately dysfunctional BAV, the presence of aortopathy and decreased aortic compliance were related to symptom status and clinical outcomes (Lee et al., 2017). Therefore, the assessment of structural and functional abnormalities of the proximal aorta and systemic vasculature is clinically important in patients with BAV.

In the present study, we evaluated vascular function using carotid VVI and presented different characteristics of carotid arterial mechanical function in patients with BAV compared to those with TAV. In general, the results from this study are consistent with the previous studies introduced above. Our findings suggest that the presence of aortopathy in a proximal ascending aorta in BAV patients is a marker of a more advanced process resulting in widespread alterations in artery elasticity (Fedak et al., 2002; Grotenhuis et al., 2007).

Detection of Vascular Dysfunction using Carotid VVI

Arterial assessment using VVI could represent a valuable new method for noninvasive quantification of vascular properties (Cannesson et al., 2006; Pirat et al., 2006). VVI allows direct assessment of angle-independent and instantaneous quantification of arterial elastic properties and vascular mechanics by measuring arterial wall strain and strain rate in both regional and segmental aspects (Kim et al., 2013). In previous studies using VVI, we characterized not only the vascular functional alterations in patients with specific vascular disorders such as Marfan syndrome or Takayasu's arteritis (Cho

et al., 2010; Yang et al., 2010), but also normal vascular aging in healthy individuals (Yang et al., 2011). FAC, average CS, and strain rate in VVI were significantly correlated with conventional parameters of arterial stiffness. Moreover, the correlations between functional variables of VVI and collagen content of the arterial wall were validated in an animal experimental study (Kim et al., 2013). Since carotid duplex ultrasound is feasible and practical, it has been widely used for detection of subclinical atherosclerosis in clinical practice. The simple addition of VVI measurement for the carotid artery could provide incremental information for assessing vascular functional changes.

Many previous studies have demonstrated a marked reduction in arterial compliance with advancing age (Boutouyrie et al., 1992; Tanaka et al., 2000). We showed an age-dependent increase in carotid IMT and decreases in FAC and GCS of CCAs in patients with TAV, but this phenomenon was not evident in patients with BAV. These observations suggest that patients with BAV have intrinsic vascular abnormalities rather than features of common vascular aging that are affected by traditional cardiovascular risk factors. Recently, structural and functional assessment of carotid arteries with ultrasound has become popular not only for detection of subclinical atherosclerosis, but also for risk stratification before cardiac surgery. This study provides insight into the different carotid structure and function in patients with BAV. Therefore, to interpret the results from carotid VVI techniques, we should consider an individual's AV phenotype and the presence of aortopathy. Conversely, if there is difficulty in distinguishing the patient's AV phenotype because of extensive calcified AV, carotid artery structural and functional assessment might provide additional information.

LIMITATIONS

Several limitations of this study should be noted. First, this study is a small size, cross-sectional study from a single center. Second, there was an age difference between the patients with BAV and those with TAV, although this was compensated by adjusting for age in the stepwise multivariate subgroup analysis. Second, all patients had significant AV dysfunction because they had been referred for carotid ultrasound as a part of preoperative carotid evaluation. Significant stenosis or regurgitation of the AV could influence carotid artery function. However, the proportion of patients with severe AS or AR and the mean systolic pressure gradient across the AV in each group were comparable. In addition, baseline left ventricular ejection fraction and stroke volume in each group were within normal ranges without any differences. Third, any circulating biomarkers relating BAV aortopathy were not assessed in the present study. Further studies are warranted for the correlation between circulating biomarkers and carotid mechanical function.

CONCLUSION

Patients with BAV have different carotid artery structure and function compared to those with TAV, suggesting intrinsic vascular abnormalities that are less affected by traditional cardiovascular risk factors and aging and more strongly related to the presence of aortopathy. This finding supports the need for comprehensive evaluation of vascular function in patients with BAV.

AUTHOR CONTRIBUTIONS

MK: Analyzed data; interpreted results; drafted manuscript; approved final version of manuscript; accountable for accuracy and integrity of the work. CS: Conception of research; design of research; analyzed data; interpreted results; prepared figures; reviewed and revised manuscript; approved final version of manuscript; accountable for accuracy and integrity of the work. SY: Design of research; analyzed data; IC: Edited and revised manuscript; GH: Conception of research; reviewed and revised manuscript; JH: Conception of research; edited and revised manuscript; NC: Edited and revised manuscript.

REFERENCES

Baumgartner, H., Hung, J., Bermejo, J., Chambers, J. B., Evangelista, A., and Griffin, B. P. (2009). American society of echocardiography; european association of echocardiography. Echocardiographic assessment of valve stenosis: E*AE/ASE recommendations for clinical practice. Eur. J. Echocardiogr.* 10, 1–25. doi: 10.1093/ejechocard/jen303

Bilen, E., Akcay, M., Bayram, N. A., Kocak, U., Kurt, M., Tanboga, I. H., et al. (2012). Aortic elastic properties and left ventricular diastolic function in patients with isolated bicuspid aortic valve. *J. Heart Valve Dis.* 21, 189–194.

Bissell, M. M., Hess, A. T., Biasiolli, L., Glaze, S. J., Loudon, M., Pitcher, A., et al. (2013). Aortic dilation in bicuspid aortic valve disease: flow pattern is a major contributor and differs with valve fusion type. *Circ. Cardiovasc. Imaging* 6, 499–507. doi: 10.1161/CIRCIMAGING.113.000528

Boutouyrie, P., Laurent, S., Benetos, A., Girerd, X. J., Hoeks, A. P., and Safar, M. E. (1992). Opposing effects of ageing on distal and proximal large arteries in hypertensives. *J. Hypertens. Suppl.* 10, S87–S91. doi: 10.1097/00004872-199208001-00023

Cannesson, M., Tanabe, M., Suffoletto, M. S., Schwartzman, D., and Gorcsan, J. (2006). Velocity vector imaging to quantify ventricular dyssynchrony and predict response to cardiac resynchronization therapy. *Am. J. Cardiol.* 98, 949–955. doi: 10.1016/j.amjcard.2006.04.045

Cho, I. J., Yang, W. I., Shim, C. Y., Kim, S. A., Chang, H. J., Jang, Y., et al. (2010). Assessment of mechanical properties of common carotid artery in Takayasu's arteritis using velocity vector imaging. *Circ. J.* 74, 1465–1470. doi: 10.1253/circj.CJ-09-0839

de Sa, M., Moshkovitz, Y., Butany, J., and David, T. E. (1999). Histologic abnormalities of the ascending aorta and pulmonary trunk in patients with bicuspid aortic valve disease: clinical relevance to the ross procedure. *J. Thorac. Cardiovasc. Surg.* 118, 588–594. doi: 10.1016/S0022-5223(99)70002-4

Fedak, P. W., David, T. E., Borger, M., Verma, S., Butany, J., and Weisel, R. D. (2005). Bicuspid aortic valve disease: recent insights in pathophysiology and treatment. *Expert Rev. Cardiovasc. Ther.* 3, 295–308. doi: 10.1586/14779072.3.2.295

Fedak, P. W., Verma, S., David, T. E., Leask, R. L., Weisel, R. D., and Butany, J. (2002). Clinical and pathophysiological implications of a bicuspid aortic valve. *Circulation.* 106, 900–904. doi: 10.1161/01.CIR.0000027905.26586.E8

Ferencik, M., and Pape, L. A. (2003). Changes in size of ascending aorta and aortic valve function with time in patients with congenitally bicuspid aortic valves. *Am. J. Cardiol.* 92, 43–46. doi: 10.1016/S0002-9149(03)00462-4

Grotenhuis, H. B., Ottenkamp, J., Westenberg, J. J., Bax, J. J., Kroft, L. J., and de Roos, A. (2007). Reduced aortic elasticity and dilatation are associated with aortic regurgitation and left ventricular hypertrophy in nonstenotic bicuspid aortic valve patients. *J. Am. Coll. Cardiol.* 49, 1660–1665. doi: 10.1016/j.jacc.2006.12.044

Kim, S. A., Lee, K. H., Won, H. Y., Park, S., Chung, J. H., Jang, Y., and Ha, J. W. (2013). Quantitative assessment of aortic elasticity with aging using velocity-vector imaging and its histologic correlation. *Arterioscler. Thromb. Vasc. Biol.* 33, 1306–1312. doi: 10.1161/ATVBAHA.113.301312

Lancellotti, P., Tribouilloy, C., Hagendorff, A., Moura, L., Popescu, P., Agricola, E., et al. (2010). European association of echocardiography recommendations for the assessment of valvular regurgitation. Part 1: aortic and pulmonary regurgitation (native valve disease). *Eur. J. Echocardiogr.* 11, 223–244. doi: 10.1093/ejechocard/jeq030

Lang, R., Bierig, M., Devereux, R., Flachskampf, F., Foster, E., Pellikka, P., et al. (2005). Recommendations for chamber quantification: a report from the American society of echocardiography's guidelines and standards committee and the chamber quantification writing group, developed in conjunction with the european association of echocardiography, a branch of the european society of cardiology. *J. Am. Soc. Echocardiogr.* 18, 1440–1463. doi: 10.1016/j.echo.2005.10.005

Lee, S. Y., Shim, C. Y., Hong, G. R., Cho, I. J., Chang, H. J., Ha, J. W., et al. (2017). Determinants and prognostic significance of symptomatic status in patients with moderately dysfunctional bicuspid aortic valves. *PLoS ONE* 12:e0169285. doi: 10.1371/journal.pone.0169285

Lee, S. Y., Shim, C. Y., Hong, G. R., Seo, J., Cho, I., Cho, I. J., et al. (2015). Association of aortic phenotypes and mechanical function with left ventricular diastolic function in subjects with normally functioning bicuspid aortic valves and comparison to subjects with tricuspid aortic valves. *Am. J. Cardiol.* 116, 1547–1554. doi: 10.1016/j.amjcard.2015.08.017

Li, Y., Deng, X. J., Bi, Y. N., Liu, J. Z., and Li, L. (2016). Evaluation of myocardial strain and artery elasticity using speckle tracking echocardiography and high-resolution ultrasound in patients with bicuspid aortic valve. *Int. J. Cardiovasc. Imaging.* 32, 1063–1069. doi: 10.1007/s10554-016-0876-2

Nistri, S., Grande-Allen, J., Noale, M., Basso, C., Siviero, P., Maggi, S., et al. (2008). Aortic elasticity and size in bicuspid aortic valve syndrome. *Eur. Heart J.* 29, 472–479. doi: 10.1093/eurheartj/ehm528

Niwa, K., Perloff, J. K., Bhuta, S. M., Laks, H., Drinkwater, D. C., Child, J. S., et al. (2001). Structural abnormalities of great arterial walls in congenital heart disease: light and electron microscopic analyses. *Circulation* 103, 393–400. doi: 10.1161/01.CIR.103.3.393

Petrini, J., Jenner, J., Rickenlund, A., Eriksson, P., Franco-Cereceda, A., Caidahl, K., et al. (2014). Elastic properties of the descending aorta in patients with a bicuspid or tricuspid aortic valve and aortic valvular disease. *J. Am. Soc. Echocardiogr.* 27, 393–404. doi: 10.1016/j.echo.2013.12.013

Petrini, J., Yousry, M., Eriksson, P., Björk, H. M., Rickenlund, A., Franco-Cereceda, A., et al. (2016). Intima-media thickness of the descending aorta in patients with bicuspid aortic valve. *IJC Heart Vasculature.* 11, 74–79. doi: 10.1016/j.ijcha.2016.03.014

Pirat, B., McCulloch, M. L., and Zoghbi, W. A. (2006). Evaluation of global and regional right ventricular systolic function in patients with pulmonary hypertension using a novel speckle tracking method. *Am. J. Cardiol.* 98, 699–704. doi: 10.1016/j.amjcard.2006.03.056

Rabkin, S. W. (2014). Differential expression of MMP-2, MMP-9 and TIMP proteins in thoracic aortic aneurysm—comparison with and without bicuspid aortic valve: a meta-analysis. *VASA* 43, 433–442. doi: 10.1024/0301-1526/a000390

Shim, C. Y., Cho, I. J., Yang, W. I., Kang, M. K., Park, S., Ha, J. W., et al. (2011). Central aortic stiffness and its association with ascending aorta dilation in subjects with a bicuspid aortic valve. *J. Am. Soc. Echocardiogr.* 24, 847–852. doi: 10.1016/j.echo.2011.04.017

Sillesen, H., Muntendam, P., Adourian, A., Entrekin, R., Garcia, M., Falk, E., et al. (2012). Carotid plaque burden as a measure of subclinical atherosclerosis: comparison with other tests for subclinical arterial disease in the high risk plaque bioimage study. *JACC Cardiovasc. Imaging* 5, 681–689. doi: 10.1016/j.jcmg.2012.03.013

Tadros, T. M., Klein, M. D., and Shapira, O. M. (2009). Ascending aortic dilatation associated with bicuspid aortic valve: pathophysiology, molecular biology, and clinical implications. *Circulation* 119, 880–890. doi: 10.1161/CIRCULATIONAHA.108.795401

Tanaka, H., Dinenno, F. A., Monahan, K. D., Clevenger, C. M., DeSouza, C. A., and Seals, D. R.,(2000). Aging, habitual exercise, and dynamic arterial compliance. *Circulation* 102, 1270–1275. doi: 10.1161/01.CIR.102.11.1270

Tzemos, N., Lyseggen, E., Silversides, C., Jamorski, M., Tong, J. H., Harvey, P., et al. (2010). Endothelial function, carotidfemoral stiffness, and plasma matrix metalloproteinase-2 in men with bicuspid aortic valve and dilated aorta. *J. Am. Coll. Cardiol.* 55, 660–668. doi: 10.1016/j.jacc.2009.08.080

Verma, S., and Siu, S. C. (2014). Aortic dilatation in patients with bicuspid aortic valve. *N. Engl. J. Med.* 370, 1920–1929. doi: 10.1056/NEJMra1207059

Wang, Y., Wu, B., Dong, L., Wang, C., Wang, X., and Shu, X. (2014). Circulating matrix metalloproteinase patterns in association with aortic dilatation in bicuspid aortic valve patients with isolated severe aortic stenosis. *Heart Vessels* 31, 189–197. doi: 10.1007/s00380-014-0593-5

Warner, P., Al-Quthami, A., Brooks, E., Kelley-Hedgepeth, A., Patvardhan, E., Kuvin, J., et al. (2013). Augmentation index and aortic stiffness in bicuspid aortic valve patients with non-dilated proximal aortas. *BMC Cardiovasc. Disord.* 13:19. doi: 10.1186/1471-2261-13-19

Wilton, E., and Jahangiri, M. (2006). Post-stenotic aortic dilatation. *J. Cardiothorac. Surg.* 1, 1–11. doi: 10.1186/1749-8090-1-7

Yang, W. I., Shim, C. Y., Bang, W. D., Oh, C. M., Chang, H. J., Chung, N., et al. (2011). Asynchronous arterial systolic expansion as a marker of vascular aging: assessment of the carotid artery with velocity vector imaging. *J. Hypertens.* 29, 2404–2412. doi: 10.1097/HJH.0b013e32834c46dd

Yang, W. I., Shim, C. Y., Cho, I. J., Chang, H. J., Choi, D., Jang, Y., et al. (2010). Dyssynchronous systolic expansion of carotid artery in patients with marfan syndrome. *J. Am. Soc. Echocardiogr.* 23, 1310–1316. doi: 10.1016/j.echo.2010.08.022

Conflict of Interest Statement: The authors declare that the research was conducted in the absence of any commercial or financial relationships that could be construed as a potential conflict of interest.

frontiers in Physiology

MINI REVIEW
published: 13 June 2017
doi: 10.3389/fphys.2017.00397

Managing Thoracic Aortic Aneurysm in Patients with Bicuspid Aortic Valve Based on Aortic Root-Involvement

Elizabeth Norton[1] *and Bo Yang*[2]*

[1] Department of Internal Medicine, Michigan Medicine, Ann Arbor, MI, United States, [2] Department of Cardiac Surgery, Michigan Medicine, Ann Arbor, MI, United States

Bicuspid aortic valve (BAV) can be both sporadic and hereditary, is phenotypically variable, and genetically heterogeneous. The clinical presentation of BAV is diverse and commonly associated with a high prevalence of valvular dysfunction producing altered hemodynamics and aortic abnormalities (e.g., aneurysm and dissection). The thoracic aortic aneurysm (TAA) in BAV frequently involves the proximal aorta, including the aortic root, ascending aorta, and aortic arch, but spares the aorta distal to the aortic arch. While the ascending aortic aneurysm might be affected by both aortopathy and hemodynamics, the aortic root aneurysm is considered to be more of a consequence of aortopathy rather than hemodynamics, especially in younger patients. The management of aortic aneurysm in BAV has been very controversial because the molecular mechanism is unknown. Increasing evidence points toward the BAV root phenotype [aortic root dilation with aortic insufficiency (AI)] as having a higher risk of catastrophic aortic complications. We propose more aggressive surgical approaches toward the BAV with root phenotype.

Keywords: aortic valve, aortic valve stenosis, aortic valve insufficiency, aortic aneurysm, aortic dissection, bicuspid aortic valve

OPEN ACCESS

Edited by:
Alessandro Della Corte, Department of Cardiothoracic Sciences—Second University of Naples, Monaldi Hospital, Italy

Reviewed by:
Daniela Carnevale, Sapienza Università di Roma, Italy
Hector Michelena, Mayo Clinic Minnesota, United States

***Correspondence:**
Bo Yang
boya@med.umich.edu

Specialty section:
This article was submitted to Vascular Physiology, a section of the journal Frontiers in Physiology

Received: *27 March 2017*
Accepted: *26 May 2017*
Published: *13 June 2017*

Citation:
Norton E and Yang B (2017) Managing Thoracic Aortic Aneurysm in Patients with Bicuspid Aortic Valve Based on Aortic Root-Involvement. Front. Physiol. 8:397. doi: 10.3389/fphys.2017.00397

INTRODUCTION

Bicuspid aortic valve (BAV) affects 1–2% of the general population (Martin et al., 2007). Diagnosis of many patients born with BAV does not happen until adulthood; however, up to 50–70% of patients with BAV experience some form of complication such as valvular insufficiency or aortic aneurysm either as children or later in life. The underlying cause of the incorrect formation of the aortic valve remains relatively uncertain; however, evidence suggests that BAV is a genetic disorder. BAV exhibits an increased prevalence in first-degree relatives of affected individuals (Martin et al., 2007). The familial clustering suggests an autosomal dominant pattern of inheritance with reduced penetrance (Martin et al., 2007). There are both single and multiplex affected families, which indicates there may be multiple means of inheritance for BAV (Martin et al., 2007). Chromosomal regions of interest for BAV include 18q, 5q, and 13q (Martin et al., 2007). Despite these probable chromosomal regions, approximately 150 genes are encoded amongst the three novel loci (Martin et al., 2007).

Abbreviations: AI, aortic insufficiency; AS, aortic stenosis; AVR, aortic valve replacement; BAV, bicuspid aortic valve; TAA, thoracic aortic aneurysm; TAV, tricuspid aortic valve; MFS, Marfan syndrome.

Despite the establishment of the heritability of BAV, the genes yielding the pathology of the aortic valve remain largely undetermined. BAV consists of a variety of morphologies and depending on which cusps are fused, blood flow patterns are impacted, which can affect the aorta in various ways. The most prominent fusion is observed between the left and right coronary cusps, followed by the right and non-coronary cusps, and very few between the left and non-coronary cusps (Bissel et al., 2013). The Sievers classification organizes BAVs based on the different subtypes; AP, Lat, R-L, R-N, N-L, and L-R/R-N (Sievers and Schmidtke, 2007).

BAVs are associated with many clinically serious abnormalities, including aortic valve insufficiency and stenosis as well as aortic dilation and dissection. The management of thoracic aortic aneurysm (TAA) in BAV has been very controversial. The ACC/AHA guidelines have been changed back and forth in the past years regarding recommendation of surgical resection of TAA based on the size of aneurysm, between 5 and 5.5 cm. BAV/TAA has been treated in a uniform manner, despite the heterogeneity of the disease. We believe BAV/TAA should be treated based on phenotype of aortic root involvement. We provide an overview of the heterogeneity of BAV, and the associated complications to improve treatment. BAV with root phenotype TAA [aortic root dilation and aortic insufficiency (AI)] should be treated more aggressively surgically; and less aggressively if the aortic root is not involved. Currently BAV/TAA is treated with a blanket approach, but additional research could lead to more phenotypic-specific guidelines to improve patient outcomes.

MATERIALS AND METHODS

We performed a search of the PubMed database for articles on BAV from inception to March 2017. Articles were limited to those written in English. Additionally, references from key articles were manually searched in a backward cumulative fashion for additional articles.

RESULTS

Genetics

While candidate genes have been identified, *NOTCH1*, *NKX2.5*, and *GATA5* are the best supported although further replication is warranted. Mutations in *NOTCH1* function both in BAV and calcific aortic disease. *NOTCH1* functions in both familial and sporadic BAV and is crucial during cardiac valve formation that promotes epithelial–mesenchymal transition (Kostina et al., 2016). For example, disruption of Notch signaling in transgenic mice is correlated with faulty neural crest cells patterning as well as unequal aortic valve leaflets with bicuspid-like morphology and aortic arch abnormalities characterized by disorganized aortic wall histology with dispersed vascular smooth muscle cells (Broberg and Therrien, 2015). While many studies have reported a linkage of BAV to *NOTCH1*, *NOTCH1* mutations do not function in BAV in all instances. In fact, the *NOTCH1* gene mutation may only be associated with a very small portion of patients with BAV. *NKX2.5*, a homeobox-containing transcription factor, is required for cardiogenic differentiation across species (Qu et al., 2014). A study that detected a novel heterozygous sequence variation found that the mutation was present in all affected family members with BAV but absent from the unaffected family members (Qu et al., 2014). *GATA5* plays an essential role in cardiac morphogenesis and aortic valve development (Nemer et al., 1999). Due to its high expression in endocardial cushions of both the outflow tract and the atrioventricular canal, *GATA5* became a candidate gene for congenital heart diseases, more specifically BAV, and mutations in *GATA5* have been associated with an increased susceptibility to BAV, but the specific detailed molecular mechanism needs to be further researched. Through a GWAS study, we also identified a coding variant of GATA4 and a non-coding variant which is 150 kb away from GATA4 are associated with BAV (Yang et al., 2017). Despite the awareness of candidate genes for the heritability of BAV, the specific genetic basis underlying BAV remains largely unknown. The involvement of many genes adds to the heterogeneity of the population of patients with BAV. In addition to the genetic source leading to the formation of BAV, the complications of BAV could also be associated with genetics. Taken together, it is clear that BAV is not a simple Mendelian trait but an accumulation of complex traits (Ellison et al., 2007; McBride et al., 2008) and is indeed heritable; therefore, we cannot treat BAV as a homogenous patient population.

Valvulopathy

The different phenotypes of valvulopathy in BAV patients also reflect the heterogeneity of this patient population. In all age groups, BAV underlies the majority of cases of aortic valve disease (Martin et al., 2007). The most common complication of BAV is valvular stenosis followed by valvular insufficiency (Pachulski and Chan, 1993). In patients that present with valvular dysfunction earlier in life (<50 years old), AI is more common; however, later in life (>50 years old) aortic stenosis (AS) is more prevalent (Pachulski and Chan, 1993). Studies have suggested a correlation between BAV phenotype and the valvular complications that develop. The overall evidence suggests that R-N BAV phenotypes have the greatest incidence of AS in both children and adults (Fernandes et al., 2004, 2007; Huang and Le Tan, 2014; Adamo and Braverman, 2015). In pediatric patients, those with the R-N BAV phenotype were more likely to have AI progression (Fernandes et al., 2004). Patients with R-N BAV have a high prevalence of AI and AS, therefore, the AI could be due to the high incidence of AS, while patients with R-L and N-L BAV phenotypes could have a high incidence of AI due to a separate mechanism (Fernandes et al., 2004, 2007). Research shows that BAV insufficiency and BAV stenosis have noticeably different characteristics. Hahn et al. (1992) demonstrated that dilation of the aortic annulus and entire aortic root is associated with AI.

Aortic Dilation/Aneurysm

Compared to the normal population, there is a significantly higher rate of dilation of the proximal aorta in patients with BAV (Della Corte et al., 2007). Della Corte et al. (2007) found that aortic dilation [an aortic ratio (measured diameter/expected diameter) >1.1] was present in 83.2% of patients with BAVs, 79%

mid-ascending dilation and 58% root dilation in adults. Aortic aneurysm commonly involves aortic root, ascending aorta, and aortic arch in clusters (Fazel et al., 2008). Researchers suggest two theories for the cause of aneurysms in patients with BAV: the hemodynamic theory and the aortopathy theory.

While the hemodynamic theory was the first explanation for BAV-associated aortic aneurysm, the genetic/aortopathy theory has become increasingly popular. Upon pairing patients with TAVs and BAVs based on sex and degree of AI, stenosis, or combined aortic valve disease, the patients with BAV were considerably younger due to the earlier onset of valvular disease and had significant aortic dilation at all levels compared to the matched patients with TAVs (Keane et al., 2000). Matching patients with TAVs and BAVs with similar degrees of valvular abnormalities reduces the effect of valvular lesions on hemodynamics and more accurately assesses the BAV (Keane et al., 2000). Hahn et al. (1992) established that aortic dilation is common in patients with BAVs even when the hemodynamic function of the valve is normal, providing support for the genetic/aortopathy theory.

The exact molecular and cellular pathways involved in BAV aortopathy remain unknown. However, MMP-2 (matrix metalloproteinase-2) has been identified as a key molecular modulator and a circulation biomarker of aortic dilation in patients with BAV. An increase in MMPs, enzymes that process or degrade the extracellular matrix, is associated with the development of aortic aneurysms (Ikonomidis et al., 2007). A study of patients with TAA comparing patients with BAVs and patients with TAVs, found that MMP-2 was increased by 34% in patients with BAVs (Ikonomidis et al., 2007). Therefore, an increase in collagen turnover and a decrease in collagen cross-linking may be a factor in the formation of aneurysms in patients with BAVs (Broberg and Therrien, 2015).

The pathological hallmark of TAA is medial degeneration; therefore, smooth muscle cells (SMCs; key component of the medial layer) function in this pathology (Milewicz et al., 2008). Mutations in SMC-specific contractile proteins could contribute to familial TAA (Milewicz et al., 2008). Various mutations in both MYH11 and ACT2A disrupt SMC contractile function causing TAA (Milewicz et al., 2008). Through the use of iPSCs modeling the BAV/TAA, we found that the defective differentiation of SMCs from neural crest stem cells, modeling the root, and ascending aortic aneurysm, manifested as decreased expression of *MYH11* and contractile function of SMCs (Jiao et al., 2016). On the other hand, the SMCs differentiated from paraxial mesoderm, modeling the descending thoracic aorta, have normal expression of contractile protein, including *MYH11* and contractile function (Jiao et al., 2016). This finding in our cellular model is consistent with clinical observation that the TAA in patients with BAV involves the root and ascending aorta but spares the descending thoracic aorta, indicating the aortopathy in BAV/TAA.

While aortopathy is important in TAA formation in patients with BAVs, the hemodynamic theory cannot be ignored. Similar to the valvulopathy, BAV subtype exhibits a correlation to the location of aortic dilation. Hope et al. (2010) found left-posterior flow jets and left-handed nested helical flow only in R-N BAVs, more distally directed flow derangement with tubular ascending and arch dilation. Hope et al. (2010) found right-anterior flow jets and right-handed nested helical flow, only seen in patients with R-L BAVs, were related to proximal flow derangement and dilation of convex side of the ascending aorta. Due to the different flow patterns produced by R-L and R-N BAVs, R-L BAVs more often cause dilation of ascending convex side while R-N BAVs cause ascending and arch dilation. BAVs compared to TAVs and different subtypes of BAV alter the hemodynamic blood flow through the valve, diversely impacting the aorta, leading to different locations of dilation. While the fusion subtypes contribute to flow patterns, so do valvular dysfunctions, such as AI and AS. Most frequently, the hemodynamic change in patients with BAV affects the ascending aorta, but not the aortic root (Tadros et al., 2009). Aortic regurgitation yields higher stroke volumes which causes higher wall tension in the ascending aorta while AS creates a high-velocity jet that increases shear stress on the ascending aorta (Tadros et al., 2009). Yet, aortic root aneurysms are still frequently seen in BAV patients (Schaefer et al., 2008). This fact supports the idea that aortopathy is the key factor of TAA in patients with BAV, and that patients with root aneurysms may be due to more severe aortopathy and less to hemodynamics. Also, patients with BAV and isolated dilation of the aortic root tend to be younger, are more likely male, and have AI (Tadros et al., 2009; Girdauskas et al., 2010, 2012; Detaint et al., 2014).

Taken together, BAV is a heterogeneous disease. Different gene mutations may cause different subtypes of BAV and exhibit different severity of aortopathy, which result in aortic aneurysm in different parts of the aorta (root, ascending aorta or arch) and at different ages with the contribution of hemodynamic change due to BAV. An asymptomatic ascending aortic aneurysm in a 60-year-old BAV patient with Sievers type 1, L-R fusion, and AS is different from an asymptomatic aortic root aneurysm in a 30-year-old BAV patient with Sievers type 0 and AI. The criteria of surgical repair of the aneurysm in these two patients should be different.

Aortic Dissection

Aortic dissection occurs 5–10 times more often among patients with BAVs than those with TAVs (Braverman, 2011), rendering it a potentially lethal disease. In patients with BAVs followed prospectively, aortic dissection has been an infrequent event; however, in patients with BAVs aortic dissection occurs an average of one decade earlier than patients with TAVs (Braverman, 2011).

A study of 56 patients with pure AI, who had an isolated AVR found that the subset of patients with a root aneurysm and AI appears to be different than the hemodynamically-triggered aortopathy seen in patients with BAV stenosis and asymmetric dilation of the tubular ascending aorta (Girdauskas et al., 2015a). This root phenotype (root aneurysm and AI) of BAV has been linked to more of a genetic/aortopathy cause, and occurs earlier in life and independent of hemodynamic factors (Della Corte et al., 2007; Girdauskas et al., 2015a). The incidence of adverse events was substantially higher in patients with the root phenotype of BAV as opposed to those with BAV/ascending aortic aneurysm and AS (Girdauskas et al., 2012). Girdauskas

et al. found that patients with BAV-AI had a 10-fold higher risk of post-AVR aortic dissection when compared to patients with BAV-AS (Girdauskas et al., 2015b). A study by Wang et al. (2016) found that patients with BAV-AI had a higher prevalence of R-L fusion phenotypes and wider aortic roots than patients with BAV-AS. Girdauskas et al. (2015a) found that 34% of participants with BAV and root phenotype suffered aortic complications after AVR and only 50% of patients in the study were unburdened by aortic complications 15 years post-AVR. Girdauskas et al. reported that 3/56 patients with root phenotype expired due to type A dissection, while 0/153 patients with stenosis and ascending aortic dilation suffered a Type A aortic dissection (Girdauskas et al., 2012, 2015a). Both Girdauskas et al. (2012) and Wang et al. (2016) found that patients with BAV-AI and root aneurysm are closer to Marfan syndrome (MFS) pathology and have a higher risk of aortic dissection and rupture. When comparing patients with BAV and MFS, Itagaki et al. (2015) found that the risk of aortic complications after AVR was 10-times higher for patients with MFS than for patients with BAV, but patients with BAV were at a significantly greater risk than patients with acquired disease of a tricuspid aortic valve. However, this study looks at all patients with BAV together, despite the proven heterogeneity of the BAV population. Therefore, though it seems that BAV finds itself in the middle of the high risk of patients with MFS and the low risk of patients with acquired valve disease of a TAV, by separating out the distinct populations of BAV, we believe those with the root phenotype (root dilation and AI) will be closer to those of MFS while those with AS and ascending dilation will be closer to those of the acquired valve disease of the TAV. Therefore, it might be reasonable to separate patients with BAV into groups to decide treatment; potentially be more aggressive when treating patients with BAV—with root phenotype (AI and root aneurysm).

We propose that when evaluating patients, patients can be classified into two separate groups; Cluster A—root phenotype (root aneurysm and AI) and Cluster B—no root involvement (no root aneurysm or AI). While the percentage of patients with Cluster A aortopathy is often less than those with Cluster B, Cluster A aortopathy is associated with a faster diametric growth rate of the ascending aorta (Della Corte et al., 2013) and high prevalence of aortic events after AVR (Girdauskas et al., 2015a). These findings suggest that this Cluster A aortopathy could be a "malignant" form of BAV that could be genetically linked; while Cluster B could be the benign form. Because patients with Cluster A aortopathy have an increased probability of life-threatening aortic events, such as aortic dissection and rupture, they could fit under the more aggressive guidelines for patients with connective tissue disorders, such as MFS (Girdauskas et al., 2015a), with recommendation of surgical resection of a root aneurysm at a diameter of 5 cm, as did Michelena et al. (2015), if asymptomatic and 4.5 cm as a concomitant surgery. Cluster B are more affected by the hemodynamics, can be treated as TAV/TAA with surgical resection at 5.5 cm if asymptomatic. Regarding those two hypothetical cases above, we would recommend a conservative approach for the first patient (60-year-old with BAV and ascending aneurysm/AS) with surgical resection when the aneurysm reaches 5.5 cm, as recommended by the current AHA/ACC guidelines; an aggressive approach for the second patient (30-year-old with aortic root aneurysm and AI) with surgical resection when the aneurysm reach 5 cm as the recommendations of current AHA/ACC guidelines for the MFS.

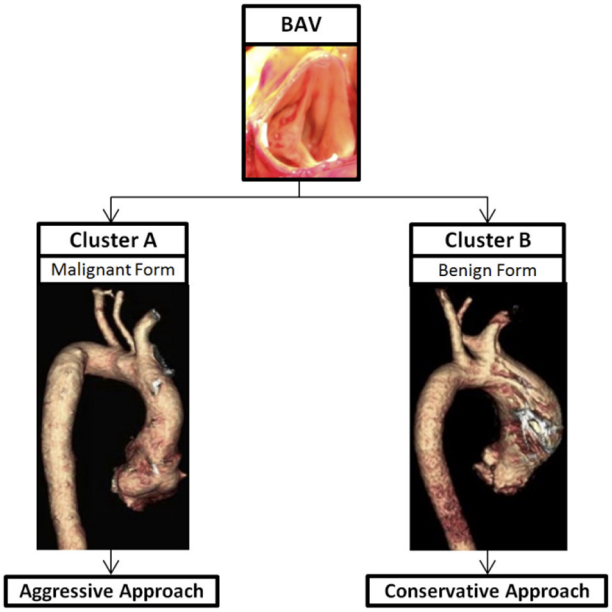

FIGURE 1 | Thoracic aortic aneurysm in BAV, a heterogeneous disease, can be divided into two clusters based on the aortic root involvement. Cluster A is BAV/TAA with aortic root aneurysm—a malignant form and should be treated more aggressively. Cluster B is BAV/TAA without aortic root dilation—a benign form and should be treated conservatively.

DISCUSSION

Patients with BAV present with different genetics, BAV subtypes, valvular complications, and areas of aortic dilation; therefore, instead of treating BAV as a homogenous disease, it should be treated based on the different subtypes and associated valvulopathy/aortopathy. Cluster A BAV (malignant form)—root phenotype with aortic root aneurysm and AI should be treated more aggressively with surgical resection at 5 cm for asymptomatic patients, as for patients with MFS, while Cluster B BAV (benign form) without aortic root aneurysm could be treated less aggressively as for patients with a tri-leaflet aortic valve with surgical resection at 5.5 cm for asymptomatic patients (**Figure 1**). Concomitant elective surgery of the aorta should be considered in both Cluster A and B when undergoing clinically indicated AVR and the aorta measures $\geq$ 4.5 cm. A study by Michelena et al. (2011) found that patients with BAV and an aortic aneurysm >4.5 cm were eight times more likely to undergo an aortic dissection. Schneider et al. (2017) found that a concomitant aortic root remodeling procedure by resecting aortic sinuses in patients with BAV undergoing an aortic valve repair when the patient's root exceeded 4.2–4.5 cm has good 10–15 year results. Therefore, when a 30-year old BAV patient needs an operation for severe AI and congestive heart failure, this

patient should undergo aortic root replacement if a root diameter $\geq$ 4.5 cm instead of an isolated AVR. While the addition of an aortic root procedure to an AVR increases technical complexity as well as cardio-pulmonary bypass time, Kim et al. found that the procedure addition did not result in an elevated operative risk, a prolonged postoperative course, or an increased blood transfusion (Kim et al., 2012). However, if surgeons are not familiar with the aortic root procedures, they should refer the case to a high-volume center of performing aortic root procedures to achieve the best outcome.

AUTHOR CONTRIBUTIONS

EN and BY substantially contributed to the conception and design of the work, the acquisition, analysis of data for the work; drafted and revised the work critically for important intellectual content; approved the final version to be published; and agree to be accountable for all aspects of the work ensuring that questions related to the accuracy or integrity of any part of the work were appropriately investigated and resolved.

ACKNOWLEDGMENTS

We would like to thank all participants of the surgical BAV (sBAV) registry, the Department of Cardiac Surgery, the Cardiovascular Health Improvement Project (CHIP) at the Frankel Cardiovascular Center (FCVC), and the University of Michigan Department of Molecular and Integrative Physiology for the support.

REFERENCES

Adamo, L., and Braverman, A. C. (2015). Surgical threshold for bicuspid aortic valve aneurysm, a case for individual decision-making. *Heart* 101, 1361–1367. doi: 10.1136/heartjnl-2014-306601

Bissel, M. M., Glaze, S. J., Pitcher, A., Robson, M. D., Barker, A. J., Myerson, S., et al. (2013). Cusp fusion pattern in bicuspid aortic valve disease predicts severity of aortic flow abnormalities. *J. Cardiovasc. Magn. Reson.* 15(Suppl. 1):o69. doi: 10.1186/1532-429x-15-s1-o69

Braverman, A. C. (2011). Aortic involvement in patients with a bicuspid aortic valve. *Heart* 97, 506–513. doi: 10.1136/hrt.2009.183871

Broberg, C. S., and Therrien, J. (2015). Understanding and treating aortopathy in bicuspid aortic valve. *Trends Cardiovasc. Med.* 25, 445–451. doi: 10.1016/j.tcm.2014.12.006

Della Corte, A., Bancone, C., Buonocore, M., Dialetto, G., Covino, F. E., Manduca, S., et al. (2013). Pattern of ascending aortic dimensions predicts the growth rate of the aorta in patients with bicuspid aortic valve. *JACC Cardiovasc. Imaging* 6, 1301–1310. doi: 10.1016/j.jcmg.2013.07.009

Della Corte, A., Bancone, C., Quarto, C., Dialetto, G., Covino, F. E., Scardone, M., et al. (2007). Predictors of ascending aortic dilatation with bicuspid aortic valve, a wide spectrum of disease expression. *Eur. J. Cardiothorac. Surg.* 31, 397–404; discussion: 404–405. doi: 10.1016/j.ejcts.2006.12.006

Detaint, D., Michelena, H. I., Nkomo, V. T., Vahanian, A., Jondeau, G., and Sarano, M. E. (2014). Aortic dilatation patterns and rates in adults with bicuspid aortic valves, a comparative study with Marfan syndrome and degenerative aortopathy. *Heart* 100, 126–134. doi: 10.1136/heartjnl-2013-304920

Ellison, J. W., Yagubyan, M., Majumdar, R., Sarkar, G., Bolander, M. E., Atkinson, E. J., et al. (2007). Evidence of genetic locus heterogeneity for familial bicuspid aortic valve. *J. Surg. Res.* 142, 28–31. doi: 10.1016/j.jss.2006.04.040

Fazel, S. S., Mallidi, H. R., Lee, R. S., Sheehan, M. P., Liang, D., Fleischman, D., et al. (2008). The aortopathy of bicuspid aortic valve disease has distinctive patterns and usually involves the transverse aortic arch. *J. Thorac. Cardiovasc. Surg.* 135, 901–907. doi: 10.1016/j.jtcvs.2008.01.022

Fernandes, S. M., Khairy, P., Sanders, S. P., and Colan, S. D. (2007). Bicuspid aortic valve morphology and interventions in the young. *J. Am. Coll. Cardiol.* 49, 2211–2214. doi: 10.1016/j.jacc.2007.01.090

Fernandes, S. M., Sanders, S. P., Khairy, P., Jenkins, K. J., Gauvreau, K., Lang, P., et al. (2004). Morphology of bicuspid aortic valve in children and adolescents. *J. Am. Coll. Cardiol.* 44, 1648–1651. doi: 10.1016/j.jacc.2004.05.063

Girdauskas, E., Borger, M. A., Kuntze, T., and Hope, M. D. (2010). Aortopathy in bicuspid aortic valve disease, is it really congenital? *Radiology* 256, 1015–1016; author reply: 1016. doi: 10.1148/radiol.101046

Girdauskas, E., Disha, K., Raisin, H. H., Secknus, M. A., Borger, M. A., and Kuntze, T. (2012). Risk of late aortic events after an isolated aortic valve replacement for bicuspid aortic valve stenosis with concomitant ascending aortic dilation. *Eur. J. Cardiothorac. Surg.* 42, 832–837; discussion: 837–838. doi: 10.1093/ejcts/ezs137

Girdauskas, E., Disha, K., Rouman, M., Espinoza, A., Borger, M. A., and Kuntze, T. (2015a). Aortic events after isolated aortic valve replacement for bicuspid aortic valve root phenotype, echocardiographic follow-up study. *Eur. J. Cardiothorac. Surg.* 48, e71–e76. doi: 10.1093/ejcts/ezv259

Girdauskas, E., Rouman, M., Disha, K., Espinoza, A., Misfeld, M., Borger, M. A., et al. (2015b). Aortic dissection after previous aortic valve replacement for bicuspid aortic valve disease. *J. Am. Coll. Cardiol.* 66, 1409–1411. doi: 10.1016/j.jacc.2015.07.022

Hahn, R. T., Roman, M. J., Mogtader, A. H., and Devereux, R. B. (1992). Association of aortic dilation with regurgitant, stenotic and functionally normal bicuspid aortic valves. *J. Am. Coll. Cardiol.* 19, 283–288. doi: 10.1016/0735-1097(92)90479-7

Hope, M. D., Hope, T. A., Meadows, A. K., Ordovas, K. G., Urbania, T. H., Alley, M. T., et al. (2010). Bicuspid aortic valve, four-dimensional MR evaluation of ascending aortic systolic flow patterns. *Radiology* 255, 53–61. doi: 10.1148/radiol.09091437

Huang, F. Q., and Le Tan, J. (2014). Pattern of aortic dilatation in different bicuspid aortic valve phenotypes and its association with aortic valvular dysfunction and elasticity. *Heart Lung Circ.* 23, 32–38. doi: 10.1016/j.hlc.2013.05.644

Ikonomidis, J. S., Jones, J. A., Barbour, J. R., Stroud, R. E., Clark, L. L., Kaplan, B. S., et al. (2007). Expression of matrix metalloproteinases and endogenous inhibitors within ascending aortic aneurysms of patients with bicuspid or tricuspid aortic valves. *J. Thorac. Cardiovasc. Surg.* 133, 1028–1036. doi: 10.1016/j.jtcvs.2006.10.083

Itagaki, S., Chikwe, J. P., Chiang, Y. P., Egorova, N. N., and Adams, D. H. (2015). Long-term risk for aortic complications after aortic valve replacement in patients with bicuspid aortic valve versus marfan syndrome. *J. Am. Coll. Cardiol.* 65, 2363–2369. doi: 10.1016/j.jacc.2015.03.575

Jiao, J., Xiong, W., Wang, L., Yang, J., Qiu, P., Hirai, H., et al. (2016). Differentiation defect in neural crest-derived smooth muscle cells in patients with aortopathy associated with bicuspid aortic valves. *EBioMedicine* 10, 282–290. doi: 10.1016/j.ebiom.2016.06.045

Keane, M. G., Wiegers, S. E., Plappert, T., Pochettino, A., Bavaria, J. E., and Sutton, M. G. (2000). Bicuspid aortic valves are associated with aortic dilatation out of proportion to coexistent valvular lesions. *Circulation* 102(19 Suppl. 3), III35–III39. doi: 10.1161/01.cir.102.suppl_3.iii-35

Kim, T. H., Park, K. H., Yoo, J. S., Lee, J. H., and Lim, C. (2012). Does additional aortic procedure carry a higher risk in patients undergoing aortic valve replacement? *Korean J. Thorac. Cardiovasc. Surg.* 45, 295–300. doi: 10.5090/kjtcs.2012.45.5.295

Kostina, A. S., Uspensky Vcapital Ie, C., Irtyuga, O. B., Ignatieva, E. V., Freylikhman, O., Gavriliuk, N. D., et al. (2016). Notch-dependent EMT is attenuated in patients with aortic aneurysm and bicuspid aortic valve. *Biochim. Biophys. Acta* 1862, 733–740. doi: 10.1016/j.bbadis.2016.02.006

Martin, L. J., Ramachandran, V., Cripe, L. H., Hinton, R. B., Andelfinger, G., Tabangin, M., et al. (2007). Evidence in favor of linkage to human chromosomal regions 18q, 5q and 13q for bicuspid aortic valve and associated cardiovascular malformations. *Hum. Genet.* 121, 275–284. doi: 10.1007/s00439-006-0316-9

McBride, K. L., Riley, M. F., Zender, G. A., Fitzgerald-Butt, S. M., Towbin, J. A., Belmont, J. W., et al. (2008). NOTCH1 mutations in individuals with left ventricular outflow tract malformations reduce ligand-induced signaling. *Hum. Mol. Genet.* 17, 2886–2893. doi: 10.1093/hmg/ddn187

Michelena, H. I., Della Corte, A., Prakash, S. K., Milewicz, D. M., Evangelista, A., and Enriquez-Sarano, M. (2015). Bicuspid aortic valve aortopathy in adults, Incidence, etiology, and clinical significance. *Int. J. Cardiol.* 201, 400–407. doi: 10.1016/j.ijcard.2015.08.106

Michelena, H. I., Khanna, A. D., Mahoney, D., Margaryan, E., Topilsky, Y., Suri, R. M., et al. (2011). Incidence of aortic complications in patients with bicuspid aortic valves. *JAMA* 306, 1104–1112. doi: 10.1001/jama.2011.1286

Milewicz, D. M., Guo, D. C., Tran-Fadulu, V., Lafont, A. L., Papke, C. L., Inamoto, S., et al. (2008). Genetic basis of thoracic aortic aneurysms and dissections, focus on smooth muscle cell contractile dysfunction. *Annu. Rev. Genomics Hum. Genet.* 9, 283–302. doi: 10.1146/annurev.genom.8.080706.092303

Nemer, G., Qureshi, S. T., Malo, D., and Nemer, M. (1999). Functional analysis and chromosomal mapping of Gata5, a gene encoding a zinc finger DNA-binding protein. *Mamm. Genome* 10, 993–999. doi: 10.1007/s003359901146

Pachulski, R. T., and Chan, K. L. (1993). Progression of aortic valve dysfunction in 51 adult patients with congenital bicuspid aortic valve, assessment and follow up by Doppler echocardiography. *Br. Heart J.* 69, 237–240. doi: 10.1136/hrt.69.3.237

Qu, X. K., Qiu, X. B., Yuan, F., Wang, J., Zhao, C. M., Liu, X. Y., et al. (2014). A novel NKX2.5 loss-of-function mutation associated with congenital bicuspid aortic valve. *Am. J. Cardiol.* 114, 1891–1895. doi: 10.1016/j.amjcard.2014.09.028

Schaefer, B. M., Lewin, M. B., Stout, K. K., Gill, E., Prueitt, A., Byers, P. H., et al. (2008). The bicuspid aortic valve, an integrated phenotypic classification of leaflet morphology and aortic root shape. *Heart* 94, 1634–1638. doi: 10.1136/hrt.2007.132092

Schneider, U., Feldner, S. K., Hofmann, C., Schope, J., Wagenpfeil, S., Giebels, C., et al. (2017). Two decades of experience with root remodeling and valve repair for bicuspid aortic valves. *J. Thorac. Cardiovasc. Surg.* 153, S65–S71. doi: 10.1016/j.jtcvs.2016.12.030

Sievers, H. H., and Schmidtke, C. (2007). A classification system for the bicuspid aortic valve from 304 surgical specimens. *J. Thorac. Cardiovasc. Surg.* 133, 1226–1233. doi: 10.1016/j.jtcvs.2007.01.039

Tadros, T. M., Klein, M. D., and Shapira, O. M. (2009). Ascending aortic dilatation associated with bicuspid aortic valve, pathophysiology, molecular biology, and clinical implications. *Circulation* 119, 880–890. doi: 10.1161/CIRCULATIONAHA.108.795401

Wang, Y., Wu, B., Li, J., Dong, L., Wang, C., and Shu, X. (2016). Impact of aortic insufficiency on ascending aortic dilatation and adverse aortic events after isolated aortic valve replacement in patients with a bicuspid aortic valve. *Ann. Thorac. Surg.* 101, 1707–1714. doi: 10.1016/j.athoracsur.2015.10.047

Yang, B., Zhou, W., Jiao, J., Nielsen, J. B., Mathis, M., Heydarpour, M., et al. (2017). Protein-altering and regulatory genetic variants near GATA4 implicated in bicuspid aortic valve. *Nat. Commun.* 8:15481. doi: 10.1038/ncomms15481

Conflict of Interest Statement: The authors declare that the research was conducted in the absence of any commercial or financial relationships that could be construed as a potential conflict of interest.

frontiers in Physiology

PERSPECTIVE
published: 10 July 2017
doi: 10.3389/fphys.2017.00475

Evolution of Precision Medicine and Surgical Strategies for Bicuspid Aortic Valve-Associated Aortopathy

*Ali Fatehi Hassanabad[1], Alex J. Barker[2], David Guzzardi[1], Michael Markl[2,3], Chris Malaisrie[4], Patrick M. McCarthy[4] and Paul W. M. Fedak[1,4]**

[1] Section of Cardiac Surgery, Department of Cardiac Sciences, Cumming School of Medicine, Libin Cardiovascular Institute of Alberta, University of Calgary, Calgary, AB, Canada, [2] Department of Radiology, Feinberg School of Medicine, Northwestern University, Chicago, IL, United States, [3] Department of Bioengineering, Feinberg School of Medicine, Northwestern University, Chicago, IL, United States, [4] Martha and Richard Melman Family Bicuspid Aortic Valve Program, Division of Cardiothoracic Surgery, Bluhm Cardiovascular Institute, Northwestern University, Chicago, IL, United States

Bicuspid aortic valve (BAV) is a common congenital cardiac malformation affecting 1–2% of people. BAV results from fusion of two adjacent aortic valve cusps, and is associated with dilatation of the aorta, known as bicuspid valve associated aortopathy. Bicuspid valve aortopathy is progressive and associated with catastrophic clinical events, such as aortic dissection and rupture. Therefore, frequent monitoring and early intervention with prophylactic surgical resection of the proximal aorta is often recommended. However, the specific pattern of aortopathy is highly variable among patients, with different segments of the ascending aorta being affected. Individual patient risks are sometimes difficult to predict. Resection strategies are informed by current surgical guidelines which are primarily based on aortic size and growth criteria. These criteria may not optimally reflect the risk of important aortic events. To address these issues in the care of patients with bicuspid valve aortopathy, our translational research group has focused on validating use of novel imaging techniques to establish non-invasive hemodynamic biomarkers for risk-stratifying BAV patients. In this article, we review recent efforts, successes, and ongoing challenges in the development of more precise and individualized surgical approaches for patients with bicuspid aortic valves and associated aortic disease.

Keywords: bicuspid aortic valve, aortopathy, MRI, biomarkers discovery, precision medicine

OPEN ACCESS

Edited by:
Alessandro Della Corte, Department of Cardiothoracic Sciences - Second University of Naples, Monaldi Hospital, Italy

Reviewed by:
Amy Banes-Berceli, Oakland University, United States
Dan Predescu, Rush University, United States

***Correspondence:**
Paul W. M. Fedak
paul.fedak@gmail.com

Specialty section:
This article was submitted to Vascular Physiology, a section of the journal Frontiers in Physiology

Received: *31 March 2017*
Accepted: *21 June 2017*
Published: *10 July 2017*

Citation:
Fatehi Hassanabad A, Barker AJ, Guzzardi D, Markl M, Malaisrie C, McCarthy PM and Fedak PWM (2017) Evolution of Precision Medicine and Surgical Strategies for Bicuspid Aortic Valve-Associated Aortopathy. Front. Physiol. 8:475. doi: 10.3389/fphys.2017.00475

INTRODUCTION

Bicuspid aortic valve (BAV) is the most common congenital heart defect, affecting 1–2% of the general population (Hoffman and Kaplan, 2002). Abnormality of the aorta is frequently associated with BAV, with thoracic aortic dilation seen in approximately 40% of patients in referral centers (Masri et al., 2016). Consequently, compared to the general population, patients with BAV are at a higher risk for acute aortic emergencies, such as aortic dissection (Januzzi et al., 2004). Given the high morbidity and mortality associated with these emergencies, identifying the optimal timing to intervene, and prevent such events is of paramount importance. However, this is a challenging process as many factors, including patient age, comorbidities, presence or absence of aortic valvular disorders, and family history of BAV, could all affect management.

Over the past three decades, it was perceived that aortopathy associated with BAV, "bicuspid aortopathy," had a similar pathophysiology to aortic disorders associated with tricuspid aortic

valve (TAV) disease. Specifically, it was believed that turbulent or eccentric flow resulting from a narrowed orifice (BAV) led to aortic dilation. However, several ensuing studies demonstrated a strong genetic component for BAV-associated aortopathy in this patient population, which in turn, significantly increases the risk of acute aortic events. These initial findings led to recommendations for more aggressive management approaches, which viewed bicuspid aortopathy in the same light as Marfan's syndrome, thereby advocating for earlier surgical intervention for patients with BAV disease. More recent research, however, has implied that genetic predisposition and hemodynamic irregularities contribute to varying degrees in different subgroups of BAV patients, and the rate of aortic complications is not as high as previously believed (Fedak et al., 2005; Hiratzka et al., 2010; Girdauskas et al., 2011; Itagaki et al., 2015; Sherrah et al., 2016). These recent studies emphasize the importance of identifying the underlying cause of bicuspid aortopathy as it has different therapeutic implications for patients with or without BAV presenting with aortic pathologies.

A few groups have considered the optimal management of BAV-associated aortopathy, and several documents have addressed it, with the first being a multi-societal set of guidelines published in 2010 (Hiratzka et al., 2010). In the more recently published guidelines by the American Heart Association/American College of Cardiology (AHA/ACC) on valvular heart disease, a more conservative set of recommendations were made (Nishimura et al., 2014). Given the significant difference in recommendations, a recent clarification statement was published (Hiratzka et al., 2016). The European Society of Cardiology has also made more conservative recommendations for the management of bicuspid aortopathy (Vahanian et al., 2012; Erbel et al., 2014). In addition, the American Association for Thoracic Surgery (AATS) will be releasing an expert consensus statement in 2017.

Emerging research is considering the genetics and molecular and cellular mechanisms underlying the disease. As Prakash and colleagues elegantly outline, autosomal-dominant transmission of BAV was observed in some 3-generation pedigrees, but there is no single-gene model which clearly explains BAV inheritance. The prevalence of BAV stands nearly 10-fold higher in primary relatives of patients with BAV than in the general population, further supporting the notion that genetics does indeed play an important role (Prakash et al., 2014). To better understand the mechanisms which drive BAV and bicuspid aortopathy, different groups are studying various molecular pathways and genetic foci. Thus far, NOTCH1 remains the only gene which has been implicated for isolated BAV identified using linkage analysis and positional cloning strategies, despite probably being the cause of small proportion of familial cases (Garg et al., 2005; Ellison et al., 2007). These studies are all in their infancy, but continued basic research in this area will undoubtedly shed more light onto the genetic building block of BAV and bicuspid aortopathy.

Bicuspid aortopathy is a very heterogeneous disorder, a feature which has added to the complexity of devising management guidelines. For example, in some instances, despite developing aortopathy, patients can be asymptomatic throughout their life. Moreover, dilation of the aorta may occur in the aortic root, ascending aorta, proximal aortic arch, or a combination of any of these three (Fazel et al., 2008). Moreover, despite ongoing research, it remains to be established if medical therapy is effective in preventing complications for patients with bicuspid aortopathy. Although supportive clinical evidence is still missing, beta-blockers and angiotensin receptor blocking agents are frequently prescribed to protect the BAV-aorta within this patient population (Danyi et al., 2011; Chun et al., 2013; Ziganshin et al., 2015). On the other hand, several groups have studied the risk of developing aneurysmal dilation of the ascending aorta over time in patients with BAV (to a size of 4.0–4.5 cm). It was shown that 20–30% of patients with BAV develop aneurysmal enlargement during 9–25 years of follow up (Michelena et al., 2008, 2014; Tzemos et al., 2008). In fact, in a recent review paper, based on eight independent studies, it was suggested that up to 84% of patients with BAV ultimately develop an aneurysm, and the risk of the aneurysm development was 80-fold higher when compared to the general population (Michelena et al., 2014; Wasfy et al., 2015).

Of clinical significance, dilatation of any or all segments of the aorta is seen in approximately 50% of patients with BAV (Fedak et al., 2005), and ascending aortic aneurysms occur in 1% of BAV patients per year. Although bicuspid aortopathy can manifest in all segments of the aorta, it is more often isolated to the aortic root, ascending aorta, or proximal aortic arch. Most patients will present with maximal dilatation of the tubular mid-ascending aorta, specifically at the greater curvature, with the aortic root and proximal arch being affected to varying degrees. Thus, resection strategies can vary greatly (Fedak et al., 2005; Della Corte et al., 2014a; Fedak and Verma, 2014; Adamo and Braverman, 2015; Moon, 2015; Sundt, 2015). In addition to deciding when to intervene in replacing the aorta in bicuspid aortopathy, assessing what to resect also poses a clinical dilemma (Fedak and Verma, 2014; Sundt, 2015). Bicuspid aortopathy is progressive, increasing the risk of aortic dissection and rupture. To date, these complications have been challenging to predict. Therefore, frequent monitoring and personalized interventions for both timing of surgery and the extent of resection are of paramount importance in preventing these clinical catastrophes and delivering optimal care (Itagaki et al., 2016).

Although different international societies and expert groups have provided unified guidelines regarding optimal management of patients with BAV disease, most surgical recommendations have primarily been based on maximal aortic diameter and growth rate (Nishimura et al., 2014). According to these guidelines, prophylactic replacement of the ascending aorta is performed in roughly 25% of BAV patients within 25 years from the time of diagnosis (Michelena et al., 2011). This has significant implications, as the burden of surgery for BAV patients in the United States exceeds 1 billion dollars per year, and surgical intervention has doubled over the past decade (Opotowsky et al., 2013). It is noted that surgical planning and decision-making for BAV patients is affected by physician bias and historical local practice within institutions, which aren't always consistent and in line with guidelines (Verma et al., 2013; Della Corte

et al., 2014b; Girdauskas and Borger, 2014; Michelena et al., 2014; Verma and Siu, 2014; Sundt, 2015; Wasfy et al., 2015). In a recent survey of 100 cardiac surgeons, it was postulated that attitudes on the etiology, inherited aortopathy vs. acquired from hemodynamic stress, rather than proven clinical evidence dictated surgical treatment of BAV aortopathy (Verma et al., 2013). Undeniably, this has complicated widely accepted and universally utilized guidelines, emphasizing the need for more translational and clinical research solely dedicated to BAV patient populations.

Fortunately, over the past 3 years, a concerted effort has been made in understanding the individual variability inherent to BAV disease and the role hemodynamic factors play in its manifestation and progression (Della Corte et al., 2014a; Fedak and Verma, 2014; Girdauskas and Borger, 2014; Martin et al., 2014; Uretsky and Gillam, 2014; Verma and Siu, 2014; Michelena, 2015; Spinale and Bolger, 2015; Itagaki et al., 2016; Sievers et al., 2016). There is a general consensus among experts regarding a critical need in developing personalized risk assessments beyond conventional aortic size and growth criteria, in delivering optimal care to BAV patients. The challenge clinicians face today is a paucity of prognostic models to inform the timing and extent of surgical intervention. To address some of these issues, our translational research group and others have focused on validating use of novel imaging techniques to establish non-invasive hemodynamic biomarkers for risk-stratifying BAV patients. In this review article, we will consider recent efforts, successes, and ongoing challenges in the development of more precise and individualized surgical approaches for patients with BAVs and associated aortic disease.

PATHOPHYSIOLOGY AND WAVERING GUIDELINES

To develop patient-specific parameters in BAV populations, researchers have considered the pathophysiology of BAV aortopathy. Like other vessels, a normal aortic wall is divided into three layers: intima, media, and adventitia. Elastin fibers, vascular smooth muscles cells, and structural extracellular matrix (ECM) comprise the medial layer. The aortic media regulates tissue biology and biomechanics (**Figure 1**). Different studies have demonstrated that BAV occurs in conjunction with degeneration of this layer. Bicuspid aortopathy involves medial ECM abnormalities which include (Della Corte et al., 2014b; Itagaki et al., 2016)

1. ECM dysregulation: altered matrix metalloproteinase expression and activity (Thompson and Cockerill, 2006; Ikonomidis et al., 2007, 2012; Wilton et al., 2008; Fedak et al., 2013; Rabkin, 2014)
2. Altered medial ECM architecture: elastin fiber degeneration (de Sa et al., 1999; Bauer et al., 2002; Cotrufo et al., 2003, 2005; Chung et al., 2007; Phillippi et al., 2014)
3. Tissue dysfunction: altered stiffness and biomechanics (Nistri et al., 2002, 2008; Schaefer et al., 2007; Pees and Michel-Behnke, 2012; Oulego-Erroz et al., 2013; Warner et al., 2013; Forsell et al., 2014; Moaref et al., 2014; Petrini et al., 2014)

As expected, the presence, severity, and location of these pathologies differs among patients. This poses a significant question: in addition to a possible genetic predisposition to dilatation, do hemodynamic conditions in the aorta contribute to its remodeling in BAV patients?

Unfortunately, the mechanisms which contribute to aortopathy in BAV patients have not been clearly elucidated (Davies et al., 2007; Tadros et al., 2009; Girdauskas et al., 2011; Michelena et al., 2011; Sievers and Sievers, 2011), and it is not known whether genetics leads to aortopathy or if the altered BAV morphology results in isolated diseased areas within the aortic wall secondary to abnormal blood flow from the valve (**Figure 2**). It is possible that it is a combination of both factors, but a unilateral focus on the genetic component has supported aggressive surgical intervention with respect to the timing and extent of aortic resection. Although previous guidelines and size thresholds for surgical resection were based on algorithms similar to those for patients diagnosed with genetic aortopathies, such as Marfan's syndrome (Bonow et al., 2008), recent clinical data strongly suggest that bicuspid aortopathy is distinct from that of Marfan's (Itagaki et al., 2015). Not surprisingly, clinical approaches in managing BAV aortopathies are highly influenced by different opinions on the varied impact of genetics and hemodynamics on disease progression (Hardikar and Marwick, 2015). Initially, a conservative cut off of 5.5 cm was used in 1998 (Tricoci et al., 2009). In 2010, surgeons were more aggressive, intervening when the aortic diameter was 4.0–4.5 cm (Warnes et al., 2008), but reverted to a more conservative approach of 5.5 cm cut off in 2014 (Svensson et al., 2013; Erbel et al., 2014; Michelena et al., 2015). Throughout this time no clinically and scientifically proven study was reported to support either a conservative or aggressive approach in surgical resection in bicuspid aortopathy (Hardikar and Marwick, 2015). To offer scientifically proven guidelines, which would consistently be used by clinicians, it is of paramount importance to continue the work on the discovery and implementation of novel aortic risk markers (Michelena et al., 2015; Spinale and Bolger, 2015).

NEW EVIDENCE ON THE PATHOPHYSIOLOGY OF BAV AORTOPATHY

Previous work studying the hemodynamic component to BAV-related aortopathy focused on the severity of aortic valve stenosis (AS) or insufficiency (AI) (Tzemos et al., 2008; Girdauskas et al., 2011; Michelena, 2015). It is now believed that these conventional hemodynamic factors alone do not reflect the impact on the aortic wall due to a malformed valve (Girdauskas et al., 2011; Sievers and Sievers, 2011; Atkins and Sucosky, 2014; Della Corte et al., 2014b; Adamo and Braverman, 2015; Michelena et al., 2015; Moon, 2015). These findings imply that the development of bicuspid aortopathy is not primarily driven by a genetic predisposition. Further supporting these results are recent studies by our group and others which have shown that altered aortic flow and valve morphology in BAV patients are related to the expression of the aortopathy

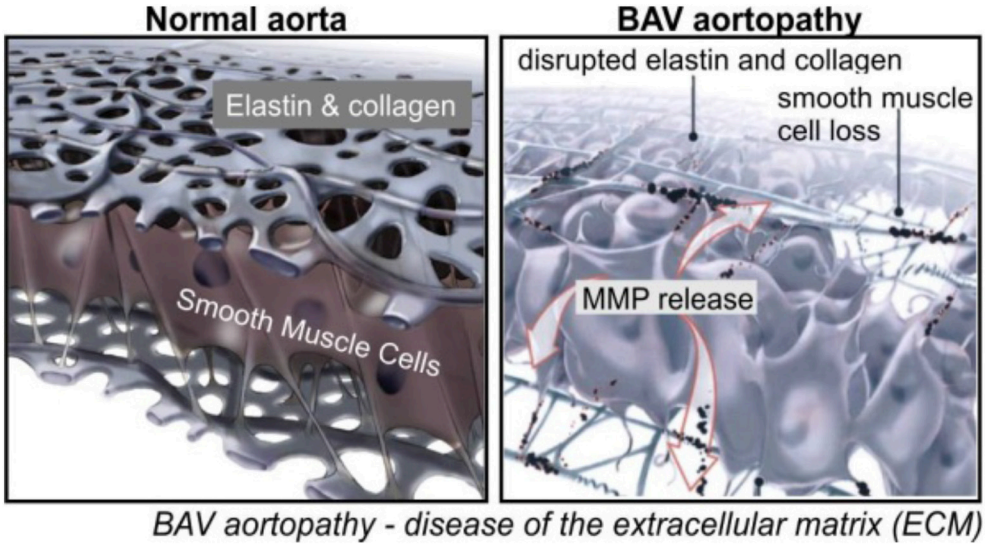

FIGURE 1 | Aortic wall degeneration in BAV (Fedak et al., 2002).

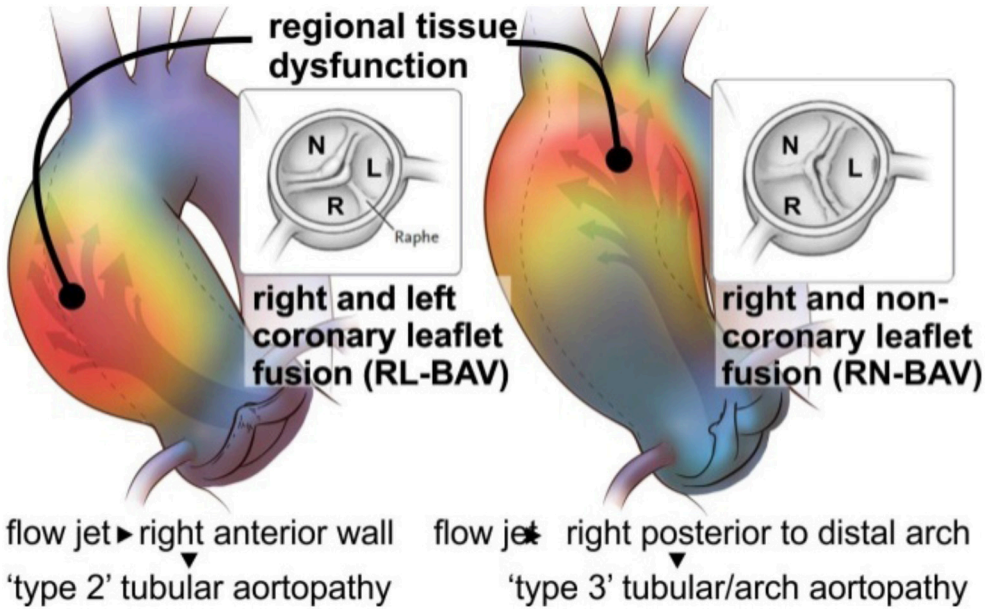

FIGURE 2 | Valve mediated hemodynamics. BAV fusion patterns lay the foundation for changes in aortic outflow and wall shear stress (WSS). Eccentric blood flow from the RL-BAV impinges on regions of dilatation at the tubular ascending aorta wall. Flow from the RN-BAV reflects off the proximal posterior wall and impinges on regions of aortic dilatation within the proximal arch. Adapted with permission (Itagaki et al., 2016).

phenotype (Kang et al., 2013; Mahadevia et al., 2014; Prakash et al., 2015). As depicted in **Figure 2**, 4-D flow MRI studies provide strong evidence that valve-mediated local flow dynamics (Barker et al., 2012) and regional differences in wall shear stress (WSS) (Mahadevia et al., 2014) are associated with changes in regional aortic wall histology and proteolytic events (Guzzardi et al., 2015), contributing to unfavorable aortic remodeling. More significantly, these preliminary data can be landmark findings in better understanding valve-mediated hemodynamics' impact on the progression of bicuspid aortopathy. They can also be a platform for clinically-proven justification in utilizing MRI-based biomarkers in risk stratification.

The dearth of prognostic models to assist in the surgical management of BAV patients is the biggest challenge clinicians face today, particularly with regards to the timing and extent of surgical repair. As mentioned, this patient population is

often offered aortic resection primarily based on maximal aortic size dimension and the rate at which the aorta expands. It is, however, now understood that measures of aortic size alone are insufficient to dictate treatment algorithms (Della Corte et al., 2012a; Verma et al., 2013; Della Corte, 2014; Michelena et al., 2014; Prakash et al., 2015; Sundt, 2015; Wasfy et al., 2015). Therefore, substantial efforts are currently being made to improve risk prediction for aortic catastrophes in BAV patients (Della Corte et al., 2007, 2012b,c, 2013; Ikonomidis et al., 2013).

Recent work has yielded strong evidence that including measures of downstream valve-mediated hemodynamics into the work-up of BAV patients has a high likelihood to circumvent current prognostic challenges (Davies et al., 2007; Rabkin, 2014; Adamo and Braverman, 2015; Song, 2015). However, conventional diagnostic modalities, such as Doppler echocardiography, 2D phase contrast [PC]-MRI, and CT scan, do not offer the means for a thorough *in-vivo* assessment of three dimensional blood flow through the aorta, which is necessary to study the role of transvalvular hemodynamics on the downstream forces experienced at the aortic wall and their impact on the progression of aortic dilatation.

INNOVATIVE TECHNOLOGY—4D FLOW MRI

Recent advances in magnetic resonance imaging have allowed for uncompromised *in-vivo* assessment of time-resolved 3D blood velocity, using a volumetric technique, referred to as 4D flow MRI (**Figure 3**). This modality provides an opportunity to quantify complex three dimensional blood flow patterns *in-vivo*, and has facilitated new insights into sophisticated cardiovascular hemodynamics (Harloff et al., 2009, 2010b; Markl et al., 2010, 2011a; Barker et al., 2012; Mahadevia et al., 2014). In particular, multidimensional 4D flow MRI data, which infers three spatial dimensions describing 3D velocity over time, permits visualization of aortic blood flow, quantification of regional velocity and flow (Markl et al., 2007, 2011b; Frydrychowicz et al., 2008a; Bock et al., 2010), and WSS (Stalder et al., 2008; Barker et al., 2010; Harloff et al., 2010a; Bock et al., 2011; Garcia et al., 2014; van Ooij et al., 2015a).

Multiple institutions have now shown that 4D flow MRI can be utilized to accurately identify altered flow patterns secondary to BAV, even if aortic stenosis is present (**Figures 3**, **4**). Among the observed hemodynamic changes are eccentric flow patterns, which result in a change of the drag forces at the vessel wall (**Figure 4**). Despite what is believed to be a multifactorial disease, recent studies have shown WSS to play a major role in bicuspid aortopathy. We now believe that WSW may change local matrix homeostasis, and consequently affect the structure of the ascending aorta (Stalder et al., 2008; Markl et al., 2009; Harloff et al., 2010a; Markl et al., 2010; Bock et al., 2011; Garcia et al., 2014; van Ooij et al., 2015a). In fact, research has shown WSS to affect cell function, implicating its role in the development of aortopathy (den Reijer et al., 2010; Hope et al., 2010a, 2011).

Our group has used non-invasive MRI techniques (2D phase contrast MRI) to show BAV-mediated alterations in flow and WSS (Barker et al., 2010). Building on the successes of our initial work, we then employed 4D flow MRI to definitively demonstrate aortic WSS was increased in BAV subjects independent of the degree of stenosis when compared to age and aortic size-matched controls ($P < 0.05$, **Figure 4**; Mahadevia et al., 2014). Also of clinical significance, we have shown that regional variation of WSS with the aorta is dependent on aortic valve fusion phenotype (Barker et al., 2012; Mahadevia et al., 2014), and is associated with the diameter of the aorta (Bissell et al., 2013). In one of our recent studies, we considered 30 BAV patients and 30 age-appropriate trileaflet aortic valve (TAV) controls, and showed that altered aortic hemodynamics may be a mechanism by which right and left coronary leaflet (RL-BAV) or right and non-coronary leaflet valve (RN-BAV) fusion influences the expression of aortopathy (Mahadevia et al., 2014).

A significant finding has been the fact that hemodynamic alterations are related to medial wall degeneration (Guzzardi et al., 2015). A pilot study was recently completed, which included both *in-vivo* 4D flow MRI and aortic tissue resection in 20 BAV patients. The study successfully demonstrated the ability to correlate *in-vivo* 4D flow derived hemodynamic biomarkers with tissue metrics of bicuspid aortopathy. In this work, 20 BAV patients undergoing aortic resection underwent pre-operative 4D flow MRI to regionally map WSS and had histologic examination of their resected tissue samples. Samples obtained from regions of both elevated and normal WSS within the same patient were paired, and compared for medial elastin degeneration by histology and ECM dysregulation by protein expression. As depicted in **Figures 6**, **7**, regions of increased WSS showed greater medial elastin degradation compared to adjacent segments with normal WSS. Moreover, multiplex protein analyses of ECM regulatory molecules revealed an increase in TGFβ-1, MMP-1, MMP-2, MMP-3, and TIMP-1 in increased WSS areas, suggesting ECM dysregulation in regions of elevated WSS. In a much larger prospective cohort, the aim will be to more comprehensively characterize aortic tissues resected from segments of abnormal WSS, further clarifying the impact of altered blood flow.

THE PROMISE OF PERSONALIZED MEDICINE FOR BAV PATIENTS

The pilot study demonstrated the potential utility of 4D flow MRI to identify areas with more advanced aortopathy in patients. Future work will focus on these significant findings, with the objectives being the discovery and validation of key hemodynamic imaging biomarkers. This should include refining aortic MRI protocols, creating "maps" or "atlases" of normal age and gender-matched imaging biomarkers of aortic hemodynamics in both BAV and TAV patients, and pushing current boundaries by carrying out a clinico-pathologic correlation study in BAV and TAV patients with aortopathy to establish imaging biomarkers predictive of aortic tissue pathology and dysfunction.

A limitation of 4D flow MRI is the acquisition time needed and its low blood-tissue contrast, which has proven a challenge for its translation to routine clinical use. Ongoing efforts to

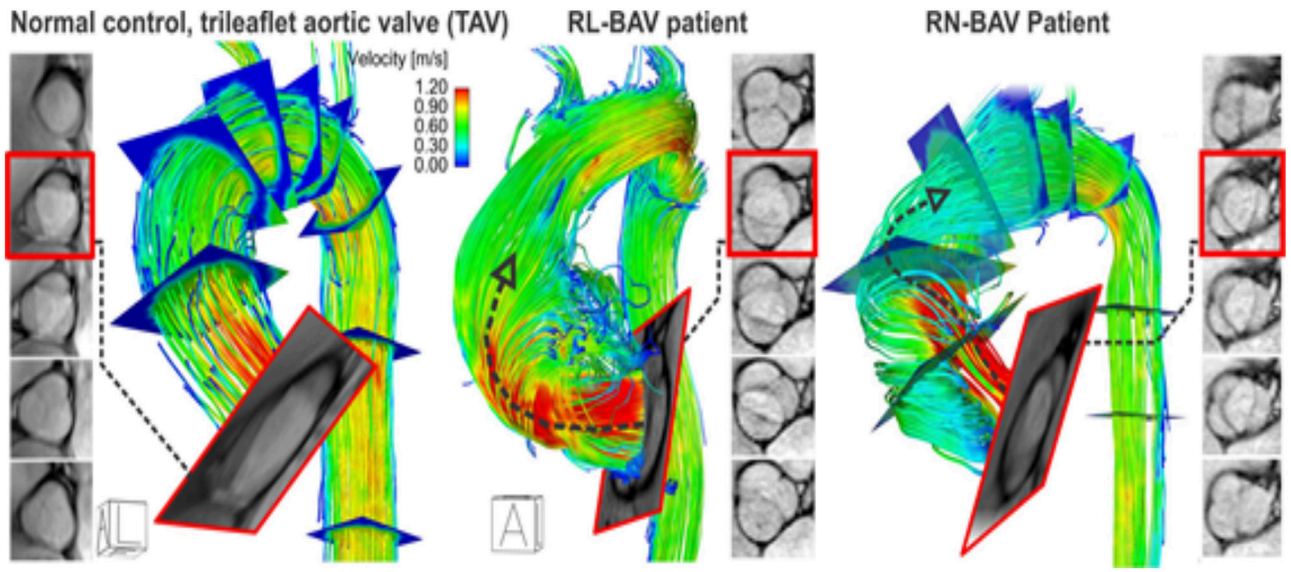

FIGURE 3 | 4D flow MRI in a control and BAV patient with a right-left (RL) fusion pattern and right-non-coronary (RN) fusion pattern. Note that the RL-BAV exerted significant eccentric aortic outflow jet (but not higher velocity, arrow) compared to TAV. The BAV phenotype (RL vs. RN) greatly influences aortic outflow, which in turn, affects aortic segments exposed to elevated WSS (**Figure 4**). Adapted with permission (Barker et al., 2012; Guzzardi et al., 2015).

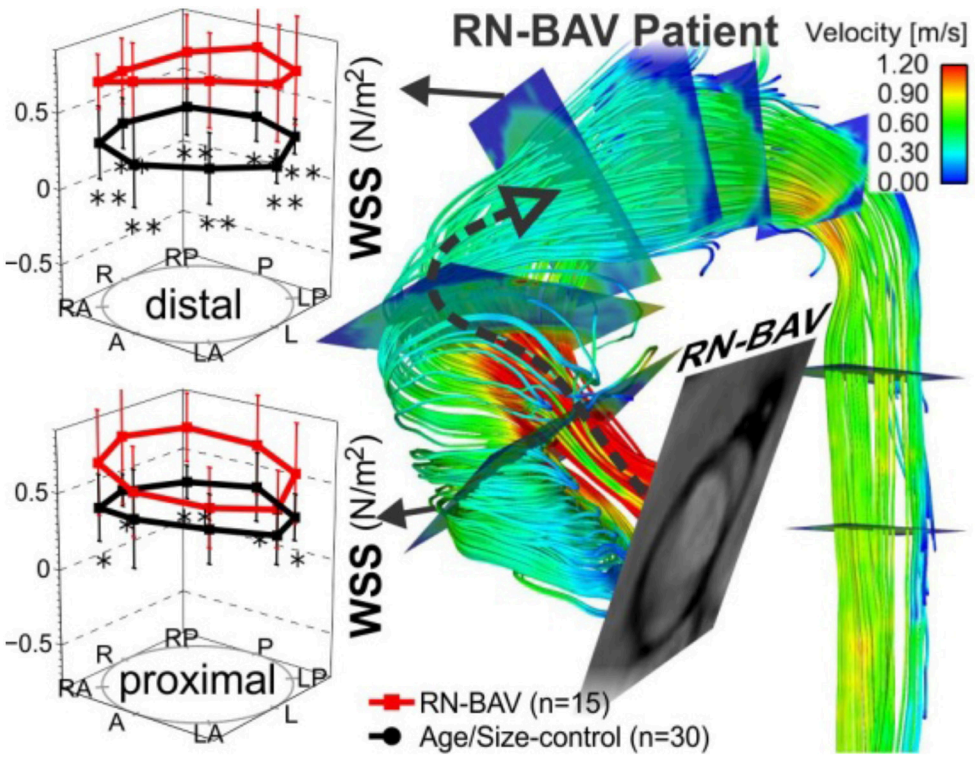

FIGURE 4 | 4D flow & WSS quantification in 15 RN-BAV patients found that 4D flow can detect significant differences (*$p < 0.05$, **$p < 0.001$) in aortic WSS distribution compared to 30 TAV controls. **(A)** Control populations and **(B)** individual BAV patient. Note the different aortic outflow pattern compared to the RL-BAV patient in **Figure 3** (Barker et al., 2012).

decrease exam time with the use of accelerated imaging strategies such as radial undersampling, k-t approaches, or compressed sensing are rapidly becoming available for the clinic (Baltes et al., 2005; Lustig et al., 2007; Moftakhar et al., 2007). This should hopefully result in reduced acquisition times for the assessment of valve dynamics and time-resolved aortic 3D geometry. Moreover, these advances should improve 3D segmentation of various parts of the aorta for precise assessment of hemodynamic imaging biomarkers, such as WSS and flow displacement, and amalgamate the analysis of aortic valve morphology (RL-, RN-BAV, etc.), geometry (orifice area), and dynamics (opening angle).

Additionally, the pilot study considered whether aortic WSS, ECM architecture and protein expression, and non-traditional hemodynamic parameters can affect regional aortic tissue function. However, it is still not known which factors associated with valve-mediated hemodynamics are most sensitive in predicting the development and progression of aortopathy. For instance, WSS gradient (WSSG) and oscillatory shear index (OSI) are also known to promote remodeling (Hope et al., 2010a; Bissell et al., 2013). Moreover, previous work studying WSS was based on two-dimensional imaging planes manually placed in the thoracic aorta (Frydrychowicz et al., 2008b, 2009; Stalder et al., 2008; Markl et al., 2010, 2011c, 2013; Harloff et al., 2010a; Hope et al., 2010b; Barker et al., 2012; Burk et al., 2012; Potters et al., 2014), and was hence, limited in calculating imaging biomarkers along the entire length of the aorta. A future goal would be to develop a comprehensive data analysis protocol.

In a recent study, an algorithm was developed to compute volumetric 3D WSS along the entire surface of the aorta (**Figure 5**; Potters et al., 2014; van Ooij et al., 2015a). Test–retest experiments for systolic WSS demonstrated excellent accuracy, with a 9% coefficient of variance, and a 6% inter-observer error (van Ooij et al., 2015b). We also now know that elevated WSS could be seen on the outer curvature of the ascending aorta in 13 BAV patients, with a significant correlation to peak systolic velocity (Cibis et al., 2015). Future work will focus on extending the methodology to incorporate additional imaging biomarkers implicated in vessel wall remodeling, such as WSSG and OSI.

Prior research on creating "heat maps" or "atlases" utilized a 3D WSS mapping technique which allowed for compact visualization of hemodynamic parameters studies across multiple subjects. This mapping, however, is limited in that it does not detect where "abnormal" values exist. Therefore, a database of healthy volunteer 4D flow MRI exams was created to produce an aortic "atlas" which established regional confidence intervals for normal physiologic WSS throughout the aorta (**Figure 5**; van Ooij et al., 2015a). Linear intra- and inter-modal brain image registration (FLIRT, Linear Image Registration Tool, FMRIB, Oxford; Jenkinson and Smith, 2001) were utilized to co-register aortic 3D WSS of 10 TAV patients with no aortic stenosis, but present aortic dilatation, and TAV patients with aortic stenosis, but no aortic dilatation, with the atlas. The dilatation cohort had significantly lower WSS on 7% of the ascending aorta, whereas the stenosis cohort showed significantly higher WSS on 34% of the ascending aorta surface (van Ooij et al., 2015a,c). A future research goal is to build on these efforts to construct age and gender matched atlases of the imaging biomarkers in a large population.

In summary, patient-specific WSS can be reliably computed and co-registered to a healthy control atlas, representing the normal ranges of physiologic WSS. These normal WSS atlases can

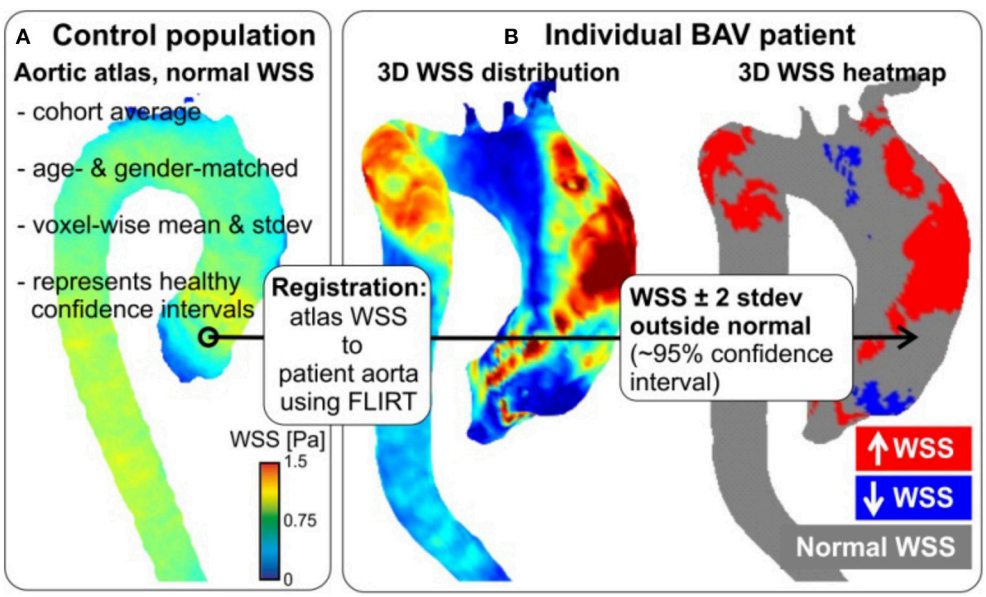

FIGURE 5 | Patient-specific WSS heat maps. Healthy atlases are registered to BAV data with tools developed for brain mapping. Maps can be reliably generated, even in patients with complex aortic geometries (as here).

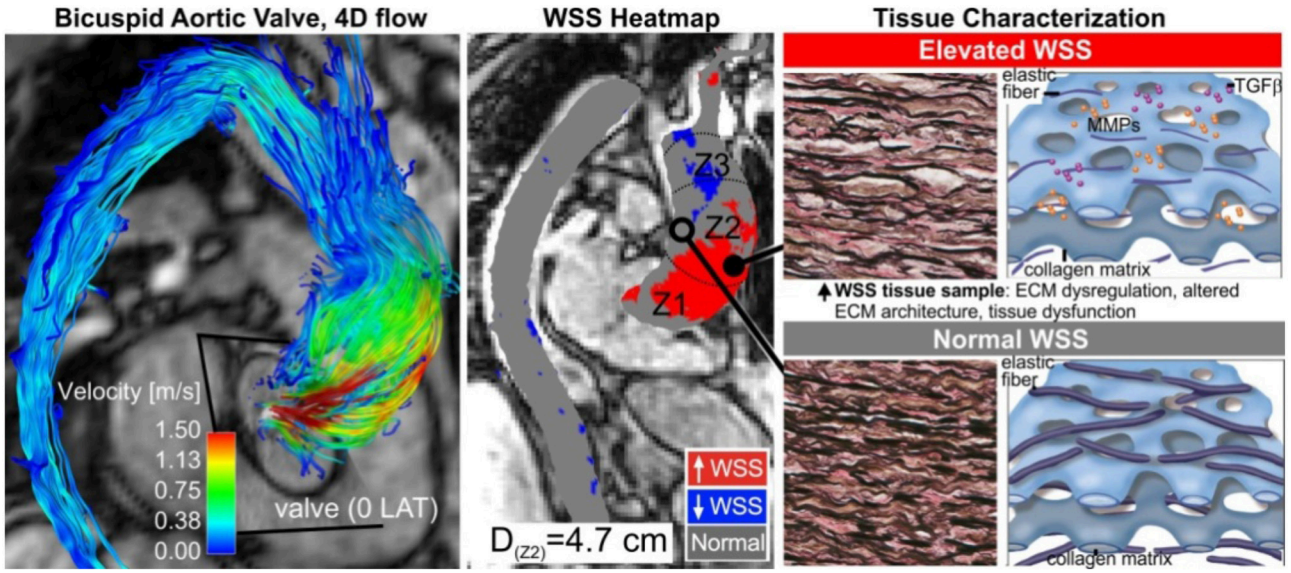

FIGURE 6 | Tissue histopathology. Aortic wall regions are exposed to elevated WSS (middle, red region), due to eccentric transvalvular BAV flow **(left)**. This manifests in the expression of abnormal tissue metrics of aortopathy **(right)**. Adapted with permission (Guzzardi et al., 2015).

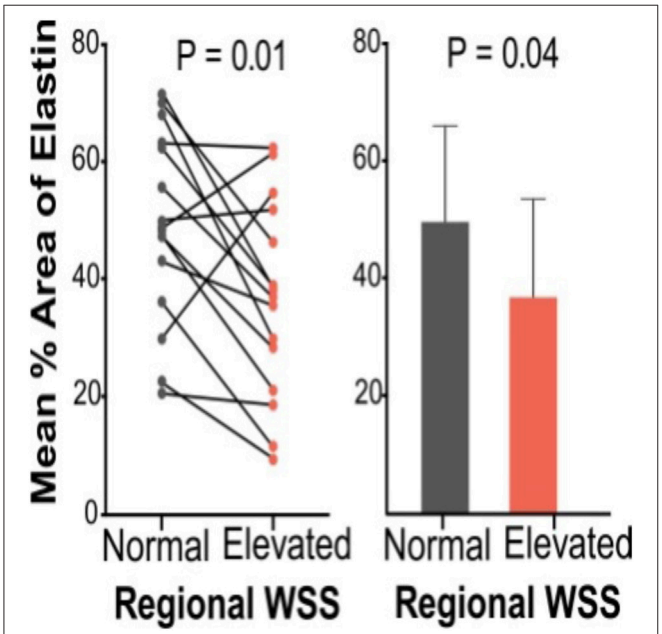

FIGURE 7 | Elastin content from Verhoeff–Van Gieson elastin staining for patient pairs and cumulative group means for aortic wall subjected to normal and elevated WSS (Guzzardi et al., 2015).

subsequently be employed to create "heat maps" which represent regions of abnormally high or low WSS in a patient in question (**Figures 5B**, **6**; van Ooij et al., 2015c). This heat map provides a foundation for thorough, yet succinct, assessment to detect regions, and segments of the aortic wall which are exposed to abnormal hemodynamics on an individual, patient-specific, basis.

IMAGING HEMODYNAMIC BIOMARKERS AND AORTIC WALL PATHOLOGY

A major component of personalized medicine is the potential utility of non-invasive biomarkers in diagnosing and prognosticating clinical risk and outcomes. The same holds true for BAV and bicuspid aortopathy; much current investigation is aimed at identifying such markers to improve the management of this patient population. For instance, Della Corte's group recently published a study which shows that the ratio of circulating Transforming Growth Factor Beta-1 to soluble endoglin is an early biomarker for bicuspid aortopathy. Although systemic biomarkers remain to be more fully validated, such investigations provide a foundation for future work in this area (Forte et al., 2017).

The focus of this review, however, is the role of novel non-invasive imaging hemodynamic biomarkers. As mentioned above, to date, most research on the hemodynamic hypothesis for bicuspid aortopathy has focused on aortic valve function, namely the severity of aortic stenosis or insufficiency (Tzemos et al., 2008; Girdauskas et al., 2012; Michelena, 2015). These factors alone, however, do not fully reflect the hemodynamic burden exacted on the aortic wall, secondary to the malformed aortic valve. Moreover, despite not being completely well-understood, there are inherent differences in the development of BAV vs. TAV aortopathy. For instance, the associated aortopathy in most patients with TAV is thought to be a result of aortic valve stenosis and altered post-valve hemodynamics. On the other hand, a strong genetic predisposition has been suggested to contribute to aortopathy in BAV patients. Interestingly, a recent study showed that TAV aortopathy was associated with more severe histologic abnormalities compared to BAV aortopathy, especially when stratified by diameter (Heng et al., 2015). Properly

assessing the diagnostic value of novel imaging biomarkers requires further work in this area to gain a better appreciation of the differences in the development of BAV vs. TAV aortopathy.

As alluded to above, recently, a correlation between WSS and regional aortic tissue remodeling in BAV patients was established (Guzzardi et al., 2015). It was concluded that elastin content and structure was significantly disrupted in areas of high WSS with a change in the expression of specific MMPs and TGF-beta. There was also an observed trend toward differences in the elastic modulus and tissue stiffness using biaxial testing. Although further clarification is required, these data promise an opportunity for utilizing valve-mediated hemodynamics as non-invasive biomarkers of aortopathy susceptibility and progression.

Despite making great strides in advancing our understanding of BAV aortopathy and its clinical implications, work has so far considered only one hemodynamic biomarker, systolic WSS, within a small sample size. Future research will need to focus on identifying the hemodynamic metric most predictive of disease severity, as well as elucidating the role other clinical factors play, in a larger population sample size. To determine the differential impact and magnitude of valve-mediated hemodynamics as compared to genetic predisposition and other non-hemodynamic factors in BAV patients, future work should compare our results to a purely hemodynamic-mediated aortopathy reference group. Finally, the pilot study was not powered to assess difference in MMP-2 expression, thus ongoing and future studies can consider MMP-2 activity, histopathology, and biomechanics in larger samples sizes.

CONCLUSION

Bicuspid aortic valve is the most common congenital cardiac defect. Multiple studies provide strong evidence for the clinical significance of this disease, especially as how it relates to pathologic abnormalities of the aorta. Many studies have also shown the devastating sequelae of aortic complications in patients with BAVs. All of these impose a highly unfavorable health and economic burden on patients and society-at-large. To better understand the etiology and pathophysiology of bicuspid aortopathy, numerous investigators have undertaken studying different aspects of the disease. These efforts have successfully elucidated critical mechanisms and factors influencing disease development and progression in bicuspid aortopathy. To an extent, the motivation for this work has been the objective of defining a uniform, safe, and evidence-based set of guidelines for the medical and surgical management of these patients. Despite key advances, more research is needed. To this end, our group and others have focused on discovering and identifying novel, non-invasive histopathologic, and hemodynamic biomarkers which could potentially play a key role in further improving the care of patients with bicuspid aortopathy. By leveraging basic and translational research techniques, novel imaging modalities, and perhaps systemic biomarkers, improved risk prediction may result in more individualized treatment options and optimal management strategies.

AUTHOR CONTRIBUTIONS

All authors listed have made a substantial, direct and intellectual contribution to the work, and approved it for publication.

FUNDING

Research reported in this publication was supported by the National Heart, Lung, and Blood Institute of the National Institutes of Health under Award Number R01HL133504. The content is solely the responsibility of the authors and does not necessarily represent the official views of the National Institutes of Health.

REFERENCES

Adamo, L., and Braverman, A. C. (2015). Surgical threshold for bicuspid aortic valve aneurysm: a case for individual decision-makin. *Heart* 101, 1361–1367. doi: 10.1136/heartjnl-2014-306601

Atkins, S. K., and Sucosky, P. (2014). Etiology of bicuspid aortic valve disease: focus on hemodynamics. *World J. Cardiol.* 6, 1227–1233. doi: 10.4330/wjc.v6.i12.1227

Baltes, C., Kozerke, S., Hansen, M. S., Pruessmann, K. P., Tsao, J., and Boesiger, P. (2005). Accelerating cine phase-contrast flow measurements using *k-t* BLAST and *k-t* SENSE. *Magn. Reson. Med.* 54, 1430–1438. doi: 10.1002/mrm.20730

Barker, A. J., Lanning, C., and Shandas, R. (2010). Quantification of hemodynamic wall shear stress in patients with bicuspid aortic valve using phase-contrast MRI. *Ann. Biomed. Eng.* 38, 788–800. doi: 10.1007/s10439-009-9854-3

Barker, A. J., Markl, M., Burk, J., Lorenz, R., Bock, J., Bauer, S., et al. (2012). Bicuspid aortic valve is associated with altered wall shear stress in the ascending aorta. *Circ. Cardiovasc. Imaging* 5, 457–466. doi: 10.1161/CIRCIMAGING.112.973370

Bauer, M., Pasic, M., Meyer, R., Goetze, N., Bauer, U., Siniawski, H., et al. (2002). Morphometric analysis of aortic media in patients with bicuspid and tricuspid aortic valve. *Ann. Thorac. Surg.* 74, 58–62. doi: 10.1016/S0003-4975(02)03650-0

Bissell, M. M., Hess, A. T., Biasiolli, L., Glaze, S. J., Loudon, M., Pitcher, A., et al. (2013). Aortic dilation in bicuspid aortic valve disease: flow pattern is a major contributor and differs with valve fusion type. *Circ. Cardiovasc. Imaging.* 6, 499–507. doi: 10.1161/CIRCIMAGING.113.000528

Bock, J., Frydrychowicz, A., Lorenz, R., Hirtler, D., Barker, A. J., Johnson, K. M., et al. (2011). *In vivo* noninvasive 4D pressure difference mapping in the human aorta: phantom comparison and application in healthy volunteers and patients. *Magn. Reson. Med.* 66, 1079–1088. doi: 10.1002/mrm.22907

Bock, J., Frydrychowicz, A., Stalder, A. F., Bley, T. A., Burkhardt, H., Hennig, J., et al. (2010). 4D phase contrast MRI at 3 T: effect of standard and blood-pool contrast agents on SNR, PC-MRA, and blood flow visualization. *Magn. Reson. Med.* 63, 330–338. doi: 10.1002/mrm.22199

Bonow, R. O., Carabello, B. A., Chatterjee, K., de Leon, A. C., Faxon, D. P., Freed, M. D., et al. (2008). 2008 Focused update incorporated into the ACC/AHA 2006 guidelines for the management of patients with valvular heart disease: a report of the American College of Cardiology/American Heart Association Task Force on Practice Guidelines (Writing Committee to Revise the 1998 Guidelines for the Management of Patients With Valvular Heart Disease): endorsed by the Society of Cardiovascular Anesthesiologists, Society for Cardiovascular Angiography and Interventions, and Society of Thoracic Surgeons. *Circulation* 118, e523–e661. doi: 10.1016/j.jacc.2008.05.007

Burk, J., Blanke, P., Stankovic, Z., Barker, A., Russe, M., Geiger, J., et al. (2012). Evaluation of 3D blood flow patterns and wall shear stress in the normal and dilated thoracic aorta using flow-sensitive 4D CMR. *J. Cardiovasc. Magn. Reson.* 14:84. doi: 10.1186/1532-429X-14-84

Chun, A. S., Elefteriades, J. A., and Mukherjee, S. K. (2013). Medical treatment for thoracic aortic aneurysm - much more work to be done. *Prog. Cardiovasc. Dis.* 56, 103–108. doi: 10.1016/j.pcad.2013.05.008

Chung, A. W., Au Yeung, K., Sandor, G. G., Judge, D. P., Dietz, H. C., and van Breemen, C. (2007). Loss of elastic fiber integrity and reduction of vascular smooth muscle contraction resulting from the upregulated activities of matrix metalloproteinase-2 and -9 in the thoracic aortic aneurysm in Marfan syndrome. *Circ. Res.* 101, 512–522. doi: 10.1161/CIRCRESAHA.107.157776

Cibis, M., Jarvis, K., Markl, M., Rose, M., Rigsby, C., Barker, A. J., et al. (2015). The effect of resolution on viscous dissipation measured with 4D flow MRI in patients with Fontan circulation: evaluation using computational fluid dynamics. *J. Biomech.* 48, 2984–2989. doi: 10.1016/j.jbiomech.2015.07.039

Cotrufo, M., Della Corte, A., De Santo, L. S., De Feo, M., Covino, F. E., and Dialetto, G. (2003). Asymmetric medial degeneration of the ascending aorta in aortic valve disease: a pilot study of surgical management. *J. Heart Valve Dis.* 12, 127–133; discussion 134–125.

Cotrufo, M., Della Corte, A., De Santo, L. S., Quarto, C., De Feo, M., Romano, G., et al. (2005). Different patterns of extracellular matrix protein expression in the convexity and the concavity of the dilated aorta with bicuspid aortic valve: preliminary results. *J. Thorac. Cardiovasc. Surg.* 130, 504–511. doi: 10.1016/j.jtcvs.2005.01.016

Danyi, P., Elefteriades, J. A., and Jovin, I. S. (2011). Medical therapy of thoracic aortic aneurysms: are we there yet? *Circulation* 124, 1469–1476. doi: 10.1161/CIRCULATIONAHA.110.006486

Davies, R. R., Kaple, R. K., Mandapati, D., Gallo, A., Botta, D. M., Elefteriades, J. A., et al. (2007). Natural history of ascending aortic aneurysms in the setting of an unreplaced bicuspid aortic valve. *Ann. Thorac. Surg.* 83, 1338–1344. doi: 10.1016/j.athoracsur.2006.10.074

Della Corte, A. (2014). The conundrum of aortic dissection in patients with bicuspid aortic valve: the tissue, the mechanics and the mathematics. *Eur. J. Cardiothorac. Surg.* 48, 150–151. doi: 10.1093/ejcts/ezu418

Della Corte, A., Bancone, C., Buonocore, M., Dialetto, G., Covino, F. E., Manduca, S., et al. (2013). Pattern of ascending aortic dimensions predicts the growth rate of the aorta in patients with bicuspid aortic valve. *JACC Cardiovasc. Imaging* 6, 1301–1310. doi: 10.1016/j.jcmg.2013.07.009

Della Corte, A., Bancone, C., Conti, C. A., Votta, E., Redaelli, A., Del Viscovo, L., et al. (2012b). Restricted cusp motion in right-left type of bicuspid aortic valves: a new risk marker for aortopathy. *J. Thorac. Cardiovasc Surg.* 144, 360–369, 369.e1. doi: 10.1016/j.jtcvs.2011.10.014

Della Corte, A., Bancone, C., Dialetto, G., Covino, F. E., Manduca, S., D'Oria, V., et al. (2014a). Towards an individualized approach to bicuspid aortopathy: different valve types have unique determinants of aortic dilatation. *Eur. J. Cardiothorac. Surg.* 45, e118–e124; discussion e124. doi: 10.1093/ejcts/ezt601

Della Corte, A., Bancone, C., Quarto, C., Dialetto, G., Covino, F. E., Scardone, M., et al. (2007). Predictors of ascending aortic dilatation with bicuspid aortic valve: a wide spectrum of disease expression. *Eur. J. Cardiothorac. Surg.* 31, 397–404; discussion 404–405. doi: 10.1016/j.ejcts.2006.12.006

Della Corte, A., Body, S. C., Booher, A. M., Schaefers, H. J., Milewski, R. K., Michelena, H. I., et al. (2014b). Surgical treatment of bicuspid aortic valve disease: knowledge gaps and research perspectives. *J. Thoracic Cardiovascular. Surg.* 147, 1749–1757. doi: 10.1016/j.jtcvs.2014.01.021

Della Corte, A., Buonocore, M., and Del Viscovo, L. (2012c). Rationale and methods for quantifying ascending aortic flow eccentricity: back to the underlying mechanism? *J. Magn. Reson. Imaging* 36, 505–506; author reply 507. doi: 10.1002/jmri.23656

Della Corte, A., De Santo, L. S., and Forte, A. (2012a). Missing link between aortic wall pathology and aortic diameter: methodological bias or worrisome finding? *Eur. J. Cardiothorac. Surg.* 42, 195–196; author reply 196. doi: 10.1093/ejcts/ezs006

den Reijer, P. M., Sallee, D., van der Velden, P., Zaaijer, E. R., Parks, W. J., Ramamurthy, S., et al. (2010). Hemodynamic predictors of aortic dilatation in bicuspid aortic valve by velocity-encoded cardiovascular magnetic resonance. *J. Cardiovasc. Magn. Reson.* 12:4. doi: 10.1186/1532-429X-12-4

de Sa, M., Moshkovitz, Y., Butany, J., and David, T. E. (1999). Histologic abnormalities of the ascending aorta and pulmonary trunk in patients with bicuspid aortic valve disease: clinical relevance to the ross procedure. *J. Thorac. Cardiovasc. Surg.* 118, 588–594.

Ellison, J. W., Yagubyan, M., Majumdar, R., Sarkar, G., Bolander, M. E., Atkinson, E. J., et al. (2007). Evidence of genetic locus heterogeneity for familial bicuspid aortic valve. *J. Surg. Res.* 142, 28–31. doi: 10.1016/j.jss.2006.04.040

Erbel, R., Aboyans, V., Boileau, C., Bossone, E., Bartolomeo, R. D., Eggebrecht, H., et al. (2014). 2014 ESC Guidelines on the diagnosis and treatment of aortic diseases: document covering acute and chronic aortic diseases of the thoracic and abdominal aorta of the adult. The Task Force for the Diagnosis and Treatment of Aortic Diseases of the ESC. *Eur. Heart J.* 35, 2873–2926. doi: 10.1093/eurheartj/ehu281

Fazel, S. S., Mallidi, H. R., Lee, R. S., Sheehan, M. P., Liang, D., Fleischman, D. et al. (2008). The aortopathy of bicuspid aortic valve disease has distinctive patterns and usually involves the transverse aortic arch. *J. Thorac. Cardiovasc. Surg.* 135, 901–907, 907.e1–2. doi: 10.1016/j.jtcvs.2008.01.022

Fedak, P. W., David, T. E., Borger, M., Verma, S., Butany, J., and Weisel, R. D., (2005). Bicuspid aortic valve disease: recent insights in pathophysiology and treatment. *Expert Rev. Cardiovasc. Ther.* 3, 295–308. doi: 10.1586/14779072.3.2.295

Fedak, P. W., de Sa, M. P., Verma, S., Nili, N., Kazemian, P., Butany, J., et al. (2013). Vascular matrix remodeling in patients with bicuspid aortic valve malformations: implications for aortic dilatation. *J. Thorac. Cardiovasc. Surg.* 126, 797–806. doi: 10.1016/S0022-5223(03)00398-2

Fedak, P. W., and Verma, S. (2014). Bicuspid aortopathy and the development of individualized resection strategies. *J. Thorac. Cardiovasc. Surg.* 148, 2080–2081. doi: 10.1016/j.jtcvs.2014.09.059

Fedak, P. W., Verma, S., David, T. E., Leask, R. L., Weisel, R. D., and Butany, J. (2002). Clinical and pathophysiological implications of a bicuspid aortic valve. *Circulation* 106, 900–904. doi: 10.1161/01.CIR.0000027905.26586.E8

Forsell, C., Bjorck, H. M., Eriksson, P., Franco-Cereceda, A., and Gasser, T. C. (2014). Biomechanical properties of the thoracic aneurysmal wall: differences between bicuspid aortic valve and tricuspid aortic valve patients. *Ann. Thorac. Surg.* 98, 65–71. doi: 10.1016/j.athoracsur.2014.04.042

Forte, A., Bancone, C., Cobellis, G., Buonocore, M., Santarpino, G., Fischlein, T. J. M., et al. (2017). A possible early biomarker for bicuspid aortopathy: circulating transforming growth factor beta-1 to soluble endoglin ratio. *Circ. Res.* 120, 1800–1811. doi: 10.1161/CIRCRESAHA.117.310833

Frydrychowicz, A., Arnold, R., Harloff, A., Schlensak, C., Hennig, J., Langer, M., et al. (2008a). *In vivo* 3-dimensional flow connectivity mapping after extracardiac total cavopulmonary connection.*Circulation* 118, E16–E17. doi: 10.1161/CIRCULATIONAHA.107.761304

Frydrychowicz, A., Berger, A., Russe, M. F., Stalder, A. F., Harloff, A., Dittrich, S., et al. (2008b). Time-resolved magnetic resonance angiography and flow-sensitive 4-dimensional magnetic resonance imaging at 3 Tesla for blood flow and wall shear stress analysis. *J. Thorac. Cardiovasc. Surg.* 136, 400–407. doi: 10.1016/j.jtcvs.2008.02.062

Frydrychowicz, A., Stalder, A. F., Russe, M. F., Bock, J., Bauer, S., Harloff, A., et al. (2009). Three-dimensional analysis of segmental wall shear stress in the aorta by flow-sensitive four-dimensional-MRI. *J. Magn. Reson. Imaging* 30, 77–84. doi: 10.1002/jmri.21790

Garcia, J., Markl, M., Schnell, S., Allen, B., Entezari, P., Mahadevia, R., et al. (2014). Evaluation of aortic stenosis severity using 4D flow jet shear layer detection for the measurement of valve effective orifice area. *Magn Reson Imaging* 32, 891–898. doi: 10.1016/j.mri.2014.04.017

Garg, V., Muth, A. N., Ransom, J. F., Schluterman, M. K., Barnes, R., King, I. N., et al. (2005). Mutations in NOTCH1 cause aortic valve disease. *Nature* 437, 270–274. doi: 10.1038/nature03940

Girdauskas, E., and Borger, M. A. (2014). Surgical threshold for bicuspid aortic valveassociated aortopathy: does the phenotype matter? *JACC Cardiovasc Imaging* 7:318. doi: 10.1016/j.jcmg.2013.12.012

Girdauskas, E., Borger, M. A., Secknus, M. A., Girdauskas, G., and Kuntze, T. (2011). Is aortopathy in bicuspid aortic valve disease a congenital defect or a result of abnormal hemodyanimcs? A critical reappraisal of a one-sided argument. *Eur. J. Cardiothorac. Surg.* 39, 809–814. doi: 10.1016/j.ejcts.2011.01.001

Girdauskas, E., Disha, K., Raisin, H. H., Secknus, M. A., Borger, M. A., and Kuntze, T. (2012). Risk of late aortic events after an isolated aortic valve replacement for bicuspid aortic valve stenosis with concomitant ascending aortic dilation. *Eur. J. Cardiothorac. Surg.* 42, 832–837; discussion 837–838. doi: 10.1093/ejcts/Ezs137

Guzzardi, D. G., Barker, A. J., van Ooij, P., Malaisrie, S. C., Puthumana, J. J., Belke, D. D., et al. (2015). Valve-related hemodynamics mediate human bicuspid aortopathy: insights from wall shear stress mapping. *J. Am. Coll. Cardiol.* 66, 892–900. doi: 10.1016/j.jacc.2015.06.1310

Hardikar, A. A., and Marwick, T. H. (2015). The natural history of guidelines: the case of aortopathy related to bicuspid aortic valves. *Int. J. Cardiol.* 199, 150–153. doi: 10.1016/j.ijcard.2015.06.059

Harloff, A., Nussbaumer, A., Bauer, S., Stalder, A. F., Frydrychowicz, A., Weiller, C., et al. (2010a). *In vivo* assessment of wall shear stress in the atherosclerotic aorta using flow-sensitive 4D MRI. *Magn. Reson. Med.* 63, 1529–1536. doi: 10.1002/mrm.22383

Harloff, A., Simon, J., Brendecke, S., Assefa, D., Helbing, T., Frydrychowicz, A., et al. (2010b). Complex plaques in the proximal descending aorta: an underestimated embolic source of stroke. *Stroke* 41, 1145–1150. doi: 10.1161/STROKEAHA.109.577775

Harloff, A., Strecker, C., Dudler, P., Nussbaumer, A., Frydrychowicz, A., Olschewski, M., et al. (2009). Retrograde embolism from the descending aorta: visualization by multidirectional 3D velocity mapping in cryptogenic stroke. *Stroke* 40, 1505–1508. doi: 10.1161/STROKEAHA.108.530030

Heng, E., Stone, J. R., Kim, J. B., Lee, H., MacGillivray, T. E., and Sundt, T. M. (2015). Comparative histology of aortic dilatation associated with bileaflet versus trileaflet aortic valves. *Ann. Thorac. Surg.* 100, 2095–2101; discussion 2101. doi: 10.1016/j.athoracsur.2015.05.105

Hiratzka, L. F., Bakris, G. L., Beckman, J. A., Bersin, R. M., Carr, V. F., Casey, D. E., et al. (2010). ACCF/AHA/AATS/ACR/ASA/SCA/SCAI/SIR/STS/SVM guidelines for the diagnosis and management of patients with Thoracic Aortic Disease. *Circulation* 121, e266–e369. doi: 10.1161/CIR.0b013e3181d4739e

Hiratzka, L. F., Creager, M. A., Isselbacher, E. M., Svensson, L. G., Nishimura, R. A., Bonow, R. O., et al. (2016). Surgery for aortic dilatation in patients with bicuspid aortic valves: a statement of clarification from the american college of cardiology/american heart association task force on clinical practice guidelines. *J. Am. Coll. Cardiol.* 67, 724–731. doi: 10.1016/j.jacc.2015.11.006

Hoffman, J., and Kaplan, S. (2002). The incidence of congenital heart disease. *J. Am. Coll. Cardiol.* 39, 1890–1900. doi: 10.1016/S0735-1097(02)01886-7

Hope, M. D., Hope, T. A., Crook, S. E., Ordovas, K. G., Urbania, T. H., Alley, M. T., et al. (2011). 4D flow CMR in assessment of valve-related ascending aortic disease. *JACC. Cardiovasc. Imaging* 4, 781–787. doi: 10.1016/j.jcmg.2011.05.004

Hope, M. D., Hope, T. A., Meadows, A. K., Ordovas, K. G., Urbania, T. H., Alley, M. T., et al. (2010a). Bicuspid aortic valve: four-dimensional MR evaluation of ascending aortic systolic flow patterns. *Radiology* 255, 53–61. doi: 10.1148/radiol.09091437

Hope, M. D., Hope, T. A., Urbania, T. H., and Higgins, C. B. (2010b). Four-dimensional flow magnetic resonance imaging with wall shear stress analysis before and after repair of aortopulmonary fistula. *Circ. Cardiovasc. Imaging* 3, 766–768. doi: 10.1161/CIRCIMAGING.110.957712

Ikonomidis, J. S., Ivey, C. R., Wheeler, J. B., Akerman, A. W., Rice, A., Patel, R. K., et al. (2013). Plasma biomarkers for distinguishing etiologic subtypes of thoracic aortic aneurysm disease. *J. Thorac. Cardiovasc. Surg.* 145, 1326–1333. doi: 10.1016/j.jtcvs.2012.12.027

Ikonomidis, J. S., Jones, J. A., Barbour, J. R., Stroud, R. E., Clark, L. L., Kaplan, B. S., et al. (2007). Expression of matrix metalloproteinases and endogenous inhibitors within ascending aortic aneurysms of patients with bicuspid or tricuspid aortic valves. *J. Thorac. Cardiovasc. Surg.* 133, 1028–1036. doi: 10.1016/j.jtcvs.2006.10.083

Ikonomidis, J. S., Ruddy, J. M., Benton, S. M., Arroyo, J., Brinsa, T. A., Stroud, R. E., et al. (2012). Aortic dilatation with bicuspid aortic valves: cusp fusion correlates to matrix metalloproteinases and inhibitors. *Ann. Thorac. Surg.* 93, 457–463. doi: 10.1016/j.athoracsur.2011.09.057

Itagaki, S., Chiang, Y., and Tang, G. H. (2016). Why does the bicuspid aortic valve keep eluding us? *Cardiol. Rev.* 24, 119–130. doi: 10.1097/CRD.0000000000000053

Itagaki, S., Chikwe, J. P., Chiang, Y. P., Egorova, N. N., and Adams, D. H. (2015). Long term risk for aortic complications after aortic valve replacement in patients with bicuspid aortic valve versus Marfan syndorme. *J. Am. Coll. Cardiol.* 65, 2363–2369. doi: 10.1016/j.jacc.2015.03.575

Januzzi, J. L., Isselbacher, E. M., Fattori, R., Cooper, J. V., Smith, D. E.,Fang, J., et al. (2004). Characterizing the young patient with aortic dissection: results from the International Registry of Aortic Dissection (IRAD). *J. Am. Coll. Cardiol.* 43, 665–669. doi: 10.1016/j.jacc.2003.08.054

Jenkinson, M., and Smith, S. (2001). A global optimisation method for robust affine registration of brain images. *Med. Image Anal.* 5, 143–156. doi: 10.1016/S1361-8415(01)00036-6

Kang, J. W., Song, H. G., Yang, D. H., Baek, S., Kim, D. H., Song, J. M., et al. (2013). Association between bicuspid aortic valve phenotype and patterns of valvular dysfunction and bicuspid aortopathy: comprehensive evaluation using MDCT and echocardiography. *JACC. Cardiovasc. Imaging* 6, 150–161. doi: 10.1016/j.jcmg.2012.11.007

Lustig, M., Donoho, D., and Pauly, J. M. (2007). Sparse MRI: the application of compressed sensing for rapid MR imaging. *Magn. Reson. Med.* 58, 1182–1195. doi: 10.1002/mrm.21391

Mahadevia, R., Barker, A. J., Schnell, S., Entezari, P., Kansal, P., Fedak, P. W., et al. (2014). Bicuspid aortic cusp fusion morphology alters aortic three-dimensional outflow patterns, wall shear stress, and expression of aortopathy. *Circulation* 129, 673–682. doi: 10.1161/CIRCULATIONAHA.113.003026

Markl, M., Bauer, S., Bock, J., Stalder, A., Frydrychowicz, A., and Harloff, A. (2009). "Wall shear stress in normal & atherosclerotic carotid arteries," in *Proceedings: 21st Annual International Conference on MR Angiography* (Lansing, MI), 68.

Markl, M., Brendecke, S. M., Simon, J., Barker, A. J., Weiller, C., and Harloff, A. (2013). Co-registration of the distribution of wall shear stress and 140 complex plaques of the aorta. *Magn. Reson. Imaging* 31, 1156–1162. doi: 10.1016/j.mri.2013.05.001

Markl, M., Geiger, J., Arnold, R., Stroh, A., Damjanovic, D., Foll, D., et al. (2011a). Comprehensive 4-dimensional magnetic resonance flow analysis after successful heart transplantation resolvescontroversial intraoperative findings and reveals complex hemodynamic alterations. *Circulation* 123, e381–e383. doi: 10.1161/CIRCULATIONAHA.110.979971

Markl, M., Geiger, J., Kilner, P. J., Foll, D., Stiller, B., Beyersdorf, F., et al. (2011b). Time-resolved three-dimensional magnetic resonance velocity mapping of cardiovascular flow paths in volunteers and patients with Fontan circulation. *Eur. J. Cardiothorac. Surg.* 39, 206–212. doi: 10.1016/j.ejcts.2010.05.026

Markl, M., Harloff, A., Bley, T. A., Zaitsev, M., Jung, B., Weigang, E., et al. (2007). Time-resolved 3D MR velocity mapping at 3T: improved navigator-gated assessment of vascular anatomy and blood flow. *J. Magn. Reson. Imaging* 25, 824–831. doi: 10.1002/jmri.20871

Markl, M., Wallis, W., and Harloff, A. (2011c). Reproducibility of flow and wall shear stress analysis using flow-sensitive four-dimensional MRI. *J. Magn. Reson. Imaging* 33, 988–994. doi: 10.1002/jmri.22519

Markl, M., Wegent, F., Zech, T., Bauer, S., Strecker, C., Schumacher, M., et al. (2010). In vivo wall shear stress distribution in the carotid artery: effect of bifurcation geometry, internal carotid artery stenosis, and recanalization therapy. *Circ. Cardiovasc. Imaging* 3, 647–655. doi: 10.1161/CIRCIMAGING.110.958504

Martin, M., Alonso-Montes, C., Florez, J. P., Pichel, I. A., Rozado, J., Andía, J. B., et al. (2014). Bicuspid aortic valve syndrome: a heterogeneous and still unknown condition. *Int. J. Cardiol.* 177:1105. doi: 10.1016/j.ijcard.2014.09.132

Masri, A., Kalahasti, V., Alkharabsheh, S., Svensson, L. G., Sabik, J. F., Roselli, E. E., et al. (2016). Characteristics and long-term outcomes of contemporary patients with bicuspid aortic valves. *J. Thorac. Cardiovasc. Surg.* 151, 1650–1659. doi: 10.1016/j.jtcvs.2015.12.019

Michelena, H. I., Desjardins, V. A., Avierinos, J. F., Russo, A., Nkomo, V. T., Sundt, T. M., et al. (2008). Natural history of asymptomatic patients with normally functioning or minimally dysfunctional bicuspid aortic valve in the community. *Circulation* 117, 2776–2784. doi: 10.1161/CIRCULATIONAHA.107.740878

Michelena, H. I., Prakash, S. K., Della Corte, A., Bissell, M. M., Anavekar, N., Mathieu, P., et al. (2014). Bicuspid aortic valve: identifying knowledge gaps and rising to the challenge from the International Bicuspid

Aortic Valve Consortium (BAVCon). *Circulation* 129, 2691–2704. doi: 10.1161/CIRCULATIONAHA.113.007851

Michelena, H. I. (2015). The bicuspid aortic valve aortopathy mystery continues: are we that mediocre? *Trends Cardiovasc. Med.* 25, 452–455. doi: 10.1016/j.tcm.2014.12.016

Michelena, H. I., Della Corte A, Prakash, S. K., Milewicz, D. M., Evangelista, A., and Enriquez-Sarano, M. (2015). Bicuspid aortic valve aortopathy in adults: incidence, etiology, and clinical significance. *Int. J. Cardiol.* 201, 400–407. doi: 10.1016/j.ijcard.2015.08.106

Michelena, H. I., Khanna, A. D., Mahoney, D., Margaryan, E., Topilsky, Y., Suri, R. M., et al. (2011). Incidence of aortic complications in patients with bicuspid aortic valves. *JAMA* 306, 1104–1112. doi: 10.1001/jama.2011.1286

Moaref, A., Khavanin, M., and Shekarforoush, S. (2014). Aortic distensibility in bicuspid aortic valve patients with normal aortic diameter. *Ther. Adv. Cardiovasc. Dis.* 8, 128–132. doi: 10.1177/1753944714531062

Moftakhar, R., Aagaard-Kienitz, B., Johnson, K., Turski, P. A., Turk, A. S., Niemann, D.B., et al. (2007). Noninvasive measurement of intra-aneurysmal pressure and flow pattern using phase contrast with vastly undersampled isotropic projection imaging. *AJNR Am. J. Neuroradiol.* 28, 1710–1714. doi: 10.3174/ajnr.A0648

Moon, M. R. (2015). Extent of distal resection for bicuspid aortopathy: Is surgical experience a factor? *J. Thorac. Cardiovasc. Surg.* 150, 125–126. doi: 10.1016/j.jtcvs.2015.04.004

Nishimura, R. A., Otto, C. M., Bonow, R. O., Carabello, B. A., Erwin, J. P. III, Guyton, R. A., et al. (2014). 2014 AHA/ACC Guideline for the Management of Patients with Valvular Heart Disease: a report of the American College of Cardiology/American Heart Association Task Force on Practice Guidelines. *Circulation* 129, 2440–2492. doi: 10.1161/CIR.0000000000000029

Nistri, S., Grande-Allen, J., Noale, M., Basso, C., Siviero, P., Maggi, S., et al. (2008). Aortic elasticity and size in bicuspid aortic valve syndrome. *Eur. Heart J.* 29, 472–479. doi: 10.1093/eurheartj/ehm528

Nistri, S., Sorbo, M. D., Basso, C., and Thiene, G. (2002). Bicuspid aortic valve: abnormal aortic elastic properties. *J. Heart Valve Dis.* 11, 369–373; discussion 373–364.

Opotowsky, A. R., Perlstein, T., Landzberg, M. J., Colan, S. D., O'Gara, P. T., Body, S. C., et al. (2013). A shifting approach to management of the thoracic aorta in bicuspid aortic valve. *J. Thorac. Cardiovasc. Surg.* 146, 339–346. doi: 10.1016/j.jtcvs.2012.10.028

Oulego-Erroz, I., Alonso-Quintela, P., Mora-Matilla, M., Gautreaux Minaya, S., and Lapena-Lopez de Armentia, S. (2013). Ascending aorta elasticity in children with isolated bicuspid aortic valve. *Int. J. Cardiol.* 168, 1143–1146. doi: 10.1016/j.ijcard.2012.11.080

Pees, C., and Michel-Behnke, I. (2012). Morphology of the bicuspid aortic valve and elasticity of the adjacent aorta in children. *Am. J. Cardiol.* 110, 1354–1360. doi: 10.1016/j.amjcard.2012.06.043

Petrini, J., Jenner, J., Rickenlund, A., Eriksson, P., Franco-Cereceda, A., Caidahl, K., et al. (2014). Elastic properties of the descending aorta in patients with a bicuspid or tricuspid aortic valve and aortic valvular disease. *J. Am. Soc. Echocardiogr.* 27, 393–404. doi: 10.1016/j.echo.2013.12.013

Phillippi, J. A., Green, B. R., Eskay, M. A., Kotlarczyk, M. P., Hill, M. R., Robertson, A. M., et al. (2014). Mechanism of aortic medial matrix remodeling is distinct in patients with bicuspid aortic valve. *J. Thorac. Cardiovasc. Surg.* 147, 1056–1064. doi: 10.1016/j.jtcvs.2013.04.028

Potters, W. V., van Ooij, P., Marquering, H., Vanbavel, E., and Nederveen, A. J. (2014). Volumetric arterial wall shear stress calculation based on cine phase contrast MRI. *J. Magn. Reson. Imaging.* 41, 505–516. doi: 10.1002/jmri.24560

Prakash, A., Adlakha, H., Rabideau, N., Hass, C. J., Morris, S. A., Geva, T., et al. (2015). Segmental aortic stiffness in children and young adults with connective tissue disorders: relationships with age, aortic size, rate of dilation, and surgical root replacement. *Circulation* 132, 595–602. doi: 10.1161/CIRCULATIONAHA.114.014934

Prakash, S. K., Bossé, Y., Muehlschlegel, J. D., Michelena, H. I., Limongelli, G., Della Corte, A., et al. (2014). A roadmap to investigate the genetic basis of bicuspid aortic valve and its complications insights from the International BAVCon (Bicuspid Aortic Valve Consortium). *J. Am. Coll. Cardiol.* 64, 832–839. doi: 10.1016/j.jacc.2014.04.073

Rabkin, S. W. (2014). Differential expression of MMP-2, MMP-9 and TIMP proteins in thoracic aortic aneurysm - comparison with and without bicuspid aortic valve: a meta-analysis. *Vasa* 43, 433–442. doi: 10.1024/0301-1526/a000390

Schaefer, B. M., Lewin, M. B., Stout, K. K., Byers, P. H., and Otto, C. M. (2007). Usefulness of bicuspid aortic valve phenotype to predict elastic properties of the ascending aorta. *Am. J. Cardiol.* 99, 686–690. doi: 10.1016/j.amjcard.2006.09.118

Sherrah, A. G., Andvik, S., van der Linde, D., Davies, L., Bannon, P. G., Padang, R., et al. (2016). Nonsyndromic thoracic aortic aneurysm and dissection: outcomes with Marfan syndrome versus bicuspid aortic valve aneurysm. *J. Am. Coll. Cardiol.* 67, 618–626. doi: 10.1016/j.jacc.2015.11.039

Sievers, H. H., and Sievers, H. L. (2011). Aortopathy in bicuspid aortic valve disease - genes or hemodynamics? or Scylla and Charybdis? *Eur. J. Cardiothorac. Surg.* 39, 803–804. doi: 10.1016/j.ejcts.2011.02.007

Sievers, H. H., Stierle, U., Hachmann, R. M., and Charitos, E. I. (2016). New insights in the association between bicuspid aortic valve phenotype, aortic configuration and valve haemodynamics. *Eur. J. Cardiothorac. Surg.* 49, 439–446. doi: 10.1093/ejcts/ezv087

Song, J. K. (2015). Bicuspid aortic valve: unresolved issues and role of imaging specialists. *J. Cardiovasc. Ultrasound.* 23, 1–7. doi: 10.4250/jcu.2015.23.1.1

Spinale, F. G., and Bolger, A. F. (2015). Fate versus flow: wall shear stress in the aortopathy associated with bicuspid aortic valves. *J. Am. Coll. Cardiol.* 66, 901–904. doi: 10.1016/j.jacc.2015.07.002

Stalder, A. F., Russe, M. F., Frydrychowicz, A., Bock, J., Hennig, J., and Markl, M. (2008). Quantitative 2D and 3D phase contrast MRI: optimized analysis of blood flow and vessel wall parameters. *Magn. Reson. Med.* 60, 1218–1231. doi: 10.1002/mrm.21778

Sundt, T. M. (2015). Aortic replacement in the setting of bicuspid aortic valve: how big? How much? *J. Thorac. Cardiovasc. Surg.* 149, S2–S9. doi: 10.1016/j.jtcvs.2014.07.069

Svensson, L. G., Adams, D. H., Bonow, R. O., Kouchoukos, N. T., Miller, D. C., O'Gara, P. T., et al. (2013). Aortic valve and ascending aorta guidelines for management and quality measures. *Ann. Thorac. Surg.* 95, S1–S66. doi: 10.1016/j.athoracsur.2012.12.027

Tadros, T. M., Klein, M. D., and Shapira, O. M. (2009). Ascending aortic dilatation associated with bicuspid aortic valve: pathophysiology, molecular biology, and clinical implications. *Circulation* 119, 880–890. doi: 10.1161/CIRCULATIONAHA.108.795401

Thompson, M., and Cockerill, G. (2006). Matrix metalloproteinase-2: the forgotten enzyme in aneurysm pathogenesis. *Ann. N. Y. Acad. Sci.* 1085, 170–174. doi: 10.1196/annals.1383.034

Tricoci, P., Allen, J. M., Kramer, J. M., Califf, R. M., and Smith, S. C., Jr. (2009). Scientific evidence underlying the ACC/AHA clinical practice guidelines. *JAMA* 301, 831–841. doi: 10.1001/jama.2009.205

Tzemos, N., Therrien, J, Yip, J., Thanassoulis, G., Tremblay, S., Jamorski, M. T., et al. (2008). Outcomes in adults with bicuspid aortic valves. *JAMA* 300, 1317–1325. doi: 10.1001/jama.300.11.1317

Uretsky, S., and Gillam, L. D. (2014). Nature versus nurture in bicuspid aortic valve aortopathy: more evidence that altered hemodynamics may play a role. *Circulation* 129, 622-624. doi: 10.1161/CIRCULATIONAHA.113.007282

Vahanian, A., Alfieri, O., Andreotti, F., Antunes, M. J., Barón-Esquivias, G., Baumgartner, H., et al. (2012). Guidelines on the management of valvular heart disease (version 2012): the Joint Task Force on the Management of Valvular Heart Disease of the European Society of Cardiology and the European Association for Cardiothoracic Surgery. *Eur. J. Cardiothoracic Surg.* 42, S1–S44. doi: 10.1093/eurheartj/ehs109

van Ooij, P., Potters, W. V., Collins, J., Carr, M., Carr, J., Malaisrie, S. C., et al. (2015c). Characterization of abnormal wall shear stress using 4D flow MRI in human bicuspid aortopathy. *Ann. Biomed. Eng.* 43, 1385–1397. doi: 10.1007/s10439-014-1092-7

van Ooij, P., Potters, W. V., Nederveen, A. J., Allen, B. D., Collins, J., Carr, J., et al. (2015a). A methodology to detect abnormal relative wall shear stress on the full surface of the thoracic aorta using four-dimensional flow MRI. *Magn. Reson. Med.* 73, 1216–1227. doi: 10.1002/mrm.25224

van Ooij, P., Powell, A. L., Potters, W. V., Carr, J. C., Markl, M., and Barker, A. J. (2015b). Reproducibility and interobserver variability of systolic blood flow velocity and 3D wall shear stress derived from 4D flow MRI in the healthy aorta. *J. Magn. Reson. Imaging* 43, 236–248. doi: 10.1002/jmri.24959

Verma, S., and Siu, S. C. (2014). Aortic dilatation in patients with bicuspid aortic valve. *N. Engl. J. Med.* 370, 1920–1929. doi: 10.1056/NEJMra1207059

Verma, S., Yanagawa, B., Kalra, S., Ruel, M., Peterson, M. D., Yamashita, M. H., et al. (2013). Knowledge, attitudes, and practice patterns in surgical management of bicuspid aortopathy: a survey of 100 cardiac surgeons. *J. Thorac. Cardiovasc. Surg.* 146, 1033–1040. doi: 10.1016/j.jtcvs.2013.06.037

Warner, P. J., Al-Quthami, A., Brooks, E. L., Kelley-Hedgepeth, A., Patvardhan, E., Kuvin, J. T., et al. (2013). Augmentation index and aortic stiffness in bicuspid aortic valve patients with non-dilated proximal aortas. *BMC Cardiovasc. Disord.* 13:19. doi: 10.1186/1471-2261-13-19

Warnes, C. A., Williams, R. G., Bashore, T. M., Child, J. S., Connolly, H. M., Dearani, J. A., et al. (2008). ACC/AHA 2008 Guidelines for the Management of Adults with Congenital Heart Disease: a report of the American College of Cardiology/American Heart Association Task Force on Practice Guidelines (writing committee to develop guidelines on the management of adults with congenital heart disease). *Circulation* 118, e714–e833. doi: 10.1161/CIRCULATIONAHA.108.190811

Wasfy, J. H., Armstrong, K., Milford, C. E., and Sundt, T. M. (2015). Bicuspid aortic disease and decision making under uncertainty: the limitations of clinical guidelines. *Int. J. Cardiol.* 181, 169–171. doi: 10.1016/j.ijcard.2014.12.020

Wilton, E., Bland, M., Thompson, M., and Jahangiri, M. (2008). Matrix metalloproteinase expression in the ascending aorta and aortic valve. *Interact. Cardiovasc. Thorac. Surg.* 7, 37–40. doi: 10.1510/icvts.2007.163311

Ziganshin, B. A., Mukherjee, S. K., and Elefteriades, J. A. (2015). Atenolol versus losartan in Marfan's syndrome. *N. Engl. J. Med.* 372, 977–978. doi: 10.1056/NEJMc1500128

Conflict of Interest Statement: The authors declare that the research was conducted in the absence of any commercial or financial relationships that could be construed as a potential conflict of interest.

Advantages of publishing in Frontiers

OPEN ACCESS
Articles are free to read, for greatest visibility

COLLABORATIVE PEER-REVIEW
Designed to be rigorous – yet also collaborative, fair and constructive

FAST PUBLICATION
Average 85 days from submission to publication (across all journals)

COPYRIGHT TO AUTHORS
No limit to article distribution and re-use

TRANSPARENT
Editors and reviewers acknowledged by name on published articles

SUPPORT
By our Swiss-based editorial team

IMPACT METRICS
Advanced metrics track your article's impact

GLOBAL SPREAD
5'100'000+ monthly article views and downloads

LOOP RESEARCH NETWORK
Our network increases readership for your article

Frontiers
EPFL Innovation Park, Building I • 1015 Lausanne • Switzerland
Tel +41 21 510 17 00 • Fax +41 21 510 17 01 • info@frontiersin.org
www.frontiersin.org

Find us on